21st Annual Combustion Research Conference

U.S. Department of Energy
Office of Basic Energy Sciences

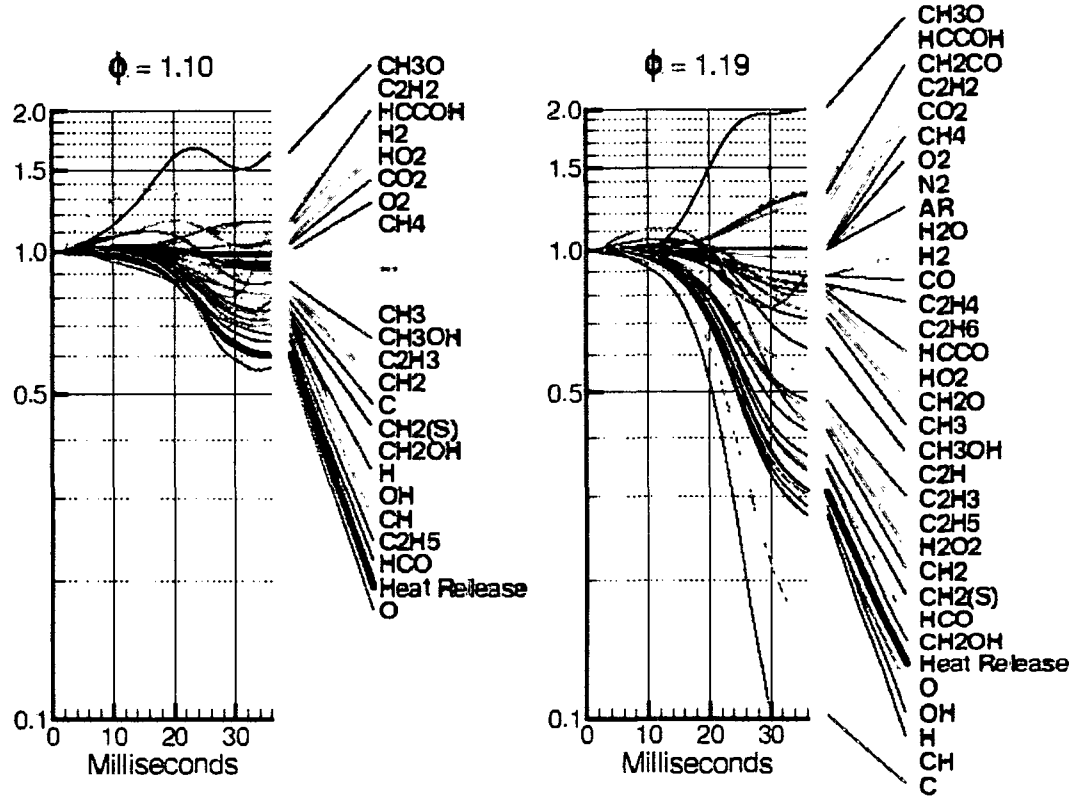

Westfields International Conference Center
Chantilly, Virginia

May 30-June 2, 2000

Cover Figure: Time history of the peak values of molar concentrations for various species, normalized to their respective values at t = 2 ms from a simulation of vortex interactions with a premixed methane flame by John Bell, Center for Computational Science and Engineering, Lawrence Berkeley National Laboratory, Combustion Teleconference, May, 2000.

Table of Contents

FOREWORD

The achievement of National goals for energy conservation and environmental protection will rely on technology more advanced than we have at our disposal today. Combustion at present accounts for 85% of the energy generated and used in the U.S. and is likely to remain a dominant source of energy for the coming decades. Achieving energy conservation while minimizing unwanted emissions from combustion processes could be greatly accelerated if accurate and reliable means were at hand for quantitatively predicting process performance.

The reports appearing in this volume present work in progress in basic research contributing to the development of a predictive capability for combustion processes. Most of the work reported herein is supported by the Department of Energy's Office of Basic Energy Sciences (BES) and a large fraction by the chemical physics program. The long-term objective of this effort is the provision of theories, data, and procedures to allow the development of reliable computational models of combustion processes, systems, and devices

The development of reliable models for combustion requires the accurate characterization of turbulent flow, chemistry, and the interaction between the two. In contributing to this end, BES supports basic research to meet a variety of needs.

- For even the simplest fuels, the chemistry of combustion consists of hundreds of reactions. Key reaction mechanisms, the means for characterizing these mechanisms and the means for determining which of the constituent reaction rates are critical for accurate characterization are all required.
- For reactions known to be important, accurate rates over wide ranges of temperature, pressure and composition are required. To assess the accuracy of measured reaction rates or to predict rates that would be too difficult to measure, theories of reaction rates and means for calculating their values either from first principles or semiempirically from known thermodynamic properties are needed.
- Energy flow and accounting must be accurately characterized and predicted.
- Methods for reducing the mathematical complexity inherent in hundreds of reactions, without sacrificing accuracy and reliability are required. Methods for reducing the computational complexity of computer models that attempt to address turbulence, chemistry, and their interdependence and also needed.

Although the emphasis in this list is on the development of mathematical models for simulating the gas phase reactions characteristic of combustion, ***such models, from the chemical dynamics of a single molecule to the performance of a combustion device, have value only when confirmed by experiment.*** Hence, the DOE program represented by reports in this volume supports the development and application of new experimental tools in chemical dynamics, kinetics, and spectroscopy.

The success of this research effort will not be measured by the quality of the research performed or the profundity of the knowledge gained, as critical as these may be. Rather it will be measured primarily by the degree to which it contributes to goals of resource conservation and

environmental stewardship. The basic research community has therefore a responsibility to be continuously attuned to the usefulness of the knowledge it creates and to optimize that usefulness wherever possible. Computational models of physical processes provide a most efficient means for ensuring the usefulness and use of basic theories and data. Although the combustion modeling and simulation initiative in the FY 2000 Department of Energy budget failed in the end to gain the support of the Congress, it is still widely recognized that modeling and simulation will play an increasing role in modern technology development. This year the budget request from the Department of Energy contains a request for additional resources for computational chemistry though at a level much reduced from last year's request.

The usefulness of the basic research programs of the Department can also benefit from closer collaboration with the technology research programs of the Department to the enrichment of both. In recognition of such benefit, this year's meeting includes presentations describing work supported by the Coal Utilization Sciences program of the Department of Energy's Office of Fossil Energy.

During the past year, the Chemical Physics program has continued to benefit from the involvement of Dr. Eric Rohlfing, program manager for the Atomic, Molecular and Optical Physics program, and Dr. Allan Laufer, team leader for the fundamental interactions programs, both of the Chemical Sciences, Biosciences, and Geosciences Division, and their contributions are hereby gratefully acknowledged. The efforts of Leila Gosslee and Kristy Duncan of the Oak Ridge Institute for Science Education in the arrangements for the meeting are also much appreciated.

William H. Kirchhoff
Fundamental Interactions Team
Chemical Sciences, Geosciences and Biosciences Division
Office of Basic Energy Sciences
e-mail: william.kirchhoff@science.doe.gov

May 30, 2000

21st Annual Combustion Research Conference
U.S. Department of Energy
Office of Basic Energy Sciences

Agenda

Tuesday, May 30

3:00 pm *Registration*

6:00 pm *Dinner*

7:30 pm *Welcoming Remarks*

7:45 pm *Invited Lecture*

Computational chemistry: not theory, not experiment. Is it science?

Dr. Karl Irikura
Physical and Chemical Properties Division
National Institute of Standards and Technology

Abstract. Throughout the R&D community, modeling and simulation are increasingly attractive economically, and are correspondingly important. This is especially evident in chemistry, where it has become unusual to find purely experimental papers in many of the pedigreed journals. A new type of scientist has emerged, who neither develops new theories of nature nor observes natural phenomena: the computational scientist. I will present some opinions about the apparent trichotomy of theory, experiment, and computation. The maturing role of computational chemistry will be illustrated using three recent technical projects in the areas of molecular spectroscopy, physical chemistry, and organic chemistry.

9:00 pm *Reception*

Wednesday, May 31
Morning Session

Special Session on Coal Utilization Sciences Research

8:00 am *"Overview of Coal Utilization Sciences (CUS) supported Research,"* Philip M. Goldberg, National Energy Technology Laboratory

8:10 am *"Thermodynamic Rules for the Self-Organization of Carbon Materials,"* Robert Hurt, Brown University

8:40 am *"Mechanisms of Coal Combustion,"* Christopher M. Hadad, Ohio State University

8:55 am *"Atomic-Level Imaging of CO_2 Disposal as a Carbonate Mineral: Optimizing Reaction Process Design,"* M.J. McKelvy, Arizona State University

9:15 am *"Atomic Level Modeling of CO_2 Disposal as a Carbonate Mineral: A Synergetic Approach to Optimizing Reaction Process Design,"* A.V.G. Chizmeshya, Arizona State University

9:30 am *"Elementary Reaction Rate Measurements at High Temperatures by Tunable-Laser Flash-Absorption,"* Jan P. Hessler, Argonne National Laboratory

10:00 am ***Break***

10:15 am *"Chemical Kinetic Data Base for Combustion Modeling,"* Wing Tsang, National Institute of Standards and Technology

10:45 am *"Mechanism and Detailed Modeling of Soot Formation,"* Michael Frenklach, Lawrence Berkeley National Laboratory

11:15 am *"Very High Pressure Single Pulse Shock Tube Studies of Aromatic Species,"* Kenneth Brezinsky, University of Illinois at Chicago

11:45 am *"Kinetics of Elementary Processes Relevant to Incipient Soot Formation"* M.C. Lin, Emory University

12:15 pm ***Lunch***

5:00 pm ***Dinner***

Wednesday, May 31
Evening Session

Joe V. Michael, Chair

6:15 pm *"Kinetics of Combustion-Related Processes at High Temperatures,"* J.H. Kiefer, University of Illinois at Chicago

6:45 pm *"Probing Flame Chemistry with MBMS, Theory, and Modeling,"* Phillip R. Westmoreland, University of Massachusetts

7:15 pm *"Comprehensive Mechanisms for Combustion Chemistry: Experiment, Modeling, and Sensitivity Analysis,"* Frederick L. Dryer, Princeton University

7:45 pm *"Gas-Phase Molecular Dynamics: Studies of the CH_3+O Radical-Radical Reaction,"* Jack M. Preses and Christopher Fockenberg, Brookhaven National Laboratory

8:15 pm ***Break***

8:30 pm *"Time-Resolved Infrared Absorption Studies of the Dynamics of Radical Reactions,"* R.G. Macdonald, Argonne National Laboratory

9:00 pm *"Spectroscopy and Kinetics of Combustion Gases at High Temperatures,"* Ronald K. Hanson and Craig T. Bowman, Stanford University

9:30 pm *"Infrared Absorption Spectroscopy and Chemical Kinetics of Free Radicals,"* Robert F. Curl, Jr. and Graham P. Glass, Rice University

10:00 pm ***Social***

Thursday, June 1
Morning Session

James Muckerman, Chair

8:00 am *"Chemical Accuracy From Ab Initio Molecular Orbital Calculations,"* Martin Head-Gordon, Lawrence Berkeley Laboratory

8:30 am *"Theoretical Studies of Molecular Systems,"* William A. Lester, Jr., Lawrence Berkeley Laboratory

9:00 am *"Electronic Structure Studies of Pyrolytic Reactions of Hydrocarbons and Their Chloro Derivatives,"* J. Cioslowski and D. Moncrieff, Florida State University

9:30 am *"Studies in Chemical Dynamics,"* Herschel Rabitz and Tak-San Ho, Princeton University

10:00 am ***Break***

10:15 am *"Reactions of Atoms and Radicals in Pulsed Molecular Beams,"* Hannah Reisler, University of Southern California

10:45 am *"Photodissociation of Free Radicals and Hydrocarbons,"* Daniel M. Neumark, Lawrence Berkeley Laboratory

11:15 am *"Universal Imaging Studies of Chemical Reaction Dynamics,"* Arthur G. Suits, Lawrence Berkeley Laboratory

11:45 am *"Chemical Dynamics and Spectroscopy at the Chemical Dynamics Beamline of the ALS,"* Tomas Baer, University of North Carolina

12:15 pm ***Lunch***

Thursday, June 1
Afternoon Session

Laurie J. Butler, Chair

4:00 pm *"Energy Partitioning in Elementary Chemical Reactions,"* Richard Bersohn, Columbia University

4:30 pm *"Theoretical Studies of the Dynamics of Chemical Reactions,"* Albert F. Wagner, Argonne National Laboratory

5:00 pm *"Theoretical Modeling of the Kinetics of Barrierless Reactions,"* Stephen J. Klippenstein, Case Western Reserve University

5:30 pm ***Break***

5:45 pm *"Ionization Probes of Molecular Structure And Chemistry,"* Philip M. Johnson, State University of New York at Stony Brook

6:15 pm *"Energy-Transfer Studies Using Tunable Picosecond Lasers,"* R.L. Farrow, D.A.V. Kliner, Fabio Di Teodoro, and Thomas A. Reichardt, Sandia National Laboratories

6:45 pm *"Flame Chemistry and Diagnostics,"* Andrew McIlroy, Sandia National Laboratories

7:15 pm *"Crossed-Molecular-Beam Ion Imaging Experiments,"* David W. Chandler, Sandia National Laboratories

8:00 pm ***Dinner***

Friday, June 2
Morning Session

George Flynn, Chair

8:00 am *"Laser Photoelectron Spectroscopy of Ions,"* G. Barney Ellison, University of Colorado

8:30 am *"Product Imaging of Combustion Dynamics,"* P. L. Houston, Cornell University

9:00 am *"Independent Generation and Study of Key Radicals in Hydrocarbon Combustion ,"* Barry K. Carpenter and Pamela A. Arnold, Cornell University

9:30 am *"Single-Collision Studies of Energy Transfer and Chemical Reaction,"* James J. Valentini, Columbia University

10:00 am ***Break***

10:15 am *"Highly Vibrationally Excited Molecules: Energy Transfer and Transient Species Vibrational Spectroscopy Through Time-Resolved IR Emission,"* Hai-Lung Dai, University of Pennsylvania

10:45 am *"Dynamical Analysis of Highly Excited Molecular Spectra,"* Michael E. Kellman, University of Oregon

11:15 am *"Vibrational State Control of Photodissociation,"* F.F. Crim, University of Wisconsin

11:45 am ***Closing Remarks***

Table of Contents

Abstracts

Analysis of Turbulent Reacting Flow

William T. Ashurst and Alan R. Kerstein
Combustion Research Facility
Sandia National Laboratories
Livermore, CA 94551-0969
Email: ashurs@ca.sandia.gov

PROGRAM SCOPE

Turbulent combustion involves processes ranging from femtosecond chemical dynamics to macroscopic flow phenomena. This project utilizes numerical simulation to study the interactions between the finest scales of fluid flow and physical and chemical effects that are simulated at the atomistic or the continuum level. The atomistic simulations use Molecular Dynamics (MD) to investigate the effects of atomic-level fluctuations on liquid atomization under diesel injection conditions. The continuum simulations use Direct Numerical Simulation (DNS) and One-Dimensional Turbulence (ODT) to investigate continuum-level fluctuation effects (e.g., turbulent eddies) at moderate and high turbulence intensity, respectively. The range of tools and of regimes examined will allow the development of a model of liquid-fuel atomization in engines that reflects the fundamental governing mechanisms, and accordingly, will provide needed predictive capabilities. MD and ODT are also used to study fundamental interactions between chemical kinetics and flow in gaseous combustion processes.

MD simulates the interactions of atoms or molecules as they move under the influence of an interaction potential. The simple Lennard-Jones pair potential is used in this work. Chemical reactions, wall effects, and global forcings (e.g., volumetric expansion) are incorporated into the simulations to reflect the corresponding features of the multiphase and combustion phenomena of interest.

DNS solves the 3D continuum equations of motion. For the atomization problem, an interface subject to surface tension is incorporated.

ODT is a 1D model formulated as a fully resolved unsteady simulation representing the time evolution of velocity profiles and advected fluid properties along a 1D line of sight in a turbulent flow. In this formulation, viscous momentum transport, species molecular transport, and chemical reactions evolve according to 1D equations of conventional form, as in 1D laminar strained flame computations. Turbulent eddies are represented by instantaneous rearrangements of property profiles on the 1D domain. The occurrence of these rearrangements is governed by a statistical sampling procedure in which event likelihoods depend on local turbulence production mechanisms (e.g., shear profile along the 1D domain). The rearrangement rules induce gradient amplification and fluid overturns that simulate reacting flow phenomena such as the unsteady evolution of multiple interacting flamelets.

RECENT PROGRESS

Atomization of a diesel fuel jet occurs over microsecond time scales and over sub-millimeter distances. The liquid jet breakup may depend upon cavitation and involves creation of new liquid surface area. Neither of these effects are well described by continuum models of fluid dynamics.

To obtain a direct numerical simulation of the atomization process, we have used the molecular dynamics (MD) method which directly computes the atomic motion [1]. Instead of the complete fuel jet breakup, we have simulated a much smaller homogeneous volume of liquid which undergoes atomization during an applied rapid expansion. In the calculations, the liquid volume is composed of 32,000 atoms, and it is expanding into a vacuum, with expansion time scales from 1 to 100 picoseconds.

It is found that the mean droplet size has a power-law dependence upon the initial expansion rate, in agreement with two continuum models of fragmentation. Extrapolation of the MD results to larger systems yields agreement with experimental results obtained with the free-jet expansion of liquid helium [2], in which the largest drop contains 40 million atoms. This comparison must be interpreted cautiously: the flow-induced strain rates created in the jet are more complex than the uniform expansion rates used in the MD simulations. An additional numerical factor of three could enter into the comparison if the estimated axial strain rate before the jet orifice is used. To provide more information, additional MD simulations [3] which used various axisymmetric expansions, instead of just the triaxial expansion described above, were done in order to more closely duplicate the expanding jet configuration. The mean droplet size in these axisymmetric cases was only a few percent larger than the symmetric-triaxial results. Thus, the axisymmetric expansion of a liquid produces fragmentation which depends strongly on the volume expansion rate, and only weakly on the composition of the expansion.

MD simulations using the Lennard-Jones energy potential have been compared with continuum solutions of reaction and diffusion in a dilute gas [4]. The reaction model is a passive one in which high energy bath atoms create a species, at dilute concentrations, which may have a very fast consumption reaction. This construction emulates typical fast reaction pathways involved in the fuel breakup in a hydrocarbon flame. Using the reaction rates and the diffusivities obtained from the molecular simulations, it is found that a continuum solution can describe the reactive atom density spatial distribution with good accuracy. Based on this agreement, it is possible to estimate which reaction rates will produce negligible diffusive spreading, and hence, which species might be assumed to be in chemical equilibrium in continuum reacting flow calculations.

The ODT methodology incorporates two features that capture the essential attributes of turbulence-microscale interaction processes. First, rearrangement events modify shear profiles, which in turn govern the occurrence of subsequent events. This two-way coupling induces complex behaviors based on the simple rules of model. In particular, rearrangements occur in sporadic bursts that obey the scaling laws of the inertial-range turbulent cascade. This is the universal or generic characteristic of the model. Second, the conventional continuous-time evolution of the 1D viscous advection-diffusion-reaction equations incorporates flow-specific behaviors through the imposed initial and boundary conditions and body forcings (e.g., buoyancy). These flow-specific behaviors include transients, spatial inhomogeneities, and energy-transfer processes that modify the cascade process in the simulations, much as in 3D Navier-Stokes turbulence.

This formulation reproduces many of the known flow-specific as well as generic scaling laws of turbulence [5]. Moreover, it reproduces remarkable large-scale structure induced by turbulence-microphysics interactions. In particular, recent work simulated the spontaneous formation of layered structure in a buoyant flow with an imposed stable salinity gradient, destabilized by heating from below [6]. The layering is a result of the difference between the molecular diffusivity of salt and heat in water. Fully resolved 3D simulation of the range of scales from thin diffusive interfaces between layers to the largest turbulent eddies is unaffordable. Models that involve spatial or temporal averaging cannot capture the physics driving structure formation.

ODT is unique in its capability to capture the relevant physics. The simulations demonstrated this capability as well as clarifying the mechanistic origins of aspects of the layering process.

As a step toward simulation of turbulent jet diffusion flames, ODT simulations of two time-developing planar free shear flows, the jet and the mixing layer, were compared to DNS results [7]. The comparisons indicate that ODT captures the principal features of free shear flow structure and energetics. Comparable performance has been demonstrated for homogeneous turbulence, wall boundary layers, and buoyancy driven flows [5, 8].

The planar jet simulation has been generalized for application to turbulent jet diffusion flame measurements at the Combustion Research Facility and other institutions involved in the Turbulent Nonpremixed Flame (TNF) workshop series and research collaboration. Comparisons of computed results to the mean evolution and fluctuation statistics of reactive species measured in turbulent diffusion flames are underway. Initial applications to H2-air and CH4-air flames indicate that the model performs as well as the available alternatives, with less empiricism [9, 10].

Another recent application involved incorporation of a multistep thermonuclear reaction mechanism into ODT in order to simulate a turbulent nuclear flame. The goal was to investigate the possibility that a combination of strain, turbulent transport, and transient flame interactions might induce thermal conditions allowing a transition to detonation, a possible mechanism for supernova explosion. The computed results suggested that this scenario may not be consistent with current estimates of conditions leading up to the explosion [11].

FUTURE DIRECTIONS

The MD fragmentation studies to date achieved a homogeneous strain rate by imposing periodic boundaries that translate at a constant rate, with adjustment of the velocity of an atom crossing a boundary to account for the spatial gradient in the imposed initial velocity. Alternatively, fragmentation can be accomplished within a constant domain by incorporating a shrinking molecular diameter along with an increasing potential well depth. Those atoms which remain close to other atoms will remain in a liquid state, and those atoms which become isolated will be in a gaseous state. This system will be simulated to determine whether the droplet distribution is the same as found in the expanding system, an equivalence that is plausible but not guaranteed.

The results may motivate further fundamental study of the fragmentation process. In particular, it is interesting to consider whether the transient evolution of the liquid state during fragmentation can be approximated in some cases by a sequence of equilibrium states. As the evolving equilibrium approaches a phase transition, enhanced fluctuations associated with the critical properties of the phase transition may be anticipated. These enhanced fluctuations may be the precursors of long-tailed fragment distributions. In fact, the enhanced fluctuations at criticality may become frozen (a departure from the assumed equilibrium) because correlation times slow down near criticality, causing the fluctuations to evolve more slowly than the time scale of the imposed expansion. Thus, the expansion would tend to trap the fluid in a critical state once criticality is reached. This proposed scenario will be analyzed to determine whether numerical or experimental tests can ascertain its validity.

A 3D continuum calculation of flow through a nozzle, followed by free jet expansion that includes both liquid and gaseous phases, has been started. These calculations will indicate which feature of the nozzle flow produces the strain rate that causes atomization.

An adaptation of the ODT approach will be developed to model liquid-jet breakup. This formulation will complement the MD and DNS methodologies because it will be applicable to larger system sizes than MD and higher injection rates than DNS. Use of three methodologies will provide an overall picture of the contributions of atomic interactions, anisotropic strain, and liquid-phase turbulence, respectively, to the atomization process.

ODT simulations will be performed in support of measurements planned in the new Turbulent Combustion Laboratory in the Combustion Research Facility. Line Raman measurements will provide 1D instantaneous species concentration profiles from turbulent diffusion flames. ODT is unique among available models in its ability to predict any quantity derivable from line Raman. It therefore allows the most thorough comparisons between model and measurement.

REFERENCES

[1] Wm. T. Ashurst and B. L. Holian, Phys. Rev. E **59**, 6742 (1999).
[2] E. L. Knuth and U. Henne, J. Chem. Phys. **110**, 2664 (1999).
[3] Wm. T. Ashurst and B. L. Holian, J. Chem. Phys. **111**, 2842 (1999).
[4] Wm. T. Ashurst, H. N. Najm and P. H. Paul, Comb. Theor. Model., accepted for publication.
[5] A. R. Kerstein, J. Fluid Mech. **392**, 277 (1999).
[6] A. R. Kerstein, Dyn. Atmos. Oceans **30**, 25 (1999).
[7] A. R. Kerstein and T. D. Dreeben, Phys. Fluids **12**, 418 (2000).
[8] T. D. Dreeben and A. R. Kerstein, Int. J. Heat Mass Transf., accepted for publication.
[9] T. Echekki, A. R. Kerstein, J-Y Chen, and T. D. Dreeben, Comb. Flame, submitted for publication.
[10] T. Echekki, A. R. Kerstein, and J-Y Chen, Comb. Flame, submitted for publication.
[11] A. M. Lisewski, W. Hillebrandt, S. E. Woosley, J. C. Niemeyer, and A. R. Kerstein, Astrophys. J., accepted for publication.

PUBLICATIONS SINCE 1998

Wm. T. Ashurst, "Flow Frequency Effect upon Huygens Front Propagation," Comb. Theor. Model., accepted.
Wm. T. Ashurst and B. L. Holian, "Droplet Formation by Rapid Expansion of a Liquid," Phys. Rev. E **59**, 6742 (1999).
Wm. T. Ashurst and B. L. Holian, "Droplet Size Dependence on Volume Expansion Rate," J. Chem. Phys. **111**, 2842 (1999).
Wm. T. Ashurst, H. N. Najm and P. H. Paul, "Chemical Reaction and Diffusion: a Comparison of Molecular Dynamics Simulations with Continuum Solutions," Comb. Theor. Model., accepted.
Y. Hu, R. Hurt, J. Calo, and A. R. Kerstein, "Kinetics of Orientational Order/Disorder Transitions and Their Application to Carbon Material Synthesis," Model. Sim. Mat. Sci. Eng. **7**, 275 (1999).
A. R. Kerstein, "One-Dimensional Turbulence - Part 2. Staircases in Double-Diffusive Convection," Dyn. Atmos. Oceans **30**, 25 (1999).
A. R. Kerstein and T. D. Dreeben, "Prediction of Turbulent Free Shear Flow Statistics Using a Simple Stochastic Model," Phys. Fluids **12**, 418 (2000).
A. M. Lisewski, W. Hillebrandt, S. E. Woosley, J. C. Niemeyer, and A. R. Kerstein, "The Distributed Burning in Thermonuclear Supernovae of Type IA," Astrophys. J., accepted.

Modeling Unimolecular Reactions Dynamics of Moderate Sized Ionic Systems

Tomas Baer (baer@unc.edu)
Department of Chemistry
University of North Carolina
Chapel Hill, NC 27599-3290

DOE Grant DE-FG02-97ER14776

Program Scope

The photoelectron photoion coincidence (PEPICO) technique is utilized to investigate the dissociation dynamics and thermochemistry of energy selected medium to large organic molecular ions. Extensive modeling of the dissociation rate constant using the RRKM theory or variational transition state theory (VTST) is necessary in order to determine the dissociation limit of energy selected ions. These are carried out with the aid of molecular orbital calculations of both the ions and the transition states connecting the ion structure to its products. The result of these investigations yield accurate heats of formation of ions and free radicals.

The PEPICO Experiment

The photoelectron photoion coincidence (PEPICO) experiment in Chapel Hill is carried out with a laboratory H_2 discharge light source. Threshold electrons are collected by passing them through a set of small holes that descriminate against electrons with perpendicular velocity components. The electrons provide the start signal for measuring the ion time of flight distribution. When ions dissociate in the microsecond time scale, their TOF distributions are asymmetric. The dissociation rate constant can be extracted by modeling the asymmetric TOF distribution.

Recent Results

A Photoelectron-Photoion Coincidence Study of the ICH_2CN Ion Dissociation: The Thermochemistry of $^{\bullet}CH_2CN$, $^{+}CH_2CN$, and ICH_2CN

The dissociation energies and dissociation dynamics of iodoacetonitrile (ICH_2CN) have been investigated by the photoelectron photoion coincidence (PEPICO) spectroscopy technique. The 0K onsets for the following products were determined: $^{+}CH_2CN + I^{\bullet}$ (12.188 ± 0.005 eV) and $^{\bullet}CH_2CN + I^{+}$ (12.345 ± 0.010 eV). From the difference between these two values the ionization energy of the $^{\bullet}CH_2CN$ was found to be 10.294 ± 0.010 eV. By using a thermodynamic cycle that involves the gas phase acidity of CH_3CN, the electron affinity of the $^{\bullet}CH_2CN$ radical, and an accurate heat of formation of acetonitrile, a $\Delta_f H^{\circ}_{298}(ICH_2CN)$ of 172.5 ± 4.0 kJ mol^{-1} is derived. This latter value is considerably higher than the best theoretical value of 153 kJ mol^{-1}.

The Dissociation Dynamics and Thermochemistry of Energy Selected $CpCo(CO)_2^{+}$ Ions

Photoelectron photoion coincidence (PEPICO) spectroscopy has been used to investigate the dissociation dynamics of cobalt pentadienyl dicarbonyl $CpCo(CO)_2^{+}$. The dissociation proceeds by the sequential loss of the two CO molecules. Both reactions proceed with no reverse activation energies and are slow near their dissociation onset. The 0K onset was determined by modeling the measured dissociation rate constants with variational transition state theory to take into account the varying location of the transition state with ion internal energy. The ionization energy of $CpCo(CO)_2^{+}$ was measured from the threshold photoelectron spectrum to be 7.35 eV.

The neutral $CpCo(CO)_2^+$ gas phase heat of formation of -117±10 kJ/mol was determined from the liquid value by measuring the heat of vaporization of 52.12±0.68 kJ/mol. The first Co-CO bond energy in the $CpCo(CO)_2^+$ was found to be 1.54±0.01 eV (148.8±1 kJ/mol) giving a gas phase heat of formation of 752±10 kJ/mol for $CpCoCO^+$. The second Co-CO bond energy in $CpCoCO^+$ was measured to be 1.49±0.01 eV (144.2±1 kJ/mol) resulting in a gas phase heat of formation of $CpCo^+$ to be 1106±10 kJ/mol.

The interest in these compounds is that they have been used extensively as catalysts for a variety of reactions important in biology and industry. Their effectiveness depends on several factors of which the availability of metal sites that can participate in the chemical reaction is of paramount importance. The metal site becomes available when one of the ligands leaves, a process that is strongly affected by the metal ligand bond. In the case of cobalt cyclopentadienyl dicarbonyl, the two weakly bound ligands are the CO groups while the cyclopentadienyl group is strongly bound to the cobalt atom. The cobalt cyclopentadienyl dicarbonyl is the parent molecule for a host of important catalysts used for a variety of organic reactions. Substation of pentamethyl cyclopentadienyl for the cyclopentadienyl group is a common modification since it has a strong +I effect resulting in stabilization of the metal orbitals. The carbonyl ligands can also be replaced by ethylene, $H_2CCHSiMe_3$, etc. groups. These organometallic compounds have recently been used to catalyze [2+2+2] cycloaddition of diynes, as well as for intramolecular hydroacylation of vinyl silanes.

Of particular interest is the possibility to determine the neutral reaction by measuring the ionization energy of CpCoCO. Heating the inlet system can generate this transient species, a fact noted a number of years ago when these compounds were first investigated by mass spectrometry. In addition, if the energy of the process:

$$CpCo(CO)_2 + h\nu \rightarrow Cp^{\bullet} + Co^+ + 2\ CO$$

can be measured, the heat of formation of the neutral organometallic complex can be determined because the heats of formation of the products are all fairly well established. The onset for this reaction is above the 14 eV available in the laboratory light source in our Chapel Hill laboratory. It will be measured at the Advance Light Source chemical dynamics facility.

Pulsed Field Ionization – Photoelectron Photoelectron Photoion Coincidence (PFI-PEPICO) Studies at the Advanced Light Source

A major advance in ion state selection was achieved at the chemical dynamics beam line of the ALS when the high-resolution capability of pulsed field ionization was coupled with ion coincidence measurements. The standard threshold photoelectron photoion coincidence (TPEPICO) technique is generally limited to 5-10 meV resolution. This resolution is only possible when using synchrotron radiation operating in the few bunch mode so that the electrons can be energy selected not only by their angular distributions, but by their time of flight as well. Because all third generation synchrotrons have great difficulty in operating in the few bunch mode because of low electron currents, 5 meV resolution cannot be practically achieved. The advance that has made possible high-resolution PEPICO studies with multi-bunch mode synchrotron radiation is based on two properties of the ALS light. First the 6.65 m monochromator can achieve the very high resolution necessary to make PFI feasible. Secondly, the pulse structure of the ring contains a 144 ns "dark" gap in which no light is generated. We have utilized this dark gap to distinguish the direct electrons from the long-lived field ionized Rydberg states. The result is a scheme that permits sub-meV resolution for ions such as CH_4.

A number of hydrocarbon systems have been investigated, including CH_4, C_2H_2, C_2H_5Br, C_3H_7Cl, C_3H_7Br, and C_3H_7I. The dissociation limits for these ions were determined with a precision of 1-5 meV. The dissociative photoionization onset for the reaction:

$$CH_4 + h\nu \rightarrow CH_3^+ + H \qquad AE = 14.323 \pm 0.001 \text{ eV}$$

By combining this onset with the accurate measurement of the IE of $CH_3^\bullet$ that was measured by Chen and White with PFI, we obtain an H-CH_3 bond energy of 4.487 ± 0.001 eV.

The study of the propyl halides resulted in a new value for the heat of formation of the $C_3H_7^+$ ion. Because the dissociation limits for halogen atom loss lie in the Franck-Condon gap, the yield of threshold electrons generated by pulsed field ionization was found to be extremely low. Nevertheless, the heat of formation of 2-$C_3H_7^+$ determined from the three molecules agreed to within 2 kJ/mol. The average and now recommended value for this heat of formation is 825.0±1.5 kJ/mol (0 K) and 807.5±1.5 kJ/mol (298 K). This can be combined with the known heats of formation of C_3H_6 and H^+ to yield a proton affinity of C_3H_6 of 742.3±1.5 kJ/mol (298 K). This new value, which is 9.3 kJ/mol lower than the recommended value of Hunter and Lias, is in much better agreement with two theoretical values (744 kJ/mol) as well as the determination of Szulejko and McMahon (746.4 kJ/mol).

The new value for the proton affinity is especially important because accurate heats of formation of ions such as $C_3H_7^+$ are used to establish this scale through the reaction:

$$C_3H_6 + H^+ \rightarrow C_3H_7^+$$

The relative proton affinities of nearly 1000 molecules are known. By anchoring the scale with accurate values for some molecules, the whole scale is placed on an absolute basis. The PA(C_3H_6) is one of the key calibrating ions and its shift by nearly 10 kJ/mol as a result of our study has a major impact on this scale.

Future Plans

In July, 2000 I will move to Berkeley in order to assume the position of Director of Long Range Planning and User Relations at the Chemical Dynamics Beam line of the Advanced Light Source. Some of the PEPICO work described here will continue at the ALS, but in addition, we plan to initiate a number of new experiments such as the photoionization of liquid He droplets with various molecules and/or free radicals dissolved in them. Another thrust will involve flame diagnostics using the continuous vacuum ultraviolet radiation from the ALS. Finally, a number of sophisticated imaging experiments will be developed to investigate the structure of new species such as CH_5^+, and to measure the ionization spectrum of vibrationally excited molecules.

Research Publications Resulting from DOE grant 1998-2000

J.W. Keister, T. Baer, R. Thissen, C. Alcaraz, O. Dutuit, H. Audier, and V. Troude, "Proton tunneling in the loss of hydrogen bromide from energy selected gas-phase 2-bromobutane cations", *J.Phys.Chem.A* **102** 1090-1097 (1998)

O.A. Mazyar and T. Baer, "Isomerization and Dissociation in Competition: the two-component dissociation rates of the energy selected methyl formate ions, *J.Phys.Chem.A* **102** 1682-1690

(1998)

J.W. Keister, P. Tomperi, and T. Baer, "Thermochemistry of gaseous ethylsilane cations" *J.Am.Soc.Mass Spectrom.* **9** 597-605 (1998)

O.A. Mazyar and T.Baer, "Theoretical and experimental studies of unimolecular dissociation of phosphorus tribromide ions", *Chem.Phys.Lett.* **288** 327-332 (1998)

O.A. Mazyar and T. Baer "Ethene loss kinetics of methyl 2-methyl butanoate ions studied by TPEPICO: The enol ion of methyl propionate heat of formation", *J.Am.Soc.Mass Spectrom.* **10** 200-208 (1999)

O.A. Mazyar and T. Baer "Isomerization and dissociation in competition: The two-component dissociation rates of methyl propionate ions", *J.Phys.Chem.* **103** 1221-1227 (1999)

T. Baer, R. Lafleur, and O.A. Mazyar, "The role of ion dissociation dynamics in the study of ion and neutral thermochemistry", in *Energetics of Stable Molecules and Reactive Intermediates*, M.E. Minas da Piedade (Ed) Kluwer Academic Publ. (1999)

G.K. Jarvis, K.M. Weitzel, M. Malow, T. Baer, Y. Song, and C.Y. Ng, "High resolution pulsed field ionization photoelectron-photoion coincidence spectroscopy using synchrotron radiation" *Rev. Sci. Instrum.* **70** 3892-3906 (1999)

K.M. Weitzel, M. Malow, G.K. Jarvis, T. Baer, Y. Song, and C.Y. Ng, "High-resolutioni pulsed field ionization photoelectron-photoion coincidence study of CH_4: Accurate 0K dissociation threshold for CH_3^+, *J.Chem.Phys.* **111** 8267-8270 (1999)

G.K. Jarvis, K.M. Weitzel, M. Malow, T. Baer, Y. Song, and C.Y. Ng, "High-resolution pulsed field ionization photoelectron photoion coincidence study of C_2H_2: Accurate 0K dissociation threshold of C_2H^+" *Phys.Chem.Chem.Phys.*, **1**, 5329-5332 (1999)

T. Baer, Y.Song, C.Y. Ng, J.Liu, and W. Chen, "The heat of formation of 2-$C_3H_7^+$ and proton affinity of C_3H_6 determined by pulsed field ionization - photoelectron photoion coincidence spectroscopy" *J.Phys.Chem.-A*, **104**, 1959-1964 (2000)

R.D. Lafleur, B. Sztaray, and T. Baer "A photoelectron-photoion coincidence study of the ICH2CN ion dissociation: The Thermochemistry of $^{\cdot}CH_2CN$, $^{+}CH_2CN$, and ICH_2CN" *J. Phys.Chem.* A **104**, 1450-1455 (2000)

Baer, Y.Song, J.Liu, W. Chen, and C.Y. Ng, "Pulsed field ionization - photoelectron photoion coincidence spectroscopy with synchrotron radiation: The heat of formation of the $C_2H_5^+$ ion" *Disc. Faraday Soc.* # 115 (2000)

Turbulence-Chemistry Interactions in Reacting Flows

Robert S. Barlow
Combustion Research Facility
Sandia National Laboratories, MS 9051
Livermore, California 94551
barlow@ca.sandia.gov

Program Scope

This experimental program is directed toward a more complete understanding of the coupling between turbulence and chemistry in both nonpremixed and premixed reacting flows. Simultaneous temporally and spatially resolved measurements of temperature and the concentrations of N_2, O_2, H_2, H_2O, CH_4, CO_2, CO, OH, and NO are obtained using the combination of Rayleigh scattering, spontaneous Raman scattering, and laser-induced fluorescence (LIF). The temperature and major species data are used to correct fluorescence signals for the effects of shot-to-shot variations in Boltzmann fraction and collisional quenching rate in turbulent flames. These detailed measurements of instantaneous thermochemical states in turbulent flames provide insights into the fundamental nature of turbulence-chemistry interactions. The emphasis of our recent work has been on the development of an internet-accessible library of data sets on turbulent nonpremixed flames that are appropriate for testing and understanding the capabilities of state-of-the-art combustion models. Experiments often involve visiting scientists, primarily from universities.

We are developing a new Turbulent Combustion Laboratory (TCL) that will include state-of-the-art capabilities for single-shot, line-imaging measurements of multiple scalar, as well as capabilities for velocity measurements and combined velocity/scalar diagnostics. This new laboratory will allow quantitative investigations of the spatial structure of turbulent flames that are being used to evaluate and develop turbulent combustion models.

In addition to our experimental work, this program plays a leading role in organizing the International Workshop on Measurement and Computation of Turbulent Nonpremixed Flames (TNF), which facilitates collaboration among experimental and computational researchers working on fundamental issues of turbulence-chemistry interactions in gaseous diffusion flames. Collaborations and interactions with several combustion modeling groups are carried out in the context of the TNF Workshop.

Progress on the TNF Model Validation Library

Wolfgang Meier (DLR Stuttgart) visited the Turbulent Diffusion Flame (TDF) lab for several weeks during 1999 to perform collaborative experiments on his turbulent $CH_4/H_2/N_2$ jet flames. These flames are useful targets for model validation because they include methane chemistry in a simple jet geometry. However, the DLR data set lacked OH and NO measurements, and their CO measurements by Raman scattering did not have sufficient accuracy to be useful for detailed evaluation of model predictions (Fig. 1). Measurements of CO by two-photon LIF, as implemented in the TDF lab, yield the level of precision needed for quantitative comparison of measured and modeled results.

Measurements of the radiative loss from turbulent flames are critical for the validation of the radiation submodels used in turbulent combustion codes. NO levels in flames are sensitive to radiation, such that the accuracy of NO predictions cannot be evaluated unless it is known that radiation has been treated with sufficient accuracy. We have measured total radiant fractions for twelve of the TNF library flames. As part of this study we confirmed that the standard black-body calibration method used for radiant heat flux probes is applicable for measurements of molecular

radiation from jet flames. We also determined that a simple emission-only model is inadequate for treatment of the 4.3 micron band of CO_2 radiation from the flames in TNF library, even though the path lengths in these flames are relatively short.

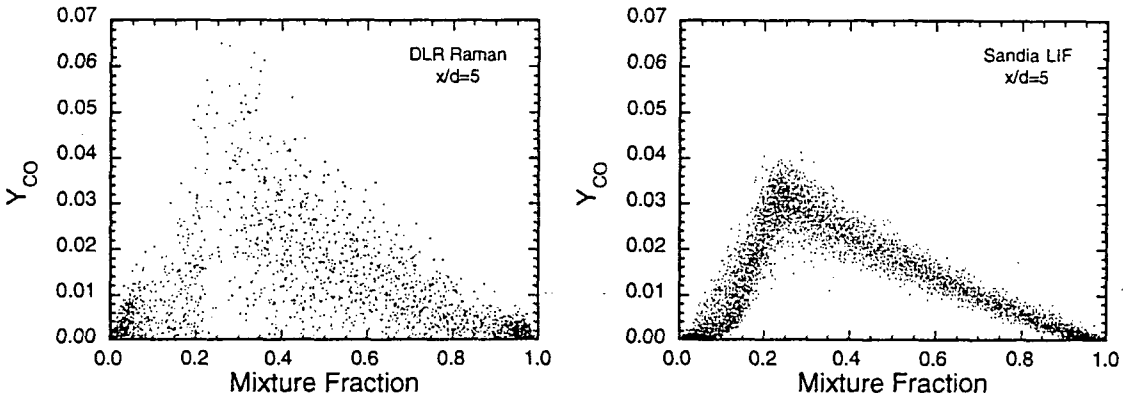

Fig. 1. Comparison of measurements of CO mass fraction based on Raman scattering (DLR setup) and two-photon LIF (Sandia setup). Single-shot results are plotted vs. the mixture fraction for the same $CH_4/H_2/N_2$ flame conditions at x/d=5.

Progress on Partially Premixed Laminar Flames

We obtained scalar measurements in several steady laminar partially premixed flames in order to allow thorough comparisons of detailed chemical mechanisms. The main issues of interest are the accurate prediction of the progress of partial oxidation of methane in fuel-rich conditions and the accurate prediction of NO throughout the flame. Preliminary comparisons with calculations using GRI Mech versions 2.11 and 3.0 show good agreement on major species, but deficiencies in the predictions of NO. This work is being done to allow for separate evaluation of critical submodels used in calculating turbulent flames.

Progress on a Shutter-Based Raman Line-Imaging System

We demonstrated a high-speed mechanical shutter for single-shot line imaging of Raman scattering from flames. This shutter was developed at the CRF in collaboration with Paul Miles of the Research in Engines Department, and it will be used in the new Turbulent Combustion Laboratory. It provides 9 μs (FWHM) gating, which is sufficient to reject luminosity from non-sooting flames, and 100% transmission when open. Combined with an imaging spectrograph and back-illuminated CCD array detector, the shutter eliminates the need for an image intensifier for gating and delivers significant improvements in quantum efficiency, dynamic range, and signal-to-noise ratio relative to intensified systems.

The shutter-based Raman line-imaging system was demonstrated in experiments on laminar jet flames. Noise statistics for measurements of species mass fractions, mixture fraction, and scalar dissipation were analyzed and scaled to account for the larger collection solid angle and laser energy in the TCL. Based on this analysis, the TCL setup should yield a factor of three improvement in SNR *and* a factor of two improvement in spatial resolution relative to Raman scattering measurements in the TDF lab. Furthermore, we project that single-shot measurements of scalar dissipation at the stoichiometric mixture fraction in methane-air flames can be achieved with relative standard deviations of 10-15% at χ_{st}~10 s^{-1} and 5-8% at χ_{st}~160 s^{-1}. This level of precision would be sufficient to differentiate among current models for the conditional scalar dissipation.

Future Plans

The new Turbulent Combustion Laboratory, with its two matched flow stations and complementary diagnostics for scalar and velocity measurements, will significantly enhance our ability to pursue fundamental investigations of reacting flows. Work in the near future will focus on three areas: i) bringing the TCL on line and fully implementing the line-imaging diagnostics, ii) continuing our investigation of turbulent flames in connection with development and evaluation of nonpremixed combustion models, and iii) continuing our investigation flow-flame interactions in steady and unsteady laminar flames. As with the work described above, we will conduct our experiments in close collaboration with computational researchers at Sandia and elsewhere.

Our first priority for scalar experiments on turbulent flames in the TCL will be to measure scalar gradients in the series of piloted CH_4/air jet flames and to extract information related to the conditional scalar dissipation. To accomplish this we will combine simultaneous line-imaging of Raman scattering, Rayleigh scattering, and CO LIF, and we will intersect that line with two laser sheets for PLIF imaging of CH (Fig. 2). The CH images (non-quantitative) will be used to determine the instantaneous orientation of the reaction zone relative to the measured line, allowing us to calculate (with some limitations) the component of scalar dissipation in the flame-normal direction. These data will help to resolved questions that have come out of model comparisons in the TNF Workshops, and they should be very useful for validation of submodels for scalar dissipation that are used in RANS and LES methods. We intend to investigate the joint statistics of mixture fraction, scalar dissipation, species mass fractions, flame curvature, and flame orientation. These statistics could be compared with results from LES and DNS calculations.

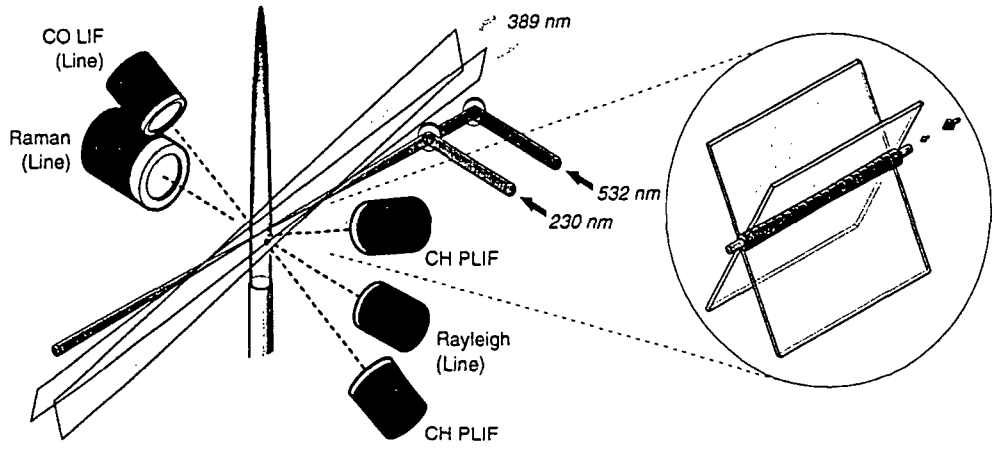

Fig. 2. Configuration for line-imaging and CH-PLIF in the TCL.

We have collaborated over the past two years with Johannes Janicka and Dirk Geyer (TU Darmstadt, Germany), Nondas Mastorakos (ICEHT, Greece), and J.-Y. Chen (UC Berkeley) on the development of an opposed-jet apparatus for fundamental studies of turbulent mixing and combustion. A copy of this burner will come to Sandia in the fall of 2000 for installation and initial experiments. The design includes optical access for laser beams along the axis of the two jets, so that line-Raman/Rayleigh/LIF measurements can be made along the mean stagnation streamline and normal to plane of the mean flame surface. We anticipate an extended collaborative experimental and modeling program based on this burner, and we expect to add opposed-jet cases to the TNF Workshop library. This geometry is of particular interest with regard to turbulent mixing, as it is modeled by both RANS and LES methods. The burner also includes a set of nozzles for laminar opposed jet flames.

BES Supported Publications (1998 - present)

R. S. Barlow and J. H. Frank, "Effects of Turbulence on Species Mass Factions in Methane/Air Jet Flames," *Twenty-Seventh Symposium (International) on Combustion*, The Combustion Institute, Pittsburgh, PA, 1998, pp. 1087-1095.

R. S. Barlow, N. S. A. Smith, J.-Y. Chen, and R. W. Bilger, "Nitric Oxide Formation in Dilute Hydrogen Jet Flames: Isolation of the Effects of Radiation and Turbulence-Chemistry Submodels," Combust. Flame, **117**, 4-31 (1999).

R. S. Barlow and P. C. Miles, "A Shutter-Based Line-Imaging System for Single-Shot Raman Scattering Measurements of Gradients in Mixture Fraction," *Twenty-Eighth Symposium (International) on Combustion*, (Edinburgh, Scotland, July 30-August 4, 2000) accepted.

R. S. Barlow, G. J. Fiechtner, C. D. Carter, and J.-Y. Chen, "Experiments on the Structure of Turbulent $CO/H_2/N_2$ Jet Flames," Combust. Flame, **120**:549-569 (2000).

B. B. Dally, A. R. Masri, R. S. Barlow, and G. J. Fiechtner, "Instantaneous and Mean Compositional Structure of Bluff-Body Stabilized Nonpremixed Flames," Combust. Flame, **114**, 119 (1998).

J. H. Frank and R. S. Barlow, "Simultaneous Rayleigh/Raman/LIF Measurements in Turbulent Premixed Methane-Air Flames," *Twenty-Seventh Symposium (International) on Combustion*, The Combustion Institute, Pittsburgh, PA, 1998, pp. 759-766.

J. H. Frank, R. S. Barlow, and C. Lundquist, "Radiation and Nitric Oxide Formation in Turbulent Nonpremixed Jet Flames," *Twenty-Eighth Symposium (International) on Combustion*, (Edinburgh, Scotland, July 30-August 4, 2000) accepted.

P. C. Miles and R. S. Barlow, "Fast Mechanical Shutter for Spectroscopic Applications," Meas. Sci. Technol. accepted (2000).

P. A. Nooren, M. Versiuis, T. H. van der Meer, R. S. Barlow, and J. H. Frank, "Raman-Rayleigh-LIF Measurements of Temperature and Species Concentrations in the Delft Piloted Turbulent Jet Diffusion Flame," Appl. Phys. B, accepted (2000).

Web-Based Information

http://www.ca.sandia.gov/tdf/Workshop.html	TNF Workshop Information
http://www.ca.sandia.gov/tdf/Lab.html	Turbulent Diffusion Flame Laboratory

Energy Partitioning in Elementary Chemical Reactions

Richard Bersohn
Department of Chemistry
Columbia University
New York, NY 10027
E-mail rb18@columbia.edu

The goals of this research are 1) to measure the yields of all the important channels of the reactions of $O(^3P)$ with unsaturated hydrocarbons and radicals and 2) by measurement of state distributions to understand the detailed mechanism. i.e. the trajectories of the atoms during the reactive collision.

I. O + alkyl alkenes: Addition to double bond *vs*. H atom abstraction from side chain

O atoms react rather slowly with ethene but the rate is considerably increased with successive alkyl radical replacement of the H atoms. (See second column of Table I) In the presence of side chains there are two different reactions, addition to one of the carbon atoms of the double bond and H atom abstraction from a side chain to form OH. Which reaction is more important? Is OH formation responsible for the increased rate constant?

LIF experiments on O atoms and OH radicals were carried out to answer this question. A mixture of SO_2 and an alkene was irradiated at 193 nm. O atom fluorescence was excited by a 130 nm laser at different times after their generation and at a fixed alkene pressure. Measurements of the decay rate were made at several pressures to obtain the rate coefficient for the loss of O atoms. Because these were nascent O atoms with an average relative kinetic energy of 5±2 kcal/mol the rate coefficients were an order of magnitude larger than the rate constants at room temperature. (See second and third columns of Table I) Cyclohexane was chosen as a comparison molecule. All OH yields were less than the OH yield from cyclohexane as shown in the fourth column of Table I. Unfortunately, the rate of decay of the O atoms in the presence of cyclohexane was so small that it could not be accurately measured. From an upper limit of the cyclohexane-O rate coefficient, we deduce that the side chain attack rate is <10% of the double bond addition rate and is probably only a few %.

Because the yield of OH from an alkyl alkene is less than that from cyclohexane but its rate constant is much larger, it is clear that side chain reaction is not important in an absolute sense. Then why does the rate constant increase so strongly with increasing alkylation? Cvetanovic explained this trend by postulating that the electrophilic O atom is attracted to a more negative site; substitution of alkyl radicals supplies electron charge to the carbon atoms forming the double bond.[1] This effect

might reduce the already small activation energies. However, an alternate explanation concentrates on the loss of energy in the C-O coordinate. There is a deep well reflecting the attraction of the O atom to the C atom. However, once the two atoms come close together, energy must be rapidly transferred to other modes or the O atom will simply bounce off. Table I shows that the order of rate coefficients is 1-hexene>1-butene>propene and cyclohexene>cyclopentene. The additional modes are proposed to change nonreactive collisions into reactive collisions. A test of this idea may be furnished by a non reactive crossed beam scattering experiment. Propene, for example, is expected to scatter O atoms at large angles, indicative of an intermediate complex formation whereas ethene may not show this effect.

TABLE I. Rate constants, rate coefficients and relative OH yields

Molecule	k(298) Units of 10^{-11} cm^3/(molecule-s)	k(fast O)	OH/OH(c-C_6H_{12})
cyclohexane	0.009	[ ]	1.00
ethene	0.068	[ ]	0
propene	0.438	7.2±3.6	0.15
1-butene	0.415	18.1	0.24
1-pentene	0.505		0.23
1-hexene	0.449	31.3	0.46
isobutene	1.78	25.3	0.34
Z-2-butene	1.84		0.24
cyclopentene	1.95	36.6	0.49
cyclohexene	2.07	40.2	0.50
E-2-butene	2.22		0.31
trimethylethene	5.41	34.0	0.27
tetramethylethene	8.01	61.8	0.34

The average relative kinetic energy of the fast O atom is ~5±2 kcal/mol. [ ] means too small to be measured, i.e. <10. k(298) data are from the NIST Chemical Kinetics Database.

II. $O(^3P) + CH_3 \rightarrow CO + H_2 + H$ (1)

The main product channel of the reaction of $O(^3P)$ with CH_3 is CH_2O + H. Seakins and Leone found the above reaction channel by observing IR emission from both CH_2O and CO.[2] Recently Preses *et al.* measured the value 0.18±0.04 for the relative yield of this channel.[3] By strongly focusing a 193 nm laser on a mixture of SO_2 and CH_3Br we were able to generate high enough reactant concentrations to be able to probe the CO state distribution with

a VUV laser. The vibrational and rotational distributions were fitted with temperatures of about 2000 K in each case. While hot, this distribution is not nearly as hot as that found by IR emission. There may be two reaction mechanisms, direct and indirect. In a direct stripping reaction the O atom captures the C atom from its ligands during the collision whereas the indirect reaction proceeds by way of an intermediate methoxyl radical, CH_3O.

III. $O(^3P) + C_2H_4 \rightarrow CH_3 + CHO$ or $H + CH_2CHO$

The fractional allocation of this reaction to the two channels is an important datum of combustion chemistry. We are trying a new method based on comparing the yields of H and HCO from C_2H_4 with the yields of D and DCO from C_2D_4. The CHO and CDO radicals were detected by their respective absorptions, A(0,9,0)<--X(0,0,0) and A(0,11,0)<--X(0,0,0) using cavity ring down spectroscopy. These absorptions were normalized to the absorptions seen in a 1/1 mixture of CH_3CHO and CD_3CDO irradiated at 308 nm. The last stage of the experiment, still in progress, is to measure the relative photochemical yields of these two isotopomers.

IV. CO(v,J) + pyrazine(hot v's) --> CO(v',J') + pyrazine

In a joint project with George Flynn, energy transfer was investigated in the collision of CO molecules with hot pyrazine (1,4-diazobenzene). The hot pyrazine is made by absorption of a 248 nm photon followed by internal conversion. The CO was probed using a pressure of 10 mTorr for each gas and a time delay of one μs. The rather astonishing result is that the v=0 CO molecules had a rotational temperature, T_R of 2200 K whereas the v=1 molecules had a T_R of 450 K. The explanation is that exchange of vibrational energy effected by the dipole-dipole interaction occurs without a direct contact between the molecules. The v=0 molecules which have not received any vibrational energy have suffered a violent collision with the vibrations of the hot pyrazine molecule. Similar results were previously found in CO_2-pyrazine collisions and the implications for energy transfer are believed to be general.[4]

An additional surprise was the finding of a strong quenching of the fluorescence of CO by cold pyrazine molecules with a cross section of ca 10000 A^2. An electronic energy transfer cross section of this magnitude between molecules has not been seen before in the gas phase. However, it is not unreasonable because of a strong overlap of two intense allowed transitions in the VUV.

Future plans

The probing of nascent CO molecules is presently carried out using the A<--X transition in the VUV near 154 nm. The required VUV light is made by combining two photons fixed at 249.63 nm whose combined energy is resonant with a xenon atom transition and a photon of variable wavelength near 646 nm. There is a danger that the relatively strong 249.63 nm light, though diverging in the reaction cell may dissociate HCO and other radicals, thus exaggerating the CO yield. An alternate probing method would use the B<--X transition. The necessary VUV is made by combining two photons at 312.85 nm in a Hg cell with one photon near 435 nm. We plan to use this method in connection with the photodissociation of acetaldehyde and with the O + alkene reactions.

In the reaction of O atoms with alkenes, vinoxy, CH_2CHO and alkyl substituted vinoxy radicals are formed. These radicals can not be probed by LIF until they have been vibrationally relaxed. We plan to use cavity ring down absorption to identify the radicals and, in a favorable case, to identify the hot mode(s) which is(are) relaxing. Extensive use would be made of the photodissociation of alkenylmethyl ethers at 193 nm which produce vinoxy type radicals.

References

1. R.J.Cvetanovic, Adv.Photochem. **1**,115(1963)
2. P.W.Seakins and S.R.Leone, J.Phys.Chem. **96**,4478(1992)
3. J.M.Preses, *et al*. J.Phys.Chem. submitted
4. C.Michaels,A.Mullin,G.W.Flynn, J.Chem.Phys.**102**,6032,6682(1995)

Publications in years 1998, 1999 and 2000

1. Reactions of $O(^3P)$ with Alkenes:H,CH_2CHO, CO and OH Channels, R.Quandt,Z.Min,X.Wong and R.Bersohn, J.Phys.Chem. **102**,60(1998)
2. Kinetic energies of hydrogen atoms dissociated from alkyl radicals, Z.Min,R.W.Quandt and R.Bersohn Chem.Phys.Lett. **296**,372(1998)
3. The CO product of the reaction of $O(^3P)$ with CH_3 radicals, Z.Min,R.W.Quandt,T-H.Wong and R.Bersohn, J.Chem.Phys. **111**,7369(1999)
4. The Reactions of $O(^3P)$ with Alkenes: The Formyl Radical Channel, Z.Min,T-H.Wong,R.W.Quandt and R.Bersohn, J.Phys.Chem.A **103**,10451(1999)

Theoretical Studies of Combustion Dynamics

Joel M. Bowman
Department of Chemistry
Emory University
Atlanta, GA 30322
bowman@euch4e.chem.emory.edu

Program Scope

The goal of my DOE-supported research is the development of (mainly) quantum mechanical methods, and the associated software, that can be used to perform reliable calculations of bimolecular and unimolecular reactions of importance in combustion. Such calculations necessarily benefit from accurate potential energy surfaces, and the development and improvement of these surfaces is a secondary, but very important additional goal of this research project. Our particular choice of reaction system is often dictated by experiment, and especially those experiments that present important challenges to theory.

Recently we have focused on unimolecular and bimolecular chemical reactions that proceed without a barrier. Such reactions are characteristic of many combustion reactions. We have focused specifically on the HOCl system, in part because of very detailed experiments by the Rizzo and Sinha groups in which the detailed quantum state dependence of the unimolecular rate to form OH+Cl was determined.[1,2] In these experiments the dissociation rates from the fifth OH-overtone as well as a nearby combination state were measured as a function of the HOCl total angular momentum and projection quantum numbers, J and K_a. The molecule is bound if J = 0 and dissociates only if it is rotating with sufficient energy to dissociate. Thus, the dissociation takes place just above the energetic threshold and, perhaps not surprisingly, it displays very non-statistical behavior with J and K_a.

The theoretical/computational study of this dissociation is extremely challenging in nearly every aspect. First, the potential energy surface has to have the correct energetics so that the molecule is indeed bound in the vibrational quantum states mentioned above, and yet dissociates with the lowest values of J and K_a, determined by experiment. Second, the dissociation rates (which are very slow compared to RRKM estimates) need to be calculated by a reliable method for values of J corresponding to experiment, e.g., J between 20 and 40 and for K_a between 0 and 4. For reasons that are well known to theorists, these are "large" values of these quantum numbers. The one important simplification is that HOCl has been shown in the experiments to be a nearly symmetric top (which is not surprising), and so various K decoupling approximations may be accurate enough to be useful.

The unimolecular dissociation of HOCl is described by a "corner" of the full potential energy surface that describes the reaction $O(^1D)+HCl \rightarrow ClO+H$, $OH+Cl$. This reaction proceeds with no potential barrier and "visits" the HOCl well, as well as the HClO isomer. Thus, this reaction is an example of the class of bimolecular reactions mentioned above. It has been studied experimentally[3-5] and theoretically.[6,7]

Thus, taken together the unimolecular dissociation of HOCl and the bimolecular reaction $O(^1D)+HCl$ present a nearly unique opportunity for theory to address two key types of chemical reactions of importance in combustion.

Recent Progress

Work on a highly accurate *ab initio*-based global potential energy surface of HOCl, including the $O(^1D)$+HCl reaction has proceeded well, in collaboration with Kirk Peterson (PNL and Washington State University). We have used this surface in quantum calculations of the dissociation rate of $HOCl(6\nu_{OH}, J, K_a)$. The quantum method we used determines the complex eigenvalues of a complex Hamiltonian for non-zero J. For these calculations we used the Adiabatic Rotation approximation[8,9] as well as the widely used Centrifugal Sudden approximation.[10,11] In addition, in collaboration with Reinhard Schinke (MPI, Göttingen), exact calculations are being done to test these two approximations. The first set of results indicates that the Adiabatic rotation approximation is more accurate than the Centrifugal Sudden ones.

The quantum calculations did find significant variation of the dissociation lifetime with J and K_a,[12] in excellent qualitative and semi-quantitative agreement with experiment. In addition, we have developed a simple model that mimics these variations based on rotationally induced "Fermi" resonance mixing of the bright state, $6\nu_{OH}$, with a background of dissociating states that necessarily are highly excited in the ClO-stretch. For $K_a = 0$ the "Fermi resonance" condition is determined from equating the rovibrational energies of $6\nu_{OH}$ state and highly excited ClO states, i.e.,

$$E_{\nu ClO}^{J=0} + \overline{B}_{\nu ClO} J(J+1) \approx E_{6\nu OH}^{J=0} + \overline{B}_{6\nu OH} J(J+1),$$

and noting that $\overline{B}_{\nu ClO} < \overline{B}_{6\nu OH}$. Thus the energy of $6\nu_{OH}$ "intersects" the energy of ClO states that are above $6\nu_{OH}$ for J = 0 for J > 0, determined by the difference between $B_{\nu ClO}$ and $B_{6\nu OH}$. If there are no intersections for a given J the rate is predicted to be relatively slow compared to the case where there are intersections. This model is clearly simplistic but does capture the flavor of the marked dependence on J (and K_a) of the unimolecular rate found in the rigorous calculations and in experiment.

We have also begun a collaboration with Stephen Gray (ANL) to apply his wavepacket code to study the reaction $O(^1D)$+HCl → ClO+H, OH+Cl on the global potential. In preliminary work we compared the quantum results for HCl(v=j=0) with those of a standard quasiclassical trajectory calcultion for J = 0.[13] The results were very encouraging for the QCT method which was found to predict the total reactivity as well as the ClO:OH branching ratio in good average agreement with the quantum calculations.

We have also collaborated with Gray on a study of the $O(^3P)$+HCl → OH + Cl reaction using the recent "S4" *ab initio* potential of Ramachandran, *et al.*[14] The results of this study are very interesting and need further analysis. They indicate very strong effects of van der Waals minima in the potential on the dynamics.

Future Plans

Our immediate plans call for more extensive quantum calculations of the $O(^1D)$+HCl reaction, in which both the J and K_a quantum numbers will be varied and in which excited rotational states of HCl (of relevance to the rate constant) will be considered. These will be very computationally demanding calculations; however, the comparisons with corresponding QCT calculations, statistical theories, and J or l-shifting theories will be very important. We also plan to collaborate with Gray on the spin-orbit coupling

between the triplet and singlet reactions. This will also require further collaboration with Kirk Peterson on the *ab initio* spin-orbit interaction.

References

1. G. Dutton, R. J. Barnes, and A. Sinha, J. Chem. Phys **111**, 4976 (1999).
2. A. Callegari, J. Rebstein, R. Jost, and T. R. Rizzo, J. Chem. Phys **111**, 7359 (1999).
3. (a) P.H. Wine, J.R. Wells, A.R. Ravishankara, J. Chem. Phys. **84** (1986) 1349; (b) Y. Matsumi, K. Tonokura, M. Kawasaki, K. Tsuji, K. Obi, J. Chem. Phys. **98** (1993).
4. (a) A.C. Luntz, J. Chem. Phys. **73** (1980) 5393; (b) C.R. Park, J.R. Wiesenfeld, Chem. Phys. Letters **163**, 230 (1989); (c) E.J. Kruus, B.I. Niefer, J.J. Sloan, J. Chem. Phys. **88**, 985 (1988).
5. N. Balucani, L. Beneventi, P. Casavecchia, G.G. Volpi, Chem. Phys. Lett. **180**, 34 (1991).
6. R. Schinke, J. Chem. Phys. **80**, 5510 (1984).
7. (a) A. Laganà, G. Ochoa de Aspuru, E. Garcia, J. Phys. Chem. **99**, 17139 (1995); (b) A. Laganà, G. Ochoa de Aspuru, E. Garcia, J. Chem. Phys. **108**, 3886 (1998); (c) M.L. Hernandez, C. Redondo, A. Laganà, G. Ochoa de Aspuru, M. Rosi, A.Sagamellotti, J. Chem. Phys. **105**, 2710 (1996).
8. (a) D. Wang and J. M. Bowman, J. Phys. Chem. **98**, 7994 (1994); (b) J. M. Bowman, Chem. Phys. Lett. **217**, 36 (1994); (b) J. Qi and J. M. Bowman, J. Chem. Phys. **107**, 9960 (1997); (c) S. Carter and J. M. Bowman, J. Chem. Phys. **98**, 4397 (1998).
9. (a) C. W. McCurdy and W. H. Miller, ACS Symp. Ser. No. 56, eds. P. R. Brooks and E. F. Hayes (American Chemical Society, Washington, D.C., 1977), pp. 239 - 242; (b) H. Wang, W. H. Thompson, and W. H. Miller, J. Chem. Phys. **107**, 7194 (1997).
10. R.T Pack, J. Chem. Phys. 60, 633 (1974).
11. P. McGuire and D. J. Kouri, J. Chem. Phys. 60, 2488 (1974).
12. S. Skokov and J. M. Bowman, J. Chem. Phys. **111**, 4933 (1999).
13. K. Christoffel, Y. Kim, S. Skokov, J. M. Bowman and S. Gray, Chem. Phys. Lett. **315**, 275 (1999).
14. B. Ramachandran, E. A. Schrader III , J. Senekowitsch, and R. E. Wyatt , J. Chem. Phys. **111**, 3862 (1999).

PUBLICATIONS SUPPORTED BY THE DOE (1998-present)

Spectator modes in resonance-driven reactions: Three-dimensional quantum calculations of HOCO resonances, F. N. Dzegilenko and J. M. Bowman, J. Chem. Phys. **108**, 511 (1998).

Three-dimensional quantum calculations of HOCO resonances, F. N. Dzegilenko and J. M. Bowman, J. Chem. Phys. **108**, 511 (1998)

Resonances: The Bridge between dynamics and spectroscopy, Feature Article, J. Phys. Chem. **102**, 3006 (1998).

Quantum calculations of inelastic and dissociative scattering of HCO by Ar J. Qi and J. M. Bowman, J. Chem. Phys. **109**, 1734 (1998).

Non-separable transition state theory for non-zero total angular momentum: Implications for J-shifting and application to the $OH+H_2$ reaction, J. M. Bowman and H. Shnider, J. Chem. Phys. **110**, 4428 (1999).

Calculation of resonance states of non-rotating HOCl using an accurate *ab initio* potential, S. Skokov, J. Bowman, and V. Mandelshtam, Physical Chemistry Chemical Physics, **1**, 1279 (1999).

Non-separable RRKM theory applied to unimolecular dissociation of HCO -> H+CO, K. Christoffel and J. M. Bowman J. Phys. Chem. **A103**, 3020 (1999).

Calculations of low-lying vibrational states of cis and trans-HOCO, J. M. Bowman, K. Christoffel, and Gabe Weinberg, J. Mol. Struct. (Theochem) **461**, 71 (1999).

Potential energy surface and vibrational eigenstates of the H_2-CN($X^2\Sigma^+$) van der Waals complex, A. L. Kaledin, M. C. Heaven, and J. M. Bowman, J. Chem. Phys. **110**, 10380 (1999).

Variation of resonance widths of HOCl(6νOH) with total angular momentum: Comparison between ab initio theory and experiment, S. Skokov and J. M. Bowman, J. Chem. Phys. **111**, 4933 (1999).

Quantum and quasiclassical reactive scattering of $O(^1D)$+HCl using an *ab initio* potential, K. Christoffel, Y. Kim, S. Skokov, J. M. Bowman and S. Gray, Chem. Phys. Lett. **315**, 275 (1999).

Wavepacket propagation for reactive scattering using real L^2 eigenfunctions with damping, S. Skokov and J.M. Bowman, PCCP **2**, 495 (2000)

Approximate time independent methods for polyatomic reactions, J. M. Bowman, "Reaction and Molecular Dynamics", Springer Lecture Notes in Chemistry, in press.

Quantum dynamics and rate constant for the $O(^3P)$+HCl reaction, S. Skokov, T. Tsuchida, S. Nambu, J. M. Bowman, and S. Gray, J. Chem. Phys., accepted.

A reduced dimensionality quantum calculation of the reaction of H_2 with diamond (111) surface, S. Skokov and J. M. Bowman, J. Chem. Phys., accepted.

"Very High Pressure

Single Pulse Shock Tube Studies of Aromatic Species"

Principal Investigator:
Kenneth Brezinsky
University of Illinois at Chicago
Department of Chemical Engineering (M/C 110)
810 South Clinton Street
Chicago, IL 60607
(312) 996-9430
(312) 996-0808 (Fax)
Kenbrez@uic.edu

Program Scope

The program focuses on shock tube studies of the oxidation and supplemental pyrolysis of benzene, toluene, cyclopentadiene, methylcyclopentadiene, dimethylcyclopentadiene, anisole, phenol and cresols. These species were chosen because of their role or the role of their radical derivatives in the mechanisms and models of benzene and toluene. The experimental data obtained from the studies of these species will be coupled with modeling of the pressure, temperature and time dependence of species concentrations. Along with the RRKM evaluation of pressure dependent rate constants, the data and modeling will help sort out and lead to further development of a comprehensive model of the oxidation and pyrolysis of aromatics.

The experimental data are acquired from a recently constructed, unique, very high-pressure single pulse shock tube. This device permits the sampling and quantitative analysis of stable species produced during the oxidation and pyrolysis experiments at pressures as high as 1000 atmospheres and temperatures as high as 2000K for nominal reaction times varying from 500 to 1500 microseconds. These conditions permit oxidation and pyrolysis reactions to be performed under very dilute conditions (low mole fractions), but with high concentrations (moles/liter). Thus secondary reactions can be controlled, temperature increases minimized, and species concentrations maintained at high enough levels for detection with advanced gas chromatography/mass spectrometry instrumentation.

Recent Progress

By operating isothermally the high-pressure shock tube facility avoids the problems that have plagued the previous use of single pulse shock tubes for the study of oxidation reactions. However, in order to accurately examine oxidation reactions, knowledge of reaction temperature is needed. The reaction temperature is obtained through calibration of shock conditions using well characterized chemical "thermometers" which minimize the need to use high pressure equations of state to deduce shock temperatures.

Much of this past year's work has been devoted to a careful determination with the chemical thermometer, CF_3CH_3, of shock temperatures as a function of incident shock velocities.. The high pressure rate constant for the unimolecular decomposition of this molecule has been established by Tsang and Lifshitz (IJCK 30, 621, 1998) for two ΔE_{down} values. These k_∞ expressions have been used in the conventional expression $conc_f/conc_i=e^{-kt}$ to back out the shock temperature from measured values of initial and final trifluoroethane concentrations, and reaction time. A plot of the results over a wide pressure range is shown in Figure 1 below

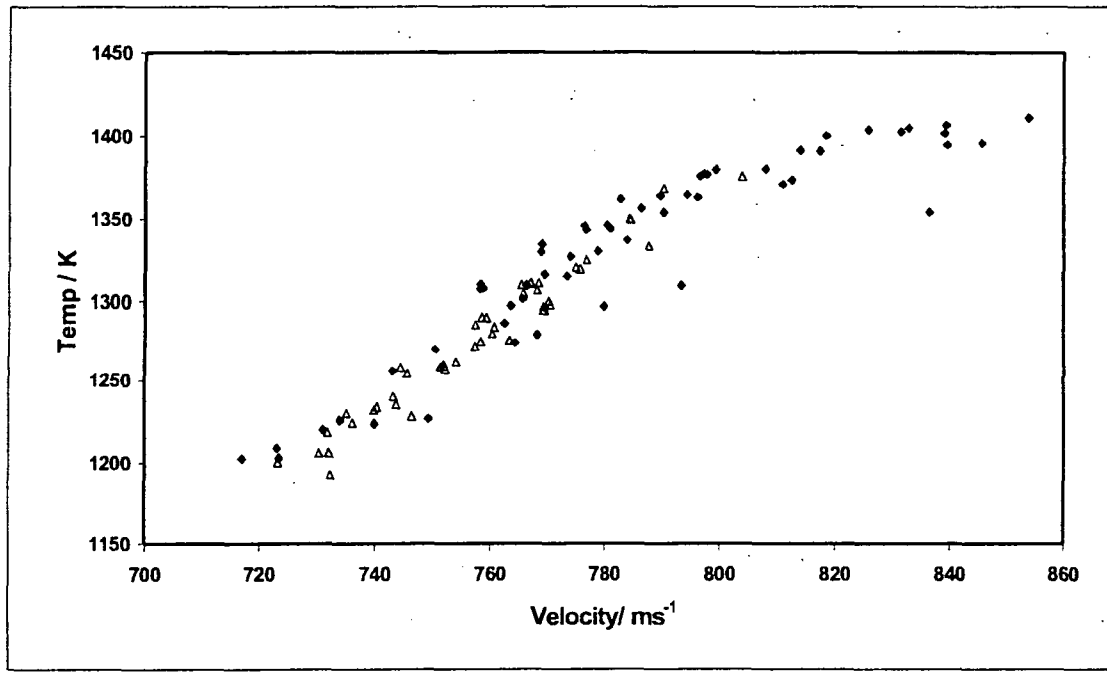

Fig. 1 Temperature determined from the unimolecular decomposition of CF_3CH_3 at 3000psi (dark diamonds) and 11,000psi (open triangles) as a function of incident shock velocity.

The temperature results in Fig. 1 indicate that the chemical thermometer provides consistent high temperature values at high pressures over this range of approximately 200-750 atmospheres. At temperatures above 1350K, the degree of conversion of CF_3CH_3 is so large that small variations in concentrations appear to lead to an artificial asymptotic approach to a maximum temperature.

In addition, to developing the correlation for temperature with respect to incident shock velocity shown above, considerable effort was expended on obtaining well defined shock profiles. A typical, optimized profile is shown in Fig. 2 below.

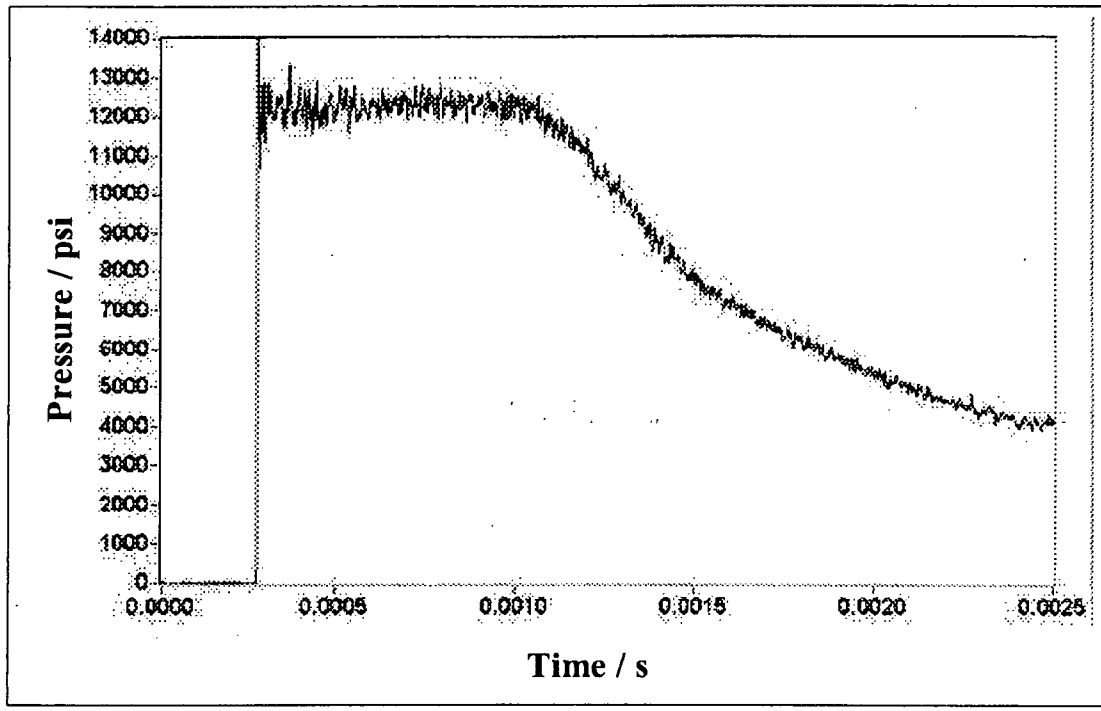

Fig. 2 Pressure trace from endwall pressure transducer. Maximum pressure = 12500 psi, 852 atm. Reaction time: approx. 1.1 ms.

This type of tailored profile was obtained by optimization of the driver section with an insert plug for a different given driven section length. In the past year, optimization tests of this type along with the temperature calibration tests described above have led to more than1200 individual shocks being performed.

Other shock tube related activities performed this year have been

a) refitted driver gas storage vessels for extremely high pressures

b) modified diaphragm section to improve shock tube performance at 1000 atmospheres

c) improved diaphragm scoring technique through the acquisition of a computerized numerical control milling machine attachment and development of a rigorous and reliable production method

d) improved chemical sampling and gas chromatography / mass spectrometry analysis for the quantification of low concentration samples.

e) installed and began modeling with CHEMKIN.

Future Work

In the very near future, shocks at 1000 atmospheres will be conducted. Preliminary attempts at this extremely high pressure have revealed a variety of system deficiencies that have now been remedied.

Chemical tests of the oxidation of toluene and benzene are also planned in the very near future. Since the shock tube has been calibrated for temperature and optimized for shock profile, high quality oxidation data is imminent. Attendant to these oxidation tests will be complementary pyrolysis studies of toluene, methane and benzene. These pyrolysis experiments will serve to both offer a reference database for the oxidation experiments and also provide opportunities to examine individual reactions.

Publications/Presentations

"A Single Pulse Shock Tube for Examination of Combustion Reactions At High Pressures", Work In Progress Poster #W1A25, Twenty-Seventh International Symposium on Combustion, August, 1998 (with R.S. Tranter, D. Fulle, E. Ikeda, P. Sarkar and J.H. Kiefer).

COMBUSTION CHEMISTRY

Principal Investigator: Nancy J. Brown

Environmental Energy Technologies Division

Lawrence Berkeley National Laboratory

Berkeley, California, 94720

510-486-4241

NJBrown@lbl.gov

PROJECT SCOPE

Combustion processes are governed by chemical kinetics, energy transfer, transport, fluid mechanics, and their complex interactions. Understanding the fundamental chemical processes offers the possibility of optimizing combustion processes. The objective of our research is to address fundamental issues of chemical reactivity and molecular transport in combustion systems. Our long-term research objective is to contribute to the development of reliable combustion models that can be used to understand and characterize the formation and destruction of combustion-generated pollutants. We emphasize studying chemistry at both the microscopic and macroscopic levels. To contribute to the achievement of this goal, our current activities are concerned with five tasks: Task 1) developing models for representing combustion chemistry at varying levels of complexity to use with models for laminar and turbulent flow fields to describe combustion processes; Task 2) developing tools to facilitate building and validating chemical mechanisms; Task 3) modeling combustion in multi-dimensional flow fields, and Task 4) determining new reaction pathways for pollutant formation. A theme of our research is to bring new advances in computing, and, in particular, parallel computing to the study of important, and computationally intensive combustion problems. Researchers who collaborate in this effort are **John B. Bell, Marcus S. Day, Michael Frenklach, Joseph F. Grcar, Nigel W. Moriarty, Richard M. Propp, Shaheen R. Tonse, and Laurent Vuilleumier.**

RECENT PROGRESS

Task 1: Developing models for representing combustion chemistry at varying levels of complexity to use with models for laminar and turbulent flow fields to describe combustion processes. Most practical combustion systems are turbulent, and the dominant computational cost in modeling turbulent combustion phenomena numerically with high fidelity chemical mechanisms is the time required to solve the ordinary differential equations associated with the chemical kinetics. To develop models that describe pollutant formation in practical fuels, the computational burden attributable to chemistry must be reduced. We have pursued an approach that can contribute to this problem, PRISM (Piecewise Reusable Implementation of Solution Mapping). PRISM has been developed as an economical strategy for implementing complex kinetics into high fidelity fluids codes. This approach to mechanism reduction draws upon factorial design, statistics and numerics, caching strategies, data structures, and long term re-use. A solution-mapping procedure is applied to parameterize the solution of the initial-value ordinary differential equation system as a set of algebraic polynomial equations. The resulting accuracy is very good, and a factor of 15 to 20 increase in computational efficiency is achieved. PRISM was ported and interfaced with the adaptive grid CFD code developed by LBNL investigators in computer sciences, and used as a tool to investigate the dimensional properties of the active portion of chemical composition space. PRISM's division of chemical composition space into hypercubes makes it an ideal tool for examining chemical composition space with varying degrees of resolution, from which the dimensionality was determined. We investigated the dimensionality for the two dimensional case of a premixed hydrogen flame propagating through an unburned turbulent mixture. The fractional dimensionality was determined as a

function of turbulent intensity, and found to be lower than the theoretical asymptote of 3 in all the cases. The significance of this research is that there are low dimensional manifolds that we hope to identify to reduce the computational complexity of PRISM. A follow-up study of this is in progress. We are currently examining the dimensionality of the manifold at instants in time. We will also measure the dimensionality for small time increments that correspond to a few of the disparate primary time-scales associated with the H_2+Air reaction mechanism to see if higher dimensions appear at short time-scales and then disappear.

We are exploring a number of ways to improve the efficiency of PRISM without sacrificing accuracy. For example, a hypercube will have high degree of reuse either through being in a portion of chemical composition space visited by the chemical trajectories of many CFD cells, or by being in a part where trajectories move relatively slowly, thus taking many steps through the hypercube. We utilized the rates at which trajectories are moving to calculate a trajectory "velocity" $\mathbf{V_{Tr}}$ and combine this with an estimated trajectory length to determine expected reuse. This allows us to identify hypercubes that would not have sufficient reuse to warrant a parametrization calculation. The cases studied were a point reaction case with zero spatial dimensions and 3 other simulations: a 1D laminar premixed H_2+Air flame, a 2D premixed H_2+Air turbulent jet and a 2D non-premixed H_2 and Air turbulent jet. We find $\mathbf{V_{Tr}}$ to be a useful indicator of reuse for the zero-dimensional case, to be somewhat less useful for laminar and turbulent pre-mixed flames, and not very effective for the turbulent non-premixed jet case.

The H_2+Air cases studied with PRISM have 11 dimensions associated with them [9 species + Temperature+ Δt]. For accurate quadratic polynomial coefficients a fractional factorial design of type 2_V^{11-4}, taken from the literature, was found to work. For CH_4 + Air combustion a factorial design of higher dimensionality is necessary. The literature contains orthogonal fractional designs only up to 13 dimensions. We have recently developed a design 2_V^{22-13} to enable us to employ PRISM on a reduced version of the GRI-Mech 1.2 mechanism with an associated 22 dimensions [20 species +Temperature + Δt]. This design has been used in preliminary PRISM calculations and gives accurate results.

Task 2: Modeling tools for building chemical mechanisms. Proper descriptions of transport properties are essential for combustion modeling. Recent research suggests that the treatment of transport in the CHEMKIN codes is outdated. To investigate the consequences of this for mechanism construction, we have performed sensitivity analysis of the observables: species concentrations, mass flow rate, and temperature to molecular diffusion coefficients and the potential parameters used in their evaluation for premixed laminar flames. Diffusion coefficients are very consequential, and their normalized sensitivities are commensurate with those associated with the most influential chemical reactions. Those that most influence species profiles are the binary diffusion coefficients of various species with molecular nitrogen. Sensitivities of observables were found to be an order-of-magnitude greater for collision diameters associated with a Lennard-Jones potential than for the corresponding well depths. These results show that we will not get the chemistry right in building chemical mechanism without an improved treatment of transport. Transport also must be dealt with at the molecular level. We are currently directing effort toward achieving an improved transport description.

Task 3: Modeling of multi-dimensional reactive flows We are collaborating with investigators in the Computer Directorate, who are funded by the Mathematics, Information, and Computational Sciences Office within the DOE Office of Science. These researchers have developed a massively parallel, high fidelity code for treating non-steady, low Mach number, reactive flows with complex chemistry that is based upon adaptive mesh refinement (AMR). The code has sufficient resolution to treat laminar, transition, and turbulent reacting flows in one, two, and three spatial dimensions. Our role in this collaboration is to contribute the chemistry

and molecular transport data for specific problems, incorporate special chemistry modules in the code (e.g., PRISM), and to contribute to the analysis and interpretation of results. We have completed a study of flame/vortex interactions (under LDRD) and reproduced behavior observed experimentally. Our current efforts in this area involve computing properties of CH_4 flames using PRISM and AMR.

Task 4: Determining New Reaction Pathways for Pollutant Formation. Combustion technology is being driven by regulations that require substantial reductions in soot. If models are to be used in the design process, better soot models are critical. Our interest has been in model benchmarking, examining soot precursor chemistry, and determining reaction pathways for aromatic ring growth. We have recently completed a study of the **hydrogen migration in the phenylethen-2-yl radical.** Our study identified a new class of reaction pathways for aromatic ring growth in combustion environments. The distinctive feature of these reaction pathways is the transfer of hydrogen atom between carbon atoms of the aromatic ring and those of the side chains. Initial calculations were performed at a semi-empirical level of quantum theory, chosen to screen a large number of mechanistic possibilities and to accommodate the large molecular size that is required for realistic modeling of PAH precursors and soot surfaces. In the past year, we turned to ab initio quantum mechanical theory to assess more accurately the feasibility of the hydrogen migration. The reaction chosen for the present study is the hydrogen migration in phenylethen-2-yl to give 2-styrene. This choice was motivated by two considerations: firstly, this reaction may play a role on its own, as both the reactant and the product are known intermediates of aromatic growth in hydrocarbon flames. Secondly, the reaction is the smallest analog of hydrogen transfer on large PAHs and soot particle surfaces and thus allows one to remain within the constraints of the available computational power. Calculations on the two radical minima and the transition state were performed at several levels of theory and basis sets. Rate coefficients and equilibrium constants are obtained using the calculated data and RRKM theory. Theoretical methods compared include PM3, MP2, B3-LYP, CASPT2 and G2MP2. The applicability of these methods was determined. Comparisons with two others, G2M and CBS-RAD, proposed to improve treatment of radicals, was also conducted. The results obtained at the most reliable level of theory produce reaction rates sufficiently fast for these reactions to play a role in high-temperature aromatic chemistry.

PUBLICATIONS

Gentile, A.C., Evensky, D.A., Durant, J.L., Brown, N.J., and Koszykowski, M.L. (1997). "Reaction Dynamics and Quantum Monte Carlo Solution of Real Time Path Integrals". in Modeling of Chemical Reactive Systems, Heidelberg, Germany, J. Warnatz, F Behrendt, eds. Univ. of Heidelberg.

Vuilleumier, L., Harley, R.A., and Brown, N.J. (1997). First-and Second-Order Sensitivity Analysis of a Photochemically Reactive System (a Green's Function Approach). Environmental Science and Technology. 31, pp 1206-1217

Brown, N.J., Li, Guoping, and Koszykowski, M.L. (1997). "Mechanism Reduction Via Principal Component Analysis". International Journal Chemical Kinetics 29, pp 393-414.

Brown, N. J., Revzan, K. L. and Frenklach, M.,(1998) "Detailed Kinetic Modeling of Soot Formation in Ethylene/Air Mixtures Reacting in Ethylene/Air Mixtures Reacting in a Perfectly Stirred Reactor," Proceedings of the Combustion Institute 27. pp 1573-1580

Frenklach, M.. Moriarty, N. L., and Brown, N.J., (1998) "Hydrogen Migration in Polyaromatic Growth," Proceedings of the Combustion Institute 27

Lazarides, A. A., Rabitz, H., Chang, J., and Brown, N. J., (1998), " Identifying Collective Dynamical Observables Bearing on Local Features of Potential Surfaces," J. Chem. Phys. Chem. 109, pp 2065-2070.

Tonse, S.R., Moriarty, N. L., Brown, N. J., Frenklach, M., (1999), "PRISM: Piecewise Reusable Implementation of Solution Mapping. An Economical Strategy for Chemical Kinetics," Israel Journal of Chemistry 39, pp 97-106. Invited paper for a special issue on Combustion Chemistry to commemorate the 70th birthday of Professor Assa Lifshitz. Also Lawrence Berkeley National Laboratory Report No. LBNL-42576

Moriarty, N. W., Brown, N.J., and Frenklach, Michael, (1999), "Hydrogen Migration in the Phenylethene-2-yl Radical," J.Phys. Chem. 103, pp 7127-7135. Also Lawrence Berkeley National Laboratory Report No. LBNL-43163

A co-author of the National Research Council Report of the Committee on Ozone-Forming Potential of Reformulated Gasoline, National Academy Press, (1999) Committee members: W.L. Chameides, C.A. Amann, R. Atkinson, N.J. Brown, J.G. Calvert, F.C. Fehsenfeld, J.P. Longwell, M.J., Molina, S.T. Rao, A.G. Russell, S.L. Saricks.

Bell, J.B., Brown, N.J., Day, M.S., Frenklach, M., Grcar, J.F., Propp, R.M., and Tonse, S.R., "Scaling and Efficiency of PRISM in Adaptive Simulations of Turbulent Premixed Flames," (1999) Accepted for publication in the Proceedings of the Combustion Institute 28. Also Lawrence Berkeley National Laboratory Report No. LBNL-44732

Bell, J.B., Brown, N.J., Day, M.S., Frenklach, M., Grcar, J.F., and Tonse, S.R., "Effect of Stoichiometry on Vortex-Flame Interactions," (1999) Accepted for publication in the Proceedings of the Combustion Institute 28. Also Lawrence Berkeley National Laboratory Report No. LBNL-44730

Dynamics of Radical Combustion Intermediates: Product Branching and Photolytic Generation

Laurie J. Butler
The University of Chicago, The James Franck Institute
5640 South Ellis Avenue, Chicago, IL 60637
LJB4@midway.uchicago.edu

I. Program Scope

Our work in the present grant period focuses on 1) investigating competing product channels in photodissociation processes used to generate radical intermediates important in combustion and 2) generalizing a new method for determining absolute branching ratios for competing radical product channels in both unimolecular and ground state bimolecular reactions in mass spectrometric experiments. We use a combination of experimental techniques including analysis of product velocity and angular distributions in a crossed laser-molecular beam apparatus and emission spectroscopy of dissociating molecules. Much of the work also serves to test and develop our fundamental understanding of chemical reaction dynamics. We focus on testing the range of applicability of two fundamental assumptions used in calculating reaction cross sections and the branching between energetically-allowed product channels: the assumption of complete intramolecular vibrational energy redistribution often used in transition state theories and the assumption of electronic adiabaticity used in defining the reaction coordinate in transition state theories and the multidimensional potential energy surface in quantum scattering calculations.

II. Recent Progress

Our work in the last year included 1) a collaborative project, with Arthur Suits and Branko Ruscic at the Advanced Light Source, characterizing the nitrogen-containing products from trimethylamine photodissociation at 193 nm,[6] 2) a combined experimental and theoretical study, with H. Guo, measuring the emission spectroscopy of SO_2 to test the excited state surfaces and calculated ground state vibrational eigenenergies,[5] and 3) a crossed laser-molecular beam photofragment scattering experiment on methylvinylether, motivated by the need to calibrate product branching in the thermal O+ ethylene reaction. The results are described in detail below.

A. Characterization of Nitrogen-Containing Radical Products from the Photodissociation of Trimethylamine at 193 nm using Photoionization Detection

Our prior work on trimethylamine photodissociation[4] served two goals. First, it provided a key calibration of the mass spectrometric sensitivity to the CH_3 and $N(CH_3)_2$ radicals important in combustion and the secondary CH_2=NCH_3 molecular product. We used the relative sensitivities calibrated in this work to calculate the product branching in N,N-dimethylformamide, whose two primary competing product channels form methyl radical in one channel and $N(CH_3)_2$ radical in the second. Such an absolute branching ratio would have normally relied on semiempirical estimates of the total ionization cross section (not reliable for polyatomic radicals) and error-prone measurement of the daughter ion cracking probabilities, but using the 1:1 production of these radicals in the separate photofragmentation calibration experiment circumvents such errors. The trimethylamine system also allowed us to test how vibrational motion influences whether a

conical intersection along the reaction coordinate is traversed adiabatically (in this case yielding excited state NR_2) or nonadiabatically (to form ground state product).

Our follow-up collaborative experiments at the ALS this year[6] used tunable VUV photoionization to characterize the nitrogen containing products, resolved by their neutral time-of-arrival spectra as in the previous work. We identified both primary and secondary neutral product channels (some of the neutral $N(CH_3)_3$ products were formed with enough internal energy to undergo secondary dissociation):

$$N(CH_3)_3 + 193\ nm \rightarrow N(CH_3)_2 + CH_3$$
$$\rightarrow CH_3N{=}CH_2 + H + CH_3$$
$$\rightarrow NC_2H_4 + H_2 + CH_3$$

We also identified the photoionization fragmentation of the ionized forms of the $N(CH_3)_2$ and $CH_3N{=}CH_2$ products, both of whose parent ions are unstable to fragmentation even upon low energy photoionization. The work combined tunable photoionization detection of the velocity resolved neutral photofragments with supporting G3 theoretical calculations of ion stabilities. $N(CH_3)_2$ primary products with very little internal energy show an experimentally observed ionization onset of 9.1±0.2 eV, but do not appear at the parent ion (*m/e*=44). Instead, the parent ion is unstable and easily fragments to *m/e*=42, where signal is observed. $N(CH_3)_2$ radicals with higher internal energies undergo H-atom loss from the neutral to give CH_2NCH_3, which has an observed ionization onset at parent (*m/e*=43) of <9.3 eV. At slightly higher ionization energies, these secondary products also appear at *m/e*=42 (where their appearance energy is roughly 9.8-9.9 eV, uncorrected for internal energy). Finally, $N(CH_3)_2$ radicals with the highest internal energy in this study appear to undergo H_2 loss as neutrals, giving rise to a species whose parent ion has *m/e*=42. The ionization onset of this species at *m/e*=42 is found to be in the range of 9.5-9.6 eV.

B. A Combined Experimental and Theoretical Study of Resonance Emission Spectra of SO_2

Our prior work[2] investigated the predissociative $\tilde{C}(^1B_2)$ state of SO_2 by cooling the SO_2 in a pulsed molecular beam and dispersing the emission upon resonant excitation into several different vibronic absorption features in the $\tilde{C}$ state between 197 and 212 nm. Unlike at lower excitation energies, the dispersed emission spectra at higher excitation energies are dominated by progressions with odd quanta in the antisymmetric stretch mode ν_3 and combination bands with up to six quanta in the bending mode ν_2. The formidable intensity for emission into vibrational states with odd quanta in the antisymmetric stretch of the jet-cooled molecule suggests that the intermediate state at high energies in the excited state is of mixed electronic character at nonsymmetric geometries, so the operative components of the transition moment for excitation and emission may be different. Our results suggested that at excitation energies near 200 nm the dissociation accesses an avoided crossing seam between the $\tilde{C}(^1B_2)$ state and a dissociative singlet state, the 3^1A_1 state. (Recent high-level *ab initio* calculations of the surfaces at these high energies have since been reported, see below, and support our conclusion that such a predissociation mechanism opens up at these energies.) The system demonstrates how such an avoided crossing seam alters commonly-accepted selection rules for optical transitions.

In order to support the best theoretical groups doing exact quantum calculations on this system, in the past year we took emission spectra at five excitation energies much lower in the $\tilde{C}$

state, 219.81, 221.16, 222.92, 224.77, and 227.73 nm.[5] Our theoretical collaborator requested this data to test the semiempirical 3-D excited state surface he had developed for the $\tilde{C}$ state of SO_2 from fitting the vibrational features of the excited state observed in laser-induced fluorescence spectra. (He also had calculated the ground electronic state vibrational eigenstates to very high energies, 15,000 cm^{-1}, and our emission spectra evidenced emission to several eigenstates not observed before but predicted at energies exact to within our experimental resolution. Thus, the work showed the empirical ground state potential of Kauppi and Halonen gives excellent predictive ability for the energies of eigenstates not previously observed.) While the calculated emission spectra at the two lowest excitation energies to the $\tilde{C}$ state agreed reasonably well with our experimental spectra, the agreement broke down at higher excitation energies. Clearly the emission spectra provide a critical test of excited state potentials. Preliminary calculations (H. Guo, private comm.) on the new *ab initio* potential for SO_2 just published by Bludsky *et al.* give much better agreement. At higher energies in the $\tilde{C}$ state, Bludsky *et al.* [Chem. Phys. Lett. 318, 607-13 (2000)] comment that their new potential strongly supports the conclusion in our earlier work[2] that a new predissociation mechanism opens up for SO_2 near 200 nm excitation, predissociation via an avoided crossing with a repulsive $^1A_1$ state.

C. The Photofragmentation Pathways of Methylvinylether: Electronic Accessibility and Calibrating Branching Ratios between the Dominant Product Channels of O + Ethylene

These experiments allow us to determine absolute branching ratios between energetically-allowed product channels in thermal bimolecular reactions, in this case O + ethylene, without relying on unreliable semiempirical estimates for the neutral products' ionization cross-sections. The experiments use a photodissociation channel of methylvinylether, $CH_2CH\text{-}O\text{-}CH_3 \rightarrow CH_2CHO + CH_3$, to directly calibrate the absolute branching between the two dominant pathways (Rxn.s 1 and 2 below) in the thermal $O(^3P) + C_2H_4$ reaction:

$$O(^3P) + C_2H_4 \rightarrow CH_3 + HCO \quad (1)$$
$$\rightarrow H + CH_2CHO \quad (2)$$
$$\rightarrow CH_2 + CH_2O \quad (3)$$

Experimental determinations of the product branching vary widely, ranging from Rxn. 1 contributing 71 (-9/+6) % of the products (assuming the yield of the third channel is small) to it contributing 44 (±15%) of the products. The reported experimental yield of 71 (-9/+6) % for Rxn. 1 comes from a crossed molecular beams scattering experiment in Y. T. Lee's group (Schmoltner *et al.*, J. Chem. Phys. 91, 6926 (1989)) at a 6 kcal/mol collision energy, so has the chance of being a benchmark for theoretical work on this system. However their branching ratio between Rxn.s 1 and 2 relied on estimating the ratio of the ionization cross sections of the vinoxy radicals and HCO radicals with an empirical method not tested for polyatomic radicals and on estimating by comparison with "related compounds" the cracking to missing masses in their daughter ion fragmentation pattern of the vinoxy radical. The experiments we have carried out this year circumvent the need to estimate ionization cross sections and daughter ion cracking patterns by instead using the 1:1 production of the methyl and vinoxy radical fragments from the photodissociation of methylvinyl ether to calibrate the mass spectrometric sensitivity to these products at the required daughter ions. (The method may be extended to calibrate the detection of

radical species in other classes of experiments, such as the measurement of concentration profiles of radical intermediates in flames using photoionization mass spectrometry or the calibration of low-energy electron impact ionization cross sections.)

Our photofragment scattering experiments on methylvinylether this year detected the vinoxy radical product at mass 42, 15 and 14 and the momentum-matched methyl radical signal at masses 15 and 14. The relative signal levels of the two radical products at any combination of daughter ion masses, corrected for the appropriate Jacobian factors and 3-D scattering, calibrate the mass spectrometric sensitivity at the CH_3^+ daughter ion for methyl radicals versus vinoxy radicals. This provides the only necessary calibration to determine an absolute branching ratio between a product channel forming methyl radical and a product channel forming vinoxy radicals, obviating the need to resort to empirical estimates of ionization cross sections and difficult measurements of daughter ion cracking probabilities. We are presently investigating possible secondary dissociation to ketene. We plan shortly to measure the relative signal levels at each parent ion upon low energy e^- impact ionization to provide a benchmark for groups who must use lower electron energies to avoid fragmentation in experiments where the products are not velocity resolved and who need our result to assess the accuracy of calculated ionization cross sections.

III. Future Plans

We plan first the completion and analysis of the methylvinylether experiments, including the low energy e^- impact ionization calibration and the determination of the O + ethylene product branching from the previously measured mass 15 spectra. Then, we plan to pursue photofragmentation experiments on vinyl and allyl iodide and its isomers. The latter is motivated by work in other groups which use allyl iodide and its isomers as a photolytic source of C_3H_5 radical isomers to study radical isomerization at resolved internal energies.

IV. Publications Acknowledging DE-FG02-92ER14305 (1998 or later)

1. Chemical Reaction Dynamics Beyond the Born-Oppenheimer Approximation, L. J. Butler, Annu. Rev. Phys. Chem. 49, 125-171 (1998).
2. Resonance Emission Spectroscopy of Predissociating SO_2 $\tilde{C}(1^1B_2)$: Coupling with a Repulsive $^1A_1$ State near 200 nm, P. C. Ray, M. F. Arendt, and L. J. Butler, J. Chem. Phys. 109, 5221-30 (1998).
3. Emission Spectroscopy of Jet-Cooled CS_2 Upon Excitation of the $^1\Sigma_g^+ \rightarrow {}^1B_2\left({}^1\Sigma_u^+\right)$ Transition in the 48 500 - 51 000 cm^{-1} Region, M. F. Arendt and L. J. Butler, J. Chem. Phys. 109, 7835-43 (1998).
4. Photodissociating Trimethylamine at 193 nm to Probe Electronic Nonadiabaticity at a Conical Intersection and to Calibrate Branching Ratios between Radical Products, N. R. Forde, M. L. Morton, S. L. Curry, S. Jarrett Wrenn, and L. J. Butler, J. Chem. Phys. 111, 4558-68 (1999).
5. A Combined Experimental and Theoretical Study of Resonance Emission Spectra of SO_2 ($\tilde{C}\,^1B_2$), B. Parsons, L.J. Butler, D. Xie, and H. Guo, Chem. Phys. Lett. 320, 499-506 (2000).
6. Characterization of Nitrogen-Containing Radical Products from the Photodissociation of Trimethylamine at 193 nm using Photoionization Detection, N. R. Forde, L. J. Butler, B. Ruscic, O. Sorkabi, F. Qi and A. Suits, submitted to J. Chem. Phys. (2000).

Independent Generation and Study of Key Radicals in Hydrocarbon Combustion (DE-FG02-98ER14857).

Barry K. Carpenter and Pamela A. Arnold
Department of Chemistry and Chemical Biology
Cornell University
Ithaca, NY 14853-1301
E-mail: bkc1@cornell.edu

1. Cyclopropyl Radical and Allyl Radical

1.1 Gas-Phase Photolysis of Cyclopropyl Iodide

We have prepared cyclopropyl iodide as a potential photochemical precursor to cyclopropyl radical. Almost all alkyl iodides are very good sources of the corresponding alkyl radical. However, cyclopropyl iodide appears to be an exception. Thus, when we supplied this compound to Carl Hayden of the Combustion Research Facility at Sandia National Laboratory, he was unable to detect any cyclopropyl radical in his time-resolved photoion-photoelectron coincidence imaging apparatus. We have consequently undertaken an investigation of the photochemistry of cyclopropyl iodide to see what does occur.

In collaboration with Paul Houston of this Department, we have subjected cyclopropyl iodide to 266nm photolysis from a quadrupled Nd:YAG laser and have imaged the ions generated from the $^2P_{1/2}$ and $^2P_{3/2}$ iodine atoms by 2+1 REMPI. Calculation of the total translational kinetic energy in the photodissociation fragments indicates that at least some of the products are formed with more than the maximum 1.86 eV kinetic energy possible for simple C–I bond fission. This upper bound in kinetic energy is predicated on a C–I bond dissocation enthalpy (BDE) of 64.5 kcal/mol – a value that is not known experimentally but can be deduced from a number of independent additivity schemes. It does not seem likely that the error in the estimated C–I BDE could be enough to account for the substantial excess kinetic energy exhibited by some of the fragments. See Figure 1 below.

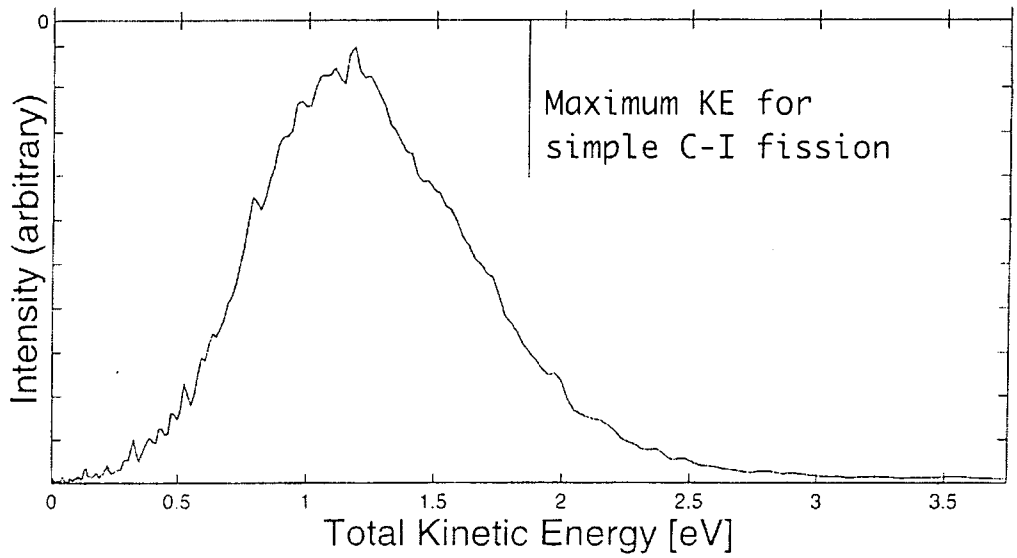

Figure 1

A plausible explanation for the result is that there is a *direct* photolysis channel from cyclopropyl iodide to allyl radical plus I*. This channel would have to be direct because the more obvious mechanism – generation of vibrationally hot cyclopropyl radical which then ring opens in a second step – could not provide excess *translational* kinetic energy to the photofragments.

That allyl radical was indeed formed in this photolysis was supported by electron imaging experiments. First, we prepared a genuine sample of allyl radical by 266 nm photolysis of allyl iodide. A 266 nm 1+1 REMPI of the allyl radical produced electrons with kinetic energy centered on 1.2 eV, in very good accord with the expectation of 1.19 eV for vertical ionization, given the known vertical I.P of 8.13 eV for allyl.[1] Significantly, the photodissociation products from cyclopropyl idodide also revealed a peak centered on 1.2 eV for the electron kinetic energy, suggesting the presence of allyl radicals.

To our knowledge, there are very few photochemical reactions that break a C–C σ bond in the primary step, and so we are investigating the matter further, using both theoretical and solution-phase experimental techniques.

The theoretical approach is to map out the S_0 and S_1 electronic potential energy surfaces of the C_3H_5I manifold and to search for conical intersections where a dissociative process of the kind proposed may occur. We are using large-basis set CASPT2//CASSCF methods, which are quite computationally intensive and time consuming, and so those calculations are still in progress. The solution-phase studies are further advanced, and the results so far are described in the next section.

1.2 Solution-Phase Photolysis of Cyclopropyl Iodide

If photolysis of cyclopropyl iodide does directly generate ally radicals, this should be kinetically discernable by bimolecular trapping in solution. Consequently we have carried out the photolysis of cyclopropyl iodide with a medium-pressure mercury lamp in benzene solution in the presence of TEMPO. The products have been fully characterized and shown to be those expected from trapping of *both* cyclopropyl radical and allyl radical (Figure 2):

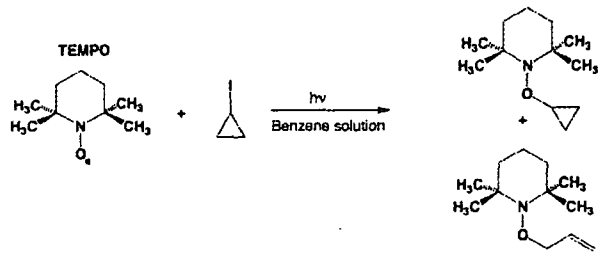

Figure 2

Of considerable significance for the mechanistic question at hand is that the ratio of the two products shows very little dependence on the concentration of TEMPO. This would not be expected if the ring-opened product were derived from a vibrationally hot cyclopropyl radical (Figure 3), since then there should be a first-order dependence of the product ratio on TEMPO concentration:

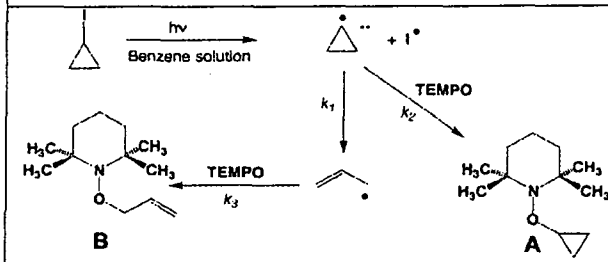

$$\frac{[A]}{[B]} = \frac{k_2}{k_1}[TEMPO]$$

Figure 3

However, the result *is* consistent with direct formation of allyl radical in the photolysis, since then the product ratio is determined solely by the ratio of the cyclopropyl to allyl radicals formed in the first step.

Whether the successful trapping of cyclopropyl radicals in solution means that they are also formed, but as yet undetected, in the gas phase, or whether it means that the photochemistry is affected by the medium remains to be determined.

2. Formyloxymethyl Radical

In computational work on the important vinyl radical + O_2 reaction, we have proposed[3] that the formation of formyl and formaldehyde occurs *via* the pathway shown in Figure 4. This mechanism can be contrasted with the previous proposal[4] (Figure 5):

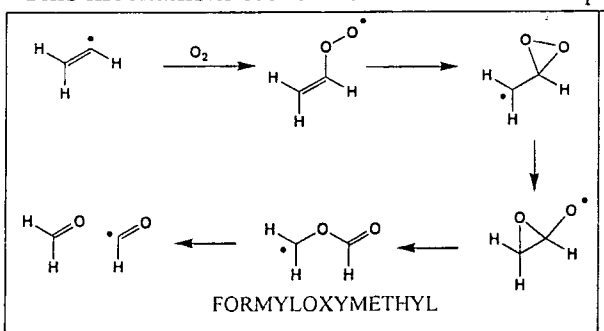

Figure 4

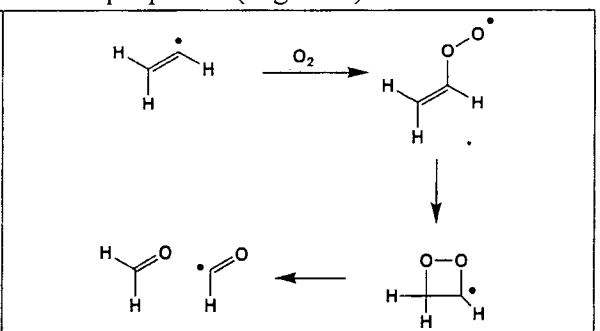

Figure 5

Subsequent calculations at a higher level than ours have supported the mechanism in Figure 4.[5] Of special significance in this mechanism is the role played by the formyloxymethyl radical. The various calculations find a barrier of 25 – 33 kcal/mol for its fragmentation to formyl plus formaldehyde. No other lower-energy unimolecular reaction has been found. This implies that formyloxymethyl could have a lifetime long enough to be interceptible by O_2 in a bimolecular process. Such a reaction would have importance for the kinetic modeling of hydrocarbon combustion. Consequently, we have undertaken a project to generate formyloxymethyl and to determine experimentally the activation barrier for its fragmentation.

During the last year we have successfully prepared a precursor to formyloxymethyl, and have shown that it does fragment to formyl and (presumably) formaldehyde, but that it is also interceptible in a bimolecular reaction. The synthesis of the precursor is shown in Figure 6 and its use in the generation and trapping of formyloxymethyl is shown in Figure 7.

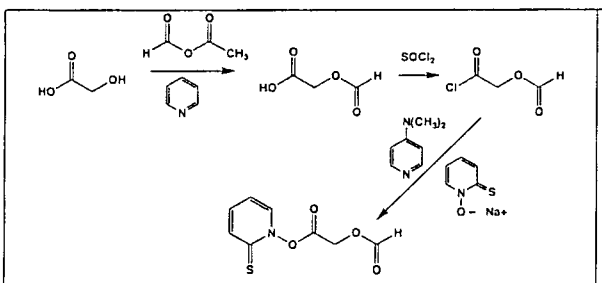

Figure 6

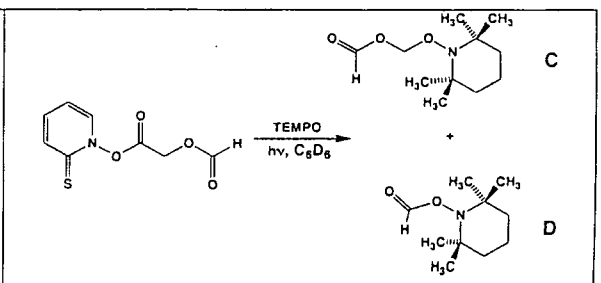

Figure 7

Compound **C** is the TEMPO trapping product of formyloxymethyl and compound **D** is the TEMPO trapping product of formyl. By studying the temperature dependence of the **C**:**D** ratio, we should be able to deduce the solution-phase activation energy for fragmenation of formyloxymethyl. A wealth of literature[6] suggests that activation parameters for radical reactions are little affected by the medium, so that this solution-phase value should also be applicable to the gas phase, and should be directly comparable to the calculated values.

Literature Citations

1. Houle, F.A.; Beauchamp, J.L. *J. Am. Chem. Soc.* **1978**, *100*, 3290.

2. Baldwin, R. R.; Lodhi, Z. H.; Stothard, N.; Walker, R. W. 23rd Int. Symp. Combust. 1991, 123.

3. Carpenter, B. K. *J. Phys. Chem.* **1995**, *99* , 9801.

4. (a) Slagle, I.R.; Park, J.-Y.; Heaven, M.C.; Gutman, D. *J. Am. Chem. Soc.* **1984**, *106*, 4357. (b) Krüger, H.; Weitz, E. *J. Chem. Phys.* **1988**, *88*, 1608. (c) Fahr, A.; Laufer, A.H. *J. Phys. Chem.* **1988**, *92*, 7229. (d) Westmoreland, P.R. *Combust. Sci. Technol.* **1992**, *82*, 151. (e) Bozzelli, J.W.; Dean, A.M. *J. Phys. Chem.* **1993**, *97*, 4427. (f) Knyazev, V.D.; Slagle, I.R. *J. Phys. Chem.* **1995**, *99*, 2247.

5. Mebel, A. M.; Diau, E. W. G.; Lin, M. C.; Morokuma, K. *J. Am. Chem. Soc.* **1996**, *118*, 9759.

6. For a recent review see: Denisov, E. *Gen. Aspects Chem. Radicals* **1999**, 79.

Crossed-Molecular-Beam Ion Imaging Experiments

David W. Chandler
Combustion Research Facility, MS 9055, Sandia National Laboratory,
chandler@ca.sandia.gov

Scope of Program

My research has focused on developing and using two-dimensional imaging techniques to study chemical dynamics. These techniques allow one to measure the velocity of state-selectively photoionized products of unimolecular and bimolecular interactions. This information is quite useful in understanding the details of chemical processes. In the last two years we have made significant improvements in these techniques with the further development of the velocity mapping technique and the utilization of a crossed molecular beam apparatus for the study of bimolecular collisions. A major effort has been to develop methods for extracting quantitative differential cross sections and alignment parameters from crossed-molecular-beam ion imaging experiments.

Recent Progress

Rotational state-resolved differential cross sections (DCS) for the j-changing collisions of HCl by Ar have been measured. A crossed-molecular beam velocity-mapped imaging apparatus is used to measure images of scattered HCl in j=0 through j=6. In the initial molecular beam the j = 0 state accounts for over 97% of the initial HCl rotational state population. From these images the full ($\theta = 0° - 180°$) DCS for $j = 0 \rightarrow j' = 1,2,..,6$ rotational energy transfer at a center-of-mass energy of ~538 cm^{-1} is determined. The scattering products are detected using state-selective ionization *via* (2 + 1) REMPI through the E-state. The images are analyzed using an iterative fitting method that produces the direct extraction of state-to-state DCS's in the center-of-mass frame.

Figure 1 is the experimental image obtained from the selective ionization of HCl j=4. Superimposed on this image is the center of mass and the relative velocity vectors of the Ar and HCl j=0 molecule that collided. Scattering intensity at $\theta=0°$ degrees represents forward-scattered products and intensity at $\theta=180°$ represents back-scattered products. The angular distributions for the experimental DCS's become increasingly backscattered as Δj increases, but do so non-monotonically, as $j' = 3$ is more forward scattered than $j' = 2$. Images for the even Δj's $0 \rightarrow 2$ and $0 \rightarrow 4$ are similar, and those for the odd Δj's $0 \rightarrow 1$ and $0 \rightarrow 3$ also have similarities. The calculated cross sections, based upon the HCl-Ar H6(4,3,0) potential of Hutson [Hudson, J. Phys. Chem. 1992, **96**, 4237-4247], agree qualitatively with the experimental cross sections and show the same non-monotonic trends in the scattering intensity. However, there are significant differences between the theoretical and experimental results, where many of the principal features in the calculated DCS's lie 10° – 30° more back scattered than the same features in the experimental DCS's. Figure 2 shows the DCS extracted from the data of Figure 1 and the corresponding DCS calculated from the H6(4,3,0) potential as well as simulated images using the two different DCSs. Comparison of the simulated images shows the sensitivity of the raw data, Figure 1, to the small differences in the DCSs of Figure 2.

This work was done in collaboration with the George McBane of Ohio State University and Paul Houston and Mike Westley of Cornell University and Thomas Lorenz, Sandia.

Other crossed-beam experiments have examined the alignment of the rotational angular momentum of scattered NO from rotationally inelastic collisions with Ar at nominally 500 cm^{-1} collision energy. The NO product is probed by polarized, two-color 1+1' REMPI through the NO $A^2\Sigma$ state. By using very low probe laser power, we avoid saturation of the resonant transition. Rotational alignment is obtained from comparison of images obtained with different polarization geometries of the probe light.

In figure 3 the velocity-mapped images of the NO $X^2\Pi_{1/2}$ (v=0, j=17/2) product, probed on the $R_{21}(17/2)$ line of the NO A $\leftarrow$ X transition are shown. In these images the NO projectile approaches from the right side of the image and the Ar target from the left. The leftmost image, labeled V, was obtained for probe light polarized perpendicular to the plane of the image. The middle image, labeled H, was obtained for probe light polarized along the horizontal axis of the image. Note that, for this product j-state, the NO is mostly forward-scattered.

The right image is the difference between V and H, normalized by their sum. This image is symmetric and shows that the forward scattered products are polarized opposite to the back scattered products. We have developed a theory to extract the angular momentum alignment from such polarization differences. There are three general types of alignment possible: wheel, frisbee and propeller. Frisbee is defined as having the j-vector perpendicular to both the recoil velocity vector and the scattering plane (defined by the center-of-mass collision vector and recoil velocity vector). Wheel is defined as j perpendicular to the recoil velocity vector and in the scattering plane. Propeller has the j vector of the scattered product parallel to the recoil velocity vector.

In the scaled difference image, lighter shading corresponds to a negative difference (V<H) and darker shading corresponds to a positive difference (V>H); the gray background shade corresponds to V=H (zero rotational alignment). The white regions of the difference image, concentrated in the backscattered region, indicate frisbee–type trajectories of the recoiling NO. The darkest regions in the difference image, concentrated in the strongly forward-scattered region, indicate propeller-type trajectories of the scattered NO. A physical picture consistent with results is that frisbee trajectories are produced by strongly repulsive collisions with all three atoms nearly in the scattering plane. Propeller trajectories originate from softer collisions in which the NO rotor is only slightly deflected in the collision.

We are currently extracting quantitative alignment parameters from difference images of this type for several rotational states of the scattered NO. The results appear similar to the alignment measurements by Meyer [H. Meyer, J. Chem. Phys. 102, 3151 (1995)] on this system. Time-of-flight experiments provide the laboratory-frame alignment parameter $A^{(2)}_0$, however, analysis of the imaging data reveals three recoil-velocity reference frame alignment parameters $A^{(2)}_0$ $A^{(2)}_{1+}$ $A^{(2)}_2$, giving give a much more complete description of the trajectory of the recoiling NO product. For example the

imaging data shows that the backscattered NO preferentially produces frisbee-type scattering, whereas the analogous TOF measurement can not distinguish between frisbee and wheel-type alignment. This work was done in collaboration with Dr. Joe Cline of the University of Nevada at Reno and Dr. Thomas Lorenz and Dr. Elisabeth Wade of Sandia.

Future Directions

We will continue to develop techniques for the study of unimolecular photochemistry and bimolecular interactions using photofragment imaging and velocity mapped crossed-molecular-beam ion imaging techniques.

Publications:

L. M. Yoder, J. R. Barker, K. T. Lorenz and D. W. Chandler, "Ion Imaging the Recoil Energy Distribution Following Vibrational Predissociation of Triplet State Pyrazine-Ar van der Waals Clusters," Chem. Phys. Lett. **302**, 602 (1999).

D. W. Neyer, A. J. R. Heck and D. W. Chandler, "Photodissociation of N_2O: *J*-dependent Anisotropy Revealed in N_2 Photofragment Images," J. Chem. Phys. **110**, 3411 (1999).

D. W. Neyer, A. J. R. Heck and D. W. Chandler, "Speed-Dependent Alignment and Angular Distributions of $O(^1D_2)$ from the Ultraviolet Photodissociation of N_2O," J. Phys. Chem. A, **103**, 10388 (1999).

M. H. M. Janssen, J. M. Teuel, D. W. Neyer, D. W. Chandler, and G. C. Groenenboom, "Imaging of State-to-State Phytodynamics of Nitrous Oxide in the Stratospheric Solar Window," *and* D. W. Chandler, J. R. Barker, A. J. R. Heck, M. H. M. Janssen, L. T. Lorenz, D. W. Neyer, W. Rotterdink, S. Stolte, and L. M. Yoder-Miller, "Ion Imaging Studies of Chemical Dynamics," *Advances in Molecular Beam Research and Applications*, ed. R. Campargue (SpringerVerlag, April 1999).

M. H. M. Janssen, J.M. Teule, D. W. Neyer, D. W. Chandler, and S. Stolte, "Comments to Dynamics of Electronic Excited States in Gaseous, Cluster, and Condensed Media," Faraday Discussions, **08**, 230 (1998).

D. W. Chandler and D. H. Parker, "Velocity Mapping of Multiphoton Excited Molecules," *Advances in Photochemistry*, Vol. 25, eds. D. C. Neckers, D. Volman, G. vonBunau (John Wiley & Sons, New York, 1999) page 59.

D. W. Chandler, D. W. Neyer, and A. J. R. Heck, "High Resolution Photoelectron Images and D^+ Photofragment Images Following 532-nm Photolysis of D_2" *Laser Techniques for State Selected and State-to-State Chemistry IV*, eds. J. Hepburn and R. Continetti, SPIE **3271**, 85 (1998).

K. T. Lorenz, M. S. Westley, D. W. Chandler, "Rotational state-to-State differential Cross sections of the HCl-Ar Collision system using velocity Mapped Ion imaging" Phys. Chem. Chem. Phys. **2**, 481 (2000).

J. M. Teule, G. C. Groenenboom, D. W. Neyer, D. W. Chandler and M. H. M. Janssen, "Long –range interaction and the alignment of O(1D2) fragments from the state to state photodynamics of nitrous oxide" Chem. Phys. Lett, submitted (2000).

D. W. Chandler and K. T. Lorenz "Velocity Mapped Imaging of Crossed Molecular Beam Scattering :The HCl-Ar system"; L. M. Yoder, J. R. Barker, K.T. Lorenz and D. W. Chandler"Recoil energy disposal in the vibrational predissociation of some van der Waals dimers"; "Crossed Molecular Beam studies of CO rotational Energy Transfer" G. C. McBane, S. Antonova, A. Lin, A. P. Tsakotellis, K. T. Lorenz and D. W. Chandler in "Imaging in Chemical Dynamics", ACS Symposium Series," edited by Arthur G. Suits and Robert E. Continetti, American Chemical Society, Washington DC., 2000.

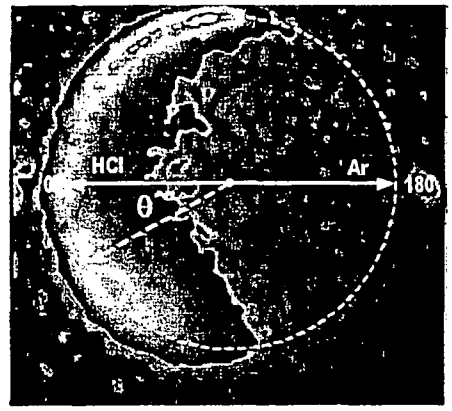

Figure 1, Image of HCl (j=4) from Ar + HCl (j=0) collision

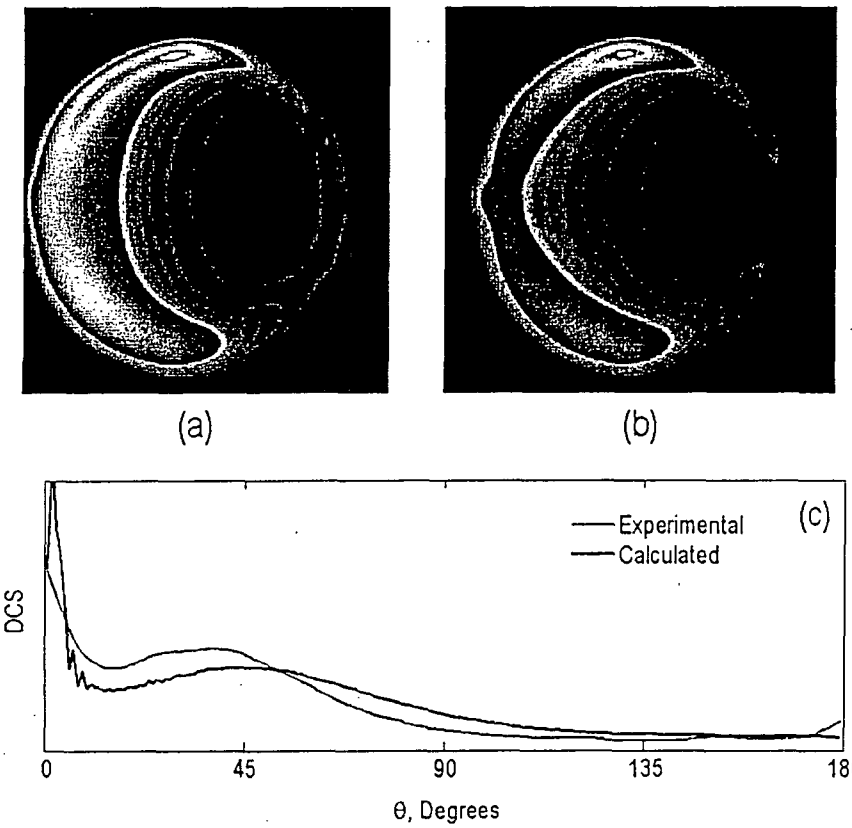

Figure 2 Simulated images from extracted (experimental) (a) and calculated (b) DCS.

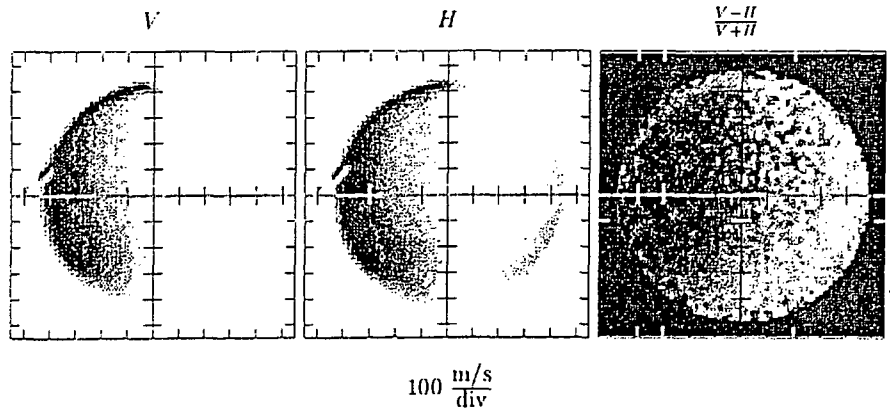

Figure 3, Image obtained using vertical and horizontal polarizations and normalized difference image

Direct Numerical Simulation and Modeling of Turbulent Combustion

Jacqueline H. Chen and Hong G. Im
Sandia National Laboratories, Mail Stop 9051
Livermore, California 94551-0969
phone: (925) 294-2586
email: jhchen@ca.sandia.gov

Program Scope

Direct numerical simulation (DNS) of turbulent and unsteady laminar flames has been an invaluable tool in the understanding of complex interactions between combustion chemistry, transport and unsteady flow in gas phase combustion. The scope of the present research is to use DNS with detailed chemical mechanisms for hydrocarbon and hydrogen fuels to simulate multi-dimensional unsteady effects in premixed, partially-premixed and nonpremixed combustion. The physical insights gained from these fundamental studies is being used to guide models of the turbulent flame speed in the flame surface density and the G-equation flame-front tracking flamelet modeling approaches for RANS and LES of practical engineering configurations.

Recent Progress

Stretch effects on the burning velocity of turbulent premixed hydrogen-air flames [1,2]

The turbulent burning velocity is a central quantity in the understanding and modeling of turbulent premixed combustion in the flamelet regime. It depends upon, not only the intrinsic thermochemistry and transport, but also on external aerodynamic stretch on corrugated flame surfaces. It is well known that stretch, through strain rate and curvature, has a profound effect on the local flame speed through coupled effects of unequal heat and mass diffusion. While experiments have confirmed the theoretical prediction that the burning velocity varies linearly with small values of stretch, the application of the linear theory to real flames with finite thickness and higher values of stretch has been more difficult and more open to debate. Outstanding issues remaining include how flame propagation is defined, the location in the flame where it is measured, transients associated with turbulent flows, and preferential/differential diffusion effects.

DNS studies of turbulent methane-air and hydrogen-air premixed flames have provided invaluable data to address the aforementioned issues, and to provide statistical information required in flamelet models. Specifically, correlations of burning velocity with strain and curvature for alternative definitions of flame speed were examined. Diffusive-thermal effects on propagation and structure for lean to rich hydrogen/air stoichiometries were found to have a dominant effect on enhancing (diminishing) flame speeds. Finally, the flame response to transient stretch is examined using multiple approaches: 1) by varying the initial turbulence intensity relative to the flame transit time in the DNS; and 2) by performing one-dimensional unsteady counterflow calculations where a time-dependent strain rate is imposed at each of the nozzle exits.

For moderate turbulence intensity DNS, $u'/S_L=5$, we found that both the local consumption and displacement speeds correlate strongly with curvature and strain rate across a wide range of thermal-diffusive mixture conditions. The results we obtain are consistent with diffusive thermal theory and differ from previous results obtained from DNS studies. We find that diffusive-thermal effects result in substantial changes in burning rate, by as much as *five* times larger than the undisturbed laminar flame speed for unstable mixtures, and by as much as *four* times lower for stable mixtures. Previous studies have indicated much more modest changes in mean burning rate due to stretch (10-30 % of S_L), even for diffusively imbalanced mixtures. Computed strain Markstein numbers we obtain range

from –5.34 to 2.85 and area-weighted expectations for the consumption speed range from $2.43S_L$ at an equivalence ratio, ϕ, of 0.4 to $0.39S_L$ at ϕ=6.5.

We also discovered that near the neutral stability point, at an equivalence ratio of ϕ=0.6, the correlation of flame speed with curvature depends upon whether heat release or fuel consumption is utilized in the consumption speed definition. Qualitative differences are observed and we attribute these differences to the physical segregation in the peak heat release and peak fuel consumption along with competing diffusional effects of H-atom and H_2. In particular, the main fuel consumption reactions are the chain-branching/carrying steps, most notably $H_2+O=H+OH$ [R2] and $H_2+OH=H_2O+H$ [R3], which favor high temperature (above 1200K), while heat release is primarily produced by the recombination step, $H_2+O_2+M=HO_2+M$ [R9], which is dominant for lower temperatures (below 900K). As such, the peak heat release occurs upstream of the location of peak fuel consumption, implying that H atom must diffuse back upstream to enhance R9. Therefore, while H_2 consumption is directly related to the focusing of H_2 at the positive cusp, heat release is affected by two competing effects, namely the focusing of H_2 and the defocusing of H-atom. For curved flame fronts the temperature and H-atom isocontours do not align due to preferential diffusion, resulting in one effect overriding the other.

For all stoichiometries considered, ϕ=0.4 to 6.5, a near linear correlation of propagation with strain is found to exist, while the correlation with curvature is nonlinear. This result implies that the theoretical results for flame propagation in the limit of weak stretch have broader applicability to turbulence situations where the strain rate is much larger. The strain contribution to the Markstein numbers for moderate turbulence intensities compares favorably with steady counterflow and experimental results. Unsteadiness, imposed by a high turbulence intensity, however, leads to an attenuation of the flame response to stretch, manifest as a reduction in the Markstein number. This is observed across a wide range of fuel-lean to fuel-rich stoichiometries.

To further clarify the role of unsteady strain rate on the burning velocity of hydrogen-air premixed flames a one-dimensional unsteady opposed nozzle configuration was studied numerically. An oscillatory and impulsive velocity forcing was applied to the exit of each of the nozzles. The Markstein number versus the frequency of oscillation was investigated for mixtures of different equivalence ratios. The general trend we observed from the counterflow simulations is that the flame speed response to strain rate fluctuation attenuates as the frequency of oscillation exceeds the inverse of the characteristic flame time, consistent with the DNS results. The increased phase delay of the flame response to strain rate causes tilting of the flame speed/Karlovitz number limit cycle, resulting in a lower Markstein number (slope of the ellipse). Unique behavior, however, was observed for some rich mixtures, in which the Markstein number exhibits a peak response for moderate frequencies. This distinct behavior disappears again as the equivalence ratio is further increased, possibly due to the effect of a reduced heat release parameter. Further comparison of the Markstein number to a case with dilution reveals that the resonance is suppressed by dilution.

Structure and propagation of triple flames in partially-premixed hydrogen-air mixtures [3,4]

Partially-premixed turbulent combustion plays an important role in many practical situations. In a direct injection diesel engine the initial stage of combustion occurs in a rich partially-premixed mode following autoignition. In a lifted turbulent jet diffusion flame it has been conjectured that the stabilization mechanism at the point of lift-off may be a partially-premixed flame known as an edge flame—*i. e.* a diffusion flame with a premixed leading edge. Turbulent diffusion flames that are highly strained and are undergoing local extinction may also have regions of partially-premixed combustion as the extinction pockets reignite and burn along the edges. In all of these situations models that adequately predict the burning rate are required. Flamelet-based models for the limiting

cases of purely premixed and purely nonpremixed flames exist and it is possible that these models may be extended to account for mixed-mode combustion.

The simplest canonical flow to study effects of partial premixing is a triple flame comprised of a curved premixed front spanning rich and lean compositions and a trailing diffusion flame formed from the excess fuel and oxidizer that survive through the premixed branches. Recently, we have used DNS with detailed chemistry to study the dynamics of triple flames interacting with unsteady vortices, along with the structure and propagation characteristics of laminar methanol-air and hydrogen-air triple flames in a scalar mixing layer configuration. From DNS of a methanol-air triple flame we discovered that triple flames have a two-stage structure, characteristic of hydrocarbon fuels, wherein the trailing diffusion flame corresponds to a CO/H_2 flame produced from stable combustion intermediates from the upstream premixed branch. We also found that the enhancement in the stabilization speed is primarily due to flow divergence, consistent with earlier studies, and that its value is proportional to the square root of the density ratio across the flame. For an unstretched flame the effect of detailed chemical kinetics on flame propagation was found to be minimal relative to heat release.

As with the DNS of methanol-air triple flames, we found that for a scalar mixing layer of diluted hydrogen/air, the triple point is near the stoichiometric line even thought the laminar flame speed of a H_2/air premixed flame is maximum for a rich mixture. For a mixing layer of undiluted hydrogen and air, the extreme asymmetric structure of the triple flames reveals some distinct features. Most notably, the maximum value of the stabilization speed, and hence the stabilization point, occurs at a location different from the triple point at which heat release and displacement speed are maximum.

The effect of unsteady flow strain on the triple flame structure and propagation was also studied by imposing a pair of counterrotating vortices in front of the flame. As the triple point encounters compressive strain in the channel between the vortices, the premixed flame front collapses onto the diffusion flame, thereby forming an edge flame. Subsequently, a shift in the heat release toward the lean premixed branch and extinction of the H-atom consumption layer at the tip were observed. The excessive strain and curvature at the triple flame tip induced by the vortical flow results in a negative displacement speed. The triple flame was subjected to vortices of different strengths. It was found that the speed at the triple point is correlated more strongly with stretch than with scalar dissipation rate.

Combined pdf-sdf approach to partially-premixed turbulent combustion [5]

Direct injection gasoline and diesel engines feature large as well as small-scale spatial fluctuations in the mixture composition. Under these conditions, a description of partially-premixed turbulent combustion is needed. From DNS studies of triple flames we learned that partially-premixed combustion occurs in two stages, with the first stage corresponding to a premixed mode, and a second stage corresponding to a diffusion flame burning the by-products of the first stage. DNS studies have shown that the premixed stage is flamelet-like while the nonpremixed stage exhibits nonflamelet behavior. Recently, a combined surface density function probability density function (SDF/PDF) formalism was developed to handle both flamelet and nonflamelet combustion regimes within a unified model [6]. As an initial attempt to extend the SDF/PDF formalism to handle partially-premixed modes of combustion, we have developed a criterion for the detection of partially-premixed finite-rate burning zones. We have defined a new single scalar variable based on geometric properties of mixture fraction and nonconserved variables observed from DNS of triple flames that allows the detection of finite-rate and triple flame domains. This scalar variable incorporates the angle between the gradients of mixture fraction and progress variable, and has been generalized to handle detailed chemistry. Using this new scalar variable the framework for a combined SDF/PDF approach has been developed that is able to treat finite-rate partially-premixed

regions in a turbulent flow by conditioning with the scalar detecting them. Future work in this area will involve developing appropriate closure models for the various terms in the new SDF/PDF approach.

Future Plans

We plan to continue our DNS studies of unsteady multi-dimensional flames with detailed hydrocarbon and hydrogen kinetics on massively parallel distributed memory computational platforms with a focus towards understanding and modeling the effects of partial premixing on flame structure and propagation, the effects of turbulent fluctuations on autoignition, and the effects of unsteady strain rate on the chemical response and propagation of premixed and partially-premixed flames.

References

[1] J. H. Chen and H. G. Im, "Stretch Effects on the Burning Velocity of Turbulent Premixed Hydrogen-Air Flames," *Twenty-Eighth Symposium (International) on Combustion*, (Edinburgh, Scotland, July 30-August 4, 2000) submitted.

[2] H. G. Im and J. H. Chen, "Effects of Flow Transients on the Burning Velocity of Hydrogen-Air Premixed Flames," *Twenty-Eighth Symposium (International) on Combustion*, (Edinburgh, Scotland, July 30-August 4, 2000) submitted.

[3] H. G. Im and J. H. Chen, "Structure and Propagation of Triple Flames in Partially-Premixed Hydrogen/Air Mixtures," *Combust. Flame*, **119**, 436 (1999).

[4] T. Echekki and J. H. Chen, "Structure and Propagation of Methanol-Air Triple Flames", *Combust. Flame*, **114:** 231-245 (1998).

[5] W. Kollmann, J. H. Chen, and H. G. Im, "Combined pdf-sdf Approach to Partially Premixed Turbulent Combustion," *Twenty-Eighth Symposium (International) on Combustion*, (Edinburgh, Scotland, July 30-August 4, 2000) submitted.

[6] L. Vervisch, E. Bidaux, K. N. C. Bray, and W. Kollmann, *Phys. Fluids*, 7:2496-2503 (1995).

[7]J. H. Chen and H. G. Im, "Correlation of Flame Speed with Stretch in Turbulent Premixed Methane-Air Flames," *Twenty-Seventh Symposium (International) on Combustion*, (The Combustion Institute, Pittsburgh, PA, 1998) pp 819-826.

[8] J. H. Chen, T. Echekki, and W. Kollmann, "The Mechanism of Two-Dimensional Pocket Formation in Lean Premixed Methane-Air Flames with Implications to Turbulent Combustion," Combust. Flame **116**,15 (1999).

[9] T. Echekki and J. H. Chen, "Analysis and Computation of the Different Contributions to Flame Propagation in Turbulent Premixed Methane-Air Flames," Combust. Flame, **118**, No. 12 (1999).

[10] H. G. Im, J. H. Chen and C. K. Law, "Ignition of Hydrogen/Air Mixing Layer in Turbulent Flows," *Twenty-Seventh Symposium (International) on Combustion*, The Combustion Institute, Pittsburgh, PA, 1998) pp. 1047-1056.

[11] H. G. Im, J. H. Chen and J.-Y. Chen, "Chemical Response of Methane/Air Diffusion Flames to Unsteady Strain Rate," Combust. Flame, **118**, 204 (1999).

[12] C. A. Kennedy, and J. H. Chen, " Mean Flow Effects on the Linear Stability of Compressible Planar Jets," Phys. Fluids, **10** 3 (1998).

[13] W. Kollmann and J. H. Chen, "Pocket Formation and Flame Surface Density Equation," *Twenty-Seventh Symposium (International) on Combustion*, The Combustion Institute, Pittsburgh, PA, 1998) pp. 927-934.

[14] N. Peters, P. Terhoeven, J. H. Chen and T. Echekki, "Statistics of Flame Displacement Speeds from Computation of 2-D Unsteady Methane-Air Flames," *Twenty-Seventh Symposium (International) on Combustion*, The Combustion Institute, Pittsburgh, PA, 1998) pp. 833-839.

Turbulent Combustion

Robert K. Cheng
Environmental Energy Technologies Div.
Lawrence Berkeley National Laboratory
70–109, 1 Cyclotron Rd.
Berkeley, CA 94720

E-mail: rkcheng@lbl.gov

Lawrence Talbot
Dept. of Mechanical Engineering
University of California at Berkeley
6173 Etcheverry Hall
Berkeley, CA 94720-1740

E-mail: talbot@me.berkeley.edu

Scope

The objective of this project is to investigate fluid mechanical processes that control combustion efficiency, power density, flame stability and formation of pollutants. In practical flames, these processes are turbulent and the flame interactions processes are not sufficiently well understood and characterized to guide the development of predictive theoretical models that include robust turbulence codes with detailed combustion chemical kinetics. Our research focuses on premixed turbulent combustion. Lean premixed combustion emits low concentrations of oxides of nitrogen (NO_x) and is a recognized energy technology for next generations heating and power systems. The main objective of our research (on the fluid mechanical processes of premixed turbulent flames) is to contribute to the development of combustion modeling and theories that will be the design tools for future clean combustion systems. This mission is relevant to the DOE programmatic goal to increase energy efficiency and to minimize adverse environmental consequences of energy production and use. Our experimental and numerical efforts are guided by a theoretical concept that separates premixed turbulent flames into regimes according to their characteristics at different levels of turbulence. The experimental configurations are designed to facilitate direct comparison with numerical models.

Recent Progress

Our current interest is to characterize the differences between flames in moderate and intense turbulence. The purpose is to test the Klimov-Williams criterion at unity Karlovitz number, $Ka = 1$. This is a theoretical threshold that separates two types of premixed turbulent flames. In wrinkled flames ($Ka < 1$), at low to moderate turbulence, the *reaction zone* of the flame front (on the order of 0.1 mm thick) remains undisturbed by turbulent eddies. The flame fronts retain many features of a laminar flame. Flames with "distributed reaction zones" ($Ka > 1$) occur at high intensity turbulence where small intense eddies may penetrate and broaden the reaction zone. As the operating conditions of most practical systems span this criterion, the problem is of interest to both fundamental and applied research. The main implication is that different flame models may be needed to simulate the combustion processes in the two regimes. This is particularly significant for modeling flames within the distributed reaction zone regime. Turbulence transport within the reaction zone imply that a very fine computational grid (at least 10 times finer that that for the wrinkled flames) may be necessary to resolve the changes in the thermal, mass transport and chemical processes.

For these investigations, we used a low-swirl burner (LSB) with a turbulence generator that produces high intensity near-isotropic turbulence of up to 3.0 m/s rms velocity. The experiments cover conditions of moderate ($u'/S_L = 3$) to intense ($u'/S_L = 12$) turbulence. For velocity measurements, we use a two-component laser Doppler anemometry system. For scalar statistics, we use laser schlieren, laser tomography, Planar Laser Induced Fluorescence for OH (OH-PLIF) and 2D Rayleigh. Methane/air flames with the same equivalence ratio ($\phi = 0.7$) have been studied. By increasing the total flow rate from 5 to 20 liters/s, the rms velocity was varied from 0.5 to 2.2 m/s.

A statistical analysis of the OH-PLIF results is complete. These images have shown that the probability of finding the smallest flame wrinkles is relatively low even under intense turbulence. This is an indication that the penetration of small intense eddies into the flame sheet, as postulated by the 'distributed reaction zone' concept, may be statistically an extremely rare event. The OH-PLIF images were also processed to determine flame wrinkle scales and curvatures. The results show that the flames respond to the increases in turbulence intensity by producing larger mean flame front curvatures. But the probability of very large mean flame curvatures (i.e., very small wrinkles) is relatively low. This gives further evidence that the influence of the smallest turbulence eddies on the flame fronts is a rare event.

The flame edges deduced from the OH-PLIF data were also analyzed to evaluate the turbulent burning rate. The method provides a two-dimensional estimate of the flame surface density, Σ (ratio of flame front length to the flame zone area) as a function of the progress variable, $\bar{c}$. This approach avoids some of the difficulties involved with previous one-dimensional methods. The integral of Σ across the flame brush is the burning rate. These results were compared with the consumption speed S_c that is equal to the turbulent flame speed, S_T, for an ideal 1D system. For the axisymmetric flame in a LSB, it is necessary to account for the radial mass fluxes to determine S_c. The results show that S_c is typically 25% of S_T indicating a large amount of outflow that occurs in the divergent flow field.

The burning rates obtained from integration of the flame surface density are found to be very similar to S_c. Both show linear increase with increasing u'/S_L. Such a similarity although to be expected intuitively, was not observed in previous comparisons of scalar burning rates and turbulent burning velocities because the displacement speed or a rms velocity was used in those comparisons. The results underline the fact that the consumption speed is the more fundamental quantity which should be used to quantify the affect of upstream conditions on the turbulent burning rate. It is clear that the scalar experiments, which are often simpler to perform than the velocity measurements, will provide a good estimate of the reactant consumption rate.

Currently, we are analyzing data obtained by simultaneous measurements of OH-PLIF and 2D Rayleigh scattering in flames stabilized in a LSB. These experiments were performed at Institut fur Techniche Mechanik in RWTH Aachen, Germany in collaboration with Professor Peters. The two methods provide complementary information. OH is a convenient marker of the reaction zone at the trailing edge of the flame front. 2D Rayleigh scattering maps the density distribution in the preheat zone at the leading edge. At the highest turbulent condition, the flame fronts shown on the 2D Rayleigh images are broadened and disrupted by turbulence. The corresponding PLIF images remain consistently less wrinkled and do not show significant broadening. These features support a new 'thin reaction zone' regime ($1 < Ka < 10$) to indicate the transition from flamelet

to distributed reaction zone at much higher Karlovitz numbers. This new regime represents the conditions under which the smallest turbulence scale is smaller that the flame thickness, d_L (about 1 mm for most atmospheric pressure hydrocarbon flames) but is still an order of magnitude larger than the reaction zone.

In addition to our experimental effort, we are also pursuing a modest numerical study of turbulent open v-flames by the discrete vortex method. This 2D method is particularly well suited for investigating the dynamics of the turbulent flow and its effects on flame wrinkling. Though other more elaborate numerical approaches have been developed for premixed turbulent flames, the discrete vortex method focuses on the fluid mechanical processes and provides a better tool to resolve dynamic flame/turbulence interactions that control the development of the turbulent flame brush. A rod-stabilized v-flame was chosen because of the wealth of experimental data on the turbulent flowfield and flame wrinkle structures that have been collected in our experimental database and are available for direct comparison with numerical results. Our collaborator on the numerical study is Prof. C. K. Chan of the Hong Kong Polytechnic University. The achievements in the past three years include improvement in the representation of outflow and lateral boundary conditions; numerical implementation of the advection algorithm; refinement and enlargement of the computation grid; and inclusion of vorticity diffusion. Considerably improved quantitative agreement with a limited set of our experimental data has also been obtained.

Summary of Planned Research

Open atmospheric pressure flame studies

We shall extend our study of burning rates and wrinkled flame front structures to different burner configurations. The burning rate is a measure of the enhancement of combustion intensity due to turbulence. From a scientific perspective, correlation of the combustion intensity with turbulence properties is essential for validating the predictive capability of theoretical or numerical models. Determining the burning rates of steady premixed turbulent flames is non-trivial and is an important unresolved scientific problem. From a practical perspective, empirical data of the mean burner rate is fundamental to scaling the combustion system.

We also plan to continue the investigation of flame front structures to verify the new concept of the thin reaction zone regime. Though the 2D Rayleigh images show strong evidence of preheat zone broadening, development of analytical methods to quantify this effect have been challenging. Different approaches are under consideration and a consistent and reproducible method will be developed. In addition to quantifying flame broadening, complementary analyses will be conducted to deduce the wrinkle scales and curvatures for different isotherms. If the thin reaction zone regime is valid, we expect that at low to moderate turbulence the wrinkle scales of the reaction zone represented by the high temperature isotherms will be consistent with those of the preheat zone. At higher turbulence intensities, the wrinkle scales of the preheat zone will be smaller than those of the reaction zone due to turbulence transport.

Flames at high pressure and temperature

We also plan to initiate a program to study lean premixed turbulent flames at high initial pressures and temperatures. The motivation is to extend our capabilities to address fundamental issues relevant to gas turbine combustion. During the past decade, the gas turbine industry has gradually been adopting lean premixed combustors to help reduce NO_x emissions. The development of the

lean premixed gas turbine has been plagued by problems such as flame stabilization, combustion oscillations and flame blowoff. As this is a relatively new technology, it has yet to generate significant interest in the scientific community to study fundamental properties of steady lean premixed turbulent flames under gas turbine operating conditions. Traditionally, high-pressure premixed turbulent flame studies have focused on non-steady flame configurations relevant to spark ignition engines. As the Combustion Fluid Mechanics Group at LBNL is one of the research pioneers for steady atmospheric premixed turbulent flames, it is a logical extension to apply our experience and expertise to a new and useful environmental energy technology.

The apparatus that will be used for studying high-pressure flames was built by funds obtained through LBNL's Laboratory Director Research and Development program. It has a test section that is designed to accept advanced laser diagnostic for probing turbulence and scalar fields. The apparatus is being commissioned and will be operational by summer of 2000.

Numerical simulation

If funding is available, we plan to use the improved discrete vortex model and extend the computations to high turbulence intensities and possible predictions of local extinction. Another extension would be to treat the problem of flame stabilization by a recirculation region behind a finite size flameholder. The model would include the effects of shear turbulence produced by the flame stabilizer and its role in the recirculation zone within the products. Formulation and exploitation of the model for the stagnation point flame configuration will also be explored. These numerical simulation developments would represent a significant and practically important advance in the prediction of premixed flame behavior by means of vortex dynamics. The numerical problems to overcome are, however, far from trivial. Additional experiments to validate the numerical predictions will also be formulated.

Publications

1. Yegian, D.T. and Cheng, R.K., "Development of Lean Premixed Low-Swirl Burner for Low NO_x Application" Combustion Science and Technology V. 139, N1-6, p. 207 (1998).
2. Cheng, R.K., Bedat, B., Shepherd I.G. and Talbot, L., "Premixed Turbulent Flame Structures in Moderate and Intense Isotropic Turbulence" to appear Combustion Science and Technology 2000.
3. Plessing, T., Kortschik, C., Mansour, M.S., Peters, N. and Cheng, R.K., "Measurement of the Turbulent Burning Velocity and the Structure of Premixed Flames on a Low Swirl Burner" submitted to 28th Symposium (International) on Combustion, 2000.
4. Shepherd, I.G., Bourguignon, E., Michou. Y. and Gokalp, I., "The Burning Rate in Turbulent Bunsen Flames" 27th International Symposium on Combustion, 1998.
5. Shepherd, I.G. and Cheng, R.K., "The Burning Rate of Premixed Flames in Moderate and Intense Turbulence" submitted to 28th Symposium (International) on Combustion, 2000.

TITLE: ATOMIC LEVEL MODELING OF CO_2 DISPOSAL AS A CARBONATE MINERAL: A SYNERGETIC APPROACH TO OPTIMIZING REACTION PROCESS DESIGN*

PIs: A.V.G. Chizmeshya° and M.J. McKelvy

INSTITUTION: Arizona State University
Center for Solid State Science and
Science and Engineering of Materials Ph.D. Program
Tempe, AZ 85287-1704
° E-mail: chizmesh@asu.edu

ABSTRACT

Modern computer based modeling of microscopic materials properties can yield critical insight into reaction processes such as CO_2 mineral sequestration (e.g., thermal activation barriers, dissociation energies, and intermediate materials stabilities). Suitably chosen first principles simulations (requiring little or no experimental input) can provide valuable predictions of properties, including mechanical stiffness and elasticity, electronic and spectroscopic response to radiation (e.g., IR, visible, x-ray), and the energetics associated with fundamental chemical reaction processes. Highly efficient (but less predictive) semi-empirical quantum mechanical methods, when properly tuned using experimental or *ab initio* data, permit very broad investigations to be performed on large systems containing 50-500 atoms.

Advanced modeling techniques are integrated with our atomic-level/microscopic mechanistic studies of $Mg(OH)_2$ dehydroxylation/carbonation processes in a synergetic way (see McKelvy, et al. abstract herein), which provides a deeper fundamental understanding than can be achieved with either approach alone. By combining first principles, semi-empirical and classical simulation techniques, we have examined the dehydroxylation reaction of $Mg(OH)_2$ (brucite) and demonstrated that metastable oxyhydroxide compounds ($Mg_{x+y}O_x(OH)_{2y}$) are expected to form along the $Mg(OH)_2 \rightarrow MgO$ reaction path. These new phases differ in free energy by only ~1-2 kcal/mol from equivalent stoichiometric mixtures of MgO and $Mg(OH)_2$ – energies small in comparison with typical local elastic strain energies associated with bending of lamella during dehydroxylation. Computed bulk moduli indicate that a rapid increase in layer stiffness occurs during dehydroxylation further increasing the elastic strain energies associated with decreasing hydroxide layer concentrations. *Ab initio* methods also provide a useful and unique point of contact with spectroscopic measurements such as EELS and x-ray, as synthetic spectra can be compared directly with those observed in order to elucidate salient bonding and structural trends. We illustrate this connection by comparing the predicted and observed signatures of carbon in different environments.

CO_2 surface reactivity has also been analyzed using judiciously chosen cluster models of MgO, $Mg_{x+y}O_x(OH)_{2y}$ and $Mg(OH)_2$ surfaces. These results provide a preliminary fundamental understanding of the early chemical events involved in the carbon dioxide mineralization process. By integrating these results with our atomic-level/microscopic imaging studies, a more comprehensive understanding of carbonation in this model Mg-rich lamellar-hydroxide mineral system is beginning to emerge. Future work will focus on extending this understanding and exploring the breadth of its application to chemically and structurally similar mineral carbonation processes, such as sepentine carbonation.

* This work is supported by DOE Fossil Energy Advanced Research managed by the National Energy Technology Laboratory.

Electronic Structure Studies of Pyrolytic Reactions of Hydrocarbons and Their Chloro Derivatives

DOE Chemical Science Grant # DE–FG02–97ER14758

J. Cioslowski

Department of Chemistry and
School of Computational Science & Information Technology
Florida State University
Tallahassee, FL 32306.

jerzy@csit.fsu.edu
(850) 644–8274

and

D. Moncrieff

School of Computational Science & Information Technology
Florida State University
Tallahassee, FL 32306.

moncrieff@csit.fsu.edu
(850) 644–4885

Program Scope

Pyrolysis of even simple substances, such as hydrocarbons and their chloro derivatives, is a complex chemical phenomenon that involves sequences of intertwined pathways connecting diverse classes of compounds. Aiming at detailed elucidation of processes responsible for the formation of various important chemicals at high temperatures, our research targets several of these pathways. A broad spectrum of theoretical approaches, ranging from very accurate interpolative schemes such as G2 to the methods of density functional theory, is employed. Stable molecules, transient intermediates, radicals, carbenes, highly strained systems, and transition states of various reactions are investigated.

The ongoing research is already producing an abundance of useful results. Reliable values of thermodynamic properties are becoming available for molecules that are not readily amenable to experimental measurements. In the near future, new mechanisms of such important reactions as the trimerization of acetylene will be revealed and several conjectured mechanisms will be either confirmed or disproved. Rules governing thermal degradation of polychlorinated hydrocarbons and heterocyclic compounds will be discovered.

Recent Progress

Five research projects were completed in 1999. These projects, which yielded data of much interest to both experimental and theoretical chemists, required very substantial computer resources.

High-level electronic structure calculations combined with empirical adjustments predicted the standard enthalpy of the C-H bond dissociation in HC≡C-CH=CH_2 to be equal 115.1±1.4 [kcal/mol], i.e. ca. 4.0 [kcal/mol] higher than that of the analogous bond cleavage in ethene [8]. This difference in bond strengths stems from resonance stabilization of the parent molecule. The standard enthalpy of formation of the 1-buten-3-yn-1-yl radical was estimated at 133.8±1.5 [kcal/mol], which is significantly higher than all of the previously published values. As in the case of polychlorinated alkanes, the BLYP approximation was found to seriously underestimate the strengths of the C-H and C-Cl bonds in chloro derivatives of HC≡C-CH=CH_2. On the other hand, the BLYP/6-311G**, MP2/6-311G**, QCISD/6-311G**, and CCSD(T)/6-311G** predictions for the standard enthalpy of ethyne dimerization all closely matched their experimental counterpart.

CCSD(T)/6-311G**//QCISD/6-311G** calculations on the concerted [2+2+2] trimerization of ethyne to benzene yielded the standard reaction enthalpy ΔH^0_{trim}(HC≡CH) = -140.2 [kcal/mol] and the standard enthalpy of activation ΔH^0_{act}(HC≡CH) = 53.1 [kcal/mol]. The corresponding transition state (TS) possesses C_2 symmetry, although both the planar D_{3h} and nonplanar D_3 structures were found to be negligibly higher in energy, indicating extreme flatness of the potential energy hypersurface along the distortion paths [9]. In agreement with the limited experimental data, the analogous trimerizations of HC≡CCl and ClC≡CCl were predicted to be considerably more exothermic. As the respective TSs cannot be located and the planar pseudo-TSs that possess several imaginary vibrational frequencies are associated with high reaction barriers, the concerted mechanism can be ruled out for these reactions.

A comprehensive set of 600 experimental standard enthalpies of formation (ΔH^0_f) were generated [10]. With its diverse species, many possessing less usual geometries and bonding situations, this compilation is capable of uncovering deficiencies in approaches of quantum chemistry that are not detectable with smaller sets of ΔH^0_f values. Its usefulness in benchmarking, calibration, and parameterization of new electronic structure methods was illustrated with the development of the B3LYP/6-311++G** bond density functional (BDF) scheme. This scheme, which is sufficiently inexpensive in terms of computer time and memory to allow predictions even for molecules as large as the C_{60} fullerene, requires only single point calculations at optimized geometries. It yields values of ΔH^0_f with the average absolute error of 3.3 [kcal/mol], rivaling more expensive methods in accuracy (especially for larger systems). A list of species that are poorly handled by typical hybrid density functional used in conjunction with moderate-size basis sets was constructed. This list is intended for rigorous testing of new density functionals.

The $C_{36}H_{36}$ spheriphane (heptacyclo[13.13.$2^{1,15}$.$2^{8,22}$. $1^{3,27}$.$1^{6,10}$.$1^{13,17}$.$1^{20,24}$]hexatriaconta-1,3(33),6,8,10(34),13,15,17(35),20,22,24(36),27-dodecaene) is a prototype of semi-rigid hydrocarbon host cages capable of selective binding of metal cations. It consists of four benzene rings linked through six -CH_2-CH_2- bridges. Electronic structure calculations carried out at the B3LYP/6-311G** level of theory revealed the existence of seven low-energy conformers of $C_{36}H_{36}$ spheriphane with symmetries ranging from C_1 to T [11]. These local minima are connected through an intricate net of reaction paths involving transition states of diverse symmetries that correspond to inversions of the C-C-C-C dihedral angles at individual -CH_2-CH_2- bridges. Barriers to these inversions were computed and vibrational spectra of conformers were predicted.

Standard enthalpies of formation of 115 IPR fullerenes with 60-180 carbon atoms that possess non-vanishing HOMO-LUMO gaps (including all the members of the C_{78}, C_{80}, C_{82}, C_{84}, and C_{86} families) were calculated at the B3LYP/6-31G* level of theory using the isodesmic reaction (N/60)C_{60}→C_N and the known value of ΔH^0_f(C_{60},g) [12]. The computed enthalpies were shown to be accurately reproduced by an additive scheme in which each hexagon is assigned a contribution

that depends on its first and second layers of neigboring rings. The availability of such an additive scheme opens an avenue to rapid predictions of stabilities of large buckyballs and bucktubes.

Future Plans

In the coming year, our research effort will be focused on reactions that are of relevance to the formation of thiophenes in fossil fuels. In particular, we will focus on the insertion of heterosulfur bridges into biaryls and angularly condensed arenes.

1. *Thermochemistry of sulfur radicals:* Little is known about the relative stabilities of radicals of sulfur that are present in the gas phase at the elevated temperatures of 350 – 400 [°C]. G2 and G3 calculations will be employed in investigation of gas-phase equilibria among sulfur rings and sulfur radicals of various degrees of catenation. These studies will identify the species responsible for the dehydrogenation of partially hydrogenated PAHs and the concomitant sulfur insertion.

2. *Thermochemistry of reactions between elemental sulfur and $AlCl_3$, and the nature of the resulting electrophilic agents:* Although it is almost certain that the insertion of sulfur into biaryls involves sulfur-containing cations, the exact nature of the pertinent electrophilic agent is unknown. Therefore, reactions of $AlCl_3$ with several sulfur rings will be studied. High-level approaches such as CCSD/6-311G**, G2, and G3 will be employed.

3. *Thermochemistry and kinetics of the model reaction* **1** + *2S* → **2** + H_2S*:* The reasons for the 2 and 2' positions of **1** being the primary sites of electrophilic attack will be elucidated. Both the CCSD/6-311G** and B3LYP/6-311G** levels of theory will be used to obtain the pertinent data. Comparison of these data will allow for a systematic correction of the predictions furnished by the latter approach for reactions involving larger PAHs.

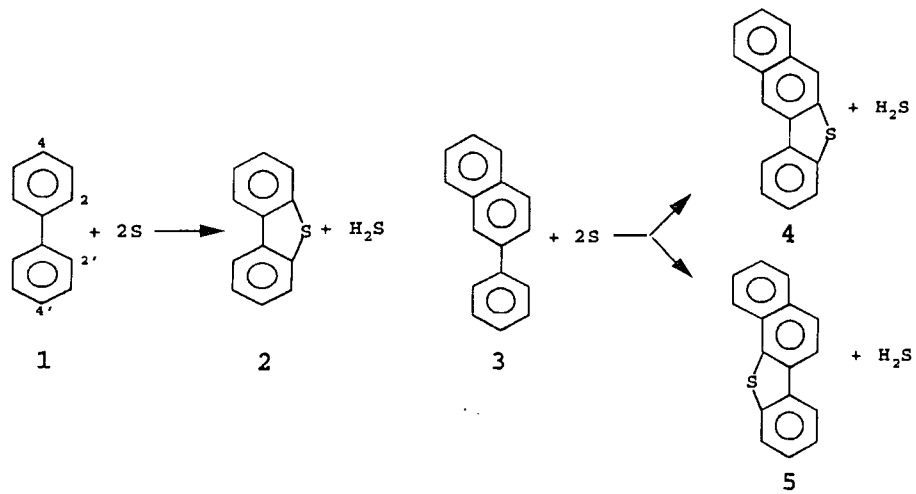

4. *Studies of sulfur insertion into 2-phenylnaphthalene, phenanthrene, and 2,2'-binaphthyl:* Electronic factors responsible for the preferential formation of **4** (rather than naphtho[1,2–*b*]benzothiophene **5**) from **3** will be investigated at the B3LYP/6-311G** level of theory. Reaction barriers and energetics of electrophilic attack at various positions in phenanthrene and 2,2'-binaphthyl will be computed in order to explain the observed failure of these PAHs to form respective annelated thiophenes.

When completed, these investigations will furnish a picture of diverse reactions responsible for the formation of bridging sulfur compounds within PAHs. These types of reactions are found under geochemical conditions and during thermal treatment of fossil fuels. Mechanisms of these processes will be elucidated in detail, opening the avenue to the control of yields of individual products through

changes in reaction conditions and the composition of the fuel itself. The ability to exert such control will undoubtedly prove invaluable in a further reduction of environmental pollution caused by the combustion of sulfur-containing substances of natural origin.

Publications Resulting From The DOE Sponsored Research (1998–2000)

1. J.Cioslowski, P.Piskorz, and D.Moncrieff: **Journal of the American Chemical Society 120 (1998) 1695.** Electronic Structure Studies of 1,2-Didehydrogenation of Arenes and Rearrangement of Arynes to Annelated Cyclopentadienylidenecarbenes.

2. J.Cioslowski, P.Piskorz, M.Schimeczek, and G.Boche: **Journal of the American Chemical Society 120 (1998) 2612.** Diversity of Bonding in Methyl Ate Anions of the First- and Second-Row Elements.

3. G.Boche, M.Schimeczek, J.Cioslowski, and P.Piskorz: **European Journal of Organic Chemistry (1998) 1851.** The Role of Ate Complexes in Halogen(Metalloid)-Lithium Exchange Reactions: A Theoretical Study.

4. J.Cioslowski, P.Piskorz, and D.Moncrieff: **Journal of Organic Chemistry 63 (1998) 4051.** Thermally Induced Cyclodehydrogenation of Biaryls: A Simple Radical Reaction or a Sequence of Rearrangements?

5. D.R. Armstrong, M.A. Beswick, N.L. Cromhout, C.N. Harmer, D. Moncrieff, C.A. Russell, P.R. Raithby, A. Steiner, A.E.H. Wheatley and D.S. Wright: **Organometallics 17 (1998) 3176.** Weakly Bonded Lewis Base Adducts of Plumbocene and Stannocene; A Synthetic and Calculational Study.

6. J. Cioslowski, G. Liu and D. Moncrieff: **Journal of Physical Chemistry A 102 (1998) 9965.** Theoretical Thermochemistry of Homolytic C-C and C-Cl Bond Dissociations in Unbranched Perchloroalkanes.

7. J. Cioslowski, M. Schimeczek, P. Piskorz and D. Moncrieff: **Journal of the American Chemical Society 121 (1999) 3773.** Thermal Rearrangement of Ethynylarenes to Cyclopentafused Polycyclic Aromatic Hydrocarbons: An Electronic Structure Study.

8. J. Cioslowski, G. Liu and D. Moncrieff: **Journal of Physical Chemistry A 103 (1999) 11465.** Theoretical Thermochemistry of the 1-Buten-3yn-1-yl Radical and it's Chloro Derivatives.

9. J. Cioslowski, G. Liu and D. Moncrieff: **Chemical Physics Letters 316 (2000) 536.** The Concerted Trimerization of Ethyne to Benzene Revisted.

10. J. Cioslowski, M. Schimeczek, G. Liu and V. Stoyanov: **Journal of Chemical Physics (submitted)** A Set of Standard Enthalpies of Formation for Benchmarking, Calibration, and Parameterization of Electronic Structure Methods.

11. J. Cioslowski and A. Szarecka: **Journal of the American Chemical Society (submitted)** Conformational Analysis of the $C_{36}H_{36}$ Spheriphane.

12. J. Cioslowski, N. Rao and D. Moncrieff: **Journal of the American Chemical Society (submitted)** Standard Enthalpies of Formation of IPR Fullerenes and Their Analysis in Terms of Structural Motifs.

Half-Collision Dynamics of Elementary Combustion Reactions
Grant DE-FG03-908ER14879

Robert E. Continetti and Hans-Jürgen Deyerl
Department of Chemistry and Biochemistry
University of California San Diego
9500 Gilman Drive
La Jolla, CA 92093-0314

rcontinetti@ucsd.edu
March 30, 2000

Program Scope

The central focus of this research program is on the study of the dynamics of hydroxyl radical reactions. Negative-ion photodetachment is used to prepare energy-selected neutral complexes in nuclear configurations near the transition-state for neutral bimolecular reactions. The products and dissociation dynamics of these complexes are then determined using translational spectroscopy. This technique of studying transition-state dynamics builds on the innovative transition-state spectroscopy experiments of Neumark[1] and Lineberger.[2] The transition-state spectroscopy experiments carried out to date yield information on the neutral potential energy surface by analysis of the photoelectron spectra of bound anion precursors. Photoelectron-photofragment coincidence spectroscopy can extend these studies significantly by allowing detailed characterization of the entire dissociative photodetachment (DPD) event that occurs when removal of an electron from a stable anion produces a neutral in a dissociative or metastable state that undergoes rapid dissociation. We plan on applying this technique to studying the OH + H_2, OH + CO and OH + F reactions, in addition to the work on OH + H_2O and OH + OH discussed below.

In the current grant period we have also continued our studies of radicals and other transient species by photoelectron spectroscopy. Specifically, we have carried out a study of the photodetachment of CF_3^-. These experiments have yielded an improved value for the electron affinity of this species.

We are also seeking to find new routes to the synthesis of anion precursors. During the current period this effort focused on laser-desorption ionization of cryogenic films. Establishment of new ion sources in the laboratory will greatly broaden the scope of the combustion-relevant systems we can study in the future.

Recent Progress

I. Transition state dynamics of the OH + H_2O hydrogen exchange reaction

The thermoneutral identity reaction OH + H_2O H $_2O$ + OH is one of the simplest hydrogen abstraction reactions by the hydroxyl radical. On a fundamental level, this reaction is one of the simpler radical-molecule reactions and thus of interest as a prototype, in addition to its significance in atmospheric problems and in combustion systems. The groundwork for this study was laid by the photoelectron studies by Arnold *et al.*[3] of the $H_3O_2^-$ anion. They observed a broad photoelectron spectrum with at least four identifiable peaks at 4.66 eV. The spectrum was observed to undergo significant changes, in both intensities and positions, upon deuteration, implying that the spectral features were primarily related to motion of the hydrogen atoms in the complex. They also carried out *ab initio* calculations and one-dimensional Franck-Condon simulations of the spectrum, confirming the role played by H atom motion in the neutral OH(H_2O) complex produced by photodetachment.

The transition-state dynamics of this reaction have been studied using dissociative photodetachment of $OH^-(H_2O)$ and $OD^-(D_2O)$ at 258 nm (4.80 eV) using photoelectron-photofragment coincidence spectroscopy.[4] The photoelectron spectra are consistent with the previous results of Neumark and co-workers,[3] and the quantum yield for dissociation of the neutral into two fragments is unity. The photoelectron-photofragment coincidence spectrum for

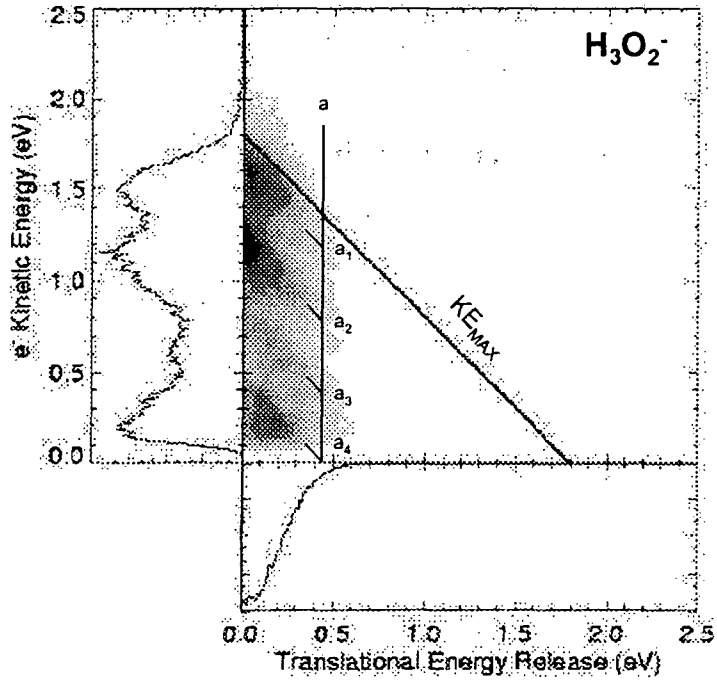

the $OH^-(H_2O)$ anion shown in fig.1 reveal considerably more information.

Fig. 1 Photoelectron-photofragment energy correlation spectrum $N(E_T, eKE)$ for $H_3O_2^-$ + hν OH + H $_2O$ + e^- at 258 nm. The $N(E_T, eKE)$ spectrum is represented as a two-dimensional gray scale histogram. The histogram along the *y*-axis shows the photoelectron spectrum (eKE) , and the *x*-axis shows the photofragment translational distribution (E_T). These are obtained by integrating the correlation spectrum over the complementary variable.

The correlation of the broad peaks in the electron kinetic energy spectrum (eKE) and photofragment translational energy release (E_T) reveals a series of four diagonal ridges. All events that lie within a single diagonal ridge have a well-defined total kinetic energy, ($E_{TOT} = E_T$ + eKE) because of energy conservation. The simplest explanation of these features is that they correspond to dissociative photodetachment (DPD) onto vibrationally adiabatic curves sensitive to the zero point energy effects of the potential. These adiabatic curves are located around the transition-state for the neutral bimolecular reaction, and correlate with the different vibrational states of the H_2O and OH products. Examination of the E_T distribution for each ridge individually shows that the width and shape of the spectrum depends on the product vibrational state. This observation is consistent with the interpretation that these diagonal ridges correspond to different adiabatic curves in the transition state region corresponding to the product states with different curvatures. The observation of five diagonal ridges in the correlation spectrum for the deuterated analog ($D_3O_2^-$) compared to four in the nondeuterated case shows the zero point effects along the hydrogen transfer coordinate on the neutral surface play a key role in the reaction dynamics of the bimolecular reaction.

Another informative way to view the $N(E_T,\text{eKE})$ correlation spectra is by examination of the total translational energy spectra generated by summing the photoelectron kinetic energy and the translational energy release for each event: E_{TOT} = eKE + E_T. In the $N(E_{TOT})$ spectra, the diagonal features in the correlation spectra appear as a resolved spectrum of the correlated product vibrational distribution. Examination of the offset of the vibrational peaks from the internal energy origin (dissociation asymptote) shows that rotational and bending excitation in the products is small. Compared to the photoelectron spectrum, the total kinetic energy spectrum shows more structure and a nicely resolved progression in the nondeuterated and deuterated case. The observed peak spacing of ~0.42 eV (3388 cm^{-1}) in $H_3O_2^-$ and ~0.33 eV (2662 cm^{-1}) in $D_3O_2^-$ are in agreement with the interpretation of excitation of the antisymmetric stretch vibration in the water product.

To aid in the analysis of the data presented above, *ab inito* calculations were performed for the anion and neutral complexes involved in these experiments. The main goal was to calculate the electronic structures of the stationary points in the anion and neutral consistently and find a method that is accurate enough for calculation of the potential energy for both the anion and the neutral.

II. Transition state dynamics of the OH + OH→ H_2O + O (^3P) reaction

The reaction between two hydroxyl radicals forming O(^3P) + H_2O is an exothermic reaction that is a minor source of H_2O in hydrocarbon flames, while the reverse reaction is a chain-branching process which results in flame acceleration at higher temperatures.[5] On a fundamental level this reaction is one of the simpler radical-radical reactions and thus of interest as a prototype. The kinetics of this reaction have been studied by Troe and co-workers.[6] There have apparently been few studies of the chemical dynamics of this reaction outside of transition-state spectroscopy experiments by Arnold *et al.*[3]

We have carried out photoelectron-photofragment coincidence studies of this reaction by dissociative photodetachment of $O^-(H_2O)$ and $O^-(D_2O)$ at 258 nm (4.80 eV). The photoelectron spectra are consistent with the previous results of Arnold *et al.*[3]

Due to the fact that dissociative photodetachment produces both OH + OH and O + H_2O products (see last progress report), the correlation spectrum $N(E_T,\text{eKE})$)shows the correlated signals for both channels. A final assignment for the diagonal ridges in the correlation spectra for $O^-(H_2O)$ and $O^-(D_2O)$ and the corresponding peaks in the total translational energy spectra will profit from an enhanced mass resolution in the photoelectron-photofragment spectrometer.

III. Photodetachment imaging studies of the Electron Affinity and Heat of Formation of CF_3

The search for new flame suppressing materials with reduced potential to destroy ozone has focused attention on fluorocarbons and hydrofluorocarbons.[7] For modeling processes in flames, accurate thermochemical data on the reacting species are required. Due to uncertainties in the thermochemistry of both CF_3 and CF_3^-, studies of the energetics and dynamics of these molecules are of continued interest. One important quantity, the adiabatic electron affinity (EA) of CF_3 is still in question. We have recorded the photoelectron spectra of trifluoromethyl anion, CF_3^-, at 355 nm and 258 nm. Simulation of the partially resolved vibrational structure is used to extract the adiabatic electron affinity EA[CF_3] = 1.80 ±0.05 eV. The heat of formation for the trifluoromethyl anion derived from the adiabatic electron affinity is $\Delta H^0_{f,298}[CF_3^-]$ = -152.9 ± 1.1 kcal/mol, which is compared to the high accuracy CBS-Q theory prediction of $\Delta H^0_{f,298}[CF_3^-]$ = -152.6 kcal/mol, after "isodesmic bond additivity" corrections (BAC). We find the CBS-Q prediction of $\Delta H^0_{f,298}[CF_3]$ = -112.1 kcal/mol after BAC, in excellent agreement with the most

recent experimental determination of the radical. The photoelectron image at 355 nm shows a "p-wave" for the photodetached electrons.

IV. Cryogenic Matrix-Assisted Laser-Desorption-Ionization Mass Spectrometry

One of the goals of this research project is the development and application of new negative ion sources. One area that we have pursued in the last year is the potential of using cryogenic matrices, both with and without absorbing matrix chromophores. In collaboration with Professor Lester Andrews of the University of Virginia, we recently demonstrated cryogenic MALDI on Ar/O_2 matrices doped with laser-ablated metal atoms. The resulting oxides, formed by reaction in the 10K Ar matrix were then analyzed by laser-desorption-ionization mass spectrometry. This observation opens the way up to potential applications of laser-desorption-ionization to a number of transient species that are unstable at room temperature.

Future Plans

In the next year we will pursue the other elementary hydroxyl radical reactions discussed in the introduction. The experimental effort will be coupled with continued studies of the potential energy surfaces for these reactions in collaboration with Dr. Peter Taylor of the San Diego Supercomputer Center. Once surfaces of reasonable accuracy are obtained, wave-packet propagation techniques will be used to simulate the photoelectron and photofragment kinetic energy distributions observed in these experiments. Our efforts on ion source development will continue with the MALDI technique, which we will extend to study methods for the generation of anion precursors to larger organic molecules including polycyclic aromatic hydrocarbons (PAHs).

Publications: August, 1998 - Present

1. H.-J. Deyerl, A. K. Luong, T. G. Clements and R. E. Continetti, Transition state dynamics of the OH + H_2O hydrogen exchange reaction studied by dissociative photodetachment of $H_3O_2^-$., Faraday Discuss. **115** (2000), in press.
2. L.S. Andrews, A.Rohrbacher, C. Laperle and R.E. Continetti, Cryogenic Laser-Desorption-Ionization Studies of Transition Metal Oxides., submitted to J. Phys. Chem. (2000).
3. H.-J. Deyerl, L. S. Alconcel and R. E. Continetti, Photoelectron imaging studies of the electron affinity of CF_3, in preparation

References

(1) R. B. Metz, S. E. Bradforth and D. M. Neumark, Adv. Chem. Phys. **81**, 1 (1992).
(2) P. G. Wenthold and W. C. Lineberger, Acc. Chem. Res. **32**, 597 (1999).
(3) D. W. Arnold, C. Xu and D. M. Neumark, J. Chem. Phys. **102**, 6098 (1995).
(4) H.-J. Deyerl, A. K. Luong, T. G. Clements and R. E. Continetti, Faraday Discuss. **115** (2000), in press.
(5) J. Warnatz, Rate coefficients in the C/H/O system, in Combustion Chemistry, ed. W.C. Gardiner, Jr., Springer-Verlag, New York, 1984, pp. 197-360.
(6) D. Fulle, H. F. Hamann, H. Hippler and J. Troe, J. Chem. Phys. **105**, 1001 (1996).
(7) M. J. Molina, Angew. Chem. Int. Ed. Engl. **35**, 1778 (1996).

VIBRATIONAL STATE CONTROL OF PHOTODISSOCIATION

F.F. Crim
Department of Chemistry
University of Wisconsin–Madison
Madison, Wisconsin 53706
fcrim@chem.wisc.edu

Our research investigates the chemistry of vibrationally excited molecules. The properties and reactivity of vibrationally energized molecules are central to processes occurring in environments as diverse as combustion, atmospheric reactions, and plasmas and are at the heart of many chemical reactions. The goal of our work is to unravel the behavior of vibrationally excited molecules and to exploit the resulting understanding to determine molecular properties and to control chemical processes. A unifying theme is the preparation of a molecule in a specific vibrational state using one of several excitation techniques and the subsequent photodissociation of that prepared molecule. Because the initial vibrational excitation often alters the photodissociation process, we refer to our double resonance photodissociation scheme as *vibrationally mediated photodissociation.* In the first step, vibrational overtone excitation or stimulated Raman scattering prepares a vibrationally excited molecule and a second photon, the photolysis photon, excites the molecule to an electronically excited state. Vibrationally mediated photodissociation provides new vibrational spectroscopy, measures bond strengths with high accuracy, alters dissociation dynamics, and reveals the properties of and couplings among electronically excited states. Our recent results on isocyanic acid illustrate the range of information available from vibrationally mediated photodissociation.

DISSOCIATION OF ISOCYANIC ACID (HNCO)

We have studied one particularly interesting molecule, isocyanic acid (HNCO), in detail because of its inherent richness and practical importance in the RAPRENOx process for removing oxides of nitrogen from combustion exhaust. Beyond controlling the branching between two chemically distinct channels (producing either NH+CO or H+NCO), we also use state selection by stimulated Raman excitation to measure of the threshold energy for breaking different bonds in HNCO. Our studies demonstrate the influence of vibrational excitation on the nonadiabatic interactions that control the competition between singlet and triplet products as well. The information we have obtained on branching ratios and dissociation thresholds has stimulated theoretical work and provided an opportunity for detailed comparison with *ab initio* calculations.

The first excited state of HNCO is a bent $^1A''$ state that has both *cis* and *trans* minima. The three decomposition channels open at the energies of the first excited state are two spin-allowed pathways producing either H + NCO or singlet NH + CO

$$\mathrm{HNCO}\,(^1A'') \rightarrow \mathrm{H}\,(X\,^2\Sigma) + \mathrm{NCO}\,(X\,^2\Pi)$$
$$\mathrm{HNCO}\,(^1A'') \rightarrow \mathrm{NH}\,(a\,^1\Delta) + \mathrm{CO}\,(X\,^1\Sigma^+),$$

and one lower energy spin-forbidden pathway producing triplet NH + CO

$$\mathrm{HNCO}\,(^1A'') \rightarrow \mathrm{NH}\,(X\,^3\Sigma^-) + \mathrm{CO}\,(X\,^1\Sigma^+).$$

Thus, our experiments probe dissociation dynamics potentially involving three different electronic surfaces (the ground state S_0, the singlet excited state S_1, and the first triplet state T_1).

VIBRATIONAL SPECTROSCOPY

Stimulated Raman Excitation

Exciting skeletal vibrations offers the possibility of exploring very different motions on the electronically excited surface, observing new vibrational transitions, determining Franck-Condon factors for electronic excitation from different vibrational states, and measuring bond dissociation energies. Using stimulated Raman excitation, we have excited three different stretching vibrations in HNCO, photodissociated the vibrationally excited molecule, and probed the NH($^1\Delta$) and NCO vibrational and rotational state populations using laser induced fluorescence. Our experiments prepare either the N–H stretch (ν_1=3538.3 cm^{-1}), the asymmetric N–C–O stretch (ν_2=2269.9 cm^{-1}), or the symmetric N–C–O stretch (ν_3=1327 cm^{-1}) by stimulated Raman excitation and provide the first gas-phase Raman spectra of HNCO. We are able to sort out perturbations in the spectra and identify strongly mixed combination bands.

The initial state selection of the Raman excitation step allows us to measure the thresholds for production of either NCO or NH in the photolysis of HNCO without interferences from thermally excited molecules. We measure a photolysis threshold for H–NCO of 38,320±140 cm^{-1} (D_0(H-NCO) ≤ 109.6±0.4 kcal/mol) and a photolysis threshold of 42,710±100 cm^{-1} (D_0(HN-CO) ≤ 122.1±0.3 kcal /mol) for HN–CO. These thresholds, which are strictly upper limits to the dissociation energy, lead to the heat of formation of HNCO when combined with other thermodynamic data.

Vibrational Overtone Excitation

We have extended our vibrationally mediated photodissociation experiments to molecules cooled in a supersonic expansion in order to simplify the vibrational spectroscopy. The analysis of the vibrational spectroscopy of HNCO molecules cooled in a supersonic expansion, using the photodissociation solely as a detection technique, is particularly informative. We have extracted molecular constants and identified interactions among vibrations in the region of three, four, and five quanta of N-H stretching excitation. The interaction matrix elements we extract agree well with *ab initio* calculations by East, Johnson and Allen [J. Chem. Phys. **98**, 1299 (1993)]. The identification of the states that are mixed into the nominal N-H stretching vibrations is important in understanding controlled photodissociation and non-adiabatic processes in the first excited state of HNCO.

ELECTRONIC SPECTROSCOPY

Excitation to the electronically excited state from vibrational states prepared with substantial bending excitation and a well-known total energy using stimulated Raman excitation locates the origin of the electronically excited state for the first time. The key is to excite near the origin of S_1 and detect the ^{3}NH product formed following the non-adiabatic transition to and decomposition on T_1. This scheme is particularly useful for detecting molecules excited near the origin of the electronically excited state, which is not accessible from the ground vibrational state, and we have combined our results with those from Reisler and coworkers, who access higher lying levels, to map out the electronic spectroscopy over more than 5000 cm^{-1}. The well-resolved spectra show clear progressions that allow us to assign the N-C stretching vibration (ω_3=1034±11 cm^{-1}), the H-N-C bending vibration

(ω_4=1192±19 cm^{-1}), and the N-C-O bending vibration (ω_5=599±7 cm^{-1}) in the excited state. Extrapolating the vibrational progressions to their origins locates the zero-point of the excited state 32,449±20 cm^{-1} above the zero-point of the ground electronic state. *Ab initio* calculations of the energy of the electronically excited state span a range from roughly 20,600 cm^{-1} to 32,970 cm^{-1}. The experimental measurements have permitted a detailed comparison with theory and have allowed the identification of a promoting mode for internal conversion from S_1 to S_0.

VIBRATIONAL CONTROL OF EXCITED STATE DYNAMICS

Controlled Bond Cleavage

We excite the N-H stretching vibration and then photodissociate the vibrationally excited molecule with light near 225 nm. The crucial comparison is between this dissociation and the one-photon dissociation *at the same added energy.* For example, one-photon dissociation with 230-nm light adds the same amount of energy to the molecule as vibrationally mediated photodissociation using $3v_{NH}$ vibrational overtone excitation and 291.5-nm photolysis light. Because this energy is barely above the threshold for producing NH, the dominant product is NCO. *Nonetheless, the relative amount of NCO increases substantially in the photolysis from the vibrationally excited state.* At energies well above the threshold for NH production, where the NH product dominates, the ability of the N-H stretch to promote dissociation of the bond is even more apparent, changing the predominant product from HN to NCO

Nonadiabatic Processes

The spin-forbidden decomposition of isocyanic acid, HNCO $\rightarrow$ NH($X\ ^3\Sigma^-$) + CO, is a nonadiabatic process that must involve coupling from the initially excited S_1 state to a triplet state. Reisler and coworkers have discussed the competition among several surfaces in the one-photon photolysis of HNCO, and we have observed a vibrational influence on the competition between spin-allowed products (^{1}NH and NCO). This observation raises the question of the influence of vibration on the competition between the spin-allowed production of ^{1}NH and the spin-forbidden production of ^{3}NH, which we explore by monitoring both the singlet and triplet products. The increased relative yield of ^{3}NH could reflect either a *enhanced* probability of crossing to T_1 (either directly or through S_0) or it could reflect a *reduced* production of ^{1}NH on the S_1. New experiments observing all three products and calculations involving multiple, coupled surfaces should sort out the mechanism as well as provide a point of comparison to theory.

FUTURE DIRECTIONS

We have recently used isocyanic acid as a test vehicle for implementing resonant multiphoton ionization (REMPI) detection of the vibrationally mediated photodissociation of HNCO molecules cooled in a molecular beam. This approach allows us to make absolute quantum yield measurements and determine the anisotropy of the fragment distribution from the decomposition of the vibrationally excited molecule. More important, the ability to use REMPI detection has allowed us to detect H atoms from the photodissociation methanol (CH_3OH) cooled in an expansion and excited in the region of either three or four quanta of O-H stretching vibration. We have made our first measurements of the kinetic energy of the products and observed slow H atoms coming from the CH_3 group. Completing and refining these measurements is the next step with similar dissociation experiments on other molecules and in clusters to follow.

PUBLICATIONS SINCE 1998 ACKNOWLEDGING DOE SUPPORT

Nonadiabatic Effects in the Photodissociation of Vibrationally Excited HNCO: the Branching between NH($a^1\Delta$) and ($X^3\Sigma^-$). H. Laine Berghout, Steven S. Brown, Ruben Delgado, and F. Fleming Crim, J. Chem. Phys. **109**, 2257 (1998),

An Experimental and Theoretical Study of the Vibrationally Mediated Photodissociation of Hydroxylamine, David Luckhaus, Jacqueline L. Scott, and F. Fleming Crim, J. Chem. Phys. **110**, 1533 (1999).

Photofragment Energy Distributions and Dissociation Pathways in Dimethyl Sulfoxide. Gail M. Thorson, Christopher M. Cheatum, Martin J. Coffey, and F. Fleming Crim, J. Chem. Phys. **110**, 10843 (1999)

Vibrational Spectroscopy and Intramolecular Energy Transfer in Isocyanic Acid (HNCO) M. J. Coffey, H.L. Berghout, E. Woods III, and F. F. Crim, J. Chem. Phys. **110**, 10850 (1999).

The Electronic Origin and Vibrational Levels of the First Excited Singlet State of Isocyanic Acid (HNCO). H. Laine Berghout, F. Fleming Crim, Mikhail Zyrianov, and Hanna Reisler, J. Chem. Phys. (In Press, 2000).

Controlling the Bimolecular Reaction and Photodissociation of HNCO through Selective Excitation of Perturbed Vibrational States. Ephraim Woods, III, H. Laine Berghout, Christopher M. Cheatum, and F. Fleming Crim, J. Phys. Chem. (Submitted, April, 2000)

INFRARED ABSORPTION SPECTROSCOPY AND CHEMICAL KINETICS OF FREE RADICALS

Robert F. Curl and Graham P. Glass
Department of Chemistry and Rice Quantum Institute
Rice University, Houston, TX 77251
(713)348-4816 (713)348-3285
rfcurl@rice.edu gglass@rice.edu

PROGRAM SCOPE

This research is directed at the detection, monitoring, and study of the chemical kinetic behavior by infrared absorption spectroscopy of small free radical species thought to be important intermediates in combustion. In the last year, infrared kinetic spectroscopy using excimer laser flash photolysis and difference frequency probing has been employed to investigate the kinetics of the NH_2 and NO_2 reaction and to measure the quantum yield of $O(^1D)$ relative to $O(^3P)$ in the 193 nm flash photolysis of NO_2. In addition, the photochemical branching in the flash photolysis of ketene has been determined in collaboration with Joe Michael of Argonne National Laboratory.

THE REACTION BETWEEN NH_2 AND NO_2

The reaction between NH_2 and NO_2 has several possible channels.

$$NH_2 + NO_2 \rightarrow NH_2O + NO \quad (\Delta H = -67 \text{ kJ/mol}) \quad (1a)$$
$$\rightarrow H_2O + N_2O \quad (\Delta H = -383 \text{ kJ/mol}) \quad (1b)$$
$$\rightarrow H_2O_2 + N_2 \quad (\Delta H = -359 \text{ kJ/mol}) \quad (1c)$$
$$\rightarrow 2OH + N_2 \quad (\Delta H = -146 \text{ kJ/mol}) \quad (1d)$$
$$\rightarrow 2HNO \quad (\Delta H = -24 \text{ kJ/mol}) \quad (1e)$$

It is generally accepted that channels (1a) and (1b) are almost completely dominant, because theoretical studies[1] suggest that the transition state energies of channels (1c-e) are higher than the energy of the reactants making them inaccessible. The branching ratio into channel (1b) has been measured several times,[2,3,4,5] but the branching ratio into channel (1a) has only been inferred by assuming that channels (1c-e) are negligible.

We have investigated this reaction using the flash photolysis of a mixture of NH_3 and NO_2 at 193 nm probing with high resolution IR spectroscopy. Because the 193 nm UV absorption cross-section of NO_2 is relatively small and the absorption cross-section of NH_3 at 193 nm is large, it is possible to produce NH_2 + H without substantial interference from the photolysis of NO_2 even with a several fold excess of NO_2 over NH_3. The photolysis products of NO_2, NO and $O(^3P)$ and $O(^1D)$ (see below), are fairly benign. NO reacts rapidly with NH_2, but cannot compete with the large excess of NO_2 as long as flow rates are large enough and repetition rates are small enough to avoid product buildup. (Our report last year was affected by product buildup.) $O(^3P)$ reacts with NO_2 producing O_2 and NO and $O(^1D)$ also reacts in this way and, in addition, reacts with NH_3 producing NH_2 and OH. This last reaction has the same net products as the photolysis of NH_3, as the H atoms produced in the photolysis of NH_3 react very rapidly with NO_2 to produce OH + NO.

This rapid creation of OH has provided a valuable probe which not only indicates that NH_2O is being formed through rapid reaction between NH_2O and OH to produce HNO + H_2O, but also provides some measure of the NH_2O production through measurement of the final HNO concentration. Our observations show that NH_2O the rate of appearance of HNO or disappearance of OH depend upon the NH_3 concentration, i.e. upon the concentration of NH_2O. We believe that reaction of NH_2O with NO_2 contributes negligibly.

Neglecting any contributions from the photolysis of NO_2, the reaction scheme is quite simple.

$NH_3 + h\nu$ (193 nm)	$\rightarrow NH_2 + H$	(2)
$H + NO_2$	$\rightarrow OH + NO$	(3)
$NH_2 + NO_2$	$\rightarrow NH_2O + NO$	(1a)
	$\rightarrow H_2O + N_2O$	(1b)
$NH_2O + OH$	$\rightarrow HNO + H_2O$	(4)
$HNO + OH$	$\rightarrow H_2O + NO$	(5)
$OH + NO_2 + M$	$\rightarrow HNO_3 + M$ (slow)	(6)

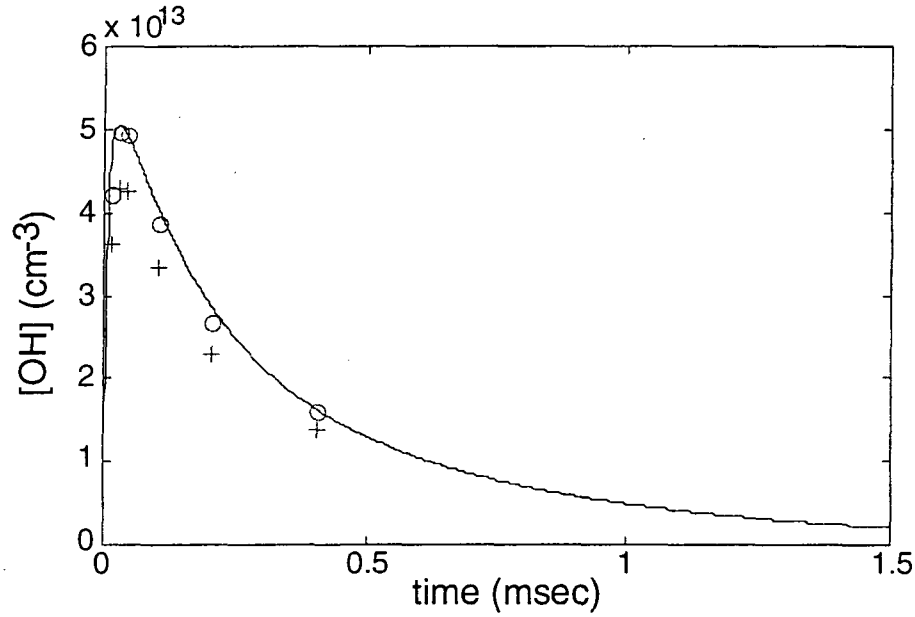

Fig. 1. OH decay calculated with the rate constants in the text with a measured NH_2 initial concentration of 5.3×10^{13} cm^{-3}. The + symbols indicate the absolute [OH], the o's after rescaling.

The stable final products on our time scale are, neglecting the small amount of HNO_3 from (6), NO, N_2O, H_2O, and HNO. As reported last year, we find a branching into channel (1b) of about 20-25% agreeing reasonably well with three of the previous four studies. Glarborg *et al*[6] have found that very little N_2 is formed at 850-1350 K in the thermal reaction of NH_3 with NO_2 effectively ruling out channels (1c) and (1d). We confirm that channel (1d) is absent as there is no prompt ground state OH. We see no prompt HNO ruling out channel (1e). Thus only channels (1a) and (1b) remain. Since (1b) is about 20-25%, (1a) must be about 75-80%. If reaction (5) were negligibly slow, we would expect that the final HNO concentration would be 75-80% of the initial NH_2 concentration. Instead we find the final HNO concentration is about 55% of the initial NH_2 concentration indicating that the rate of reaction (5) is not negligible.

To obtain a crude estimate of the rates of reactions (4) and (5), we have adjusted them to fit the observed $([HNO]/[N_2O])_{final}$ and data for the decay of OH. The resulting rates are $k_4 \approx 1.2 \times 10^{-10}$ and $k_5 \approx 3 \times 10^{-11}$ $cm^3 s^{-1}$. In Fig. 1 above, the initial concentration of NH_2 was obtained from photolysis without NO_2. There is a small discrepancy between the [OH] and $[NH_2]_o$. To show that the time behavior is reproduced, the [OH] was rescaled to give the circle points.

$O(^1D)$ QUANTUM YIELD AT 193 NM

We have measured the quantum yield of $O(^1D)$ compared with the total quantum yield for the destruction of NO_2 in the flash photolysis of NO_2 by measuring the ratio of the yield of OH upon the photolysis of NO_2 in the presence of a large excess of H_2 to the loss of NO_2 in the absence of H_2. We find this ratio is 0.41. Each $O(^1D)$ should produce two OH molecules through the reaction sequence

$NO_2 + h\nu$ (193 nm)	$\rightarrow NO + O(^1D)$	(7)
$O(^1D) + H_2$	$\rightarrow OH + H$	(8)
$H + NO_2$	$\rightarrow OH + NO$	(9)

The rate of reaction (8) at 298 K is[7] 1.1×10^{-10} $cm^3 sec^{-1}$ so that even if the reaction of $O(^1D)$ with NO_2 is gas kinetic it is easily flooded out by H_2. The photolysis of NO_2 in the absence of H_2 destroys two NO_2 molecules for each O atom created

$NO_2 + h\nu$ (193 nm)	$\rightarrow NO + O(^1D \ \& \ ^3P)$	(10)
$O + NO_2$	$\rightarrow NO + O_2$	(11)

The rate of reaction (11) is[7] 9.7×10^{-11} and is the dominant fate of O atoms in low pressure mixtures of NO_2 and He. Thus $[O(^1D)]/[NO_2]_{phot} = 0.4_1$.

PHOTOLYSIS PRODUCT QUANTUM YIELDS OF KETENE AT 193 nm

The photolysis of ketene at 193 nm was studied by measuring the amount of atomic hydrogen produced when very dilute ketene/Ar and ketene/H_2 mixtures were irradiated by a single pulse from an ArF excimer laser. Absolute concentrations of atomic hydrogen were monitored over a time interval of 1-3 ms by using Lyman α H atom resonance absorption spectroscopy (ARAS).

Four different photo-dissociation channels of ketene were identified,

$H_2CCO + h\nu$ (193 nm)	$\rightarrow CH_2 (\tilde{X}\ ^3B_1) + CO$	(12a)
	$\rightarrow CH_2(\tilde{a}\ ^1A_1) + CO$	(12b)
	$\rightarrow H + HCCO$	(12c)
	$\rightarrow C_2O(^1\Sigma) + H_2$	(12d)

The quantum yields for these channels were measured as $\phi_a = 0.63$, $\phi_b = 0.19$, $\phi_c = 0.11$, and $\phi_d = 0.07$. In order to explore the secondary chemistry that occurred when using higher pressure ketene/Ar mixtures, a mechanism was constructed that used well documented reactions, and for most processes, rate constants that had already been accurately determined. Modeling studies using this mechanism showed the hydrogen atom/ time profile to be determined largely by the rate of reaction of HCCO with H.

$$H + HCCO \rightarrow CH_2 + CO \qquad (13)$$

An excellent fit to all the experimental data was obtained when a value of k_{13} of $(1.7 \pm 0.2) \times 10^{-10}$ $cm^3 molecule^{-1} s^{-1}$ was used.

A paper has been submitted for publication on this work.

FUTURE PLANS

We are preparing papers on the reaction system NH_2+NO_2 and the $O(^1D)$ yield from NO_2. Our efforts this year to observe the NH stretch of NH_2O have so far been fruitless, but we have carried out B3LYP calculations on NH_2O which indicate that although the antisymmetric NH stretch is weak (7.2 km/mol) it should be observable. This year we have rebuilt our apparatus with a Herriott cell arrangement. We expect that this may improve our sensitivity by as much an order of magnitude through better overlap of the probe and excimer beams. With clear evidence that NH_2O is present, we propose to attempt to observe it again. We plan to search for the highest frequency NH stretching vibration of N_2H_3, which is predicted to be three times stronger (23.1 km/mol) than the strongest NH stretch of NH_2O. We also plan searching for a CH stretch of CH_3OCH_2 which has a band strength a factor of two higher yet. The reaction OH + CH_3CHO may have, in addition to the abstraction channel producing H_2O + CH_3CO, an addition channel producing CH_3 + HCOOH. We plan to search for methyl as a reaction product, and, if CH_3 is found, to measure the branching ratio between these channels.

---

[1] A. M. Mebel, C.-C. Hsu, M. C. Lin, and K. Morokuma, *J. Chem. Phys.* **103**, 5640 (1995).

[2]H. Meurier, P. Pagsberg, and A. Silleson, *Chem. Phys. Lett.* **261**, 277 (1996).

[3]J. Park and M. C. Lin, *Int. J. Chem. Kinetics* **28**, 879 (1996).

[4]R. W. Quandt and J. F. Herschberger, *J. Phys. Chem.* **100**, 9407 (1996).

[5]N. Lindhom and J. F. Herschberger, *J. Phys. Chem.*, **101**, 4991 (1997)

[6]P. Glarborg, K. Dam-Johansen, and J. A. Miller, *Int. J. Chem. Kinetics* **27**, 1207 (1995).

[7]Atkinson *et al, J. Phys. Chem. Ref. Data* **26**, 1326 (1997).

Publications

1. "Analysis of the K-subband Structure of the ν_1 Fundamental of Propargyl Radical $H_2CC{\equiv}CH$," Li Yuan, John DeSain, and R. F. Curl, *J. Mol. Spectrosc.* **187**, 102-108 (1998).

2. "The Rotationally Resolved Infrared Spectrum of the ν_1 Stretch of the Allyl Radical," J. D. DeSain, R. I. Thompson, S. D. Sharma, R. F. Curl, *J. Chem. Phys.* **109**, 7803-7809 (1998).

3. "Rotational Analysis of ν_{13} of Allyl Radical," J. D. DeSain and R. F. Curl, *J. Mol. Spectrosc.* **196**, 324-328 (1999).

4. "Kinetics of the Reaction of Propargyl Radical with Nitric Oxide," J. D. DeSain, P.Y. Hung, R. I. Thompson, G. P. Glass, G. Scuseria and R. F. Curl, *J. Phys. Chem. A* (accepted and available on the JPC web site).

Highly Vibrationally Excited Molecules: Energy Transfer and Transient Species Vibrational Spectroscopy Through Time-Resolved IR Emission

Hai-Lung Dai
Department of Chemistry, University of Pennsylvania, Philadelphia PA 19104-6323
dai@sas.upenn.edu

I. Program Scope

Currently in our effort to understand the chemical properties of highly vibrationally excited molecules, we are concentrating on characterizing the collision energy transfer dynamics and the structure and spectroscopy of transient, vibrationally excited species. Experimentally, the time-resolved Fourier transform emission spectroscopy has been developed and used for probing the energy content as well as the structure of the molecules excited with a laser pulse.

In energy transfer studies, we have found that collision energy transfer from highly vibrationally excited molecules, such as NO_2, SO_2, CS_2 and pyrazine with energies as high as 40,000 cm^{-1}, is dominated by long range interactions through transition dipoles. Experimental evidence from time-resolved IR emission studies shows that energy loss per collision increases dramatically with the excitation energy and is proportional to the transition dipole of the excited molecule. There appear to be thresholds in the excitation energy that coincide with the origins of intramolecular vibronic coupling, which enhances the transition dipoles. The energy transfer efficiency in V-T collisions also increases with polarizability. Furthermore, relaxation cross section, measured through kinetic quantum beat spectroscopy, of highly excited molecules is found to be much larger than the Lennard-Jones cross section. The long-range interactions become important at high energies because of the relaxation of the resonance condition and the increase of transition dipole, all resulted from strong intramolecular coupling and high level density.

In a new development, an approach for detecting the vibrational spectrum of transient species is demonstrated on the vinyl radical. Photodissociation of carefully chosen precursors at selected photolysis wavelengths produces highly vibrationally excited radicals. IR emission from these radicals is then measured by time-resolved Fourier Transform Spectroscopy with nanosecond time resolution. All 9 vibrational bands of the vinyl radical, generated from 4 different precursors, are obtained and reported here for the first time.

II. Transient Species Vibrational Spectroscopy through Time-Resolved Fourier Transform IR Emission

Vibrational spectroscopy of radicals, because of their unstable and transient nature and because they may generally be produced only in small quantities, is usually challenging. A variety of experimental techniques have been devised to utilize the generally stronger electronic transitions. The radical species are usually generated by a photolysis light pulse and excited to an electronically excited state through a second light pulse. The downward transitions are then measured either through fluorescence dispersion or through stimulated emission to give the vibrational levels in the electronic ground state. These approaches rely on the existence of a stable excited state accessible by available laser wavelengths. The vibrational levels can of course be probed directly by high sensitivity

absorption techniques based on IR lasers. Such direct absorption techniques are most effective for high-resolution spectroscopy if it is known *a priori* where to scan the narrow line width IR lasers to search for the rovibrational transitions.

Information on IR active modes can in principle be acquired through emission spectroscopy provided the radicals are produced with excess vibrational energy. Time-Resolved Fourier Transform Emission Spectroscopy (TR FTES) has proven to be a viable method for resolving the emission spectra in calibrated absolute frequencies over a wide frequency range with sufficient frequency and time resolution. Within the past year we have demonstrated an approach which applies TR FTES to disperse the IR emission of radicals produced in their electronic ground state but with vibrational excitation. This approach is particularly useful for detecting previously unknown vibrational modes of a radical.

The radical species is generated through photodissociation of selected precursor molecules. The precursor and photolysis wavelength are chosen such that, due to the exothermicity of the reaction, the radical is produced with excess vibrational energy. Time resolution allows observation of the nascent emission, as well as evolution of the emission features in time to ensure the assignment of the spectral features to the radical species. A non-reactive quenching gas is used at a pressure much higher than the precursor to promote collision induced vibrational relaxation so the transition frequencies and intensities of the radical can eventually be observed as close as possible to the fundamental transitions. The spectral resolution is expected to be limited by the rotational bandwidth of the molecules, as the molecules have a room temperature rotational state distribution. The resultant spectrum using this approach should reveal all of the IR active modes and serve as a guide for high-resolution studies.

III. The Vinyl Radical

This strategy is demonstrated first on the vinyl radical (C_2H_3). Due, in part, to its important role in the free radical addition and polymerization of acetylene as well as in the decomposition of ethenoid compounds, vinyl has been the subject of numerous experimental and theoretical studies. Yet, despite the effort so far, only one electronic ground state vibrational mode has been optically detected while spectroscopy of excited electronic states has been more successful. This may be a result of the dissociative behavior of the first electronic excited state that hindered vibrational spectroscopy through electronic transitions. The only definite identification of a ground state level was performed by Kanamori, Endo and Hirota using an IR diode laser absorption measurement in the region of 820 - 960 cm^{-1} of vinyl produced by photodissociation of vinyl halides.

In our experiments, the vinyl radical was produced by 193 nm photolysis of several precursor molecules which give the common product of vinyl as well as various additional products. The precursor molecules selected were vinyl bromide (VBr), vinyl chloride (VCl), methyl vinyl ketone (MVK) and butadiene (BD). The dissociation reactions of all these precursors are sufficiently exothermic to produce vinyl radical with excess internal energy. Furthermore, at low pressures, the 193 nm dissociation quantum yield for all of the precursor molecules is expected to be close to unity and would not produce excited precursor molecules which may contribute to the emission spectra. The IR emission signal was directed through the FTIR Interferometer and onto a mercury cadmium telluride (MCT) detector that has a 500 ns rise time and a spectral response of 700 to 8000 cm^{-1}. The Fourier Transform spectrometer was run in step scan mode with 50 laser shots averaged and digitized at each mirror position of the movable mirror. The spectra were taken at 50 ns time intervals.

Figure 1 shows the infrared emission spectra from the photodissociation products of VBr. Selected time slices from 0.5 to 18.5 ms following the photolysis pulse are shown. The spectra shown have been corrected for the detector response function. To confirm which emission peaks are from vinyl we compare spectra from photodissociation products generated from different precursor molecules, VBr, VCl, MVK and BD. The peaks that are common to each of these spectra are assigned to vinyl. This data represents the first experimental report of the entire set of 9 vibrational mode frequencies and relative intensities.

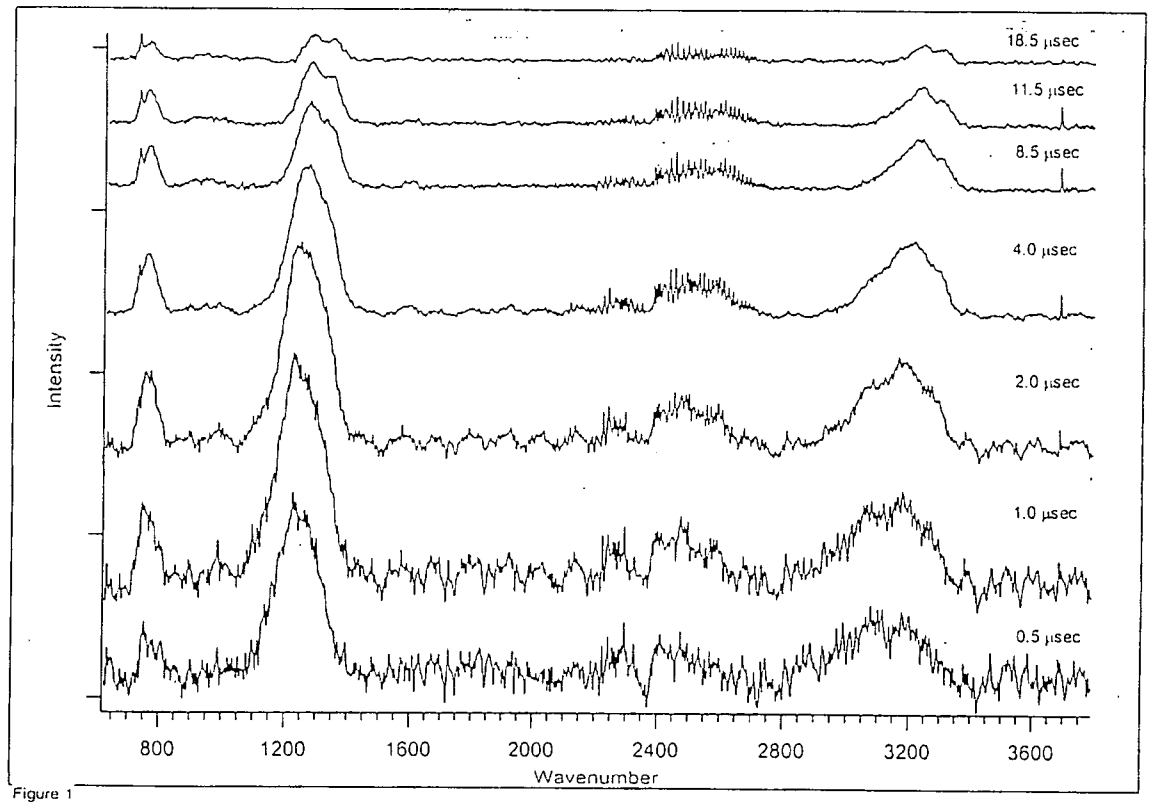

Figure 1

IV. Future Plans

We have two directions, both are related to the structure and dynamics of excited molecules and both use the time-resolved FTIR emission approach, to move along at this point. One is to continue the investigation of collision energy transfer dynamics of highly vibrationally excited molecules. The present emphasis is on the energy transfer behavior of large molecules such as pyrazine. The second direction is highlighted in this report and will be continued with the following molecules: vinylidene, acetyl, and other small oxygen or CN containing radicals.

V. Publications of DOE Sponsored Research since 1998

Stimulated Emission Pumping (SEP) Spectroscopy
in "Nonlinear Spectroscopy for Molecular Structure Determination", a monograph published by the Int. Union of Pure and App. Chem. (Blackwell Science, Malden, MA, 1998), Ed. S. Tsuchiya et al., Chapt. 3, pp. 55-74
Hai-Lung Dai

Nanosecond Time-Resolved FTIR Emission Spectroscopy: Monitoring the Energy Distribution of Highly Vibrationally Excited Molecules during Collisional Deactivation
J. Chem. Phys., 108, 1297-1300 (1998)
Charles Pibel, Egor Sirota, Jerrel Brenner, and Hai-Lung Dai

Interfacing a Transient Digitizer to a Fourier Transform Spectrometer for Nanosecond Time-Resolved Spectroscopy
Rev. Sci. Inst., 70, 18-22 (1999)
Laura T. Letendre, Hai-Lung Dai, Ian A. McLaren, and Timothy J. Johnson

Structure and Dynamics of Highly Excited Molecules from Time-Resolved FTIR Emission Spectroscopy
Proceedings of the 12th International Conference on FT Spectroscopy (Waseda University Press, Tokyo, Japan, 1999), pp. 115-8
L. Letendre, D. K. Liu, C. D. Pibel, J. B. Halpern, and H. L. Dai

Vibrational Spectroscopy of a Transient Species through Time-Resolved Fourier Transform Emission Spectroscopy: The Vinyl Radical
J. Chem. Phys., [communication], in press
L. Letendre, D-K. Liu, C. D. Pibel, J.a B. Halpern and H. L. Dai

V-V Energy Transfer from Highly Vibrationally Excited Molecules through Transition Dipole Coupling: A Semi-QuantitativeTest on SO_2 to $SF_6(3_1)$
J. Phys. Chem. (C. B. Moore special issue), submitted
Dong Qin, Gregory V. Hartland and Hai-Lung Dai

A Time Resolved Fourier Transform Emission Spectroscopy Study of the Collisional Deactivation of Highly Vibrationally Excited SO_2
Z. Phys. Chem. (J. Troe special issue), submitted
D. Qin, G.V. Hartland, H.L. Dai, and C.L. Chen

Geometric approach to multiple–time–scale kinetics

Michael J. Davis

Chemistry Division
Argonne National Laboratory
Argonne, IL 60439
Email: davis@tcg.anl.gov

Research in this program focuses on three interconnected areas. The first involves the study of intramolecular dynamics, particularly of highly excited systems. The second area involves the use of nonlinear dynamics as a tool for the study of molecular dynamics and complex kinetics. The third area is the study of the classical/quantum correspondence for highly excited systems, particularly systems exhibiting classical chaos.

Recent Progress

Some work was done in this period to complete an earlier project on the assignment of highly excited vibrational eigenstates. The first 133 eigenstates were assigned, well into the classically chaotic region of phase space. Several interesting features of highly excited eigenstates were elucidated, including a memory effect for resonant eigenstates, which results in different shapes and transition moments for overtone resonant eigenstates.

Several small projects were completed which demonstrate the utility of low-dimensional manifolds in several types of kinetic systems: 1) complex chemical kinetics, 2) nonlinear master equations for vibrational relaxation, and 3) coagulation-fragmentation kinetics, which is useful for soot modeling, and was studied for a sample problem of micelle kinetics. This work was done in collaboration with Rex Skodje. We were able to demonstrate that there were low-dimensional manifolds in the nonlinear master equation and that there was no simple exponential rate of relaxation except very close to equilibrium. There are also low-dimensional manifolds in the micelle kinetics and this explains the well known presence of a fast and slow relaxation in micelle kinetics. Additional progress has been made to improve the algorithms used to generate low-dimensional manifolds and a better understanding of the global structure of phase space for a full mechanism of the H_2/O_2 system has been elucidated, compared to the reduced model studied earlier.

A project on low-dimensional manifolds in partial differential equations was started. This project is a collaboration with Tasso Kaper (Mathematics, Boston University), and Hans Kaper and Paul Fischer (Mathematics and Computer Science, Argonne). Low-dimensional manifolds so far have been used to reduce complex chemical kinetics, which is described by a set of coupled, nonlinear ordinary differential equations. However, a full modeling of combustion systems also involves fluid dynamics, which is described by a set of coupled nonlinear partial differential equations. The focus of this project has been trying to understand the structure of nonlinear partial differential equations. A few numerical results have been generated, but most of the effort has been devoted to a study of the literature. There are several approaches in the applied mathematics literature which suggest it will be possible to generate low-dimensional manifolds for such systems in a reasonably rigorous fashion.

A major project was undertaken to understand the geometry of the phase space for nonlinear master equations describing association and dissociation reactions, with an application to $CH_3 + CH_3 \leftrightarrow C_2H_6$. This work is being done in collaboration with Stephen Klippenstein. In addition to this reaction an investigation of the phase space structure of the phenomenological rate law and the Lindemann mechanism for association/dissociation has been completed. It was demonstrated that there are one-dimensional manifolds in the

discrete version of the master equation for the methyl recombination reaction with dissociation. This manifold is the nonlinear analogue of the least negative eigenvector for the linear master equation. It was demonstrated that generally the dynamics of the master equation follows the phenomenological rate law along the manifold, but there can be deviations in the fall-off region and at high pressure when methyl radical is not very dilute in the Argon buffer gas (~ 1 – 5%), particularly at high temperatures.

It was also demonstrated in this project that rate constants could be estimated efficiently by properly analyzing the linearization of the nonlinear master equation. This method involves matrix diagonalization, so like the linear counterpart, allows for certain diagnostics, based on the relative sizes of the eigenvalues. It was demonstrated how rate constants could be obtained over a wide range of temperatures, pressures, and values of ΔE_d, without resort to a change of methods (it is difficult to calculate dissociation rate constants at low temperature in this reaction, and methods for directly approximating association rate constants may break down at high temperature). Deviations from the phenomenological rate constant were also analyzed within this framework.

The accompanying figure demonstrates some of the features of the project. In the top panel a low-dimensional manifold is shown for the methyl/ethane master equation. The calculation was done with 531 bins of width 100cm^{-1} for ethane. The fraction of density of reactive species in the first bin (g_1) is plotted vs. the fraction of density that is methyl radical (g_d). Equilibrium is at the open circle and ρ describes the density of reactive species. On one side of the equilibrium the reaction along the manifold is dominated by dissociation (g_d smaller than equilibrium) and on the other side by association. The plot demonstrates that the manifold is linear and passes very close to (1.0, 0.0), indicating that there is no transient behavior for the reaction with all the density started in the methyl radical. The linearity is indicative of a Boltzmann distribution along the manifold for a fraction of the low lying bins.

In the middle panel the situation has changed as the total density of reactive species is increased (dilution is ~ 5% in Argon). Here the manifold (solid line) is clearly nonlinear and does not pass through (1.0, 0.0). Equilibrum is near (0, 0) for this case. The dashed line shows that an initially pure mixture of methyl takes awhile to reach the manifold (~ 2.5 μs). The curvature also indicates non-Boltzmann behavior along the manifold. The combination of these effects indicate that typical estimates of the association rate constant will fail away from equilibrium. Such a failure is further indicated in the bottom panel where the instantaneous rate constant is estimated along the trajectory, and shown with a solid line. The dashed line shows the asymptotic rate constant, indicating that the instantaneous and aysmptotic rate can differ by as much as ~30%.

Future Plans

The low-dimensional manifold work will continue. An increased effort to understand and implement low-dimensional manifolds for partial differential equations will be undertaken with Tasso and Hans Kaper. It is anticipated that, in collaboration with John Kiefer, the vibrational relaxation of several molecules studied by Kiefer and co-workers will be investigated with a nonlinear master equation. A new project will be initiated to study stochastic methods for describing nonlinear master equations and coagulation-fragmentation kinetics in collaboration with Rex Skodje. The feasibility of incorporating stochastic kinetics in certain types of combustion problems will be undertaken in collaboration with Sharath Girimaji.

Publications

A. Callegari, H. K. Srivastava, U. Merker, K. K. Lehmann, G. Scoles, and M. J. Davis, "Eigenstate resolved infrared-infrared double-resonance study of intramolecular vibrational relaxation in benzene: First overtone of the CH stretch, J. Chem. Phys. **106**, 432 (1997).

M. J. Davis, "Chaotic dynamics and approximate semiclassical quantization: Assigning highly excited vibrational eigenstates", J. Chem. Phys. **107**, 106 (1997).

M. J. Davis, "Investigating intramolecular dynamics: Hierarchical analysis and the topography of energy flow", J. Chem. Phys. **107**, 4507 (1997).

C. C. Martens, M. J. Davis, and G. S. Ezra, "Comment on 'Local frequency analysis and the structure of classical phase space of LiNC/LiCN' [J. Chem. Phys. **108**, 63 (1998).", J. Chem. Phys. **109**, 6507 (1998).

M. J. Davis and R. T. Skodje, "Geometric investigation of low-dimensional manifolds in systems approaching equilibrium", J. Chem. Phys. **111**, 859 (1999).

M. J. Davis, "Assignment of highly excited vibrational eigenstates", Phys. Chem. Chem. Phys.. (submitted).

M. J. Davis and R. T. Skodje, "Geometric approach to multiple-time-scale kinetics", to be submitted.

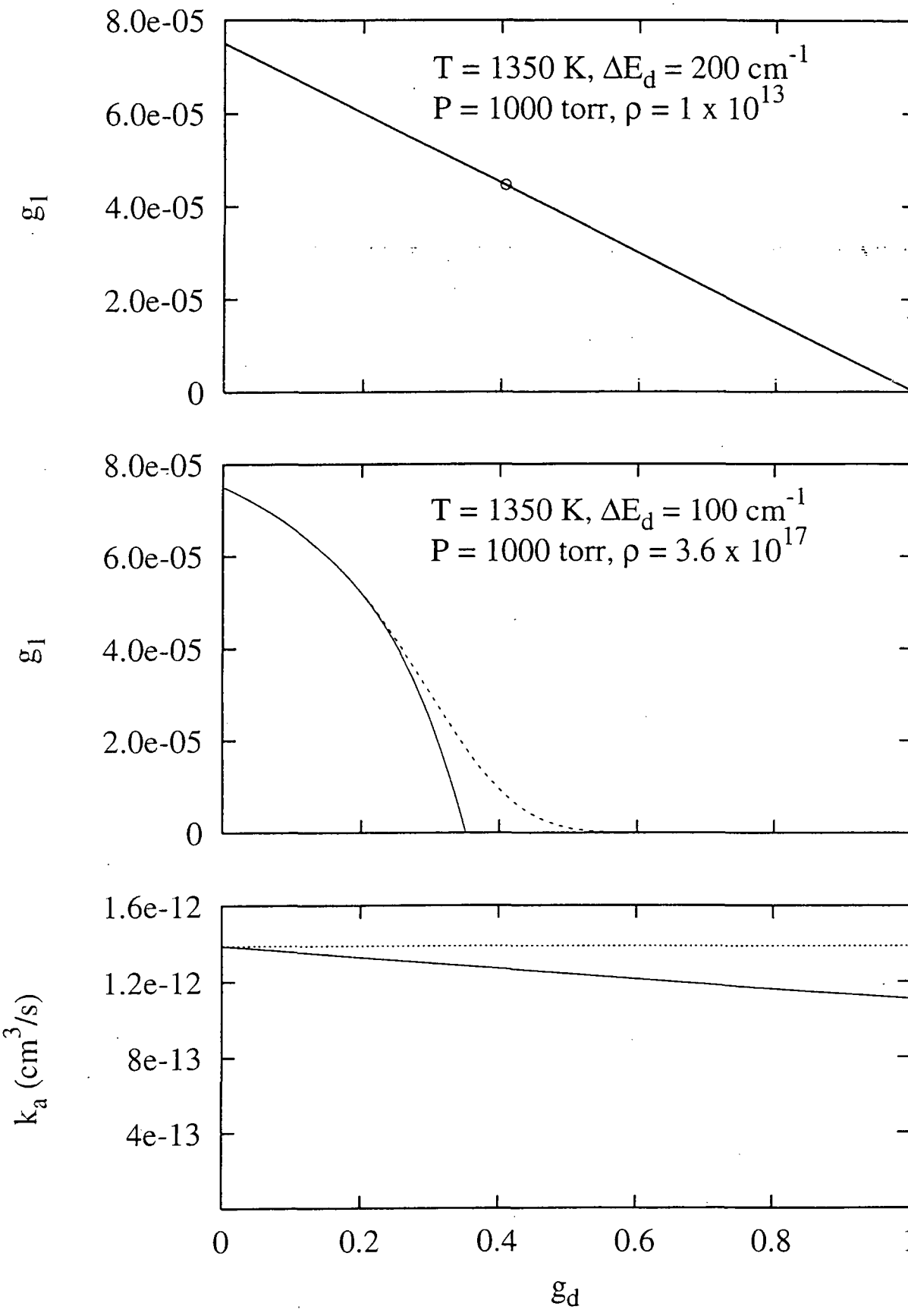
8.0e-05
6.0e-05
4.0e-05
2.0e-05
0
g_l
T = 1350 K, ΔE_d = 200 cm^{-1}
P = 1000 torr, ρ = 1 x 10^{13}
8.0e-05
6.0e-05
4.0e-05
2.0e-05
0
g_l
T = 1350 K, ΔE_d = 100 cm^{-1}
P = 1000 torr, ρ = 3.6 x 10^{17}
1.6e-12
1.2e-12
8e-13
4e-13
k_a (cm^3/s)
0
0.2
0.4
0.6
0.8
1
g_d

COMPREHENSIVE MECHANISMS FOR COMBUSTION CHEMISTRY: EXPERIMENT, MODELING, AND SENSITIVITY ANALYSIS

Frederick L. Dryer
Department of Mechanical and Aerospace Engineering
Princeton University, Princeton, New Jersey 08544-5263
fldryer@princeton.edu

Grant No. DE-FG02-86ER-13503

Program Scope

The experimental aspects of our work are conducted in 10 cm-diameter flow reactors, at pressures from 0.3 to 20 atmospheres, temperatures from 500 K to 1200 K, and with observed reaction times from 10^{-2} to 2 seconds. Measurements of stable reactant, intermediate, and product species provide a significantly constrained set of kinetic data for elucidating mechanistic behavior and validating detailed kinetic mechanisms. The experimental data guide the development of kinetic-mechanisms that are utilized for deriving/testing rate-parameter selections, for interpreting observations, for extending the predictive range of mechanism constructs (by comparison with generated as well as literature data from other kinetic experiments), and to study the effects of diffusive transport coupling on reaction behavior in pre-mixed and diffusion flames. Continuing efforts of this program are: (1) utilizing the perturbations of the H_2/O_2 and CO/H_2O/Oxidant-reaction systems by the addition of small amounts of other species to further clarify elementary reaction properties and refine these important kinetic mechanisms; (2) further elucidating the reaction mechanisms for the pyrolysis and oxidation of small hydrocarbons (alkanes and olefins) and hydrocarbon oxygenates (aldehydes, alcohols, and ethers). Below, we detail recent progress on portions of this work.

Recent Progress

Recent progress, including summaries of published works, those in press, those in review for publication and some of the efforts currently underway are presented below.

1. M.A. Mueller, T.J. Kim, R.A. Yetter, and F.L. Dryer, "Flow Reactor and Kinetic Modeling Studies of the H_2/O_2 Reaction", Int. J. Chem. Kin., 31, 113 (1999).

Profile measurements of the H_2/O_2 reaction have been obtained using a variable pressure flow reactor over pressure and temperature ranges of 0.3 to 15.7 atm and 850 to 1040 K, respectively. These data span the explosion limit behavior of the system and place significant emphasis on HO_2 and H_2O_2 kinetics. The explosion limits of dilute $H_2/O_2/N_2$ mixtures extend to higher pressures and temperatures than those previously observed for undiluted H_2/O_2 mixtures. In addition, the explosion limit data exhibit a marked transition to an extended second limit, which runs parallel to the second limit criteria calculated by assuming HO_2 formation to be terminating. The experimental data and modeling results show that the extended second limit remains an important boundary in H_2/O_2 kinetics. Near this limit, small increases in pressure can result in more than a two order of magnitude reduction in reaction rate. At conditions above the extended second limit, the reaction is characterized by an overall activation energy much higher than in the chain explosive regime.

The overall data set, consisting primarily of experimentally measured profiles of H_2, O_2, H_2O, and temperature, further expand the database used for comprehensive mechanism development for the H_2/O_2 and $CO/H_2O/O_2$ systems. Several rate constants recommended in an earlier reaction mechanism have been modified using recently published rate constant data for $H+O_2(+N_2) = HO_2(+N_2)$, $HO_2+OH = H_2O+O_2$, and $HO_2+HO_2 = H_2O_2+O_2$. When these new rate constants are incorporated into the reaction mechanism, model predictions are in very good agreement with the experimental data.

2. M.A. Mueller, R.A. Yetter, and F.L. Dryer, "Flow Reactor Studies and Kinetic Modeling of the H_2/O_2 /NO_x and $CO/H_2O/O_2/NO_x$ Reactions", Int. J. Chem. Kin., 31, 705 (1999).

Flow reactor experiments were performed over wide ranges of pressure (0.5-14.0 atm) and temperature (750-1100 K) to study H_2/O_2 and $CO/H_2O/O_2$ kinetics in the presence of trace quantities of NO and NO_2. The promoting and inhibiting effects of NO reported previously at near atmospheric pressures extend throughout the range of pressures explored in the present study. At conditions where the recombination reaction $H+O_2(+M)=HO_2(+M)$ is favored over the competing branching reaction, low concentrations of NO promote H_2 and CO oxidation by converting HO_2 to OH. In high concentrations, NO can also inhibit oxidative processes by catalyzing the recombination of radicals. The experimental data show that the overall effects of NO addition on fuel consumption and conversion of NO to NO_2 depend strongly on mixture pressure and stoichiometry. The addition of NO_2 was also found to promote H_2 and CO oxidation but only at conditions where the reacting mixture first promoted the conversion of NO_2 to NO.

Experimentally measured profiles of H_2, CO, CO_2, NO, NO_2, O_2, H_2O, and temperature were used to constrain the development of a detailed kinetic mechanism consistent with the previously studied H_2/O_2, $CO/H_2O/O_2$,

H_2/NO_2, and $CO/H_2O/N_2O$ systems. Model predictions generated using the reaction mechanism presented here are in good agreement with the experimental data over the entire range of conditions explored.

3. M.A. Mueller, J.L. Gatto, T.J. Kim, R.A. Yetter, and F.L. Dryer, "Hydrogen/Nitrogen Dioxide Kinetics: Derived Rate Data for the Reaction H_2+NO_2 = HONO+H at 833 K", Combust. and Flame 120, 589 (1999).

Flow reactor experiments were performed at temperatures near 833 K and pressures ranging from 1.2-5.0 atm to study the kinetics of the $H_2/NO_2/N_2$ reaction. Model predictions of NO_2, NO, and H_2O were compared with experimental measurements to derive rate data for the reaction H_2+NO_2 = HONO+H which are a factor of 30 lower than the critical evaluation of Tsang and Herron (J. Phys. Chem. Ref. Data 20:609-663 (1991)), but within 12% of the recent theoretically predicted rate expression of Park et al. (J. Phys. Chem. 102A:10099-10105 (1998)).

4. J. S. Lee, R.A. Yetter, F.L. Dryer, A.G. Tomboulides, and S. A. Orszag, "Simulation and Analysis of Laminar Flow Reactors", Combust. Sci. and Tech. (2000). In Press.

Laminar flow reactors are frequently used to experimentally study an isolated elementary reaction step as well as chemical kinetic mechanisms of many coupled reactions. This classical method is effective in measuring kinetic rate parameters when the effects of mass diffusion and wall surface reactions can be neglected or accurately assessed. We perform a series of two-dimensional direct numerical simulations to investigate issues related to the operation of this classical apparatus. By utilizing a well-established gas phase kinetic mechanism for moist CO oxidation and a commonly used sub-model for multi-component diffusive transport, we investigate a virtual elementary kinetic experiment. In particular, we extract data from the simulations and evaluate the rate parameters of the reaction $CO+OH \rightarrow CO_2 + H$ as one would in an actual experiment. We show that under appropriate operating conditions, the desired elementary reaction rate parameters can be recovered accurately with minimal efforts in analyzing the experimental data. We also demonstrate that two-dimensional simulations can be useful in refining the operating conditions of an experiment to minimize uncertainties in the determined rate parameters. Numerical results confirm that operating conditions that differ from the classical "plug flow" condition can yield more accurate results. Finally, we investigate laminar reactor operating conditions typical of those used in the literature to study reacting systems of many coupled elementary reactions. Using the same CO oxidation mechanism as an example, we show that for oxidation experiments conducted at one atmospheric pressure, the coupling between transport and chemical kinetics results in a highly two-dimensional reacting flow field. Interpreting these results on a one-dimensional basis can lead to significant inaccuracies in the evaluated rate parameters.

5. H.J. Curran, S.L. Fischer, and F.L. Dryer, "A Flow Reactor Study of Dimethyl Ether. I: High Temperature Pyrolysis and Oxidation", Accepted for Publication, November 1999 in the Int. J. Chem. Kin.

Dimethyl ether pyrolysis was studied in a variable-pressure flow reactor (VPFR) at 2.5 atmospheres and 1118 K. A second, near-pyrolysis experiment was performed in an atmospheric-pressure flow reactor (APFR) at 1060 K. In addition, the APFR was used to study the oxidation of dimethyl ether at an average temperature of 1086 K, with the equivalence ratios of 0.32 to 3.4. All experiments were performed with approximately 98% nitrogen dilution. On-line extractive sampling with FTIR, NDIR (for CO and CO_2), and electrochemical (for O_2) analyses were performed to quantify species at specific locations along the axis of the turbulent flow reactors. Species concentrations were correlated against residence time in the reactor and these species evolution profiles were compared to the predictions of a previously published detailed kinetic mechanism. Some minor changes were made to the model in order to simulate the present experimental data. In addition, this model is able to reproduce the high temperature kinetic data obtained in a jet-stirred reactor (JSR).

6. H.J. Curran, S.L. Fischer, and F.L. Dryer, "A Flow Reactor Study of Dimethyl Ether. II: Low Temperature Oxidation", Accepted for Publication, January 2000 in the Int. J. Chem. Kin.

Dimethyl ether oxidation has been studied in a VPFR over an initial reactor temperature range of 550 to 850 K, in the pressure range 12 to 18 atm, at equivalence ratios of 0.7 to 4.2, and with nitrogen diluent of approximately 98.5%. On-line extractive sampling in conjunction with FTIR, NDIR (CO and CO_2), and electrochemical (for O_2) analyses were performed to quantify species at specific locations along the axis of the reactor. Product species concentrations were correlated against residence time (at constant inlet temperature) and against temperature (at fixed mean residence time). Formic acid was observed as a major intermediate of dimethyl ether oxidation at low temperatures. The experimental species evolution profiles were compared to the predictions of a previously published detailed kinetic mechanism (Curran et al., 1998). This mechanism did not predict the formation of formic acid. In the current study we have included chemistry leading to formic acid formation (and oxidation). This new chemistry is discussed and is able to reproduce the experimental observations with good accuracy. In addition, this model is able to reproduce low temperature kinetic data obtained in a jet-stirred reactor (Dagaut et al., 1998) and high temperature shock tube results (Pfahl et al., 1997).

7. J.J. Scire, Jr., R.A. Yetter and F.L. Dryer, "Flow Reactor Studies of Methyl Radical Oxidation Reactions in Methane Perturbed Moist Carbon Monoxide Oxidation at High Pressure with Model Sensitivity Analysis", Submitted to Int. J. Chem. Kin., March 3, 2000.

New rate constant determinations for the reactions

$$CH_3+HO_2 \rightarrow CH_3O+OH \quad (1)$$

$$CH_3+HO_2 \rightarrow CH_4+O_2 \quad (2)$$

$$CH_3+O_2 \rightarrow CH_2O+OH \quad (3)$$

were made at 1000 K by fitting species profiles from high pressure flow reactor experiments on moist CO oxidation perturbed with methane. These reactions are important steps in the intermediate temperature burnout of hydrocarbon pollutants, especially at super-atmospheric pressure. The experiments used in the fit were selected to minimize the uncertainty in the determinations. These uncertainties were estimated using local model sensitivity coefficients, derived for time-shifted flow reactor experiments, along with literature uncertainties for the unfitted rate constants. The experimental optimization procedure significantly reduced the uncertainties in each of these rate constants over the current literature values. The new rate constants and their uncertainties were determined to be:

Reaction	k_i (at 1000 K) ($cm^3gmol^{-1}s^{-1}$)	Uncertainty Factor Estimate		
		Local	Global* Lower	Global* Upper
1	$1.48(10)^{13}$	2.24	2.11	1.69
2	$3.16(10)^{12}$	2.89	2.84	2.76
3	$2.36(10)^{8}$	4.23	3.16	2.11

**from Monte Carlo global analysis discussed in 8, below.*

There are no direct and few indirect measurements of reactions 1 and 2 in the literature. There are few measurements of reaction 3 near 1000 K. These results therefore represent an important refinement to radical oxidation chemistry of significance to methane and higher alkane oxidation.

The model sensitivity analysis, used in the experimental design, was also used to characterize the mechanistic dependence of the new rate constant values. Linear sensitivities of the fitted rate constants to the unfitted rate constants were determined. The above determinations were found to depend primarily on the rate constant values chosen for the reactions $CH_3+CH_3+M \rightarrow C_2H_6+M$ and $CH_2O+HO_2 \rightarrow HCO+H_2O_2$. Uncertainties in the rate constants of these two reactions are the primary contributors to the uncertainty factors reported above. Further reductions in the uncertainties of these assigned specific rates would lead to significant reductions in the uncertainties in the rate constants determined for k_1, k_2, and k_3.

8. Comparison of Global and Local Sensitivity Techniques for Rate Constants Determined Using Complex Reaction Mechanisms

A comparison of local gradient and Monte Carlo sensitivity techniques was made for rate constants determined by fitting a complex reaction mechanism to experimental data. Local techniques, because of their computational efficiency, have been used in various studies to show how the fitted rate constants depend on the other rate parameters in the mechanism. The local sensitivity results can be used to select experiments to best determine rate constants, given the uncertainties in the remaining model parameters. In addition, the analysis provides detailed information about the mechanistic dependence of the determinations. However, this method only utilizes local, first order sensitivities. In this study the local sensitivity technique was compared with Monte Carlo calculations of sensitivities averaged over the full range of allowable parameter values. Importance sampling was implemented to make the Monte Carlo calculation tractable. The technique developed was used to examine the applicability of the local analysis for the large uncertainties and coupled reactions typical of kinetic mechanisms. In follow-on work to Item 7 (above), local sensitivity techniques were compared with Monte Carlo calculations of sensitivities averaged over the full range of allowable parameter values. The "global" uncertainties for k_1, k_2, and k_3 that resulted are reported above. The rigorous uncertainty limits from the Monte Carlo calculation are narrower than those of the local technique, especially for reaction 3. The Monte Carlo results revealed that the error in the local analysis results primarily from strong higher order sensitivities and show that the rate constant distributions are skewed toward lower rate constant values. The local uncertainty estimates appear to be of sufficient accuracy for experimental design, but are subject to error when the local linear sensitivities vary significantly from the globally fit linear model. Techniques for improving the efficiency of the global method are also under investigation.

9. The Oxidation of Methyl Formate in a Flow Reactor at 3 atm: Experiments and Modeling

Methyl formate and dimethyl ether are formed as intermediates in the oxidation of dimethoxymethane (DMM), an oxygenate under consideration as an alternative fuel for diesel applications. The reaction kinetics of methyl formate were studied in a variable-pressure flow reactor at 3 atm. Experiments were performed under highly dilute conditions of 0.5% fuel with the equivalence ratio (ϕ) varying from $0.5 < \phi < 1.6$ at 900 K. On-line, continuous

extractive sampling, in conjunction with FTIR, NDIR (CO and CO_2), and electrochemical (O_2) analyses were performed to quantify species at specific locations along the axis of the turbulent flow reactor. Species concentrations were correlated against residence time in the reactor and these profiles were compared to a detailed kinetic mechanism. It was found that the fuel mainly undergoes a three-centered unimolecular elimination reaction to yield methanol and carbon monoxide directly. Overall, good agreement was obtained between the experimental results and the detailed kinetic mechanism, except for intermediate concentrations of methanol. Experimental studies over a wider range of conditions and modeling efforts in collaboration with Dr. H.J. Curran are continuing.

10. Oxidation and Pyrolysis Study of Ethanol.

Literature data on the oxidation of ethanol is restricted to observations near atmospheric pressure, and there are few data on the pyrolysis of ethanol at temperatures accessible in flow reactors. Our earlier studies of oxidation (Norton and Dryer, *Int. J. Chem. Kin.*, 24:319, 1992) were performed using gas chromatography to determine intermediate reaction species; as a result, formaldehyde and water, important ethanol oxidation intermediates, were not quantified. Additional studies have been performed in the same atmospheric pressure flow reactor (APFR) utilized by Norton and Dryer, but using on-line chemical analysis based upon Fourier Transform Infrared (FTIR) detection. Oxidation data are in good agreement with earlier measurements, but with improved uncertainties. Additional oxidation studies over a range of pressures (1-15 atm) and temperatures (550-1100 K) are underway in a variable pressure flow reactor (VPFR).

Recent modeling efforts reported by Marinov (*Int. J. Chem. Kin.*, 31:183, 1999) suggest that ethanol decomposition contributes significantly to the destruction of ethanol, even under oxidative conditions at the temperatures of our investigations. Marinov predicts that the most important decomposition channel at these temperatures and atmospheric pressure is that forming C_2H_4 and H_2O. However, there are no pyrolysis data or measurements of the various ethanol decomposition channels at flow reactor temperatures presently appearing in the literature. Initial "oxidative" pyrolysis experiments in the APFR (T_i = 1089 K, P = 1atm, and $C_2H_5OH_i$ = *0.545%, background* $O_2 \approx 0.03\%$), show significant pyrolysis at these conditions. While the Marinov model predicts a reasonable rate of ethanol destruction in comparison to the experiments, the product distribution, particularly those for C_2H_4 and H_2O are in disagreement with the experiment. Further experimental efforts are planned to isolate the specific decomposition channel contributions using radical trapping techniques similar to those applied in shock tube studies.

The additional pyrolysis and oxidation data will be used to further refine understanding and validate comprehensive mechanisms for ethanol pyrolysis and oxidation.

Plans

Reaction systems of present interest over the coming year, in addition to those discussed above, include the pyrolyses and oxidations of formaldehyde, acetaldehyde, methyl formate, dimethoxy methane, ethylene, and ethanol.

Publications, 1998 - Present

1. J.J. Scire, Jr., F.L. Dryer, and R.A. Yetter, "Flow Reactor Studies of Methyl Radical Oxidation Reactions in Methane Perturbed Moist Carbon Monoxide Oxidation at High Pressure with Model Sensitivity Analysis", Submitted to Int. J. Chem. Kin., March, 2000.
2. H.J. Curran, S.L. Fischer, and F.L. Dryer, "A Flow Reactor Study of Dimethyl Ether. I: High Temperature Pyrolysis and Oxidation", Accepted for Publication, November 1999 in the Int. J. Chem. Kin.
3. H.J. Curran, S.L. Fischer, and F.L. Dryer, "A Flow Reactor Study of Dimethyl Ether. II: Low Temperature Oxidation", Accepted for Publication, January 2000 in the Int. J. Chem. Kin.
4. J. S.Lee, R.A. Yetter, F.L. Dryer, A.G. Tomboulides, and S. A. Orszag, "Simulation and Analysis of Laminar Flow Reactors", Combust. Sci. and Tech. (2000). In Press.
5. M.A. Mueller, J.L. Gatto, T.J. Kim, R.A. Yetter, and F.L. Dryer, "Hydrogen/Nitrogen Dioxide Kinetics: Derived Rate Data for the Reaction $H_2+NO_2 = HONO+H$ at 833 K", Combust. and Flame 120, 589 (1999).
6. Mueller, M.A., Kim, T.J., Yetter, R.A., and Dryer, F.L. (1999). "Flow Reactor and Kinetic Modeling Studies of the H_2/O_2 Reaction", Int. J. Chem. Kin., 31, 113.
7. Mueller, M.A., Yetter, R.A., and Dryer, F.L. (1999). "Flow Reactor Studies and Kinetic Modeling of the $H_2/O_2/NO_x$ and $CO/H_2O/O_2/NO_x$ Reactions", Int. J. Chem. Kin., 31, 705.
8. M. A. Mueller, R.A. Yetter, and F.L. Dryer, "Measurement of the Rate Constant of $H+O_2+M=HO_2+M$ (M=N_2, Ar) Using Kinetic Modeling of the High Pressure $H_2/O_2/NOx$ Reaction", 27th Symposium (Intn'l) on Combustion, The Combustion Institute, Pittsburgh, PA., 1998. p. 177.
9. T. Amano and F.L. Dryer, "Effect of Dimethyl Ether, NOx, and Ethane on CH_4 Oxidation; High Pressure, Intermediate Temperature Experiments and Modeling", 27th Symposium (Intn'l) on Combustion, The Combustion Institute, Pittsburgh, PA., 1998. p. 309.
10. T.J. Held and F.L. Dryer, "A Comprehensive Mechanism for Methanol Oxidation", Int. J. Chem. Kin.., 30, 805 (1998).

LASER PHOTOELECTRON SPECTROSCOPY OF IONS

G. Barney Ellison
Department of Chemistry & Biochemistry
University of Colorado
Boulder, CO 80309-0215
Email: **barney@JILA.colorado.edu**

Peroxyl Radicals

Following our photoelectron study of the peroxyl radicals, HO_2 and $(CH_3)_3CO_2$, [J. Chem. Phys. **109**, 10293-10310 (1998)] we have found two applications of organic peroxyl radicals in atmospheric chemistry. The first paper is a general model of organic aerosols which establishes that reactions of radicals with hydrocarbon films are an important process in cloud nucleation. [J. Geophys. Res., **104**, 11633-11643 (1999).] Our model is very general and will apply to most organic aerosols. In particular it will describe the organic aerosols that are produced by internal combustion engines. These aerosols are believed to be responsible for roughly 20% of all continental aerosols [Jacobson *et al*, Rev. Geophys. (in press, 2000)].

Near IR photochemistry ($\hbar\omega \cong 1$ eV) of simple organic peroxyl radicals, such as CH_3O_2, may be responsible for the release of OH and CH_2O into the atmosphere at sunrise. [J. Phys. Chem. A, **103**, 10169-10178 (1999)]

Molecular Resonances and Organic Nitrenes

We have observed the negative ion photoelectron spectrum of the methylnitrene ion, CH_3N^-, and we have measured the electron affinity of methylnitrene, $EA(CH_3N)$ = 0.022 ± 0.009 eV. In addition to detaching the methylnitrene anion to the ground state of $CH_3N(\tilde{X}\ ^3A_2)$, we also detect the first electronically excited state of methylnitrene, $\tilde{a}\ ^1E$. We measure the singlet/triplet splitting to be $\Delta E(\tilde{a}\ ^1E \leftarrow \tilde{X}\ ^3A_2) = 1.352 \pm 0.011$ eV. The photoelectron spectrum of $CH_3N\ \tilde{a}\ ^1E$ contains relatively sharp vibronic structure. Unlike the spectra from H_2CC^-, the photoelectron spectra for CH_3N^- show no evidence for a barrier separating the rearrangement of singlet methylnitrene to methyleneimine: $^1[CH_3N] \rightarrow CH_2{=}NH$. [J. Chem. Phys. **111**, 5349-5360 (1999)]

The dynamical nature of $^1[CH_3N]$ has been studied computationally. In J. Chem. Phys. **111**, 5349-5360 (1999) we analyzed our experimental CH_3N^- spectra and concluded that $\tilde{a}\ ^1E\ CH_3N$ is a "resonance" and is not a bound species. Extensive *ab initio* electronic structure calculations find, in contrast, that this species is bound by roughly 500 cm^{-1}. [J. Am. Chem. Soc. **122**, 122-124 (2000)]

Electron Affinities of Oxides of Carbon

Over the last year conversations with Prof. H.F. Schaefer III suggested that an earlier set of *EA* measurements of ours were incorrect. We collaborated with Schaefer's group and have revised our experimental findings. We conclude that $EA(C_3O)$ = 0.93 ± 0.10 eV and $EA(C_4O)$ = 2.99 ± 0.10 eV. [J. Phys. Chem. A **104**, 2273-2280 (2000)]

This Year's Planned Experiments

1. We have extensive photoelectron spectra of the $[HCCN]^-$, $[DCCN]^-$, $[HCNC]^-$, and $[DCNC]^-$ ions. Photodetachment of the $[HCCN]^-$ ion, m/z 39, reveals a pair of electronic states of the HCCN diradical which are labeled $\tilde{X}\ ^3A''$ and $\tilde{a}\ ^1A'$ HCCN. Our photoelectron spectra reveal: $\Delta E(\tilde{a}\ ^1A' \leftarrow \tilde{X}\ ^3A'') \geq 0.512$ eV. Detachment of $HCCN^-\ \tilde{X}\ ^2A''$ leads to $EA(HCCN\ \tilde{X}\ ^3A'') \leq 2.005 \pm 0.011$ eV. We have also observed the isocyanomethylene, HCNC, as well. Methylisocyanide reacts with oxide anion to afford us the desired ion: $[O]^- + CH_3NC \rightarrow [HCNC]^- + H_2O$. Detachment of $HCNC^-\ \tilde{X}\ ^2A''$ leads to $EA(HCNC\ \tilde{X}\ ^3A'') = 1.879 \pm 0.013$ eV and $\Delta E(\tilde{a}\ ^1A' \leftarrow \tilde{X}\ ^3A'') \leq 0.14$ eV. Our spectra suggest that both the HCCN and HCNC carbenes are quasilinear species.
2. In collaboration with W.C. Lineberger, M. Okmurua, and V.M. Bierbaum, we have produced and detached beams of $CH_3O_2^-$ and $CD_3O_2^-$. Extension of our chemistry to include $CH_3CH_2O_2^-$ seems straightforward.
3. We have studied both the {NCN, HNCN} and {CNN, HCN_2} radicals earlier. This coming year we will attempt to generate the diaziryl anion, *c*-HCN_2, from diazirine, *c*-CH_2N_2.
4. In May, 2000 we will finish a collaboration with H. F. Schaefer's group to publish a review article (in *Chemical Reviews*) that discusses all computational methods to calculate electron affinities and collects the experimental electron affinities of 1,100 different atoms and molecules that have been measured by photoelectron spectroscopy.
5. Peter Chen's hyperthermal nozzle has developed into a versatile source of organic radicals for us. We have initiated a collaboration with B. K. Carpenter to study the vibrational spectroscopy of several fundamental species such allyl (CH_2CHCH_2) and its isomer, cyclopropyl (*c*-C_3H_5). As an example of the use of this technology to study aryl radicals, we have produced the phenyl radical, C_6H_5, by decomposition of C_6H_5I in a hyperthermal nozzle. During the last 12 months we have used this radical source and an FTIR to measure the vibrational spectra of phenyl in an argon matrix at 5 K. In addition to the measurement of the fundamental frequencies $\{\nu\}_{1\text{-}27}$ and IR intensities $\{A\}_{1\text{-}27}$, we have used a polarized laser to photo-orient the C_6H_5 radicals and report the polarizations of the vibrational fundamentals. In the Figure the solid lines depict the experimental FTIR spectrum with dots (•) marking the C_6H_5 fundamentals and the superimposed dotted lines depict the [unscaled] harmonic modes computed from a UB3LYP/6-311G(d,p) *ab initio* calculation.

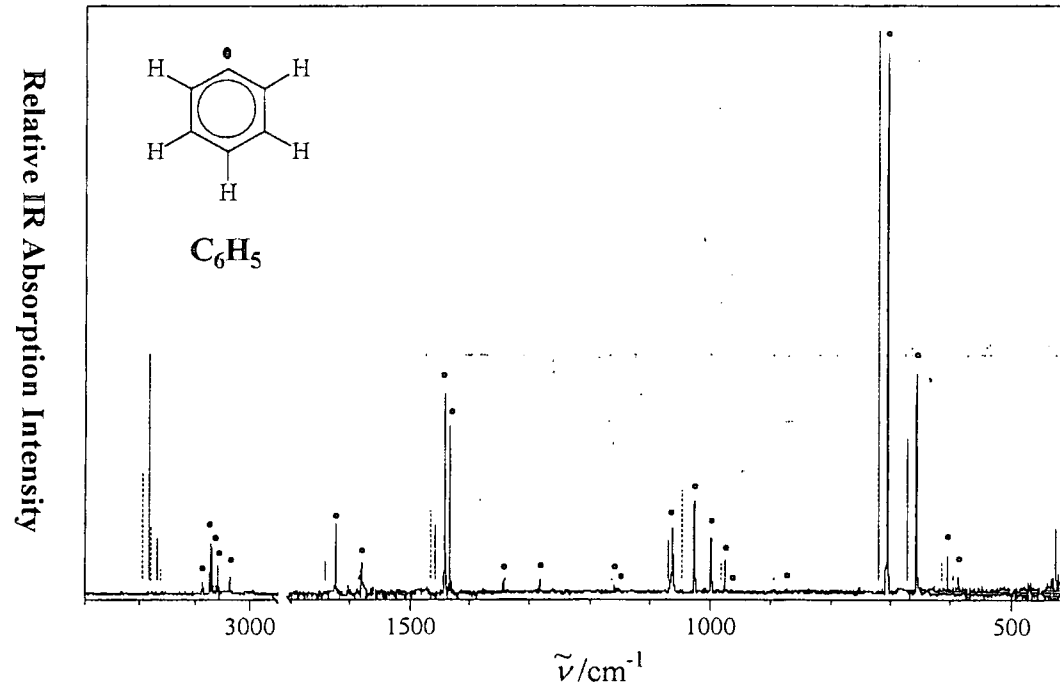
Relative IR Absorption Intensity
H
H
H
H
H
C_6H_5
3000
1500
1000
500
$\tilde{\nu}$/cm^{-1}

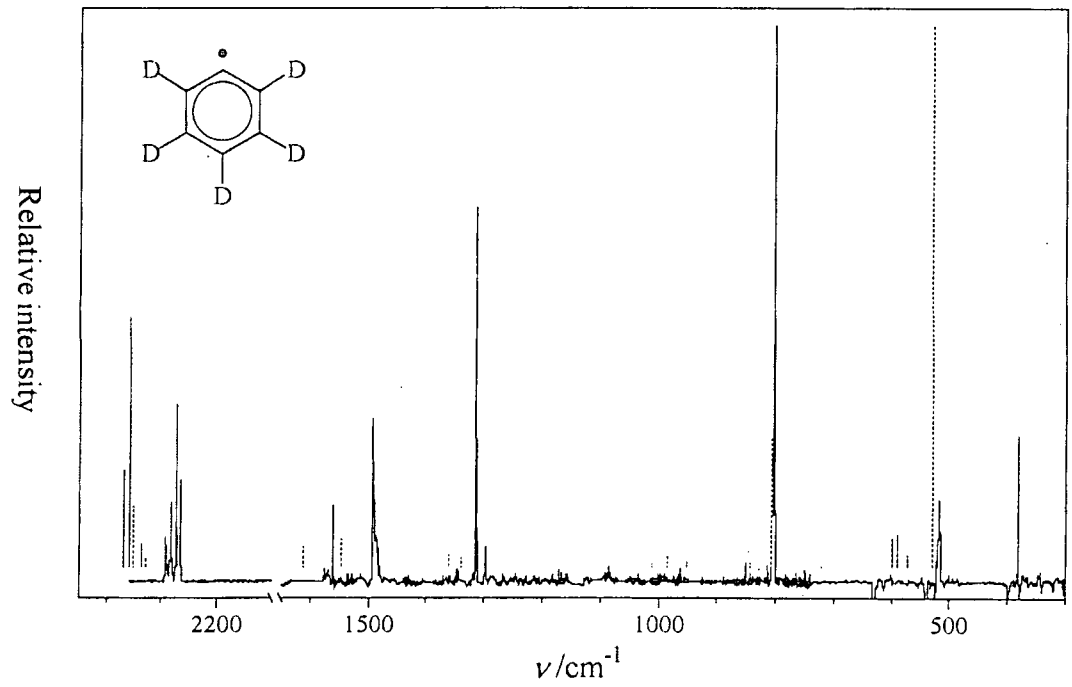
Relative intensity
D
D
D
D
D
2200
1500
1000
500
ν/cm^{-1}

Publications

- Eileen P. Clifford, Paul G. Wenthold, W. C. Lineberger, G. Barney Ellison, Cun X. Wang, Joseph J. Grabowski, Fernando Vila, and Kenneth D. Jordan, "Properties of Tetramethyleneethane (TME) as Revealed by Ion Chemistry and Ion Photoelectron Spectroscopy," J. Chem. Soc. Perkin Trans. 2, 1015-1022 (1998).
- Eileen P. Clifford, Paul G. Wenthold, W. Carl Lineberger, George A. Petersson, Katherine M. Broadus, Steven R. Kass, Shuji Kato, Charles H. DePuy, Veronica M. Bierbaum, and G. Barney Ellison, "The Properties of Diazocarbene [CNN] and the Diazomethyl Radical [HCNN] *via* Ion Chemistry and Spectroscopy," J. Phys. Chem. A **102**, 7100-7112 (1998).
- Eileen P. Clifford, Paul G. Wenthold, Roustam Gareyev, W. Carl Lineberger, Charles H. DePuy, Veronica M. Bierbaum, G. Barney Ellison, "Photoelectron Spectroscopy, Gas Phase Acidity, and Thermochemistry of *tert*-butyl hydroperoxide: Mechanism for the rearrangement of peroxyl radicals", J. Chem. Phys. **109**, 10293-10310 (1998).
- G. Barney Ellison, Adrian F. Tuck, and Veronica Vaida, "Atmospheric Processing of Organic Aerosols," J. Geophys. Res., **104**, 11633-11643 (1999).
- Michael J. Travers, Daniel C. Cowles, Eileen P. Clifford, G. Barney Ellison and Paul C. Engelking, "Photoelectron Spectroscopy of the CH_3N^- Ion," J. Chem. Phys. **111**, 5349-5360 (1999).
- Gregory J. Frost, G. Barney Ellison, and Veronica Vaida, "Organic peroxyl radical photolysis in the near-infrared: Effects on tropospheric chemistry," J. Phys. Chem. A, **103**, 10169-10178 (1999).
- Carl R. Kemnitz, G. Barney Ellison, William L. Karney, and Weston Thatcher Borden, "CASSCF and CASPT2 *Ab Initio* Electronic Structure Calculations Find Singlet Methylnitrene Is an Energy Minimum", J. Am. Chem. Soc. **122**, 122-124 (2000)]
- Jonathan C. Rienstra-Kiracofe, G. Barney Ellison, Brian C. Hoffman, and Henry F. Schaefer III, "The Electron Affinities of C_3O and C_4O," J. Phys. Chem. A **104**, 2273-2280 (2000).

Thermochemistry of Hydrocarbon Radicals: Guided Ion Beam Studies

Kent M. Ervin
Department of Chemistry/216
University of Nevada, Reno
Reno, Nevada 89557
Telephone: 775-784-6676
E-mail: ervin@chem.unr.edu

Project Scope

Gas phase negative ion chemistry methods are employed to determine enthalpies of formation of small hydrocarbon radicals that are important in combustion processes. Using guided ion beam tandem mass spectrometry, we measure collisional threshold energies of endoergic proton transfer and hydrogen atom transfer reactions of hydrocarbon molecules with negative reagent ions. In the absence of reverse activation energies, the measured threshold energies for proton transfer reactions yield the relative gas phase acidities. In an alternative methodology, competitive collision-induced dissociation of proton-bound ion–molecule complexes provides accurate gas phase acidities relative to a reference acid. Combined with the electron affinity of the R· radical, the gas phase acidity yields the RH bond dissociation energy of the corresponding neutral molecule, or equivalently the enthalpy of formation of the R· organic radical. The threshold energy for hydrogen abstraction from a hydrocarbon molecule yields its hydrogen atom affinity relative to the reagent anion, providing the RH bond dissociation energy directly. Electronic structure calculations are used to evaluate the possibility of potential energy barriers or dynamical barriers along the reaction path, and as input for RRKM model calculations.

Recent Progress

During the third year of this project, we finished work on competitive threshold collision-induced dissociation (TCID) of proton-bound dimers of simple alcohols with alkoxide, hydroxide, and fluoride anions. These measurements yield refined RO–H bond dissociation energies for ethanol, *iso*-propyl alcohol, and *tert*-butyl alcohol.[1] We recently reported the first experimental determination of the bond dissociation energy of diacetylene,[2] HC≡C–C≡CH. A study[3] of the endoergic hydrogen atom abstraction reaction of $S^-(^2P)$ with molecular hydrogen yielded new gas phase acidities for HS and H_2S.

Bimolecular endoergic proton transfer. Our previous work on bimolecular endoergic proton transfer reactions of F and Cl with H_2O and small alcohols[4,5] yielded threshold energies that were 5–9 kJ/mol higher than expected from literature gas phase acidities. This implies either that there are small reverse activation energies, which is not supported by ab initio calculations of the proton transfer surfaces, or that the usual threshold analysis that assumes that all internal degrees of freedom are active is inadequate. It is clear that vibrational energy of the reactants can promote reaction, but the new results[6] on a larger range of proton transfer test systems suggests that the rotational energy

does not. If we do not include the rotational energy distribution in the threshold analysis, agreement with literature gas phase acidities is regained.

Threshold collision-induced dissociation of proton-bound complexes. Because of these issues with threshold measurements of bimolecular proton transfer, we have developed an alternate experimental protocol, competitive TCID of proton-bound clusters such as shown below:

$$ROH \cdot F^- + Xe \rightarrow RO^- + HF + Xe$$
$$\rightarrow ROH + F^- + Xe$$

The threshold behavior for the two product channels are analyzed using a RRKM model that accounts for the energy-dependent product branching ratios.[7,8] The difference in threshold energies between the two channels yields the gas phase acidity of ROH relative to HF. A gas-phase acidity ladder is developed, shown in Figure 1, with multiple determinations of the alcohol acidities and anchored at both ends, to HF and H_2O. With remeasured electron affinities of the RO alkoxy radicals from the Lineberger group,[9] we have derived new accurate values for the O–H bond dissociation energies of the alcohols.[10] Values for *iso*-propyl alcohol and *tert*-butyl alcohol are slightly higher than previous values based on pyrolysis kinetics of ethers and peroxides.

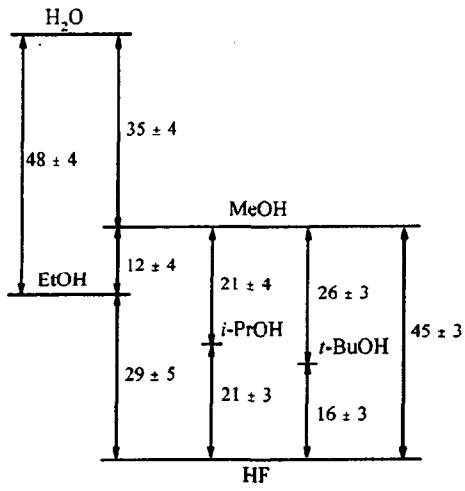

Figure 1. Gas-phase acidity ladder (kJ/mol) for the alcohols from competitive TCID measurements.

Sulfur anion chemistry for hydrogen atom abstraction. We have examined the endoergic hydrogen atom abstraction by S^- anions from molecular hydrogen,[3]

$$S^- + H_2 \rightarrow HS^- + H.$$

The reaction threshold energy can be related by well-known electron affinities to the bond dissociation energy of HS. Our value matches previous experiments, with small error bars related to the uncertain role of the hydrogen rotational energy and the S (^2P_J) spin-orbit states in promoting the abstraction reaction. This endoergic reaction occurs at the thermochemical threshold despite the existence of the strongly exoergic associative detachment channel,

$$S + H_2 \rightarrow H_2S + e .$$

Our CCSD(T) calculations of the reaction potential energy surfaces[3] show that there is an energy barrier for this channel, in agreement with previous experiments showing no associative detachment reaction at thermal energies.

It was hoped that hydrogen atom abstraction by S^- would be a general method for obtaining hydrocarbon bond energies. Unfortunately, in validation experiments on small alkanes and alkenes it was found that there are substantial reverse activation energies in some cases.[11]

Bond dissociation energy of diacetylene. We produce carbon cluster ions, C_n and C_nH (n = 3–8), which are believed to be linear chains in this size range, with a high voltage dc discharge using a graphite cathode, with hydrogen added in the discharge to make the C_nH^- ions, or with a microwave discharge with acetylene precursor gas. The ions are thermalized in our flow tube reactor source by

about 10^5 collisions with the helium and argon buffer gas mixture. We observe the endoergic proton transfer reaction,

$$C_4H^- + HCCH \rightarrow C_4H_2 + C_2H^-,$$

and find a 0 K threshold energy, $E_0 = 77 \pm 8$ kJ/mol. Using electron affinities from Neumark and coworkers,[12,13] this gives a lower limit for the bond dissociation energy of diacetylene, $D_0(HC_4–H) \geq 531 \pm 8$ kJ/mol. However, ab initio calculations of the reaction path for this proton transfer reaction show a double-well potential, which may lead to dynamic restrictions and cause the threshold energy to be higher (and the apparent bond energy lower) than the thermodynamic value.

As a alternative measurement, we used the competitive TCID method. The proton-bound complex of C_4H^- with acetaldehyde was prepared in the flow tube ion source. This complex undergoes collision-induced dissociation with xenon target gas to give the two possible proton-transfer products:

$$[HC_4^-\cdot\cdot H\cdot\cdot CH_2CHO] + Xe \rightarrow HC_4^- + CH_3CHO$$
$$\rightarrow HC_4H + {}^-CH_2CHO$$

The cross section data are shown in Figure 2. We model the competitive threshold data with RRKM theory, which gives the product branching ratio as a function of available energy.[7,8] Ab initio calculations are used to determine the transition state parameters for the two channels. In agreement with the observed crossing of the two product channels at about 0.9 eV, the lower-energy channel to form C_4H^- goes through a tight transition state for dissociation and the higher-energy channel has a loose transition state. The threshold energy difference is obtained by a least-squares fit of the data with the RRKM theory model. The extracted gas phase acidity difference between diacetylene and acetaldehyde is 18 ± 3 kJ/mol. Using the literature value for the gas phase acidity of acetaldehyde[14] and known electron affinities, we obtain[2] $D_0(HC_4–H) = 539 \pm 12$ kJ/mol, for which most of the uncertainty comes from the acidity of acetaldehyde. This value is the same or slightly smaller than the well-established dissociation energy of acetylene,[15] $D_0(HCC–H) = 551.2 \pm 0.1$ kJ/mol.

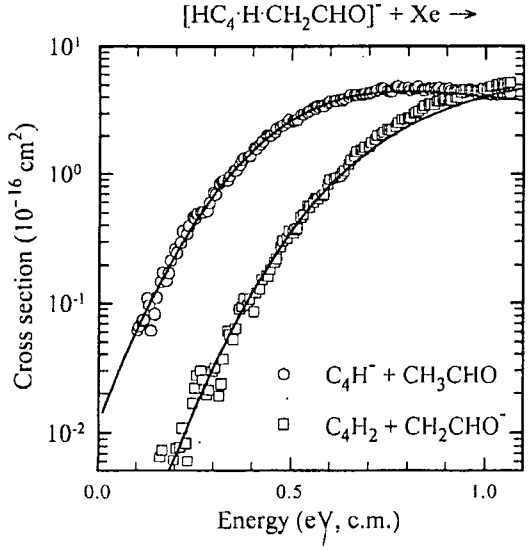

Figure 2. Competitive TCID cross sections. Lines show RRKM fits.

Future Plans

We are performing other proton transfer and TCID measurements with different proton transfer and hydrogen atom transfer reagents that hopefully will allow us to refine the bond energy of diacetylene, and to determine both first and second CH bond dissociation energies of longer $HC_{2n}H$ polyynes. We are also pursuing measurements of the kinetic energy release of products in the hydrogen atom transfer reactions, which can provide an independent experimental means to measure reverse activation energies. We are also collaborating with W. C. Lineberger to measure radical electron affinities and gas phase acidities of polycyclic aromatic hydrocarbons. Preliminary photoelectron spectra have been obtained for naphthide and corenene.

References

[1]V. F. DeTuri and K. M. Ervin, J. Phys. Chem. A **103**, 6911 (1999).

[2]Y. Shi and K. M. Ervin, Chem. Phys. Lett **318**, 149 (2000).

[3]K. Rempala and K. M. Ervin, J. Chem. Phys. **112**, 4579 (2000).

[4]V. F. DeTuri and K. M. Ervin, Int. J. Mass Spectrom. **175**, 123 (1998).

[5]V. F. DeTuri, M. A. Su, and K. M. Ervin, J. Phys. Chem. A **103**, 1468 (1999).

[6]V. F. DeTuri, Ph.D. Dissertation, University of Nevada, Reno, 1999.

[7]M. T. Rodgers, K. M. Ervin, and P. B. Armentrout, J. Chem. Phys. **106**, 4499 (1997).

[8]M. T. Rodgers and P. B. Armentrout, J. Chem. Phys. **109**, 1787 (1998).

[9]T. M. Ramond, G. E. Davico, R. L. Schwartz, and W. C. Lineberger, J. Chem Phys. **112**, 1158 (2000).

[10]V. F. DeTuri and K. M. Ervin, J. Phys. Chem. A **103**, 6911 (1999).

[11]K. Rempala, M.S.Thesis, University of Nevada, Reno, 1999.

[12]D. W. Arnold, S. E. Bradforth, T. N. Kitsopoulos, and D. M. Neumark, J. Chem. Phys. **95**, 8753 (1991).

[13]T. R. Taylor, C. Xu, and D. M. Neumark, J. Chem. Phys. **108**, 10018 (1998).

[14]S. G. Lias, J. E. Bartmess, J. F. Liebman, J. L. Holmes, R. D. Levin, and W. G. Mallard. 1988. Gas-Phase Ion and Neutral Thermochemistry. *J. Phys. Chem. Ref. Data* 17(Supplement 1).

[15]D. H. Mordaunt and M. N. Ashfold, J. Chem. Phys. **101**, 2630 (1994).

Publications, 1998-present

"Proton transfer between Cl and C_6H_5OH. O–H bond energy of phenol", V. F. DeTuri and K. M. Ervin, *Int. J. Mass Spectrom.* **175**, 123-132 (1998).

"Dynamics of endoergic bimolecular proton transfer reactions. F + ROH → HF + RO (R = H, CH_3, CH_3CH_2, $(CH_3)_2CH$, and $(CH_3)_3C$)", V. F. DeTuri, M. A. Su, and K. M. Ervin, *J. Phys. Chem. A.* **103**, 1468-1479 (1999).

"Orientational effects in the direct Cl^- + CH_3Cl S_N2 reaction at elevated collision energies: Hard-ovoid line-of-centers collision model", K. M. Ervin, *Int. J. Mass Spectrom.* **185/186/187**, 343-350 (1999).

"Competitive threshold collision-induced dissociation: Gas phase acidities and bond dissociation energies for a series of alcohols", V. F. DeTuri and K. M. Ervin, *J. Phys. Chem. A* **103**, 6911-6920 (1999).

"Microcanonical analysis of the kinetic method. The meaning of the 'effective temperature'", K. M. Ervin, *Int. J. Mass Spectrom.* **195/196**, 271-284 (2000).

"Gas phase acidity and C–H bond energy of diacetylene", Y. Shi and K. M. Ervin, *Chem. Phys. Lett.* **318**, 149-154 (2000).

"Collisional activation of the endoergic hydrogen atom transfer reaction S (^2P) + H_2 → SH + H", K. Rempala and K. M. Ervin, *J. Chem. Phys.* **112**, 4579-4590 (2000).

Low Energy Ion-Molecule Reactions

James M. Farrar
Department of Chemistry
University of Rochester
Rochester, NY 14627
E-mail: farrar@chem.rochester.edu

Program Scope

This project is devoted to studying the dynamics of the interactions of low energy ions important in combustion with small molecules and with liquid hydrocarbon surfaces. The first of these topics is a long-standing project in our laboratory devoted to elucidating the key features of potential energy surface topology that control chemical reactivity. The project provides detailed information on such concepts as the utilization of specific forms of incident energy, the role of preferred reagent geometries, and the disposal of total reaction energy into product degrees of freedom. We employ crossed molecular beam methods under single collision conditions, at collision energies from below one eV to several eV, to probe potential surfaces over a broad range of distances and interaction energies. In so doing, we test and extend dynamical models describing chemical reactivity, extending the predictive capabilities of theory in realistic systems, including combustion. We infer intimate details about the nature of collisions leading to chemical reaction by measuring the angular and energy distributions of the reaction products with vibrational state resolution. We employ the crossed beam low energy mass spectrometry methods that we have developed over the last several years. In the past year, we have made a significant transition in the nature of this program as we have begun to apply both the methods and concepts of gas phase dynamics to the study of interactions of low energy ions with liquid hydrocarbon surfaces. Those experiments are now operational, and we report on preliminary results below.

Recent Progress

Over the past year, we have completed a series of measurements in the $OH^- + D_2$ system, focusing special attention on isotope exchange and non-reactive scattering channels. We discussed preliminary results on that work at last year's Contractor's Meeting, and that work is now in press in the *Journal of Chemical Physics*. One of the most interesting results of that study is the appearance of specific modes of energy transfer in the nonreactive scattering. Especially at low energy, data for which are shown to the left, we observe that the product kinetic energy distributions for nonreactively scattered OH^- are structured and that the structures in the lab distributions are consistent

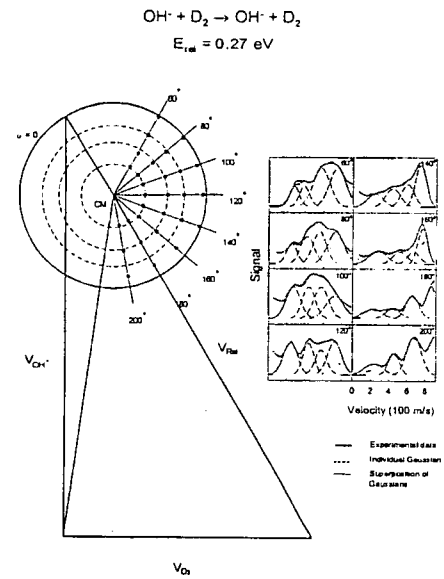

with the formation of OH^-/D_2 products with specific amounts of product rotational excitation. Although there is some correlation between the product rotational states we observe and the bending vibrational energy levels of the $[OHD_2^-]$ intermediate complex, theoretical work to sharpen this interpretation is necessary.

We have begun to apply the experimental techniques that have been developed in our laboratory over the years to the very interesting, but relatively unexplored problem of dynamics of gas-liquid surface interactions. Although the orthodox view of the combustion of fuel droplets[1] is that the actual combustion process is a homogeneous gas phase process, both the heating phase and the fuel evaporation phase are poorly understood and require an understanding of collision processes occurring at interfaces. Using methods developed by Nathanson and collaborators[2], we have begun experiments in which the O^- species collides with a freshly-prepared liquid surface of the long chain hydrocarbon squalane, $C_{30}H_{62}$. The initial experiments, performed at an angle of incidence of 45° with respect to the surface normal, involve measurements of nonreactive scattering distributions, in order to assess accommodation of kinetic energy at the droplet surface and the nature of direct collisions with surface molecules. In the left panel of the figure shown below, we plot results of angular distribution measurements at a fixed angle of incidence. The data show sharp, near-specular scattering, with a width that provides information about the role thermal motion plays in roughening the surface. The right panel shows kinetic energy distributions that reveal a very large energy transfer component to the surface, resulting in a high degree of local heating. More than 75% of the incident kinetic energy goes into internal degrees of freedom of the liquid. By measuring energy distributions as function of angle, a simple kinematic analysis[3] allows us to calculate the "effective surface" mass for the interaction of O^- with squalane. This rudimentary calculation suggests an effective mass of approximately 40 mass units, suggesting that the incoming ion interacts with the three methyl groups that orient themselves at the surface of the liquid.

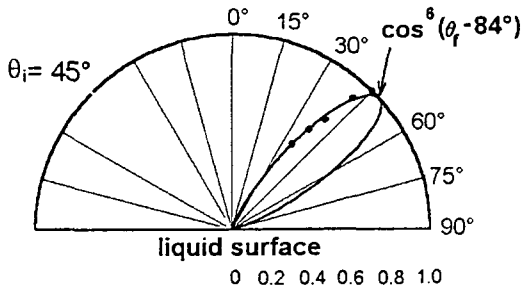

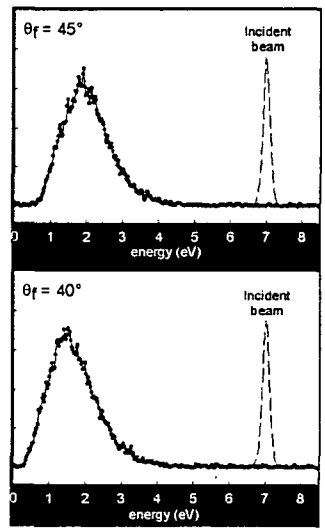

1 J. Warnatz, U. Maas, and R. W. Dibble, *Combustion* (Springer, Berlin, 1996), pp. 205-209

2 See, for example, M. E. Saecker, S. T. Govoni, D. V. Kowalski, M. E. King, and G. M. Nathanson, *Science*, **252**, 1421 (1991).

3 T. K. Minton, private communication

Future Plans

This work is just beginning to bear fruit, and we will continue a series of measurements with O^- and squalane over a collision energy range from 1 eV to 10 eV, with liquid surface temperatures varied over reasonable limits. In addition, we will examine collisions of other ions, including OH^-, C^+, and CH^+ to probe inelastic scattering and chemical reaction.

Publications, 1997-2000

M. A. Carpenter and J. M. Farrar, "Vibration State-Resolved Study of the $O^- + D_2$ Reaction: Low Energy Dynamics from 0.25 to 0.37 eV", *J. Phys. Chem.* **101**, 6475 (1997).

M. A. Carpenter and J. M. Farrar, "Vibration State-Resolved Study of the $O^- + D_2$ Reaction: Direct Dynamics from 0.47 to 1.20 eV", *J. Phys. Chem.* **101**, 6870 (1997).

M. A. Carpenter and J. M. Farrar, "Dynamics of Hydrogen Atom Abstraction in the $O^- + CH_4$ Reaction: Product Energy Disposal and Angular Distributions", *J. Chem. Phys.* **106**, 5951 (1997).

Susan Troutman Lee and James M. Farrar, "Vibrational State-Resolved Study of the $O^- + H_2$ Reaction: Isotope Effects on the Product Energy Partitioning", *J. Chem. Phys.* **111**, 7348 (1999).

Susan Troutman Lee, Elizabeth Richards O'Grady, Michael A. Carpenter, and James M. Farrar, "Dynamics of the Reaction of O^- with D_2 at Low Collision Energies: Reagent Rotational Energy Effects", *Phys. Chem. Chem. Phys.*, **2**, 679 (2000).

Susan Troutman Lee and James M. Farrar, "Dynamics of the $OH^- + D_2$ Isotope Exchange Reaction: Reactive and Nonreactive Decay of the Collision Complex", *J. Chem. Phys.* **112**, XXXX (2000).

Energy-Transfer Studies Using Tunable Picosecond Lasers

R. L. Farrow, D. A. V. Kliner, Fabio Di Teodoro,* and Thomas A. Reichardt*
Combustion Research Facility, P.O. Box 969, MS 9055
Sandia National Laboratories
Livermore, CA 94551-0969
Telephone: (925)294-3259, email: farrow@ca.sandia.gov

Program Scope

Spectroscopic diagnostic methods are widely used for quantitative detection of atoms and molecules in combustion studies and a variety of other applications. Our research involves the development of linear and nonlinear optical diagnostics, including basic investigations of the physical and chemical phenomena underlying the techniques. Many of the relevant processes occur at rates of 10^9 s^{-1} or faster, including collisional energy transfer, photo-ionization, and predissociation. We recently established a new laboratory equipped with subnanosecond lasers and fast (>1 GHz) detectors to allow direct measurements of these processes. Because laser sources with the requisite combination of spectral and temporal characteristics are not available commercially, we have developed tunable visible/uv lasers with 60-100 ps pulse durations and transform-limited linewidths. Two widely tunable, synchronized laser systems are planned for this facility, which is open to visiting researchers collaborating with CRF staff. As discussed below, the first experiments in the new laboratory have investigated rotational energy transfer of OH in collisions with Ar, N_2, O_2, and H_2O and electronic quenching of CO in a variety of bath gases at room temperature. Future experiments will extend these energy-transfer studies to higher temperatures. We will also investigate the use of picosecond lasers for minimizing the effect of the collisional environment on various optical diagnostic methods.

Recent Progress

Our original laser system consists of an amplified, frequency-doubled, distributed-feedback dye laser (DFDL). This source has sufficient spectral resolution (≈0.15 cm^{-1}) for excitation of individual molecular transitions, while providing pulses short enough (≈100 ps) to resolve processes occurring at atmospheric-pressure collision rates. For applications not requiring transform-limited pulses, we have developed a novel picosecond laser based on a spectrally filtered, broadband, dye oscillator (see Fig. 1). The oscillator and dye amplifiers are pumped by a short-pulse (115-ps fwhm) frequency-doubled, Nd:YAG laser operating at 20 Hz. The spectrally filtered laser has excellent passive wavelength stability and does not require active stabilization as does the DFDL. The bandwidth at the fundamental wavelength of 690 nm was measured to be 0.7 cm^{-1}. We obtained pulse durations of ≈85 ps and pulse energies of 6 mJ. With frequency tripling using BBO crystals, pulse energies of 0.4 mJ were obtained at 230 nm.

Two-photon excitation of CO via B–X(0,0) followed by detection of the B–A fluorescence is being used by several groups for both point measurements and imaging of CO in flames. Quantitative implementation of this detection scheme requires knowledge of the effective lifetime of the excited B state, which depends on the photoionization, collisional quenching, and spontaneous emission rates. The latter two processes are being investigated in the present work. We have measured the electronic quenching rate of CO $B\ ^1\Sigma^+$ by various collision partners, including noble gases (He, Ne, Ar, Kr, Xe) and molecular combustion species (H_2, H_2O, CH_4, CO_2, O_2, N_2) using time-resolved LIF. Using the frequency-tripled output of the filtered broadband dye laser, two-photon excitation at 230 nm from the CO ground $X\ ^1\Sigma^+$ state to the $B\ ^1\Sigma^+$ state in a room-temperature cell was performed. Blue-green fluorescence in the Angstrom bands ($B\ ^1\Sigma^+ \rightarrow A\ ^1\Pi$)

*Sandia Post-Doctoral Appointee

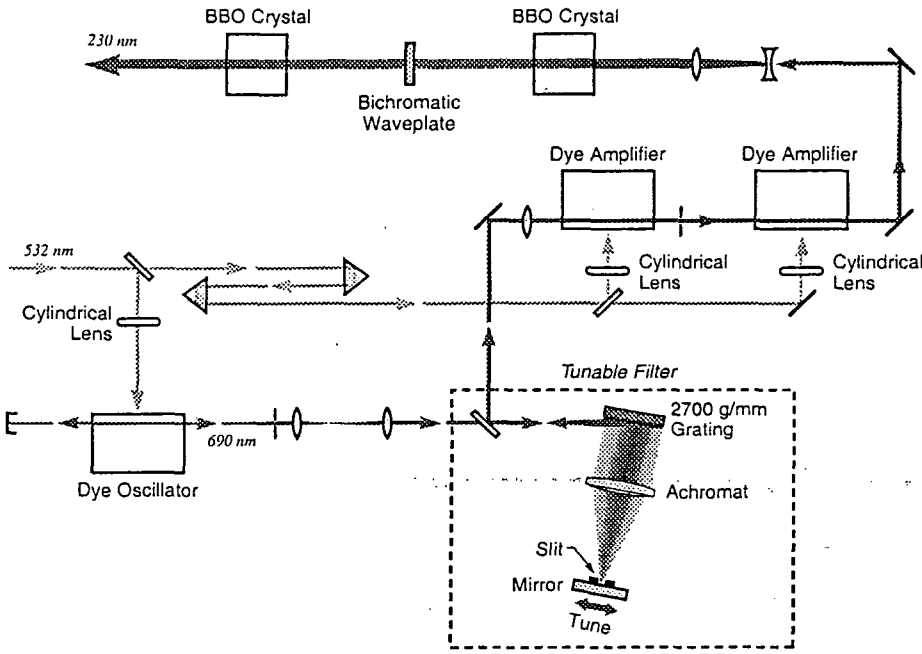

Fig. 1. Tunable picosecond laser system based on amplification of the filtered output of a broadband oscillator, followed by frequency tripling. The pump source has a pulse duration of 115 ps (fwhm). The filter design is based on the time-compensated filter of Hung *et al.*,[1] which does not temporally broaden the transmitted pulses.

was detected using a microchannel-plate photomultiplier tube (400-ps falltime) and a 1-GHz digital oscilloscope. Fluorescence quenching rates observed for various pressures of 12 quenching gases are plotted in Fig. 2. Quenching rate coefficients derived from these data range from 1.4×10^5 s^{-1} $Torr^{-1}$ (Ne) to 4.2×10^7 s^{-1} $Torr^{-1}$ (H_2O). Accurate values of the radiative lifetime (22.4 ns) and the self-quenching rate coefficient (8.1×10^6 s^{-1} $Torr^{-1}$) were obtained by modeling the nonlinear dependence of the fluorescence lifetime on CO pressure (caused by radiation trapping of the $B\,^1\Sigma^+ \rightarrow X\,^1\Sigma$ emission).

We have begun pump/probe measurements of state-to-state RET rate constants of OH in its ground electronic state. Using two single-mode lasers (a pulse-amplified, ring-dye laser and a single-mode, frequency-doubled Nd:YAG laser), we prepared selected rotational levels of OH $X\,^2\Pi_{3/2}$ with Λ-doublet- and spin-orbit-state resolution by stimulated Raman pumping (SRP). The ring-dye (Stokes) laser was tuned to excite rotational levels N''=1-6 in the v''=1 state via vibrational

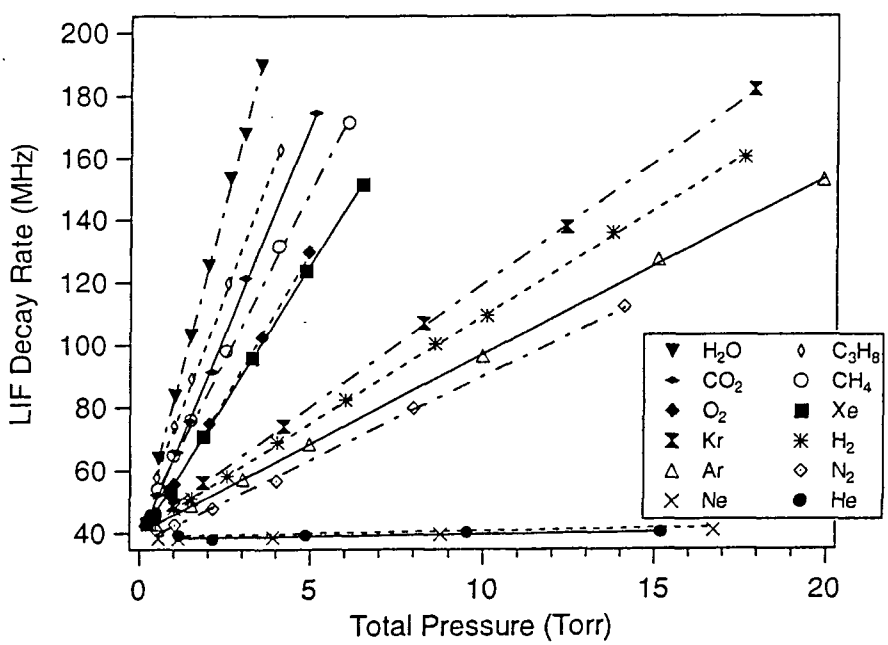

Fig. 2. Fluorescence decay rates at various pressures of the CO-quencher mixture (the CO pressure was held constant at 0.005 Torr). The lines are linear fits.

Q-branch transitions. Using the frequency-doubled DFDL, we detected $v''=1$ rotational level populations using LIF via A-$X(1,1)$ R_1-branch transitions. Figure 3 shows LIF spectra obtained by tuning the Stokes laser through resonance with the Λ-doubled $Q(5)$ Raman transition. With a small pump-probe delay, a LIF signal was detected when the e level was excited, seen as the indicated peak in the uppermost spectrum. When the f level was excited, (indicated by the second arrow in the spectrum) very little signal was seen since the R_1-branch LIF probes only e-level populations. With larger pump-probe delays, Λ-doublet-changing collisions moved population from the f to the e level, causing a peak to appear at the f excitation frequency (see additional spectra). By modeling the time-dependent populations extracted from the spectra, we determined Λ-doublet-changing and population-removal rate constants for the $N''=5$ level in collisions with H_2O. We have similarly determined these rate constants for $N''=2$–4, and 6. We have also observed inelastic, state-to-state transfer ($\Delta N''=+1$, and -1 to -4) by exciting the $N''=5$ level and probing levels with $N''=1$–6.

These results demonstrate for the first time that SRP can selectively excite a single parity level of an OH rotational level split by Λ-type doubling. Since our previous work demonstrated that Λ-doublet transfer is a significant RET channel (and hence contributes to pressure broadening of OH transitions), this ability will be crucial to measuring Λ-resolved state-to-state energy-transfer rates important in LIF diagnostics of OH. Several preliminary conclusions can already be drawn for collisions of OH with H_2O:

1) The state-to-state rate constants for nearly elastic ($\Delta N''=\Delta J''=0$) Λ-doublet-changing collisions are of comparable magnitude to the largest inelastic ($\Delta N''\neq 0$) rate constants.
2) The rate constant for Λ-doublet-changing elastic collisions decreases with increasing N''.
3) For inelastic collisions, there is generally a preference to conserve the Λ-doublet label, but this propensity decreases with increasing $\Delta N''$.

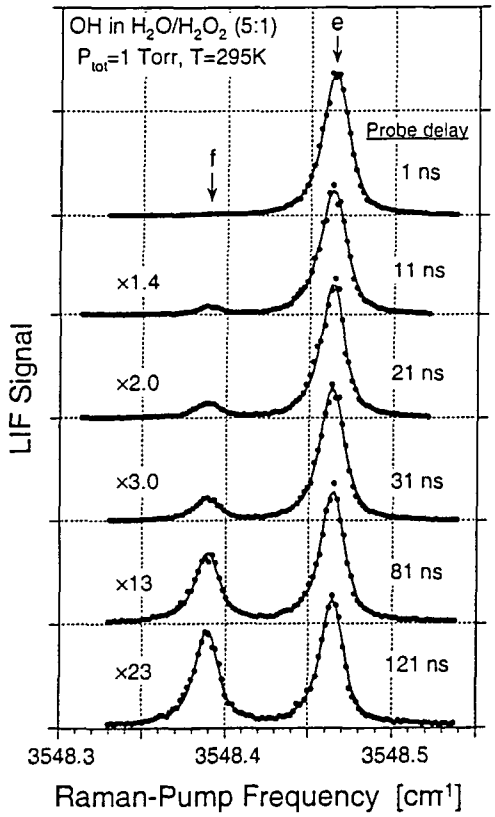

Fig. 3. LIF spectra recorded as the SRP Stokes laser was tuned through a vibrational Raman Q-branch transition of OH $X\ ^2\Pi_{3/2}$, sequentially exciting the two Λ-doublet levels of the $N''=5$ rotational level ($v''=1$). The LIF probe detected the population of the Λ-doublet e-level after various delays between the SRP and LIF pulses. The peak at the e excitation frequency results mainly from detection of the prepared population in e. The growth of a peak at the f excitation frequency results from detection of e population following Λ-doublet-changing transfer from $f \rightarrow e$. Note the indicated vertical scale multipliers. The decline of both peaks at large delays results from collisional removal of population to other rotational levels. The solid lines are fits using Lorentzian profiles.

Future work

Although surveys of CO quenching rates in flames have been reported,[2] additional data are needed over wider temperature ranges and for individual quencher species. We will determine the quenching rates of CO $B\ ^1\Sigma^+$ by various collision partners by measurement of LIF decays from $B\ ^1\Sigma^+ \rightarrow A\ ^1\Pi$ following excitation by a picosecond laser. The experiments will be performed using a furnace-heated, backscatter LIF cell at temperatures from 295 K to 1200 K. These data will be analyzed with the aim of developing a predictive model for the quenching cross-sections. Using a similar setup, we will also perform measurements of the effective cross section for photolyzing CO_2 to produce CO that constitutes an interference to TP-LIF at 230 nm. We will incorporate the quenching and photolysis models and an LIF rate-equation model (based on our recent results for absorption, broadening, and photoionization cross-sections) into a comprehensive LIF simulation code, which will be made available to interested users.

Our initial SRP experiments have demonstrated that this approach can provide quantitative state-to-state RET rate constants for OH in the ground electronic state with full Λ-doublet and spin-orbit state resolution. We plan to complete the room-temperature experiments to obtain the full RET rate matrix for collisions with H_2O. We will determine Λ-doublet-changing rates, Λ-doublet propensities for inelastic RET, and the dependence of both on initial and final spin-orbit state. We will investigate the validity of various RET models in the literature, which are used to interpret OH LIF spectra obtained in flames and other combustion environments. In addition, we will extend the SRP experiments to other bath gases relevant to combustion diagnostics (particularly N_2 and O_2) and to rare gases (for which theoretical calculations are available). We will later begin experiments to measure state-to-state rates at elevated temperatures.

References

1. N. D. Hung, Y. Segawa, Y. H. Meyer, P. Long, L. H. Hai, App. Phys. B **62**, 449-55 (1996).
2. See, for example, S. Agrup and M. Aldén, Appl. Spectrosc. **48**, 1118 (1994).

BES-Supported Publications, 1998-present

1. T. A. Reichardt, R. P. Lucht, P. M. Danehy, R. L. Farrow, "Theoretical Investigation of the Forward Phase-Matched Geometry for Degenerate Four-Wave Mixing Spectroscopy," J. Opt. Soc. Am. B **15**, 2566-2572 (1998).
2. D. A. V. Kliner and R. L. Farrow, "Measurements of Ground-State OH Rotational Energy-Transfer Rates," J. Chem. Phys. **110**, 412-22 (1999).
3. R. L. Farrow and D. J. Rakestraw, "Analysis of Degenerate Four-Wave Mixing Spectra of NO in a $CH_4/N_2/O_2$ Flame," Appl. Phys. B, **68**, 741-47 (1999).
4. M. D. Di Rosa and R. L. Farrow, "Cross Sections of Photoionization and Ac Stark Shift Measured from Doppler-free B←X (0,0) Excitation Spectra of CO," J. Opt. Soc. Am. B. 16, 861-70 (1999).
5. M. D. Di Rosa and R. L. Farrow, "Two-Photon Excitation Cross section of the $B \leftarrow X$ (0,0) Band of CO Measured by Direct Absorption," J. Opt. Soc. Am. B. **16**, 1988-94 (1999).
6. P. P. Yaney, D. A. V. Kliner, P. E. Schrader, and R. L. Farrow, "Distributed-Feedback Dye Laser for Picosecond UV and Visible Spectroscopy," Rev. Sci. Instr. **71**, 1296-1305 (2000).
7. M. D. Di Rosa and R. L. Farrow, "Temperature-Dependent Collisional Broadening and Shift of Q-branch Transitions in the $B \leftarrow X$ (0,0) Band of CO Perturbed by N_2, CO_2, and CO," accepted, J. Quant. Spectrosc. Radiat. Transfer, Feb. 2000.
8. T. A. Reichardt, F. Di Teodoro, R. L. Farrow, S. Roy, and R. P. Lucht, "Collisional Dependence of Polarization Spectroscopy with a Picosecond laser," submitted, J. Chem. Phys, March, 2000.

Spectroscopic and Dynamical Studies of Highly Energized Small Polyatomic Molecules

Robert W. Field and Robert J. Silbey
Massachusetts Institute of Technology
Cambridge, MA 02139

Program Definition. Our research program is centered on the development and application of experimental and theoretical methods for studying the dynamics (Intramolecular Vibrational Redistribution and Isomerization) and kinetics of combustion species. Our primary focus is the dynamics of acetylene at internal energies above which acetylene–vinylidene isomerization becomes feasible.

Recent Progress

Acetylene Unimolecular Dynamics. Based on our study of the normal isotopomer, $^{12}C_2H_2$, two new studies of the $^{13}C_2H_2$ and C_2HD isotopomers have been initiated. ~15 cm^{-1} and ~7 cm^{-1} resolution Dispersed Fluorescence (DF) data sets for the $^{12}C_2H_2$, $^{13}C_2H_2$, and C_2HD isotopomers have been recorded and carefully calibrated. Since all isotopomers share the same electronic potential surface, complementary diagnostic features of the same potential can be mapped out by studies of different isotopomers.

New DF data sets of $^{12}C_2H_2$ have been recorded, which cover the internal energy range from 15,000 cm^{-1} to well above the acetylene⇔vinylidene isomerization barrier (estimated to be at ~16,000 cm^{-1}). Analysis of these data sets has revealed that there exists a series of vibrational levels up to at least 18,000 cm^{-1} that can be labeled with normal mode quantum numbers. These account for only a small fraction of the states at high internal energy, but their existence implies that IVR is highly state-specific, with some states exhibiting virtually no IVR (on a time scale faster than ~1 ps, which corresponds to the ~7 cm^{-1} resolution of our spectra) even when acetylene-vinylidene isomerization is energetically feasible. This is in accord with predictions from our effective Hamiltonian model of DF spectra for internal energies up to 15,000 cm^{-1}.

By examining the nodal structures of eigenfunctions of the effective Hamiltonian of acetylene, we discovered a qualitative difference between the eigenfunctions at low internal energy and those at high internal energy. As expected, at low vibrational energy the eigenfunctions have well-defined nodal co-ordinates and can be assigned normal mode quantum numbers. More surprising is that at high internal energy (15,000 cm^{-1}), many of the eigenfunctions also have simple, well-defined nodal coordinates, but these nodal coordinates are qualitatively distinct from those at low internal energy, which are organized by the normal modes. That is, the eigenfunctions demonstrate the emergence of new types of stable vibrational motions at high internal energy.

Two specific classes of vibrational motion are demonstrated to be particularly important at high internal energy, as depicted in Figure 1. The first is called "local bend", which involves the bending of one hydrogen atom while the other remains co-linear with the CC bond. The second is called "counter-rotation", in which the two hydrogen atoms undergo circular motions on opposite ends of the CC bond. Both of these motions are a natural result of a transition from normal to local mode behavior in the bending dynamics of acetylene that occurs near 9,000 cm^{-1}. In summary, the normal mode model is a better zero-order representation at low energy, while the local mode model is superior at high energy.

The collaboration with Professors Howard Taylor (USC) and Christof Jung (UNAM), with the goal of exploiting quantum-classical correspondences, contributed to our understanding of the large-amplitude bending dynamics of acetylene. Classical periodic orbits calculated by Jung have revealed the same qualitative changes as the eigenfunction analysis. At low internal energy, the periodic orbits exhibit *trans* and *cis* bending motions;

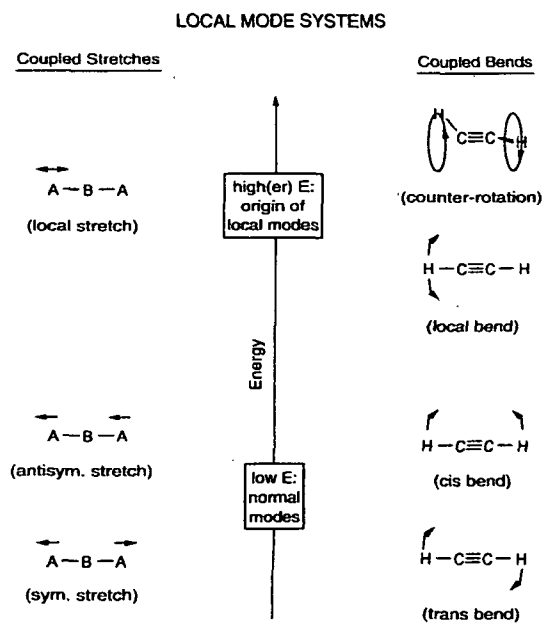

Figure 1. Comparison between the stretching modes and bending modes.

while in the >9,000 cm^{-1} regime, the periodic orbits bifurcate and form new classes of periodic orbits which correspond to local bend and counter-rotation motion.

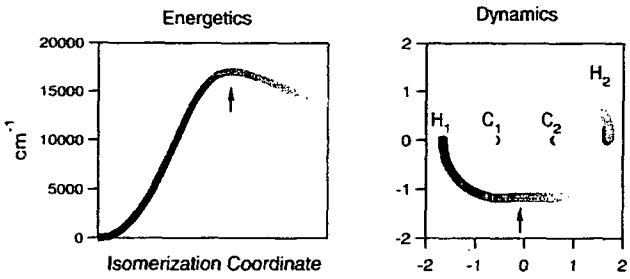

Figure 2. Energetics and dynamics of the acetylene⇔vinylidene isomerization

Figure 2 provides a closer look at the minimum energy isomerization pathway from acetylene to vinylidene, as represented by the Halonen, Child, and Carter surface. The left panel depicts the vibrational energy along the minimum energy isomerization path, and the right panel represents the vibrational motion along that path. The motion of each atom is depicted, and the shading of the lines in the right panel matches the shading in the left, such that black represents acetylene and light gray represents vinylidene. Note that hydrogen #2 moves very little during most of the isomerization motion from acetylene to the transition state, while hydrogen #1 bends well past 90°. That is, the approach to the isomerization transition state is well described as a local bend motion.

The overall picture that emerges from Figure 2 is that, although neither pure *trans* nor pure *cis* bend motions promote isomerization of acetylene to vinylidene, the large amplitude local bend motions, which have been demonstrated to be highly stable at ~15,000 cm^{-1}, are essential to isomerization.

The C_2HD molecule is of particular interest for the study of local mode motions. The CCH vs. CCD mass difference causes the *trans* and *cis* normal modes to be replaced by CCD and CCH localized normal modes. Consequently, local mode motions are expected to occur at much lower internal energy in C_2HD than in the symmetric isotopomers. In other words, the C_2HD molecule is intrinsically a local mode molecule.

However, there are complications in the study of C_2HD. In C_2H_2, the *trans* bending motion in the upper electronic state is symmetric with respect to inversion; while the *cis* bending motion in the ground electronic state is anti-symmetric; thus there will be no Franck-Condon allowed transitions from the *trans* bent electronic state to the *cis* bending vibrations in the ground electronic state (the *cis* bend is Franck-Condon dark). In fact, there is only one bright state per polyad. However, in the case of C_2HD, there will be multiple bright states in each polyad.

Figure 3 shows five DF spectra recorded from $2\nu_3'$, $4\nu_3'$, $\nu_2'+\nu_3'$, $\nu_2'+2\nu_3'$ and $2\nu_3'+\nu_6'$ of the first excited electronic state of C_2HD.

Despite the complicated appearance of the spectra, and the practical difficulties addressed above, we were able to assign normal mode quantum numbers to almost all peaks observed in the $4\nu_3'$ spectrum at internal energies below 10,000 cm^{-1}. However, although most sharp features are assignable in the $4\nu_3'$ DF spectrum, some weaker peaks do not coincide with any of the bright modes (CC stretch and both of the bends). We believe this is due to coupling of the CH bend with the CH stretch. This coupling is inconsistent with the expectation that IVR in C_2HD is non-existent. We are setting up a suitable effective Hamiltonian to describe the frequencies and relative intensities of the "dark" transitions.

Studies of $^{12}C_2H_2$ completed over the past year have resolved several questions raised by previous DF investigations. The "extra features", which cannot be associated with any set of polyad quantum numbers, are due to K-changing collisions. A pressure study of the DF by

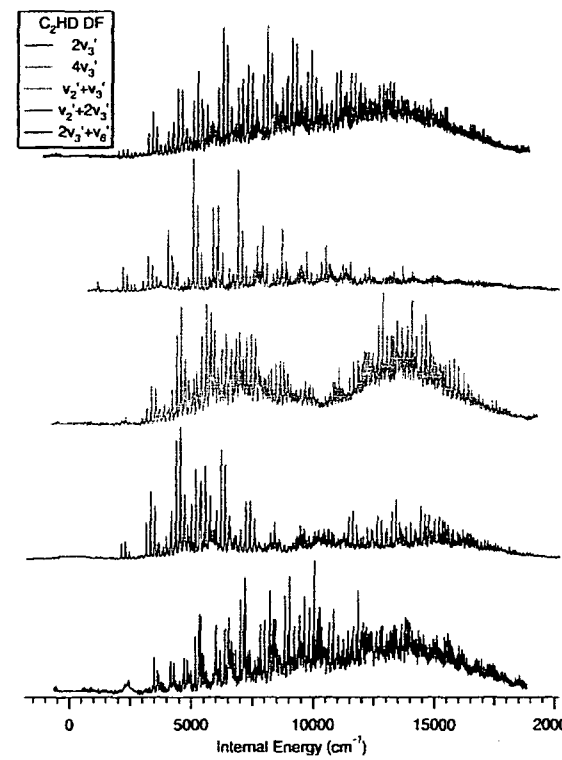

Figure 3. C_2HD DF spectra recorded from five vibrational levels of the first excited electronic state.

pumping a hotband indicates that the "unexpected transitions" are pressure-induced transitions that originate from various K in the upper state. The fact that it is pressure-dependent and that its intensity is distributed among $\Delta K=0$, ±1, ±2, ±3 transitions, determines that this is a collisional effect rather than a spectroscopic phenomenon. Higher quality DF spectra are being recorded to confirm our kinetic model of the K-changing process.

In principle, tunneling splittings can occur in spectra of $^{13}C_2H_2$ whereas one member of each tunneling doublet has zero statistical weight in $^{12}C_2H_2$. The size, energy positions, and mode-specificity of the tunneling splittings are sensitive to the height and shape of the acetylene⇔vinylidene barrier and to the locations of vinylidene vibrational levels. Our first step in the study of $^{13}C_2H_2$ has been to record high quality LIF and DF data sets. We have recorded LIF and DF spectra from 8 different vibrational intermediate levels and have used our pattern recognition algorithms (Extended Cross Correlation) to gain an overview of the short-time vibrational dynamics. Upon close inspection, the dynamics in $^{13}C_2H_2$ are noticeably *simpler* than the dynamics in $^{12}C_2H_2$. This implies a nearly complete absence of energy flow from the bend modes of $^{13}C_2H_2$ to the stretch modes. The stretch-bend interactions in $^{13}C_2H_2$ are "turned off" because one anharmonic interaction that is responsible for these interactions in $^{12}C_2H_2$ is detuned from resonance in $^{13}C_2H_2$. The relative simplicity of the dynamics in $^{13}C_2H_2$ is particularly noticeable above 15,000 cm^{-1}. This is beneficial for observing the sudden changes in the unimolecular dynamics that we expect will be related to isomerization. We have developed a $\mathbf{H}^{eff}$ model for the pure bending polyads in $^{13}C_2H_2$ based on the DF data obtained in the past year. The major features of the DF spectra remain unchanged up to ~18,000 cm^{-1}, indicating no major participation of vinylidene in the short-time dynamics (≤1 ps) sampled by the relatively low-resolution DF spectra. This is a preliminary result, higher resolution SEP spectra are required in order to probe the changes in vibrational dynamics which would accompany the onset of isomerization.

We have also completed a preliminary search for tunneling splittings in SEP spectra of $^{13}C_2H_2$ at ~22,000 cm^{-1}. The higher resolution and sensitivity of SEP relative to DF allow us to probe the influence of vinylidene at a much longer timescale. Nonetheless, this preliminary search, in which we observed hundreds of eigenstates, did not reveal any tunneling splittings, indicating that, for the states that we observed, vinylidene plays a negligible role in the dynamics for ~100 ps. Since this experiment probed the energy region >5000 cm^{-1} above the barrier to isomerization, it is clear that the rate of acetylene⇔vinylidene isomerization is highly mode-selective and mandates careful selection of the intermediate state in further SEP experiments.

We have collaborated with Professors Kevin Lehmann and Giacinto Scoles at Princeton in a search for tunneling splittings in highly excited vibrational states of $^{13}C_2H_2$. In these sub-Doppler IR-visible double resonance experiments, acetylene was seeded in a jet expansion and then excited from the vibrationless ground state to the $(1,0,1,0^{+1},0^{-1})$ level with a color center laser and subsequently excited to the $(2,1,3,1^{+1},1^{-1})$ level using a Ti:Sapphire laser. The (21311) state has not been observed previously, however, using our $\mathbf{H}^{eff}$ model for $^{13}C_2H_2$, we were able to accurately predict the position of the $(2,1,3,1^{+1},1^{-1})$ state. Within the ~17 MHz resolution of these experiments, no nuclear permutation splittings were observed.

Our collaboration with Professors John Hall and Jun Ye at JILA/NIST will allow us to investigate the $(2,1,3,1^{+1},1^{-1})$ level with much higher resolution. Previous Noise Immune Cavity Enhanced Optical Heterodyne Molecular Spectroscopy (NICE-OHMS) studies on acetylene have demonstrated a transit time limited resolution of 400 kHz and an integrated absorption sensitivity of 5.2×10^{-13} @ 1s. Over the past year a double resonance NICE-OHMS experiment has been designed to observe the nuclear permutation splittings in $^{13}C_2H_2$. The NICE-OHMS spectrometer, assembled for this double resonance experiment, has been tested on the 820 nm band of water and the noise equivalent integrated absorption sensitivity is clearly shot noise limited at 2×10^{-11}. The use of a higher finesse cavity, (for instance a finesse of 100,000 instead of the current finesse of 16,000) will push the sensitivity well into the 10^{-13} regime. Ms. Silva is currently locking a tunable IR diode laser onto a rovibrational line of the (10111) band and searching for the low-J levels in the (21311) level.

Kinetics and Spectroscopy of Combustion Free Radicals. Recently we have initiated collaboration with Professor William H. Green (MIT, Dept. of Chemical Engineering) with the goal of investigating some reactions of free radicals involved in combustion chemistry. The radicals are generated by flash photolysis and monitored using ultra-sensitive absorption-based techniques. Most of the spectra of these radicals have been poorly characterized, and some have never been observed in the gas phase. Initial survey scans and kinetic measurements are being performed using a Herriott cell. The Herriott cell mirrors cover a broad spectral range (240-350 nm) that is well suited for survey scans. The cell geometry also allows good overlap between the photolysis laser and the multipass probe beam.

Future Directions

A complete analysis of the $^{13}C_2H_2$ LIF spectra must be performed in order to understand and eventually exploit the anharmonic perturbations observed in those spectra. We have already identified perturbations in the LIF spectra of the $3\nu_3$' and $4\nu_3$' upper states. In addition, a global $\mathbf{H}^{eff}$, which takes into account all DF data obtained for $^{13}C_2H_2$, will be developed to complement the $\mathbf{H}^{eff}$ modeling of the pure-bending polyads.

SEP spectra will be recorded at other energies, using our knowledge of the short-time dynamics from the DF spectra, to identify states that might be expected to have the greatest probability of interacting with vinylidene on an observable timescale. For instance, SEP spectra recorded via the perturber of the $3\nu_3$' level, which we believe exhibits local bending structure at the vibrational turning points, may reveal large tunneling splittings. Execution of such a local bender "pluck" of S_0 acetylene will induce large amplitude motions directly along the minimum energy isomerization path and directly sample the isomerization transition state.

Recent DOE-Supported Publications (Since 1998)

1. J.P. O'Brien, M.P. Jacobson, J.J. Sokol, S.L. Coy, and R.W. Field, "Numerical Pattern Recognition in Acetylene Dispersed Fluorescence Spectra," J. Chem. Phys. 108, 7100-7113 (1998).

2. M.P. Jacobson, J.P. O'Brien, R.J. Silbey, and R.W. Field, "Pure Bending Dynamics in the Acetylene $\tilde{X}^1\Sigma_g^+$ State to 15,000 cm^{-1} of Internal Energy," J. Chem. Phys. 109, 121-133 (1998).

3. A.J. Marr, S.W. North, T.J. Sears, L. Ruslen, and R.W. Field, "Laser Transient Absorption Spectroscopy of Bromomethylene," J. Mol. Spectrosc. 188, 68-77 (1998).

4. M.P. Jacobson, J.P. O'Brien, and R.W. Field, "Anomalously Slow IVR in the $\tilde{X}^1\Sigma_g^+$ State above 10,000 cm^{-1}," J. Chem. Phys. 109, 3831 - 3840 (1998).

5. M.P. Jacobson, R.J. Silbey, and R.W. Field, "Local Mode Behavior in the Acetylene Bending System," J. Chem. Phys. 110, 845 - 859 (1999).

6. M.P. Jacobson, C. Jung, H.S. Taylor, and R.W. Field, "State-by-State Assignment of the Bending Spectrum of Acetylene at 15,000 cm^{-1}: A Case Study of Quantum-Classical Correspondence," J. Chem. Phys. 111, 600-618 (1999).

7. D.B. Moss, Z. Duan, M.P. Jacobson, J.P. O'Brien, and R.W. Field, "Observation of Coriolis Coupling Between $\nu_2+4\nu_4$ and $7\nu_4$ in C_2H_2 by Stimulated Emission Pumping Spectroscopy," J. Mol. Spectrosc. 199, 265-274 (1999).

8. M.P. Jacobson and R.W. Field, "Acetylene at the Threshold of Isomerization," J. Phys. Chem. (feature article).

9. M.P. Jacobson and R.W. Field, "Visualizing IVR: Expectation Values of Resonance Operators," Chem. Phys. Lett. 000, 0000-0000 (2000).

Laser Studies of Chemical Reaction and Collision Processes

George Flynn, Department of Chemistry, Columbia University
Mail Stop 3109, 3000 Broadway, New York, New York 10027
flynn@chem.columbia.edu

Introduction and Overview

Our work involves the study of energy transfer during collisions between molecules. We have focussed our attention on what we believe is the most important energy transfer problem in current studies of chemical and collision dynamics: the collisional cooling of molecules with "chemically significant" amounts of vibrational energy. A molecule with "chemically significant" energy is one that is sufficiently energetic to undergo chemical reaction or bond rupture. Our efforts are aimed at determining both a qualitative and quantitative picture of these collision processes. The qualitative picture constitutes the "mechanism" that controls relaxation for these high energy collision events. By mechanism we mean the quantum state resolved picture of the quenching process, which in turn provides insight into the relative effectiveness of short and long range forces in mediating the energy transfer. The quantitative measure of these collision events is contained in the energy transfer probability distribution function, P(E,E'), which gives the probability for transferring an amount of donor internal energy $\Delta E=E-E'$ during a collision.[1-14] A key result of our efforts over the past few years has been the development of a method to invert our data and obtain directly significant portions of this distribution function. P(E,E') is the *sine qua non* for meaningful comparisons between experimental data and theoretical calculations. Despite its close connection to theoretical descriptions of energy transfer processes, this function is also of enormous practical significance since kinetic models of unimolecular reactions employing master equation techniques require P(E,E') as input. We have had some notable successes in determining both the qualitative, mechanistic energy transfer picture for these high energy collision events and the quantitative shape and magnitude of P(E,E'). These results have left a number of well posed, unanswered questions about energy transfer for molecules with chemically significant amounts of energy that we plan to investigate over the next year. We hope through these experiments to improve our basic understanding of photochemical and photophysical phenomena and to provide dynamical and mechanistic data of fundamental interest for combustion and atmospheric reaction processes.

Our effort to understand and develop a quantum state resolved picture of the quenching of unimolecular reactions is one aspect of the more general field of vibrational energy transfer, the process by which molecules transfer their internal vibrational energy during collisions. The high energy of the quenched species distinguishes the present experimental studies from those vibrationally quantum state resolved investigations involving donors with only a few quanta of internal vibrational energy, carried out in the 1960's and 1970's at the dawn of the laser/energy transfer era. Similarly, the truly remarkable spectral resolution of the present experiments, providing as it does deep physical insight into the quenching process for these high energy molecules, distinguishes these investigations from most of the unimolecular reaction quenching studies carried out from roughly 1925 through 1990.

Experimental Approach

Our success in obtaining new levels of understanding about these high energy collision events has been based on the use of infrared diode lasers to probe the post collision quantum state population distributions of one of the collision partners.[1,12-14] The application of infrared diode lasers to study time-dependent dynamic events was developed in our

laboratory under D.O.E. sponsorship. The technique as applied to studies of dynamic molecular processes is by now well established. In brief, in the experimental approach that we are using to study these energy transfer processes, substrates (S) of essentially arbitrary complexity are produced with high energy by laser pumping methods. The collision processes that relax these highly excited S* molecules are investigated by probing the quantum states of the bath molecules B' produced by the interaction between S* and B. By using relatively simple bath molecules and sophisticated laser probe methods to follow the quantum states of B', the nature of the mechanism for energy loss by S* can be "seen" through the behavior of the (small) energy acceptor molecule, B. To fully analyze the deactivation process for such highly vibrationally excited molecules as S*, however, the level of excitation, rotational profiles and translational recoils of *different* vibrational modes of the bath acceptor B' are required. Furthermore, the amount of energy transferred to the rotational and translational degrees of freedom of the *ground* (vibrationless) state of the bath molecules is also of interest. Our technique is capable of supplying all of this extremely valuable information.

Results

Probing Angular Momentum Constraints

There are two kinds of angular momentum constraints for which we have tantalizing evidence in our experiments to date. These include constraints for both impulsive collisions and constraints for soft collisions mediated by long range forces.

For impulsive collisions we find a direct, linear correlation between the velocity recoil of a CO_2 bath molecule and its rotational angular momentum quantum number for collisions with highly excited pyrazine or methyl pyrazine having 5 eV of internal vibrational energy. Such behavior can be understood if the velocity recoil and angular momentum imparted to the bath molecule arise predominantly from an impact along the length of the CO_2 molecule at some distance **b** from the center of mass (the C atom). The impact in this case, of course, comes from one of the vibrating atoms on the highly excited donor molecule. Although there are a number of possible values for **b**, its maximum is set by the dimension of the molecule to be the distance from the center of mass to the end of the molecule, or roughly the CO bond distance for collisions of CO_2 with pyrazine and methyl pyrazine. For CO_2 this leads to observed final rotational states of the ground vibrationless state (00^00; J) with J values as high as 80 when the mean thermal J is roughly 22 (a maximum ΔJ of about 60)! Larger ΔJ values would require either harder hits or a "longer" molecule (larger distance from the center of mass to the end of the molecule).

The above simple concepts can be tested by a number of straightforward experiments. For example, CO is a molecule where the center of mass is about half way between the C and O atoms so that the maximum impact length, **b**, is about half the length of the C≡O triple bond [(1/2)1.128 Å ≈ 0.6Å]. This is slightly less than half the maximum **b** for the CO_2 molecule, which is roughly equal to the length of a C=O double bond [1.23 Å]. We have performed experiments to study this kind of process that can be described by the following equations:

$$C_4N_2H_4 + h\nu\ (248\ nm) \rightarrow C_4N_2H_4^{(E)}\ [Excitation]$$

$$C_4N_2H_4^{(E)} + CO\ (v=0;\ J',V') \rightarrow C_4N_2H_4^{(E-\Delta E)} + CO\ (v=0;J,V)\ [Quench]$$

$$CO(v=0;\ J,V)+h\nu\ (4.8\mu m) \rightarrow CO(v=1;J\pm1,V)[Diode\ Laser\ Probing]$$

In the first step, pyrazine ($C_4N_2H_4$) is excited by a pulsed laser to an electronically excited state from which it rapidly intersystem crosses/internally converts to ground electronic state, highly vibrationally excited pyrazine $\{C_4N_2H_4^{(E)}\}$ with roughly 5 eV of vibrational energy. In the second step a collision of this species with ground state CO distributed in a number of thermally occupied rotational levels, J', produces rotationally excited CO in the v=0 level with angular momentum J and velocity recoil V. Given the above impact parameter arguments, we expect the maximum J observed for CO(v=0, J) to be about 40 since the mean initial J is about 10 at room temperature, and the upper limit of ΔJ should, therefore, be around (0.6/1.23)60=29, where 60 is approximately the maximum ΔJ observed for the CO_2 case. 0.6 Å and 1.23 Å are, respectively, the maximum impact length, **b**, for CO and CO_2. We have already obtained preliminary results for this system that suggest this simple picture is qualitatively correct, but complete rotational state profiles as a function of temperature are needed to asses the accuracy of these early results. It should also be possible to test these concepts further by studying the maximum angular momentum produced in the bath molecule as a function of the excitation energy of the donor molecule. Higher energies correspond to larger amplitude motion for the atoms in the donor and hence a harder hit on the bath acceptor molecule. Pyrazine and methyl pyrazine have relatively broad absorption bands allowing studies at a number of different initial excitation energies, E.

Present and Future Experimental Program

Experimental laser studies of a series of interconnected bimolecular quenching processes are planned or in progress to study high energy collisions of large donor molecules with small bath molecules. The high resolution, high speed infrared diode laser probe technique will be used to determine final vibrational, rotational, and translational energy distributions for bath product species formed as the result of a collision event. In particular quantum state and velocity distributions will be determined for carbon monoxide, acetylene, and hydrogen halide molecules recoiling from high energy donor molecules such as 1-phenylpyrrole, pyrazine and methylpyrazine containing chemically significant amounts of vibrational energy (4-6 eV). In these experiments special emphasis will be placed on determining the nature and importance of angular momentum constraints that limit the total energy transfer in such collisions. These studies are expected to provide information about the impact parameter dependence of the mechanism for quenching unimolecular chemical reactions. In addition the quantitative shape and magnitude of the energy transfer distribution function, P(E,E'), will be extracted from these experiments, extending our recently successful initial efforts[1,12-14] to obtain this distribution directly from laboratory data. Model trajectory calculations will be performed to determine the dependence of the shape and magnitude of the energy transfer distribution function, P(E,E'), on initial collision excitation energy, E, on angular momentum, and on the initial quantum state of the bath molecule.

References

1. C. A. Michaels and G. W. Flynn, J. Chem. Phys. 106, 3558 (1997)
2. I. Oref and D.C. Tardy, Chem. Rev. 90, 1407 (1990)
3. J. R. Barker, J. D. Brenner, and B. M. Toselli, Advances in Chemical Kinetics and Dynamics, 2B, 393-425 (1995); John Barker, Ed.; JAI Press Inc., Greenwich, CT
4. I. Oref, Advances in Chemical Kinetics and Dynamics, 2B, 285-298 (1995); John Barker, Ed.; JAI Press Inc., Greenwich, CT
5. F. A. Lindemann, *Trans. Faraday Soc.*, 1922, 17, 598.
6. D. C. Tardy and B. S. Rabinovitch , Chem. Rev. 77, 369(1977)
7. J. Troe, J. Chem. Phys. 66, 4745 (1977).

8. T. Lenzer, K. Luther, J. Troe, R. G. Gilbert, and K. F. Lim, J. Chem. Phys. 103, 626 (1995).
9. J. Troe, J. Chem. Phys. 97, 288 (1992).
10. V. Bernshtein and I. Oref, J. Phys. Chem. 97, 12811 (1993).
11. J. R. Barker, J. Phys. Chem., 96, 7361(1992); J. D. Brenner, J. P. Erinjeri, and J. R. Barker, Chem. Phys. 175, 99 (1993).
12. Chris A. Michaels, Amy S. Mullin, Jeunghee Park, James Z. Chou, and George W. Flynn, J. Chem. Phys., 108, 2744-2755 (1998)
13. C. A. Michaels, Z. Lin, A. S. Mullin, H. C. Tapalian, and G. W. Flynn, J. Chem. Phys., 106, 7055-7071 (1997)
14. G. W. Flynn, C. A. Michaels, H. C. Tapalian, Z. Lin, E. Sevy, and M. A. Muyskens in *Highly Excited Molecules: Relaxation, Reaction, and Structure*, ACS Symposium Series, 678, pp134-149, Eds. Amy Mullin and George Schatz, American Chemical Society, Washington, DC, 1997

DOE Publications

(1998-2000)

1. Chris A. Michaels, Amy S. Mullin, Jeunghee Park, James Z. Chou, and George W. Flynn, "The Collisional Deactivation of Highly Vibrationally Excited Pyrazine by a Bath of Carbon Dioxide: Excitation of the Infrared Inactive (10^00), (02^00), and (02^20) Bath Vibrational Modes", J. Chem. Phys., 108, 2744-2755 (1998)

2. E.T. Sevy, M.A. Muyskens, S.M. Rubin, and G.W. Flynn, "Competition Between Photochemistry and Energy Transfer in UV-excited Diazabenzenes: I. Photofragmentation Studies of Pyrazine at 248 nm and 266 nm", J. Chem. Phys., 112, 5829-43 (2000)

3. E.T. Sevy, C. A. Michaels, H. C. Tapalian, and G.W. Flynn, "Competition between Photochemistry and Energy Transfer in UV-excited Diazabenzenes: II. Identifying the Dominant Energy Donor for 'Supercollisions'", J. Chem. Phys., 112, 5844-51 (2000)

4. George W. Flynn, "Energy Transfer in Gases", Encyclopedia of Chemical Physics and Physical Chemistry, in press

5. E. T. Sevy, Seth Rubin, Z. Lin, and G. W. Flynn, "Translational and Rotational Excitation of the $CO_2(00^00)$ Vibrationless State in the Collisional quenching of Highly Vibrationally Excited 2-Methylpyrazine: Kinetics and Dynamics of Large Energy Transfers", J. Chem. Phys. (accepted)

6. Jack M. Preses, Christopher Fockenberg, and George Flynn, "A Measurement of the Yield of Carbon Monoxide from the Reaction of Methyl Radicals and Oxygen Atoms", (submitted)

7. E. T. Sevy, M. A. Muyskens, Z. Lin, and G. W. Flynn, "Competition between Photochemistry and Energy Transfer in UV-excited Diazabenzenes: III. Photofragmentation, Quenching, and "Supercollisions" in 2-Methylpyrazine", (submitted)

Quantitative Imaging Diagnostics for Reacting Flows

Jonathan H. Frank and Phillip H. Paul
Combustion Research Facility
Sandia National Laboratories, MS 9051
Livermore, CA 94551
jhfrank@ca.sandia.gov

Program Scope

The primary objective of this project is the development and application of laser-based imaging diagnostics for studying reacting flows. Imaging diagnostics provide temporally and spatially resolved measurements of species, temperature, and velocity distributions over a wide range of length scales. Multi-dimensional measurements are necessary to determine spatial correlations, scalar and velocity gradients, flame orientation, curvature, and connectivity. Our current efforts focus on planar laser-induced fluorescence (PLIF) techniques for probing the detailed structure of isolated flow-flame interactions. These basic interactions are of fundamental importance in understanding the coupling between turbulence and chemistry in turbulent flames. These studies have required the development of a new suite of imaging diagnostics, to measure key species in the hydrocarbon-chemistry mechanism as well as to image rates of reaction.

Recent Progress

Recent research has continued to emphasize the development of novel PLIF diagnostics for probing the detailed structure of reaction zones during flow-flame interactions. The coupling of measurements with simulations remains an essential element of this program. Research activities have included the following: i) An initial demonstration of simultaneous OH/CO PLIF for reaction-rate imaging. ii) An initial study of a new imaging diagnostic for CH_3O to provide insight into carbon conversion through low-temperature oxidation pathways. iii) Measurements and modeling of quenching processes in CH_2O and CO for improving the quantitative interpretation of PLIF signals from these molecules.

Reaction-rate imaging An initial demonstration of joint CO/OH PLIF imaging shows promise for measuring the forward reaction rate of the reaction CO+OH $\Rightarrow$ CO_2 + H. This reaction represents the primary pathway for the formation of CO_2 in a methane-air flame. The forward rate can be written $R_f = n_{OH} n_{CO} k_f(T)$, where n is molecular number density, and the forward rate constant is $k_f(T) \propto T^{1.5} e^{-E/RT}$, where T is temperature and E is the activation energy. The basic concept of the diagnostic involves using the product of simultaneous OH and CO PLIF measurements to obtain a signal that is proportional to R_f. The product of LIF signals from OH and CO can be approximated by $S_{fOH} S_{fCO} \propto n_{OH} n_{CO} (g_{OH}(T) g_{CO}(T))$, where the temperature dependence of the LIF signals is represented by $g(T)$. The exact functional dependence of $g(T)$ depends on the particular transition(s) employed, the spectral characteristics of the detection system, and the temperature dependence of the quenching cross section. For reaction-rate imaging, the strategy is to select pump/detection schemes such that $g_{OH}(T) g_{CO}(T) \propto k_f(T)$. The temperature dependence of OH LIF is well characterized, and thus $g_{OH}(T)$ is known for a given pump/detection scheme. However, the temperature dependence of two-photon CO LIF is not well understood and is a current limitation to this technique. In our initial investigation,

$g_{CO}(T)$ was estimated using key observations from published data combined with experimental results of R. Farrow. Estimates using laminar flame calculations indicate that it is possible to choose a combination of pump/detection schemes for CO and OH PLIF such that $g_{OH}(T)g_{CO}(T) \propto k_f(T)$.

C_2 imaging* In performing CO imaging, Swan-band emission from laser-created C_2* presents a significant fluorescence interference. This is a known interferent traditionally attributed to photolysis of acetylene. To obtain quantitative CO results, it is necessary to take additional images of this emission to correct the CO images. These background LIF correction images are in fact of relatively high signal and quality. Dispersed LIF spectra of the laser-induced C_2* produced in a methane-air flame showed emission only from the first few vibrational levels of the *d*-triplet. This observation, combined with a consideration of the energies involved appears to preclude acetylene as the source (requiring three-photon excitation that would show emission from higher states of C_2* as well as from CH*). Of the other potential sources in the flame only vinyl radical satisfied both the issues of energy vs. emitting states and spatial location. The likely mechanism is a near-resonant 1+1 photon process through a state that predissociates to excited vinylidene. This suggests that it may be possible to obtain single-pulse PLIF images of vinyl radical that would offer unique information as to the flux of carbon through $C_{(2)}$ pathways. Efforts are underway to confirm this mechanism.

Planar LIF imaging of polyatomic species To quantify PLIF images requires knowledge of the temperature and collisional bath dependencies inherent in the LIF signal. In PLIF, the objective is to select an excitation/detection strategy to minimize these effects. For polyatomic species, these issues are significant considerations in image interpretation. However, if these dependencies are known, then direct comparisons to model results can be made by mapping the model results into LIF signal. A significant effort in the laboratory has been directed at measurement and modeling of collisional quenching cross-sections. Experimental studies of dispersed CH_2O LIF spectra at 300K and under flame conditions were recorded and analyzed to better understand the relative effects of excited state VET and collisional quenching, and to obtain rate coefficient data. These data were used to construct a more accurate model of the CH_2O LIF signal.

Methoxy-radical imaging Diagnostic development efforts have included an initial investigation of a new PLIF imaging diagnostic for CH_3O. Data on methoxy provide unique insight into carbon conversion through low-temperature oxidation pathways. The technique has been applied to imaging in both methane- and dimethylether-air flames. PLIF images taken in a steady laminar methane-air flame show significant differences between measurement and model regarding both methoxy concentration and spatial profile.

New Laboratory Construction Completed The new Advanced Imaging Laboratory in CRF Phase II was completed during the past year. This laboratory represents the state-of-the-art in imaging diagnostics capabilities. A broad range of laser diagnostics can now be implemented using a variety of lasers, including Nd:YAG-pumped optical parametric oscillators (OPO), excimer-pumped dye laser systems, and an injection-seeded excimer laser. Multiple UV-sensitive image intensified CCD cameras are available for image acquisition. Combinations of lasers and detectors can be used at three test stations, which accommodate a wide range of burners and flow configurations. The new facility provides increased opportunities for visitor interactions.

Future Plans

In the near term, we will continue to expand our studies of flow-flame interactions in highly reproducible, building-block flames using novel laser-based imaging diagnostics. The longer-term goals are to use imaging diagnostics to apply our understanding of these building-block flames to turbulent flow-flame interactions. In all of these endeavors, we will strive to couple our experimental measurements with simulation and modeling efforts.

Diagnostics Development We plan to continue the development of diagnostics that provide imaging measurements of reaction-rates and heat-release rates. Further studies using HCO, CH_2O/OH, and CO/OH measurements are planned in reproducible flow-flame interactions. In addition, we plan to investigate techniques for instantaneous images of reaction rates in turbulent flames.

The quantitative interpretation of CO PLIF images is limited in part by a lack of knowledge about quenching processes. To provide more quantitative CO imaging measurements, we plan to investigate the species-specific temperature dependence of CO quenching in collaboration with R. Farrow.

Plans are underway to extend a multi-year collaborative effort between Yale University, The University of Sydney, and Sandia to develop techniques for mixture fraction imaging. The primary motivation for developing such a diagnostic is to provide information on flame structure and scalar dissipation, which is determined from the gradient of the mixture fraction. While considerable progress has been made in developing schemes for obtaining images of mixture fraction in both H_2 and CH_4 flames, there remain challenges that need to be addressed for further use of these techniques. We plan to continue pursuing a mixture fraction imaging technique that can be verified with the line Raman/Rayleigh/LIF measurements performed with R. Barlow in Sandia's Turbulent Combustion Laboratory. One of our goals is to obtain mixture fraction imaging measurements in the series of flames being used for model validation in the Turbulent Non-premixed Flame (TNF) Workshop. A comparison of these measurements with large eddy simulations (LES) could provide guidance in developing subgrid scale models. Experiments will be performed in collaboration with M. Long of Yale University.

Flame-Vortex Interactions Further studies on flame-vortex interactions will extend the range of operating conditions to examine the effects of N_2 dilution levels as well as vortex size and speed. Additional measurements will include joint CO/OH PLIF imaging, and particle-imaging velocimetry. Experiments will continue to be coupled with numerical simulations by H. Najm.

Effects of Transient Strain The combined effect of unsteady strain and curvature complicates our efforts to resolve discrepancies between computations and experiments of flame-vortex interactions. To isolate the effect of transient strain, we plan to perform a series of measurements in a pulsed opposed flow burner.

Triple Flames Our efforts to understand fundamental flame structures and their interaction with unsteady flows will include an investigation of triple flames. Triple flames occur when a flame propagates through a fuel-concentration gradient, and they may play an important role in the stabilization of non-premixed and partially premixed lifted flames. In collaboration with R. Schefer, we will conduct a detailed investigation of triple flames using a laminar triple-flame burner. We plan to implement reaction-rate and heat-release rate diagnostics in this laminar triple-flame burner. These experiments may help to define an observable signature for a triple-flame that could be used to identify their presence and structure in turbulent flames. Experimental investigations will be coupled with numerical simulations by J. Chen and H. Najm.

DOE Supported Publications

J. H. Frank and R. S. Barlow, "Simultaneous Rayleigh, Raman, and LIF measurements in turbulent premixed methane-air flames," *Twenty-Seventh Symposium (International) on Combustion*, The Combustion Institute, Pittsburgh, 1998, pp. 759-766.

R. S. Barlow and J. H. Frank, "Effects of turbulence on species mass fractions in methane/air jet flames," *Twenty-Seventh Symposium (International) on Combustion*, The Combustion Institute, Pittsburgh, 1998, pp. 1087-1095.

P. A. Nooren, M. Versluis, T. H. van der Meer, R. S. Barlow, and J. H. Frank, "Raman-Rayleigh-LIF measurements of temperature and species concentrations in the Delft piloted turbulent jet diffusion flame," accepted to *Applied Phys. B.*

J. H. Frank, R. S. Barlow, and C. Lundquist, "Radiation and nitric oxide formation in turbulent nonpremixed jet flames," *Twenty-Eighth Symposium (International) on Combustion*, The Combustion Institute, (Edinburgh, Scotland, July 30-August 4, 2000), accepted.

H. N. Najm, P. H. Paul, C. J. Mueller, and P. S. Wyckoff, "On the Adequacy of Certain Experimental Observables as Measurements of Flame Burning Rate," *Combust. Flame*, 113:312-332 (1998).

H. N. Najm, O. M. Knio, P.H. Paul, and P. S. Wyckoff, "A Study of Flame Observables in Premixed Methane-Air Flames," *Combust. Sci. Technol.* 140:369-403 (1999).

P. H. Paul and H. N. Najm, "Planar Laser-Induced Fluorescence Imaging of Flame Heat Release Rate," *Twenty-Seventh Symposium (International) on Combustion*, The Combustion Institute, Pittsburgh, 1998, pp. 43-50.

P. H. Paul and J. Warnatz, "A Re-evaluation of the Means Used to Calculate Transport Properties of Reacting Flows," *Twenty-Seventh Symposium (International) on Combustion*, The Combustion Institute, Pittsburgh, 1998, pp. 495-504.

H. N. Najm, P. H. Paul, O. M. Knio, and A. McIlroy, "A Numerical and Experimental Investigation of Premixed Methane-Air Flame Transient Response," *Twenty-Eighth Symposium (International) on Combustion*, (Edinburgh, Scotland, July 30-August 4, 2000) submitted.

J. E. Rehm and P. H. Paul, "Reaction Rate Imaging," *Twenty-Eighth Symposium (International) on Combustion*, (Edinburgh, Scotland, July 30-August 4, 2000) submitted.

W. T. Ashurst, H. N. Najm and P. H. Paul, "Chemical Reaction and Diffusion: A Comparison of Molecular Dynamics Simulations with Continuum Solutions," *Combust. Theory. Model.* submitted.

MECHANISM AND DETAILED MODELING OF SOOT FORMATION

Principal Investigator:Michael Frenklach

Department of Mechanical Engineering
The University of California
Berkeley, CA 94720-1740

Phone: (510) 643-1676; E-mail: myf@me.berkeley.edu

Project Scope: Soot formation is one of the key environmental problems associated with operation of practical combustion devices. Mechanistic understanding of the phenomenon has significantly advanced in recent years, shifting the focus of discussion from conceptual possibilities to specifics of reaction kinetics. However, along with the success of initial models comes realization of their shortcomings. The project focuses on fundamental aspects of physical and chemical phenomena critical to the development of predictive models of soot formation in combustion of hydrocarbon fuels, as well as on the computational techniques for development of predictive reaction models and their economical application to CFD simulations. The work includes theoretical and numerical studies of gas-phase chemistry of gaseous soot particle precursors, soot particle surface processes, particle aggregation into fractal objects, and development of economical numerical approaches to reaction kinetics.

Recent Progress:

Scaling and Efficiency of PRISM in Adaptive Simulations of Turbulent Premixed Flames (with J. B. Bell, N. J. Brown, M. S. Day, J. F. Grcar, R. M. Propp, and S. R. Tonse).

The dominant computational cost in modeling turbulent combustion phenomena numerically with high fidelity chemical mechanisms is the time required to solve the ordinary differential equations associated with chemical kinetics. One approach to reducing that computational cost is to develop an inexpensive surrogate model that accurately represents evolution of chemical kinetics. One such approach, PRISM (Piecewise Reusable Implementation of the Solution Mapping), develops a polynomial representation of the chemistry evolution in a local region of chemical composition space. This representation is then stored for later use. As the computation proceeds, the chemistry evolution for other points within the same region are computed by evaluating these polynomials instead of calling an ordinary differential equation solver. If initial data for advancing the chemistry is encountered that is not in any region for which a polynomial is defined, the methodology dynamically samples that region and constructs a new representation for that region. The utility of this approach is determined by the size of the regions over which the representation provides a good approximation to the kinetics and the number of these regions that are necessary to model the subset of composition space that is active during a simulation. In the present study, we tested further the PRISM methodology by applying it to simulations of tow-dimensional turbulent premixed hydrogen flames. We considered a range of turbulent intensities ranging from weak turbulence that has little effect on the flame to strong turbulence that tears pockets of burning fluid from the main flame. For each case, we explored a range of sizes for the local regions and determine the scaling behavior as a function of region size and

turbulent intensity. The results indicate that the range of chemical compositions is restricted to a low-dimensional subset of chemical compositions (a 2- to 3-dimensional manifold) and that the region can be effectively represented by a modest number of hypercubes. Conservative choice of hypercube size allows high-fidelity simulation with more than an order of magnitude reduction in computational cost.

Ab Initio Study Of Naphthalene Formation By Addition Of Vinylacetylene To Phenyl (with N. W. Moriarty)

Reaction pathways leading to the formation of naphthalene by the addition of vinylacetylene to phenyl were examined using density functional theory B3-LYP functionals with the standard triple-zeta basis set, 6-311G(d,p). The chemically-activated reaction dynamics were examined employing time-dependent solution of master equations. The addition of phenyl to the triple bond of vinylacetylene was computed to be relatively slow, due to a substantial energy barrier of the intermediate double-bond rotation. Addition of phenyl to the other end of a vinylacetylene molecule produced more favorable results. Yet, the most promising pathway appeared to be the two-step reaction sequence via the formation of a phenyl-butatriene molecule. The reaction rate evaluated for this pathway is very close to the value tested in prior flame simulations that demonstrated a dominant character of such a step for naphthalene formation. This indicates that the formation of naphthalene from phenyl and vinylacetylene may play a significant role in flame modeling of aromatic growth, and that the more favorable mechanism of the reaction may be a two-step sequence via the formation of a stable molecular intermediate rather than a "single" chemically-activated path. The time-dependent solution of master equations revealed that at flame conditions typical of aromatic growth the reaction system does not reach a steady state on a time of scale of 1 ms, suggesting that dynamics of energy redistribution in such "elementary" reaction systems may need to be treated with inclusion of bimolecular reactions between energized adducts and gaseous partners.

Propargyl Radical: An Electron Localization Function Study (with X. Krokidis, N. W. Moriarty, and W. A. Lester, Jr.)

Bonding in the C_3H_3 radical has been determined using the topological analysis of the electron localization function (ELF) calculated with various wavefunctions (HF, LSDA, MP2, CASSCF, QCISD, BLYP, B3LYP). Not only is ELF independent of quantum chemical approximation, but also produced topologically equivalent molecular partitions. The ELF partition of space into localization domains provides an objective characterization of bonding in C_3H_3, supporting a resonance description of almost equal contributions of propargyl and allenyl forms. Moreover, it explains the reported difference between the frequencies of the in-plane and out-of-plane bending modes ($\angle C_{(2)}C_{(3)}H_{(3)}$) arising from the topology of the $C_{(2)}C_{(3)}$ bonding region.

On Unimolecular Decomposition of Phenyl Radical (with H. Wang, A. Laskin, and N. W. Moriarty)

The unimolecular decomposition of the phenyl radical leading to ortho-benzyne formation and the concerted decomposition of ortho-benzyne yielding acetylene and diacetylene were examined

by ab initio quantum chemical calculations using the Complete Active Space Self-Consistent Field approach, Rice-Ramsperger-Kassel-Marcus calculations, and numerical simulation of published shock-tube data of nitrosobenzene and benzene pyrolysis. The rate constant of C–H fission in the phenyl radical was determined from the rates of H-atom production during the pyrolysis of nitrosobenzene for $1450 < T < 1730$ K and $1.5 < p < 7$ atm. The experimental rate constant was successfully reproduced and extrapolated with RRKM calculations. It was demonstrated that a revised Bauer-Aten mechanism of the thermal decomposition of benzene, featuring H-ejection from phenyl followed by the concerted decomposition of o-benzyne, is capable of reproducing the published data of benzene decomposition in a single-pulse shock tube.

The Effect of Stoichiometry on Vortex Interactions (with J. B. Bell, N. J. Brown, M. S. Day, J. F. Grcar, and S. R. Tonse)

The interaction of a vortex pair with a premixed flame serves as an important prototype for premixed turbulent combustion. In this study, we investigated the interaction of a counter-rotating vortex pair with an initially flat premixed methane flame. We focussed on characterizing the mechanical nature of the flame-vortex interaction and on the features of the interaction strongly affected by fuel equivalence ratio, ϕ. We compared computational solutions obtained using a time-dependent, two-dimensional adaptive low Mach number combustion algorithm that incorporated GRI-Mech 1.2 for the chemistry, thermodynamics and transport of the chemical species. We found that the circulation around the vortex scours gas from the preheat zone in front of the flame, making the interaction extremely sensitive to equivalence ratio. For cases with $\phi \approx 1$, the peak mole fraction of CH across the flame was relatively insensitive to the vortex whereas for richer flames we observed a substantial and rapid decline in the peak CH mole fraction, commencing early in the flame-vortex interaction. The peak concentration of HCO was found to correlate, in both space and time, with the peak heat release across a broad range of equivalence ratios. The model also predicted a measurable increase in C_2H_2 as a result of interaction with the vortex, and a marked increase in the low temperature chemistry activity.

Formation of Cyclopentadienyl from Addtion of Acetylene to Propargyl (with N. W. Moriarty, X. Krokidis, and W A. Lester, Jr.)

The addition of acetylene and propargyl has been investigated using several DFT methods including B3-LYP, B3-PW91 and B&H-H&LYP. The optimized geometries were calculated using the 6-31G(d,p) and the cc-pVTZ basis sets. Quantum Monte-Carlo (QMC) calculations were performed at the B3-LYP/cc-pVTZ optimized geometries. A number of other theoretical methodologies including CBS-RAD, G2, G3 and their economical variations were used to study some important features of the potential energy surface and thermochemistry of the cyclopentadienyl radical.

The RRKM rate constants were determined for the reactions leading to the formation of the cyclo-C5H5 radical. A detailed analysis of the reaction pathways was performed using the MultiWell suite of codes to provide time dependence and efficiency of the overall reaction which

has three major paths of four or more reaction steps. The heat of formation and rate of decomposition of the radical were determined and compared with experiment. The critical and interesting hydrogen migration common to all paths was examined using Bonding Evolution Theory (BET) concepts applied to the Electron Localization Function (ELF). The results support the feasibility of this step for aromatic formation, and show that this pathway should be competitive with other accepted channels.

Future Plans

1. *Numerical Approaches to Reaction Kinetics*: Further investigation of approaches to increase the economy of the PRISM method: (a) Using the "gradient" of the reaction trajectory to estimate a priori whether a hypercube is likely to be used a sufficient number of times to warrant its construction; (b) Selection of the hypercube size based on species sensitivities; (c) To reduce the number of dimensions in the factorial design; (d) To test the method in 2D- and 3D-CFD simulations and on a larger chemical model, that of natural gas combustion with a set of about 20 chemical species. (In collaboration with Bell, Brown, and Grcar).
2. *Soot Modeling*: To perform two-dimensional CFD calculations of turbulent combustion with soot model included. The objective is to investigate interaction between turbulence and such a complex chemical reaction model as soot formation. (In collaboration with Bell, Brown, and Grcar).
3. *Soot Chemistry*: To continue ab initio quantum-chemical analysis of reactions critical to the development of kinetic models of aromatic growth. After the completion of the propargyl + acetylene $\rightarrow$ cyclopentadiene, we will focus on the next step of this reaction pathway: cyclopentadiene + acetylene system. (In collaboration with Lester).
4. *Particle Aggregation*: To complete the ongoing investigation of the relationship between instantaneous volume, surface area, and fractal dimension of the growing soot particle, and, based on these data, develop a mathematical model that capture the essential physics of the particle dynamics undergoing simultaneous coagulation and surface growth.

Publications

1. "Monte Carlo Simulation of Soot Particle Aggregation with Simultaneous Surface Growth—Why Primary Particles Appear Spherical," P. Mitchell and M. Frenklach, *Twenty-Seventh Symposium (International) on Combustion*, The Combustion Institute, Pittsburgh, PA, 1998, pp. 1507–1514.
2. "Hydrogen Migration in Polyaromatic Growth," M. Frenklach, N.L. Moriarty, and N.J. Brown, *Twenty-Seventh Symposium (International) on Combustion*, The Combustion Institute, Pittsburgh, PA, 1998, pp. 1655–1661.
3. "PRISM: Piecewise Reusable Implementation of Solution Mapping. An Economical Strategy for Chemical Kinetics," S.R. Tonse, N.W. Moriarty, N.J. Brown and M. Frenklach, *Israel Journal of Chemistry* **39**, 97–106 (1999).
4. "Hydrogen Migration in the Phenylethen-2-yl Radical," N. W. Moriarty, N. J. Brown, and M. Frenklach, *J. Phys. Chem. A* **103**, 7127–7135 (1999).
5. "Propargyl Radical: An Electron Localization Function Study," X. Krokidis, N. W. Moriarty, W. A. Lester, Jr., and M. Frenklach, *Chem. Phys. Lett.* **314**, 534–542 (1999).
6. "Kinetic Modeling of Soot Formation with Detailed Chemistry and Physics: Laminar Premixed Flames of C_2 Hydrocarbons," J. Appel, H. Bockhorn, and M. Frenklach, *Combust. Flame* 121, 122–136 (2000).

Multiresonant Spectroscopy and the High-Resolution Threshold Photoionization of Combustion Free Radicals

Edward R. Grant
Department of Chemistry
Purdue University
West Lafayette, IN 47907
edgrant@purdue.edu

Program Definition/Scope

In this research we apply methods of multiresonant spectroscopy and rotationally resolved threshold photoionization to characterize the structure, thermochemistry and intramolecular dynamics of excited neutrals and cations derived from combustion free radicals. The objectives of this work are: (1) To measure ionization potentials with wavenumber accuracy for a broad set of polyatomic molecules of relevance to combustion and combustion modeling; (2) To determine vibrational structure for cations as yet uncharacterized by ion absorption and fluorescence spectroscopy, including the study of anharmonic coupling and intramolecular vibrational relaxation at energies approaching thresholds for isomerization; (3) By threshold photoionization scans, referenced in double resonance to specific cation rovibrational states, to obtain information on originating-state level structure useful for the development of neutral-species diagnostics; (4) To measure rotationally detailed state-to-state photoionization cross sections for comparison with theory; and (5) To spectroscopically study near-threshold electron-cation scattering dynamics of relevance, for example, to plasma processes such as dissociative recombination, by acquiring and analyzing rotationally resolved high-Rydberg spectra.

Recent Progress

Appearance of the $A\ ^1\Pi$ -- $X\ ^1\Sigma^+$ transition in the(1+2)-photon ionization-detected absorption spectrum of BH

We have obtained the first resonance-enhanced multiphoton ionization (REMPI) spectrum of diatomic boron hydride. BH fragments are formed by the 193 nm photolysis of B_2H_6 entrained in H_2 in a pulsed free-jet expansion. Over the spectral range from 368 to 372 nm, we find rotational line features at cation masses m = 12 ($^{11}BH^+$), m = 11 ($^{10}BH^+$, $^{11}B^+$) and m = 10 ($^{10}B^+$). Figure 1 shows an example for mass m = 12. All lines observed in this spectrum and the ones recorded for lighter masses can be assigned to the one-photon transition, $A\ ^1\Pi$ ($v' = 2$) -- $X\ ^1\Sigma^+$ ($v'' = 0$), in ^{11}BH or its less-abundant isotopemer, ^{10}BH. Because cation production at these wavelengths requires three photons, the structure exhibited here must arise from resonant one-photon absorption followed by two-photon ionization in a (1+2)-photon process. Examination of the energy spacing of electronically excited states in BH shows that this (1+2)-photon ionization pathway is likely assisted by a near-resonance with the v = 1 level of the $B\ ^1\Sigma^+$ state at the second-photon level. The efficiency of this ionization route suggests that the $A\ ^1\Pi$ excited state will serve as an effective gateway in two- and three-color strategies to probe the structure and dynamics of the higher excited states of this reactive intermediate.

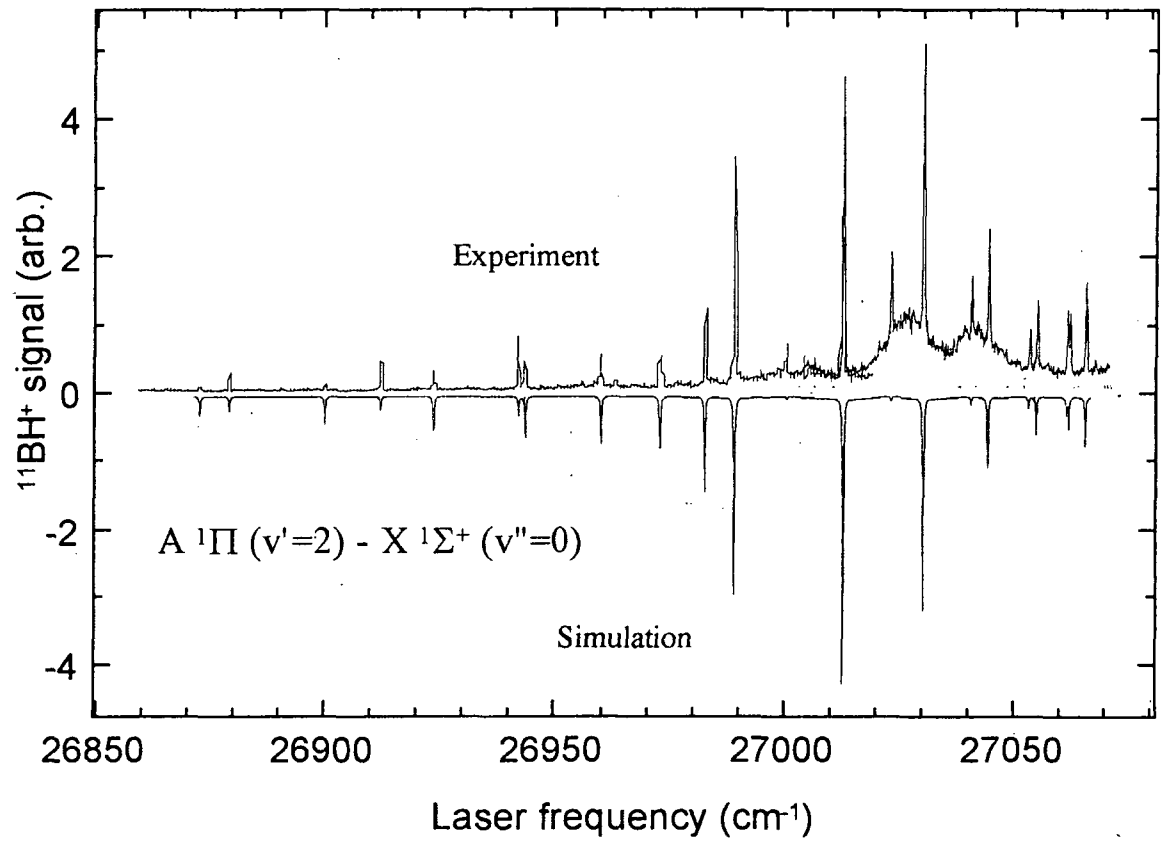

Figure 1. Mass-resolved (1+2)-photon ionization-detected absorption spectrum of ^{11}BH (upper trace). Simulation of the one-photon A $^1\Pi$ (v' = 2) – X $^1\Sigma^+$ (v" = 0) transition for a bimodal rotational state distribution characterized by temperatures of 40 K (0.9) and 600 K (0.1) (lower trace). Low-temperature BH radicals are detected downstream by (1+2)-photon resonant ionization following 193 nm pulsed-jet photolysis. The additional higher-temperature contribution to the BH spectrum is thought to arise from probe-laser-induced photolysis of higher boron hydride fragments (probably BH_2) in the extraction region of the mass spectrometer. Near double resonance with the B $^1\Sigma^+$ state at the level of the second photon enhances the cross section for two-photon ionization of photopopulated A-state levels.

Experimental Characterization of the Higher Vibrationally Excited States of HCO^+: Determination of ω_2, x_{22}, g_{22} and $B_{[030]}$

We have analyzed high Rydberg series of HCO built on the (030) vibrational state of the core in an effort to establish rovibrational state-detailed thresholds for the (030) level of HCO^+. UV-visible laser double resonance rovibrationally isolates series for assignment. Strongly vertical Rydberg-Rydberg transitions from photoselected N′ = 0 and N′ = 2 rotational levels of the Σ^- Renner-Teller vibronic component of the 3pπ $^2\Pi$ (030) complex define individual series converging to rotational levels, N^+ = 1 through 5 and 3 through 5 of the HCO^+ vibrational states (03^10) and (03^30), respectively. Figure 2 shows a portion of the spectrum observed from 3pπ $^2\Pi$ (030) Σ^- N' = 0, together with a simulation. Prominent resonances can be identified which have quantum defects closely related to ones identified in a comprehensive assignment of series converging to the (010) state of HCO^+.

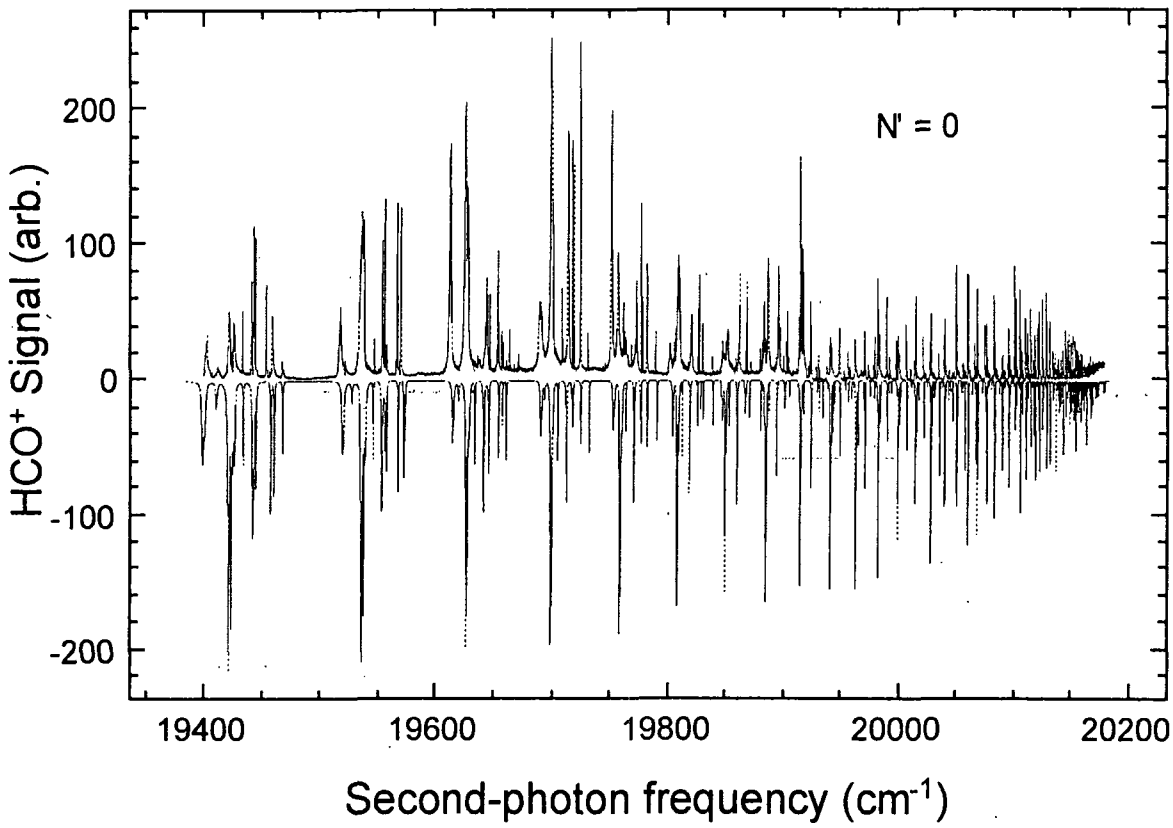

Figure 2. Spectrum of HCO autoionization resonances obtained in transitions from the N' = 0 level of the Σ^{--} component of the 3pπ $^2\Pi$ (030) system (upper trace). Simulation drawn from quantum defects established by analogy to our comprehensive assignment of Rydberg series built on the (010) state of HCO^+.

Extrapolation of autoionizing series in the (030) spectrum locates the positions of HCO^+ rovibrational states associated with the second bending overtone to within ± 0.01 cm^{-1}. The use of this information combined with precise ionization limits for lower vibrational states determined from earlier Rydberg extrapolations and spectroscopic information available from infrared absorption measurements enables us to accurately estimate the force-field parameters for HCO^+ bending. Parameters derived from our measurements include the harmonic bending frequency, ω_2, the vibrational angular momentum splitting constant, g_{22}, and the diagonal bending anharmonicity, x_{22}, separated from the off-diagonal contribution, x_{12}, by reference to *ab initio* calculations. These results are tabulated below together with comparisons to recent theoretical predictions.

In preliminary work on new combustion free-radicals, we have obtained REMPI signals establishing the production of OH and HCO from formic acid, and begun a collaborative effort with Barney Ellison to explore carbonyl-nitrites as a precursors for substituted formyl radicals such as HOCO and NH_2CO.

Table 1. New vibrational constants for HCO^+ derived from state-detailed ionization thresholds

	Experiment	Puzzarini ('96) MRCI	Lee ('93) CCSD(T)/ cc-pVTZ	Lee ('93) CCSD(T)/ cc-pVQZ	Schmatz ('98) CCSD(T)/ cc-pVQZ
ν_1	3088.73	3090.4	3087.9		3085.58
ν_2	829.72	830.7	824.2		830.74
ν_3	2183.95	2182.7	2166.0		2179.09
$2\nu_2$	1643.73[a]	1641.1			
$3\nu_2$	2462.35[a]	2458.9			
ω_1		3243.1	3229.6	3223.1	3223
ω_2	842.57[a]	852.4	832.5	841.9	845
ω_3	2208.1[b]	2216.2	2195.8	2209.3	2209
x_{11}		-54.039	-54.204		
x_{22}	-2.53[a]	-3.575	-0.860		
x_{33}	-10.055	-10.003	-9.963		
x_{12}		-22.044	-22.034		
x_{13}		-25.878	-22.201		
x_{23}	0.134	0.459	1.112		
g_{22}	3.26[a]	4.589	4.776		

[a] This work

[b] Oka, JMS **128**, 236 (1988) {based on theoretical $x_{13} = -8.4$}

References to publications of DOE sponsored research (1998-2000)

Double-Resonance Spectroscopy of the High Rydberg States of HCO II. Mode Specificity in the Dynamics of Vibrational Autoionization via CO-Stretch versus Bend, E. E. Mayer, H. G. Hedderich and E. R. Grant, *J. Chem. Phys.* **108**, 1886 (1998).

Double-Resonance Spectroscopy of the High Rydberg States of HCO III. Multiple Pathways in the Vibrational Autoionization of the Bending Overtone, E. E. Mayer, H. G. Hedderich and E. R. Grant, *J. Chem. Phys.* **108**, 8429 (1998).

On the high Rydberg states of the formyl radical and the dynamics of vibrational autoionization in triatomic molecules, E. R. Grant in, *The Role of Rydberg States in Spectroscopy and Reactivity*, C. Sandorfy, ed. (Kluwer Academic Publishers, Dordrecht, 1998)

A characterization of vibrationally excited NO_2^+ by ZEKE high-resolution threshold photoionization spectroscopy, G. K. Jarvis, Y. Song, C. Y. Ng and E. R. Grant, *Advanced Light Source Compendium 1998* (Lawrence Berkeley Laboratory, Berkeley, CA, 1999).

A characterization of vibrationally and electronically excited NO_2^+ by high-resolution threshold photoionization spectroscopy, G. K. Jarvis, Y. Song, C. Y. Ng and E. R. Grant, *J. Chem. Phys.* **111**, 9568 (1999).

Experimental Characterization of the Higher Vibrationally Excited States of HCO^+: Determination of ω_2, x_{22}, g_{22} and $B_{[030]}$, R. J. Foltynowicz, J. D. Robinson, E. J. Zückerman, H. G. Hedderich and E. R. Grant, *J. Mol. Spectrosc.* **199**, 147-157 (2000).

CHEMICAL DYNAMICS IN THE GAS PHASE: QUANTUM MECHANICS OF CHEMICAL REACTIONS

Stephen K. Gray
Chemistry Division
Argonne National Laboratory
Argonne, IL 60439

E-mail: gray@tcg.anl.gov

PROGRAM SCOPE

This research focuses on the development and application of accurate quantum mechanical methods to describe gas phase chemical reactions and highly excited molecules. Emphasis is placed on time-dependent or iterative quantum approaches that, in addition to computational simplifications, yield mechanistic insights. Applications to systems of current experimental and theoretical interest, and relevance to combustion, are emphasized. The results of these calculations also allow one to gauge the quality of the underlying potential energy surfaces and the reliability of more approximate theoretical approaches such as classical trajectories and transition state theories.

RECENT PROGRESS

The role of electronic non-adiabacity in the $O(^1D) + H_2 \rightarrow OH + H$ reaction was explored with three-dimensional wave packet calculations that included two relevant potential energy surfaces and their non-adiabatic coupling (Gray, Petrongolo, Drukker and Schatz, 1999). The previously developed real wave packet approach (Gray and Balint-Kurti, 1998), owing to its favorable memory and computational requirements, was found to be extremely useful for this study. A novel nonadiabatic mechanism for reactivity at relatively low collision energies was identified, and estimates of the contribution of excited state and nonadiabatic dynamics to the thermal rate constant were made. Another interesting reaction involving $O(^1D)$ atoms, $O(^1D) + HCl \rightarrow OH + Cl$ was also studied successfully with the real wave packet approach in collaboration with Bowman's group (Christoffel *et al.*, 1999).

An efficient theoretical approach to the quantum mechanical calculation of bimolecular rate constants was developed (Forsythe and Gray, 1999). The approach makes use of Miller's cumulative reaction probability [1] and Zhang and Light's [2] interpretation of it as a sum over "transition state wave packets". The approach involves implementation of the transition state wave packet idea within the real wave packet formalism. The method was illustrated with full dimensional (including fully coupled, total angular momentum $J > 0$) wave packet calculations of the rate constant for the $D + H_2 \rightarrow HD + H$ exchange reaction.

Bound and resonance states of H_2O were be investigated with a variety of quantum mechanical techniques including Lanczos and Chebyshev iterations. Three dimensional calculations based on an accurate *ab initio* potential surface developed by Ho *et al.* [3] were carried out. Resonances above the OH + H threshold were found that represented the direct continuation of local mode progressions in the bound states.

FUTURE PLANS

Recent experimental developments [4] have suggested that excited state and nonadiabatic dynamics may influence the relative reactivity of j = 0 and j = 1 initial rotational states in the $O(^1D) + H_2$ (v=0,j) $\rightarrow$ OH + H reaction. Our previous work focused on v = j = 0 and total nuclear angular momentum J = 0 (Gray, Petrongolo, Drukker and Schatz, 1999) but with additional computational effort it is possible to obtain reasonably accurate quantum cross sections and to directly connect with these interesting new experimental results. Preliminary calculations suggest that an interesting, subtle picture exists regarding the collision energy dependence of the ratio of the j = 1 and 0 cross sections that could have interesting experimental implications.

Accurate adiabatic quantum mechanical studies of several other three-atom systems will be undertaken using the real wave packet and related iterative methods previously developed. The quantum dynamics of the $O(^3P)$ + HCl reaction will be studied on a new *ab initio* potential surface, and comparison with experimental rate constants will be made. A study of a variety of ro-vibrational states of different electronic surfaces of HCP will also be undertaken with Nanbu, to elucidate the nature of highly excited electronic states in this system. The scattering dynamics of several four-atom systems, including the combustion important CH + H_2 $\rightarrow$ CH_2 + H and OH + OH $\rightarrow$ H_2O + O systems, will be investigated in collaboration with Goldfield and Nanbu.

A project on the *ab initio* dynamics of singlet ketene dissociation, $CH_2CO \rightarrow CH_2 + CO$, with the hope of eventually making connection with experiments from Hall's group [5], will be initiated (in collaboration with S. J. Klippenstein). The experiments have pointed to interesting deviations from phase space theories and it is hoped that the direct dynamics will shed light on the origin of these deviations.

---

[1] W. H. Miller, S. D. Schwartz, and J. W. Tromp, J. Chem. Phys. 79, 4889 (1983).
[2] D. H. Zhang and J. C. Light, J. Chem. Phys. 106, 551 (1996).
[3] T. S. Ho, T. Hollebeek, H. Rabitz, L. B. Harding, and G. C. Schatz, J. Chem. Phys. **105**, 10472 (1996).
[4] S. H. Lee and K. Liu, J. Chem. Phys. 111, 4351 (1999).
[5] G. E. Hall, private communication.

PUBLICATIONS, S. K. Gray (1998-2000)

1. S.K. Gray and G.G. Balint-Kurti, Quantum dynamics with real wave packets, including application to three-dimensional (J=0) D + H_2 $\rightarrow$ HD + H, J. Chem. Phys. **108**, 950(1998).

2. R. Lehoucq, S.K. Gray, D-H. Zhang, and J.C. Light, Vibrational eigenstates of four-atom molecules: A parallel strategy employing the implicitly restarted Lanczos algorithm, Comp. Phys. Comm. **109**, 15 (1998).

3. G.G. Balint-Kurti, A.I. Gonzalez, E.M. Goldfield, and S.K. Gray, Quantum reactive scattering of $O(^1D)+H_2$ and $O(^1D)+HD$, Faraday Discussions **110**, 169 (1998).

4. A.J.H.M. Meijer, E.M. Goldfield, S.K. Gray, and G.G. Balint-Kurti, Flux analysis for calculating reaction probabilities with real wave packets, Chem. Phys. Lett. **293**, 270 (1998).

5. S. Skokov, J. Qi, J.M. Bowman, C-Y. Yang, S.K. Gray, K.A. Peterson, and V.A. Mandelshtam, Accurate variational calculations and analysis of the HOCl vibrational energy spectrum. J. Chem. Phys. **109**, 10273 (1998).

6. K. Runge, B.G. Sumpter, D.W. Noid, S.K. Gray and C-Y. Yang, Electron propagation along a nanowire: a study in chattering, Nanotechnology **9**, 365 (1998).

7. S.K. Gray, E.M. Goldfield, G.C. Schatz, and G.G. Balint-Kurti, Helicity decoupled quantum dynamics and capture model cross sections and rate constants for $O(^1D) + H_2 \rightarrow OH + H$ Phys. Chem. Chem. Phys. **1**, 1141 (1999).

8. S. K. Gray, C. Petrongolo, K. Drukker and G. C. Schatz, Quantum wave packet study of nonadiabatic effects in $O(^1D)+H_2 \rightarrow OH + H$, J. Phys. Chem. A **103**, 9448-9459(1999).

9. K. M. Christoffel, Y. Kim, S. Skokov, J. M. Bowman and S. K. Gray, Quantum and quasiclassical reactive scattering of $O(^1D)$ + HCl using an *ab initio* potential, Chem. Phys. Lett. **315**, 275-281(1999).

10. K. M. Forsythe and S. K. Gray , A transition state real wavepacket approach for obtaining the cumulative reaction probability, J. Chem. Phys. **112**, 2623 (2000).

Computer-Aided Construction of Chemical Kinetic Models

William H. Green, Jr.
Department of Chemical Engineering
Massachusetts Institute of Technology
Cambridge, MA 02139-4307
whgreen@mit.edu

Industrial Collaborators: A.M. Dean & J.M. Grenda, Exxon Research & Engineering Co.

Project Scope

The combustion chemistry of even simple fuels can be extremely complex, involving hundreds or thousands of kinetically significant species. Even relatively minor species can play an important role in the formation of undesirable emissions. A number of researchers [1-8] have recognized that the most reasonable way to deal with this complexity is to use a computer not only to numerically solve the kinetic model, but also to construct the model in the first place. We are developing the methods needed to make this feasible, particularly focusing on the need for reliable computer estimates of pressure dependent rates, and methods for handling situations where the reaction conditions change significantly with time or with spatial position.

Recent Progress

We previously devised [8] the first general algorithm for constructing kinetic models appropriate to particular reaction conditions, by numerically testing whether particular species are significant under those conditions. This algorithm can very rapidly and reliably construct rather complex kinetic schemes, testing hundreds of thousands for reactions to find the smaller set which is actually important. It is much less prone to inadvertently omitting an important reaction than other model construction techniques. It has the advantage of clarifying the relationship between the reaction conditions and the kinetic model required. Unfortunately, the existing algorithm is explicitly designed for perfectly mixed, isothermal, isobaric simulations. Relaxing these restrictions raises a number of issues.

The key issue in constructing any kinetic model, of course, is how to reliably estimate the rate constants required. Fortunately, many of the important rates for light alkane combustion are known experimentally, though usually over a restricted range of temperatures and pressures (e.g. moderate temperatures, atmospheric or sub-atmospheric pressure). We have found that in many cases the largest error in *ab initio* rate estimates comes from errors in the calculated barrier height, so one should use the available experimental data to determine the barrier height, and the quantum calculation to estimate the Arrhenius "A" factor (which may be T-dependent). We recently published a demonstration that this approach allows rather accurate extrapolations to different temperatures, using relatively simple density functional theory calculations and conventional transition state theory.[16]

However, in some situations, the A factor cannot be computed accurately using the conventional separability assumptions, due to the effects of specific floppy motions coupled to the reaction coordinate. One very common situation arises in combustion

reactions of resonantly-stabilized radicals, where motion along one or more torsional coordinate can break the resonance by destroying the alignment of the p-orbitals involved. We have recently constructed the appropriate Hamiltonian for the case where a single large amplitude torsional coordinate is strongly coupled to the reaction coordinate (and to many small-amplitude coordinates), and solved the Hamiltonian by integrating out the fast motions corresponding to the small-amplitude coordinates. We have applied this technique to several reactions involving resonantly stabilized radicals, presented our results at the American Chemical Society meeting in March, and are now preparing this work for publication. We find that the A factor is indeed affected by the large amplitude motion, but due to cancellation of error and thermal averaging, the A factor computed using the conventional separability approximation is more accurate than one might initially expect.

For many reactions, pressure-dependent fall-off and chemical-activation effects are very significant. In collaboration with the Exxon researchers, we are currently automating the process of computing pressure-dependent rate constants, so that the computer can do this "on-the-fly" as it constructs the kinetic model. A large piece of this work has been completed and presented at the SIAM Numerical Combustion meeting in March by Jeff Grenda of Exxon, and we are currently preparing a manuscript demonstrating its effectiveness by comparison with experimental data on methane pyrolysis. For systems involving larger molecules, efficient methods for screening out unimportant chemically-activated isomerizations will be necessary, and we are currently working to demonstrate that our chosen screening criteria are valid for a variety of different types of cases.

As a first step, we have automated the inverse-Laplace-transform [9] method (which gives predictions very similar to QRRK [10]), and have applied it to several pressure-dependent reactions where there is some controversy [11,12] about the rates. Our calculations on $OH+NO_2$ have recently been published.[17] We are also examining other methods for estimating pressure-dependence, and attempting to assess the errors introduced by the various approximations. Curiously, for $OH+NO_2$ at atmospheric conditions, the error appears to be dominated by uncertainty about the details of the coupling of the overall rotational energy with the reaction coordinate, rather than details about the potential energy surface or the pressure-dependence model used. We have recently submitted several manuscripts [18-21] predicting pressure-dependent rates for larger radicals involved in combustion where no experimental data are available.

In combustion, the overall rate of reaction is usually controlled as much by mixing as by any rate constant. Conventional reacting-flow simulation techniques can only be used if the chemistry model is very small, since they typically attempt to solve for the concentration of every chemical species in the model at every spatial position and at every time point in the simulation. Since the computer can rapidly construct kinetic models adapted to each reaction condition, it should be possible to construct an "adaptive chemistry" reacting flow simulation, where different truncated kinetic models are used at different spatial positions and times. This could dramatically reduce the number of equations which must be solved in the simulation. We have developed an adaptive chemistry algorithm, and have successfully applied it to 0-d (time-dependent) problems. We presented these results at the SIAM Numerical Combustion conference in March. We are currently extending this approach to 1-d and 2-d flame simulations.

As a first step towards developing such a simulation, we have been examining how one could in practice develop truncated kinetic schemes known to be reliable over a specific range of reaction conditions. We have reformulated the scheme-reduction problem as a type of mixed-integer dynamic optimization problem, and are currently working on the numerical solution of that problem in collaboration with Paul I. Barton.

Future Plans

In the coming year we will coupling the pressure-dependent rate modules with the existing kinetic-modeling package, and testing the results on a variety of applications. In collaboration with Exxon, we have devised a general algorithm which constructs every chemically-activated and stabilization pathway, and so can construct and solve the equations which describe the pressure dependence. The required k(E)'s and ρ(E)'s can be obtained from the high-pressure limit k(T)'s and the group-additivity heat capacities by the inverse Laplace transform technique [9] and the "3-frequency" technique [13] respectively. The pressure dependence can be estimated in many different ways ranging from simple approximations to full-blown time-dependent master equations; we have begun to explore the tradeoffs between accuracy and computational speed. At least initially, we will use the exponential-down model for energy transfer, and the corresponding Troe $\beta k_s[M]$ approximation.[14] For large molecules there are a very large number of possible reaction pathways, and some pruning will be necessary. This can be done by setting a criterion for kinetic significance which suppresses the most minor channels, and we are currently testing that such pruning does not significantly reduce accuracy. Once one has constructed the pressure-dependence model, it can be solved for a range of pressures and for different initial energy distributions of the activated complex (corresponding to different entrance channels and temperatures). We will test this new tool by computing the pressure dependence of a large number of reactions; in performing these validations we have already found some surprises.

The longer term challenge is to develop reliable methodology for constructing and solving "adaptive chemistry" reacting-flow simulations. Initially, we will focus on the "model-reduction" and related "range-of-applicability" problems for truncated kinetic models. We will also test various approximations we have devised for dealing with the boundaries between finite elements with different kinetic schemes (involving different numbers of species). For the numerical solution, we draw heavily on numerical methods for solving differential-algebraic equations with discrete control variables recently developed at MIT [15]. Initially, we will construct the reacting flow simulations by hand, for very simple geometries. Once we demonstrate that the "adaptive chemistry" approach provides a significant advantage over current approaches, we can begin to incorporate the technology developed by others for adaptive gridding etc. that would be required for reacting flows through complex geometries.

Literature Cited

1) L. Haux, P.-Y. Cunin, M. Griffiths, & G.-M. Come, *J. Chim. Phys.* **85** (1988) 739-43.
2) S.J. Chinnick, D.L. Baulch, & P.B. Ayscough, *Chemom. Itell. Lab. Syst.* **5** (1988) 39-52.
3) E. Ranzi, A. Sogaro, P. Gaffuri, G. Pennati, C.K. Westbrook, & W.J. Pitz, *Combust. Flame* **99** (1994) 210-211.
4) E.S. Blurock, *J. Chem. Inf. Comput. Sci.* **35** (1995) 607-616.
5) L.J. Broadbelt, S.M. Stark, and M.T. Klein, *Comput. Chem. Eng.* **20** (1996) 113-129.
6) M. Nehse, J. Warnatz, and C. Chevalier, *Twenty-Sixth Symposium (International) on Combustion* (The Combustion Institute: Pittsburgh 1997).
7) D.J. Klinke and L.J. Broadbelt, *A.I.Ch.E. J.* **43** (1997) 1828.
8) R.G. Susnow, A.M. Dean, W.H. Green, P. Peczak, & L.J. Broadbelt, *J. Phys. Chem. A* **101** (1997) 3731-3740.
9) W. Forst, *J. Phys. Chem.* **76** (1972) 342-8.
10) A.M. Dean, *J. Phys. Chem.* **89** (1985) 4600-4608.
11) (a) T.J. Dransfield, K.K. Perkins, N.M. Donahue, J.G. Anderson, M.M. Sprengnether, K.L. Demerjian, *Geophys. Res. Lett.* **26** (1999) 687-690; (b) N.M. Donahue, M.K. Dubey, R. Mohrschladt, K.L. Demerjian, J.G. Anderson, *J. Geophys. Res.-Atm.* **102** (1997) 6159-6168.
12) D. Fulle, H.F. Hamann, H. Hippler, & J. Troe, *J. Chem. Phys.* 108 (1998) 5391-5397.
13) J.W. Bozzelli, A.Y. Chang, and A.M. Dean, *Int. J. Chem. Kinet.* 29 (1997) 161-170.
14) R.G. Gilbert, K. Luther, and J. Troe, *Ber. Bunsenges. Phys. Chem.* 87 (1983) 169.
15) Park T. and P. I. Barton, *ACM Trans. Mod. Computer Sim.* **6** (1996) 137-165.
16) R.G. Susnow, A.M. Dean, and W.H. Green, *Chem. Phys. Lett.* **312** (1999) 262.
17) D.M. Matheu and W.H. Green, *Int. J. Chem. Kinet.* **32** (2000) 245-262.
18) H. Richter, T.G. Benish, O.A. Mazyar, W.H. Green, and J.B. Howard, "Formation of Polycyclic Aromatic Hydrocarbons and their Radicals in a Nearly Sooting Premixed Benzene Flame", *Proc. Combust. Inst.* (accepted).
19) J.L. DiNaro, J.B. Howard, W.H. Green, J.W. Tester, and J.W. Bozzelli, "Analysis of an Elementary Reaction Mechanism for Benzene Oxidation in Supercritical Water", *Proc. Combust. Inst.* (accepted).
20) J.L. DiNaro, J.B. Howard, W.H. Green, J.W. Tester, and J.W. Bozzelli, "Elementary Reaction Mechanism for Benzene Oxidation in Supercritical Water", *J. Phys. Chem. A* (submitted).

Publications of DOE sponsored research

1) D.M. Matheu and W.H. Green, *Int. J. Chem. Kinet.* **32** (2000) 245-262.
2) H. Richter, T.G. Benish, O.A. Mazyar, W.H. Green, and J.B. Howard, "Formation of Polycyclic Aromatic Hydrocarbons and their Radicals in a Nearly Sooting Premixed Benzene Flame", *Proc. Combust. Inst.* (accepted).

Christopher M. Hadad
Department of Chemistry
Ohio State University
100 West 18th Avenue
Columbus, OH 43210-1173
hadad.1@osu.edu

Mechanisms of Coal Combustion

Coal is a very important energy source for electric power generation in the United States. However, the mechanistic steps in the combustion of coal is not well understood due to its large and complex nature. With Department of Energy support, we are using computational chemistry in order to examine the individual constituents of coal in order to probe the important aspects of reactivity for large polycyclic aromatic hydrocarbons and to understand the mechanism of their oxidation. We have examined the energy required to cleave C-H and N-H bonds in representative monocyclic and polycyclic aromatic rings so as to understand the specific thermodynamic preferences for oxidative reactivity on representative moieties for coal.

We have calculated C–H bond dissociation enthalpies (BDEs) for small to medium sized PAHs.[1] We have evaluated monocyclic rings as models for larger PAHs as well as to calibrate theoretical methods that could be applied to thermodynamic and kinetic issues for large aromatic hydrocarbons. In comparison to benzene, the C-H BDEs are lower for nitrogen-containing six-membered rings (such as pyridine, pyridazine, pyrimidine and pyrazine), but the BDEs in five-membered rings are larger than for benzene. We have examined the origins of these effects and besides providing quantitative data, we have also examined the geometrical and spin density changes in these systems. Furthermore, we have noted that one can use C-H BDE data for the small, monocyclic rings to predict the BDE values in the larger PAHs to within 1 kcal-mol^{-1} on average. The B3LYP/6-31G(d) method seems to be very well suited to calculating accurate C-H BDEs in the larger systems and also at a reasonable cost.

The modes of attack for radicals of importance to combustion (O, OH, and H) have not been fully explored, especially for polycyclic aromatic hydrocarbons. We have examined H-atom abstraction vs radical addition to the aromatic units of coal.[2] Hydroxyl radical (OH) is significantly more reactive (kinetically and thermodynamically) than H or O for H-atom abstraction from the monocyclic aromatic rings. In general, radical addition is more favored at low temperatures, but H-atom abstraction becomes more favorable at high temperatures due to the entropic effect. The cross-over temperature between addition vs H-atom abstraction is dependent on the reacting radical as well as the aromatic ring. We have extended these approaches to examine H-atom abstraction and radical addition to larger carbonaceous PAHs, such as naphthalene, phenanthrene and corannulene.[3] In particular, we have observed that reactions at the edges of the aromatic rings are significantly more favored (kinetically and thermodynamically) than chemistry at the bridgehead positions.

We have explored the decomposition pathways for the combustion of aryl radicals to generate the products of combustion, i.e. CO and CO_2. Two papers have already

resulted from this aspect of the project.[4,5] In the first paper of this series,[4] predominantly thermodynamic information for the decomposition pathways of phenyl, pyridinyl, furanyl, and thiophenyl radicals with O_2 were presented. In these pathways, we explored some different options for phenyl radical with O_2, including dioxiranyl, dioxetanyl, phenoxy and other pathways, along the previously suggested mechanisms by Carpenter.[6] We were able to show that the dioxiranyl pathway would be the most energetically favorable in order to decompose the aromatic radicals. We were able to demonstrate the formation of oxidized carbon as well as other noxious products, such as HCN.

For phenyl radical with O_2, we followed our predominantly thermodynamic study[4] with an exhaustive study of the potential energy surface (including transition states) for dioxiranyl, dioxetanyl, phenoxy and other mechanistic pathways.[5] From this exhaustive study, we were able to discern that the dioxiranyl pathway will be the most favored means for decomposing phenyl radical in the presence of O_2 to about 1000 K. However, at temperatures above that, the phenoxy radical and O-atom pathway becomes more dominant.

We have since extended these studies to explore the oxidation of aryl radicals derived from the nitrogen-containing six-membered rings (pyridine, pyridazine, pyrimidine, and pyrazine)[7] and the five-membered rings (furan, pyrrole, thiophene and oxazole).[8] Once again, we have explored the temperature dependence for formation of the arylperoxy radicals and their subsequent decomposition via the dioxiranyl, dioxetanyl and aryloxy radical pathways. There are significant differences between the reactivity of the five- and six-membered rings, especially with regard to arylperoxy radical formation.

We are currently extending these approaches to larger PAHs of relevance to coal. Also, further work will focus on the formation of NO_x and SO_x from oxidation of fuel nitrogen and sulfur in model compounds.

Acknowledgments: We gratefully acknowledge support by DOE Fossil Energy Advanced Research managed by the National Energy Technology Laboratory.

References:

[1] Barckholtz, C.; Barckholtz, T. A.; Hadad, C. M. *J. Am. Chem. Soc.* **1999**, *121*, 491.
[2] Barckholtz, C.; Barckholtz, T. A.; Hadad, C. M. *J. Phys. Chem. A*, manuscript in preparation.
[3] Broughton, P. S.; Barckholtz, C.; Hadad, C. M. *J. Phys. Chem. A*, to be submitted.
[4] Barckholtz, C.; Fadden, M. J.; Hadad, C. M. *J. Phys. Chem. A* **1999**, *103*, 8108-8117.
[5] Fadden, M. J.; Barckholtz, C.; Hadad, C. M. *J. Phys. Chem. A*, **2000**, *104*, 3004.
[6] Carpenter, B. K. *J. Am. Chem. Soc.* **1993**, *115*, 9806.
[7] Fadden, M. J.; Hadad, C. M. *J. Phys. Chem. A*, submitted.
[8] Fadden, M. J.; Hadad, C. M. *J. Phys. Chem. A*, submitted.

SPECTROSCOPY AND KINETICS OF COMBUSTION GASES AT HIGH TEMPERATURES

Ronald K. Hanson and Craig T. Bowman
Department of Mechanical Engineering
Stanford University, Stanford, CA 94305-3032
hanson@me.stanford.edu, bowman@navier.stanford.edu

Program Scope

This program involves two complementary activities: (1) development and application of cw laser absorption methods for the measurement of species concentrations and fundamental spectroscopic parameters of species of interest in combustion; and (2) shock tube studies of reaction kinetics relevant to combustion. Species investigated in the spectroscopic portion of the research include: NO_2, which is being investigated using fixed-frequency laser absorption; H_2O, using tunable diode laser absorption; CH_3, using narrow-linewidth ring dye laser absorption; and NH_2 and OH, using frequency-modulation laser absorption methods. Reactions of interest in the shock tube kinetics research include: $NH_2 + NO \rightarrow$ Products; $NH_2 + NH_X \rightarrow$ Products; $H + O_2 + M \rightarrow HO_2 + M$, with M = Ar, N_2, H_2O; $C_2H_6 \rightarrow CH_3 + CH_3$; and $CH_3 + O_2 \rightarrow$ Products.

Recent Progress

Shock Tube Chemical Kinetics

We have continued investigation of the pressure-dependent reaction

$$H + O_2 + M \rightarrow HO_2 + M, \quad \text{with M = Ar, } N_2\text{, and } H_2O, \qquad (1)$$

using a high-pressure shock tube facility. This reaction plays a significant role in the ignition process and in the noncatalytic process for NO-removal (SNCR) from combustion products. Reaction (1) can be kinetically isolated by monitoring NO_2 concentrations in relatively low temperature (1200 - 1400 K), but high pressure (10 - 150 atm) $NO/H_2/O_2/Ar$ shock tube experiments. Values of k_1 are inferred from comparisons of measured NO_2 concentration profiles, whose plateau values show a strong sensitivity to this rate coefficient, with profiles modeled using the GRI-Mech mechanism. Errors attributable to the calibration were reduced by a careful study of the temperature and pressure dependence of the absorption coefficient of NO_2 at the Ar^+ laser wavelength 472.7 nm. To measure the reaction rate for M=N_2 or H_2O, some of the argon is replaced by N_2 or H_2O. The present results for k_1 exhibit significantly reduced scatter compared with previous literature values, and when used with the k_∞ and F_{cent} values suggested by Cobos et al. (1985), and the lower temperature values of Ashman and Haynes (1998), give an improved description of the rate coefficient.

We have used a low-pressure shock tube facility to investigate the two primary channels of the reaction of NH_2 and NO,

$$NH_2 + NO \rightarrow OH + NNH \qquad (2a)$$
$$NH_2 + NO \rightarrow N_2 + H_2O \qquad (2b)$$

The branching ratio, $\alpha = k_{2a}/(k_{2a}+k_{2b})$, of these two primary channels is an important parameter in the modeling of NO_X reduction by the Thermal $DeNO_X$ process. Our approach is to take advantage of the very high sensitivity of NH_2 detection available with frequency-modulation (FM) spectroscopy methods to establish accurate high-temperature values of both the overall rate and the branching ratio. In particular, using low (ppm level) concentrations of NH_2 generated by excimer laser photolysis of NH_3/NO/Ar mixtures, it is possible at certain conditions to effectively eliminate the dependence of α on the overall rate coefficient. This results in a very accurate determination of the branching ratio near $\alpha = 0.5$. The best-fit curve of selected recent determinations over the temperature range 300 –2000 K is given by $\alpha = 0.057 + 7.01 \times 10^{-6} \times (T/K)^{1.503}$.

The overall rate coefficient of the reaction $NH_2 + NO \rightarrow$ products is being determined in shock tube experiments using FM detection of NH_2. The source of the NH_2 radicals in the experiments to date is the thermal decomposition of CH_3NH_2, monomethylamine. To determine k_{2a+2b}, a perturbation strategy is employed that is based on changes in the NH_2 profiles when NO is added to the CH_3NH_2/Ar mixtures. Sensitivity analysis shows that NH_2 profiles in the CH_3NH_2/NO/Ar mixtures are sensitive primarily to the overall rate, with significantly lower sensitivity to the branching ratio and other NH_2 reactions. The measured NH_2 profiles are interpreted by detailed kinetic modeling to obtain k_{2a+2b}-values in the temperature range 1716-2507 K; a summary of the data is given in Fig. 1.

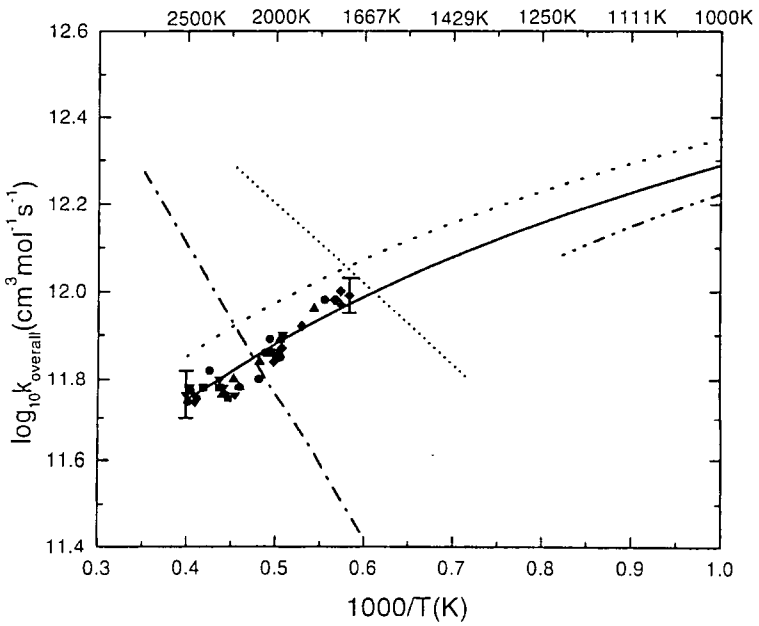

Fig. 1. Summary of high temperature values of k_{2a+2b}. Solid symbols are from the present investigation: ♦ 0.2%NO; ■ 0.25% NO; ● 0.3% NO; ▲ 0.4% NO; ▼ 0.5% NO. ———, best fit expression; ·····, Deppe et al. (1999); - - - -, Miller and Glarborg (1999) and Lesclaux et al. (1975) ; — · —, Roose et al. (1981); — - - —, Silver and Kolb (1982).

The present k_{2a+2b}-values are consistent with recent theoretical results of Miller and co-workers. There is no evidence for a positive activation energy for this reaction at elevated temperatures as reported in several other high-temperature experimental studies. Combining the present high-

temperature data with lower temperature determinations yields the following simple expression for the overall reaction rate,

$$k_{2a+2b} = 2.34 \times 10^{16} T^{-1.36} \text{ cm}^3/\text{mol-s}$$

for the temperature range 300-2500K.

Absorption Diagnostics and Spectroscopy

We are applying FM absorption spectroscopy methods to NH_2 detection. This method, similar to that used by Sears and colleagues at Brookhaven, allows direct subtraction of the noise caused by the interaction of the laser beam and the shock-induced flow. Using this method we have achieved a minimum detectable absorption of 0.01% in a single-pass configuration. This represents a factor of 10-20 improvement in detection sensitivity over conventional laser absorption.

We are reviewing and investigating the collision-width and -shift parameters of several rotational lines in the OH A-X transition that are accessible with our laser configuration in an effort to extend the useful range of the OH laser absorption diagnostic. We are continuing to improve signal-to-noise ratio of these laser absorption measurements through installation of a low-noise, solid-state cw pump laser for the ring dye laser system, the use of an electro-optic modulator for laser noise reduction, and large area detectors to permit operation at high pressures where beam steering effects are greatest.

Measurement of the rate coefficient for $H+O_2+H_2O$ requires accurate measurements of water concentration in the shock tube. Determination of pre-shock water vapor concentration is performed using semiconductor diode laser absorption at wavelengths near 1405 nm. Very little experimental collision-broadening data exists in the literature on these transitions, and hence we have conducted a series of tests over an extended range of temperature (300-2000 K) to acquire these data. We have also measured the pressure-shift of these transitions using shock waves to generate step changes in pressure.

Future Plans

A. Shock Tube Kinetics

Work will proceed on several fronts. 1) Continue studies of the reaction $NO + NH_2 \rightarrow$ products, including determination of the overall reaction rate and branching ratio; 2) Investigate the use of benzylamine, $C_6H_5\text{-}CH_2\text{-}NH_2$, as a precursor for NH_2 radicals; 3) Complete RRKM studies of the reaction $H + O_2 + M \rightarrow HO_2 + M$ with M = H_2O, N_2, and Ar; 4) Initiate studies of the reaction $CH_3 + O_2 \rightarrow$ products, using high-sensitivity FM laser absorption methods; and 5) Initiate studies of the reactions $NH_2 + NH_X \rightarrow$ Products using detection of NH_2, NH_3 and NH, as required.

B. Fundamental Spectroscopy and Laser Diagnostics Development

Work will proceed on three fronts. 1) Develop second-generation improvements to the frequency modulation absorption diagnostic used in the NH_2 studies at 597 nm. 2) Develop techniques to measure CH_3 quantitatively at high pressures using laser absorption at 216 nm. 3) Continue modeling and measurement of collision-broadening and -shift parameters of OH near 306 nm at low and high pressures, including possible use of FM Spectroscopy.

Publications of DOE Sponsored Research (1998-2000)

1. D. F. Davidson and R. K. Hanson, "Spectroscopic Diagnostics," in *Handbook of Shock Waves*, Academic Press, San Diego, in press.

2. S. Song, R. K. Hanson, C. T. Bowman, and D. M. Golden, "Shock Tube Determination of the Overall Rate of NH_2+NO $\rightarrow$ Products at High Temperatures," accepted for publication in the Twenty-eighth Symposium (International) on Combustion.

3. E. L. Petersen and R. K. Hanson, "Non-Ideal Effects Behind Reflected Shock Waves in a High-Pressure Shock Tube," Shock Waves, submitted for publication.

4. V. Nagali, D. F. Davidson and R. K. Hanson, "Measurements of Temperature-Dependent Argon-Broadened Half-Widths of H_2O Transitions in the 7117-cm-1 region," J. Quant. Spectrosc. Radiat. Transfer 64, 651-655 (2000).

5. M. Votsmeier, S. Song D. F. Davidson and R. K. Hanson, " A Shock Tube Study of Monomethylamine Thermal Decomposition and NH_2 High Temperature Absorption Coefficient," Int. J. Chem. Kinet. 31, 323-330 (1999).

6. M. Votsmeier, S. Song, D. F. Davidson and R. K. Hanson, "Sensitive Detection of NH_2 in Shock Tube Experiments using Frequency Modulation Spectroscopy," Int. J. Chem. Kinet. 31, 445-453 (1999).

7. M. Votsmeier, S. Song, R. K. Hanson and C. T. Bowman, "A Shock Tube Study of the Product Branching Ratio for the Reaction NH_2+NO using Frequency-Modulation Detection of NH_2," J. Phys. Chem. A 103, 1566-1571 (1999).

8. D. F. Davidson, R. Bates, E. L. Petersen and R. K. Hanson, "Shock Tube Measurements of the Equation of State of Argon," J. Thermophysics **19**, 1585-1594 (1998).

Theoretical Studies of Potential Energy Surfaces*

Lawrence B. Harding
Chemistry Division
Argonne National Laboratory
Argonne, IL 60439
harding@tcg.anl.gov

The goal of this program is to calculate accurate potential energy surfaces for both reactive and non-reactive systems. Our approach is to use state-of-the-art electronic structure methods (MR-CI, CCSD(T), etc.) to characterize multi-dimensional potential energy surfaces. Depending on the nature of the problem, the calculations may focus on local regions of a potential surface (for example, the vicinity of a transition state), or may cover the surface globally. A second aspect of this program is the development of techniques to fit multi-dimensional potential surfaces to convenient, global, analytic functions that can then be used in dynamics calculations. Finally a third part of this program involves the use of direct dynamics for high dimensional problems to by-pass the need for surface fitting.

Initiation Reactions: Little is known about the reactions responsible for the initiation of combustion even in the simplest systems (H_2-O_2). This is partly because these reactions are so slow, that measurement of the rates is quite challenging. This year we undertook joint theoretical-experimental studies of two initiation reactions. The following are brief summaries of the key findings from these studies.

(A) $H_2+O_2 \rightarrow HOO+H$: Extensive searches using both CCSD(T) and MR-CI methods were made for transition states for reactions (1)-(3).

$$H_2+O_2 \rightarrow HOO+H \quad (1)$$
$$H_2+O_2 \rightarrow 2HO \quad (2)$$
$$H_2+O_2 \rightarrow O+H_2O \quad (3)$$

No transition states could be found for reactions (2) and (3). High level electronic structure calculations, CCSD(T)/cc-pvqz, on reaction (1), coupled with conventional transition state theory calculations yielded rate constants in good agreement both with new high temperature measurements by Michael and with older low temperature measurements on the reverse reaction by Kaufman, Keyser and others.

(B) $H_2CO+O_2 \rightarrow HOO+HCO$: In the second joint theoretical/experimental project, the reaction of formaldehyde with molecular oxygen was examined using CCSD(T)/cc-pvdz calculations. The calculations predict a loose long range complex on the product side, bound by 5.3 kcal/mole relative to HOO+HCO. The barrier separating the complex and the reactants is predicted to lie slightly below the energy of the products. Conventional transition state theory using the ab initio transition state parameters were found to yield a rate constant in good agreement both with new high temperature measurements by Michael and earlier low temperature measurements by Baldwin.

Potential Surfaces: A feature of this program is the development of analytic potential surfaces that can be used in subsequent dynamical studies. This year progress was made on two such surfaces. The following are brief summaries of these efforts.

(A) $CH_4 \rightarrow CH_3+H$: Methane dissociation is an important prototype for unimolecular dissociation/recombination reactions. This year we completed a four dimensional surface for this reaction based on accurate, high level (CAS+1+2/aug-cc-pvtz) calculations. The four dimensions included consist of the dissociating CH bond distance, the two transitional modes for the

departing hydrogen atom and the CH_3umbrella mode. The new surface is somewhat more attractive than the Hase-Hirst potential. Two collaborative efforts are now underway using this new surface in dynamical studies. Statistical adiabatic channel (SACM) calculations are being done by Sibert (University of Wisconsin) and variable reaction coordinate transition state theory calculations are being done by Klippenstein (Case-Western Reserve).

(B) $CH + HCCH \rightarrow C_3H_3$: Propargyl radical is thought to be a precursor to soot formation in flames. As such there is considerable interest in reactions leading to the formation of propargyl. One such reaction is CH+HCCH. Previous theoretical studies have focused on the barriers to rearrangement separating various C_3H_3 isomers. The present calculations focus in the long range interaction between CH and HCCH. The coordinate system used is as shown,

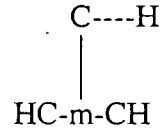

where m is the center of mass of the HCCH fragment. The results show attractive, long-range, interactions for all values of the C-m-C angle. For C-M-C angles near ninety degrees the preferred orientation of the CH is parallel to the HCCH (as shown above) while for C-m-C angles near zero the preferred orientation is colinear, HCCH---CH. A three dimensional (the C-m distance, the H-C-m angle and the C-m-C angle) analytic surface is now in progress. A preliminary two dimensional contour plot of this surface is shown in Figure 1.

Direct Dynamics Studies: Current techniques for the analytic representation of multi-dimensional potential surfaces can be routinely applied to systems of at most four atoms. To go beyond this limit we have been investigating (in collaboration with Stephen Klippenstein) the use of techniques in which the ab initio energies are input directly into the dynamical calculations, without using analytic representations. Last year we completed a direct dynamics study of the CH_3+CH_3 recombination reaction. This year work has focused on two reactions:

$$HNNOH \rightarrow HNN + OH \qquad (4)$$
$$CH_3OH \rightarrow CH_3 + OH \qquad (5)$$

The first of these is a key step in the Thermal De-NO_x process. The second is the lowest, simple bond cleavage pathway for the decomposition of methanol, which is thought to compete with several, non radical-producing, pathways. For both reactions the dynamical bottlenecks occur in parts of the potential surface where two surfaces are quite close in energy. To treat this near-degeneracy, MR-CI calculations are being done using state-averaged CAS orbitals.

Future Plans: In addition to continuing work on the CH+HCCH potential surface described above, we plan to extend our direct dynamics studies in several areas. First, direct dynamics techniques now make it feasible to study more complicated radical-radical reactions such as CH_3+C_2H_3 and C_2H_3+C_2H_3. Second, we plan to use direct dynamics to explore mechanistic questions. For example, there remains an unresolved dispute between theory and experiment regarding the products resulting from the decomposition of CH_3O; experimental evidence suggests that CO is produced, while no theoretical calculations have been able to locate a transition state leading to CO. A direct dynamics study may be able to resolve this question.

*Work performed under the auspices of the Office of Basic Energy Sciences, Division of Chemical Sciences, U.S. Department of Energy, under Contract W-31-109-Eng-38.

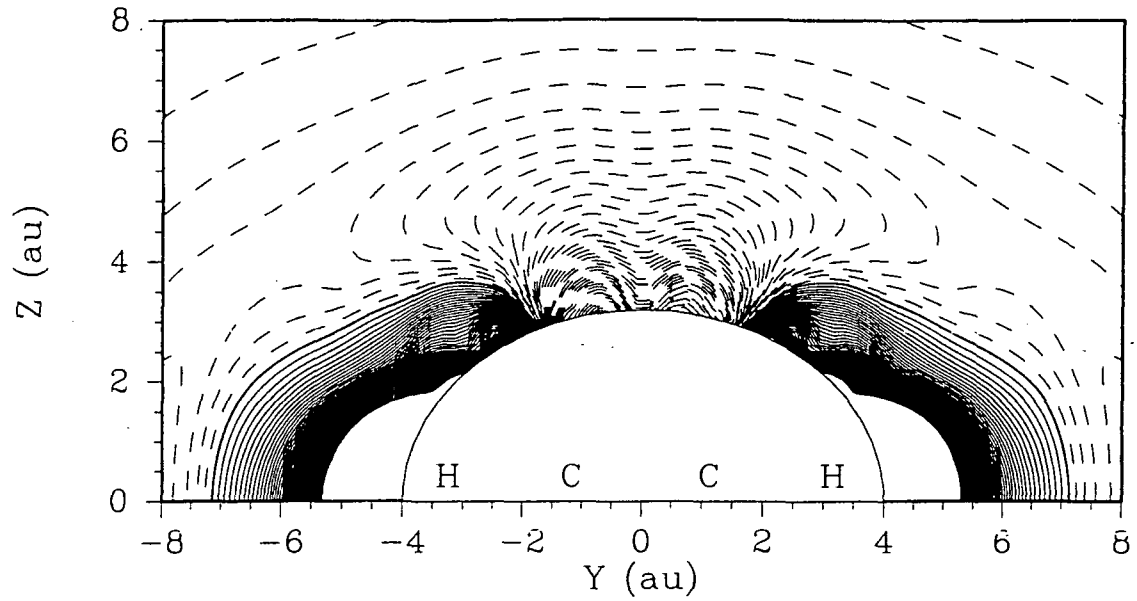

Figure 1: Two dimensional contour plot of the planar CH+HCCH interaction potential for the $^2A''$ potential. The internal coordinates of both the HCCH and CH fragments are kept fixed. The (y,z) coordinates depict the location of the CH carbon in a cartesian coordinate system centered on the HCCH fragment (as shown). At each point the m-C-H angle is optimized. The contour increment is 0.5 kcal/mole, dashed contours are attractive, solid contours are repulsive.

PUBLICATIONS (1997 - Present):

A Theoretical Study of Solid Hydrogens Doped with Atomic Oxygen,
Z.L. Li, V.A. Apkarian and L.B. Harding, *J. Chem. Phys.* **106**, 942-953 (1997)

Ab Initio Calculations of Force Fields for H_2CN and ClHCN and Vibrational Energies of H_2CN,
S. Carter, J.M. Bowman and L.B. Harding, *Spectrochimica Acta* **Part A 53**, 1179-1188 (1997)

Potential Energy Surfaces for CH Bond Cleavage Reactions,
L.B. Harding, *Berichte der Bunsen-Gesellschaft fur Physikalische Chemie* **101**, 363-371 (1997)

The Influence of Hindered Rotations on Recombination/Dissociation Kinetics,
A.F. Wagner, L.B. Harding, S.H. Robertson, and D.M. Wardlaw,
Berichte der Bunsen-Gesellschaft fur Physikalische Chemie **101**, 391-399 (1997)

A Global A-State Potential Energy Surface for H_2O: the Influence of Excited States on the $O(^1D)+H_2$ Reaction, T.-S. Ho, T. Hollebeek, H. Rabitz, L.B. Harding, and G.C.Schatz,
J. Chem. Phys. **107**, 2340-2350 (1997)

Thermal Rate Constant and Branching Ratio for CN+HD→HCN/DCN+D/H from T=293 to 375K
G. He, I. Tokue, L.B. Harding, and R.G. Macdonald, *J. Phys. Chem.* **102**, 7653-7661 (1998)

A Theoretical Analysis of the Reaction of H with C_2H_5, L.B. Harding and S.J. Klippenstein *Comb. Symp.* **27**, 151-157 (1998)

New Studies of the Unimolecular Reaction $NO_2 \rightarrow O+NO$. II. Relation between High Pressure Rate Constants and Potential Parameters, L. B. Harding, H. Stark, J. Troe, and V.G. Ushakov *Phys. Chem. Chem. Phys.* **1**, 63-72 (1999)

A Theoretical Study of the Kinetics of C_2H_3+H, S.J. Klippenstein and L.B. Harding *Phys. Chem. Chem. Phys.* **1**, 989-997 (1999)

Exploring the Reactions Dynamics of Nitrogen Atoms: A combined Crossed Beam and Theoretical Study of $N(^2D)+D_2 \rightarrow ND+H$, M. Alagia, N. Balucani, L. Cartechini, P. Cassavecchia, G.G. Volpi, L.A. Pederson, G.C. Schatz, G. Lendvy, L.B. Harding, T. Hollebeek, T.-S. Ho and H. Rabitz, *J. Chem. Phys.* **110**, 8857-8860 (1999)

Reaction of H with Vibrationally Excited Water: Activated or Not ?, G.C. Schatz, G. Wu, G. Lendvay, D.-C. Fang, L.B. Harding, *Faraday Discussions* **113**, 151-165 (1999)

A Direct Transition State Theory Based Study of Methyl Radical Recombination Kinetics S.J. Klippenstein and L.B. Harding, *J. Phys. Chem.* **103**, 9388-9398 (1999)

An Empirical Potential Surface for the Ne-OH/D Complexes, H.-S. Lee, A.B. McCoy, L.B. Harding, C.C. Carter and T.A. Miller, *J. Chem. Phys.* **111**, 10053-10060 (1999)

Potential Energy Surface and Quasiclassical Trajectory Studies of the $N(^2D)+H_2$ Reaction L.A. Pederson, G.C. Schatz, T.-S. Ho,T. Hollebeek, H. Rabitz, L.B. Harding and G. Lendvy *J. Chem. Phys.* **110**, 9091-9100 (1999)

Classical Trajectory Calculations of the High Pressure Limiting Rate Constants and of Specific Rate Constants for the Reaction $H+O_2 \rightarrow HO_2$: Dynamic Isotope Effects Between Tritium+O_2 and Muonium+O_2, L.B. Harding, J. Troe, and V.G. Ushakov *Phys. Chem. Chem. Phys.* **2**, 631-642 (2000)

Potential Energy Surface of the A State of NH_2 and the role of Excited States in the $N(^2D)+H_2$ Reaction, L.A. Pederson, G.C. Schatz, T. Hollebeek, T.-S. Ho, H. Rabitz and L.B. Harding *J. Phys. Chem.* 104,2301-2307(2000)

A Summary of "A Direct Transition State Theory Based Study of Methyl Radical Recombination Kinetics", S.J. Klippenstein and L.B. Harding *J. Phys. Chem.* **104**,2351-2354(2000)

Femtosecond Laser Studies of Ultrafast Intramolecular Processes

Carl Hayden
Combustion Research Facility, MS9055
Sandia National Laboratories
Livermore, CA 94551-0969
CCHAYDE@SANDIA.GOV

Program Scope

Our research focuses on studies of ultrafast energy relaxation and unimolecular reaction processes in very highly excited molecules. The goal of these studies is to provide measurements of the time scales for elementary chemical processes that play critical roles in the reaction mechanisms of highly excited reaction intermediates. The development of new techniques that take advantage of the time resolution provided by femtosecond lasers for studies of chemical processes is an integral part of this research. Over the past several years we have developed femtosecond time-resolved photoelectron spectroscopy and combined this with photoionization yield measurements to study the pathways of ultrafast processes.

Currently, we are working to develop methods for time-resolved dynamics studies of vibrationally hot free radical species. One of the only methods for creating hot radicals with subpicosecond time-resolution is through photodissociation of appropriate precursors. Thus, we have extended our photoionization techniques to study photodissociation processes and the subsequent time evolution of the resulting highly excited photofragments. We are using a time-resolved photoelectron-photoion coincidence imaging apparatus that is specifically designed for studying unimolecular processes, such as isomerization, in vibrationally hot free radicals produced by photolysis. This new technique combines ion imaging to determine fragment internal energies with photoelectron spectroscopy for time-resolved characterization of the photoproducts, enabling measurements of internal energy resolved reaction rates.

Recent Progress:

Photoelectron Angular Distributions in the Molecular Frame of a Dissociating Molecule

For the purpose of developing the coincidence imaging technique we have been studying the dissociative multiphoton ionization (DMI) pathways for NO_2 with femtosecond pulses in the wavelength region around 375 nm. Our experiments on NO_2 have provided a detailed picture of the DMI process in this molecule, revealing a totally unexpected mechanism. An energy level diagram illustrating this process is shown in Figure 1. Over the past year we have greatly enhanced our ability to measure and analyze time-resolved photoelectron angular distributions (PADs) referenced to the dissociation axis of the molecule. This capability gives us a new way to probe ultrafast dynamics.

In our experiments, 100 fs laser pulses at 375.3 nm are split into two paths so that the ionization probe pulse may be time-delayed with respect to the pump pulse. The two beams are then recombined and focused into the apparatus. The femtosecond laser beam is crossed with a continuous molecular beam (2% NO_2 in Ar) in the horizontal plane. The pump pulse dissociates and the probe pulse ionizes the molecules. After an ionization event, the photoelectron is accelerated towards one time- and position-sensitive detector. After a 100 ns time delay, during which the electrons are detected, a voltage pulse accelerates the ions toward a second time- and position-sensitive detector. Each detector records the arrival time, and hence velocity, of the particle in one dimension, while the position supplies the other two dimensions of the particle

velocity. In the case of the ion, the arrival time also provides mass selection. The particles are detected in coincidence, such that the ion-electron pair originates from the same ionization event. Using the position and arrival time together, the recoil velocity vectors for the photofragment and photoelectron are calculated for each detected event. After the detection of many coincident events, complete three-dimensional photofragment and photoelectron energy and angular distributions can be constructed due to the 4π acceptance solid angles of both detectors.

To extract molecular frame PADs, we determine the angle between the electric vector of the light and the fragment ion velocity vector, and the angle between the fragment ion and coincident electron velocity vectors, for each detected event. If we consider only events in which the ion recoil direction is parallel ($\pm 10^{\circ}$) to the pump and probe laser polarizations, the resulting three-dimensional electron angular distributions are azimuthally isotropic about the ion recoil axis. In Figure 2, the PADs are displayed as polar plots of the electron intensity (per unit solid angle) as a function of the angle between the ion and electron recoil directions. The earliest stages of the dissociation are probed with zero pump-probe time delay. In this case, the dissociation and ionization both occur within the duration of a single laser pulse (100 fs). Pump-probe time delays of 350 fs, 500 fs, and 10 ps probe progressively later stages of the dissociation. The experimental PAD for zero time delay [Fig. 2(a)] is strongly forward-backward asymmetric with higher intensity in the direction of NO^+ recoil. A prominent lobe is observed at about 30° from the ion recoil direction. As the pump-probe time delay is increased to 350 fs and then to 500 fs [Fig. 2(b) and (c) respectively] the asymmetry decreases and the lobe becomes less prominent. At a time delay of 10 ps [Figs. 2(d], the PAD is symmetric and the lobe at 30° is absent.

The strong forward-backward asymmetry and the lobe at 30° from the O-NO dissociation axis, observed in the PADs at short time delays, are primarily attributed to scattering of the ejected electron from the highly non-spherical potential created by the close proximity of the O and NO fragments when ionization occurs to yield NO^+. As the dissociation proceeds, the PAD features rapidly evolve as the effect of the departing O-atom on the ionization weakens. After 1 ps, the dissociation is complete and the PADs correspond to ionization of free NO(C). These are the first measurements of femtosecond time-resolved PADs in the molecular frame of a dissociating molecule. The PADs for a dissociating molecule provide an entirely new approach for probing dissociation processes. In addition, they are an excellent test for recent theoretical treatments of photoelectron angular distributions.

Femtosecond VUV Photoelectron Spectroscopy

For time-resolved studies of unimolecular processes in radicals following photolysis of radical precursors, the ionization of vibrationally hot molecules is a crucial step. We have successfully detected hot allyl radicals using femtosecond two-photon ionization near 250nm. However, for a more general ionization method we have focused on development of femtosecond VUV ionization. The VUV photon energy must be below the precursor ionization potential but sufficient to ionize the radical. We have developed a femtosecond VUV source with a photon energy less than 9.5 eV (131 nm). Operated under proper conditions, the femtosecond VUV source produces vibrationally resolved photoelectron spectra of cold molecules, such as benzene. Changes in the photoelectron spectrum as the molecule is heated (as high as 2000 K) are readily observed. A pulsed pyrolysis source[2] has been constructed to heat molecules and also to thermally generate radicals from precursors. Using this source and femtosecond VUV ionization we have measured photoelectron spectra of hot radicals such as propargyl, allyl and benzyl.

Future Plans

One of the main purposes for developing the coincidence imaging technique is to study isomerization in hot radicals. Radical isomerization processes are difficult to study directly because such studies would require the generation of a sample of hot, thermodynamically unstable radicals and then the detection of their isomeric form as a function of time. Photolysis of precursor molecules produces hot radicals, but with a wide distribution of internal energies. Normally this would preclude studies of internal energy specific reaction rates. However, if the radical fragment is photoionized then we can determine the fragment recoil energy, and hence internal excitation, for individual radicals using our arrival-time and position-sensitive ion imaging technique. The electron produced in the photoionization probe step is collected in coincidence and its energy determined. Thus, collection of many coincident ions and electrons provides time-resolved photoelectron spectra over a range of radical internal energies. From the photoelectron spectrum of a radical, its isomeric form can usually be determined. Thus, by collecting coincident ion and electron images at a range of time delays between generation of the radicals by photolysis and their detection by photoionization, we will be able to follow the progress of radical isomerization processes in time as a function of internal energy.

Our studies of radical isomerization processes will focus initially on isomers of the allyl radical. Isomerization of cyclopropyl radical to allyl is a simple example of ring opening, while methylvinyl isomerization to allyl radical is a simple hydrogen migration. We have performed initial studies on the photolysis of cyclopropyl iodide, but the two photon ionization approach we applied did not detect cyclopropyl radicals. Therefore, the initial products from the photolysis are, at present, not known. We are currently working to use our VUV source to ionize the photolysis products. The next step is to push the VUV generation to still longer wavelengths to avoid precursor ionization. When this is accomplished, VUV ionization can be used with coincident detection of the recoiling radical fragment ions. The combination of photolysis with VUV ionization will provide a very general capability for studying radical processes.

References

1. J. A. Davies, J. E. LeClaire, R. E. Continetti, and C. C. Hayden, J. Chem. Phys. **111**, 1 (1999).
2. D. W. Kohn, H. Clauberg, and P. Chen, Rev. Sci. Instrum. **63**, 4003 (1992).

Publications: 1997-Present

C. C. Hayden and A. Stolow, "Non-Adiabatic Dynamics Studied by Femtosecond Time-Resolved Photoelectron Spectroscopy", in *Adv. Ser. in Phys. Chem., Vol. 10: Photoionization and Photodetachment*, edited by C. Y. Ng, (World Scientific, Singapore, 1999) in press.

J. A. Davies, J. E. LeClaire, R. E. Continetti, and C. C. Hayden, "Femtosecond Time-Resolved Photoelectron-Photoion Coincidence Imaging Studies of Dissociation Dynamics", J. Chem. Phys. **111**, 1 (1999).

J. A. Davies, R. E. Continetti, D. W. Chandler, and C. C. Hayden, "Femtosecond Time-Resolved Photoelectron Angular Distributions Probed During Photodissociation of NO_2", Phys.Rev. Lett. Submitted (2000).

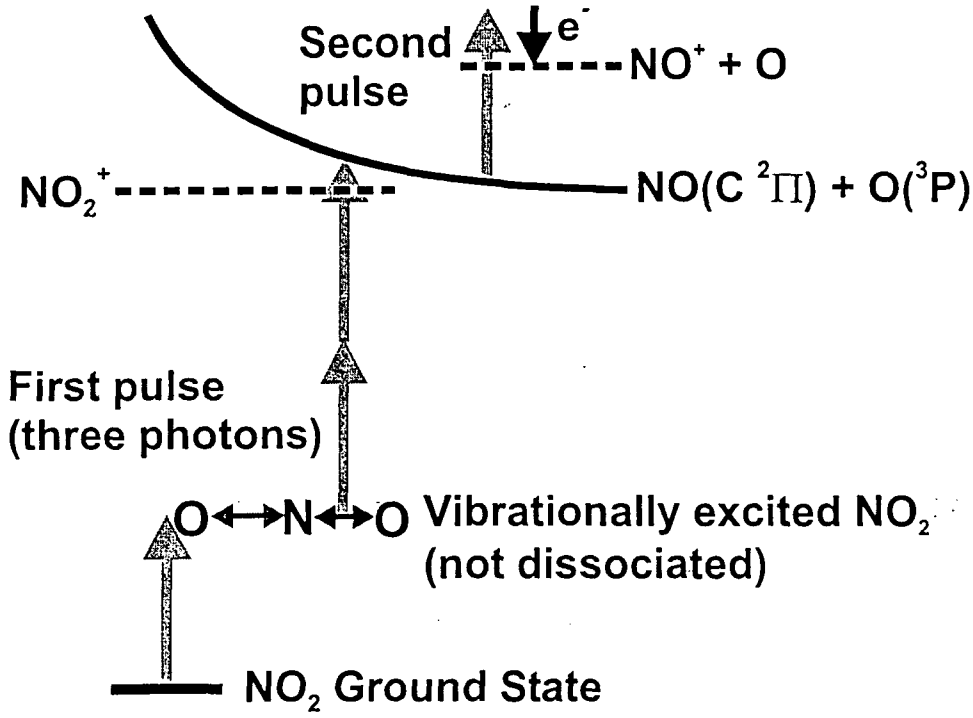

Figure 1. Energy level diagram for multiphoton ionization of NO_2. With femtosecond pulses at 375 nm three-photon excitation occurs through intermediate states to a dissociative state above the NO_2 IP. One-photon ionization follows directly to produce $NO^+ + O$

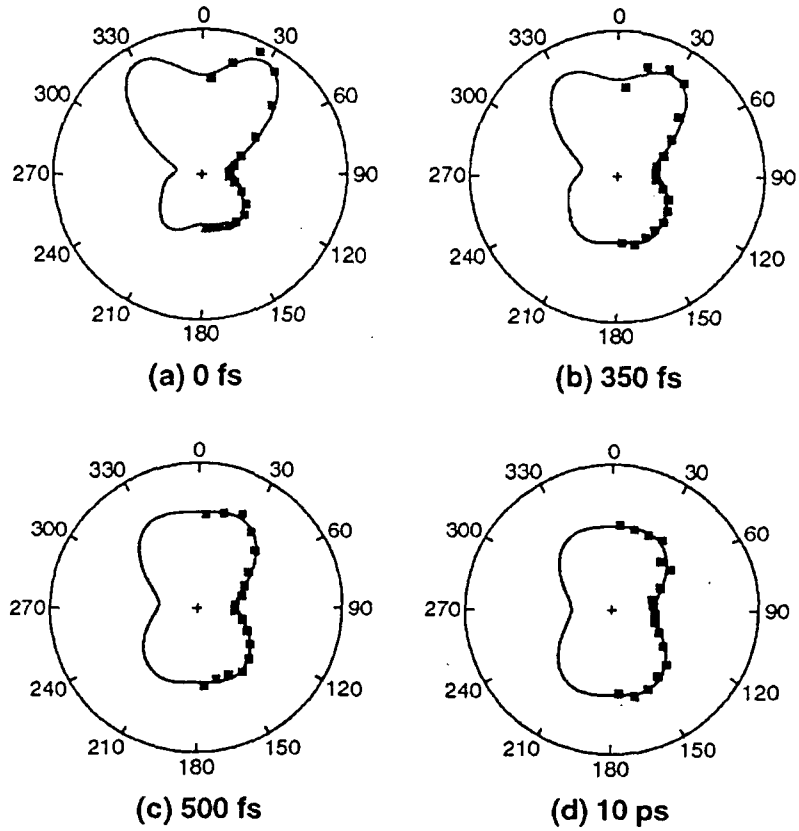

Figure 2. Time-resolved photoelectron angular distributions from the ionization of dissociating NO_2. The electron intensity is represented by the distance between the experimental data points and the origin of the polar plot. It is plotted as a function of angle between the direction of the NO^+ (0 degrees) and the direction of the electron recoil. The electric vectors for the pump and probe laser polarizations are parallel to the ion recoil direction and dissociation axis.

CHEMICAL ACCURACY FROM AB INITIO MOLECULAR ORBITAL CALCULATIONS

Martin Head-Gordon
Department of Chemistry, University of California, Berkeley, and,
Chemical Sciences Division, Lawrence Berkeley National Laboratory,
Berkeley, CA 94720.
mhg@cchem.berkeley.edu

1. Scope of Project.

Short-lived reactive radicals and intermediate reaction complexes are believed to play central roles in combustion, interstellar and atmospheric chemistry. Due to their transient nature, such molecules are challenging to study experimentally, and our knowledge of their structure, properties and reactivity is consequently quite limited. To expand this knowledge, we develop new theoretical methods for reliable computer-based prediction of the properties of such species. We apply our methods, as well as existing theoretical approaches, to study prototype radical reactions, often in collaboration with experimental efforts. These studies help to deepen understanding of the role of reactive intermediates in diverse areas of chemistry. At the same time, these challenging problems sometimes reveal frontiers where new theoretical developments are needed in order to permit better calculations in the future.

2. Summary of Recent Major Accomplishments.

2.1 Density functional theory for ground and excited states of radicals.

We have probed the applicability of density functional theory for the ground and excited states of radicals. For the ground state, traditional wavefunction-based methods are plagued with symmetry-breaking problems for radicals. We have shown that density functional methods can alleviate this problem, and a basic explanation for their improved stability was uncovered [13]. For excited states, time-dependent density functional theory (TDDFT) provides a formally exact framework for the calculation of excitation energies. In practice, however, approximate functionals are employed and the adiabatic approximation is invoked. We have shown [14,17,18,19] that low-lying excited states of radicals can usually be adequately described using TDDFT with existing functionals. This is a particularly exciting result because such states often involve substantial double excitation character which is tremendously difficult to describe within wavefunction-based approaches. The positive results of these investigations significantly expand the range of radicals which are amenable to simulation by electronic structure methods.

2.2 Radical reactions.

Experimentally it is often not possible or feasible to characterize the short-lived intermediates which are transiently formed during the radical neutral reactions that play important roles in combustion and interstellar chemistry. Theoretical methods are ideal

for this purpose however, and therefore the combination of experimental data and calculations together can yield deeper insight than either separately. We have completed a joint theoretical and experimental study [1,2,3,8,16] of the reaction of H_2S + atomic C, with the objective of characterizing the intermediate H_2CS species, the reaction pathway, and the relative propensity for forming HCS and HCS as products. This reaction is an interesting model system for the sulfur-based chemistry that can arise in the presence of reactive atomic species, which is controversial in such contexts as the chemistry induced in the Jovian atmosphere by cometary collisions, and the generation of organosulfur compounds as combustion byproducts.

3. Summary of Research Plans.

3.1 Density functional theory for excited states of radicals.

We are planning further development and application of the time-dependent density functional (TDDFT) approach to excited states of large molecules, particularly radicals. Based on our emerging understanding of how TDDFT performs with present day functionals, it appears that a wide range of interesting applications concerning the nature of low-lying valence excited states in large unsaturated molecules may now be feasible. Such applications will produce useful chemical information, and further sharpen our understanding of TDDFT's present strengths and weaknesses, as a basis for future theoretical work.. We are undertaking a study of excited states of the phenyl peroxy radical. Experiments on this radical in solution by the Ingold group (NRC), and in the gas phase by Lim (Emory) showed that it exhibits an absorption in the visible. This is in dramatic contrast to the corresponding vinyl peroxy radical which only absorbs in the UV, based on experiments by Fahr and Lauffer. There is also current experimental interest within the combustion program by Green (MIT) on other radicals isoelectronic to the phenyl peroxy species (eg. Ph-C2H3, etc), which we shall also examine.

We are also examining the behavior of TDDFT for the so-called dark excited states of polyene oligomers such as butadiene, hexatriene, and octatetraene. These are states which have proved enormously difficult to calculate by conventional wavefunction methods, because of their substantial double excitation character. We are beginning to work on extensions of TDDFT to explore excited potential energy surfaces via gradient and possibly hessian evaluation, extending the techniques we have successfully developed for CIS [19]. We also plan to examine the improved functionals, to better describe the Rydberg excited states for which current functionals perform poorly.

3.2 A new standard of accuracy for electronic structure calculations?

In the words of Thom Dunning at the last American Conference on Theoretical Chemistry, the CCSD(T) coupled cluster method is the present "gold standard of quantum chemistry". However, this is based on a series of calculations on closed shell atoms and molecules. The situation may well be substantially less satisfactory for radicals. We are engaged in a comprehensive benchmark study to assess the comparative performance of CCSD(T) for radicals versus closed shell species, using roughly a dozen well-characterized radicals. At the same time we will obtain benchmark data for the

performance of current density functional theory (DFT) methods. Preliminary indications are that the performance of CCSD(T) for unsaturated radicals is considerably worse than for the closed shell species. This seems to be because CCSD(T) has its origin in Moller-Plesset (MP) perturbation analysis at 4^{th} and 5^{th} orders. It is well-known that the convergence of the MP series is substantially poorer for radicals than for neutrals.

We are also developing a new correction to coupled cluster theory based on a direct second order correction to the CCSD reference problem. It is possible to construct a reference Hamiltonian which the CCSD problem exactly solves. This Hamiltonian is found as a similarity transformation of the normal Hamiltonian, followed by a partitioning. The correction to CCSD is then based on second order perturbation theory using as a perturbation the difference between the full transformed Hamiltonian, and the partitioned transformed Hamiltonian. This correction contains not only normal one and two body operators, but the effect of three and four body operators as well. As such this perturbation series has a substantially different grouping of terms to CCSD(T). At second order, it is already a superset of the CCSD(T) terms, because quadruple substitutions enter, and the overall cost appears to be roughly twice as great. If this method can improve CCSD(T), this will be a very significant and exciting development.

3.3 Unravelling radical reaction chemistry.

We intend to continue to study systems of current experimental interest within the combustion program, using electronic structure methods. We are implementing the direct simulation of a polyatomic neutral-radical reaction by ab initio "on-the-fly" quasiclassical trajectories, with density functional calculation of the energies and gradients on the potential energy surface. The objective is to gain insight into the reaction mechanism, rather than to produce rate constants. This is particularly important for polyatomic radical neutral reactions that involve multiple barriers, multiple intermediate complexes, and of course multiple chemically distinct exit channels. Accurate ab initio calculations such as we perform using coupled cluster methods may not give direct insight into the reaction mechanism, particularly when there are many saddle points of similar energy.

A series of initial trajctories will be performed for carbon plus acetylene where we have previously performed accurate calculations. We anticipate future joint theoretical and experimental studies in which highly accurate coupled cluster calculations of stationary points are supplemented by qualitative trajectory information to elucidate the origin of experimental measurements of product distributions. If reasonable success is achieved with the initial applications, we shall plan to examine new systems of experimental interest within the program, and also attempt to extend the technique to multiple surfaces using time-dependent density functional theory. Finally, we hope that the tools we are building for this trajectory effort will lead to natural collaborations that enable the use of more advanced dynamical methods such as semiclassical techniques and reaction path Hamiltonian models, together with "on-the-fly" generated potentials.

4. Publications from DOE Sponsored Work, 1998-present.

[1] "The Formation of HCS and HCSH Molecules and Their Role in the Collision of Comet Shoemaker-Levy 9 with Jupiter", R.I.Kaiser, C.Ochsenfeld, M.Head-Gordon and Y.T.Lee, Science 279, 1181-1184 (1998).

[2] "Fourier Transform Millimeter Wave Spectroscopy of the HCS Radical in the 2A' Ground Electronic State", H.Habara, S.Yamamoto, C.Ochsenfeld, M.Head-Gordon, R.I.Kaiser, and Y.T.Lee, J. Chem. Phys. 108, 8859-8863 (1998).
[3] "Combined Crossed Molecular Beams and Ab Initio Investigation of the Formation of Carbon-bearing Molecules in the Interstellar Medium via Neutral-Neutral Reactions", R.I.Kaiser, C.Ochsenfeld, D.Stranges, M.Head-Gordon and Y.T.Lee, Faraday Discussions 109, 183-204. (1998).
[4] "Shifted Contour Auxiliary Field Monte-Carlo for Electronic Structure: Straddling the Sign Problem", R.Baer, M.Head-Gordon, and D.Neuhauser, J. Chem. Phys. 109, 6219-6226 (1998).
[5] "A Multipole Acceptability Criterion for Electronic Structure Theory", E.Schwegler, M.Challacombe, and M.Head-Gordon, J. Chem. Phys 109, 8764-8769 (1998).
[6] "Energy Renormalization Group Method for Electronic Structure of Large Systems", R.Baer and M.Head-Gordon, Phys. Rev. B 58, 15296-15299 (1998).
[7] "Electronic Structure of Large Systems: Coping with Small Gaps Using the Energy Renormalization Group Method", R.Baer and M.Head-Gordon, J. Chem. Phys. 109, 10159-10168 (1998).
[8] "Crossed-beam Reaction of Carbon Atoms with Sulfur Containing Molecules I: Chemical Dynamics of Thioformyl (HCS; X^2A') Formation From Reaction of C (^3P_j) with Hydrogen Sulfide, H_2S (X^1A_1)", R.I.Kaiser, C.Ochsenfeld, M.Head-Gordon and Y.T.Lee, J. Chem. Phys. 110, 2391-2403 (1999).
[9] "Quasidegenerate Second Order Perturbation Corrections to Single Excitation Configuration Interaction for Excitation Energies", M.Head-Gordon, M.Oumi, and D.Maurice, Mol. Phys. 96, 593-602 (1999)
[10] "Ab Initio Molecular Orbital Calculations of the Excited States of Chalcone", M.Oumi, D.Maurice and M.Head-Gordon, Spectrochim. Acta 55A, 525-537 (1999).
[11] "Accurate Calculations on Excited States: New Theories Applied to the –OX –XO, and –XO2 (X=Cl and Br) Chromophores and Implications for Stratospheric Bromine Chemistry", T.J.Lee, S.Parthiban and M.Head-Gordon, Spectrochim. Acta 55A, 561-574 (1999).
[12] "Neutral-Neutral Reactions in the Interstellar Medium. II. Isotope Effects in the Formation of Linear and Cyclic C3H and C3D radicals in Interstellar Environments", R.I.Kaiser, C.Ochsenfeld, M.Head-Gordon, and Y.T.Lee, Astrophys. J. 510, 784-788 (1999).
[13] "On the Performance of Density Functional Theory for Symmetry Breaking Problems", C.D.Sherrill, M.S.Lee and M.Head-Gordon, Chem. Phys. Lett. 302, 425-430 (1999).
[14] "Time-dependent Density Functional Theory for Radicals: An Improved Description of Excited States with Substantial Double Excitation Character", S.Hirata and M.Head-Gordon, Chem. Phys. Lett. 302, 375-382 (1999).
[15] "Analytical Second Derivatives for Electronic Excited States using the Single Excitation Configuration Interaction Method: Theory and Application to Benzo[a]pyrene and Chalcone", D.Maurice and M.Head-Gordon, Mol. Phys. 96, 1533-1541 (1999).
[16] "A Coupled Cluster Ab Initio Investigation of Singlet/triplet CH2S Isomers, and the Reaction of Atomic Carbon with Hydrogen Sulfide to HCS/HSC", C.Ochsenfeld, R.I.Kaiser, Y.T.Lee, and M.Head-Gordon, J. Chem. Phys. 110, 9982-9988 (1999).
[17] "Time-dependent Density Functional Study of the Electronic Excitation Energies of Polycyclic Aromatic Hydrocarbon Radical Cations of Napthalene, Anthracene, Pyrene and Perylene", S.Hirata, T.J.Lee, and M.Head-Gordon, J. Chem. Phys. 111, 8904-8912 (1999).
[18] "Time-dependent Density Functional Theory within the Tamm-Dancoff Approximation", S.Hirata and M.Head-Gordon, Chem. Phys. Lett. 314, 291-299 (1999)
[19] "Configuration Interaction Singles, Time-dependent Hartree-Fock, and Time-dependent Density Functional Theory for the Electronic Excited States of Extended Systems", S.Hirata, M.Head-Gordon and R.J.Bartlett, J. Chem. Phys. 111, 10774-10786 (1999).

Infrared Laser Studies of the Combustion Chemistry of Nitrogen

John F. Hershberger

Department of Chemistry
North Dakota State University
Fargo, ND 58105
hershber@prairie.nodak.edu

Time-resolved infrared diode laser spectroscopy is used in our laboratory to study the kinetics and product channel dynamics of several chemical reactions of importance in the gas-phase combustion chemistry of nitrogen-containing radicals. This program is aimed at improving the kinetic database of reactions crucial to the modeling of NO_x control strategies such as Thermal de-NO_x, RAPRENO$_x$, and NO-reburning. The data obtained is also useful in the modeling of propellant chemistry. The emphasis in our study is the quantitative measurement of product branching ratios. For example, in recent years we have quantitatively measured the branching ratios of the CN+NO_2, NCO+NO, NCO+NO_2, and CD+NO reactions. Work during the last year has concentrated on the HCCO + NO and HCC+NO reactions, as well as LIF and infrared studies of NCS+NO_x and HCCl+NO_x kinetics.

A. HCCO+NO Reaction

We have completed our study of the branching ratio of the HCCO+NO reaction. This reaction is of major interest to several laboratories because of its role in NO-reburning mechanisms. In particular, the amount of HCNO formed has a major effect on the subsequent chemistry in NO-reburning models. The most likely possible products include:

$$\text{HCCO + NO} \rightarrow CO_2 + \text{HCN} \quad (1a)$$
$$\rightarrow \text{CO + (HCNO)} \quad (1b)$$

We used infrared diode lasers to probe CO and CO_2 product yields in this reaction. A major difficulty in this system is the lack of ideal photolytic precursors. In combustion systems, HCCO is primarily formed as one channel of the O+C_2H_2 reaction, which is unfortunately quite slow. In earlier work, we attempted to form HCCO from the CN+H_2CCO reaction, but found that CN does not abstract H atoms from ketene, but instead reacts via an addition-elimination mechanism. Work by Curl and Glass,[1] however, has shown that HCCO + H is a significant minor channel in the 193 nm photodissociation of ketene, in addition to the better known CH_2 + CO channel. We have used this approach, even though the CO produced in the dissociation represents a background signal that must be subtracted from the total CO observed in order to obtain the CO yield from the title reaction. (Note that isotopic $N^{18}O$ labeling, previously used in several studies in our laboratory, will not work here because it would likely produce $HCN^{18}O + C^{16}O$, not $HCN^{16}O + C^{18}O$.) Neither of the detected products can originate from the CH_2+NO secondary reaction, which primarily produces HCNO+H.

Our results showed that the CO_2+HCN product channel is produced in the surprisingly low yield of 12±4%, and that CO+(HCNO) dominates this reaction. The (HCNO) presumably appears as fulminic acid, but we cannot rule out contributions from isocyanic acid (HNCO) as well. Our CO_2

yield is somewhat lower than other experimental studies of the Peeters[2] and Temps[3] groups, which reported 23 and 28 %, respectively. All three groups that have conducted direct experimental measurements on this reaction are in qualitative agreement that CO+(HCNO) is the major channel. This is in significant disagreement, however, with ab initio calculations and kinetic modeling of Miller et al,[4-6] which predicted a CO_2 yield of 81% at 300K, with a moderate decrease at higher temperatures. It appears at this time that the potential surface for this reaction as well as the detailed kinetic model of the NO-reburning process need significant refinement.

B. HCCl + NO_x

We are currently investigating reactions of HCCl using both laser-induced fluorescence and infrared absorption techniques. This radical is of interest in modeling the combustion of chlorinated hydrocarbons. We form HCCl from 193-nm photolysis of $HCClBr_2$, and detect it by LIF spectroscopy at 602.53 nm. As of this writing, we have measured room temperature rate constants for HCCl + NO and HCCl + NO_2. The HCCl + NO rate constant is in reasonable agreement with the one previous study of H. Gg. Wagner et al.[7] No previous literature data are available for HCCl + NO_2 kinetics. Rate constant measurements at elevated temperatures are planned in the near future.

For HCCl+NO, several product channels are possible:

HCCl + NO	→ HCNO + Cl	(2a)
	→ HNCO + Cl	(2b)
	→ NCO + HCl	(2c)
	→ HCN + ClO	(2d)
	→ CN + HOCl	(2e)
	→ CO + HNCl	(2f)

So far, we have detected HCNO, but been unable to detect HNCO. We have also detected N_2O and CO_2 which we believe to be secondary products of the NCO + NO reaction. Thus we have evidence that at least two channels are active. In the near future, we will use deuterated reagents to look for DCN and DCl products.

C. HCC + NO

We have performed some product yield measurements on the HCC+NO reaction:

HCC (or DCC) + NO	→ HCN (or DCN) + CO	(3a)
	→ CN + HCO (or DCO)	(3b)

We produce HCC from the 193-nm photolysis of acetylene. Products detected by infrared absorption include CO and DCN (from deuterated precursor). We have also detected CN by LIF spectroscopy, although quantifying the absolute yields by LIF is difficult. In principle, the infrared experiment alone should provide the branching ratio, because any HCO produced in the second channel should produce additional CO via the HCO+NO→CO+HNO reaction. Our data, however, indicates that DCN production exceeds CO production, suggesting that a secondary source of DCN is present. This is surprising, as CN+C_2D_2 is not expected to proceed by D atom abstraction, but via an addition-elimination mechanism, producing DCCCN+D. It is possible that secondary chemistry involving DCCCN produces DCN.

We have also tried indirect detection of CN by adding small amounts of NO_2, and detecting N_2O from the reaction sequence $CN+NO_2 \rightarrow NCO+NO$ followed by $NCO+NO_x$. Kinetic modeling of these results is consistent with significant CN formation, but reliable determination of the branching ratio has so far proved difficult because of unknown secondary chemistry. An alternative approach that we may try in the near future is to photolyze a mixture of C_2H_2, NO, and C_6D_{12} (or some other large deuterated hydrocarbon). The HCC+NO reaction would form HCN+CO and CN+HCO as before, but then $CN+C_6D_{12} \rightarrow DCN + C_6D_{11}$ would occur. By measuring [CO] and [DCN] at different reaction conditions, we be able to obtain the branching ratio, although several other secondary reactions are present here as well.

D. $NCS+NO_x$ Reactions

We have completed the first reported measurements of the kinetics of the NCS radical, which may be an intermediate in the combustion of sulfur-containing fuels.
NCS is apparently an extremely weak infrared absorber, but has a well characterized laser-induced fluorescence spectrum near 375 nm. We have therefore used a tunable dye laser to perform LIF measurements. Two difference methods of producing NCS were used:

$$ICN + h\nu\ (248\ nm) \rightarrow I + CN \qquad (4)$$
$$CN + OCS \rightarrow NCS + CO \qquad (5)$$

$$C_2H_5NCS + h\nu\ (193\ nm) \rightarrow C_2H_5 + NCS \qquad (6)$$

For NCS reactions, we obtain the following rate constants at low total pressure (~2.0 Torr):

$k\ (NCS+NO) = (4.1\pm1.4)\times10^{-15}\ \exp[(1561.5\pm116)/T]$ over the range 296-468 K

$k\ (NCS+NO_2) = (7.0\pm0.6)\times10^{-12}\ \exp[(579\pm39.4)/T]$ over the range 296-620 K.

In addition, we have examined the pressure dependence of these reactions using helium buffer gas. The $NCS+NO_2$ rate constant is not significantly pressure dependent, but the NCS+NO rate constant increases roughly linearly with pressure over the range 0-500 Torr of He, reaching a value of 2.9×10^{-11} cm^3 $molecule^{-1}$ s^{-1} at 500 Torr.

We have also used infrared detection to attempt to detect products. The most likely channels are:

$$NCS + NO \rightarrow N_2O + CS \qquad (7a)$$
$$\rightarrow OCS + N_2 \qquad (7b)$$
$$\rightarrow NCSNO \qquad (7c)$$
$$NCS + NO_2 \rightarrow N_2O + OCS \qquad (8a)$$
$$\rightarrow NCSNO_2 \qquad (8b)$$

We have been unable to detect N_2O or OCS products in either of these reactions. Based on this fact as well as the pressure dependence of the total rate constants, we conclude that the association channels (7c) and (8b) dominate these reactions.

We have also briefly investigated the $NCS+O_2$ and $NCS+C_2H_2$ reactions. No measureable rate was observed, and we estimate upper limits for rate constants of 1×10^{-14} cm^3 $molecule^{-1}$ s^{-1} at 296 K.

References

1. 4. R.F. Curl and G.P. Glass, report of the 1997 Combustion Contractors Meeting.
2. W. Boullart, M.T. Ngugen, and J. Peeters, J. Phys. Chem. **98**, 8036 (1994).
3. U. Eickhoff and F. Temps, Phys. Chem. Chem. Phys. **1**, 243 (1999).
4. J.A. Miller, J.L. Durant, P. Glarborg, Symp. (Int.) Combust. Proc. **26**, 235 (1998).
5. P. Glarborg, M. U. Alzueta, K. Dam-Johansen, J.A. Miller, Combust. Flame **115**, 1 (1998).
6. L. Prada, J.A. Miller, Combust. Sci. Technol. **132**, 225 (1998).
7. R. Wagener, H. Gg. Wagner, Z. Phys. Chem. **175**, 9 (1992).

Publications acknowledging DOE support (1998-present)

"Product Branching Ratios of the HCO+NO_2 Reaction", K.T. Rim and J.F. Hershberger, J. Phys. Chem. A **102**, 5898 (1998).

"A Diode Laser Study of the Product Branching Ratios of the CH+NO_2 Reaction", K.T. Rim and J.F. Hershberger, J. Phys. Chem. A **102**, 4592 (1998).

"Kinetics of the CN+CH_2CO and NCO+CH_2CO Reactions", M. Edwards and J.F. Hershberger, Chem. Phys. **234**, 231 (1998).

"Kinetics of the CN+OCS Reaction", J. Park and J.F. Hershberger, Chem. Phys. Lett. **295**, 89 (1998).

"Reaction of NCO and NCS Radicals", J.F. Hershberger, book chapter in "N-Centered Radicals", A.B. Alfassi, ed., Wiley (1998).

"Temperature Dependence of the Product Branching Ratio of the CN+O_2 Reaction", K.T. Rim and J.F. Hershberger, J. Phys. Chem. A **103**, 3721 (1999).

"Kinetics of the NCS Radical", R.E. Baren and J.F. Hershberger, J. Phys. Chem. A **103**, 11340 (1999).

"Product Branching Ratio of the HCCO+NO Reaction", K.T. Rim and J.F. Hershberger, J. Phys. Chem. A **104**, 293 (2000).

Elementary Reaction Rate Measurements at High Temperatures by Tunable-Laser Flash-Absorption

Jan P. Hessler

Chemistry Division, Argonne National Laboratory
9700 South Cass Avenue, Argonne, Illinois 60439-4831
E-mail: hessler@anl.gov

1. Scope

The major objective of this program is to measure thermal rate coefficients and branching ratios of elementary reactions. To perform these measurements, we have constructed an ultrahigh-purity shock tube to generate temperatures between 1000 and 5500 K. The tunable-laser flash-absorption technique[1] is used to measure the rate of change of the concentration of species which absorb below 50,000 cm^{-1} (*e.g.*, OH, and CH_3). This technique is being extended to utilize multiphoton excitation techniques so we can study atomic species (*e.g.*, H, C, O, N, and Cl) and molecular species (*e.g.*, OH, NO, CO, NH_3, and CF_3).

2. Recent Progress

2.1. Measurements of OH + OH → H_2O + O at High Temperatures and a Reduction of the Data from 230 to 3400 K

The above reaction is chain terminating in the forward direction and chain-branching in the reverse direction and, therefore, influences flame propagation. Recently, we monitored the temporal behavior of hydroxyl in a mixture of 400 ppm C_3H_8 with 4% O_2 in a mixture of He and Kr from 1900 to 3400 K. Our results for the forward rate coefficient are shown in figure 1 along with those of Wooldridge, Hanson, and Bowman[2] and the FP-RF results from Sutherland, Patterson, and Klemm[3]. The solid line in the figure represents a reduction of data from 230 to 3400 K to obtain the phenomenological expression

$$k(cm^3s^{-1}) = 3.22 \times 10^{-20} T^{2.49} \exp[995/T] + 6.63 \times 10^{-8} \exp[-26017/T].$$

The dashed curve represents another fit based on conventional transition-state theory with Eckart tunneling[4]. The parameters of the CTST are the moments of inertia

calculated from the geometries of the two transition states ($^3A'$ and ^3A") calculated by Harding and Wagner[5] and their vibrational frequencies. The well depth of the OH-OH complex was adjusted and found to be -1700 K (-3.4 kcal/mole) whereas the height of the barrier to the lowest triplet surface is 2569 K (5.1 kcal/mole). The second triplet surface was found to be 1256 K (2.5 kcal/mole) above the first surface. Tunneling through both of these surfaces was modeled with the same Eckart length, l, of 0.309 Å. To obtain a good fit the vibrational frequencies of the lower transition state had to be increased by 10% while those of the upper state by only 0.3%. Although the CTST reproduces all of the data between 230 and 2500 K it can not reproduce the rapid increase above 2500 K. Attempts to associate this increase with the onset of the $O(^1D) + H_2O$ channel are not consistent with the measured reverse rate coefficient and equilibrium constant.

2.2. The Reaction $CH_3 + O_2$: The Product Channels Untwined

In the latest study of the two product channels for the above reaction, Rabinowitz and his colleagues state[6], "However, we believe that the two channels are stubbornly linked, and no study to date has been able to untwine them." Recently, we simultaneously extracted the rate coefficients for both the $CH_3O + O$ and the $H_2CO + OH$ channels from time-dependent profiles of the hydroxyl radical and, thereby, untwined the product channels. Our results agree with the recent results of Michael, Kumaran, and Su[7] and Hwang, Ryu, De Witt, and Rabinowitz[6] for the methoxy plus atomic-oxygen channel. For the formaldehyde plus hydroxyl channel our measurements extend from 1174 to 2157 K, reproduce our previous results, and suggest that at high temperatures the rate coefficient goes through a maximum.

Our results are obtained in experiments where the initial molecular oxygen to methyl precursor ratio is much larger than all previous studies that monitor the hydroxyl radical. Furthermore, we use a methyl precursor that dissociates quickly, azomethane. In addition, we used an improved detector scheme that utilizes two linear-array detectors to monitor simultaneously a signal and reference profile and a new injection seeded Nd:YAG plus dye laser to generate the light used to probe the system. These improvements allow us to produce more stable profiles of the probe beam and to obtain reliable data over the entire length of the array detector.

Above 1687 K we can extract rate coefficients for both channels because the duration of our measurements extends over the time interval needed for the system to come to a stable chemical state. Under these conditions, nearly all of the carbon contained in the methyl radicals has been converted to carbon monoxide. Sensitivity analysis shows that the initial slopes of these profiles are sensitive to the rate coefficient for the formaldehyde

plus hydroxyl channel. The branching ratio between the two product channels and the hydroxyl-hydroxyl reaction to form water and atomic-oxygen determine the height and location of the peaks of the profiles. Therefore, because we can accurately monitor the hydroxyl profile over most of the time needed for both primary and secondary chemistry to run to completion we can untwine the rates of the two product channels.

3. Future Plans

Recently, Randall E. Winans, Soenke Seifert, Thomas H. Fletcher (Bringham Young University), and I used the small angle X-ray scattering instrument at the Basic Energy Sciences Synchrotron Radiation Center (BESSRC) of Argonne's Advanced Photon Source (APS) to observe the early formation of soot spherules during the pyrolysis of toluene. These new results bridge the gap between fluorescent images of polycyclic aromatic hydrocarbon emissions and elastic scattering of light in the optical region. In particular, soot particles that range in size between 1 and 50 nm were observed.

Our results point to an opportunity to directly observe the temporal behavior of soot at its earliest stages of formation. To accomplish this we are designing a detector specifically for SAXS studies of spherules that will have a temporal resolution that will match the revolution time of an electron bunch at the APS, 3.68 μs. With this detector we will be able to monitor the formation of soot in a shock tube in the critical period that is not accessible to elastic scattering in the optical region.

Work performed under the auspices of the U.S. Department of Energy, Office of Basic Energy Sciences, Division of Chemical Sciences, under Contract No. W-31-109-ENG-38.

References

[1] VonDrasek, W. A., Okajima, S., Kiefer, J. H., Ogren, P. J., and Hessler, J. P. *Appl. Opts.* **29**, 4899–4906 (1990).

[2] Wooldridge, M. S., Hanson, R. K., and Bowman, C. T. *Int. J. Chem. Kinet.* **26**, 389 (1994).

[3] Sutherland, J. W., Patterson, P. M., and Klemm, R. B. *Int. Symp. on Comb.* **22**, 51–57 (1990).

[4] Eckart, C. *Phys. Rev.* **35**, 1303–1309 (1930).

[5] Harding, L. B. and Wagner, A. F. *Int. Symp. on Comb.* **22**, 983–989 (1988).

[6] Hwang, S. M., Ryu, S. O., Witt, K. J. D., and Rabinowitz, M. J. *J. Phys. Chem. A* **103**, 5942–5948 (1999).

[7] Michael, J. V., Kumaran, S. S., and Su, M. C. *J. Phys. Chem. A* **103**, 5942–5948 (1999).

Publications Supported by this Program 1998-present

Calculation of Reactive Cross Sections and Microcanonical Rates from Kinetic and Thermochemical Data
J. P. Hessler, *J. Phys. Chem.*, **102**, 4517-4526 (1998).

New empirical rate expression for reactions without a barrier: Analysis of the reaction of CN with O_2
J. P. Hessler, *J. Chem. Phys.*, **111**, 4068-4076 (1999).

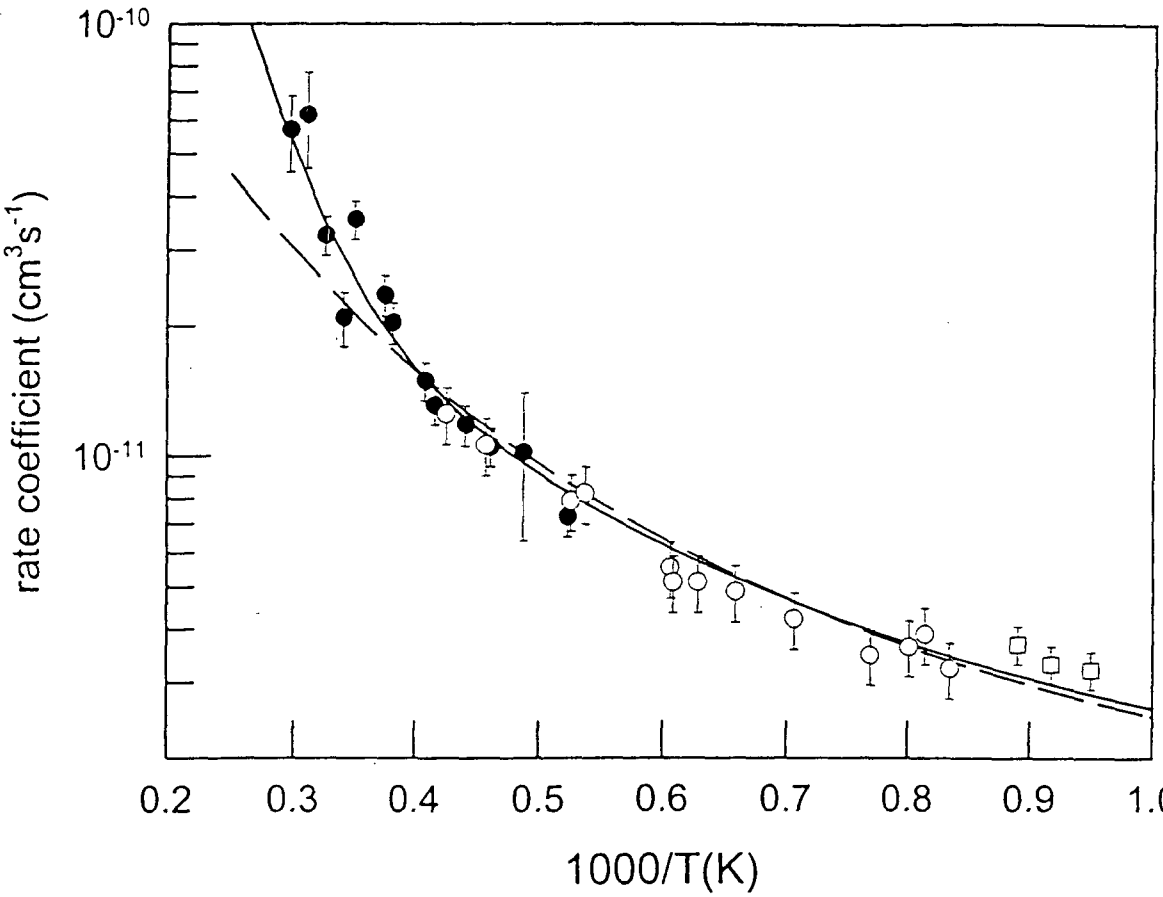

Figure 2.1: Rate coefficient for OH + OH -> H_2O + O. The solid points are from this work, the open circles from reference [2] and the open squares from reference [3].

PRODUCT IMAGING OF COMBUSTION DYNAMICS

P. L. Houston
Department of Chemistry
Cornell University
Ithaca, NY 14853-1301
plh2@cornell.edu

Program Scope

The technique of product imaging is being used to investigate several processes important to a fundamental understanding of combustion. The imaging technique produces a "snapshot" of the three-dimensional velocity distribution of a state-selected reaction product. Research in three main areas is planned. First, the imaging technique will be used to measure rotationally inelastic energy transfer on collision of closed-shell species with several important combustion radicals. Such measurements improve our knowledge of intramolecular potentials and provide important tests of *ab initio* calculations. Second, product imaging will be used to investigate the reactive scattering of radicals or atoms with species important in combustion. These experiments, while more difficult than studies of inelastic scattering, are now becoming feasible. They provide both product distributions of important processes as well as angular information important to the interpretation of reaction mechanisms. Finally, experiments using product imaging at the Advanced Light Source will explore the vacuum ultraviolet photodissociation of CO_2 and other important species. Little is known about the highly excited electronic states of these molecules and, in particular, how they dissociate. These studies will provide product vibrational energy distributions as well as angular information that can aid in understanding the symmetry and crossings among the excited electronic states.

Recent Progress

a. The NO vibrational distribution in the reaction $O(^1D) + N_2O \rightarrow 2\ NO$

The vibrational distribution of NO products from the reaction $O(^1D) + N_2O \rightarrow 2\ NO$ has been measured from v=0 to v=12.[1] The measurement was performed in a molecular beam apparatus, in which the product NO was rotationally but not vibrationally cooled. The NO was detected by REMPI at wavelengths from 220-315 nm. A differentially pumped detection chamber helped to minimize the amount of thermal background NO from previous reactions. As shown in Fig. 1, the measured vibrational population is found to be peaked at v=7, with only a small amount of NO in v=0. This result contrasts sharply with some earlier measurements of the vibrational distribution. Based on this distribution, the amount of vibrational energy in the NO products ($<E_{vib}>$ between 24000 and 28000 cm^{-1}) is much greater than previously reported. The vibrational distribution presented in this work is inconsistent with the dominance of either a stripping or a statistical mechanism producing a substantial fraction of the product NO.

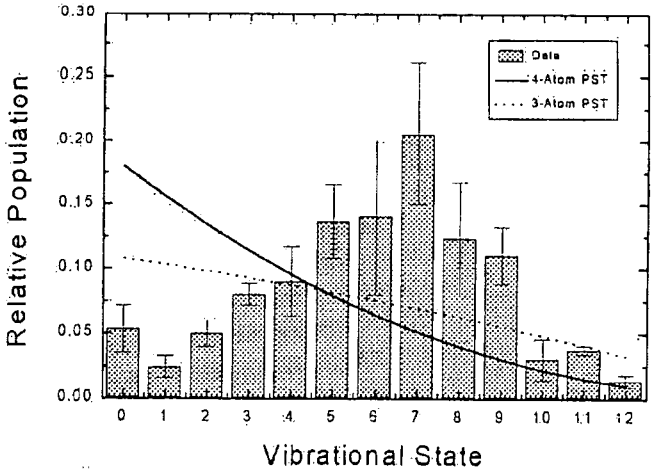

Fig. 1 The measured vibrational distribution of NO products from the reaction of $O(^1D)$ with N_2O along with the predictions of 3-atom phase space theory (dashed line) and 4-atom phase space theory (solid line).

b. Differential Cross Sections for Rotationally Inelastic Collisions of NO(v=0,J)

The differential cross sections (DCS) for rotationally inelastic collisions of NO with He and D_2 were measured for an initial rotational quantum number of J=0.5 and for final quantum numbers of J=2.5 to J=12.5. The measurements were performed in a crossed molecular beam laser ionization, time-of-flight mass spectrometer ion imaging apparatus recently constructed at Sandia National Laboratory.

The apparatus is described in some detail in a forthcoming paper.[2] Basically, a molecular beam of NO is prepared by expanding a 2% NO, 98% Ar gas mixture through a pulsed molecular valve, which produces a rotationally cooled NO molecular beam (>98% in the lowest rotational level). This beam passes through two collimating apertures before it enters the interaction chamber, which is maintained at a pressure less than 5 x 10^{-7} torr during the experiments. This NO beam intersects a similarly collimated beam of either He or D_2 in the center of the interaction chamber. NO molecules that undergo rotationally inelastic collisions are excited to a higher rotational level and are then ionized by a 226-nm laser passing through the intersection point of the two molecular beams. The NO^+ ions are extracted and velocity mapped onto an microchannel plate/phosphor detector.

The extraction of the DCS from the 2-D velocity-mapped ion image was performed using a new numerical integration image simulation program and a basis set of simulated images. For a given set of experimental parameters, the simulation program uses an newly developed algorithm that takes advantage of the geometric constraints of the problem to quickly evaluate the 9-D integral to produce a simulated image. Rather than produce a single simulated image, the simulation program creates a non-orthogonal basis set of images that can be used to simulate quickly an image by matrix multiplication and addition. The DCS is extracted from the data image by iteratively varying the DCS input to the simulated image until an integrated annular region on the data image matches the same integrated annulus on the simulated image. A correspondence between this annular region's angular dependence and the DCS makes the technique robust.

The extracted DCS's have a single rainbow peak that monotonically progresses from forward to backward scattering with increasing J and that occurs in a slightly more forward scattered direction with D_2 than with He. This simple dependence suggests that a simple hard ellipse model may be sufficient to predict the scattering DCS. A comparison with the NO + He PES by Alexander is underway.

c. Allyl and Cyclopropyl Radicals

We have investigated the gas phase photodissociation of cyclopropyl iodide in collaboration with Professor B. K. Carpenter and his student Pam Arnold. Cyclopropyl iodide photodissociates to produce a cyclopropyl radical and an iodine radical. We have been interested in determining whether the highly excited cyclopropyl radical formed in this dissociation process undergoes ring opening, and, if it does, what the time scale for such a process is. Ion and electron imaging have been our main tools.

One goal of our initial investigation was to determine the internal energy distribution of the resulting alkyl radical of cyclopropyl iodide by imaging iodine fragments ($^2P^o_{3/2}$ and $^2P^o_{1/2}$ states) formed from the 266-nm photodissociation of cyclopropyl iodide. The results we obtained were unexpected. According to calculation, the maximum possible total kinetic energy for the system is 1.86 eV. We found that a non-negligible portion of the fragments surpassed this value. If the calculation is correct, a possible explanation is that the cyclopropyl iodide might dissociate directly into lower energy channel giving an allyl radical and iodine radical. By using electron imaging we showed that the photodissociation of allyl iodide at 266 nm and the photodissociation of cyclopropyl iodide at 266 nm, gave, on a time scale of 8 ns, electrons that were ejected with the same energies: one velocity peak in the image corresponded to the ionization of iodine atoms while a second presumably corresponded to the ionization of vibrationally excited allyl radicals. The data thus suggest that allyl radical is indeed present as a product from cyclopropyl iodide photodissociation on an 8 ns time scale.

d. Rotational Differential Cross Sections for Vibrational Excited States

We have begun to measure state-resolved *differential* cross sections for collisions of rare gases with NO(J=0.5) in specific vibrational levels v = 4-7. The impetus for this experiment came both from the possible of comparison to theory and from two experimental advances, both mentioned in the prior

results section above. First, we learned that we could produce NO(v, J=0.5) by dissociating ozone/N_2O mixtures in a carrier gas near to the expansion nozzle. Second, Mike Westley of our group has been studying He and H_2 inelastic differential cross sections for the ground vibrational of NO during visits to Sandia. Figure 2 shows the apparatus used to obtain differential cross sections for collisions of NO(v,J=0.5) with argon .

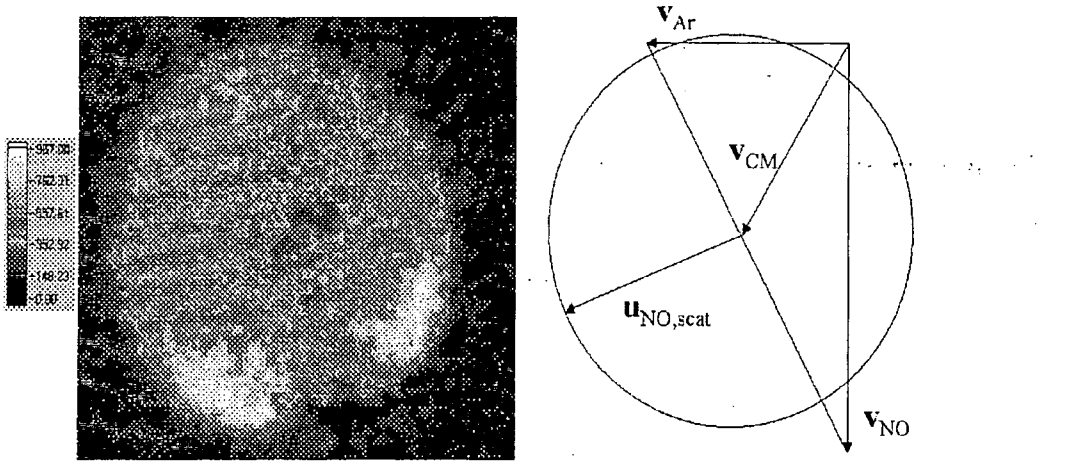

Fig. 2 Image for scattering of NO(v=5, J=0.5) from argon detecting NO(v=5, J= 10.5); Newton diagram for the collision is at right.

An example of a differential cross section image is shown in Fig. 2. The image clearly shows the rotational rainbows associated with rotationally inelastic collisions; in this case theyare located in the forward NO hemisphere, although the position changes with final rotational state and collision energy. The data shown took 1-3 hours of integration time at a laser repetition rate of 10 Hz.

Future Directions

Our success in measuring differential cross sections for rare gas collisions with the densities of NO(v,J) that we can produce in our photolysis source gives us confidence that we can use the capabilities of our source to study differential cross sections for collisions of rare gas atoms with various radical species. Members of our group (as well as others) have extensive experience in creating radicals by photolysis, and many of these can be ionized by simple REMPI schemes. For example, for comparison to the work of Bowman and co-workers,[3] we could create HCO from 308 nm photolysis of acetaldehyde and detect the product rotational states by ionization. Other systems ammenable to study by this technique include collisions of rare gases or small molecules with the following radicals: SO, SH, PO, NH, CH_3 and CH_3O.

We also plan to investigate differential cross sections for reactive collisions. A start has been made on the $O(^1D) + N_2O$ system and the OH + CO system, but improvements to the apparatus will be required to make these practical.

A third area of future investigation is determination of vibrational distributions following VUV photodissociation of small molecules. Despite the large absorption coefficients of small molecules in the vacuum ultraviolet region of the spectrum, little is known either about their excited states or about the products they dissociate to. The availability of a beam line at the Advanced Light Source now makes it possible to investigate the dynamics of energy release for small molecules following absorption of a VUV photon. Typical absorption cross sections in the region from 110-140 nm are on the order of 1 x

10^{-16} cm^2. For triatomics, multiphoton ionization of the atomic photodissociation fragment can be performed with very high efficiency. It should thus be possible using the product imaging facilities of End Station Three at the ALS to image the atomic fragment, thereby determining the vibrational distribution of the sibling diatomic fragment. Such information should help in understanding what bonds in addition to the dissociative one either lengthen or bend during the dissociation process. Angular distributions of products also provide information about the symmetry of the excited state and the time scale for dissociation.

References

1. P. J. Pisano, M. S. Westley and P. L. Houston, "The NO vibrational state distribution in the reaction $O(^1D) + N_2O$ -2 NO," *Chem. Phys. Lett.* **318**, 385-392 (2000).
2. K. T. Lorenz, M. S. Westley, and D. W. Chandler, "Rotational State-to-state Differential Cross Section for the HCl-Ar Collisional System Using Velocity-Mapped Ion Imaging," *PCCP* **2**, 481-494 (2000).
3. J. Qi and J. M. Bowman, "Quantum calculations of inelastic and dissociative scattering of HCO by Ar," *J. Chem. Phys.* **109**, 1734-1742 (1998).

Publications Prepared with DOE Support 1998-2000

B.-Y. Chang, R. C. Hoetzlein, J. A. Mueller, J. D. Geiser, and P. L. Houston, "Improved 2D Product Imaging: The Real-Time Ion-Counting Method," Rev. Sci. Instrum. **69**, 1665-1670 (1998).

J. A. Mueller, S. A. Rogers, and P. L. Houston, "Zero Kinetic Energy Photofragment Spectroscopy: The Threshold Dissociation of NO_2,"J. Phys. Chem. A **102**, 9666-9673 (1998).

P. J. Pisano, M. S. Westley and P. L. Houston, "The NO vibrational state distribution in the reaction $O(^1D) + N_2O$ -2 NO," *Chem. Phys. Lett.* **318**, 385-392 (2000).

K. T. Lorenz, M. S. Westley, and D. W. Chandler, "Rotational State-to-state Differential Cross Section for the HCl-Ar Collisional System Using Velocity-Mapped Ion Imaging," *PCCP* **2**, 481-494 (2000).

AROMATICS OXIDATION AND SOOT FORMATION IN FLAMES

J. B. Howard
MIT 66-454
77 Massachusetts Avenue
Cambridge, MA 02139-4307
Email: jbhoward@mit.edu

Scope

This project is concerned with the kinetics and mechanisms of aromatics oxidation and soot and fullerenes formation inflames. The overall objective of the aromatics oxidation work is to extend the study of benzene oxidation by measuring concentration profiles for important benzene decomposition intermediates such as phenyl and phenoxy radicals which could not be adequately measured with molecular-beam mass spectrometry to permit definitive testing of benzene oxidation mechanisms. The focus includes polycyclic aromatic hydrocarbons (PAH) radicals which are of major importance under fuel-rich conditions although their concentrations are in many cases too low to permit measurement with conventional molecular beam mass spectrometry. The radical species measurements are used in critical testing and improvement of benzene oxidation and PAH growth mechanisms. The overall objective of the research on soot formation is to extend the measurement of radicals into the overlapping region of large molecular radicals and small soot particles with radical sites. The ultimate goal is to understand how nascent soot particles are formed from high molecular weight compounds, including the roles of planar and curved PAH and the relationships between soot and fullerenes. The specific aims are to characterize both the high molecular weight compounds involved in the nucleation of soot particles and the structure of soot including internal nanoscale features indicative of contributions of planar and/or curved PAH to particle inception.

Recent Progress

PAH Radicals in Flames. The study of polycyclic aromatic hydrocarbon radicals was continued using a radical-scavenging flame sampling method similar to that used by Haussman *et al.* (1992). Low-pressure flat flames were probed using a quartz sampling nozzle and low pressure expansion chamber somewhat like those used in molecular beam mass spectrometry. A radical scavenger, dimethyl disulfide (DMDS), is injected into the expanding sample stream, and radicals are trapped along with the scavenger in a frozen matrix. The scavenger reacts with the radicals upon warming the trap to produce methylthio adducts, stable compounds that can be identified using chromatography:

$$R\cdot + CH_3SSCH_3 \Rightarrow R\text{-}SCH_3 + CH_3S\cdot$$

The condensable species including scavenged radicals were washed from the trap with dichloromethane and identified using a GC/MS and a GC with a sulfur chemiluminescence detector which gives an equimolar response to sulfur-containing compounds. To measure compounds in trace quantities, some of the collected solutions were first concentrated under nitrogen.

The study of low-pressure, fuel-rich premixed benzene flames was continued with an emphasis on detailed quantitation of both PAH and PAH radicals. Fifty-five compounds were measured throughout the PAH formation and consumption region of the flames. Many of the compounds have not previously been unequivocally measured in these flames, including 1- and 2-ethynylnapthalene, biphenylene, 1-and 5-ethynlacenapthalene, and the acenapthyl, fluoranthenyl, and pyrenyl radicals. Chromatographic separation of some of these compounds required the use of a more polar column than is typically used for PAH analysis. Particular care had to be taken in handling flame samples to prevent evaporation and

condensation of the compounds of interest, which would drastically affect the quantitation and interpretation of the data.

PAH analysis by this radical scavenging technique showed that PAH are in significantly higher concentrations in a benzene flame than were measured by molecular beam/mass spectrometry (MB/MS) (Bittner and Howard, 1981), presumably because of difficulties in calibrating the MB/MS system for PAH. The observed differences scale with the size of the PAH and ranges from 20% to a factor of 10. The inventory of PAH less than 300 amu does not change significantly by increasing the equivalence ratio past the sooting limit of the flame, even though the concentration of high molecular weight species (>800 amu) increases by two orders of magnitude. If PAH are the precursors to soot inception, then increasing the sooting potential of a flame speeds up both the formation and consumption pathways of PAH by the same amounts.

Vinyl-PAH radicals that could be produced by acetylene addition of PAH were not detected, nor were π radicals that could result from ring closures. But this observation does not exclude their importance in PAH growth pathways, as they may be too reactive to exist in detectable concentrations. Acenapthalene appears to be formed by the addition of C_2H_2 to the 1-napthyl radical, which is supported by the relative concentrations observed for the napthyl radical isomers and the ethynylnapthalenes. The formation of acenapthylene is a reasonable explanation for the preferential consumption of the 1-naphthyl species, and is verified by kinetic modeling of this mechanism. However, the soot model also suggests that another acenapthylene formation pathway is necessary in the benzene flame to account for high concentrations of acenapthylene. A reaction between two phenyl radicals (or a reaction between phenyl and benzene) and subsequent rearrangements has been postulated as the dominate pathway for the formation of acenaphthylene in the benzene flames. The occurrence of phenyl-phenyl reactions is supported by the high concentration of biphenyl in flames, while the rearrangement of biphenyl and biphenylene into acenaphthylene has been seen to occur readily at temperatures as low as 1100 °C and 900 °C respectively.

The concentration of the PAH radicals measured in this study are 5% to 30% of the values predicted by an assumption of equilibrium of PAH radicals with H and H_2 at the point in the flame where PAH concentrations are at their maxima. This suggest that kinetic mechanisms dominate over thermodynamics in the PAH growth and consumption region of the flame, but that thermodynamic considerations can be significant. Thermodynamics predicts that the percentage of PAH that contain a radical site depends almost exclusively on the number of C-H bonds on the periphery of each molecule. At least in the early stages of the flame, this prediction can be significantly incorrect, presumably because of kinetic effects.

Formation of PAH, Fullerenes and Soot. Ab initio density function calculations show that the aryl C-H bond dissociation energies around the periphery of PAH are roughly the same as those for benzene, regardless of the size of the PAH. The σ radicals created by hydrogen abstraction from PAH are unaffected by the resonance π structures of the PAH. This adds some credibility to the application of the hydrogen abstraction and acetylene addition rate coefficients, experimentally measured only for benzene, to the rest of the PAH inventory. The vinyl-type C-H bonds in the five-membered rings of PAH are computed to be about 4-kcal/mol stronger than their aryl counterparts. The high bond dissociation energy of these vinyl groups many be a result of the inability of the already strained C-C bonds of the 5-membered ring to relax upon loss of the hydrogen, unlike what is observed in the vinyl groups of linear hydrocarbons, or to a lesser extent, the less-strained six-membered rings of PAH. The C-H bonds of the methylene-type 5-membered rings of cyclopenta[def]phenanthrene are computed to be 32 kcal/mol weaker than the aryl C-H bonds due in part to the stabilization by the adjacent π system.

An existing kinetic model describing the formation of PAH was updated and improved. Recently published kinetic data describing the oxidation of six- and five-membered ring species were implemented and thermodynamic data for key species involved in the growth process were determined using ab initio

quantum mechanical computations. Different radical sites could be distinguished. The kinetics of acetylene addition to PAH radicals was deduced by means of transition state theory and the relative importance of ring closure leading to five-membered ring species such as acenaphtylene was determined. Using ab initio quantum-mechanical computations. Different radical sites could be distinguished. The kinetics of acetylene addition to PAH radicals was deduced by means of transition state theory and the relative importance of ring closure leading to five-membered ring species such as acenaphthylene was determined. A QRRK treatment allowed the computation of rate constants at the pressure of the present study. The prediction of the kinetic model has been tested against experimental data from the nearly sooting low-pressure premixed benzene/oxygen/argon flame in which radical and stable PAH concentration profiles were measured in this project. The availability of experimental concentration profiles of intermediate, often radical, species increased significantly the level of confidence in conclusions about reaction pathways and their elementary reactions responsible for PAH growth. Thermodynamic limitations of PAH growth via hydrogen-abstraction/acetylene-addition sequences were found to be important. Ring closure via the reaction of PAH-C_2H radicals with acetylene was shown to be a net consumption pathway of napthalene, phenanthrene and corresponding radicals. A general feature of the model prediction is that the consumption of PAH-C_2H species is too slow compared to the experimental data. This observation along with the underprediction of larger PAH and the lack of acetylene consumption beyond the reaction zone indicate the necessity of additional thermodynamically favorable PAH growth and acetylene consumption pathways. The results also indicate there are important contributions of cyclopentadienyl and phenyl in the formation of naphthalene, phenanthrene (via biphenyl), and benzo [b]fluoranthene. The implication of these radicals in the formation of larger PAH which are not considered in the present model may be an explanation for the overprediction of these radicals. A reaction sequence leading from benzyne dimerization and isomerization to acenaphthylene was tested with encouraging results. The participation of benzyne-type species seems to be promising and would deserve further investigation.

Soot samples collected as bulk solids and by thermophoretic sampling at different residence times in a fullerene-forming premixed benzene/oxygene flat flame (C/O = 0.96, P = 5.34 kPa, 10% argon, v = 25 cm/s) were analyzed by high resolution electron microscopy. The samples contained soot particles that were composed to some extent of amorphous and fullerenic carbon (e.g., curved layers and fullerene-molecule-sized closed-shell structures). Qualitative and quantitative analyses of residence-time resolved samples showed that the length of curved layers increases and their radius of curvature decreases with increasing residence time in the flame. The number of closed-shell structures in the soot as well as the concentration of fullerene molecules in the gas phase increase with increasing residence time, consistent with fullerenes concentration increasing with residence time, and fullerenes being consumed by reaction with soot. The data suggest that the formation of amorphous and fullerenic carbon occurs in milliseconds, with the fullerenic carbon becoming more curved as a soot particle traverses the length of the flame. Conversely, the formation of highly ordered carbon nanostructures, such as tubes and onions, appears to require much longer residence times, perhaps seconds or minutes depending on the temperature, in the flame environment.

FuturePlans

The research on aromatic compounds in flames will involve the continued application of the radical scavenging method and use of the experimentally measured concentration profiles to test and improve critical submechanisms in the overall model of aromatic oxidation and PAH and fullerenes formation. Specific objectives are to resolve differences between radical concentration measurements in this project and previous measurements; to extend the measurement of radicals concentration profiles to larger PAH radicals than have been measured previously and to additional radicals of interest in studies of PAH growth mechanisms but whose identities could not be confirmed to date in this project; to measure concentration profiles of oxygen-containing PAH pertinent to the modeling of aromatic oxidation; and to extend and

improve the present model of PAH and fullerene formation in flames building on the additional and improved concentration profiles of stable and radical PAH and oxygen-containing PAH obtained in the experimental work.

The research on soot and fullerenes formation in flames will involve the method of assessing curved structure within soot particles to determine the kinetics of the development of fullerenic structure and to test the hypothesis that fullerenes formation within soot particles is a significant mechanism of fullerenes formation in flames. In addition, the modeling of PAH, fullerenes and soot formation will be extended to include improved treatment of PAH-soot and fullerene-soot reactions.

References

Haussman, M., Hebgen, P., and Homann, K.H., 1992. *Proc. Combust. Inst.*, **24**: 793-801.

Bittner, J.D. and Howard, J.B., 1981. *Proc. Combust. Inst.*, **18**: 1105-1116.

Publications of DOE Sponsored Research, 1998-2000

Lafleur, A. L., Howard, J.B., Plummer, E., Taghizadeh, K., Scott, L.C., Necula, A. and Swallow, K.C.: "Identification of Some Novel Cyclopenta-Fused Polycyclic Aromatic Hydrocarbons in Ethylene Flames," *Polycyclic Aromatic Compounds*, **12**, 223-237, 1998.

Shandross, R.A., Longwell, J.P. and Howard, J.B.: "Net Rate Analysis Method for Assessment and Improvement of Flame Models," *Combust. Flame*, **112**, 371-386, 1998.

Grieco, W.J., Lafleur, A.L., Swallow, K.C., Richter, H., Taghizadeh, K. and Howard, J.B.: "Fullerenes and PAH in Low Pressure Premixed Benzene/Oxygen Flames," *Twenty-Seventh Symposium (International) on Combustion*, The Combustion Institute, Pittsburgh, 1669-1675, 1998.

Pope, C.J., Shandross, R.A. and Howard, J.B.: "Variation of Equivalence Ratio and Element Ratios with Distance from Burner in Premixed One-Dimensional Flames," *Combust. Flame*, **116**, 605-614, 1999.

Richter, H., Grieco, W.J. and Howard, J.B.: "Formation Mechanism of Polycyclic Aromatic Hydrocarbons and Fullerenes in Premixed Benzene Flames," *Combust. Flame* **119**, 1-22, 1999.

Richter, H. Benish, T.G., Ayala, F. and Howard, J.B.: "Kinetic Modeling of the Formation of Polycyclic Aromatic Hydrocarbons", *A.C.S. Fuel Chem. Div. Preprints* **45(2)**, 273-277,2000.

Grieco, W.J., Howard, J.B., Rainey, L.C. and Vander Sande, J.B.: "Fullerenic Carbon in Combustion-Generated Soot," *Carbon* **38**, 597-614, 2000.

Richter, H., Benish, T.G., Mazyar, O.A, Green, W.H. and Howard, J.B.: "Formation of Polycyclic Aromatic Hydrocarbons and Their Radicals in a Nearly Sooting Premixed Benzene Flame", *Twenty-Eighth Symposium (International) on Combustion*, The Combustion Institute, Pittsburgh, (accepted).

Richter, H. and Howard, J.B.: "Formation of Polycyclic Aromatic Hydrocarbons and their Growth to Soot – A Review of Chemical Reaction Pathways", *Prog. Energy and Combust. Sci.* (accepted).

Title: Thermodynamic Rules for the Self-Organization of Carbon Materials

By: Robert Hurt
Brown University, Box D
Providence, RI 02912
e-mail robert_hurt@brown.edu

Abstract

Carbon atoms organize themselves in a variety of structures, from the tetrahedra of diamond, to the stacked planes of graphite, to the celebrated Fullerene spheres and nanotubes. The graphite family alone includes a rich variety of materials, including some of special importance to energy applications, such as soot, solid fuel chars, pyrolytic carbons, and carbon fibers for energy efficient vehicles. These materials exhibit a rich variety of properties and functions, arising in part from differences in the size and spatial arrangement of polyaromatic clusters that form the basic building blocks of carbons — i.e. the carbon nanostructure.

This talk addresses the origin of carbon nanostructure with emphasis on thermodynamic approaches to identify the equilibrium order modes. A model will be presented that treats the order / disorder transitions in ensembles of disk-like molecules by combining elements from liquid crystal theory and regular solution theory. Nonequilibrium effects will be discussed briefly as will liquid crystal surface anchoring in fluid carbon precursors. A new theory on the origin of shell / core nanostructures in primary soot particles will also be presented.

* This work is supported by DOE Fossil Energy Advanced Research managed by the National Energy Technology Laboratory, and by National Science Foundation, Chemical and Transport Systems.

IONIZATION PROBES OF MOLECULAR STRUCTURE AND CHEMISTRY

Philip M. Johnson
Department of Chemistry
State University of New York, Stony Brook, NY 11794
Philip.Johnson@sunysb.edu

PROGRAM SCOPE

Photoionization processes provide very sensitive probes for the detection and understanding of molecules and chemical pathways relevant to combustion processes. Laser based ionization processes can be species-selective by using resonances in the excitation of the neutral molecule under study or by exploiting the fact that different molecules have different sets of ionization potentials. Therefore the structure and dynamics of individual molecules can be studied, or species monitored, even in a mixed sample. We are continuing to develop methods for the selective spectroscopic detection of molecules by ionization, to use these spectra for the greater understanding of molecular structure, and to use these methods for the study of some molecules of interest to combustion science.

RECENT PROGRESS

The exploitation of Rydberg molecules has enabled orders-of-magnitude increases in the resolution available for recording the spectra of molecular ions. These spectra provide information equivalent to photoelectron spectra, but contain much more information by virtue of that resolution and the versatility of laser preparation of the states involved.

We have developed techniques called mass analyzed threshold ionization spectroscopy (MATI) and photoinduced Rydberg ionization spectroscopy (PIRI) to provide high resolution access to the spectroscopy of the electronic states of ions. To accomplish this we create high Rydbergs state just below an ionic threshold. A small field is used to separate the prompt ions from the Rydberg molecules and then after a delay of a few microseconds either a small electrical pulse field ionizes the Rydbergs (MATI) or a tunable laser beam is sent through the Rydberg molecules (PIRI). In the latter, if this laser is resonant with a transition of the ionic core, core-excited Rydberg molecules are created which promptly autoionize. These ions are again separated from the remaining Rydbergs and after a further few microseconds the various ion packets are sent into a TOF mass spectrometer, where they arrive as a distinct groups whose intensity can be recorded as the either the Rydberg preparation laser or the final laser is scanned. The resonant nature of MATI and PIRI are of great use in sorting out the vibrational structure of some ionic states.

Aromatic molecules such as benzene have played a vital role in the understanding of molecular orbitals and therefore of chemistry in general. They are also important constituents in many combustion processes. In spite of the enormous amount of work that has gone into their study, there are still some outstanding questions concerning even the rough ordering of the molecular orbitals of aromatic molecules.

I. Photoinduced Rydberg ionization spectroscopy of halobenzenes.

Excited states of polyatomic molecular ions have been of great interest because their study

provides information about occupied molecular orbitals, among other reasons. Assignment of these states is essential to confirm the accuracy of electronic structure calculations and is fundamental to our understanding of molecular bonding. In many cases in the past, spectroscopic studies have been hampered by either poor resolution or lack of selectivity which prevented unambiguous analysis of the excited ionic states. We are addressing the issue of the symmetry assignment of the second excited state (the $\tilde{B}$ state) of halobenzene cations, molecules which provide insight into the perturbative effects of substitution of strongly electronegative atoms onto the benzene ring.

Numerous photoelectron spectroscopy (PES) studies have attempted to assign the state symmetries of the excited states of fluorobenzene and chlorobenzene cations, but were hampered by a lack of vibrational resolution in most bands. Various other low resolution studies have also been performed in an effort to elucidate the state ordering of these ionic states; for instance, Penning Ionization Electron spectroscopy (PIES), and emission spectroscopy. It has been inferred that symmetries of the $\tilde{B}$ states are $^2B_2$, which leads to electronically forbidden transitions from the $\tilde{X}$ states ($^2B_1$). However, due to the proximity of the $\tilde{B}$ and $\tilde{C}$ states, the assignment of the $\tilde{B}$ state is difficult. The most convincing arguments are based on fluorescence emission studies, which have indicated that the $\tilde{B}$ state of fluorobenzene cation is a half -filled $^2B_2$ σ-state corresponding to the conclusively assigned σ-state appearing approximately at the same energy in benzene cation. This conclusion stems from the observation that the fluorescence quantum yield of the ion is very small ($< 10^{-5}$), similar to that of benzene, in which the $\tilde{B}$ state does not fluoresce. Others have also assigned the second excited ionic state to be a σ-state, based on mass-selected ion dip spectroscopy. An alternate assignment, indicated to be possible from *ab initio* calculations, is for the state to be a $^2B_1$ π state since the two states (π and σ) are very close in energy.

In order to resolve the issue of the B state assignment, vibrationally resolved PIRI spectra of the $\tilde{B}$ state of fluorobenzene cation via the origin, 16a, 6b and 11 vibrational modes in the ground ionic state require a reassignment of the accepted state symmetry. Based on lower resolution studies, the $\tilde{B}$–$\tilde{X}$ transition has been previously assigned as an electronically forbidden $^2B_2$– $^2B_1$ transition. Vibrational analyses of the spectra observed via various ground state non-symmetric vibrations, particularly from the 16a vibrational mode, unambiguously locate the origin of the transition at 21075 cm^{-1}, resulting in the reassignment of the $\tilde{B}$ ionic state as $^2B_1$. *Ab initio* calculations, while not conclusive, also indicate that $\tilde{B}$–$\tilde{X}$ transition is an allowed π to π transition.

Chlorobenzene is a much more difficult molecule for PIRI because of very short excited state lifetimes and a propensity to dissociate. However we have recorded very good spectra from several vibrational levels of the cation. Spectra of the $\tilde{B}^+$ state of the chlorobenzene cation were recorded via the origin, 6b and 16a16b vibrations of the cation ground state ($\tilde{X}^+$). The REMPD spectrum of $\tilde{B}^+$–$\tilde{X}^+$ transition of the chlorobenzene cation was also obtained during this study. To date it has been thought that $\tilde{B}^+$–$\tilde{X}^+$ is an electronically forbidden transition (C_{2v} symmetry), taking place from the $^2B_1$ ground state to a $^2B_2$ excited state. The ability of PIRI to provide spectra from specific lower state vibrational levels allowed this hypothesis to be tested, since the 16a vibration would be the primary inducing mode in the transition. Assuming a forbidden transition, a comparison between the spectrum from the ground state origin and that from the 16a16b vibration would necessitate an assignment which gives unlikely vibrational frequencies. It is therefore concluded that the $\tilde{B}^+$–$\tilde{X}^+$ transition of chlorobenzene is electronically allowed. CIS and CASSCF calculations with 6-31G** basis sets were performed to ascertain the symmetry assignments of the excited ionic states. These resulted in the possibility that there lies at least one excited state of the cation of $^2B_1$ symmetry below any state of $^2B_2$ symmetry. Hence, we propose that the ionic transition observed in the acquired PIRI/REMPD

spectra of the cation is an allowed transition to a $^2B_1$ state, thus giving rise to the observation of the origin of the $\tilde{B}^+$ state at 18219 cm^{-1}.

II. Infrared laser spectroscopy of ethyl radical

In conjunction with Trevor Sears at Brookhaven National Laboratory, we have been studying the high resolution IR spectrum of ethyl. This molecule is an important prototype for molecular physics because it has an internal rotor where the two parts have almost equal masses, leading to an extremely complicated rotational manifold.

Recently, additional assignments of rotational lines, refinements of the data set, and the measurement of additional spectral regions have enabled the determination of almost all the constants in the model Hamiltonian and resulted in a good simulation of the spectrum.

Measurements of the ethyl radical -CH_2 out-of-plane rocking vibrational fundamental by transient diode laser absorption spectroscopy have provided information on the structure of, and the barrier to internal rotation in, the radical, and how these quantities change on vibrational excitation. We find that the effective barrier decreases from approximately 17 cm^{-1} in the zero point level to 10 cm^{-1} in the excited vibrational level. The assigned data set now contains approximately 450 rotation-torsional transitions and has been fit to a model effective Hamiltonian. The derived molecular parameters generally reproduce the measured line positions to better than 0.01 cm^{-1}, but this does not approach the estimated measurement accuracy of 0.001 - 0.002 cm^{-1}.

In order to understand these results it has been necessary to come to terms with what a torsional barrier really is when the rest of the molecule is moving around (because of relaxation and vibrational motion) as the rotors are turning.

For molecules such as ethyl radical which have a small torsional barrier, the interaction between the internal rotation and the other normal modes of the molecule can have a substantial effect on the magnitude of the barrier itself. In ethyl this is experimentally demonstrated by a large change in the torsional barrier on vibrational excitation of the methylene group inversion motion. A simple method was applied to ethyl, involving the use of electronic structure calculations to estimate both the electronic and vibrational contributions to the barrier. Good agreement is found with experimental results from the infrared spectrum of the rocking vibration of the ethyl radical .

With the combination of experimental and calculational work, we now have a rather complete understanding of the interactions in this vibrating-rotating molecule, which will serve as a model for other systems.

III. The Jahn-Teller effect in benzene

The cation of benzene provides a prototype system for the detailed study of the Jahn-Teller effect in highly symmetric molecules. The cation ground state has shown a remarkable agreement with theory for the energies of the lowest few vibrational levels. However, above 1000 cm^{-1} the mode mixing gets so extreme that experimental vibrational assignments are impossible from frequency considerations alone. In order to get more information about assignments by exploiting optical selection rules and isotope shifts, we have recorded the MATI spectra of C_6H_6 and C_6D_6 using both VUV single photon excitation from the neutral ground state and pump-probe excitation through S_1. Peaks with angular momentum 3/2 in ν_6 are forbidden in the former and allowed in the latter. This effect, along with a different vibrational pattern in the deuterated molecule and PIRI spectra to the

electronic B^+ state (the subject of previous work) from each vibrational level will be coupled with multimode Jahn-Teller calculations to provide a much more reliable description of the vibrational motion in ground state benzene cation.

DOE PUBLICATIONS

"Photoinduced Rydberg ionization(PIRI) spectroscopy of phenol: The structure and assignment of the B state of the cation", J. E. LeClaire, R. Anand, and P. M. Johnson, J. Chem. Phys., **106,** 6785 (1997) .

"The observation of strong pseudo-Jahn-Teller activity in the benzene cation B $^2E_{2g}$ state", J. G. Goode, J. D. Hofstein and P. M. Johnson, J. Chem. Phys., **107**, 1703 (1997).

"Photoinduced Rydberg Ionization (PIRI) Spectroscopy of the B-state of Fluorobenzene Cation," Richa Anand, Jeffrey E. LeClaire, and Philip Johnson, J. Phys. Chem.A, **103**, 2618 (1999).

"Assignment Of The $\tilde{B}^+$ State Of The Chlorobenzene Cation: Photoinduced Rydberg Ionization (PIRI) Spectroscopy", Richa Anand, J. D. Hofstein, Jeffrey E. LeClaire, Philip Johnson, and Claudina Cossart-Magos, J. Phys. Chem. A, **103**, 8927-8934 (1999).

"Infrared spectrum of the -CH_2 out of plane fundamental of C_2H_5," Trevor J. Sears, Philip M. Johnson and Joanne BeeBe-Wang, J. Chem. Phys., **111**, 9213-9221 (1999).

"Vibrational effects on the torsional motion of ethyl radical," Philip M. Johnson and Trevor J. Sears, J. Chem. Phys., **111**, 9222-9226 (1999).

"Reassessing the orbitals of pi systems using photoinduced Rydberg ionization spectroscopy," Philip Johnson, Richa Anand, Jason Hofstein and Jeffrey LeClaire, J. Electron Spect. and Related Phenom., *in press*.

"Mass-analyzed cation spectroscopy using Rydberg states: MATI and PIRI", Philip M. Johnson, Adv. Ser. in Phys. Chem.,Vol. 10A, *Photoionization and Photodetachment*, edited by C. Y. Ng (World Scientific, Singapore, 2000), *in press*.

DYNAMICAL ANALYSIS OF HIGHLY EXCITED MOLECULAR SPECTRA

Michael E. Kellman
Department of Chemistry, University of Oregon, Eugene, OR 97403
541-346-4196 Kellman@Oregon.Uoregon.Edu

PROGRAM SCOPE:

Spectra of highly excited molecules are essential to understanding intramolecular processes of fundamental importance for combustion. Our program applies theoretical methods to analyze highly excited vibrational spectra. Because of the breakdown of the standard normal modes picture in highly excited states, new theoretical tools are needed to unlock and interpret the information about ultrafast internal molecular motion encoded in high energy spectra.

In highly excited states, strong anharmonicity and multiple Fermi resonance couplings induce marked departures from ordinary normal mode behavior, including the birth in bifurcations of new anharmonic modes, and the onset of widespread chaotic classical dynamics. In a bifurcation, a normal mode changes character, with an abrupt change in the natural motions of the molecule. This involves a branching, or bifurcation, into new types of anharmonic motion.

Our methods, based on bifurcation analysis of molecular Hamiltonians obtained from experimental spectra, are now being applied in collaboration with several experimental and theoretical groups to understand ultrafast dynamics. Recently this has developed to include reaction modes in "isomerization spectroscopy" of molecules undergoing unimolecular rearrangement. Our methodology started in the frequency domain of high resolution spectroscopy, and is now being extended to analysis of experiments using ultrafast laser pulses. We thus have a unique perspective on ultrafast dynamics, whether viewed through the frequency domain of traditional spectroscopy, or the time domain of ultrafast spectroscopy.

RECENT PROGRESS:

Significant recent progress falls into four main areas: 1) isomerization spectroscopy; 2) bending spectra of acetylene with several modes and multiple couplings; 3) a new methodology called the "dressed basis" approach for simplifying analysis of larger molecules, whose complexity grows exponentially with size. 4) semiclassical quantization of chaotic systems.

1) ISOMERIZATION SPECTROSCOPY: Isomerizing species are of crucial importance in understanding combustion processes, and their spectroscopic observation has been a long-standing goal. Spectroscopy experiments and theory are now probing isomerizing systems such as HCP and HCN. Experimental "isomerization spectra" of HCP have been observed by R.W.Field (MIT) and subsequently examined in more detail by H. Ishikawa (Tokyo). Analysis of results of the latter indicates a bifurcation to an "isomerization mode", indicated by the observation of a spectral pattern originally predicted by our group, as follows.

Predictions confirmed: spectral patterns of bifurcating normal modes. When normal modes change character at high energy, an abrupt change in the natural motions of the molecule can take place. This involves a branching, or bifurcation, into new types of anharmonic motion. A key problem is identifying spectral patterns associated with this change. Our group has applied bifurcation analysis to spectral patterns in systems with Fermi resonance. A clear hallmark of a bifurcation in the spectral pattern was predicted by our work: a minimum in the spacing of levels

assigned sequential quantum numbers in our new assignment procedure. Exactly this pattern, connected to the onset of the "isomerization mode", was observed by Ishikawa in analysis of experimental spectra of isomerizing HCP. The data of Ishikawa were not complete, however. We analyzed a complete set of "data" consisting of a vibrational spectrum calculated from a molecular potential surface by Schinke and co-workers, who were puzzled by odd patterns in their spectra. We have explained these in an analysis which confirms our earlier predictions about spectral patterns in Fermi resonance systems. All the evidence now ties together into the conclusion of an abrupt birth in a bifurcation of an isomerization mode. This shows the potential of our methods to unlock information about ultrafast processes, and begins to make connections with notions of reaction pathways. A publication [6] has appeared in J. Chem. Phys. of a five-way collaboration of groups from MIT (Field), Tokyo (Ishikawa), Gottingen (Schinke), Grenoble (Joyeux), and my student V. Tyng and myself.

2) BENDING SPECTRA OF ACETYLENE: BIFURCATION ANALYSIS, ISOMERIZATION PATHWAYS: Many-mode bifurcation analysis, assignment, and spectral patterns of chaotic molecules. A key accomplishment of 1995-1997 of Rose, Lu, and Kellman [1] was to extend our methodology of bifurcation analysis, quantum number assignment, and spectral pattern identification, originally developed for systems with just a single important coupling, to systems with many modes coupled by multiple resonances, with chaotic dynamics, in polyatomics such as H_2O. This forms the basis for all of the work outlined below involving three or more interacting modes. An important part of this is a "diabatic correlation diagram" technique of Rose and Kellman (J. Chem. Phys. 1996) for assigning spectra.

Applications to C_2H_2: spectral patterns, energy transfer pathways within polyads. The groups of R.W. Field (MIT) and M. Herman (Brussels) have used our earlier "polyad" analysis of complex molecules to unravel polyad groupings in C_2H_2 dispersed fluorescence spectra. We have explored further unraveling of these polyads into subpolyads representing energy flow pathways by extending to bending spectra of C_2H_2 the diabatic correlation diagram method described above for H_2O. A very preliminary account has appeared [3]; detailed publications are in preparation [10,11]. We find that there are novel energy and intensity patterns within subpolyads of the polyads with 10, 12, and 14 quanta of bending vibration. We are able to account for these patterns with a Hamiltonian that describes energy flow along the ``primary" energy transfer pathway induced by an effective Darling-Dennison coupling.

3) DRESSED BASIS METHOD FOR SIMPLIFYING LARGER MOLECULES: This new methodology is an outgrowth of our work on diabatic correlation diagram assignments. It allows us to simplify the analysis of a very complicated system, with multiple resonance couplings between many interacting modes. We are able to view the system from several simplified perspectives, each involving effectively a single resonance coupling. We then recombine the different views into an overall picture of the dynamics in their full complexity. This methodology has developed into a powerful new tool for simplifying the spectral analysis of the larger molecules we are now trying to encompass with detailed bifurcation analysis. The dressed basis approximately resolves the system into sub-systems of simple effective couplings and energy transfer pathways, even in chaotic systems. Extremely positive results have been obtained [8,9] for H_2O.

4) SEMICLASSICAL QUANTIZATION OF CHAOTIC SYSTEMS: Our work on assigning spectra of chaotic systems has been based on the semiclassical hypothesis of quantizing structures with classical properties corresponding to approximate quantum numbers. We have been testing the notion that the quantizing structures are cantori—chaotic remnants of tori, so-called because mathematically the cantori are fractal Cantor sets. Quantization of tori is well-established and in fact is the basis of our work on spectral patterns (above). M.J. Davis in pioneering work has shown

that applying an approximate quantization condition to cantori can give energy levels comparable in accuracy to those in the regular regime. We have been investigating the much more uncertain question whether one can obtain a semiclassical wave function for a chaotic cantorus structure. This would constitute a major in advance in understanding of semiclassical dynamics of chaotic systems. As a first step, a paper in Phys. Rev. A [5] presents a new method for semiclassical wave functions of systems corresponding to invariant tori.. We have now tested this method with success for weakly chaotic models of coupled molecular vibrations. The wave functions we obtain agree well with the exact quantum wave functions, which show significant effects due to the chaos.

FUTURE PLANS: Work is planned in three areas.

1) Dressed basis, energy transfer pathways, and isomerization modes for C_2H_2. A complete treatment of the C_2H_2 spectrum along the lines initiated in [3,10,11] is now a plausible goal. This will involve a full-blown application of the dressed basis approach, combined with a complete bifurcation analysis of the spectroscopic Hamiltonian of the kind we have performed earlier for triatomics. The bifurcation analysis is now largely complete in recent work with graduate student V. Tyng (see Fig. 1). Further challenges include using spectra to elucidate the pathway to the acetylene-vinylidene isomerization. The power of bifurcation analysis of spectra for ultrafast intramolecular rearrangement processes has been demonstrated for the isomerization spectrum of HCP [6]. If successful, this should contribute an important tool to using spectroscopy to unravel the reaction paths in isomerization processes. Already, H. Taylor and co-workers have identified bifurcation phenomena in one of the highest polyads (22 bend quanta) accessed in the experiments of the MIT group of R.W. Field. This part of the spectrum involves only the bends and their mutual couplings, however. An important part of the C_2H_2 dynamics involves the stretching motion as well, more readily accessed in the Brussels absorption experiments. Earlier work of Rose and Kellman (J. Chem. Phys. 1995) analyzed a resonance coupling, important in the absorption spectrum, between the C-H and C-C stretches and the bends, and this has been seen to be important in simulations by J. Muckerman. There is also evidence from ab initio calculations that the true transition state in the C_2H_2 isomerization involves the stretching motion. It is therefore important to understand the bifurcation phenomena due to all interacting modes and their couplings, a problem of greater complexity than attempted previously by any group. A danger is that it can be done in a "brute force" way, but with loss of the understanding gained for simpler systems. To surmount this, we are using the dressed basis approach. This will give us qualitative knowledge of how each coupling affects the natural motions of the molecule through bifurcations. We expect to be able to identify clearly how the isomerization pathway is generated through bifurcations.

2) Ultrafast dynamics. The methods we have developed are being widely used to unlock internal molecular dynamics from frequency domain spectra. These are ultrafast dynamics, as shown especially by the power of our techniques when applied to isomerization spectra. It is now a completely natural step to consider the observation of dynamics behavior, such as the birth of new modes in bifurcation, in ultrafast, time-domain experiments. However, until now, no one has attempted to make this link. In 1997 Lu and Kellman (J. Chem. Phys.) analyzed bifurcation behavior in ClO_2. In ultrafast experiments, the group of P. Reid at the University of Washington has observed a sudden transformation of energy transfer processes from ClO_2 to a surrounding solvent. At first, with about 15 quanta of antisymmetric stretch, there is slow energy transfer to the solvent; suddenly, with about 8 quanta of bend remaining, there is rapid IVR within the ClO_2. They have speculated that this might be due to the bifurcation predicted by us in 1997. An important future direction of our work is to provide interpretation and explanation for these observations of ultrafast experiments.

3) Quantization of strongly chaotic systems. As mentioned above, a paper has been submitted [5] on a new method for obtaining semiclassical wave functions, which we have now applied for

chaotic remnants of tori. This is an important issue of principle in understanding what it means to assign spectra of strongly coupled systems; it possibly has practical ramifications in spectral assignment as well. Our work so far has encompassed weakly chaotic systems. We are planning to extend this to much more strongly chaotic systems, in light of the unexpectedly good success we have had so far.

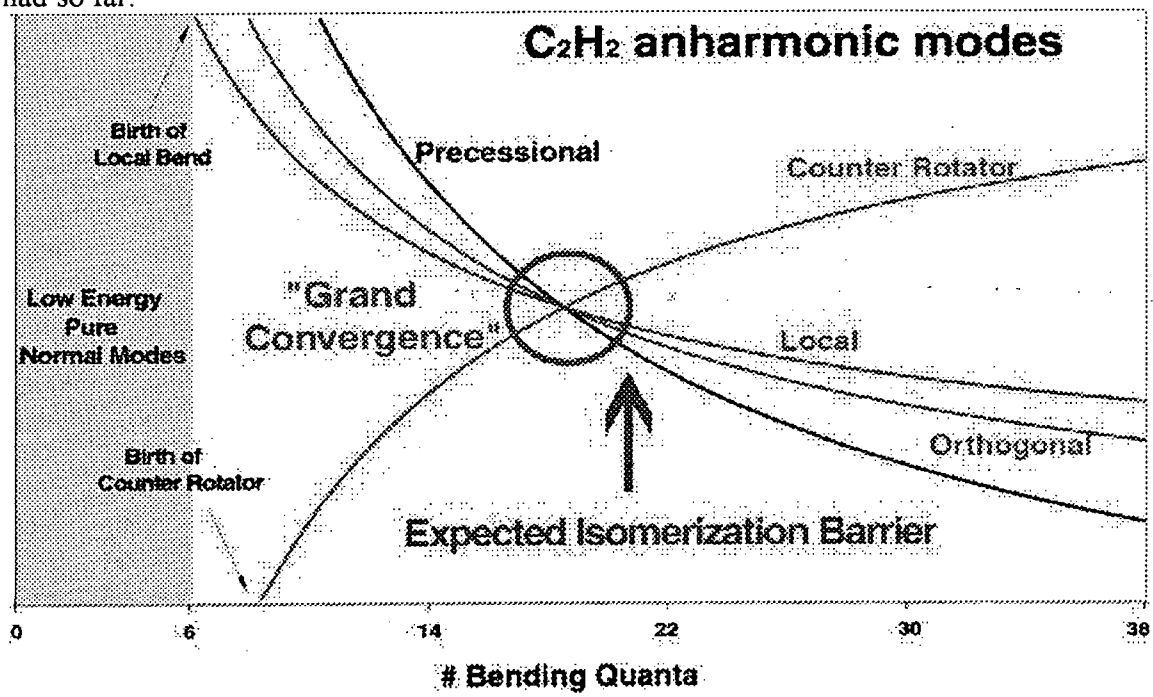

1. "Phase Space Structure of Triatomic Molecules", Z.-M. Lu and M.E. Kellman, J. Chem. Phys., 107, 1-15 (1997).
2. "Nonrigid Systems in Chemistry: A Unified View", M.E. Kellman, Int. J. of Quantum Chem. 65, 399-409 (1997).
3. "General Discussion on Regular and Irregular Features in Unimolecular Spectra and Dynamics" Solvay Conference Proceedings, M.E. Kellman, Adv. Chem. Phys. 101, 590-594 (1997).

PUBLICATIONS WITH DOE SUPPORT, 1998-2000:

4. M.E. Kellman, article on "Correlation", McGraw-Hill 1999 Yearbook of Science and Technology (McGraw-Hill, New York, 1999).
5. M. Joyeux, D. Sugny, V. Tyng, M.E. Kellman, H. Ishikawa, and R.W. Field, "Semiclassical Study of the Isomerization States of HCP", J. Chem. Phys. 112, 4162 (1999).
6. S. Yang and M.E. Kellman, "Direct Trajectory Method for Semiclassical Wavefunctions", in press, Phys Rev A.
7. M.E. Kellman, "Internal Molecular Motion", in press, Encyclopedia of Chemical Physics and Physical Chemistry, J.H. Moore, Ed. (Institute of Physics, London).
8. M.E. Kellman and M.W. Dow, "Dressed Basis for Highly Excited Molecular Vibrations", submitted to J. Chem. Phys.
9. M.E. Kellman and Mark W. Dow, "Representation Choice for Dressed Basis", submitted to Chem. Phys. Lett.
10. J.P. Rose and M.E. Kellman, "Spectral Patterns of Chaotic Acetylene", submitted to J. Phys. Chem.
11. J.P. Rose and M.E. Kellman , "Spectral Patterns and Dynamics of Planar Acetylene", to submitted, European Physical Journal D : Atoms, Molecules and Clusters.

SHOCK TUBE STUDIES OF THERMAL DECOMPOSITIONS OF FUELS AND THEIR RELEVANCE TO THE SOOT FORMATION PROCESS

R.D. Kern, H.J. Singh and Q. Zhang

Department of Chemistry
University of New Orleans
New Orleans, LA 70148
rdkern@uno.edu

Program Scope

From its inception some 21 years ago, our program has focused on the identification and temporal behavior of radical intermediates formed during the combustion and pyrolysis of gaseous fuels. The goals have been the elucidation of the kinetic pathways to soot formation, proposing and testing the pertinent reaction mechanisms, and providing realistic rate constants as functions of temperature and pressure. The basic apparatus employed by us has been a shock tube coupled to a time-of-flight mass spectrometer which provided dynamic analysis of reactants, products and intermediates. The TOF data were often combined with the invaluable observations of laser schlieren densitometry (LS) obtained by Professor John Kiefer and his research group at the University of Illinois at Chicago (UIC). Their contributions involved precise measurements of the decay rate of the reactant as a function of temperature and pressure, determined whether reaction profile shapes were diagnostic of radical or molecular processes, and identified late-time exothermic excursions associated with recombination reactions. Some other helpful information is furnished from the static analysis of single pulse shock tube work: high-pressure unimolecular dissociation rate constants and quantitation of trace species (for examples see refs 1-3). Atomic resonance absorption spectroscopy (ARAS) measurements of H-atom profiles assist in the formulation and testing of mechanisms; a recent example is that of cyclopentadiene decomposition (see refs 4 and 5). A recent addition by Professor Kiefer to the arsenal of shock tube techniques is the development of the incident-shock, quench-tank (ISQT) experiment which allows GC/MS analysis of the gas sample as studied by LS; application to methylcyclopentadiene pyrolysis is described in ref 6. Lastly, theoretical calculations by Drs. Branko Jursic at the University of New Orleans (UNO) and Larry Harding and Al Wagner at Argonne National Laboratory of the energetics and structures of intermediate species have played important roles in the investigations of the pyrolyses of acetylene[7], allene and propyne[8], aromatic azines[9], and cyclopentadiene.[5, 10]

Recent Progress

The thermal decomposition of methylcyclopentadiene (MCP) has been investigated utilizing several of the techniques described above; namely, TOF work at UNO and LS and ISQT experiments at UIC. For the TOF work, MCP was obtained as a middle distillate from the dimer. The mixture of MCP and Ne used for the TOF shock tube experiments was

analyzed for the presence of dimer and other impurities present in the MCP purchased from Aldrich. Neither were detected. However, the MCP sample is comprised of three isomers:

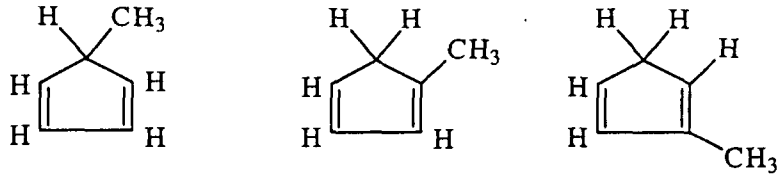

The first two isomers shown above, 1-MCP and 2-MCP, have the same heat of formation; 5-MCP is ~ 1.5 kcal higher.[11]

TOF experiments with a 2% MCP-98% Ne mixture were performed over reflected shock zone temperatures of 1250 – 1600 K and total pressures of 145 – 225 Torr. The primary products observed are C_2H_2, benzene, CH_4 and C_2H_4. Reaction profiles are depicted for a run at 1283K and 152 Torr. The solid lines represent model calculations with a mechanism developed from the results of the TOF, LS and ISQT techniques. One disturbing aspect is the low carbon atom balance recorded throughout the temperature range; 30% at the lowest temperatures increasing to 50% at 1600 K. The TOF carbon balance is determined by establishing the initial carbon atom concentration from the MCP at time zero. In the accompanying figure, that value is 24 x 10^{-8} C/cm^3. The final [C] is taken from the observable product plateaus. It has been the practice in the past to attribute the "missing" carbon atoms to soot and polycyclic aromatics. This contention now has support: the ISQT runs confirm the presence of copious amounts of naphthalene and other PCAH species as well as the major products and, in particular, C_6H_6 (m/e 78) is identified as benzene by GC/MS analysis. There is also serious mass loss in the ISQT experiments. The scatter in the TOF profiles shown is attributed in part to the carbon atom imbalance.It is concluded that the main pathway for MCP decomposition is C-C fission emanating solely from the 5-MCP isomer. The experiments and modeling support the proposals for the efficient production of benzene via reactions of the cyclopentadienyl radical [11,12] and the production of naphthalene via dimerization.[11] This work will be presented at the 28th Combustion Symposium.

A chapter written for the Handbook of Shock Waves entitled "Mass Spectrometric Methods for Chemical Kinetics in Shock Tubes" covers the 21 years of Department of Energy supported work as well as earlier studies of gas phase isotopic exchange reactions funded by the National Science Foundation.

References

1. A. Lifshitz, M. Bidani and S. Bidani, J. Phys. Chem. 90, 5373 (1986).
2. P.P. Organ and J.C. Mackie, J. Chem. Soc., Faraday Trans. 87, 815 (1991).
3. D. Fulle, A. Dib, J.H. Kiefer, Q. Zhang, J. Yao and R.D. Kern, J. Chem. Phys. A, 102, 7480 (1998).
4. K. Roy and P. Frank, 21st Int. Symp. On Shock Waves, Vol I, p. 403, (1997).
5. R.D. Kern, Q. Zhang. J. Yao, B.S. Jursic, R.S. Tranter, M.A. Greybill and J.H. Kiefer, 27th Symp. (Int.) on Combustion, p. 143 (1998).
6. E. Ikeda, R.S. Tranter, J.H. Kiefer, R.D. Kern, H.J. Singh and Q. Zhang, 28th Symp. (Int.) on Combustion, accepted.

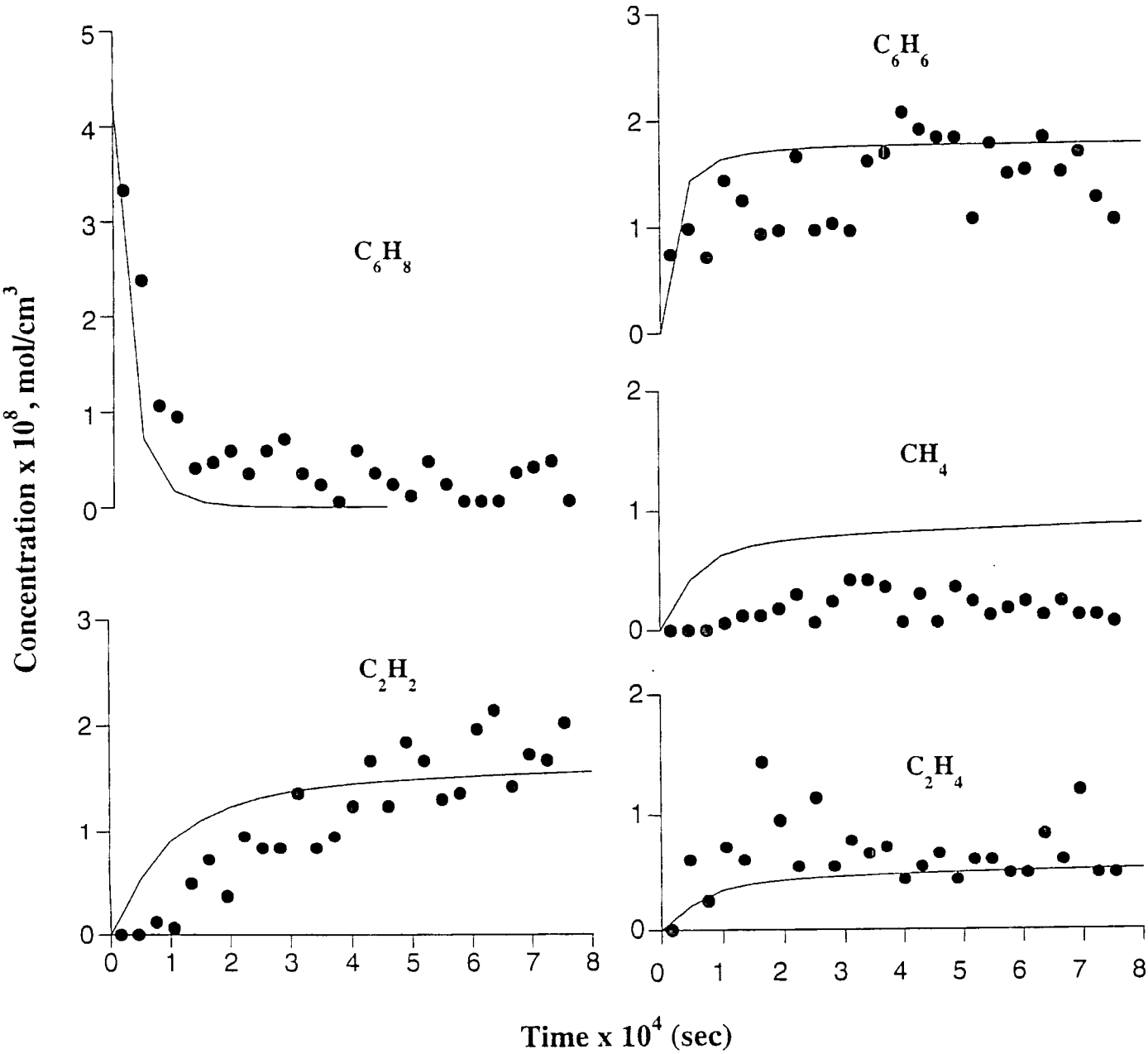
Concentration x 10^8, mol/cm^3
C6H8
C6H6
CH4
C2H2
C2H4
Time x 10^4 (sec)

7. J.H. Kiefer, S.S. Sidhu, R.D. Kern, K. Xie, H. Chen and L.B. Harding, Combust. Sci. Tech. 82, 101 (1992).
8. J. H. Kiefer, P.S. Mudipalli, S.S. Sidhu, R.D. Kern, B.S. Jursic, K. Xie and H. Chen, J. Phys. Chem. A, 101, 4057 (1997).
9. J.H. Kiefer, Q. Zhang, R.D. Kern, B.S. Jursic, H. Chen and J. Yao, J. Phys. Chem. A, 101, 7061 (1997).
10. R.D. Kern, H.J. Singh, Q. Zhang, B.S. Jursic, J.H. Kiefer, R.S. Tranter, E. Ikeda and A.F. Wagner, 22nd Int. Symp. on Shock Waves, in press.
11. C.F. Melius, J.A. Miller and E.M. Evleth, 24th Symp. (Int.) on Combustion, p. 261 (1992).
12. L.V. Moskaleva, A.M. Mebel and M.C. Lin, 26th Symp. (Int.) on Combustion, p. 521 (1996).

Future Plans

The TOF shock tube laboratory at the University of New Orleans will be dismantled and the principal investigator will retire from the university this year.

Publications of DOE Sponsored Research During 1998-2000

R.D. Kern, J. Yao and Z. Zhang, "Inhibition of C_2H_2 Pyrolysis at High Temperatures by H_2 and HCl". 21st International Symposium on Shock Waves, Volume I, Panther Publishing House and Printing Canberra, Australia, 1998, p. 269-272.

D.F. Fulle, A. Dib, J.H. Kiefer, Q. Zhang, J. Yao and R.D. Kern, "Pyrolysis of Furan at Low Pressures: Vibrational Relaxation, Unimolecular Dissociation and Incubation Times". J. Phys. Chem., 102, 7480 – 7486 (1998).

R.D. Kern, Q. Zhang. J. Yao, B.S. Jursic, R.S. Tranter, M.A. Greybill and J.H. Kiefer, "Pyrolysis of Cyclopentadiene: Rates for Initial C-H Bond Fission and the Decomposition of c-C_5H_5 Radical". 27th Symposium (International) on Combustion, The Combustion Institute, Pittsburgh, PA, 1998, p. 143-150.

R.D. Kern, H.J. Singh, Q. Zhang, J.H. Kiefer, R.S. Tranter, E. Ikeda and A.F. Wagner, "Thermolysis of Cyclopentadiene in the Presence of Excess Acetylene or Hydrogen", 22nd International Symposium on Shock Waves, in press.

E. Ikeda, R.S. Tranter, J.H. Kiefer, R.D. Kern, H.J. Singh and Q. Zhang, "The Pyrolysis of Methylcyclopentadiene: Isomerization and Formation of Aromatics", 28th Symposium (International) on Combustion, The Combustion Institute, Pittsburgh, PA, accepted.

R.D. Kern, H.J. Singh and Q. Zhang, "Mass Spectrometric Methods for Chemical Kinetics in Shock Tubes", Handbook of Shock Waves, Academic Press, accepted.

KINETICS OF COMBUSTION-RELATED PROCESSES AT HIGH TEMPERATURES

J. H. Kiefer
Department of Chemical Engineering
University of Illinois at Chicago
Chicago, IL 60607
(kiefer@uic.edu)

Program Scope

As it has for some years, this program involves the use of the shock tube with laser-schlieren and laser-flash absorption diagnostics to explore reactions and energy transfer processes over an extremely wide range of temperatures and pressures. Recently we have added a new diagnostic facility, a quench-tank for incident-shock product analysis, and some improvements in our laser-schlieren apparatus. Some theory is motivated by the experiments. The work described below was greatly assisted by collaboration with J. V. Michael and A. F. Wagner at Argonne, and by R. D. Kern and B. S. Jursic at UNO.

Recent progress

Facilities development:

A large expansion tank (100L), a 'quench tank' (QT), has been added to the end of the driven section of the low-pressure shock tube to allow post-incident shock samples to be withdrawn for analysis by GC/MS. The purpose of the tank is to prevent the incident shock from being reflected at the end-wall of the tube thus reheating the gas. The distribution of products now found will usually be close to that at completion/equilibrium.

To establish that that the incident shock is fully dissipated in the tank we have examined the simple molecular decomposition reactions of cyclohexene [1] and c-C_4F_8 [2], both of which have well-determined rate coefficients over the temperature range of interest in this application. Shock conditions were selected such that the temperature in the incident wave was insufficient to cause measurable reaction but that of the reflected shock was high enough to cause complete decomposition. Analysis of samples from these experiments has confirmed that there was indeed no significant reflected-shock heating of these samples.

For laser-schlieren (LS) experiments we have purchased a new laser, a Uniphase "μgreen" solid-state device with 20mw output at 532nm. This laser has very low noise, and the shorter wavelength translates to improved collimation with greater sensitivity and resolution. At the same time we have taken the opportunity to improve our data acquisition system with the introduction of a new computer, a 12-bit digitizer and redesigned software. The new data acquisition system has a GAGE Applied sciences 12100 DAQ card in a 450 MHz Pentium III computer equiped with 128MB ram. The 12100 DAQ card is a 12-bit AD converter which can scan two channels at 50 MHz each or one at 100MHz. Software using LabVIEW 5.1 and Visual Basic 6.0 for processing has been developed. This apparatus has just been put into use.

The study of early precursors to soot formation:

It is widely believed that aromatic rings are essential for soot generation. To further the understanding of their formation we have been examining the decomposition of some C5 ring

compounds recently proposed as precursors to aromatics in aliphatic systems [3]. These studies now include the pyrolysis of cyclopentadiene (CPD) and methylcyclopentadiene (MCP). Both have been observed in shock waves with time-of-flight mass-spectrometry (TOF), quench-tank (QT) analysis, and laser-schlieren densitometry (LS). The low-temperature LS and TOF experiments offer consistent rate constants for the initial C-H fission of CPD, indicating a barrier of 84 ± 2 kcal/mol. Rates were also estimated for the important secondary reaction c-C_5H_5 → C_3H_3 + C_2H_2. High-level density-functional calculations show that the unexpectedly large rates uncovered are a consequence of a low barrier of 61.9 kcal/mol and a twenty-fold reaction path degeneracy for the rate-controlling 1,2 H-atom shift in c-C_5H_5.

As part of the above work we calculated a new set of thermodynamic functions for the cyclopentadienyl radical which are consistent with the highest-level *ab initio* structural calculations of its Jahn-Teller distortion [4]. The large increase in entropy originally predicted by Wang and Brezinsky [5] is not supported; the thermochemical values are actually much closer to some earlier estimates which did not consider pseudorotation [6]. Unfortunately, there is a continuing disagreement between experimental [7,8] and theoretical [4] results on the size of the Jahn-Teller distortion. The issue remains under investigation.

The pyrolysis of MCP shows the expected initial C-C fission and subsequent exothermic reaction from methyl-radical recombination. Rate constants for this were reported in last-years abstract. QT-GC/MS distributions of the three rapidly interconverted isomers (1-,2- and 5-MCP) find the 5-MCP just 1.2 kcal/mol above the other two isoenergetic isomers, but only 0.01 of the total. Only the 5-MCP can readily dissociate so the high-pressure rate is reduced by ~ 100 from normal C-C fission. However, the low-pressure rate, dependent only on energy-transfer rates, is unaffected.

A large number of aromatic species are generated in this pyrolysis as shown in the attached QT analysis. The abundant benzene at the lowest temperatures suggests that chain decomposition to fulvene (H + MCP → C_6H_6 + H_2 + H and/or CH_3 + c-C_5H_5 → C_6H_6 + 2H), and thence to benzene [9], is indeed efficient in this decomposition. This is consistent with the near absence of benzene in CPD decomposition. The large naphthalene production in both pyrolyses supports the c-C_5H_5 dimerization path, in full accord with recent theory [9].

In addition to the above, we have begun a study of the decomposition of the three xylenes. So far we have extensive LS and QT data on the para-compound, and this is being analysed.

Chemical thermometers for the K. Brezinsky high-pressure tube:

A large set of LS and QT experiments has been performed on the decomposition of perfluorocyclobutane. The intention is to characterize falloff and secondary reactions, e.g., C_2F_4 → $2CF_2$, to improve its reliability as a high-P, high-T chemical thermometer.

Future Plans

We plan to continue our efforts on the c-C5 compounds with dimethylcyclopentadiene decomposition. Here the conversion to benzene should occur at even lower temperatures. Perhaps we can then identify fulvene in the products. We also plan an investigation of dissociation rates, secondary reactions, and gaseous products from the pyrolysis of C_4H_2. This molecule evidently plays a key role in soot formation in many instances, and its decomposition really needs a fuller characterization at high temperatures.

References

1) Kiefer, J. H. & Shah, J.N., J. Phys. Chem. **91**, 3024 (1987).
2) Tsang, W. & Lifshitz, A., Int. J. Chem. Kinet. **30**, 621 (1998).
3) L. V. Moskaleva, A. M. Mebel, and M. C. Lin, 26th (Int'l) Symp. on Comb., The Combustion institute, Pittsburgh, 1996, p. 521; C. F. Melius, M. E. Colvin, N. M. Marinov, W. J. Pitz, and S. M. Senkan, ibid, p. 685.
4) Borden, W. T. & Davidson, E. R., J. Am Chem. Soc. **101**, 3771 (1979).
5) Wang, H. & Brezinsky, K., J. Phys. Chem. **102**, 1530 (1998).
6) Burcat, A.& McBride, B., Ideal Gas Thermodynamic data for Combustion and Air-pollution use. Technion Eng. Rpt. TAE804:71 (1997).
7) Lu, L., Cullin, D. W., Williamson, J. M. & Miller, T. A., J. Chem. Phys. **98**, 2682 (1993).
8) Engelking, P. C & Lineberger, W. C., J. Chem. Phys. **67**, 1412 (1977).

Publications of DOE Sponsored Research During 1998-2000.

"Pyrolysis of Cyclopentadiene: Rates for Initial C-H bond Fission and the Decomposition of the Cyclopentadienyl Radical", R.D. Kern, Q. Zhang, J. Yao, B.S. Jursic, R.S. Tranter, M.A. Greybill, and J.H. Kiefer, 27th International Symposium on Combustion, The Combustion Institute, Pittsburgh (1998), p.143.

Invited topical review: "Some Unusual Aspects of Unimolecular Falloff of Importance in Combustion Modeling" J.H. Kiefer, 27th International Symposium on Combustion, The Combustion Institute, Pittsburgh (1998), p.113.

"Reaction Mechanism for the Thermal Decomposition of BCl_2/H_2 Mixtures", S.J. Harris, J.H. Kiefer, Q. Zhang, A. Schoene, and K.-W. Lee, J. Electrochem. Soc. 145, 3203 (1998).

"Pyrolysis of Furan at Low Pressures: Vibrational Relaxation, Unimolecular Dissociation, and Incubation Time", D. Fulle, A. Dibb, J.H. Kiefer, Q. Zhang, and R.D. Kern, J. Phys. Chem. 102, 7480 (1998).

"The Pyrolysis of Methylcyclopentadiene: Isomerization and Formation of Aromatics", E. Ikeda, R.S. Tranter, J.H. Kiefer, R.D. Kern, H.J. Singh, and Q. Zhang, submitted to the 28th International Symposium on Combustion (1999).

"Observation and Analysis of Nonlinear Vibrational Relaxation of Large Molecules in Shock Waves", J.H. Kiefer, L.L. Buzyna, A. Dibb, and S. Sundaram, accepted for J. Chem. Phys. (1999).

"Thermolysis of Cyclopentadiene in the Presence of Excess Acetylene or Hydrogen", R.D. Kern, H.J. Singh, Q. Zhang, B.S. Jursic, J.H. Kiefer, R.S. Tranter, E. Ikeda, and A.F. Wagner, 22nd International Symposium on Shock Waves (1999), to be published.

"The Application of Densitometric Methods to the Measurement of Rate Processes in Shock Waves", J. H. Kiefer, in "Handbook of Shock Waves", Academic Press, New York; to be published.

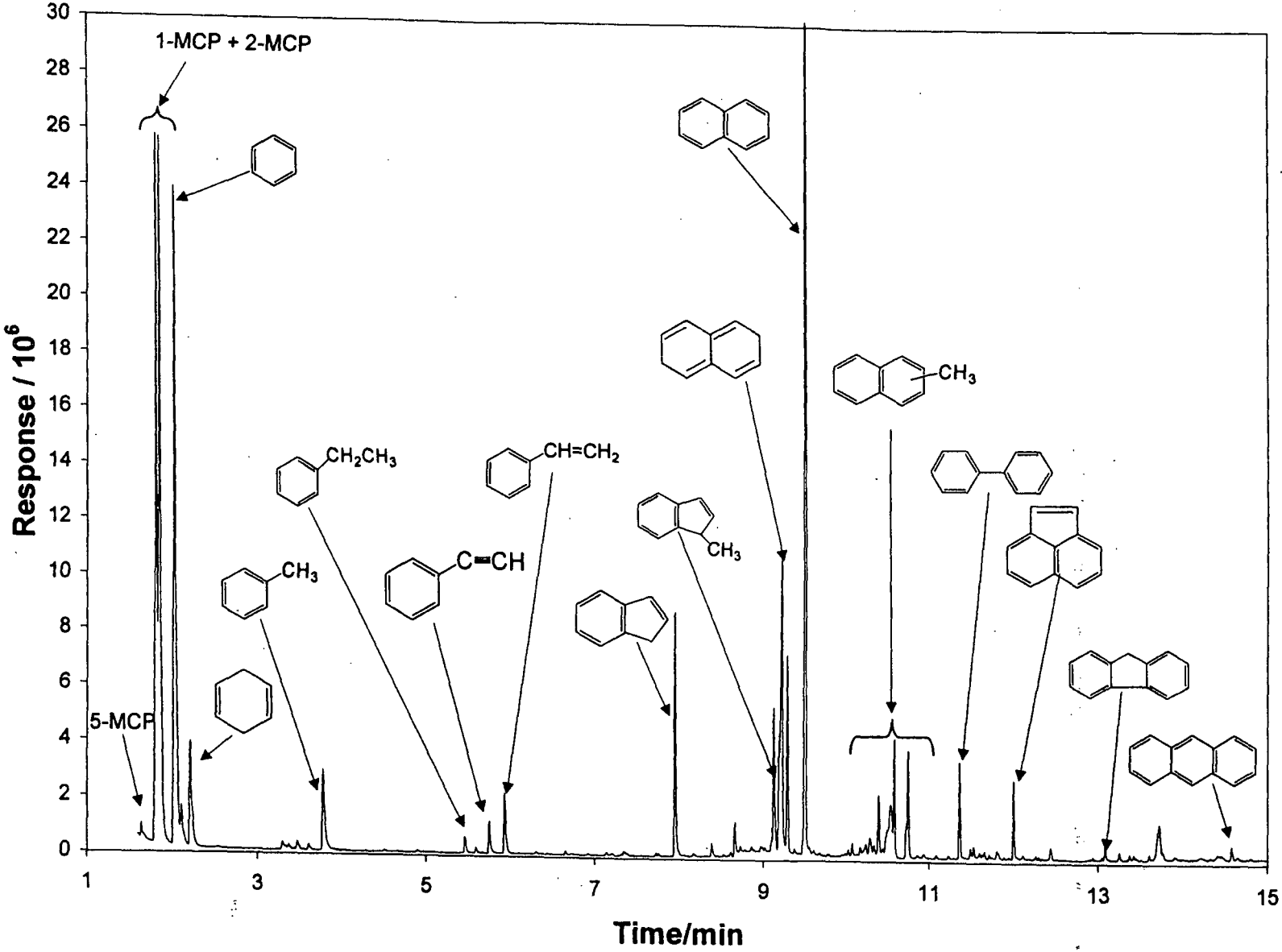

QT-GC/MS product analysis for larger species from an incident shock at 1079 K and 624 torr in 4.5% MCP/Ar. Note the extensive formation of large aromatics, benzene and naphthalene in particular. These results should be regarded as but semiquantitative because of heavy soot formation and consequent carbon imbalance.

Theoretical Modeling of the Kinetics of Barrierless Reactions

Stephen J. Klippenstein
Chemistry Department
Case Western Reserve University
Cleveland, OH, 44106-7078
E-mail: sjk5@po.cwru.edu

Program Scope

This research program aims to develop and apply sophisticated transition state theory based models for the kinetics of barrierless reactions of importance in combustion. Our current applications involve the coupling of the variable reaction coordinate (VRC) transition state theory (TST) methodology [1,2] with (i) *ab initio* quantum chemical potential energy surface evaluations in the transition state region, and/or (ii) master equation based simulations of the pressure dependence. Our continuing developments of the VRC-TST methodology include further generalizations of the transition state dividing surface. We also intend to probe the effects of collision induced transitions in angular momentum on the pressure dependence of the reaction kinetics.

Recent Progress

VariFlex

The first version of a general purpose computer code (VariFlex) for modeling the temperature/energy and pressure dependence of the kinetics of barrierless reactions is now available [3]. This package implements VRC-TST at the canonical and E/J resolved levels as well as standard rigid-rotor harmonic-oscillator TST and phase space theory. This package also allows for the direct incorporation of the TST estimates into master equation and RRKM simulations of pressure dependent rate constants. It includes simple general forms for the potential and allows for the treatment of both neutral and ionic reactions. Continuing developments for the VariFlex package include multichannel master equation simulations and an improved treatment of internal hindered rotor modes of the fragments.

High Pressure Recombination Rate Constants

We have now completed, in collaboration with Larry Harding (Argonne), an analysis of the addition kinetics of H with propargyl and allyl radicals (7). Grid based fits of wide-ranging *ab initio* simulations at the CAS+1+2/cc-pvdz level provided analytic representations of the transitional mode potentials in the transition state region. Estimates for the high pressure limiting recombination rate constants were then obtained on the basis of VRC-TST calculations employing these potentials.

For the H + propargyl reaction, the theoretical predictions are in quantitative agreement with the most recent experimental study at room temperature. However, they differ from earlier kinetic modeling results by an order of magnitude, near 1500 K. The propyne formation channel is predicted to be the dominant channel, with the allene channel contributing about 40% of the total rate. Further *ab initio* simulations, at the CAS+1+2/cc-pvtz level along the reaction path, yield a basis set correction of only about 15%.

For the H + allyl reaction, the theoretical predictions are again in quantitative agreement with the experimental results at room temperature. The H + allyl and H + propargyl addition rate constants are essentially identical.

Interestingly, these addition rate constants are actually greater than those obtained in our related calculations for the H + vinyl and H + ethyl addition reactions (1-2). Instead, one might have expected them to be somewhat lower due to the resonance stabilization of the allyl and propargyl radicals. However, the decrease in rate for a given addition channel due to the resonance stabilization is more than

compensated by the overall increase due to the presence of twice as many addition channels. Thus, the enhanced populations of such resonantly stabilized radicals in flames does not appear to be the result of decreased addition rates.

For these H + radical reactions the optimized transition state dividing surfaces were found to be closely correlated with the contours of the radical orbitals. The optimized pivot points in the VRC-TST evaluations were generally found to lie somewhere along the radical orbital. Recent experimental studies of kinetic isotope effects for CH addition reactions (and CCH + O_2) provide a reasonably direct verification of such pivot point locations [4]. In particular, in joint work with Craig Taatjes (Sandia), we have examined the dependence of VRC-TST predictions for the kinetic isotope effect on the location of the pivot point [5]. Quantitative agreement with experiment is found for pivot points located about 1 Å away from the C atom. In contrast, pivot points located at the center-of-mass yield kinetic isotope effects that are even in the wrong direction.

Direct Statistics

The application of VRC-TST to the recombination of a nonlinear fragment with a linear fragment requires a 5-dimensional potential describing the inter-fragment interactions. The accurate development of such a potential is difficult and time-consuming. An alternative is to directly generate the potential values from *ab initio* simulations solely for the specific geometries required to converge the configurational integrals. In collaboration with Larry Harding and De-Cai Feng, this direct statistics procedure has been implemented in the determination of the transition state partition functions for (i) CH_3 + OH [6], and (ii) HNN + OH [7]. For both reactions the orientation dependent energetics were determined at the CAS+1+2/cc-pvdz level. Further calculations with the aug-cc-pvtz basis set were performed along a restricted number of paths to obtain corrections for limitations in the basis set size.

For the CH_3 + OH reaction, the resulting predictions for the high pressure recombination rate constant are in reasonable agreement with various experimental results near room temperature. However, the majority of the experiments, including the recent direct experiments of Pilling and coworkers [8], observe a rapid decrease with increasing temperature, whereas the direct VRC-TST calculations predict a nearly temperature independent rate constant. This deviation between the theoretical and experimental rate constants for the CH_3 + OH recombination may be an indication of a failure to reach the high pressure limit in the experimental studies.

In collaboration with Jim Miller (Sandia), we intend to examine the pressure dependence of this association via master equation simulations. As a first step in this analysis we are performing a direct statistics study of the $^1CH_2$ + H_2O channel [9]; which provides an additional barrierless decay channel for the CH_3OH complex. Preliminary results for the high pressure association along this channel are a factor of two greater than recent measurements [10] of the decay rate of the ground vibrational state of CH_2. However, the experimental results for the decay of the first excited vibrational state are in much better agreement, being only 20 to 30% lower than the theoretical predictions. This improved agreement for the higher vibrational state may again be an indication that the experimental observations for the ground vibrational state are not in the high pressure limit. Interestingly, the observed and predicted temperature dependence is essentially identical, decreasing by a factor of 1.8 from 255 to 475 K. This comparatively large decrease in the rate constant with increasing temperature is related to the presence of a saddle point corresponding to a major structural change from a hydrogen bonded structure to a CO bonded structure.

Our modeling study of the NH_2 + NO reaction (5), performed in collaboration with Jim Miller, indicated the importance of the temperature dependence for the HNN + OH reaction in determining the branching between the N_2 + H_2O and HNN + OH products. This strong dependence led to the implementation of a direct statistical analysis of this channel [7]. This analysis indicates that the high pressure rate constant for the HNN + OH channel decreases by a factor of 1.7 from 300 to 1000 K, in reasonable agreement with our empirical modeling which employed a rate which decreased by a factor of two. We are now in the process of implementing these direct statistics results for the HNN + OH channel

into the modeling of the overall NH_2 + NO process. The preliminary results *a priori* are in good agreement with the nominal case results from our modeling study.

Pressure Dependent Multichannel Reactions

In collaborative studies with Jim Miller and Struan Robertson we have examined the pressure dependence of the C_2H_5 + O_2 reaction (6) and the C_2H_3 + C_2H_2 reaction [11] on the basis of time dependent master equation simulations employing *ab initio* properties for the transition states. For both reactions the transition state energetics were evaluated with both Gaussian-2 like calculations and with B3LYP density functional theory.

For the C_2H_5 + O_2 reaction, a decrease in the key transition state energy by 1.3 kcal/mol, yields theoretical predictions for the temperature and pressure dependence of the kinetics which are in reasonable agreement with the experimental observations. The theoretical results suggest three separate temperature regimes for the kinetics. At low temperatures, below about 600 K, the time evolution is exponential and the rate coefficient and branching fraction (between stabilization and C_2H_4 + HO_2 products) are functions of temperature and pressure. Above 700 K, the reaction can be written as an elementary step $C_2H_5 + O_2 \rightarrow C_2H_4 + HO_2$ with a pressure independent rate coefficient, even though the reaction goes through an intermediate complex which may suffer numerous collisions. At intermediate temperatures (between 600 and 700 K) the time behavior is decidedly non-exponential and it is impossible to rigorously extract a rate coefficient from the calculations. In this temperature regime, the redissociation of the $C_2H_5O_2$ complex begins to compete with the stabilization process and the C_2H_4 + HO_2 branching fraction rapidly rises towards unity as the temperature increases.

The reaction of vinyl radicals with acetylene is somewhat more complicated due to the presence of multiple energetically accessible low-lying wells for the complex. The inclusion of up to three separate wells in a multi-well master equation analysis yields valid predictions for the time-dependence of the reactants and products. One novel result of this analysis is an indication of the significance of the cyclic-C_4H_5 complex. A minor decrease of one key barrier height by 0.5 kcal/mol again yields good agreement between the theoretical predictions and experimental observations. Interestingly, at least qualitatively, our results for the C_2H_3 + C_2H_2 reaction are remarkably similar to those discussed above for the reaction of ethyl radicals with oxygen. In particular, there are again three separate temperature regimes, with the intermediate temperature regime now corresponding to 700 to 900 K.

We have also collaborated with Mike Davis (Argonne) on a nonlinear master equation based analysis of the pressure dependence of the methyl radical recombination kinetics [12].

Future Plans

In collaboration with Larry Harding, we are beginning a more quantitative analysis of the kinetic isotope effects for the CH + acetylene reaction, which has been examined experimentally by Craig Taatjes and coworkers. This work will require a generalization of the VRC-TST methodology to allow for the placement of pivot points off the diatomic axis. The generation of non-spherical dividing surfaces for the H + radical reactions is also planned as a means to more thoroughly examine the correlation between the contours of the radical orbitals and the optimal dividing surfaces.

In collaboration with Jim Miller, we are in the process of examining some other propargyl radical reactions. In particular, we are currently considering the temperature, pressure, and time dependence of the product distributions for the recombination of propargyl radicals. Preliminary calculations, implementing BAC-MP4 energetic estimates of Melius and coworkers, have demonstrated the feasibility of this study and final results should be available in the near future. We are also performing a G2-like analysis of the energetics of the C_3H_3 + O_2 reaction, for subsequent use in master equation based simulations [13]. We have also discovered an inadequacy in the available procedures for averaging over the total angular momentum in generating the one-dimensional master equation for bimolecular reactions.

We plan to present an improved procedure and to include this as part of the VariFlex package together with various developments for multiwell reactions.

We also intend to continue to explore possible explanations for the apparent deviations between experimental observations and theoretical predictions for the high pressure limit rate constants. One possible explanation involves a directly repulsive component of the dynamics. Direct dynamics simulations may provide a useful procedure for examining the magnitude of this component. In collaboration with Stephen Gray and Kelsey Forsythe (Argonne) we are performing such a direct dynamics study of the $^1CH_2 + CO$ reaction [14]. Related direct dynamics studies of the $CH_3 + CH_3$ are also planned. Another explanation involves the possible conservation of the orbital angular momentum in addition to the total angular momentum. VRC-TST studies incorporating this constraint are planned.

References

[1] S. J. Klippenstein, *Chem. Phys. Letts.* **170**, 71 (1990); J. Chem Phys. **94**, 6469 (1991); J.Chem. Phys. **96**, 367 (1992); Chem. Phys. Letts. **214**, 418 (1993); J. Phys. Chem. **98**, 11459 (1994).

[2] S.H. Robertson, A. F. Wagner, and D. M.Wardlaw, *Faraday Disc.* **102,** 65 (1995).

[3] S. J. Klippenstein, A. F. Wagner, S. H. Robertson, R. C. Dunbar, D. M. Wardlaw, *VariFlex*, version 1.0, July 1999; http://chemistry.anl.gov/variflex/.

[4] H. Thiesemann, J. McNamara, and C. A. Taatjes, *J. Phys. Chem. A*, **101**, 1881 (1997); C. A. Taatjes, *J. Phys. Chem.* **100**, 17840 (1996); H. Thiesemann, and C. A. Taatjes, *Chem. Phys. Letts.* **270**, 580 (1997).

[5] C. A. Taatjes and S. J. Klippenstein, manuscript in preparation.

[6] D.-C. Feng, L. B. Harding, and S. J. Klippenstein, manuscript in preparation.

[7] D.-C. Feng, L. B. Harding, S. J. Klippenstein, and J. A. Miller, work in progress.

[8] R. D. A. Pereira, D. L. Baulch, M. J. Pilling, S. H. Robertson, and G. Zeng, *J. Phys. Chem. A*, **101**, 9681 (1997).

[9] B. J. Serve and S. J. Klippenstein, work in progress.

[10] H. H. Carstensen and H. G. Wagner, *Ber. Bunsen. Phys. Chem.* **99**, 1539 (1995).

[11] *A Theoretical Analysis of the Reaction Between Vinyl and Acetylene*, J. A. Miller S. J. Klippenstein, and S. H. Robertson, J. Phys. Chem. A, *submitted*, (2000).

[12] M. J. Davis and S. J. Klippenstein, manuscript in preparation.

[13] D. K. Hahn, S. J. Klippenstein, and J. A. Miller, work in progress.

[14] K. Forsythe, S. K. Gray, and S. J. Klippenstein, work in progress.

DOE Supported Publications

(1) A Theoretical Analysis of the Reaction of H with C_2H_5, L. B. Harding and S. J. Klippenstein, *Twenty-Seventh Symp. (Int.) Comb.*, 151 (1998).

(2) A Theoretical Study of the Kinetics of $C_2H_3 + H$, S. J. Klippenstein and L. B. Harding, *Phys. Chem. Chem. Phys.*, **1**, 989 (1999).

(3) Angular Momentum Conservation in the $O + OH \leftrightarrow O_2 + H$ Reaction, J. A. Miller and S. J. Klippenstein, *Int. J. Chem. Kinet.*, **31**, 753 (1999).

(4) A Direct Transition State Theory Based Study of Methyl Radical Recombination Kinetics, S. J. Klippenstein and L. B. Harding, *J. Phys. Chem. A*, **103**, 9388 (1999).

(5) Theoretical Considerations in the $NH_2 + NO$ Reaction, J. A. Miller and S. J. Klippenstein, *J. Phys. Chem. A,* **104**, 2061 (2000).

(6) A Theoretical Analysis of the Reaction Between Ethyl and Oxygen, J. A. Miller, S. J. Klippenstein, and S. H. Robertson, *Twenty-Eighth Symp. (Int.) Comb.*, in press, (2000).

(7) *Theoretical Kinetic Estimates for the Recombination of Hydrogen Atoms with Propargyl and Allyl Radicals*, S. J. Klippenstein, and L. B. Harding, Twenty-Eighth Symp. (Int.) Comb., in press, (2000).

TIME-RESOLVED FTIR EMISSION STUDIES OF LASER PHOTOFRAGMENTATION AND RADICAL REACTIONS

Stephen R. Leone
JILA and Department of Chemistry and Biochemistry
University of Colorado
Boulder, Colorado 80309-0440
(303) 492-5128 srl@jila.colorado.edu

Scope of the Project

This research involves the study of laser-initiated radical reaction kinetics and dynamics, photofragmentation, and energy transfer processes related to problems in combustion dynamics. The vibrationally excited species generated in such processes are probed by time-resolved Fourier transform infrared (FTIR) emission spectroscopy. Time resolution of the dynamics is obtained by coupling a high repetition rate pulsed excimer laser to a Fourier transform infrared spectrometer with appropriate synchronization electronics. This is a relatively unique facility, and the FTIR method has been previously applied in our laboratory to study photofragmentation processes, the dynamics of energy transfer, radical-molecule reactions, and radical-radical reactions. The method permits the study of photofragmentation processes under jet-cooled conditions and single collision energy transfer events.

The current research involves several major thrusts. One is to study radical reactions to determine the nascent product species and states formed in a variety of important radical-radical and radical-molecule processes. The other is to develop studies of collisional energy transfer and photofragmentation involving polyatomic molecules and radical species with nascent vibrational and rotational state detail.

Experimental Advances

Through a generous equipment grant supplement from DOE, we procured a new step-scan FTIR for this research. Not only does this new instrument have much better optical stability (because of a very stable mechanical/optical layout in contrast to the dynamic mirror alignment of the old instrument), but in addition, the data-taking can be accomplished much faster and with many more resultant time windows of spectra per scan. Comparing time-resolved scans taken at the same laser repetition rate, the signal-to-noise is estimated to be improved by approximately a factor of five over the old instrument. In addition, the data for 20 coadditions is acquired in 4 hours compared to 10 hours with the old instrument under identical 0.2 cm^{-1} resolution, since there is less dead time due to mirror fly back. In addition, up to 200 time slices of the complete spectrum can be obtained in one measurement, whereas for the old instrument only 6-8 time slices could typically be obtained. For rapid scan continuous signals, the results show more than an order of magnitude improvement for the same time of data acquisition. The rapid scan mode is used for several aspects of studies on the $O + C_2H_5I$ reactions that proceed through five-membered ring transition states. Thus the impressive improvements of the step scan technology and the better optical stability of the instrument permit more difficult projects. Another important technological improvement has been the development of a jet-cooled source for photolysis preparation of radicals. With this source we have been able to study the jet-cooled photofragmentation of ammonia and deuterated ammonia molecules with elegant rotational and vibrational detail.

Atom-Molecule Reactions: 5-Member Ring Transition States

The product branches of atom-molecule reactions are important in combustion processes. There are relatively few examples of 5-membered ring transition states in the gas phase; the most well-

known, based on theoretical calculations, is the 5-member ring in the reaction of alkyl radicals with O_2. New studies involve the remarkable gas phase reaction discovered in our laboratory that proceeds through a 5-member ring transition state, the reaction of $O(^3P)$ atom with C_2H_5I, which forms vibrationally excited HOI. In this reaction, the O atom attacks the iodine, forming a quasibound complex that survives long enough for the O atom to undergo elimination of an H atom on the β-carbon along with the iodine. Forming the double bond between the two carbon atoms supplies sufficient energy to drive the reaction to vibrationally excited products. We obtained the first completely vibrationally and rotationally resolved spectrum of HOI, taken at 0.03 cm^{-1} unapodized resolution in emission, as well as the vibrational product state distributions in the O-H stretch of HOI for a series of reactions. The power of the FTIR method is aptly demonstrated by this discovery, due to its ability to analyze broad regions of infrared vibrational frequencies simultaneously, permitting new species to be detected.

Recent studies involved O atom reactions with a series of ring compounds and partially fluorinated iodide compounds, designed to probe the effect of ring strain on the formation of the C=C double bond and to determine whether 6-membered and 7-membered ring transition states can also occur. The 6- and 7-membered ring transition states must proceed through a diradical, which could only release the necessary additional reaction energy if the diradical undergoes closure. A number of important results were found. Reactions of cyclopentyl iodide and cyclohexyl iodide compounds both produce vibrationally excited HOI by the normal β–elimination pathway, with surprisingly similar vibrational product state distributions compared to O + ethyl iodide. The cyclopentyl and cyclohexyl rings have little effect on the rates of formation or vibrational excitation of the HOI. Reaction of $CF_3CH_2CH_2I$ produces HOI, but with a slightly but distinctly lower vibrational excitation in the HOI product. We attribute this to the strongly electron withdrawing CF_3 group, which weakens the β–hydrogen and lowers the vibrational excitation. Compounds like $CH_3CF(CF_3)CF_2I$ do not produce any vibrationally excited HOI, and no other vibrationally excited products are observed in this reaction. Thus a 7–membered ring transition state to produce HOI and the diradical does not appear to be favorable - at least it does not produce vibrationally excited HOI. However, neopentyl iodide $(CH_3)_3CCH_2I$, which has only a 6-membered ring pathway available, does produce some vibrationally excited HOI, and this may indicate formation of a cyclopropane product in one step. Most surprisingly, a new type of reaction was observed for O atoms reacting with compounds like $CHF_2CF_2CH_2I$ and CF_3CH_2I, which efficiently produce highly vibrationally excited HF(v) (not vibrationally excited HOI) by a complex addition-elimination pathway involving a common FC–C(H)I functional group. Fluorinated compounds that lack an iodine or bromine substituent fail to yield HF, suggesting that the presence of an I or Br atom is essential to the course of the HF-generating reaction. Presently one explanation is that the O atom attacks the iodine and can then switch places with the iodine forming an activated FC–C(H)OI species that has sufficient energy to overcome the endothermicity to eliminate HF across the C–C bond. The formation of the COI bonding configuration can liberate approximately 240 kJ $mole^{-1}$.

O + C_2H_5 Radical-Radical Reactions

Previously, we completed an extensive study of the radical-radical reaction $C_2H_5 + O(^3P) \rightarrow OH(v) + C_2H_4$ and the related *n*- and *i*-propyl radical reactions, in which we studied the OH product. In the O + ethyl radical system, inverted vibrational distributions in the OH product were observed, atypical of the usual monotonically decreasing vibrational state distributions of an addition-elimination pathway. Recently, Paul Zittel from Aerospace Corporation indicated that his measurements of room temperature O atom + hydrocarbon flow tube infrared emission combustion systems contain unexpected CO(v) emission components and that his results would be best fit if the O atom reactions with larger hydrocarbons also produced a CO(v) product channel, analogous to the CO(v) channel we reported for the $CH_3 + O$ reaction. Our observation for $CH_3 + O \rightarrow CO(v) + H_2 + H$ was initially met with some skepticism, since there were conflicting experimental results and potential surface calculations that indicated the formaldehyde product has a unit yield.

However, recently, two new independent studies have confirmed that CO(v) is produced in the CH_3 + O reaction, possibly with a 20% yield. In recent experiments, we have confirmed the CO(v) product of the O + C_2H_5 reaction. The experiment required a careful blend of kinetics analysis, timing, and tailoring of concentration conditions to determine if this pathway does occur. The products of a reaction RCH_2 + O could be CO(v) + H + RH or CO(v) + R + H_2, the former requiring an H atom migration and the latter giving the corresponding one-carbon-smaller hydrocarbon radical. All these reactions are sufficiently exothermic (330-370 kJ $mole^{-1}$) to form the vibrationally excited CO product channel. Reactions with secondary hydrocarbon radicals, such as RC˙HR', would require an atom or radical migration to form CO + RH + R', and these will also be explored.

Spectroscopic Pattern Recognition of Product State Distributions

The method of time-resolved FTIR spectroscopy permits the experimentalist to study the progress of many simultaneous reaction pathways, monitoring the infrared-emitting product state distributions and branching ratios of different reaction channels. While this can be a fundamental advantage of this technique, detailed analyses of the spectroscopic data obtained, and their variation with reaction conditions, are a necessary prerequisite to the interpretation of the chemical system under study. In some cases, the parallel reaction pathways under study can become so convoluted and the spectroscopy so complex that it may be difficult to readily gain any clear understanding from the analysis.

A spectral pattern recognition technique developed by Field and coworkers for the systematic study of equilibrium states, has been extended to the realm of reactive product state distributions. The simplest reaction to consider is a photodissociation in which branching ratios of vibrational and rotational states for different bond cleavages are of key importance. The method was applied to a study of ammonia and deuterated ammonia species. In the case considered in this work, not only was the competition for products from different parent molecules investigated (e.g. ND_2 from ND_3 or from ND_2H), but the technique was applied to separate out the product state distributions arising from all four deuterated parent molecules undergoing simultaneous dissociation to give up to six different final state distributions. This is the first application of the spectral pattern deconvolution procedure to dynamical product state distributions.

The separation of fragment distributions by this method of pattern recognition not only yields spectral patterns which are less complicated to assign, but it also reveals physical insights into the chemical process without even assigning the product spectra. For example, we have demonstrated that it is possible to estimate relative quantum yields or branching ratios for breaking various bonds in the photochemical process. Also, key features of the product state distributions can be immediately observed by viewing the graphical representation of the pattern correlation. The pattern recognition method can be applied to study systems for which any well-defined experimental variable can be altered in a systematic way. In this work, the variables chosen were the reactant ratios and the temperature of the photodissociation event.

The dissociation of NH_2D and ND_2H show that the competing nature of the adiabatic and non-adiabatic processes influences the dissociation dynamics. Quantum yields calculated from the pattern recognition technique suggest that the yield of the ND_2 excited fragment produced from the dissociation of ND_2H, is much higher than that from ND_3, with an exceptional enhancement of a factor of approximately 6±1 in the bending excitation of the product ND_2(v=1). The large increase in the ND_2 quantum yield on comparing ND_2H and ND_3 may be due to the increased tunneling probability with the breaking of an N-H bond as opposed to an N-D bond. Some ND_2(v=2) is also observed, reflecting the available energy, since the N-H bond is the weakest and the bending frequency of ND_2 the lowest. The rotational distributions of the products from the dissociation of NH_2D and ND_2H have also been obtained. Surprisingly, little NHD product is observed from the dissociation of either NH_2D or ND_2H, although the lack of transition moments for NHD prohibits

the calculation of an accurate branching ratio.

As well as yielding dynamical information about the dissociation event and improving our understanding of it, these studies have permitted new information to be gained on the electronic spectroscopy of the fragments NH_2, NHD and ND_2. Little information existed on the first electronic excited states of NHD and ND_2 and this study has enabled a manifold of states to be observed and transitions to be spectroscopically assigned.

New Directions

New studies will emphasize a variety of radical-radical and radical-molecule reactions, such as C_2H + NO, HCO + O_2, NH_2 + NO, C_2H + O, CH_3 + N and additional work on five-member ring intermediates and O + larger alkyl radicals to study the CO products.

Publications

J. Lindner, R. A. Loomis, J. J. Klaassen, and S. R. Leone, "A laser photolysis/time-resolved Fourier transform infrared emission study of OH(X 2Π,v) produced in the reaction of alkyl radicals with O(3P)," J. Chem. Phys. **108**, 1944 (1998).

R. A. Loomis, M. K. Gilles, and S. R. Leone, "Novel five-membered ring intermediates in gas phase reactions," Research on Chem. Intermediates **24**, 707 (1998).

R. A. Loomis, J. P. Reid, and S. R. Leone, "Photofragmentation of ammonia at 193.3 nm: Bimodal rotational distributions and vibrational excitation of $NH_2(\tilde{A})$," J. Chem. Phys. **112**, 658 (2000).

Jonathan P. Reid, Richard A. Loomis and Stephen R. Leone, "Characterization of dynamical product-state distributions by spectral extended cross-correlation: Vibrational dynamics in the photofragmentation of NH_2D and ND_2H," J. Chem. Phys. **112**, 3181 (2000).

Jonathan P. Reid, Charles X.W. Qian and Stephen R. Leone, "Probing the cyclic transition state in the reaction $O(^3P)$ + alkyl iodides to form HOI: Electronic, steric and thermodynamic factors influencing the reaction pathway," Phys. Chem. Chem. Phys. **2**, 853 (2000).

INTERMOLECULAR INTERACTIONS OF HYDROXYL RADICALS AND OXYGEN ATOMS ON REACTIVE POTENTIAL ENERGY SURFACES

Marsha I. Lester
Department of Chemistry
University of Pennsylvania
Philadelphia, PA 19104-6323
milester@sas.upenn.edu

PROGRAM SCOPE

A primary new objective of the DOE supported work in this laboratory is to examine the interaction potential and reaction dynamics of the CH_4 + OH system, one of the key initiation steps in the combustion of methane. The goal of this study is to map out the reaction pathway from the entrance valley through the transition state via spectroscopic and dynamical studies of CH_4-OH entrance channel complexes. Our approach is to stabilize the CH_4 + OH reactants in a weakly bound complex in the entrance channel to reaction and then to use stimulated Raman, infrared, and/or electronic excitation for spectroscopic characterization of the system. Vibrational or electronic excitation of one of the reactants induces a reactive and/or inelastic scattering process that starts from a well-defined initial state under the restricted geometric conditions imposed by the complex. We explore these dynamical processes through the lifetime of the vibrationally activated complexes and the quantum state distribution of the products. The results of these experiments, particularly when coupled with theoretical calculations of the experimental observables, yield a wealth of new information on the $CH_4 + OH \rightarrow CH_3 + H_2O$ potential energy surface. Finally, pre-reactive complexes of OH radicals (and O atoms) with other molecular partners of combustion importance are being investigated.

VIBRATIONAL SPECTROSCOPY OF CH_4-OH

Vibrational spectroscopy has been utilized to examine the structure and vibrational decay dynamics of CH_4-OH complexes that have been trapped in the entrance channel to the CH_4 + OH hydrogen abstraction reaction. Infrared spectra of the CH_4-OH complexes have been obtained in the OH fundamental and overtone regions using an IR pump – UV probe scheme, in which the OH fragments from vibrational predissociation are detected by UV laser-induced fluorescence.[1] Pure OH stretching bands have been identified at 3563.45(5) and 6961.98(4) cm^{-1} (origins), shifted 5.02 and 9.36 cm^{-1} to lower energy of the corresponding Q(3/2) transitions in free OH. Structural parameters derived from the rotationally resolved spectra indicate that CH_4-OH adopts a C_{3v} minimum energy structure in which the H-end of OH points toward a tetrahedral face of CH_4, consistent with high-level *ab initio* calculations by Lendvay.[1] Combination bands have also been detected (at 41 and 54 cm^{-1} to higher energy) that likely involve intermolecular bending excitation of OH and may access configurations that resemble the transition state to reaction.

The infrared spectra exhibit extensive homogeneous broadening arising from the rapid decay of vibrationally activated CH_4-OH complexes due to vibrational relaxation and/or reaction. Homogeneous line widths of 0.14(2) and 0.21(2) cm^{-1} have been observed for the pure OH stretching bands in the fundamental and overtone bands (as compared to an instrumental line

width of less than 0.04 cm^{-1}), corresponding to 38 and 25 ps lifetimes for vibrationally activated complexes with one and two quanta of OH stretching excitation. The lifetimes are surprisingly short and suggest that both inelastic and reactive channels contribute to the rapid decay of CH_4-OH (ν_{OH}) and ($2\nu_{OH}$) as found in a recent collision study of OH (v=1, 2) + CH_4.[2] The nascent distribution of the OH products from vibrational predissociation has been evaluated by probe laser-induced fluorescence measurements. The dominant inelastic decay channel involves the transfer of one quantum of OH stretch to the pentad of CH_4 vibrational states with energies near 3000 cm^{-1}.

In addition, the vibrational spectrum of CH_4-OH in the CH_4 symmetric stretching region (ν_1) has been obtained using stimulated Raman excitation (SRE).[3] SRE transitions were detected via a fluorescence depletion scheme with the probe laser fixed on a previously identified CH_4-OH electronic transition in the OH *A-X* 1-0 region at 35390 cm^{-1}. The SRE spectrum of CH_4-OH consists of a primary feature at 2912.5 cm^{-1}, which is shifted 4.0 cm^{-1} to lower energy of the ν_1 stretch in free CH_4, and a secondary shoulder at 2911.8 cm^{-1}. These features are likely due to two distinct forms CH_4-OH, corresponding to different internal rotor states of the methane subunit within the complex. The OH product rotational distribution reveals that CH_4-OH (ν_1) decays via intramolecular vibrational energy transfer within the CH_4 monomer; the possibility of reactive decay has not yet been explored. Ongoing studies are focused on infrared excitation of the C-H stretching modes of CH_4-OH, as quantum dynamics calculations have predicted a large enhancement in the rate of the bimolecular reaction upon C-H vibrational excitation.[4] Preliminary infrared spectra of CH_4-OH have already been obtained in the CH_4 symmetric (ν_1) and asymmetric (ν_3) stretching regions near 3 μm.

REACTIVE QUENCHING OF OH $A\ ^2\Sigma^+$ BY H_2/D_2

Another goal of the current grant period is to initiate the hydrogen abstraction reaction between H_2/D_2 and OH in its ground $X\ ^2\Pi$ and excited $A\ ^2\Sigma^+$ electronic states through vibrational and electronic excitation of OH-H_2/D_2 reactant complexes, and to probe the H/D-atom products of chemical reaction directly. Towards this end, we have investigated the reactive quenching of electronically excited OH $A\ ^2\Sigma^+$ radicals in collisions with molecular hydrogen.[5] *Ab initio* calculations have predicted that the potential energy surfaces for H_2 interacting with OH in its ground $X\ ^2\Pi$ and excited $A\ ^2\Sigma^+$ electronic states cross by means of a conical intersection in the T-shaped HO-H_2 orientation.[6,7] Two pathways exit from the conical intersection: the nonreactive quenching pathway follows down to OH $X\ ^2\Pi$ + H_2 and the reactive pathway generates H + H_2O.

We have used Doppler spectroscopy of H-atoms via two-photon laser-induced fluorescence[8] to demonstrate that reactive quenching is indeed a significant decay channel and to characterize the translational energy distribution of the H-atom products. We find a bimodal distribution, which is fit to Gaussian functions with translational temperatures of 900 K and 13000 K, indicating that the H-atoms are produced with two distinct kinetic energy distributions. The bimodal distribution most likely originates from two different dynamical pathways through the conical intersection region. In addition, isotopic substitution studies have shed further light on the mechanism for this nonadiabatic reaction by revealing that both D- and H-atoms are produced in the reactive quenching of OH $A\ ^2\Sigma^+$ by D_2. Thus, both abstraction and insertion mechanisms are operative as the reactants are funneled through the conical intersection region.

FUTURE PLANS

During the coming year, we plan to continue our in depth investigation of fundamental hydrogen abstraction reactions of combustion relevance. Specifically, we will continue mapping the CH_4 + OH potential energy surface through infrared and stimulated Raman excitation of the CH_4-OH entrance channel complexes in the CH_4 symmetric (ν_1) and asymmetric (ν_3) stretching regions. We will also be evaluating the rates and product state distributions for inelastic scattering and chemical reaction following infrared, stimulated Raman, and electronic excitation of CH_4-OH and H_2-OH reactant complexes. Our aim is to probe the products of these chemical reactions directly. Finally, we will begin exploring the potential energy surface for the CH_4 + O system via similar methodologies. This includes the stabilization and spectroscopic characterization of CH_4-O reactant complexes.

REFERENCES

1. M. D. Wheeler, M. Tsiouris, M. I. Lester, and G. Lendvay, *J. Chem. Phys.* **112**, xxxx (2000).
2. K. Yamasaki, A. Watanabe, T. Kakuda, N. Ichikawa, and I. Tokue, *J. Phys. Chem. A* **103**, 451 (1999).
3. M. Tsiouris, M. D. Wheeler, and M. I. Lester, *Chem. Phys. Lett.* **302**, 192 (1999).
4. G. Nyman and D. C. Clary, *J. Chem. Phys.* **101**, 5756 (1994).
5. D. T. Anderson, M. W. Todd, and M. I. Lester, *J. Chem. Phys.* **110**, 11117 (1999).
6. M. I. Lester, R. A. Loomis, R. L. Schwartz, and S. P. Walch, *J. Phys. Chem. A* **101**, 9195 (1997).
7. D. R. Yarkony, *J. Chem. Phys.* **111**, 6661 (1999).
8. T. W. Hansch, S. A. Lee, R. Wallenstein, and C. Wieman, *Phys. Rev. Lett.* **34**, 307 (1975).

DOE SUPPORTED PUBLICATIONS
1998-2000

1. D. T. Anderson, R. L. Schwartz, M. W. Todd, J. M. Hossenlopp, and M. I. Lester, "Infrared Spectroscopy of Entrance Channel Complexes", Proc. SPIE-Int. Soc. Opt. Eng. (1998), 3271 (Laser Techniques for State-Selected and State-to-State Chemistry IV), 164-168.

2. D. T. Anderson, R. L. Schwartz, M. W. Todd, and M. I. Lester, "Infrared Spectroscopy and Time-Resolved Dynamics of the *ortho*-H_2-OH Entrance Channel Complex", *J. Chem. Phys.* **109**, 3461-3473 (1998).

3. P. J. Krause, D. C. Clary, D. T. Anderson, M. W. Todd, R. L. Schwartz, and M. I. Lester, "Time-Resolved Dissociation of the H_2-OH Entrance Channel Complex", *Chem. Phys. Lett.* **294**, 518-522 (1998).

4. J. M. Hossenlopp, D. T. Anderson, M. W. Todd, and M. I. Lester, "State-to-State Inelastic Scattering from Vibrationally Activated OH-H_2 Complexes", *J. Chem. Phys.* **109**, 10707-10718 (1998).

5. M. D. Wheeler, M. W. Todd, D. T. Anderson, and M. I. Lester, "Stimulated Raman Excitation of the *ortho*-H_2-OH Entrance Channel Complex", *J. Chem. Phys.* **110**, 6732-6742 (1999).

6. M. D. Wheeler, D. T. Anderson, M. W. Todd, M. I. Lester, P. J. Krause, and D. C. Clary, "Mode-Selective Decay Dynamics of the *ortho*-H_2-OH Complex: Experiment and Theory", *Mol. Phys.* **97**, 151-158 (1999).

7. M. Tsiouris, M. D. Wheeler, and M. I. Lester, "Stimulated Raman and Electronic Excitation of CH_4-OH Reactant Complexes", *Chem. Phys. Lett.* **302**, 192-198 (1999).

8. D. T. Anderson, M. W. Todd, and M. I. Lester, "Reactive Quenching of Electronically Excited OH Radicals in Collisions with Molecular Hydrogen", *J. Chem. Phys.* **110**, 11117-11120 (1999).

9. M. D. Wheeler, M. Tsiouris, M. I. Lester, and G. Lendvay, "OH Vibrational Activation and Decay Dynamics of CH_4-OH Entrance Channel Complexes", *J. Chem. Phys.* **112**, xxxx (2000).

10. M. D. Wheeler, D. T. Anderson, and M. I. Lester, "Probing Reactive Potential Energy Surfaces by Vibrational Activation of H_2-OH Entrance Channel Complexes", *Int. Rev. Phys. Chem.* (invited review), in press (2000).

Theoretical Studies of Molecular Systems

William A. Lester, Jr.
Chemical Sciences Division, Ernest Orlando Lawrence
Berkeley National Laboratory and Chemistry Department
University of California, Berkeley
Berkeley, California 94720-1460
walester@cchem.berkeley.edu

Program Scope

This research program is directed at extending fundamental knowledge of atoms and molecules. The approach combines the use of ab initio basis set methods and the quantum Monte Carlo (QMC) method to describe the electronic structure, energetics, and reaction pathways of systems of combustion interest.

Recent Progress

Quantum Monte Carlo and Density Functional Theory Study of the Reaction of Propargyl Radical with Acetylene to Form Cyclopentadienyl Radical (with N. W. Moriarty, X. Krokidis, and M. Frenklach)

The addition of acetylene and propargyl has been investigated using several DFT methods including B3-LYP, B3-PW91 and B&H-H&LYP. The optimized geometries were calculated using the 6-31G(d,p) and the cc-pVTZ basis sets. Quantum Monte Carlo (QMC) calculations were performed at the B3-LYP/cc-pVTZ optimized geometries. A number of other theoretical methodologies including CBS-RAD, G2, G3 and their variations were used to study some important features of the potential energy surface and thermochemistry of the cyclopentadienyl radical.

The RRKM rate constants were determined for the reactions leading to the formation of the cyclo-C_5H_5 radical. The heat of formation and rate of decomposition of the radical are determined and compared with experiment. A detailed analysis of the reaction pathways is performed using the Bonding Evolution Theory (BET) concepts applied to the Electron Localization Function (ELF).

Theoretical Study of the Reaction of Cl + CH_3OH (with O. Couronne and F. Gilardoni)

A crossed molecular beam study of the present reaction has been carried out by A. G. Suits and coworkers and shows that the reaction implies direct, close collisions. As a first step in the study of this system, restricted open-shell Moeller-Plesset second-order pertubation theory (ROMP2) calculations have been carried out using a 6 311++G** basis set. In contrast to previous theoretical findings which suggested an intermediate complex, the present work is consistent with

the experiment of Suits and coworkers.

Stability of NO dimer (with X. Krokidis, French Institute of Petroleum, J. Grossman, LLNL, and Ken Hass, Ford Motor Co.)

We are engaged in carrying out large scale calculations for the NO dimer to resolve ongoing debate regarding a) the optimal structure of the triplet conformation, b) the spin multiplicity of the dimer ground state, and c) the binding energy of the singlet and of the triplet states. This system is of particular interest for automotive combustion, where it plays a key role in several important catalytic reaction steps. Calculations are being performed using the Hartree-Fock, local spin density, B3LYP DFT, CCSD(T), and DMC approaches. Findings to date indicate strong disagreement among mean-field approaches for the singlet/triplet separation. The energy of the triplet state is also shown to be highly sensitive to geometry.

Future Plans

Future work will continue primarily in the direction of establishing fundamental understanding of mechanisms leading to soot formation as well as other molecular species of combustion interest.

DOE Supported Publications 1998-2000

1. C. W. Greeff and W. A. Lester, Jr., "A Soft Hartree-Fock Pseudopotential for Carbon with Application to Quantum Monte Carlo," J. Chem. Phys. 109, 1607 (1998).
2. W. A. Lester, Jr. and R. N. Barnett, "Quantum Monte Carlo Methods for Electronic Structure", in "The Encyclopedia of Computational Chemistry", P. v. R. Schleyer; N. L. Allinger, T. Clark; J. Gasteiger; P. A. Kollman; H. F. Schaefer, III; P. R. Schreiner (Eds.); John Wiley & Sons: Chichester, 1998, vol. 3, 1735.
3. A.L. Almeida, J. B. L. Martins, C.A. Taft, E. Longo, and W.A. Lester, Jr., "Ab Initio and Semiempirical Studies of the Adsorption and Dissociation of Water on Pure, Defective, and Doped MgO (001) Surfaces", J. Chem. Phys. 109, 3671 (1998).
4. A.C. Pavão, T.C.F. Guimarães, S.K. Lie, C.A. Taft, and W.A. Lester, Jr., "Modeling the Adsorption and Dissociation of CO on Transition Metal Surfaces*, J. Mol. Struct. (Theochem) 458, 99 (1999).
5. A.L. Almeida, J.B.L. Martins, C.A. Taft, E. Longo, and W.A. Lester, Jr., *Theoretical Study of Water Coverage on MgO Surfaces", Int. J. Quantum Chem. 71, 153 (1999).
6. J.C. Grossman, W.A. Lester, Jr., and S.G. Louie, "Cyclopentadiene Stability: Quantum Monte Carlo, Coupled Cluster, and Density Functional Theory Determinations", Mol. Phys. 96, 629 (1999)
7. C.A. Taft, T.C.F. Guimarães, A.C.Pavão, and W.A. Lester, Jr., "Adsorption and Dissociation of Diatomic Molecules on Transition Metal Surfaces", Int. Rev. Phys. Chem. 18, 163 (1999).

8. T.C.F. Guimarães, A.C. Pavão, C.A. Taft, and W.A. Lester, Jr., "Dissociation of N_2 on Chromium Alloys: A General Mechanism for Dissociation of Diatomic Molecules", Phys. Rev. B 60, 11789 (1999).

9. X. Krokidis, N.W. Moriarty, W.A. Lester, Jr., and M. Frenklach, "Propargyl Radical: An Electron Localization Function Study", Chem. Phys. Letters 314, 541 (1999).

10. J.C. Grossman, W.A. Lester, Jr., and S.G. Louie, "Quantum Monte Carlo and Density Functional Theory Characterization of 2-Cyclopentenone and 3 Cyclopentenone Formation from $O(^3P)$ + Cyclopentadiene", J. Am. Chem. Soc. 122, 705 (2000).

Quantum Dynamics of Fast Chemical Reactions - DE-FG02-87ER13679

April - 2000

Principal Investigator, John C. Light
University of Chicago
5640 S. Ellis, Chicago, IL 60637
j-light@uchicago.edu

I. PROGRAM SCOPE

The aims of this research are to develop a theoretical understanding and predictive abiility for a variety of processes occurring in the gas phase and on surfaces. These include bimolecular chemical exchange reactions, photodissociation, predissociation resonances and unimolecular reactions. The focus is both on the development and applications of new methods and approaches to the problems above as well as to their applications. The techniques developed and used are primarily quantum mechanical which permits us to focus on the potential energy surfaces of the systems and the effects of the internal states of reactants and internal state distributions and branching ratios for products. Efficient methods to look at thermal rates of exchange of light atoms with tunneling have been developed. A variety of basis set (L^2) and time dependent correlation function methods have been developed and used to study such processes as exchange reactions, predissociation resonances, unimolecular dissociation and potential energy inversion.

II. RECENT PROGRESS

A major goal of the research under this proposal has been to simplify the theoretical evaluation of chemical reaction rate information, whether that information is at the level of state-to-state reaction probabilities, cumulative reaction probabilities, or thermal rate constants. In the past decade great progress has been made toward these goals both by our group and others. With respect to exact quantum methods for calculating dynamical information, there have been a number of recent developments including: better representations such as the Discrete Variable Representation (DVR) [1,2]; sequential diagonalization/truncation methods [3,4,2] for eigenvalues and eigenfunctions; development of square integrable (L^2) approaches to quantum scattering [5–7]; correlation function formulations of the rate constants and cumulative reaction probabilities [8,9]; improved time dependent approaches to quantum scattering [10–12]; and use of optical potentials [13], etc.

Simple time independent methods were developed for evaluation state-to-state scattering in L^2 bases via pointwise projection using the finite range scattering wavefunction (FRSW) method [14] and/or the artificial boundary inhomogeneity (ABI) method [14–16]. The ABI method has been applied to the 3-D calculation of resonances (from the lifetime matrix) for HCO (J=0, 1, and 3) [17]. This latter was combined with a quantum/classical time dependent SCF calculation of the vibrational transition probabilities and collisional dissociation of HCO in collisions with Ar [18],

An alternative approach is via time dependent quantum scattering using either initial state wave packets or transition state wave packets combined with correlation function formulations of the reaction probabilities. Initial state selected cumulative reaction probabilities [19] and state-to-state reaction probabilities have been calculated via time evolution of initial state selected wave packets (ISSWP) [20] for the H + H_2O [21] reaction as well as for the H + HOD reaction [22].

Some recent projects have been very successful. Since they were reported before, we merely list them:

- the quantum transition state (TSWP) method [23,24] for evaluation of the cumulative reaction probabilities, N(E), or state selected cumulative reaction probabilities, N_i(E), This was applied to several reactions including the H_2 + CN [25] reaction.
- a quantum transition state theory (QTST), evolved from the TSWP approach for larger systems, in this case diffusion of H atoms on non-rigid Cu(100). In this case we determined that in which only one (or a few) transition state wavepackets need be propagated [26] and that the full rate constant could be obtained accurately from this information combined with a sum over adiabatic transition states.

- a mixed quantum/classical calculation of the collision induced dissociation of HCO (J=0) in collisions with Ar [18].

III. RECENT RESULTS:

There are three other areas of research on which we spent substantial effort over the past year. Of these, one failed, one had modest success, and the third, still under intensive investigation, is succeeding very well. These three projects are the calculation of N(E) by cross correlation methods starting with a single "random" transition state wavepacket; the use of semi-classical IVR methods with forward-backward time evolution using the Møller operator to define the S matrix elements; and finally, the development of highly correlated pseudo-random Gaussian bases for highly excited vibrational bound states and resonances of polyatomic molecules.

A. Cross correlation TSWP for N(E):

One of the proposed projects, about which I was very enthusiastic, did not succeed despite substantial efforts. This was the combination of the TSWP approach with a cross correlation method for determining the sum of the contributions to N(E) from all transition states from a single wavepacket propagation. I will describe the approach and our findings briefly.

Earlier we [23,21] found a simple but important reformulation of N(E) which is conceptually pleasing and computationally highly advantageous, the transition state wavepacket (TSWP) approach. In this approach a set of TS wavepackets are defined on the N-1 dimensional space defining the dividing surface between reactants and products. The direct product of these with the eigenfunctions of the flux operator provide a rapidly convergent basis set for evaluation of N(E). Many fewer TS wavepackets are usually required for evaluation of N(E) than reactant wave packets, for example.

Recently Mandelshtam demonstrated formally and for examples, that propagation of a single suitably chosen initial state and evaluation of the autocorrelation function and cross correlation functions with asymptotic initial and final states could, with effort, yield the entire S matrix for all energies [27]. Since far fewer correlation functions between TSWP's than initial states are required for convergence of N(E) as noted above, we re-formulated Mandelshtam's harmonic inversion cross correlation approach to apply to the TSWP approach to N(E).

Although the approach worked for 1-D Eckhart potentials, demonstrating the correctness of the formulation, and with difficulty for the collinear H + H_2 reactive scattering model, we could not develop a stable algorithm for the required harmonic inversion either by using Mandelshtam's approach or the more stable Prony's method. After substantial investigation using exact eigenfunctions of the Hamiltonian and optical potentials, we found an interesting cause of the failure. The method requires an extraordinarily accurate fitting of a time series by a harmonic series, e.g. evaluation of d's and ω's in the series representation of a correlation function:

$$c(t) = \Sigma_k \quad d_k \quad e^{-i\omega_k t} \tag{1}$$

For reactive scattering with transition state wavepackets, the correlation functions decay rapidly (ω's are complex). Thus the coefficients, d_k could not be fit very accurately since the time series contains primarily real exponential decays. These do not have the nice properties of Fourier series. In order to extract the scattering information accurately from this approach, the complex d's must be known very accurately which was not possible for any but the simplest systems.

Ironically, the very attributes which make the TSWP approach efficient and accurate, short time propagation and few wave packets, make it inappropriate for use with cross correlation approaches where very accurate harmonic expansions are required. Prony's method, which permits limitations of the number of terms in the time series and least squares fitting of the correlation functions, was tried in the hope that it might be sufficiently stable. Unfortunately, we found that it was not. We are not working on this project at this time although the idea is still appealing; there must be a way to extract the relatively few TSWP cross correlation functions required from the single propagation cross correlation approach. We may figure out a stable way to do it in the future.

B. Forward-backward IVR evaluation of Møller wave operators:

The semi-classical evaluation of reaction probabilities accurately is a highly desired approach to the dynamics of larger systems. It is, however, beset by many practical problems. The "initial value representation" (IVR) for the formal semi-classical propagator solves one major problem, namely the erstwhile matching of initial and final actions to integral values of h. Two major remaining problems, however, are that the normalization (monodromy) matrix may be ill conditioned or difficult to calculate, and that the phase space integrals are over integrands containing rapidly varying oscillatory exponentials of the action integrals. These conditions make the convergence of the phase space integrals very demanding in terms of the number of classical trajectories required. Makri [28] and Miller [29] have recently shown that the oscillatory integrand problem can be greatly ameliorated for squares of matrix elements by combining forward and backward propagations. This greatly reduces the magnitude of the action contributing to the oscillatory integrand. These applications, however, require an additional semi-classical approximation or expansion of the action.

We investigated the use of similar forward-backward cancellation in the evaluation of gas phase reactive scattering using an IVR semi-classical representation of Møeller wave operators. One general improvement in these IVR calculations was the evaluation of the monodromy matrix via direct integration along the classical trajectory using the unitary property of the matrix. This permitted the matrix to be evaluated over long periods of time both efficiently and accurately. The approach worked well for simple problems, the Eckart barrier and collinear $H + H_2$. However, the number of classical trajectories required for convergence was large. In the case of 3-d reactive scattering, the convergence with number of trajectories was quite slow, requiring 10^4 to 10^5 trajectories for marginal convergence. We are still considering variations which will permit more complete cancellation of the oscillations of the integrand and thus more rapid convergence.

C. Random Gaussian Bases

All quantum dynamical calculations of molecular vibrations, chemical reactions, etc. require a representation of the Hamiltonian describing the quantum system. As noted in the introduction DVR's are widely used for direct product representations for systems of up to six degrees of freedom (tetra-atomic systems). (See our recent review article for a discussion of multi-dimensional direct product bases, including DVR's [30]). However, the size of "primitive" direct product bases must scale exponentially with dimension since a separate basis is required for each dimension. Truncation of the DVR's to energies below some cut-off reduces the size considerably but adds complexity and errors of uncertain magnitude. Since DVR basis sizes scale roughly as $N_{basis} \simeq n^d$ with d = dimension and n $\sim$ 10 or more, there appears to be a practical limit of 4 atoms for calculation of large amplitude motions (5 atoms implies d = 9, $N_{basis} \sim 10^9$).

Many years ago we [31] demonstrated on simple one and two dimensional problems that distributed Gaussian bases (DGB's) were efficient and accurate. They are still used for some problems [32]. However, since optimization seemed difficult for multi-dimensional problems and there are concerns over linear dependence, the basis has not been widely studied as is the case for DVR's for example. However, DGB's are multidimensional basis functions and may offer much better scaling with dimension than DVR's.

We have thus examined the possibility of using *localized correlated* basis sets which combine the advantage of easy evaluation of potential and kinetic energy matrix elements with tailoring to the multi-dimensional potential. The basis of choice appears to be multi-dimensional distributed Gaussian basis functions (DGHB's) perhaps combined with very low order polynomials which borders on linear dependence!

We have determined that very efficient DGB's can be easily obtained for the distance coordinates in multidimensional problems and are easily combined with DVR's in angles as suggested much earlier [33]. However the Gaussian distribution and exponents are now chosen to yield much more efficient bases. A maximum desired energy, E_{max} leads to a local maximum desired kinetic energy, $T_{max,i}$ = (E_{max} - $V(\mathbf{r}_i)$). Simple arguments show that the Gaussian exponents must be proportional to $T_{max,i}$, and the density of Gaussian centers proportional to the square root of the inverse of $T_{max,i}$. The latter is accomplished by testing coordinate points chosen from Sobol sequence(s) and rejecting with a Monte Carlo procedure based on the desired local density. After the positions of the desired number of Gaussians are fixed, all the (different) exponents are scaled by a given factor to reduce the condition number of the overlap matrix to between 10^{-9} - 10^{-12}, a value which yields excellent accuracy of all states below E_{max} for an adequate number of basis functions. The number of basis

functions required is remarkably small, about 2^d times the number of accurate eigenvalues desired (5 or more significant figures). This approach has just been tested on the water molecule for which all 250 or so levels up to about 25000 cm^{-1} were obtained to about 0.1 cm^{-1} accuracy from a 3-D basis (2-d DGB, 1-d DVR) of less than 2500 functions. A single diagonalization/truncation step but no symmetrization was used.

This research is continuing, in particular with respect to optimizing localized bases for angular coordinates which now represent one bottleneck in calculations on larger systems. This approach has significant implications for quantum dynamic calculations using L^2 approaches and may be used with iterative approaches as well as standard diagonalization methods.

---

[1] J. V. Lill, G. A. Parker, and J. C. Light, Chem. Phys. Lett. **89**, 483 (1982).
[2] J. C. Light, R. M. Whitnell, T. J. Park, and S. E. Choi, in *Supercomputer Algorithms fo Reactivity, Dynamics and Kinetics of Small Molecules*, edited by A. Lagana (Kluwer, Dortdrecht, 1989), Vol. 277, pp. 187–214, nATO ASI Series C.
[3] Z. Bacic and J. C. Light, J. Chem. Phys. **85**, 4594 (1986).
[4] R. M. Whitnell and J. C. Light, J. Chem. Phys. **89**, 3674 (1988).
[5] W. H. Miller and B. J. op de Haar, jcp **86**, 6213 (1987).
[6] T. Seideman and W. H. Miller, J. Chem. Phys. **96**, 4412 (1992).
[7] J. Z. H. Zhang *et al.*, J. Chem. Phys. **88**, 2492 (1988).
[8] W. H. Miller, J. Chem. Phys. **61**, 1823 (1974).
[9] W. H. Miller, S. D. Schwartz, and J. W. Tromp, J. Chem. Phys. **79**, 4889 (1983).
[10] R. Kosloff, J. Phys. Chem. **92**, 2087 (1988).
[11] D. J. Kouri and R. C. Mowrey, J. Chem. Phys. **86**, 2087 (1987).
[12] D. H. Zhang and J. Z. H. Zhang, J. Chem. Phys. **101**, 3671 (1994).
[13] D. Neuhauser and M. Baer, J. Chem. Phys. **90**, 4351 (1989).
[14] H. W. Jang and J. C. Light, J. Chem. Phys. **99**, 1057 (1993).
[15] H. W. Jang and J. C. Light, J. Chem. Phys. **102**, 3262 (1995).
[16] H. W. Jang and J. C. Light, Chem. Phys. Lett. **242**, 62 (1995).
[17] G. S. Whittier and J. C. Light, J. Chem. Phys. **107**, 1816 (1997).
[18] G. S. Whittier and J. C. Light, J. Chem. Phys. **110**, 4280 (1999).
[19] D. H. Zhang and J. C. Light, J. Chem. Phys. **104**, 4544 (1996).
[20] D. H. Zhang and J. Z. H. Zhang, J. Chem. Phys. **99**, 5615 (1993).
[21] D. H. Zhang and J. C. Light, J. Chem. Phys. **105**, 1291 (1996).
[22] D. H. Zhang and J. C. Light, J. Chem. Soc. Farad. Trans. **93**, 691 (1997).
[23] D. H. Zhang and J. C. Light, J. Chem. Phys. **104**, 6184 (1996).
[24] D. H. Zhang and J. C. Light, J. Chem. Phys. **106**, 551 (1997).
[25] J. C. Light and D. H. Zhang, Faraday Discuss. **110**, 105 (1998).
[26] D. H. Zhang, J. C. Light, and S. Y. Lee, J. Chem. Phys. **111**, 5741 (1999).
[27] V. Mandelshtam, J. Chem. Phys. **108**, 9999 (1998).
[28] K. Thompson and N. Makri, J. Chem. Phys. **110**, 1343 (1999).
[29] H. Wang, M. Thoss, and W. H. Miller, J. Chem. Phys. **112**, 47 (2000).
[30] J. C. Light and T. Carrington, Jr., Adv. Chem. Phys. ((In Press)).
[31] I. P. Hamilton and J. C. Light, J. Chem. Phys. **84**, 306 (1986).
[32] S. Schmatz and M. Mladenovic, Phys. Chem. Chem. Phys. **101**, 372 (1997).
[33] Z. Bacic and J. C. Light, Ann. Rev. Phys. Chem. **40**, 469 (1989).

 # DOE supported publications, 1998-2000

See above References # 18, 25, 26, and 30.

Kinetics of Elementary Processes Relevant to Incipient Soot Formation

M. C. Lin
Department of Chemistry
Emory University
Atlanta, GA 30322
chemmcl@emory.edu

I. Program Scope

Soot formation and abatement processes are some of the most important and challenging problems in hydrocarbon combustion. The key reactions involved in the formation of polycyclic aromatic hydrocarbons (PAH's), the precursors to soot, remain elusive. Small aromatic species such as C_5H_5, C_6H_6 and their derivatives are believed to play a pivotal role in incipient soot formation.

The goal of this project is to establish a kinetic database for elementary reactions relevant to soot formation in its incipient stages. In the past year, our major focus has been placed on the experimental studies on several metathetical reactions of C_6H_5 with primary and tertiary alkanes and small aromatic hydrocarbons and a computational study on the unimolecular decomposition of C_6H_6.

II. Recent Progress

A Experimental studies

We have developed three complementary methods for determination of the kinetics and mechanisms for C_6H_5 reactions with combustion species, including small alkanes, CO, CH_2O and small aromatics. Combination of these methods: CRDS, P/FTIR and PLP/MS, allows us to cover a broad temperature range, 300 - 1000 K. The results of our studies are briefly summarized below.

1. $C_6H_5 + C_2H_6$ and *neo*-C_5H_{12}

The rate constants for the $C_6H_5 + C_2H_6/neo\text{-}C_5H_{12} \rightarrow C_6H_6 + C_2H_5/neo\text{-}C_5H_{11}$ reactions have been measured by PLP/MS experiments in the temperature range of 583-1003 K.[1] The purpose of this study lies in the establishment of the rate constant for the C_6H_5 attack at primary C-H bonds (p-CH) of larger alkanes. As employed for the $C_6H_5 + H_2/CH_4$ reactions,[2,3] the C_6H_5 radical was generated by the photolysis of $C_6H_5COCH_3$ at 193 nm, the reaction rates were determined by the kinetic modeling of the absolute yields of C_6H_6 and $C_6H_5CH_3$ products. The results can be represented by k (C_2H_6) = $10^{11.28 \pm 0.05}$ exp [(-2185 ± 80)/T] ; k (C_5H_{12}) = $10^{11.34 \pm 0.05}$ exp[(-1884 ± 88)/T] cm^3 mol^{-1} s^{-1}. These two sets of data give the primary C-H rate constant per bond, k (p-CH) = $10^{10.40 \pm 0.06}$ exp[(-1790±102)/T) cm^3 mol^{-1} s^{-1}, which convolutes all errors from the individual experiments.

2. $C_6H_5 + i\text{-}C_4H_{10}$, $(CH_3)_2CHCH(CH_3)_2$ and $(CH_3)_2CHCH(CH_3)CH(CH_3)_2$

The kinetics of the C_6H_5 reaction with i-C_4H_{10} has been measured by CRDS and PLP/MS covering the temperature range 290 – 1000 K.[4] Combination of these two sets of data gives k (C_4H_{10}) = $10^{11.45 \pm 0.10}$ exp [(-1512 ± 44)/T] cm^3 mol^{-1} s^{-1}. The good agreement between the results obtained by the two different methods provides a strong support for the reliability of the PLP/MS technique as has been demonstrated by our previous study on the $C_6H_5 + H_2/CH_4$ reactions. Similar measurements by CRDS for 2,3-dimethyl butane (C_6H_{14}) and 2,3,4-trimethyl pentane (C_8H_{18}) at temperatures between 290 and 500 K gave k (C_6H_{14}) = $10^{11.72 \pm 0.75}$ exp[(-1007 ± 124)/T] and k (C_8H_{18}) = $10^{11.83 \pm 0.13}$ exp[(-428 ± 108)/T] cm^3 mol^{-1} s^{-1}. It should be pointed out that these three sets of kinetic data, after subtracting the primary C-H contributions with the k (p-CH) equation given above, lead to 3 distinct rate constants per t-CH bond from C_4H_{10} to C_8H_{18}, with decreasing A-factors and temperature coefficients and increasing absolute values.

3. $C_6H_5 + CO \rightarrow C_6H_5CO$

The kinetics of the C_6H_5 reaction with CO has been studied by the CRDS technique in the temperature range 295-500 K at 12-120 Torr pressure using Ar as the carrier gas.[5] The reaction was found to occur near the high-pressure limit above 40 Torr. A weighted least-squares analysis of all data gives the rate constant for the association reaction, $k = 10^{11.93\pm0.14}$ exp[-(1507 ± 109)/T] $cm^3 mol^{-1} s^{-1}$. Our result can be satisfactorily correlated with the kinetic data reported by Solly and Benson for the reverse process[6] with the RRKM theory using the transition-state parameters computed quantum mechanically by the MP2 method with the 6-31G(d,p) basis set.

Combination of the forward and reverse reaction data gives ΔH_6° = -24.6 ± 0.8 kcal/mol at 0 K and $k_6^\infty = 5.3 \times 10^{14}$ exp(-14,600/T) s^{-1} for the temperature range 300 - 670 K. The heat of reaction, combining with the known heats of formation the reactants, leads to $\Delta_f H_0^\circ(C_6H_5CO)$ = 32.5 ± 1.5 kcal/mol, which agrees reasonably with existing values within the error limits, ± 3 kcal/mol.[7,8]

4. $C_6H_5 + CH_2O \rightarrow$ products

The kinetics and mechanism for the $C_6H_5 + CH_2O$ reaction was investigated by CRDS and PLP/MS methods at temperatures between 298 and 1083 K.[9] With the CRDS method, the rate constant was measured by monitoring the decay of C_6H_5, whereas in the PLP/MS experiment at higher temperatures, the rate constant was determined by kinetic modeling of the absolute yields of C_6H_6. The values of the rate constants obtained by the two different methods agree closely, suggesting that the abstraction reaction, $C_6H_5 + CH_2O \rightarrow C_6H_6 + CHO$, is the dominant channel.

A weighted least-squares analysis of the two sets of data gave $k = (8.55 \pm 0.25) \times 10^4 T^{2.19\pm0.25} \times$ exp[-(19±13)/T] $cm^3 mol^{-1} s^{-1}$ for the temperature range studied. The mechanism for the $C_6H_5 + CH_2O$ reaction has been elucidated with a quantum-chemical calculation employing a hybrid density functional theory using the augmented correlation consistent aug-cc-PVTZ basis set. The theory predicts the barriers for the abstraction producing C_6H_6 and the addition giving $C_6H_5CH_2O$ and $C_6H_5OCH_2$ to be 0.8, 1.4 and 9.1 kcal/mol, respectively. The rate constant calculated for the H-abstraction process, using the 0.8 kcal/mol barrier with a small tunneling correction, agrees closely with the experimental result.

5. $C_6H_5 + C_6H_6 \rightarrow C_6H_5C_6H_6 \rightarrow C_{12}H_{10} + H$

The absolute rate constants for the $C_6H_5 + C_6H_6$ and C_6D_6 reactions have been measured by CRDS at temperatures between 298 and 495 K at a constant 40-Torr Ar pressure.[10] These results, which reveal no detectable kinetic isotope effect, can be represented by the equation, $k = 10^{11.91\pm0.13}$ exp [-(2102 ± 106)/T] $cm^3 mol^{-1} s^{-1}$. Our low-temperature data for the addition/stabilization process, $C_6H_5 + C_6H_6 \rightarrow C_{12}H_{11}$, can be correlated with those obtained in a low-pressure, high-temperature Knudsen cell study for the addition/displacement reaction,[11,12] $C_6H_5 + C_6H_6 \rightarrow C_{12}H_{10} + H$, by the RRKM theory using the molecular and transition-state parameters computed at the B3LYP/6-311G(d,p) level of theory. Combination of the two sets of data gives $k = 10^{(11.98\pm0.03)}$ exp [-(2168 ± 34)/T] $cm^3 mol^{-1} s^{-1}$ covering the temperature range 298 - 1330 K.

The RRKM theory also correlates satisfactorily the forward reaction data with the high-temperature shock-tube result for the reverse H-for-C_6H_5 substitution process[13] with 2.7 and 4.7 kcal/mol barriers for the entrance ($C_6H_5 + C_6H_6$) and reverse ($H + C_{12}H_{10}$) reactions, respectively.

B. Computational Studies

1. $H + C_6H_5 \rightarrow$ products and related unimolecular decomposition of C_6H_6

In collaboration with the Institute of Atomic and Molecular Sciences in Taiwan, we have investigated the association of H with C_6H_5 and the decomposition of C_6H_6 in detail.[14] The potential energy surface of the system, including the direct abstraction of a hydrogen atom at the ortho, meta and para positions from the radical center, has been computed with the ab initio G2M(cc,MP2) method. The results show that, besides the direct emission of a hydrogen atom occurring without exit

barrier, benzene molecule can undergo sequential 1,2-hydrogen shifts to *o*-, *m*-, and *p*- C_6H_6, respectively, and then lose an H atom with exit barriers of about 6 kcal/mol. *o*-C_6H_6 can eliminate a hydrogen molecule with a barrier of 121.4 kcal/mol relative to benzene. *o*- and *m*- C_6H_6 can also isomerize to acyclic isomers, ac- C_6H_6, with barriers of 110.7 and 100.6 kcal/mol, respectively, but in order to form *m*- C_6H_6 from benzene the system has to overcome a barrier of 108.6 kcal/mol for the 1,2-H migration from *o*- C_6H_6 to *m*- C_6H_6.

The bimolecular H + C_6H_5 reaction is shown to be more complicated than the unimolecular fragmentation reaction due to the presence of various metathetical processes, such as H-atom abstraction or addition to different sites on the ring. The addition to the radical site is barrierless, the additions to the *o*-, *m*-, and *p*-positions have entrance barriers of about 6 kcal/mol and the abstraction channel leading to *o*-benzyne + H_2 has a barrier of 7.6 kcal/mol.

The RRKM and TST methods were used to compute the total and individual rate constants for various channels of the forward and reverse reactions under different temperature/pressure conditions. A fit of the calculated rate constant for the unimolecular benzene decomposition producing H + C_6H_5 with no coupling with the isomerization processes gave the first-order high-pressure rate constant, 8.43×10^{15} exp(-58710/T) s^{-1}, according to the result of our canonical variational RRKM calculation. However, convolution of all possible unimolecular processes gave the expression for the total rate constant for H-atom production, 3.22×10^{13} exp(-53440/T) s^{-1} for T = 1000-3000 K and atmospheric pressure, *which is significantly different from the rate constant recommended presently assuming only the H + C_6H_5 product channel, 9.0×10^{15} exp(-54060/T) s^{-1}.*[15] At T =1000 K, the branching ratio of the H + C_6H_5 products is 45%, and the reaction is dominated by benzene isomerization to *ac*- C_6H_6. The H + C_6H_5 become the major products at T $\geq$ 1200 K. The total rate for the bimolecular H + C_6H_5 reaction is predicted to be 1×10^{-10} cm^3 $molecule^{-1}$ s^{-1} for the broad range of temperatures (300-3000 K) and pressures (100 Torr - 10 atm), in close agreement with experiment.[16,17]

2. New mechanism for prompt NO formation

Recently we have investigated the reaction of CH radicals with N_2 in conjunction with our study of azide polymer combustion reactions.[18] The result of our extensive ab initio MO calculation on this important "**prompt NO**" precursor process at the G2M(RCC)//B3LYP/6-311G(d,p) level of theory reveals that the CH + N_2 reaction produces primarily the spin-allowed H + NCN, instead of the long assumed spin-forbidden HCN + N products, originally proposed by Fenimore in 1971.[19] In a recent comprehensive calculation by Cui, Morokuma, Bowman and Klippenstein[20], the rate constant for the HCN + N production was predicted to be two orders of magnitude smaller than the high-temperature shock-tube results of Hanson, Bowman, Roth and their cowerkers,[21,22] contrary to the earlier conclusion of Miller and Walch[23] who did not consider the detrimental effect of surface crossing associated with the spin change.

The results of our multi-channel RRKM calculation for the production of NCN over the spin-conserved ground electronic doublet surface gave quantitative agreement with the high-temperature shock-tube data obtained by monitoring CH decay[21] or N-atom production.[22] The prompt NO is believed to be formed by the facile, exothermic oxidation of NCN by O_x and HO_x (x = 1,2). Kinetic studies of NCN reactions will be carried out theoretically and experimentally. The reason that the NCN production rate constant is greater than that for HCN production is readily understandable. First of all, the spin change associated with the latter channel reduces the transmission probability; secondly, the transition state leading to the production of HCN + N is tighter and also energetically higher than H + NCN, which are formed barrierlessly via a loose transition state.

III. Future Plans

In the next year, we will continue the acquisition of kinetic data for C_6H_5 reactions by CRDS and PLP/MS techniques to determine the reactivity of the phenyl toward s-CH bonds and larger aromatics such as styrene and phenyl acetylene. Computationally, we will carry out high-level *ab initio* MO

calculations to improve our predictive capability for the rate constants and product branching ratios of C_6H_5 reactions with C_2H_2, C_2H_4 and O_2. We also plan to extend the calculations to include the reactions of phenylvinyl radical with C_2H_2 and phenyl acetylene at a lower level of theory.

IV. References (DOE publications, 1998-present, denoted by #)

1. # J. Park, S. I. Gheyas, M. C. Lin, "Kinetics of the $C_6H_5 + C_2H_6$/*neo*-C_5H_{12} Reactions", *Int. J. Chem. Kinet.*, submitted.
2. J. Park, I. V. Dyakov, and M. C. Lin., *J. Phys. Chem.* A, **101**, 8839 (1997).
3. # I. V. Tokmakov, J. Park, S. Gheyas and M. C. Lin, *J. Phys. Chem. A* **103,** 3636-3645 (1999).
4. # J. Park, S. I. Gheyas and M. C. Lin, *Int. J. Chem. Kinet.* **31**, 645 (1999).
5. # Gi-Jung Nam, W. Xia, J. Park and M. C. Lin, *J. Phys. Chem.* A, **104**, 1233 (2000).
6. R. K. Solly, S. W. Benson, S. W. *J. Am. Chem. Soc.* **93,** 2127 (1971).
7. H. Q. Zhao, Y. S. Cheung, C. L. Liao, C. Y. Ng, and W. K. Li, J. Chem. Phys., **107**, 7230 (1997).
8. J. A. M. Semoes and D. Griller, Chem. Phys. Lett., **158**, 175 (1989).
9. # Y. M. Choi, Wensheng Xia, J. Park and M. C. Lin, "Kinetics and Mechanism for the Reaction of Phenyl Radical with Formaldehyde", JPC, submitted.
10. # J. Park, S. Burova, A. S. Rodgers and M. C. Lin, *J. Phys. A,* **103**, 9036 (1999).
11. A. Fahr, .S. E. Stein,. *Twenty-Second Symposium (International) on Combustion*; The Combustion Institute; Pittsburgh, PA, 1989; p 1023.
12. A. Fahr, W. G. Mallard, W. E. Stein, *Twenty-First Symposium (International) on Combustion*; The Combustion Institute; Pittsburgh, PA, 1988, p 825.
13. J. A. Manion, W. Tsang, Proceedings of Chemical and Physical Processes in Combustion, 1996 Fall Technical Meeting, p. 527.
14. # A. M. Mebel, M. C. Lin, D. Chakraborty, J. Park, S. H. Lin and Y. T. Lee, "Ab Initio and RRKM Study of Multichannel Rate Constants for the H + C_6H_5 Reaction and the Unimolecular Decomposition of Benzene," *J. Am. Chem. Soc.* submitted.
15. D. L. Baulch, C. J. Cobos, R. A. Cox, C. Esser, P. Frank, Th. Just, J. A. Kerr, Pilling, J. Troe, R. W. Walker, J. Warnatz, *J. Phys. Chem. Ref. Data* **21**, 411-429 (1992)
16. L. Ackermann, H. Hippler, P. Pagsberg, C. Reihs, J. Troe, *J. Phys. Chem.* **94**, 5247 (1990)
17. M.Braun-Unkhoff, P. Frank, Th. Just, *22th Symp. Int. Combust.* Proc. 1053 (1989)
18. # L. V. Moskaleva and M. C. Lin, "The Spin-Conserved Reaction CH + N_2 $\longrightarrow$ H + NCN: A Major Pathway to Prompt NO Studied by Quantum/Statistical Theory Calculations and Kinetic Modeling of Rate Constant" *28th Symposium (Int'l) on Combustion*, submitted.
19. C. P. Fenimore, *13th Symp. (Int.) Combust. Proc.* 1971, pp. 373-79.
20. Q. Cui, K. Morokuma, J. M. Bowman and S. Klippenstein, *J. Chem. Phys.* **110**, 9469, (1999).
21. A. J. Dean, R. K. Hanson, C. T. Bowman, *23th Symp. (Int.) Combust. Proc.,* 1991, p. 259.
22. D. Lindackers, M. Burmeister, P. Roth, *23th Symp. (Int.) Combust. Proc.,* 1991, p. 251.
23. J. A. Miller, S. P. Walch, *Int. J. Chem. Kinet.* **29**, 253-259 (1996).

Other DOE Publications Not Cited in the Text:

1. A. M. Mebel, L. V. Moskaleva, and M. C. Lin, NH_2 Reactions in the Gas Phase, *in N-Centered Radicals,* Z. B. Alfassi, ed., pp. 467-514, John Wiley and Sons, N. Y., 1998.
2. A. M. Mebel, L. V. Moskaleva and M. C. Lin, *J. Mol. Struct.* (THEOCHEM), **461/462**, 223 (1999).
3. A. M. Mebel and M. C. Lin, *J. Phys. Chem. A* **103,** 2088 (1999).
4. L. V. Moskaleva and M. C. Lin, *PCCP*, **1**, 3967 (1999).
5. L. V. Moskaleva and M. C. Lin, *J. Phys. Chem. A* **102**, 4687 (1998).
6. J. Park and M. C. Lin "Kinetic Studies of Aromatic Radical Reactions by Cavity Ringdown Spectrometry" *in Cavity-Ring-Down Spectrometry-A New Technique for Trace Absorption Measurements*, ACS Publication Series **720**, Chap. 13, 196 (1999).
7. J. Park and M. C. Lin, *Recent Res. Develop. in Phys. Chem.*, Transworld Research Network, **2**, 965 (1998).
8. M. D. Brioukov, J. Park and M. C. Lin, *Int. J. Chem. Kinet.* **31**, 577 (1999)
9. I. V. Tokmakov, J. Park, S. Gheyas and M. C. Lin, *J. Phys. Chem. A* **103,** 3636 (1999).
10. J. Park, D. Chakraborty, D. M. Bhusari and M. C. Lin, *J. Phys. Chem. A.* **103,** 4002 (1999).
11. L. V. Moskaleva and M. C. Lin, "Unimolecular Isomerization/Decomposition of Cyclopentadienyl and Related Bimolecular Reverse Process: Ab Initio MO/Statistical Theory Study" *J. Comput. Chem.* in press.

INVESTIGATION OF POLARIZATION SPECTROSCOPY AND DEGENERATE FOUR-WAVE MIXING FOR QUANTITATIVE CONCENTRATION MEASUREMENTS

Principal Investigator: Robert P. Lucht
Graduate Students Supported: Sherif Hanna and Sukesh Roy
Department of Mechanical Engineering, Texas A&M University, Mail Stop 3123, College Station, TX 77843-3123 (rlucht@tamu.edu)

I. PROGRAM SCOPE

Degenerate four-wave mixing (DFWM) and polarization spectroscopy (PS) are techniques that show great promise for sensitive measurements of transient gas-phase species, and diagnostic applications of these techniques are being pursued actively at laboratories throughout the world. However, significant questions remain regarding strategies for quantitative concentration measurements using DFWM and polarization spectroscopy. The objective of this research program is to develop and test strategies for quantitative concentration measurements in flames. We are investigating the physics of these processes by direct numerical integration (DNI) of the time-dependent density matrix equations that describe the resonant interaction. Significantly fewer restrictive assumptions are required using this DNI approach compared with the assumptions required to obtain analytical solutions. A very significant accomplishment over the last couple of years has been the incorporation of the Zeeman state structure of the laser-coupled rotational levels into our computational analysis. In addition, we have now successfully incorporated the multi-axial-mode laser structure that is characteristic of commercial dye lasers into our polarization spectroscopy calculations.

II. RECENT PROGRESS

A. Picosecond Polarization Spectroscopy

The potential advantages of short-pulse laser excitation for reducing or eliminating the effects of collisions in laser diagnostic measurements in combustion have long been recognized. However, the lack of reliable and affordable tunable laser sources with pulse lengths on the order of 10-100 psec has hindered the development of picosecond-laser-based diagnostic techniques. A laser with a nominal pulse length of 10-100 psec is ideal for diagnostics of atmospheric pressure flames because the laser pulse length is shorter than the characteristic collisional times in the medium. In addition, the nominal laser bandwidth (Fourier transform limit) of 1.5 to 0.15 cm^{-1} is low enough that the laser radiation can couple efficiently with molecular resonances. Recently a tunable distributed-feedback dye laser (DFDL) system with pulse lengths on the order of 100 psec and a near-Fourier transform-limited bandwidth has been developed at Sandia National Laboratories.[1] The tuning of the DFDL laser is computer-controlled and the wavelength of the laser is feedback-stabilized to within 0.02 cm^{-1}, allowing the laser wavelength to be scanned over resonance lines or placed accurately at line center. Frequency-doubling of the DFDL is very efficient because of the high peak powers resulting from the short pulse length.

During a visit to the Combustion Research Facility at Sandia National Laboratories during the summer of 1999, the potential of short-pulse polarization spectroscopy for quantitative concentration measurements was investigated.[2] PS signal intensities from the $P_1(2)$ rotational transition in the (0,0) band of the $A^2\Sigma^+ - X^2\Pi$ electronic transition of OH were measured at in a room-temperature H_2O_2 photolysis cell[3] at room temperature for pressures ranging from 10 to 500 Torr. The results of these measurements are shown in Fig. 1. The ratio of the PS signal to the OH concentration dropped by only about a factor of three for the high intensity PS measurements; the low-intensity PS measurements also showed a dependence on collisional rates that was much less than would have been expected for nanosecond laser excitation.

The DNI numerical methodology that we have developed over the last few years is particularly well-suited for the investigation of the physics of picosecond-laser-based diagnostic techniques. We have incorporated the Zeeman state structure of the resonances into our calculations. Using our DNI numerical

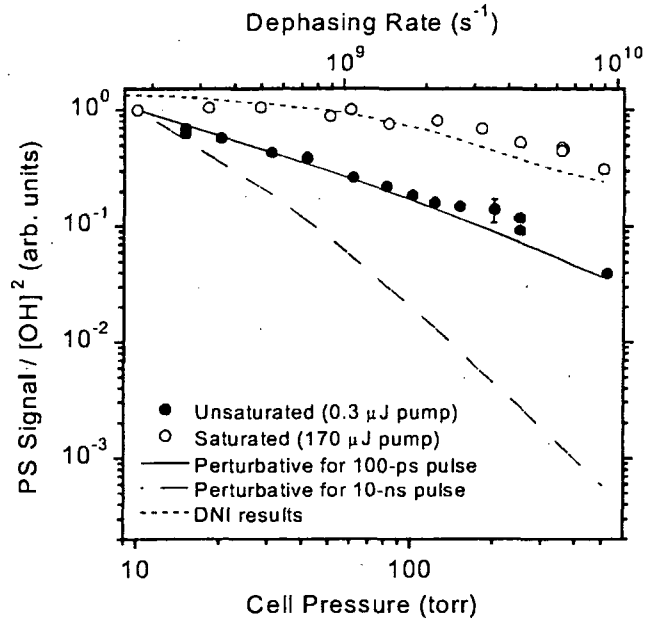

Fig. 1. Dependence of the ratio of the PS signal to the square of the number density of OH from the H_2O_2-photolysis experiments of Reichardt et al.[2] The DNI results are indicated by the short-dashed line.

methodology we can investigate the laser excitation dynamics in detail by examining the temporal dependence of the Zeeman populations and the induced coherences for the allowed Zeeman transitions. The picosecond PS calculations are performed with a modified version of our DFWM code[4] rather than with our previous PS code.[5] As pointed out by Suvernev et al.,[6] PS can be regarded as a special case of DFWM where the resonance interacts with the pump beam twice. The PS signal is calculated from the time-dependent third-order polarization rather than directly from the induced anisotropic absorption and phase shift terms as in Reichardt and Lucht.[5] This is necessary in general for picosecond pulses because the system is so far from steady state and in some cases most of the PS signal will be generated after the pump and probe beams have passed through the probe volume. The results of DNI calculations of the pressure dependence of the OH PS signal in the photolysis cell are shown in Fig. 1.

As an example of detailed information that can be obtained from the DNI analysis, the PS signal pulses and the temporal dependence of the upper energy level population (sum over all Zeeman states) are shown in Fig. 3 for low- and high-intensity excitation of the $P_1(2)$ resonance for a 100-psec laser pulse. For both low- and high-intensity excitation most of the signal pulse is generated after the pump and probe pulses have passed through the medium. Rabi beating is evident for the high-intensity case.

B. Multi-Axial-Mode Effects in Polarization Spectroscopy

The effects of multi-frequency-mode laser radiation on polarization spectroscopy signal generation were investigated by direct numerical integration of the time-dependent density matrix equations.[7] The numerical solution of the density matrix equations allows us to incorporate a physically reasonable model for a pulsed dye laser radiation in our analysis of the laser-resonance interaction. The inclusion of the multi-mode laser structure into our density matrix equations represents a significant advance in modeling the nonlinear interaction of laser radiation with atomic or molecular resonances. The laser radiation is modeled as the sum of electric fields from a finite number of modes that are assumed to have random pulse-to-pulse phases. The effect of the multi-mode laser radiation on polarization spectroscopy line shapes and saturation curves was investigated parametrically for different values of the laser bandwidth and mode spacing and resonance collision and Doppler widths.

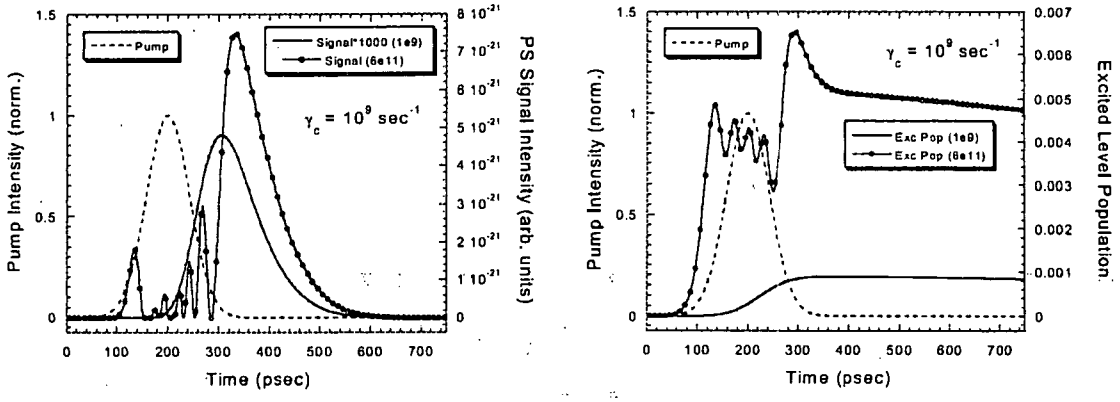

Fig. 2. Temporal structure of the PS signal pulses (left) and of the upper laser-coupled-level population (right) are shown for low-intensity (10^9 W/m^2) and high-intensity ($6x10^{11}$ W/m^2) pump pulses. The probe intensity is 1% of the pump intensity and the dephasing rate is 10^9 sec^{-1}.

The effect of the ratio of the laser linewidth and the homogeneous (collisional) linewidth on the saturation behavior and noise statistics of a homogeneously broadened PS resonance is shown in Fig. 3. When the laser linewidth is greater than the collisional linewidth, the effective saturation intensity for the resonance increases and the pulse-to-pulse fluctuations in PS signal intensity are much higher than for the case where the laser and collisional widths are comparable. For the case where $\Delta\omega_C = 0.01$ cm^{-1}, ten times less than the laser linewidth, the fluctuations are huge and the single-pulse signal levels are always less for the multi-mode case than for the single-mode case. When the collisional linewidth is significantly greater than the multi-mode laser linewidth, the single-pulse multi-mode PS signal levels are always greater than the single-mode PS signal levels; the resonance can respond to even the fastest fluctuations in the laser intensity, and the PS signal is enhanced by the multi-mode intensity spiking.

III. FUTURE WORK

Our investigation of the physics of picosecond PS will continue; the reduced dependence of the picosecond PS signal on collision rate for both low and high laser intensities is very encouraging. Theoretical work on the effect of multi-axial-mode structure on PS signal generation will also continue. The experimental systems that were used for PS and DFWM measurements at the University of Illinois have been transferred and are now in operation at Texas A&M University. We will perform PS measurements in low-pressure flames for comparison with the multi-mode calculations and investigate the potential of two-color PS for sensitive concentration measurements. The generation of DFWM signals from molecules with anisotropic Zeeman state distributions[8] will be investigated theoretically.

IV. REFERENCES

1. P. P. Yaney, D. A. V. Kliner, and R. L. Farrow, Rev. Sci. Instr., accepted for publication (2000).
2. T. A. Reichardt, F. Di Teodoro R. L. Farrow, S. Roy, and R. P. Lucht, J. Chem. Phys., submitted (2000).
3. D. A. V. Kliner and R. L. Farrow, J. Chem. Phys. **110**, 412-422 (1999).
4. T. A. Reichardt and R. P. Lucht, J. Chem. Phys. **111**, 10008-10020 (1999).
5. T. A. Reichardt and R. P. Lucht, J. Chem. Phys. **109**, 5830-5843 (1998).
6. S. S. Suvernev, R. Tadday, and T. Dreier Phys. Rev. A **58**, 4102-4115 (1998).
7. W. C. Giancola, T. A. Reichardt, and R. P. Lucht, J. Opt. Soc. Am. B, submitted (2000).
8. T. Müller, T. A. W. Wasserman, P. H. Vaccaro, and B. R. Johnson **108**, 7713-7738 (1998).

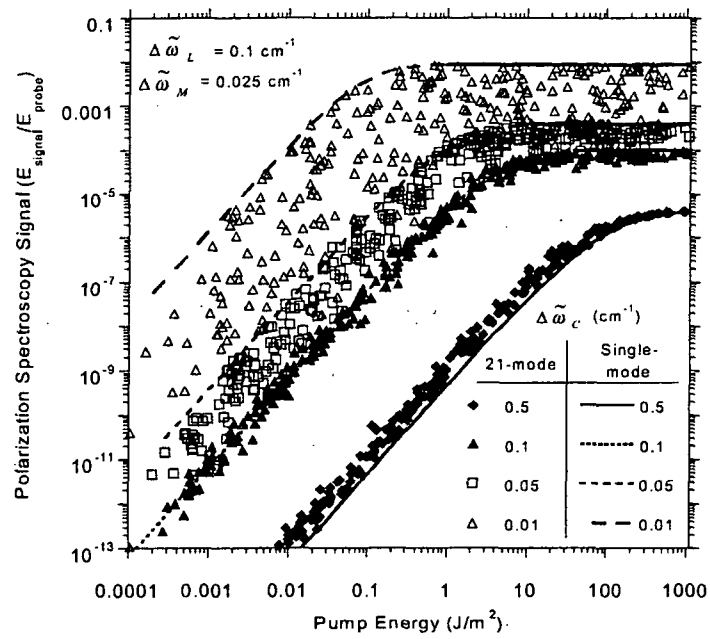

Fig. 3. PS saturation curves for the $P_1(2)$ resonance for a laser linewidth of 0.1 cm^{-1} and different values of the collisional linewidth.

V. BES-SUPPORTED PUBLICATIONS 1998-2000

1. T. A. Reichardt and R. P. Lucht, "Theoretical Calculation of Lineshapes and Saturation Effects in Polarization Spectroscopy," J. Chem. Phys. **109**, 5830-5843 (1998).
2. T. A. Reichardt and R. P. Lucht, "Investigation of the Forward Phase-Matched Geometry for Degenerate Four-Wave Mixing Spectroscopy," J. Opt. Soc. Am. B **15**, 2566-2572 (1998).
3. T. A. Reichardt and R. P. Lucht, "Resonant Degenerate Four-Wave Mixing Spectroscopy of Transitions with Degenerate Energy Levels: Saturation and Polarization Effects," J. Chem. Phys. **111**, 10008-10020 (1999).
4. T. A. Reichardt, W. C. Giancola, C. M. Shappert, and R. P. Lucht, "Experimental Investigation of Saturated Degenerate Four-Wave Mixing for Quantitative Concentration Measurements," Appl. Opt. **38**, 6951-6961 (1999).
5. T. A. Reichardt, W. C. Giancola, and R. P. Lucht, "Experimental Investigation of Saturated Polarization Spectroscopy for Quantitative Concentration Measurements," Appl. Opt., accepted for publication, to appear in April 20 issue (2000).
6. W. C. Giancola, T. A. Reichardt, and R. P. Lucht, "Multi-Axial-Mode Laser Effects in Polarization Spectroscopy," J. Opt. Soc. Am. B, submitted for publication (2000).
7. T. A. Reichardt, F. Di Teodoro R. L. Farrow, S. Roy, and R. P. Lucht, "Collisional Dependence of Polarization Spectroscopy with a Picosecond Laser," J. Chem. Phys., submitted for publication (2000).

VI. GRADUATE DISSERTATIONS RESULTING FROM DOE/BES SUPPORT 1998-2000

1. Thomas A. Reichardt, "Investigation of Degenerate Four-Wave Mixing and Polarization Spectroscopy for Quantitative Measurements in Combustion Environments," Ph.D. Thesis, University of Illinois at Urbana/Champaign (1999).
2. William C. Giancola, "Theoretical Investigation of Polarization Spectroscopy in Multi-Axial-Mode Fields," M.S. Thesis, University of Illinois at Urbana/Champaign (1999).

Time-Resolved Infrared Absorption Studies of the Dynamics of Radical Reactions

R. G. Macdonald
Chemistry Division
Argonne National Laboratory
Argonne, IL 60439
Email: macdonald@anlchm.chm.anl.gov

Background

There is very little information available about the dynamics of radical+radical interactions. These processes are important in combustion being chain termination steps as well as generating new molecular species. To study these processes, a new experimental apparatus has been constructed to investigate radical-radical dynamics. The first radical or atomic species is produced with a known concentration in a microwave discharge flow system. The second is produced by pulsed laser photolysis of a suitable photolyte. The time dependence of individual rovibrational states of the product is followed by absorption of a continuous infrared laser. This approach will allow the reaction of interest to be differentiated from other radical reactions occurring simultaneously. The experimental approach is highly versatile, being able to detect a number of molecular species of particular interest to combustion processes such as water, methane, acetylene etc. at the state specific level. State specific infrared absorption coefficients of radicals can be measured in situ allowing for the determination of the absolute concentrations, and hence branching ratios for reactions having multiple reaction pathways.

Recent Results

Over the past several years an investigation into the detailed dynamics of a family of reactions involving translationally energetic H atoms with CN containing compounds has been initiated. The reactions under investigation have been

$$\begin{aligned} H + XCN &\rightarrow HNC + X && 1(a) \\ &\rightarrow HCN + X && 1(b) \\ &\rightarrow HX + CN && 1(c) \end{aligned}$$

where X is Cl, Br or CN. This series of reactions illustrates the rapid increase in the complexity of the reaction dynamics as one goes from the study of atom + diatom systems into reactions leading to polyatomic products. One of the most intriguing aspects of these systems is the possibility of multiple product channels, as illustrated by reaction 1. The potential energy surfaces governing such reaction systems are very complicated involving multiple minima and transition states, for example, Harding[1] has characterized the energetics and geometries of 14 minima and 9 transition states for the HClCN four atom system. As a first step in characterizing the reaction dynamics of these systems, the determination of the branching ratios has been undertaken.

An important aspect of determining branching ratios for radical-radical or radical-molecule reactions is the need for the measurement of absolute concentrations of radicals

or transient species and stable molecules, and a great deal of effort has been made to measure the transition moments for the various transient species involved in these reaction systems, i.e. Br, CN and HNC. The use of time-resolved infrared absorption spectroscopy is a highly versatile method for carrying out such measurements, as is well demonstrated by this series of reactions. Four species Br, HNC, HCN and HCl were detected by tunable infrared laser radiation from a color center laser, and the fifth CN, detected using CN "red" system , $A\ ^2\Pi \leftarrow\ ^2\Sigma^+$ (2-0) band near 790 nm.

Hydrogen atoms with 22 kcal mol^{-1} translational energy were created by 248 nm photolysis of CH_3SH, and the concentration of the products from reaction 1 determined by time- and frequency- resolved absorption spectroscopy. The channels 1(a) and (b) can be considered to be addition of the H atom to the appropriate N or C atom followed by molecular elimination, while channel 1(c) arises from direct abstraction.

Previous determinations of the branching ratios for the various reaction systems relied on setting the probe laser at the line-center of a spectroscopic transition and recording the complete time profile of the species of interest. In the current experiments, a frequency scan of a spectral feature of the probed species was recorded at fixed times. The latter experiment eliminated uncertainties in finding the exact line center, and allowed for a more accurate determination of the species concentration. It was also found that the CN radical reacted with CH_3SH to produce HNC, and the branching fraction for the CN + $CH_3SH \rightarrow$ HCN/HNC + products reaction was measured. These new measurements confirm the earlier determination of the branching fractions for the H + XCN reaction systems. For H + BrCN and ClCN the HNC channel accounts for about 75% of the reaction product even though the HCN channel is 15 kcal mol^{-1} more exothermic; thus features of the potential energy surface and the dynamics rather than pure energetics dominate the outcome of a reactive encounter.

Another probe of the reaction dynamics for these systems comes from the determination of product state distributions for the various channels in reaction 1. In all three systems the CN bond behaves as a spectator bond. In the case of H + BrCN and ClCN, the CN radical product state distribution reflects the dynamics of the direct abstraction channel, and in the case of H + $(CN)_2$ the CN radical product state distribution reflects the dynamics of the dominant HCN + CN channel. The H + ClCN system, channel 1(c) has been studied previously,[2,3] using translationally energetic H atoms, and the CN(v,J) product state distribution measured by LIF detection. In the current experiment, the CN (v=0, J) product state distribution was determined for all three systems by time- and frequency-resolved absorption spectroscopy of CN(v=0,J) at 790 nm. The experiments were carried out under bulk conditions, but at low pressures and short delay times following the initiation of the reaction so that the products were measured under nearly collision-free conditions. An important aspect of these measurements was the determination of the product translational energy released in the probed reaction. Both the translational energy release and the CN(v=0, J) distribution provide information on the internal energy excitation in the unobserved product. The global dynamical features of these reactions are quite similar to those for the related three atom systems H + XY, where X and Y are halogen atoms. Furthermore, the absolute reaction cross section was also measured for each reaction channel.

For the H + $(CN)_2 \rightarrow$ HCN/HNC + CN reaction the HNC channel is endothermic by 1.5 kcal mol^{-1} assuming reaction with H atoms having 22 kcal mol^{-1} translational energy; thus only a few vibrational levels can be populated in the reaction. The HNC (v, J) product was probed by time- and frequency-resolved absorption spectroscopy and the

complete rotational state distribution was measured for HNC(00^00) and HNC(01^10). No other vibrational levels were detected so these measurements determine the vibrational state distribution as well. Again, the product translational energy was also determined. The fact that the HNC product is seen indicates that there is little or no activation energy above the reaction endothermicity. About 40% of the observed HNC molecules were in the HNC(01^10) bending vibration strongly indicating that the reaction proceeds through bent configurations. As well, a large fraction of the reaction exothermicity appeared as bending excitation, again indicating reaction proceeding through bent configurations. The global energy partitioning was found to be remarkably similar to that for the three atom H + Cl_2 system.

Future Work

For the H +$(CN)_2$ system, further work will be needed to be able to determine the complete HCN(v, J) product state distribution. The CN + CH_3SH reaction is gas kinetic so that improvements in the detection sensitivity will be necessary to detect the HCN produced in the H + $(CN)_2$ reaction without interference from the secondary reaction. Future effort will also be directed to determining some of the HNC(v, J) product state distributions from the H + ClCN reaction.

Effort is underway to study the CN + OH radical-radical reaction. Both species will be produced by cophotolysis of suitable precursor molecules, and the CN and OH species monitored simultaneously following the photolysis laser pulse. This radical-radical process is an attractive candidate for study because only a few electronic states are involved in the interaction, $^{1,3}A'$ and $^{1,3}A''$, and these should be amenable to theoretical calculations. There are four possible exothermic reaction channels leading to HNC + O, HCN +O, NCO + H and NH + CO, in increasing exothermicity. All except the NCO + H channel can be probed directly by the laser systems currently available. The absolute concentration of the reactants and the product channels are determined in the time- and frequency-resolved measurements so that the branching into the four channels can be determined.

References

1) L. B. Harding, J. Phys. Chem. **100**, 10123 (1996).
2) J. de Juan, S. Callister, H. Reisler, G. A. Seagull, and C. Wittig, J. Chem. Phys. **89**, 1977 (1988).
3) G. W. Johnston and R. Bersohn, J. Chem. Phys. **90**, 7096 (1989).

Publications 1998-2000.

The thermal rate constant for the CN + H_2/D_2 → HCN/DCN + H/D reaction from T =293 K to 380 K.
- G. He, I. Tokue, and R.G. Macdonald
J. Phys. Chem. A. 102, 4585-4591 (1998).

The initial vibrational level distribution of HCN $X^1\Sigma^+(v_1,0,v_3)$ in the CN($X,^2\Sigma$) + H_2 → HCN + H reaction system.
- G. A. Bethardy, F.J. Northrup, G. He, I. Tokue, and R. G. Macdonald
J. Chem. Phys. 109, 4224-4236 (1998).

The thermal rate constant and branching ratio for CN + HD → HCN/DCN + D/H reaction from T =293 K to 375 K.
- G. He, I. Tokue, and R.G. Macdonald
J. Phys. Chem.A. 102, 7653-7661 (1998).

Experimental measurement of the transition moment for the (2,0) band of the CN $A\,^2\Pi \leftarrow {}^2\Sigma$ *red system at 789.5 nm.*
- G. He, I. Tokue, and R.G. Macdonald
J. Chem. Phys. 109, 6312-6319 (1998).

Experimental determination of the υ_1 *fundamental vibrational transition moment for HNC.*
-G. He and R.G. Macdonald
Chem. Phys. Lett. 301, 175-182 (1998).

Experimental and theoretical determination of the magnetic dipole transition moment for $Br(4p^5)$ $(^2P_{1/2} \leftarrow {}^2P_{3/2})$ *fine-structure transition and the quantum yield of* $Br(^2P_{1/2})$ *from the 193 nm photolysis of BrCN.*
-G. He, M. Seth, I. Tokue, and R. G. Macdonald
J. Chem. Phys. 110, 7821-7831 (1999).

Rotational and translational energy distributions of CN(v=0,J) from the hot atom reactions: H + XCN → HX + CN(v=0,J), where X = Br, Cl. And CN.
-G. He, I. Tokue, and R. G. Macdonald
J. Chem. Phys. April 15 (2000).

Rotational and vibrational state distribution of $HNC(0\,v_2^l\,0)$ *from the hot H atom reaction:* $H + (CN)_2 \rightarrow HNC + CN$.
-R. G. Macdonald
J. Phys. Chem. Submitted (2000).

Flame Chemistry and Diagnostics

Andrew McIlroy
Combustion Research Facility
Sandia National Laboratories, MS 9055
Livermore, CA 94551-0969
Phone: (925) 294-3054
Email: amcilr@sandia.gov

Program Scope

The goal of this program is to elucidate the chemical mechanisms of combustion through a combination of experiments based on state-of-the-art diagnostics and detailed chemical kinetic modeling. The experimental program concentrates on the development and application of combustion diagnostics for the measurement of key chemical species concentrations. Although much work has been done to develop diagnostics for combustion species, many common radicals such as CH_3 and CH_2 remain difficult to study on a routine basis and many larger radicals remain difficult to detect at all. Comparison of experimental data to models employing detailed chemical kinetics allows us to determine the important chemical kinetic pathways for combustion, to test the accuracy of published models, and to develop new models. For the development and validation of chemical kinetic models, low pressure, one-dimensional laminar flames are studied. Transport issues are minimized in this configuration and well-developed models including detailed chemical kinetics, such as the Sandia PREMIX code, are available. As turbulent combustion models become increasingly sophisticated, accurate chemical kinetic mechanisms will play a larger role in computations of realistic combustion systems. Validated and well-characterized models will be required as inputs to these reactive flow codes. Only after rigorous comparisons of calculated and experimental results for a given chemical kinetic flame model over a wide range of steady conditions can these models be used with any confidence in turbulent codes. Recent studies of transiently strained flame structure indicate that even this stringent level of validation may be insufficient[1].

Recent Progress

Recently, we have carried out work in three general areas: the measurement of spectroscopic data needed for new flame diagnostics, the development and application of new laser and mass spectrometer diagnostics, and the testing of chemical kinetic models of combustion by careful measurements of stable species and radical intermediates. This work is briefly summarized below.

To develop the data needed for the quantitative detection of the vinyl radical, we have continued our investigation of the electronic spectroscopy and dynamics of vinyl using cavity ringdown spectroscopy. Although a small and ubiquitous radical in combustion, little is known of vinyl spectroscopy. Our initial studies indicated that fluorescence quenching due to intramolecular dynamics might have inhibited previous attempts to detect this radical by optical means. We have obtained high signal-to-noise ratio (S/N) spectra of the vinyl radical in a photolysis cell in the range 520-390 nm[2]. Modeling of the rovibrational band structure indicates that vinyl rapidly predissociates in the A-state on a picosecond time scale. We are

building a pulsed slit discharge molecular beam source to better investigate the intramolecular dynamics of vinyl and other combustion intermediates.

Spatially resolved cavity ringdown spectroscopy methods have recently been developed in our lab to detect the combustion intermediate CH. We have measured absolute methylidyne (CH) radical concentrations in a series of rich 31.0-Torr (4.13 kPa) methane-oxygen-argon flames. Probing via the CH $A^2\Delta$-$X^2\Pi$ transition near 430 nm gives a sensitivity of $3x10^9$ cm^{-3} for our experimental conditions, yielding a signal-to-noise ratio greater than 1000 for the strongest transitions observed. We measure profiles of CH mole fraction as a function of height above a flat-flame burner for rich flames with equivalence ratios of 1.0, 1.2, 1.4, and 1.6. These flames are modeled using the following mechanisms: 1) the GRI Mech 2.11[3], 2) a mechanism by Prada and Miller[4], 3) a modified GRI 2.11 mechanism, which employs a more realistic increased CH + O_2 rate coefficient, and 4) the new GRI Mech 3.0[5]. Generally good agreement between the models and the data is found, with the GRI 3.0 and modified 2.11 mechanism best reproducing the data. The greatest discrepancies are observed at the richest stoichiometry, where all of the models predict a wider CH profile shifted further from the burner than experimentally observed.

In order to produce a more general flame diagnostic while maintaining high selectivity and sensitivity, we have built a novel molecular-beam sampling mass spectrometer (MBMS) to probe the structure of low-pressure flames. This system features single-photon, VUV photoionization and time-of-flight mass spectroscopy (PI-TOF-MS), as well as laser diagnostics and an electron impact, quadrupole mass spectrometer (EI-Q-MS). The PI-TOF-MS portion is similar in concept to that of Cool and coworkers[6,7]. Single photon ionization near threshold eliminates many of the difficulties inherent in EI ionization. With modern nonlinear mixing schemes, vuv laser light can be produced that is both tunable and intense. We use resonant sum-difference frequency mixing in krypton to produce tunable light in the range 6.2-10.3 eV[8]. Tripling of Nd:YAG third harmonic in xenon gives an additional vuv source at 10.5 eV. With these sources of vuv light, we can easily tune over the ionization threshold of most radicals and can use this information to identify many of the isomeric species. Since ionization cross sections rise rapidly near threshold, but fragmentation does not, operating near threshold will allow us to maximize the yield of parent ions, simplifying our mass spectra and assisting in assignment. Rapid data collection is achieved with a 100 Hz laser system and TOF-MS. Both analog and ion-counting detection are employed where appropriate. Species with ionization energies above 10.5 eV are detected with an online EI-Q-MS. Since these species are generally stable, small molecules or radicals, electron impact ionization is acceptable. Laser diagnostics are used for temperature profiling and for the detection of specific radicals.

We have studied the oxidation of dimethyl ether (DME) in low-pressure, premixed flames using this new instrument. Two 30.0-Torr (4.00 kPa), premixed DME/oxygen/argon flames with stoichiometries of 0.98 and 1.20 were investigated. The profiles of flame temperature, nine stable species, and two radicals were measured as a function of height above the burner. The temperature and OH radical profiles were measured by OH laser-induced fluorescence. The remaining species were studied with the MBMS system. The experimental results were compared to the predictions of the detailed chemical kinetic reaction mechanism of Curran *et al.* [9]. Generally good agreement was found between the model and data. The model stable species profiles tracked the experimental data well. The largest discrepancies were found for the methyl radical profiles where the model predicts

qualitatively different trends in the methyl concentration with stoichiometry than observed in the experiment. The model predicts an increase in methyl mole fraction with increasing stoichiometry, whereas the experiment shows a decrease.

Future Plans

The photoionization system will be ideal for studying the formation of soot precursors such as polycyclicaromatic hydrocarbons (PAH), which are easily fragmented by other ionization techniques. After our dimethyl ether studies, we plan to move on to more complex fuels of current scientific and practical interest. In order to investigate the formation of the first aromatic ring in rich combustion, we will use several simple unsaturated fuels. Acetylene, ethylene, and allene all provide excellent opportunities to investigate the initial stages of molecular weight growth. Benzene, a component of gasoline, is a fuel that easily produces high concentrations of PAHs and soot. It has been used in a number of studies by Howard's group[10-15] and others[16,17] to investigate the mechanism of formation of PAHs and fullerenes. These fuels have been investigated by traditional sampling EI-Q-MS and in optical studies, however, our new photoionization instrument will be better able to detect many of the low concentration, larger molecular weight species that are not well quantified in these previous studies.

Unlike our commonly employed lab flames, many practical combustion devices do not use premixed fuel and oxidizer, but rather employ diffusion flames. In such devices, a much wider range of stoichiometries is present and with different temperature profiles than in premixed combustion. Thus mechanisms developed with reference solely to premixed data may fail for diffusion flames. To investigate these effects, a counterflow diffusion burner will be constructed in collaboration with Roger Farrow (Sandia). Initially, this system will rely on non-intrusive laser diagnostics. Studies will investigate the kinetics of methanol and dimethylether flames. Both of these oxygenated fuels are considered as direct-injection diesel fuels. In such engines, mixing is relatively poor and diffusion flames play an important role.

In parallel with our premixed and diffusion flame structure studies, we will continue to develop laser and mass spectrometer diagnostic methods to detect selected atomic and polyatomic radicals in low-pressure flames. We place particular emphasis on linear, absorption-based laser techniques, which are inherently easier to interpret than many fluorescence-based or non-linear methods. Cavity ringdown studies of new radicals such as vinyl will be undertaken as opportunities are identified. Other absorption-based techniques will also be investigated. Candidate methods include frequency-modulated (fm) diode laser absorption in multi-pass cells[18,19] and cavity-locked, fm spectroscopy using cw lasers[20,21].

Recent BES Publications

A. McIlroy, "Direct measurement of $^1CH_2$ in flames by cavity ringdown laser absorption spectroscopy," *Chemical Physics Letters* **296**, 151 (1998).

C. D. Pibel, A. McIlroy, C. A. Taatjes, S. Alfred, K. Patrick, and J. B. Halpern, "The vinyl radical ($\tilde{A}^2A'' \leftarrow \tilde{X}^2A'$) spectrum between 530 and 415 nm measured by cavity ring-down spectroscopy, " *Journal of Chemical Physics* **110**, 1841 (1999).

A. McIlroy, "Laser studies of small radicals in rich methane flames: OH, HCO and $^1CH_2$," *Israel Journal of Chemistry*, **39**, 55 (1999).

J. W. Thoman, Jr., A. McIlroy, "Absolute CH Concentrations in Rich Low-Pressure Methane-Oxygen-Argon Flames via Cavity Ringdown Spectroscopy of the $A^2\Delta$-$X^2\Pi$ Transition," *Journal of Physical Chemistry*, accepted 2000.

A. McIlroy, T. Hain, H. Michelsen, and T. A. Cool, "A Laser and Molecular Beam Mass Spectrometer Study of Low-Pressure Dimethyl Ether Flames," *Twenty-Eighth International Symposium on Combustion*, accepted 2000.

Cited Refernces

[1] H. N. Najm, O. M. Knio, P. H. Paul, and P. S. Wyckoff, *Combustion Theory and Modelling* **3,** 709-725 (1999).

[2] C. D. Pibel, A. McIlroy, C. A. Taatjes, S. Alfred, K. Patrick, and J. B. Halpern, *J. Chem. Phys.* **110,** 1841-1843 (1999).

[3] G. P. Smith, M. Frenklach, H. Wang, C. T. Bowman, D. Golden, W. Gardiner, V. Lissianski, and R. Serauskas, (sponsored by the Gas Research Institute, available at http://www.me.berkeley.edu/gri-mech/,).

[4] L. Prada and J. A. Miller, *Comb. Sci. Tech.* **132,** 225-250 (1998).

[5] G. P. Smith, D. M. Golden, M. Frenklach, N. W. Moriarty, B. Eiteneer, M. Goldenberg, C. T. Bowman, R. Hanson, S. Song, J. W. C. Gardiner, V. Lissianski, and Z. Qin, (sponsored by the Gas Research Institute, available at http://www.me.berkeley.edu/gri-mech/,).

[6] J. H. Werner and T. A. Cool, *Chem. Phys. Lett.* **275,** 278-282 (1997).

[7] J. H. Werner and T. A. Cool, *Chem. Phys. Lett.* **290,** 81-87 (1998).

[8] J. P. Marangos, N. Shen, H. Ma, M. H. R. Hutchinson, and J. P. Connerade, *J. Op. Soc. Am.* **7,** 1254-1259 (1990).

[9] H. J. Curran, W. J. Pitz, C. K. Westbrook, P. Dagaut, J. C. Boettner, and M. Cathonnet, *Int. J. Chem. Kinet.* **30,** 229-241 (1998).

[10] J. B. Howard, J. T. McKinnon, M. E. Johnson, Y. Makarovsky, and A. L. Lafleur, *J. Phys. Chem.* **96,** 6657-6662 (1992).

[11] J. B. Howard, in *Twenty-Fourth Symposium (International) on Combustion* (The Combustion Institute, Pittsburgh, 1992), pp. 933-946.

[12] C. J. Pope and J. B. Howard, in *Twenty-Fifth Symposium (International) on Combustion* (The Combustion Institute, Pittsburgh, 1994), pp. 671-678.

[13] H. Richter, K. Taghizadeh, W. J. Grieco, A. L. Lafleur, and J. B. Howard, *J. Phys. Chem.* **100,** 19603-19610 (1996).

[14] J. T. McKinnon and J. B. Howard, in *Twenty-Fourth Symposium (International) on Combustion* (The Combustion Institute, Pittsburgh, 1992), pp. 965-971.

[15] C. B. Vaughn, J. B. Howard, and J. P. Longwell, *Combust. Flame* **87,** 278-288 (1991).

[16] M. Bachman, W. Wiese, and K.-H. Homann, *Combust. Flame* **101,** 548-550 (1995).

[17] R. D. Smith and A. L. Johnson, *Combust. Flame* **51,** 1-22 (1983).

[18] J. T. Farrell and C. A. Taatjes, *J. Phys. Chem. A* **102,** 4846-4856 (1998).

[19] C. A. Taatjes and D. B. Oh, *Appl. Opt.* **36,** 5817-5821 (1997).

[20] J. Ye, L. S. Ma, and J. L. Hall, *J. Op. Soc. Am. B* **15,** 6-15 (1998).

[21] L. Gianfrani, R. W. Fox, and L. Hollberg, *J. Op. Soc. Am. B* **16,** 2247-2254 (1999).

TITLE: ATOMIC-LEVEL IMAGING OF CO_2 DISPOSAL AS A CARBONATE MINERAL: OPTIMIZING REACTION PROCESS DESIGN*

PIs: M.J. McKelvy,° R.W. Carpenter and R. Sharma

INSTITUTION: Arizona State University
Center for Solid State Science and
Science and Engineering of Materials Ph.D. Program
Tempe, AZ 85287-1704
° E-mail: mckelvy@asu.edu

ABSTRACT

Whereas, many other proposed CO_2 sequestration technologies provide long-term storage, mineral carbonation provides permanent disposal in the form of geologically stable mineral carbonates. Mineral carbonation avoids the ongoing problems and costs associated with long-term storage, which include guaranteeing permanent containment, avoiding adverse environmental consequences, and the ongoing cost of site monitoring. The primary goal for mineral carbonation is cost-competitive process development. Enhancing carbonation reaction rates is crucial to process cost. Mg-rich lamellar-hydroxide minerals (e.g., $Mg(OH)_2$ and serpentine-based minerals) provide an intriguing class of materials for enhancing carbonation reactivity, as the associated dehydroxylation process can disrupt the mineral structure at the atomic level. $Mg(OH)_2$ was chosen as a model Mg-rich lamellar-hydroxide mineral system to study the relationship between dehydroxylation/rehydroxylation processes and gas-solid carbonation reactivity.

$Mg(OH)_2$ carbonation is a complicated solid-state process in which dehydroxylation/water evolution occurs together with carbonation. As the overall carbonation process involves dehydroxylation, carbonation and the potential competition between them, developing an atomic-level understanding of the dehydroxylation process was first targeted to provide a foundation from which to explore the overall carbonation process. Environmental-cell (E-cell) dynamic high-resolution transmission electron microscopy (DHRTEM) has been used to directly image the dehydroxylation process at the atomic level for the first time. These studies have been complemented by a variety of in-situ and ex-situ experimental investigations and advanced computational modeling (see Chizmeshya, et al. abstract herein) to develop a better fundamental understanding of dehydroxylation/rehydroxylation processes and begin to explore their role in carbonation reactivity. We have discovered $Mg(OH)_2$ dehydroxylation is best described as a lamellar nucleation and growth process, which can access, at least locally, a broad range of new lamellar oxyhydroxide intermediate materials, $Mg_{x+y}O_x(OH)_{2y}$, during dehydroxylation. These intermediates provide access to a broad new range of carbonation reaction pathways. Controlled formation of such intermediates via dehydroxylation/rehydroxylation has been observed to substantially enhance carbonation reactivity, with substantial carbonation rates observed at ambient temperature and CO_2 pressure. Similar mechanisms may be more generally applicable for enhancing Mg-rich lamellar-hydroxide-based mineral (e.g., serpentine-based minerals) carbonation processes. These mechanisms offer excellent potential for enhancing carbonation reactivity and lowering CO_2 sequestration process costs via materials and reaction engineering.

* This work is supported by DOE Fossil Energy Advanced Research managed by the National Energy Technology Laboratory.

FLASH PHOTOLYSIS-SHOCK TUBE STUDIES

Joe V. Michael

Gas Phase Chemical Dynamics Group, Chemistry Division
Argonne National Laboratory, Argonne, IL 60439
e-mail: michael@anlchm.chm.anl.gov

During the past year, rate studies on two bimolecular and one termolecular reactions have been completed. In these studies, the atomic resonance absorption spectroscopic (ARAS) method was used for atom detection in reflected shock waves experiments.

In our recent study on $CH_3 + O_2 \rightarrow CH_3O + O$, a fast reaction between $H_2CO + O_2 \rightarrow HCO + HO_2$ was postulated.[1] Using trioxane as a thermal source of H_2CO, O-atom ARAS was used to observe absolute $[O]_t$ from this reaction under conditions of low $[H_2CO]_0$ so that most secondary reactions were negligible.[2] Unambiguous determinations of rate constants were possible by concentrating on initial rate analyses. The *ab initio* electronic structure calculations of Fang and Harding[3] were extended and used without change to estimate the thermal rate behavior using conventional transition state theory (CTST). Within ±6% for 500-3000 K, the theoretical results can be expressed by,

$$k_1^{th} = 4.4929 \times 10^{-20} T^{2.9116} \exp(-18692/T) \text{ cm}^3 \text{ molecule}^{-1} \text{ s}^{-1}.^2 \quad (1)$$

The transition state is non-linear and quite loose giving rise to the substantial non-linear behavior indicated by Eqn. (1). This equation is in moderate agreement with the directly determined[2] and previously inferred[1] values for the rate constants. In addition, it agrees quite well with values previously reported by Baldwin et al.[4] Hence, we suggest that Eqn. (1) be used in chemical models of combustion.

In our recent study on H_2CO decomposition, the products, $H_2 + CO$, compared to $H + HCO$, were found to be in the ratio of 85% to 15%, respectively.[5] Hence, H_2 is the major product. In our $CH_3 + O_2 \rightarrow CH_3O + O$ study,[1] H_2 formation from this decomposition was considered to be a dead end because the potentially important reaction, $H_2 + O_2$, was considered to be negligible. We therefore directly measured O-atom formation from $H_2 + O_2 \rightarrow$ products in order to check this assumption.[6] It is worth noting that this reaction is also the primary initiation reaction in H_2 oxidation by O_2. On kinetics grounds alone, the most probable products are $H + HO_2$. HO_2 instantaneously decomposes to $H + O_2$, and the free H-atoms then react with excess O_2 to give the observed O-atoms. This scheme was entirely corroborated with very high level *ab initio* electronic structure calculations. The products, OH + OH, were found to be of negligible importance. The measured rate constants, along with earlier values from Baldwin et al.[7] and transformed values from the back reaction,[8] were compared to a CTST calculation based on the *ab initio* potential energy surface. The theoretical results can be expressed by,

$$k_2^{th} = 1.228 \times 10^{-18} T^{2.4328} \exp(-26926 \text{ K/T}) \text{ cm}^3 \text{ molecule}^{-1} \text{ s}^{-1},^6 \quad (2)$$

to within ±2% over the T-range, 400-2300 K. Eqn. (2) is in excellent agreement with all of the experimental data including the present,[6] Baldwin et al.,[7] Sridharan et al.,[8] and Keyser.[8] We suggest that $H_2 + O_2 \rightarrow H + HO_2$ is the only significant initiation reaction in H_2 oxidation by O_2 and that Eqn. (2) be used to describe its rate.

The reaction of I with H_2 has been studied in reflected shock waves between 1755-2605 K[9] using I-atom ARAS[10] yielding,

$$k = (3.92 \pm 1.50) \times 10^{-9} \exp(-21398 \pm 658\ K/T)\ cm^3\ molecule^{-1}\ s^{-1}. \quad (3)$$

Combining the present results with earlier values from Sullivan[11] and transformed direct data from the back reaction, H + HI,[12-14] the data can be expressed in Arrhenius form over the T-range, 230-2605 K, as,

$$k = (4.52 \pm 0.34) \times 10^{-10} \exp(-17070 \pm 34\ K/T)\ cm^3\ molecule^{-1}\ s^{-1}. \quad (4)$$

Various theoretical models were investigated in order to explain this result. Even with scaling of both the activation barrier and bending frequencies, no previously considered potential energy surface was sufficient to describe the data. The best description over ~30 orders of magnitude is the experimental Arrhenius expression given in Eqn. (4). This has led us to suggest that detailed and accurate *ab initio* evaluation of anharmonicities of bending vibration frequencies may be necessary if high temperature thermal rate constants are to be theoretically rationalized.

The third-order reaction, H + O_2 + M, was directly studied in reflected shock waves with N_2 and Ar bath gases between ~450-700 K using the Laser Photolysis-Shock Tube (LP-ST) technique, and the results were reported in last year's contractors meeting. In these experiments, H atom depletion was observed with H-atom ARAS.[15] This study was extended to include a room temperature determination for H + O_2 + H_2O and a temperature dependent determination for H + O_2 + O_2.[16] The measured room temperature rate constants for bath gases, H_2O, N_2, O_2, Ar, Kr, Ne, and He, are (50 ± 3), (4.32 ± 0.28), (3.13 ± 0.06), (2.16 ± 0.14), (2.10 ± 0.10), (1.40 ± 0.04), and (1.80 ± 0.07), all with 2σ errors and in units of 10^{-32} cm^6 $molecule^{-2}$ sec^{-1}, respectively. The room temperature values were combined with the T-dependent values for N_2, Ar, and O_2 yielding,

$$k_{ter}^{N_2}(T) = (4.82 \pm 1.03) \times 10^{-29}\ T^{-1.232\pm0.036}\ cm^6\ molecule^{-2}\ s^{-1}, \quad (5)$$

$$k_{ter}^{Ar}(T) = (1.26 \pm 0.27) \times 10^{-29}\ T^{-1.120\pm0.035}\ cm^6\ molecule^{-2}\ s^{-1}, \quad (6)$$

and,

$$k_{ter}^{O_2}(T) = (1.57 \pm 0.38) \times 10^{-29}\ T^{-1.094\pm0.040}\ cm^6\ molecule^{-2}\ s^{-1}. \quad (7)$$

in substantial agreement with Mueller, Yetter, and Dryer[17] and also with Bates, Hanson, Bowman, and Golden.[18]

Data have also been obtained with G. P. Glass on the room temperature photodissociation quantum yields at 193 nm in ketene.[19] Absolute H-atom profiles were measured in the presence of either excess H_2 or Ar. From $[H]_0$ values, the quantum yield to give H + HCCO relative to $CH_2(^1A_1)$ + CO could be determined. Two additional photodissociation processes were identified, $CH_2(^3B_1)$ + CO and $C_2O(^1\Sigma)$ + H_2, from longer time profile considerations. These involved fitting the profiles to a chemical mechanism where most rate constants were previously known from direct studies. The rate constant for H + HCCO → products was additionally determined to be 1.7 x 10^{-10} cm^3 $molecule^{-1}$ s^{-1}.[19]

CH_3 profiles have also been measured at 214 nm using the recently described multipass optical system with and without added O_2.[20] Though complete, these data are

still being analyzed. We also plan to extend our capabilities with the multipass system to investigate reactions of other radical species (e.g., CH radicals).

Additional atom and radical with molecule reaction studies (e. g. Cl + hydrocarbons, OH + hydrocarbons, CF_2 + O_2, etc.) and, also, thermal decomposition investigations (e. g. C_2H_5, C_2H_3, etc.) are in the planning stage at the present time. These reaction studies are of theoretical interest to chemical kinetics and of practical interest in hydrocarbon combustion or waste incineration.

This work was supported by the U. S. Department of Energy, Office of Basic Energy Sciences, Division of Chemical Sciences, under Contract No. W-31-109-ENG-38.

References

1. J. V. Michael, S. S. Kumaran, and M.-C. Su, J. Phys. Chem. A, **103**, 5942 (1999).
2. J. V. Michael, M.-C. Su, J. W. Sutherland, D.-C. Fang, L. B. Harding, and A. F. Wagner, J. Phys. Chem., submitted.
3. D.-C. Fang and L. B. Harding, private communication, October, 1998.
4. R. R. Baldwin, D. H. Langford, M. J. Matchan, R. W. Walker, and D. A. Yorke, The Thirteenth Symposium (International) on Combustion **13**, 251 (1971); R. R. Baldwin, A. R. Fuller, D. Longthorn, and R. W. Walker, J. Chem. Soc. Faraday Trans. 1 **70**, 1257 (1974).
5. S. S. Kumaran, J. J. Carroll, and J. V. Michael, Twenty-Seventh Symposium (International) on Combustion **27**, 125 (1998).
6. J. V. Michael, J. W. Sutherland, L. B. Harding, and A. F. Wagner, The Twenty-Eighth Symposium (International) on Combustion, accepted.
7. R. R. Baldwin and R. W. Walker, The Seventeenth Symposium (International) on Combustion **17**, 525 (1979); R. R. Baldwin, M. E. Fuller, J. S. Hillman, D. Jackson, and R. W. Walker, J. Chem. Soc. Faraday Trans. 1 **70**, 635 (1974).
8. U. C. Sridharan, L. X. Qui, and F. Kaufman, J. Phys. Chem. **86**, 4569 (1982); L. F. Keyser, J. Phys. Chem. **90**, 2994 (1986).
9. J. V. Michael, S. S. Kumaran, M.-C. Su, and K. P. Lim, Chem. Phys. Lett. **319**, 99 (2000).
10. S. S. Kumaran, M.-C. Su, K. P. Lim, and J. V. Michael, Chem. Phys. Lett. **243**, 59 (1995).
11. J. H. Sullivan, J. Chem. Phys. **39**, 3001 (1963); and references therein.
12. K. Lorenz, H. Gg. Wagner, and R. Zellner, Ber. Bunsenges. Phys. Chem. **83**, 556 (1979).
13. H. Umemoto, S. Nakagawa, S. Tsunashima, and S. Sato, Chem. Phys. **124**, 259 (1988).
14. S. Vasileiadis and S. Benson, Int. J. Chem. Kinet. **29**, 915 (1997).
15. K. P. Lim and J. V. Michael, The Twenty-Fifth Symposium (International) on Combustion **25**, 713 (1994).
16. J. V. Michael, J. J. Carroll, J. W. Sutherland, and M.-C. Su, in preparation.
17. M. A. Mueller, R. A. Yetter, and F. L. Dryer, The Twenty-Seventh Symposium (International) on Combustion **27**, 177 (1998).
18. R. W. Bates, R. K. Hanson, C. T. Bowman, and D. M. Golden, Paper 159, First Joint Meeting of the U. S. Sections of the Combustion Institute, March 14-17, 1999, Washington, D. C.
19. G. P. Glass, S. S. Kumaran, and J. V. Michael, J. Phys. Chem., submitted.
20. M.-C. Su, S. S. Kumaran, K. P. Lim, and J. V. Michael, Rev. Sci. Inst. **66**, 4649 (1995).

PUBLICATIONS FROM DOE SPONSORED WORK FROM 1998-2000

■ *Thermal Decomposition Studies of Halogenated Organic Compounds*, J. V. Michael and S. S. Kumaran, Fifth International Congress on Toxic Combustion Byproducts, Combust. Sci. Tech. **134**, 31 (1998).

■ *Thermal Decomposition of CF_3Br Using Br-atom Absorption,* J. Hranisavljevic, J. J. Carroll, M.-C. Su, and J. V. Michael, Int. J. Chem. Kinet. **30**, 859 (1998).

■ *Rate Constants for $CF_3 + H_2 \rightarrow CF_3H + H$ and $CF_3H + H \rightarrow CF_3 + H_2$ Reactions in the Temperature Range 1100 K To 1600 K*, J. Hranisavljevic and J. V. Michael, J. Phys. Chem. **102**, 7668 (1998).

■ *Simultaneous Adjustment of Experimentally Based Enthalpies of Formation of CF_3X, X = nil, H, Cl, Br, I, CF_3, CN, and a probe of G3 Theory*, Branko Ruscic, Joe V. Michael, Paul C. Redfern, Larry A. Curtiss, and Krishnan Raghavachari, J. Phys. Chem. **102**, 10889 (1998).

■ *$H + CH_2CO \rightarrow CH_3 + CO$: A High Pressure Chemical Activation Reaction with Positive Barrier*, J. Hranisavljevic, S. S. Kumaran, and J. V. Michael, Twenty Seventh Symposium (International) on Combustion, The Combustion Institute, 1998, pp. 159-166.

■ *The Branching Ratio in the Thermal Decomposition of H_2CO*, S. S. Kumaran, J. J. Carroll, and J. V. Michael, Twenty Seventh Symposium (International) on Combustion, The Combustion Institute, 1998, pp. 125-133.

■ *Rate Constants for $CH_3 + O_2 \rightarrow CH_3O + O$ at High Temperature and Evidence for $H_2CO + O_2 \rightarrow HCO + HO_2$*, J. V. Michael, S. S. Kumaran, and M.-C. Su, J. Phys. Chem. A **103**, 5942 (1999).

■ *Thermal Rate Constants over Thirty Orders of Magnitude for the $I + H_2$ Reaction*, J. V. Michael, S. S. Kumaran, M.-C. Su, and K. P. Lim, Chem. Phys. Lett. **319**, 99 (2000).

■ *Atomic Resonance Absorption Spectroscopy with Flash or Laser Photolysis in Shock Waves Experiments*, Handbook of Shock Waves, J. V. Michael and Assa Lifshitz, Academic Press, New York, in press.

CHEMICAL KINETICS AND COMBUSTION MODELING

James A. Miller
Combustion Research Facility
Sandia National Laboratories
Livermore, CA 94551-0969
Email: jamille@ca.sandia.gov

PROGRAM SCOPE

The goal of this program is to gain qualitative insight into how pollutants are formed in combustion systems and to develop quantitative mathematical models to predict their formation rates. The approach is an integrated one, combining low-pressure flame experiments, chemical kinetics modeling, reaction rate theory, and kinetics experiments (microscopic and macroscopic) to gain as clear a picture as possible of the processes in question. My efforts and those of my collaborators are focused on problems involved with the nitrogen chemistry of combustion systems and the formation of soot and PAH in flames, as well as on general problems in hydrocarbon combustion.

RECENT PROGRESS

A Theoretical Analysis of the Reaction Between Ethyl and Molecular Oxygen (with Stephen J. Klippenstein, Case Western Reserve University, and Struan H. Robertson, Molecular Simulations, Inc., Cambridge, England)

Using a combination of electronic-structure theory, variational transition-state theory, and solutions to the *time-dependent* master equation, we have studied the kinetics of the title reaction theoretically over wide ranges of temperature and pressure. The agreement between theory and experiment is quite good. By comparing the theoretical and experimental results describing the kinetic behavior, we have been able to deduce a value for the $C_2H_5 - O_2$ bond energy of ~34 kcal/mole and a value for the exit-channel transition-state energy of –4.3 kcal/mole (measured from reactants). These numbers compare favorably with our electronic-structure theory predictions of 33.9 kcal/mole and –3.0 kcal/mole, respectively. The master-equation solutions show three distinct temperature regimes for the reaction, discussed extensively in our paper. Above $T \approx 700$ K, the reaction can be written as an elementary step, $C_2H_5 + O_2 \leftrightarrow C_2H_4 + HO_2$, with the rate coefficient,

$$k(T) = 3.19 \times 10^{-17} T^{1.02} \exp(2035/RT) \text{ cm}^3\text{/molec.-sec.},$$

independent of pressure even though the intermediate collision complex may suffer any number of collisions.

A Theoretical Analysis of the Reaction Between Vinyl and Acetylene: Quantum Chemistry and Solution of the Master Equation (with Stephen J. Klippenstein, Case Western Reserve University, and Struan H. Robertson, Molecular Simulations, Inc., Cambridge, England)

We have studied the reaction between vinyl and acetylene theoretically using electronic structure theory (DFT-B3LYP and a G2-like method) to calculate properties of stationary points on the potential, RRKM theory to compute microcanonical rate coefficients, and solutions to the *time-dependent, multiple-well* master equation to extract

information about the thermal rate coefficient and product distribution as a function of temperature and pressure. For the temperature range,
$300K \leq T \leq 700K$, both the total rate coefficient $k_1(T,p)$ and the products are functions of pressure. For $700K \leq T \leq 900K$, $k_1(T,p)$ is not always well defined in that the reactants can exhibit non- exponential decays in time. At sufficiently high pressure, the dominant product of the reaction changes from n-C_4H_5 to c-C_4H_5 (a four-numbered ring) to C_4H_4+H, where C_4H_4 is vinyl acetylene, as the temperature is increased from 600K to 900K. For $T > 900K$, the reaction can be written as an elementary step,

$$C_2H_3+C_2H_2 \rightarrow C_4H_4+H, \qquad (R1)$$

with a rate coefficient, $k_1=2.19\times10^{-12}T^{0.163}\exp(-8312/RT)$ cm^3/molecule-sec, *independent of pressure*, even though the intermediate collision complex may suffer numerous collisions. We interpret our results in terms of the eigenvalues and eigenvectors of the G matrix, i.e. the relaxation/reaction matrix of the master equation. For $T > 900K$, $k_1(T,p)$ always corresponds to the largest eigenvalue of G, which in turn corresponds to the zero-pressure limit rate coefficient $k_0(T)$. The situation is more complicated at lower temperatures. Our predictions are in good agreement with the limited amount of experimental information available on the reaction.

The quantum chemistry calculations indicate that both c-C_4H_5 and i-C_4H_5 are more stable than n-C_4H_5. The G2-like method gives results for the $\Delta H_f^{(0)}(0K)$ of c-C_4H_5 and i-C_4H_5 that are lower that that of n-C_4H_5 by 9.5 and 11.2 kcal/mole, respectively. The DFT-B3LYP results show similar differences of 6.0 kcal/mole and 13.7 kcal/mole, respectively.

Exploring Old and new Benzene Formation Pathways in Low-Pressure Premixed Flames of Aliphatic Fuels (with Christopher J. Pope)

We have performed a modeling study of benzene and phenyl radical formation is performed for three low-pressure premixed laminar flat flames having an unsaturated C_2 or C_3 hydrocarbon fuel (acetylene, ethylene, and propene). Predictions using three published detailed elementary-step chemical kinetics mechanisms were tested against MBMS species profile data for all three flames. The differences between the three mechanisms' predictive capabilities were explored, with an emphasis on benzene formation pathways. A new chemical kinetics mechanism was created combining features of all three published mechanisms. Included in the mechanism are several novel benzene formation reactions involving combinations of radicals such as C_2H+C_4H_5, C_2H_3+C_4H_3, and C_5H_3+CH_3. Reactions forming fulvene (a benzene isomer) are included, such as C_3H_3+C_3H_5, as well as fulvene-to-benzene reactions.

Predictions using the new mechanism show virtually all of the benzene and phenyl radical to be formed by reactions of either C_3H_3+C_3H_3 or C_3H_3+C_3H_5, with the relative importance being strongly dependent upon the fuel. C_5H_3+CH_3 plays a minor role in fulvene formation in the acetylene flame. The C_2H_x+C_4H_x reactions do not contribute noticeably to benzene or phenyl radical formation in these flames, sometimes being a major decomposition channel for either fulvene or phenyl radical. The formation pathways for C_3H_3 and C_3H_5 are delineated for the three flames; while the key reactions differ from flame to flame, $^1CH_2+C_2H_2 \Leftrightarrow C_3H_3+H$ is important for all three flames.

FUTURE DIRECTIONS

Our work on solving the time-dependent, multiple-well master equation in the last year has been leading up to an attempt to predict the rate coefficient and product distribution for the recombination of 2 propargyl radicals. This is a seven-well problem. We have already obtained interesting preliminary results for $T \geq 1500K$ and for $p \leq 1$ atm. Under these conditions, **benzene is not formed as a direct product.** The only significant products are fulvene and phenyl + H, with 2-ethynyl-1,3-butadiene formed as a minor product under some conditions. Continuing this analysis will be the primary focus of our attention in the next year.

In addition to our work on master equations, we shall continue to improve our kinetic model for the formation and growth of aromatic hydrocarbons in combustion, focusing primarily on the pressure dependence of key reactions. We shall also remain interested in the nitrogen chemistry of combustion, particularly the modeling of NO_x control techniques such as Thermal De-NO_x, RAPRENO$_x$, and reburning.

Publications of James A. Miller
1998 – Present

J.A. Miller, S.J. Klippenstein, and S.H. Robertson, "A Theoretical Analysis of the Reaction Between Ethyl and Molecular Oxygen," submitted to *Twenty-Eighth International Combustion Symposium* (2000)

J.A. Miller, S.J. Klippenstein, and S.H. Robertson, "A Theoretical Analysis of the Reaction Between Vinyl and Acetylene: Quantum Chemistry and Solution of the Master Equation," submitted to *J. Phys. Chem A* (2000)

C.J. Pope and J.A. Miller, "Exploring Old and New Benzene Formation Pathways in Low-Pressure Premixed Flames of Aliphatic Fuels," *submitted to Twenty-Eighth International Combustion Symposium* (2000)

C.J. Pope and J.A. Miller, "Variation of Equivalence Ratio and Element Ratios in Low-Pressure Premixed Flames of Aliphatic Fuels," *Combustion and Flame,* submitted (2000)

J.A. Miller and S.J. Klippenstein, "Theoretical Considerations in the NH_2 + NO Reaction," *J. Phys. Chem A* **104**, 2061-2069 (2000)

J.A. Miller and P. Glarborg, "Modeling the Thermal De-NO_x Process: Closing in on a Final Solution," *International Journal of Chemical Kinetics* **31**, 757-765 (1999)

J.A. Miller and S.J. Klippenstein, "Angular Momentum Conservation in the O +OH $\leftrightarrow$ O_2 + H Reaction, " *International Journal of Chemical Kinetics* **31**, 753-756 (1999)

P. Glarborg, A.B. Bendtsen, and J.A. Miller, "Nitromethane Dissociation: Implications for the CH_3 + NO_2 Reaction," *International Journal of Chemical Kinetics* **31**, 591-602 (1999)

J.A. Miller, J.L. Durant, and P. Glarborg, "Some Chemical Kinetics Issues in Reburning: The Branching Fraction of the HCCO + NO Reaction," *Twenty-Seventh Symposium (International) on Combustion*, pp. 235-243 (1998)

P. Glarborg, M.U. Alzueta, M. Ostberg, K. Dam-Johansen, and J.A. Miller, "The Recombination of Hydrogen Atoms with Nitric Oxide at High Temperature," *Twenty-Seventh Symposium (International) on Combustion*, pp. 219-226 (1998)

P. Glarborg, M.U. Alzueta, K. Dam-Johansen, and J.A. Miller, "Kinetic Modeling of Hydrocarbon/Nitric Oxide Interactions in a Flow Reactor," *Combustion and Flame* **115**, 1-27 (1998)

L. Prada and J.A. Miller, "Reburning Using Several Hydrocarbon Fuels: A Kinetic Modeling Study," *Comb. Sci. Tech.* **132**, 225-250 (1998)

J.A. Miller, C.F. Melius, and P. Glarborg, "The CH_3 + NO Rate Coefficient at High Temperatures: Theoretical Analysis and Comparison with Experiment," *International Journal of Chemical Kinetics* **30**, 223-228 (1998)

Reaction Dynamics in Polyatomic Molecular Systems

William H. Miller

Department of Chemistry, University of California, and
Chemical Sciences Division, Lawrence Berkeley National Laboratory
Berkeley, California 94720-1460
Ph: 510-642-0653; Fax: 510-642-6262
miller@neon.cchem.berkeley.edu

Program Scope or Definition

The goal of this program is the development of theoretical methods and models for describing the dynamics of chemical reactions, with specific interest for application to polyatomic molecular systems of special interest and relevance. There is interest in developing the most rigorous possible theoretical approaches and also in more approximate treatments that are more readily applicable to complex systems.

Recent Progress

Much progress has been made in recent years in developing ways to calculate the thermal rate constant k(T) (and also k(E), the microcanonical rate) for chemical reactions both 'directly', i.e., without having to solve the complete state-to-state reactive scattering problem, and yet also 'correctly', i.e., fully quantum mechanically and without any inherent approximation. The approach, which involves calculation of reactive flux correlation functions and which has qualitative vestiges of (and efficiencies related to) transition state theory, has been applied successfully to a number of small (3 or 4 atom) molecule chemical reactions. Ref. 2 provides a review of both the methodology and its applications.

To employ these approaches for more complex reactions, we have recently begun to explore use of the *semiclassical* (SC) *initial value representation* (IVR) to approximate the flux correlation functions. For example, the exact quantum expression for the 'flux-side' correlation function (the long time limit of which gives the thermal rate constant) is

$$C_{fs}(t) = \mathrm{tr}\left[\hat{F}(\beta)\, e^{i\hat{H}t/\hbar}\, \hat{h}\, e^{-i\hat{H}t/\hbar}\right], \qquad (1)$$

where $h = h(\mathbf{q})$ is the Heaviside function that is 0(1) on the reactant (product) side of a dividing surface, $\hat{F}(\beta) = e^{-\beta\hat{H}/2}\,\hat{F}\,e^{-\beta\hat{H}/2}$, and $\hat{F} = \frac{1}{\hbar}[\hat{H},\hat{h}]$ is the flux operator. The semiclassical approximation to it is obtained by using the SC-IVR to approximate the time evolution operators $\exp(\pm i\hat{H}t/\hbar)$ in Eq. (1). The coherent state IVR, for example, gives the propagator as (for a system of F degrees of freedom)

$$e^{-i\hat{H}t/\hbar} = (2\pi\hbar)^{-F}\int d\mathbf{p}_0 \int d\mathbf{q}_0\, C_t(\mathbf{p}_0,\mathbf{q}_0)\, e^{iS_t(\mathbf{p}_0,\mathbf{q}_0)/\hbar}\, |\mathbf{p}_t,\mathbf{q}_t\rangle\langle\mathbf{p}_0,\mathbf{q}_0|, \qquad (2)$$

where $(\mathbf{p}_0,\mathbf{q}_0)$ are the initial conditions for classical trajectories, $(\mathbf{p}_t,\mathbf{q}_t)$ are the momenta at time t that result from this trajectory, $S_t(\mathbf{p}_0,\mathbf{q}_0)$ is the action integral along the trajectory, and $C_t(\mathbf{p}_0,\mathbf{q}_0)$ is the square root of a determinant involving the various monodromy matrices (cf. refs. 10, 14, and many others listed below). Straight-forward use of the SC-IVR, Eq. (2), to evaluate the correlation function, Eq. (1), thus leads to a *double* phase space average (over the initial conditions

of two trajectories),

$$C_{fs}(t) = (2\pi\hbar)^{-F} \int d\mathbf{p}_0 \int d\mathbf{q}_0 \, (2\pi\hbar)^{-F} \int d\mathbf{p}_0' \int d\mathbf{q}_0' \, C_t(\mathbf{p}_0,\mathbf{q}_0) \, C_t(\mathbf{p}_0',\mathbf{q}_0')^*$$

$$e^{i[S_t(\mathbf{p}_0,\mathbf{q}_0)-S_t(\mathbf{p}_0',\mathbf{q}_0')]/\hbar} \langle \mathbf{p}_0,\mathbf{q}_0|\hat{F}(\beta)|\mathbf{p}_0',\mathbf{q}_0'\rangle \langle \mathbf{p}_t',\mathbf{q}_t'|\hat{h}|\mathbf{p}_t,\mathbf{q}_t\rangle \, . \qquad (3)$$

This may be contrasted with the fully *classical* expression for the correlation function,

$$C_{fs}^{CL}(t) = (2\pi\hbar)^{-F} \int d\mathbf{p}_0 \int d\mathbf{q}_0 \; F_\beta^{CL}(\mathbf{p}_0,\mathbf{q}_0) \, h(\mathbf{q}_t) \, , \qquad (4)$$

which involves only a single phase space average over initial conditions, and more significantly, does not have the oscillatory integrand that Eq. (3) involves.

Our most significant recent accomplishment has been to show how the *two* semiclassical propagators in Eq. (3) can be combined into *one* effective propagator, from 0 to t and from t back to 0, and thus only a single phase space average over initial conditions (refs. 14, 19). The resulting expression for the flux correlation function is

$$C_{fs}(t) = \int_{-\infty}^{\infty} dp_s \, (2\pi i p_s)^{-1} \, (2\pi\hbar)^{-F} \int d\mathbf{p}_0 \int d\mathbf{q}_0 \, C_0(\mathbf{p}_0,\mathbf{q}_0) \, e^{iS_0(\mathbf{p}_0,\mathbf{q}_0)/\hbar} \langle \mathbf{p}_0,\mathbf{q}_0|\hat{F}(\beta)|\mathbf{p}_0',\mathbf{q}_0'\rangle \, , \qquad (5)$$

where the classical trajectory begins with initial conditions $(\mathbf{p}_0,\mathbf{q}_0)$ and is propagated to time t, arriving at the phase point $(\mathbf{p}_t,\mathbf{q}_t)$; here the momentum is changed,

$$\mathbf{p}_t \rightarrow \mathbf{p}_t + p_s \frac{\partial s(\mathbf{q}_t)}{\partial \mathbf{q}_t} \, , \qquad (6)$$

and the trajectory propagated back to time 0; $(\mathbf{p}_0',\mathbf{q}_0')$ is the final phase point, and S_0 and C_0 the corresponding action integral and determinant pre-factor. Eq. (5) involves only a single phase space average over initial conditions, plus a one-dimensional integral over the magnitude of the 'jump parameter' p_s. Note that the direction of the 'momentum jump' at time t, Eq. (6), is in the direction of the reaction coordinate (i.e., normal to the dividing surface defined by $s(\mathbf{q}) = 0$); thus any degrees of freedom not significantly coupled to the reaction coordinate will largely cancel out in the forward-backward time evolution, a self-cancellation that makes the integrand of Eq. (5) much less oscillatory than that of Eq. (3). Application of this approach to systems of up to 50 degrees of freedom have been satisfactorily carried out (ref. 26).

Future Plans

Further development of the SC-IVR methodology is happening rapidly, and its application to a variety of dynamical phenomena in complex systems is envisioned.

1998 - 2000 (to date) DOE Publications

1. V. S. Batista and W. H. Miller, Semiclassical Molecular Dynamics Simulations of Ultrafast Photodissociation Dynamics Associated with the Chappuis Band of Ozone, J. Chem. Phys. **108**, 498 (1998); LBNL-40715.

2. W. H. Miller, "Direct" and "Correct" Calculation of Microcanonical and Canonical Rate Constants for Chemical Reactions, J. Phys. Chem. **102**, 793 (1998); LBNL-40716.

3. A. Viel, C. Leforestier, and W. H. Miller, Quantum Mechanical Calculation of the Rate Constant for the Reaction $H + O_2 \rightarrow OH + O$, J. Chem. Phys. **108**, 3489 (1998); LBNL-41150.

4. W. H. Miller, Quantum Theory of Chemical Reaction Rates, in Encyclopedia of Computational Chemistry, ed. P. v. R. Schleyer, J. Wiley & Sons, Ltd., U.K., Vol. 4, 1998, pp. 2375-2380; LBNL-39602.

5. W. H. Miller, The Semiclassical Initial Value Representation for Including Quantum Effects in Molecular Dynamics Simulations, in Classical and Quantum Dynamics in Condensed Phase Simulations, ed. B. J. Berne, G. Ciccotti, and D. F. Coker, World Scientific, Singapore, 1998, pp. 617-627; LBNL-40896.

6. X. Sun and W. H. Miller, Semiclassical Initial Value Representation for Rotational Degrees of Freedom: The Tunneling Dynamics of HCℓ Dimer, J. Chem. Phys. **108**, 8870 (1998); LBNL-41166.

7. W. H. Miller, Quantum Theory of Reactive Scattering and Chemical Reaction Rates, in Photonic, Electronic, and Atomic Collisions, ed. F. Aumayr and H. Winter, World Scientific, Singapore, 1998, pp. 441-451; LBNL-40714.

8. D. E. Skinner, T. C. Germann, and W. H. Miller, Quantum Mechanical Rate Constants for $O + OH \leftrightarrow H + O_2$ for Total Angular Momentum $J > 0$, J. Phys. Chem. **102**, 3828 (1998); LBNL-41297.

9. H. Wang, W. H. Thompson, and W. H. Miller, 'Direct' Calculation of Thermal Rate Constants for the $F + H_2 \rightarrow HF + H$ Reaction, J. Phys. Chem. **102**, 9372 (1998); LBNL-41296.

10. H. Wang, X. Sun, and W. H. Miller, Semiclassical Approximations for the Calculation of Thermal Rate Constants for Chemical Reactions in Complex Molecular Systems, J. Chem. Phys. **108**, 9726 (1998); LBNL-41295.

11. T. C. Germann and W. H. Miller, Quantum Mechanical Calculation of Resonance Tunneling in Acetylene Isomerization via the Vinylidene Intermediate, J. Chem. Phys. **109**, 94 (1998); LBNL-41438.

12. X. Sun, H. Wang, and W. H. Miller, On the Semiclassical Description of Quantum Coherence in Thermal Rate Constants, J. Chem. Phys. **109**, 4190 (1998); LBNL-41644.

13. X. Sun, H. Wang, and W. H. Miller, Semiclassical Theory of Electronically Nonadiabatic Dynamics: Results of a Linearized Approximation to the Initial Value Representation, J. Chem. Phys. **109**, 7064 (1998); LBNL-41756.

14. W. H. Miller, Quantum and Semiclassical Theory of Chemical Reaction Rates, Faraday Disc. Chem. Soc. **110**, 1 (1998); LBNL-42153.

15. D. Skinner and W. H. Miller, Application of the Semiclassical Initial Value Representation and Its Linearized Approximation to Inelastic Scattering," Chem. Phys. Lett. **300**, 20 (1999); LBNL-42302.

16. V. S. Batista, M. T. Zanni, B. J. Greenblatt, D. M. Neumark, and W. H. Miller, Femtosecond Photoelectron Spectroscopy of the I_2^- Anion: A Semiclassical Molecular Dynamics Simulation Method, J. Chem. Phys. **110**, 3736 (1999); LBNL-42303.

17. M. T. Zanni, V. S. Batista, B. J. Greenblatt, W. H. Miller, and D. M. Neumark, Femtosecond Photoelectron Spectroscopy of the I_2^- Anion: Characterization of the $\tilde{A}'\,^2\Pi_{g,1/2}$ Excited State, J. Chem. Phys. **110**, 3748 (1999); LBNL-42304.

18. H. Wang, X. Song, D. Chandler and W. H. Miller, Semiclassical Study of Electronically Nonadiabatic Dynamics in the Condensed-Phase: Spin-Boson Problem with Debye Spectral Density, J. Chem. Phys. **110**, 4828 (1999); LBNL-42176.

19. X. Sun and W. H. Miller, Forward-Backward Initial Value Representation for Semiclassical Time Correlation Functions, J. Chem. Phys. **110**, 6635; LBNL-42426.

20. V. Guallar, V. S. Batista and W. H. Miller, Semiclassical Molecular Dynamics Simulations of Excited State Double-Proton Transfer in 7-Azaindole Dimers, J. Chem. Phys. **110**, 9922; LBNL-42679.

21. H. Wang and W. H. Miller, Analytic Continuation of Real-Time Correlation Functions to Obtain Thermal Rate Constants for Chemical Reaction, Chem. Phys. Lett. **307**, 463 (1999); LBNL-42906.

22. W. H. Miller, Generalization of the Linearized Approximation to the Semiclassical Initial Value Representation for Reactive Flux Correlation Functions, J. Phys. Chem. **103**, 9384 (1999); LBNL-43208.

23. Y. Guo, D. L. Thompson and W. H. Miller, Thermal and Microcanonical Rates of Unimolecular Reactions from an Energy Diffusion Theory Approach, J. Phys. Chem. **103**, 10308 (1999); LBNL-43207.

24. D. E. Skinner and W. H. Miller, Application of the Forward-Backward Initial Value Representation to Molecular Energy Transfer," J. Chem. Phys. **111**, 10787 (1999); LBNL-44187.

25. W. H. Miller, Using Mechanics in a Quantum Framework: Perspective on "Semiclassical Description of Scattering", Theo. Chem. Accts. **103**, 236 (2000); LBNL-42905.

26. H. Wang, M. Thoss, and W. H. Miller, Forward-Backward Initial Value Representation for the Calculation of Thermal Rate Constants for Reactions in Complex Molecular Systems, J. Chem. Phys. **112**, 47 (2000); LBNL-44637.

27. E. A. Coronado, Victor S. Batista, and W. H. Miller, Nonadiabatic Photodissociation Dynamics of *ICN* in the $\tilde{A}$ Continuum: A Semiclassical Initial Value Representation Study, J. Chem. Phys. (accepted); LBNL-44723.

28. M. Thoss, W. H. Miller and G. Stock, Semiclassical Description of Nonadiabatic Quantum Dynamics: Application to the S_1-S_2 Conical Intersection in Pyrazine, J. Chem. Phys. (accepted); LBNL-44877.

Selective Photochemistry*

C. Bradley Moore, Investigator
Chemical Sciences Division,
Lawrence Berkeley National Laboratory and
Department of Chemistry,
University of California, Berkeley, California 94720-1460
cbmoore@socrates.berkeley.edu

Program Scope

The fundamental goals of this work are to elucidate the molecular dynamics of energy transfer and chemical reaction processes. Lasers are used to prepare molecules in selected excited states and a variety of spectroscopic probes are used to follow energy transfers and chemical reactions with quantum-state resolution. Ideally, all quantum numbers are resolved in the initial excitation and for each of the product states. By exploring the dependence of processes on quantum state and other experimentally controllable parameters it is usually possible to establish a physical model for the process. Optimally, accurate benchmarks are established for the quantitative test of first principles theory and the validation of quantitative models for combustion and atmospheric chemistry.

In molecules with low energy barriers to bond breaking, the assumption of rapid and fully statistical flow of vibrational energy, upon which the statistical transition state theory (e.g. RRKM theory) is based, comes into question. Results on HCO and on HFCO are illustrative. Dissociations of free radicals generally have low barriers because breaking a single bond is accompanied by an increase in the strength of another bond, e.g.,

$$H_3C\text{-}O \rightarrow H_2C{=}O + H.$$

Thus there is a large class of reactions of great importance in chemical combustion for which transition state theory may give very poor predictions of reaction rates. The rates of some or all of these reactions may be limited by the rates and detailed paths of energy flow. A study of the vibrational spectroscopy of free radicals in cooled pulsed jets is underway in preparation for state-resolved dynamical studies of ir photofragmentation of free radicals. With sufficiently short and intense pulses of ir it may be possible to drive a molecule along a selected reaction coordinate on a timescale short compared to IVR times.

Lasers are particularly useful in studying the highly reactive species important in complex chemical processes. Flash photolysis with a laser provides a controlled source of these species for study in gases or liquids. Laser spectroscopy provides excellent wavelength and time resolution for observation of the spectrum and study of the kinetics. Studies here, in collaboration with Robert Bergman, Heinz Frei and Charles Harris focus on diazo compounds and on coordinatively unsaturated organometallics important in CH activation chemistry.

Recent Progress

Vibrational Spectroscopy, Energy flow and Dissociation of Free Radicals
A. Bragg, X. Chen, I. Kalinovski, A. Mann and C. B. Moore

Infrared spectra of the fundamental and first overtone of the CH stretches of methoxy and its deuterated isotopomers have been recorded at high resolution by fluorescence depletion spectroscopy in a cooled pulsed jet. Methoxy is produced by uv photolysis of methyl nitrite at the nozzle of a free jet expansion. It then cools in the expansion and is excited on a single rovibronic uv transition. The fluorescence-excitation spectra have been recorded and analyzed. These spectra are severely complicated by the simultaneous operation of the spin-orbit interaction and the Jahn-Teller effect. The isotopic data have been particularly revealing in this regard. If an infrared pulse excites molecules out of the same rovibrational level of the ground

* This work was supported by the Director, Office of Energy Research, Office of Basic Energy Sciences, Chemical Sciences Division of the U. S. Department of Energy under Contract No. DE-AC03-76SF00098.

electronic state that the uv laser is tuned to excite, the uv fluorescence intensity is depleted. The spectra show evidence of significant, but very far from statistical, vibrational mixing at v_{CH} =2. The CHD_2O molecule is an ideal candidate for study of mode selectivity in the bond breaking reaction to form H and CD_2O. The threshold for this reaction is near the energy of the 2nd C-H overtone.

In order to study the dynamics of infrared-driven unimolecular reactions of free radicals, the enhanced detection sensitivity and increased information content of state-selective REMPI (resonance-enhanced multiphoton ionization) imaging detection is required. A molecular beam machine has been designed and built for this purpose. This system will also allow us to return to studies of ketene photofragmentation and isomerization with full resolution of the rotational energy levels of the reactant and products.

Flash Infrared Kinetics of the Photochemistry of Tp*Rh(CO)$_2$ and Bp*Rh(CO)$_2$ in Liquid Xenon Solution

J. S. Yeston, B. K. McNamara, R. G. Bergman, and C. B. Moore

The photochemistry of Tp*Rh(CO)$_2$ (1) [Tp*=hydridotris(3,5-dimethylpyrazolyl)borate] in liquid xenon solution at –50 °C has been examined by flash IR kinetic spectroscopy. IR spectra of the solution taken 2 μs after 308 nm photolysis exhibit two transient bands at 1976–1980 cm^{-1} and 1994–1998 cm^{-1}, respectively, both of which decay with the same first-order rate constant (k=2 x 10^4 s^{-1}). In the presence of excess CO, the rates of decay of both of these bands increase by an order of magnitude and correlated with the rate of recovery of the CO stretch of the parent complex. Photolysis of xenon solutions of Bp*Rh(CO)$_2$ (**5**) [Bp*=dihydrobis(3,5-dimethylpyrazolyl)borate] produces a transient species with a single IR absorption at 1996–2000 cm^{-1}. Upon addition of pyridine to the solution, this transient photoproduct reacts to form the new, stable complex Bp*Rh(CO)(pyridine), with an IR absorption at 1978 cm^{-1}. On the basis of these results, the 1978 cm^{-1} and 1996 cm^{-1} bands observed upon photolysis of **1** are attributed to (η^3–Tp*)Rh(CO)•Xe and (η^2–Tp*)Rh(CO)•Xe solvates **2•Xe** and **3•Xe**. Preliminary kinetic data for the reaction of **1** with cyclohexane in xenon solution indicate that both the 1978 cm^{-1} and 1996 cm^{-1} transient bands still appear, and that their rates of decay correlate with formation of the Rh alkyl hydride product Tp*Rh(CO)(cyclohexyl)(H) (**4**) absorbing at 2032 cm^{-1}.

Future Plans

A series of experiments on the vibrational spectroscopy and photochemistry of free radicals has been initiated. It should be possible to map out many vibrational levels at energies well above the threshold for dissociation. Product fragments will be detected by LIF and by REMPI imaging. For reactions requiring four or more C—H quanta, e.g., vinyl radical, a two-step ir (two tunable high-resolution ir lasers) excitation scheme is needed to approach saturation and therefore to be useful in dynamics experiments. The REMPI ion imaging molecular beam system will be used to measure reaction rates and product state properties for dissociation of free radicals using ir excitation. High-resolution one- and two-step ns ir excitation and ps ir multiphoton excitation will be used. A picosecond IR optical parametric amplifier (OPA) has been completed in collaboration with the Institute for Spectroscopy of the Russian Academy of Sciences in Moscow. This needs to be modified to produce pulses with transform-limited resolution rather than the 20 cm^{-1} resolution now available.

fs ir-driven reaction coordinate experiments will be attempted for small polyatomic free radicals and for modest-sized mono- and di-functional diazo compounds. The latter studies will be commenced in room temperature liquid solvents. This work will utilize the fs ir laser system in the lab of our collaborator Karl Kompa in Munich.

Xe has been shown to bind to a wide variety of metal centers. However, very few studies have probed the interaction between this noble gas and reactive hydrocarbon fragments. A picosecond pump-probe study of UV-induced carbene formation in liquid xenon or Xe-saturated media will explore the possibility of Xe binding to the unsaturated carbon center. This also prepares for real-time detection in the fs ir-driven chemistry experiments above.

The sensitivity of the ion-imaging machine will be exploited to study the dynamics at rotationally selected transition states of ketene following high resolution ir+uv excitation.

Publications 1998, 1999, 2000

A. Mellinger, M.V. Ashikhmin, and C.B. Moore, "Experimental Evidence for K-Conservation in the Dissociation of Singlet Ketene," *J. Chem. Phys.*, **108**, 8944 (1998).

M.V. Ashikhmin, A. Mellinger, and C.B. Moore, "The Photodissociation of Singlet Ketene: Transition State Tightening and K-Conservation," *SPIE Proceedings*: **3271**, 67-70, Laser Techniques for State-Selected and State-to-State Chemistry IV, (1998).

B.K. McNamara, J.S. Yeston, R.G. Bergman, and C.B. Moore, "The Effect of Alkane Size on Rates of Photoinduced C-H Bond Activation by $Cp^*Rh(CO)_2$ in Liquid Rare Gas Media: An Infrared Flash Kinetics Study," *J. Am. Chem. Soc.* In press (1999).

M.A. Hall, "I. Singlet Photodissociation of Ketene: The Effects of K-Conservation. II. Promoting Understanding of Thermodynamics: The Role of Student Explanation and Integration of Ideas," Ph.D. Thesis, University of California, Berkeley, (1999).

J.S. Yeston, B.K. McNamara, R.G. Bergman, and C.B. Moore, "Flash Infrared Kinetics of the Photochemistry of $Tp^*Rh(CO)_2$ and $Bp^*Rh(CO)_2$ in Liquid Xenon Solution," submitted to *Organometallics*, 02/22/00.

GAS-PHASE MOLECULAR DYNAMICS: EXPERIMENTAL AND THEORETICAL STUDIES OF SPECTROSCOPY AND DYNAMICS

James T. Muckerman (muckerma@bnl.gov), Trevor J. Sears (sears@bnl.gov)
and Gregory E. Hall (greghall@bnl.gov)
Chemistry Department, Brookhaven National Laboratory, Upton, NY 11973-5000

PROGRAM SCOPE

The goal of this research is the understanding of elementary chemical and physical processes important in the combustion of fossil fuels. Interest centers on reactions and properties of short-lived chemical intermediates. High-resolution, high-sensitivity, laser absorption methods are augmented by high-temperature, flow-tube reaction kinetics studies with mass-spectrometric sampling. These experiments provide information on the energy levels, structures and reactivity of molecular free radical species and, in turn, provide new tools for the study of energy flow and chemical bond cleavage in radicals involved in chemical systems. The experimental work is supported by theoretical and computational work using time-dependent quantum wavepacket calculations, which provide quantitative and qualitative insight into energy flow between the vibrational modes of polyatomic molecules.

RECENT PROGRESS

The infrared spectrum of the ethyl radical in the region of the CH_2 out-of-plane rocking fundamental was recorded some time ago, but only recently completely understood. The spectrum consists of numerous torsion-rotation sub-bands and their assignment and analysis has resulted in the first definitive measurement of the torsional barrier and its change on vibrational excitation in an alkyl radical. The interaction between the torsion and the other modes of vibration in the radical has a substantial effect on the magnitude of the barrier. A simple model, using the results of high level electronic structure calculations for estimating electronic and vibrational contributions to the barrier was developed. It gives good agreement with the experimental results and should be generally useful for predicting the barrier in larger alkyls where experimental information is unlikely to be available in the near future.

Continuing work on methylene, new spectra in the singlet band system of the molecule near 9400 cm^{-1} were recorded, using a near infrared diode laser-based spectrometer employing the transient frequency modulation technique developed at BNL. The spectra give information on levels close to the barrier to linearity that have not before been accessed by any spectroscopic technique. Comparison of the energy levels derived to the best available calculations, which are themselves optimized by refinements based on previous spectroscopic results, suggest that some refinement of the shape of the upper singlet potential surface is needed. We are collaborating with Professor Per Jensen (Wuppertal) on this aspect of the project.

Bromomomethylene, HCBr, provides a revealing contrast to CH_2 itself because the lowest state is now of singlet character, and the triplet state corresponding to the ground state of methylene lies to slightly higher energy in the brominated compound. The position of this triplet state is not accurately known and one of the aims of our work is its location via the observation of perturbations in the energy levels of the lower singlet state. Rotational analyses of 9 vibronic bands in the near infrared spectrum of HCBr have now been completed. Since the spectra involve levels with $0 \leq v_2 \leq 2$ in the $\tilde{A}$ and $\tilde{X}$ states of both HCBr and DCBr, a nearly complete picture of the rovibronic structure near the minima of both states is now available. In the excited state, K=0 levels are generally regular, but exhibit a few localized perturbations, while higher K levels are often seriously perturbed. These perturbations have made analysis of the spectra rather time consuming, but in many cases additional spectroscopic transitions to the perturbing levels were identified. In the ground state, we have not detected any discrete perturbations, but there are unusual rotational and vibrational level spacings that suggest the zero point level of the triplet lies between 1700 and 2300 cm^{-1} above the ground (000) level. We have also begun electronic structure calculations on

HCBr with the aim of computing a bending potential surface that can be used as a starting point for a refinement based on the experimental level positions.

Experiments in which spectra of metal-containing radicals were created in a free jet cooled laser ablation source and detected by direct absorption of a frequency modulated Ti:sapphire laser have also been completed. The prototypical diatomics PtC and TiS were detected in collaboration with Prof. T. Steimle (Arizona State). These results are an important prelude to work on more complex systems where laser induced fluorescence, the usual spectroscopic experiment of choice, cannot be used due to poor fluorescence quantum yields.

Assessing the role of non-adiabatic interactions in the branching of chemical reactions on multiple potential energy surfaces is a central topic in the development of predictive codes for combustion modeling. We have used transient FM Doppler spectroscopy to characterize the mixed adiabatic/diabatic branching in the photodissociation of ICN in unprecedented detail. This prototype multiple-surface system provides direct comparisons of high-level quantum dynamics calculations with an information-rich set of experimental observables.

Multisurface quantum dynamical calculations on the photodissociation of ICN in which the polarization of the excited molecules is explicitly taken into account were carried out in conjunction with the experimental effort in our group. Previous wavepacket calculations took into account the polarization of the population in the various excited electronic states only during the excitation process, but not the mixing of these polarized populations as a consequence of nonadiabatic transitions between electronic states far from the Franck-Condon region. They could not, therefore, address such observables as the product-state-dependent anisotropies that are measured in the Doppler spectroscopy studies in our group. Our approach was to describe the population in each electronic state in terms of a two-component nuclear wavefunction: one component corresponding to parallel polarization, the other to perpendicular polarization. The nonadiabatic interaction induces coupling only between nuclear wavefunction components of the same polarization (*i.e.*, a change of electronic state cannot cause the ICN molecule to instantaneously flip its axis by roughly 90 degrees). This approach allowed us to make detailed comparisons between theory and experiment that revealed deficiencies in the potential energy surfaces.

In further investigations of ICN photodissociation, we sought insight into the implicit assumptions made in the previous wavepacket studies. In this work we carried out wavepacket calculations as a function of the angle between the molecular axis and a space-fixed axis corresponding to the electric field of the excitation laser. At each value of this angle (except for 0, $\pi/2$ and π), the initial wavepacket contains components corresponding to both parallel and perpendicular transitions. There are two "magic angles" (symmetrically located about $\pi/2$) at which the populations of the parallel and perpendicular components in the initial wavepacket are proportional to the squares of their transition moments. The previous wavepacket studies can be interpreted as having been carried out at one of these magic angles (but not both). The fact that the subsequent nonadiabatic interaction is different for the two magic angles gives rise to quantitative errors in the previous results.

The development of the experimental methods of ion imaging, metastable tagging, time-of-flight, and Doppler spectroscopy for the measurement of the angular dependence of polarized reaction products has been beset with a confusing proliferation of notations and frameworks. The quantities represented offer direct connection with the most basic quantum mechanical observables, yet no consensus has yet been reached on the most convenient or insightful representation to use. We have had extensive collaboration with members of the Zare group (Stanford) to clarify the connection between the older, bipolar moment formalism, and the more recent notation originated in the Zare group. The two formalisms have been shown to be equivalent, and the way in which coherent effects appear in the semiclassical formalism has been made clear.

We have succeeded in performing photoinitiated reactions with transient FM Doppler probing of the reaction products in a supersonic slit jet. The barrierless unimolecular dissociation of ketene to form

singlet methylene and carbon monoxide has in this way been studied at the coincident state level of detail. A high-quality and distinctive data set shows some startling deviations from low-level approximate theories of barrierless reactions. Ongoing theoretical work by S. Gray (ANL) and S. Klippenstein (Case Western Reserve) related to these measurements bears on questions of energy-dependent mode coupling and the fundamental approximations of statistical unimolecular theory.

FUTURE PLANS

The difference in energy between the ground, triplet, and first excited, singlet, states of CH_2 is important with regard to the chemical properties of the radical. It is also of fundamental interest as methylene has been a benchmark for advances in theoretical techniques for the past 40 years. The current best estimate (with an error of $\pm$ 5 cm^{-1}) comes from detailed analysis of perturbed transitions in the far infrared spectrum of the radical combined with theoretical estimates of the energy of excited bending vibrations in the triplet state. Due to improvements in experimental techniques and our knowledge of the lowest energy levels of the singlet, it is now feasible to attempt to measure perturbed-singlet from triplet vibrational rotation transitions in the bending overtone spectrum of the triplet. Such transitions are predicted by theory to be weak, but should be observable given currently achievable sensitivities. We are setting up an experiment to attempt to measure such transitions in the 3-5 micron region.

A relatively unexplored method of optical spectroscopy exists in a world between cavity ring-down spectroscopy and multi-pass transient FM spectroscopy. Building on recent work from J. Hall (JILA), we plan to explore means of combining high-Q resonant cavities with FM detection of transient species. Compared to single-pass FM spectroscopy, detection limits can in principle be reduced by an additional factor of the cavity Q. The useful enhancement is ultimately limited by the chemical transient lifetime, providing an upper bound on the cavity-Q or ring-down-time for which cavity enhancements will lead to sensitivity improvement.

As applications of transient FM spectroscopy spread to reaction kinetics, the boundaries of validity for the simplified theory used for intensity calibration need to be better defined. For high enough probe laser intensity, or strong enough molecular transition strengths, unexplained line shapes and temporal patterns in the transient FM spectra have been observed, probably related to the strongly driven populations and coherences in multilevel systems. We will pursue a combined experimental and theoretical approach to the characterization of the onset of optical saturation effects in transient FM spectroscopy.

The new effort aimed toward the *ab initio* calculation of molecular free radicals will continue with emphasis on species such as CHBr being studied experimentally in our program. It is anticipated that theoretical information from these calculations will aid in the assignment of the complicated spectra exhibited by such systems and permit inversion of the observed energies to potential surfaces.

The CO product from the CH_3 + O reaction is likely to be produced by one of two pathways: (1) the elimination of an H atom from the CH_3O adduct to form vibrationally excited formaldehyde (CH_2O) which in turn eliminates H_2 to form CO; or (2) the elimination of H_2 from the adduct to form vibrationally excited HCO which subsequently eliminates an H atom to form CO. We will explore the CH_3O potential energy surface for these scenarios using a high level of *ab initio* electronic structure theory in search of transition states and steepest-descent reaction paths. Using transition states, reaction paths and energetics obtained from these calculations, we will compute rate constants and branching fractions for the various channels in the reaction of CH_3 radicals with O atoms. These results will be compared with results from ongoing experimental TOFMS and diode laser transient absorption studies in our program.

ACKNOWLEDGMENT

This research was carried out at Brookhaven National Laboratory under Contract DE-AC02-98CH10886 with the U.S. Department of Energy and supported by its Division of Chemical Sciences, Office of Basic Energy Sciences.

PUBLICATIONS SINCE 1998

Fockenberg, C., Sears, T. J., and Chang, B.-C.
Near-Infrared High Resolution Diode Laser Spectrum of the CH_2 $b\ ^1B_1 \leftarrow a\ ^1A_1$ Transition
J. Molec. Spectrosc. **187**, 119-125 (1998)

Marr, A. J., North, S. W., Sears, T. J., Ruslen, L., and Field, R. W.
Laser Transient Absorption Spectroscopy of Bromomethylene
J. Molec. Spectrosc. **188**, 68-77 (1998)

Blank, D. A., Suits, A. G., Lee, Y. T., North, S. W., and Hall, G. E.
Photodissociation of Acrylonitrile at 193 nm: A Photofragment Translational Spectroscopy Study using Synchrotron Radiation for Product Photoionization
J. Chem. Phys. **108**, 5784-5794 (1998)

Blank, D. A., Sun, W., Suits, A. G., Lee, Y. T., North, S. W., and Hall, G. E.
Primary and Secondary Processes in the 193 nm Photodissociation of Vinyl Chloride
J. Chem. Phys. **108**, 5414-5425 (1998)

North, S. W., and Hall, G.
Transient Frequency-Modulated Spectroscopy: Application to the Measurement of Vector and Scalar Correlations in Molecular Photodissociation
SPIE Proceedings San Diego 1998 Meeting, San Diego, CA, Jan. 26-28, 1998

Bergmann, K., Carter, R. T., Hall, G. E., and Huber, J. R.
Resonance Enhanced Multiphoton Ionization Time-of-Flight Study of CF_2I_2 Photodissociation
J. Chem. Phys. **109**, 474-483 (1998)

Chen, R., Guo, H., Liu, L., and Muckerman, J. T.
Symmetry-Adapted Filter-Diagonalization: Calculation of the Vibrational Spectrum of Planar Acetylene from Correlation Functions
J. Chem. Phys. **109**, 7128-7136 (1998)

Marr, A. J., Sears, T. J., and Chang, B.-C.
Near Infrared Spectroscopy of CH_2 Frequency Modulated Diode Laser Absorption
J. Chem. Phys. **109**, 3431-3442 (1998)

Furlan, A., and Hall, G. E.
Photoproducts Ejected from Liquid Surfaces: The Importance of Photochemical, Diffusional, Kinetic and Surface Structural Effects
J. Chem. Phys. **109**, 10390-10399 (1998)

Liu, L., and Muckerman, J. T.
Strong-Field Optical Control of Vibrational Dynamics: Vibrational Stark Effect in Planar Acetylene
J. Chem. Phys. **110**, 2446-2451 (1999)

Weston, R. E.
Anomalous or Mass-Independent Isotope Effects
Chem. Rev. **99**, 2115-2136 (1999)

Marr, A. J., and Sears, T. J.
Hot Band Spectroscopy of DCBr Near 0.96 μm
Molec. Phys. **97**, 185-193 (1999)

Fockenberg, C., Bernstein, H. J., Hall, G. E., Muckerman, J. T., Preses, J. M., Sears, T. J., and Weston, R. E., Jr.
Repetitively Sampled Time-of-Flight Mass Spectrometry for Gas-Phase Kinetics Studies
Rev. Sci. Instrum. **70**, 3259-3264 (1999)

Fockenberg, C., Hall, G. E., Preses, J. M., Sears, T. J., and Muckerman, J. T.
Kinetics and Product Study of the Reaction of CH_3 Radicals with $O(^3P)$ Atoms using Time Resolved Time-of-Flight Spectrometry
J. Phys. Chem. A **103**, 5722-5731 (1999)

Costen, M. L., North, S. W., and Hall, G. E.
Vector Signatures of Adiabatic and Diabatic Dynamics in the Photodissociation of ICN
J. Chem. Phys. **111**, 6735-6749 (1999)

Rakitzis, T. P., Hall, G. E., Costen, M. L., and Zare, R. N.
Relationship Between Bipolar Moments and Molecule-Frame Polarization Parameters in Doppler Photofragment Spectroscopy
J. Chem. Phys. **111**, 8751-8754 (1999)

Nolte, J., Wagner, H. G., Sears, T. J., and Temps, F.
The Far Infrared Laser Magnetic Resonance Spectrum of CH_2F
J. Molec. Spectrosc. **195**, 43-53 (1999)

Marr, A. J., and Sears, T. J.
Vibronic Reassignment of the $A\ ^1A'' \leftarrow X\ ^1A'$ Band System of Bromomethylene
J. Molec. Spectrosc. **195**, 367-370 (1999)

Sears, T. J., Johnson, P. M., and Beebe-Wang, J.
Infrared Spectrum of the -CH_2 out of Plane Fundamental of C_2H_5
J. Chem. Phys. **111**, 9213-9221 (1999)

Johnson, P. M., and Sears, T. J.
Vibrational Effects on the Torsional Motion of Ethyl Radical
J. Chem. Phys. **111**, 9222-9226 (1999)

Steimle, T. C., Costen, M. L., Hall, G. E., and Sears, T. J.
Transient Frequency Modulation Absorption Spectroscopy of Molecules Produced in a Laser Ablation Supersonic Expansion Source
Chem. Phys. Lett. **319**, 363-367 (2000)

Hall, G. E., and North, S. W.
Transient Laser Frequency Modulation Spectroscopy
Annu. Rev. Phys. Chem. (in press)

Sevy, E. T., Muyskens, M. A., Rubin, S. M., Flynn, G. W., and Muckerman, J. T.
Competition Between Photochemistry and Energy Transfer in UV-Excited Diazabenzenes:
I. Photofragmentation Studies of Pyrazine at 248 nm and 266 nm
J. Chem. Phys. (in press)

Kobayashi, K., Pride, L. D. and Sears, T. J.
Absorption Spectroscopy of singlet CH_2 near 9500 cm^{-1}
J. Phys. Chem. (in press)

Chang, B. -C., Costen, M. L., Marr, A. J., Ritchie, G. Hall, G. E. and Sears, T. J.
Near-Infrared Spectroscopy of Bromomethylene in a Slit Jet Expansion
J. Molec. Spectrosc. (in press)

Reacting Flow Modeling with Detailed Chemical Kinetics

Habib N. Najm

Combustion Research Facility
Sandia National Laboratories, MS 9051
Livermore, CA 94551
hnnajm@ca.sandia.gov

1. Program Scope

This project focuses on the study of unsteady flame-flow interaction in multi-dimensional reacting flow using numerical modeling with detailed chemical kinetics and transport. The objectives are to provide improved understanding of the interaction between flames and turbulent flow, and to generate information leading to the development of predictive turbulent combustion models. Unsteady flow-flame interaction in turbulent combustion has a significant effect both on overall combustion efficiency and on pollutant generation. Concerns about air quality and atmospheric pollution necessitate improved understanding of turbulent reacting flow in order to enable continued reduction of pollutant emissions in practical combustion systems.

2. Recent Progress

Recent progress is outlined below as pertaining to both numerical methods development and reacting flow studies.

2.1 Numerical Methods

We have continued developments towards more efficient operator-split implementations, in collaboration with Prof. O. Knio of Johns Hopkins. By using extended stability explicit time integrators in split diffusional half-steps, and by improving cache utilization, we have achieved another factor of 5 speedup in 2D reacting flow computations with detailed kinetics. Global time steps on the order of $1\mu s$ are now feasible, allowing computations of unsteady 2D methane-air flames with GRImech1.2 with length and time scales comparable to those in existing experimental data.

We have also continued development of numerical methods for coupled Lagrangian-Eulerian time integration. This is in the context of our Adaptive Mesh Refinenment (AMR) code capability for large-scale reacting jet flow computations. We have recently implemented a second-order construction for coupling baroclinic vorticity generation with Lagrangian particle motion [1]. We have also incorporated CVODE as a stiff integrator for the chemical source terms. This necessitated splitting of the diffusion and reaction terms. With this approach, reacting flow jet computations using stiff detailed kinetics have been enabled.

We have also had a collaborative project involving the modeling of 1D transient flames with Prof. A. Ghoniem of MIT. This involved joint development of robust implicit 1D solvers for transient 1D flames with an ILU preconditioned BICGSTAB krylov-space iterative construction that exhibits both fast and robust convergence properties [2,3].

2.2 Transient Premixed Flame Response and Stoichiometry

We studied the effect of equivalence ratio Φ on the transient response of 2D premixed methane-air flames under a range of flow time scales [4,5]. Results indicate significant changes in flame response depending on Φ. Our findings are summarized as follows.

- The heat release response time decreases as Φ increases from $\Phi = 0.8$ to 1.2. In contrast with results for 1D flames under sinusoidal stretching, the slower propagating rich flame responds faster than the stoichiometric flame. Meanwhile, the lean flame responds at a slightly slower rate than the stoichiometric flame. Consequently, the response time scale does **not** generally correlate with peak heat release rate or the fuel consumption rate. The response of the heat release rate appears to be governed by the roles of H and OH in the kinetics. As Φ increases, fuel consumption pathways are dominated by H due to the scarcity of OH, and thus respond at the faster H time scales.
- Both numerical and experimental results show faster response of CH and OH in the rich, versus stoichiometric, case. In general, results suggest that the global premixed flame time scale based on flame thermal thickness and burning speed is inadequate for describing transient flame response. The rich flame, with slower burning speed, responds faster to the imposed strain-rate than the stoichiometric flame.
- We report experimental measurements of peak HCO evolution by P. Paul of Sandia, that are in agreement with the decay rates of numerical peak HCO. The robustness of the experimental HCO signal suggests continued burning despite the collapse of the CH signal. We continue to find different response of CH and OH in the experiment versus the computed CH and OH.
- In a collaboration [6] with Profs. M. Valorani, Univ. Rome, and D. Goussis, ICEHT-Greece, we have used Computational Singular Perturbation (CSP) analysis of existing flame-vortex databases to investigate the roles of specific reactions in the transient flame dynamics. Results indicate that diffusion and convection do not have important roles in the transient dynamics of CH or OH, suggesting that the above described discrepancies are due to the chemical mechanism. Specific reactions with dominant roles have been identified, and will be likely targets of further study.

2.3 Lifted Jet Diffusion Flame

Using the AMR code, we studied lifted non-premixed jet flame dynamics using a global, and a C_1 reaction mechanism, with a focus on the flame base structure and dynamics [7].

- A triple flame was observed at the lifted flame base with the global mechanism. On the other hand, the C_1 mechanism exhibits a flame edge structure with a lean branch but no rich branch, in agreement with recent experimental CO, OH PLIF data from P. Paul at Sandia, and with numerical results of M. Smooke at Yale.
- We examine the interaction of jet vortices with the flame base using a global mechanism. We observe entrainement, stretching and contortion of the flame base by the vortex flow field. The flame base dynamics exhibit robustness consistent with earlier studies of vortex interaction with triple flames. These dynamics and robustness of the flame base are crucial for the stability of the lifted jet flame.

2.4 One-Dimensional Transient Flame

In a collaboration with Prof. A. Ghoniem of MIT, 1D transient flame studies were conducted using detailed kinetics and compared to existing flame-vortex results as pertains to the role of strain-rate on flame response [2,3]. Results were used to guide the development of imbedded flame submodels, to be used in the context of large-scale combustion device simulations.

2.5 Molecular Dynamics Study of Diffusion and Reaction

In a collaboration with Wm. Ashurst of Sandia, a Molecular Dynamics (MD) study of

diffusion and reaction was conducted, with comparisons to continuum results [8]. The conventional description of the rate of diffusive transport of a reactive molecule presumes many diffusional collisions before a reactive collision is expected. This assumption breaks down for molecules with near gas-kinetic reaction rates. The present study investigated the modification to the conventional diffusion coefficient for species with very fast dissociation rates, approaching gas kinetic collision rates. We find that the diffusivity of the reactive species is generally within 20% of the non-reacting, conventional, diffusivity under all conditions examined. This is remarkable, given the large changes in reactivity explored.

3. Future Plans

Future plans are outlined as pertaining to numerical methods and flame studies.

3.1 Numerical Methods

Further advances in the formulation and implemention of advanced numerical methods will be pursued in order to enhance our modeling efficiency, while maintaining accuracy. We plan to pursue further validation, and optimization of extended stability explicit schemes for the operator-split diffusion half-steps. We also plan to reduce integration costs by utilizing inexact Jacobians in the stiff-integration procedure. Jacobians are used only to direct the solver towards the solution, and are not required to high accuracy. We also plan to enhance the accuracy of our models by using an efficient implementation of mixture-averaged transport properties. We will also continue optimization of the stiff operator-split reaction-diffusion construction in the AMR code.

3.2 Flame Studies

We plan to continue studies of transient premixed flame response. We will examine the validity of computed transients in CH_3O and other species in the low temperature region, during flame-vortex interactions, using improved mechanisms that better account for the chemical pathways relevant in this part of flame. We will also investigate parametric space in the flame-vortex interaction problem, as regards the role of flow length and time scales and mixture composition on the long-time flame dynamics, flame reconnection, and pocket formation. We will also use mixture-averaged transport properties to investigate transient flame response in flame-vortex studies. In collaboration with Valorani & Goussis, we will extend our CSP studies of flames toward automatic spatially and temporally-localized reduction of mechanisms using CSP analysis. We will also work with Prof. W. Green of MIT on utilization of adaptive chemistry approaches in multidimensional reacting flow computations.

Using the AMR code we will conduct studies of the steady-state structure and transient dynamics of the flame base of a lifted methane-air jet flame, using detailed kinetics. Both premixed and non-premixed jets will be studied, and results will be compared to experimental results of R. Schefer and P. Paul, Sandia. We will also use the AMR code to study large-scale jet flame behaviour, with a focus on the role of jet structures in modulation and extinction of the diffusion flame.

We will use the 1D transient flame code developed by A. Ghoniem of MIT to conduct parametric runs with different chemical mechanisms, strain-rate time histories, mixture compositions, and transport coefficients. These studies, afford an easier way (vs. 2D studies) of traversing parametric space in various dimensions.

References

[1] Najm, H.N., Milne, R.B., Ray, J., Devine, K.D., and Kempka, S.N., *J. Comput. Phys.* (2000) submitted.

[2] Marzouk, Y.M., Ghoniem, A.F., and Najm, H.N., *Twenty-Eighth Symposium (International) on Combustion*, The Combustion Institute, submitted, (2000).

[3] Marzouk, Y.M., Ghoniem, A.F., and Najm, H.N., *AIAA 2000-0866* (2000) AIAA 38^{th} Aerospace Sciences Meeting and Exhibit, Reno, NV.

[4] Knio, O.M., and Najm, H.N., *Twenty-Eighth Symposium (International) on Combustion*, The Combustion Institute, submitted, (2000).

[5] Najm, H.N., Paul, P.H., Knio, O.M., and McIlroy, A., *Twenty-Eighth Symposium (International) on Combustion*, The Combustion Institute, submitted, (2000).

[6] Valorani, M., Goussis, D., and Najm, H., Using CSP to Analyze Computed Reacting Flows, Eighth International Conference on Numerical Combustion, SIAM, (2000).

[7] Ray, J., Najm, H.N., Milne, R.B., Devine, K.D., and Kempka, S.N., *Twenty-Eighth Symposium (International) on Combustion*, The Combustion Institute, submitted, (2000).

[8] Ashurst, Wm.T., Najm, H.N., and Paul, P.H., *Combustion Theory and Modeling* (2000) submitted.

Publications

1. Najm, H.N., Knio, O.M., Paul, P.H., and Wyckoff, P.S., "Response of Stoichiometric and Rich Methane-Air Flames to Unsteady Strain-Rate and Curvature", *Combustion Theory and Modelling*, 3, no. 4, pp. 709-726, (1999).
2. Knio, O.M., Najm, H.N., and Wyckoff, P.S., "A Semi-Implicit Numerical Scheme for Reacting Flow. II. Stiff Operator-Split Formulation", *J. Comput. Phys.*, 154, pp. 428-467, (1999).
3. Najm, H.N., Azoury, P.H., and Piasecki, M., "Hydraulic Ram Analysis: A New Look at an Old Problem". *J. Power and Energy, Proc. Inst. Mech. Eng. A*, 213(A2), pp. 127-141, (1999).
4. Najm, H.N., Milne, R.B., Devine, K.D., and Kempka, S.N., "A Coupled Lagrangian-Eulerian Scheme for Reacting Flow Modeling", ESAIM Proc., 7, pp. 304-313, (1999).
5. Najm, H.N., Knio, O.M., Paul, P.H., and Wyckoff, P.S., "A Study of Flame Observables in Premixed Methane-Air Flames", *Comb. Sci. Tech.*, 140(1-6), pp. 369-403, (1998).
6. Paul, P.H. and Najm, H.N., "Planar Laser-Induced Fluorescence Imaging of Flame Heat Release Rate", in *Twenty-Seventh Symposium (International) on Combustion*, pp. 43-50, The Combustion Institute, (1998).
7. Najm, H.N., Paul, P.H., Mueller, C.J., and Wyckoff, P.S., "On the Adequacy of Certain Experimental Observables as Measurements of Flame Burning Rate". *Combustion and Flame*, 113(3), pp. 312-332, (1998).
8. Najm, H.N., Wyckoff, P.S., and Knio, O.M., "A Semi-Implicit Numerical Scheme for Reacting Flow. I. Stiff Chemistry". *J. Comput. Phys.*, 143(2), pp. 381-402, (1998).

Photodissociation of Free Radicals and Hydrocarbons

Daniel Neumark
Chemical Sciences Division
Lawrence Berkeley National Laboratory
Berkeley, CA 94720
neumark@cchem.berkeley.edu

This research program is aimed at elucidating the photodissociation dynamics and bimolecular chemistry of free radicals and hydrocarbons. Particular emphasis is placed on radicals that play a role as reactive intermediates in combustion mechanisms. Our experiments yield bond dissociation energies, heats of formation, and excited state dynamics for these important species.

While the photodissociation experiments on many closed-shell radicals have been carried out, far fewer studies of free radicals have been published because the techniques developed for stable molecules are not easily extended to reactive free radicals. We have developed a photodissociation experiment uniquely suited to free radicals, in which radicals are generated by photodetachment of mass-selected anions and then are photodissociated. A second component of our research program focuses on the photodissociation of hydrocarbons on a crossed molecular beams apparatus in our campus laboratory and at the Advanced Light Source. These experiments enable us to distinguish between photoproducts of the same mass but with different ionization potentials.

Recent progress:

Photodissociation of NCN, CNN, and HNCN: These radicals were all studied on our fast radical beam spectrometer. They are of interest as possible reactive intermediates in low energy combustion pathways for production of N atoms from N_2 which are subsequently oxidized to form NO. The primary photochemistry and product state distributions were determined for all three species. Although NCN is linear in its ground and excited electronic states, it dissociates primarily to C + N_2, implying passage through a bent (possibly C_{2v}) transition state. CNN also dissociates to C + N_2, but with considerably more rotational energy in the N_2 fragment than occurs in NCN dissociation. HNCN dissociates to CH + N_2, with substantial vibrational excitation of the N_2 fragment but little rotational excitation. These results imply that dissociation occurs via an HCN_2 transition state with near C_{2v} symmetry.

Photodissociation of carbon clusters: The photodissociation of mass-selected linear carbon clusters (C_n, n = 4 – 6) is studied using fast beam photofragment translational spectroscopy. The photofragment yield (PFY) spectra consist of several continua spanning the whole visible and ultraviolet region. The product mass distributions for dissociation of C_n clusters are dominated by C_3 and its partner fragment C_{n-3}. Translational energy P(E_T) distributions for the C_3 + C_{n-3} channel were measured at several photolysis energies. The PFY spectra and P(E_T) distributions indicate that multi-

photon dissociation occurs at photon energies below the dissociation threshold, and that both single- and multi-photon dissociation occur above the threshold. The one-photon components of the P(E_T) distributions can be modeled by phase space theory (PST), suggesting that photoexcitation is followed by internal conversion to the ground state. The PST analysis yields dissociation energies for $C_n \rightarrow C_n + C_{n-3}$ in reasonable agreement with recent Knudsen effusion mass spectrometry measurements..

Photodissociation of the ethoxy radical: This species was investigating on the fast radical beam instrument. The ethoxy radical is generated by photodetachment of $C_2H_5O^-$ and subsequently dissociated by photon absorption in the range of 270-220 nm; no dissociation is seen at higher wavelengths. The photofragment yield (PFY) spectrum is structureless, but exhibits abrupt increases in intensity at 260 and 225 nm. The product mass distribution shows that C_2H_5O dissociates into vinyl radical (C_2H_3) and H_2O throughout the entire absorption band. We propose that these products are formed by isomerization and dissociation on electronically excited surfaces rather than by internal conversion to the ground state. The translational energy P(E_T) distributions for this channel are largely insensitive to photon energy. However, at the two highest photon energies (5.51 and 5.96eV), a new feature appears at $E_T \leq 0.3$eV which is assigned as production of an excited state of C_2H_3.

Photodissociation of allene and propyne: The photodissociation dynamics of propyne and allene were investigated in two molecular beam/photodissociation instruments, one using electron impact ionization and the other using tunable vacuum ultraviolet (VUV) light to photoionize the photoproducts. The primary dissociation channels for both reactants are $C_3H_3 + H$ and $C_3H_2 + H_2$. Measurement of the photoionization efficiency curves on the VUV instrument shows that the C_3H_3 product from propyne is the propynyl (CH_3CC) radical, whereas the C_3H_3 product from allene is the propargyl (CH_2CCH) radical. The C_3H_2 primary product from both reactants is the propadienylidene (H_2CCC) radical. We also observe a small amount of C_3H_2 product from photodissociation of the C_3H_3 radicals in both cases.

Photodissociation of 1,3-butadiene, 1,2-butadiene, and 2-butyne: The 193 nm photodissociation of these three molecules (all with chemical formula C_4H_6) have been investigated using electron impact VUV ionization. Five dissociation channels are seen from 1,3-butadiene: $H + C_4H_5$, $H_2 + C_4H_4$, $CH_3 + C_3H_3$, $C_2H_2 + C_2H_4$, and $C_2H + C_2H$. Measurements on isotopically substituted (d_1,d_2,d_5,d_6) 1,3-butadiene and measurements of product ionization potentials at the Advanced Light Source have aided in identifying the products. In 1,2-butadiene, only the first three channels are observed, and in 2-butyne, only H atom loss and CH_3 loss are observed.

Future plans:

Photodissociation experiments on NCS, NCO, HCNN, and CH_3CH_2S radicals are planned for the fast radical beam apparatus. In addition, a new detector will be installed that will enable detection of three-body dissociation, and will also improve our collection efficiency for photofragments formed with low kinetic energy.

Efforts on our crossed beam instrument will focus on the development of radical sources based on pyrolysis and photolysis. These sources will be used in photodissociation and crossed molecular beams experiments. We are particularly interested in the ethoxy and propargyl radicals.

References to publications of DOE sponsored research that have appeared in 1997, 1998 and 1999 or have been accepted for publication.

D. L. Osborn, H. Choi, D. H. Mordaunt, R. T. Bise, D. M. Neumark, and C. M.Rohlfing, "Fast beam photodissociation (Spectroscopy and dynamics of the vinoxy radical," J. Chem. Phys. 106, 3049-66 (1997).

D. L. Osborn, D. H. Mordaunt, H. Choi, R. T. Byse, D.M. Neumark, and C.M. Rohlfing, "Photodissociation spectroscopy and dynamics of the HCCO free radical," J. Chem Phys.106, 10087 (1997).

D. L. Osborn, H. Choi, and D. M. Neumark, "Photodissociation spectroscopy and dynamics of the vinoxy (CH_2CHO) radical," Adv. Chem. Phys. 101, (1997).

D. L. Osborn, D. J. Leahy and D. M. Neumark, "Photodissociation spectroscopy and dynamics of CH_3O and CD_3O," J. Phys. Chem., 101, 6583, (1997).

L.R. Brock, B. Mischler, Eric A. Rohlfing, Ryan T. Bise and D. M. Neumark, "Laser-Induced fluorescence spectroscopy of the ketenyl radical," J. Chem. Phys. 107, 665, (1997).

D.H. Mordaunt, D.L. Osborn, and D. M. Neumark, "Nonstatistical unimolecular dissociation over a barrier," J. Chem. Phys. 108, 2448, (1998).

H. Choi, D. H. Mordaunt, R. T. Bise, T. R. Taylor and D. M. Neumark, "Photodissociation of triplet and singlet states of the CCO radical," J. Chem. Phys. 108, 4070, (1998).

R. T. Bise, H. Choi, H. B. Pedersen, D. H. Mordaunt and D. M. Neumark, "Photodissociation spectroscopy and dynamics of the methylthio radical (CH_3S)," J. Chem Phys. 110, 805, (1999).

W. Sun, K. Yokoyama, J. Robinson, A. Suits and D. M. Neumark, "Discrimination of product isomers in the photodissociation of propyne and allene at 193mm," J. Chem. Phys. 110, 4363, (1999).

R. T. Bise, H. S. Choi, and D. M. Neumark, "Photodissociation dynamics of singlet and triplet states of the NCN radical," J. Chem. Phys. 111, 4923, (1999).

H. Choi, R. T. Bise, A. A. Hoops, D. H. Mordaunt, D. M. Neumark, "Photodissociation of Linear Carbon Clusters C_n (n=4-6)," J. Phys. Chem. A 104, 2025, (2000).

R. T. Bise, A. A. Hoops, H. Choi, D. M. Neumark, "Photoisomerization and photodissociation dynamics of the NCN, CNN and HNCN free radicals". (ACS Symposium in press)

H. Choi, R. T. Bise, D. M. Neumark, "Photodissociation dyamics of the ethoxy radical (C_2H_5O)". (J. Phys. Chem. in press)

H. Choi, R. T. Bise, A. A. Hoops, D. M. Neumark, "Photodissociation dynamics of the triiodide anion (I_3^-)". (Submitted to J. Chem. Phys.)

Photoionization and Photoelectron Studies of Combustion Species

C. Y. Ng
Ames Laboratory, USDOE and Department of Chemistry
Iowa State University, Ames, Iowa 50011 (Email: CYNG@AMESLAB.GOV)

I. Program Scope

The goals of this program are: (1) to obtain accurate thermochemical and spectroscopic data, such as ionization energies (IEs), bond dissociation energies at 0 K (D_0's) and rovibronic constants, for neutral polyatomic molecules, radicals, and their ions; and (2) to study the photoionization and photodissociation dynamics of molecules and radicals induced by the absorption of ultraviolet and vacuum ultraviolet (VUV) photons. Our recent studies have emphasized radicals and molecular systems relevant to combustion, catalysis, and atmospheric chemistry.

II. Recent Progress

Photoelectron spectroscopy is a major technique for research in Physical Sciences. The development of the laser based pulsed field ionization (PFI)-photoelectron (PFI-PE) technique has revolutionized the field of photoelectron spectroscopy, demonstrating a resolution close to the laser optical resolution. Nevertheless, the full potential of this technique has not been realized due to the limited tunable range accessible by lasers. The real impact of this technique to chemistry requires a high-resolution, broadly tunable VUV source.

In the past few years, we have established such a high-resolution VUV facility at the Chemical Dynamics Beamline of the Advanced Light Source. This facility consists of a 6.65-m Eagle-mounted monochromator, which has demonstrated the resolving power of 100,000 in the range of 6-30 eV, is currently the highest resolution scanning VUV monochromator in the World. This resolving power is close to that achieved in common VUV laser systems. However, the (pulsed) laser based PFI-PE technique has traditionally required a delay of $\approx$1-3 μs for the dispersion of prompt background electrons. Thus, this approach is not directly applicable to PFI-PE measurements using synchrotron radiation, which is essentially a continuous light source. We have developed a novel synchrotron based PFI-PE scheme overcoming the delay requirement and have attained resolution of 2-5 cm^{-1} (FWHM). In the past year, we have improved the PFI-PE resolution and prompt electron discrimination by introducing the time-of-flight (TOF) detection scheme. This method has achieved a PFI-PE resolution of 1 cm^{-1} (FWHM) at 12 eV, which is also similar to that attained in laser-based PFI-PE studies. The ease of tunability of this ALS synchrotron source has made rotationally resolved PFI-PE measurements for many molecules a routine operation. The high sensitivity of this photoelectron-photoion apparatus of the Chemical Dynamics Beamline has allowed the measurements of rotationally resolved photoelectron spectra of many diatomic molecules, covering vibrational levels up to the dissociation limits of the corresponding diatomic ions.

During the 1999 fiscal year, we have succeeded in developing the PFI-PE-photoion coincidence scheme, which makes possible the internal state selection for cations to a resolution of 4.8 cm^{-1} (FWHM) limited only by the PFI-PE measurement. By employing this high-resolution PFI-PE-PICO scheme, together with the supersonic beam technique for rotational cooling of gaseous samples, we show that accurate 0 K ion dissociation thresholds can be determined unambiguously by the disappearing energy of the parent ion. As a demonstration experiment, we have measured the 0 K dissociative photoionization thresholds for the formations of CH_3^+ from CH_4 and C_2H^+ from C_2H_2 to the accuracy of $\pm$0.001 eV. These measurements, when combined with accurate IE values for CH_3, CH_4, and C_2H_2 obtained by PFI-PE measurements, make possible the determination of highly accurate D_0 values for H-CH_3, H-CH_3^+, and H-C_2H^+ with the values of 4.487$\pm$0.001, 1.705$\pm$0.004, and 5.957$\pm$0.001 eV, respectively.

Since these newly developed synchrotron-based PFI-PE and PFI-PEPICO methods are generally applicable to all gaseous molecules, we expect their application to have a significant impact in spectroscopic and energetic studies of neutrals and cations. Furthermore, this development has

established a sound foundation for future experimentation concerning PFI-PEPICO studies of radicals and state-selected ion-molecule reaction dynamics relevant to plasma and planetary chemistry.

II. Future Plans

In the Ames Laboratory, we have recently developed a comprehensive high-resolution VUV laser system, together with a state-of-the-art molecular beam photoionization-photoelectron apparatus. This new VUV laser system consists of two dye lasers pumped by a frequency-doubled or tripled Nd-YAG laser, a vacuum chamber for nonlinear wavelength mixing, and a VUV monochromator for wavelength separation. By four-wave-mixing techniques, coherent VUV radiation can be generated in the range of 650-2000 Å with a resolution of 0.15 cm^{-1} (FWHM). We plan to use this VUV laser system to perform high-resolution VUV PIE and PFI-PE studies of cold polyatomic molecules and radicals. We have previously developed a versatile supersonically cooled polyatomic radical source by combining the excimer laser photodissociation and supersonic beam methods. Since the VUV laser is operated at low repetition rate, it is ideal to combine this excimer-laser-photolysis radical source and the VUV laser for PIE and PFI-PE measurements. Considering that many excimer laser photodissociation processes are highly selective, it is possible to prepare radicals with specific isomeric structures for experimental studies. Using appropriate precursor molecules, many sulfur-, oxygen-, and halogen-containing radicals relevant to combustion chemistry can be prepared by the excimer laser photodissociation source. The sulfur-containing radicals of interest are SO, CS, CH_3S, CH_3CH_2S, CH_3SCH_2, CH_2CH_2SH, CH_3SS, C_6H_5S, which can be prepared in abundance by excimer laser photodissociation of SO_2, CS_2, CH_3SH (or CH_3SCH_3), $CH_3CH_2SCH_2CH_3$, $HSCH_2CH_2SH$, CH_3SSCH_3, and C_6H_5SH (or $C_6H_5SCH_3$), respectively. The series of oxygen-containing radicals CH_3O, C_2H_3O, CH_3CH_2O, CH_3CO, and C_6H_5CO can also be prepared by photodissociation. Most of these radicals are important intermediates in combustion and atmospheric processes. To our knowledge, these radicals, except SO and CH_3S, have not been subjected to high-resolution PFI-PE studies. The halogen-containing radicals of interest are CCl_2, CBr_2, CClBr, CFBr, $CHBr_2$, and CF_3O. Studies of these radicals are relevant to atmospheric degradation of halohydrocarbons. In addition to the above radical systems, we are also interested in the PIE and PFI-PE studies of simple hydrocarbon radicals C_2H, C_2H_3, and C_2H_5. The PIE and photoelectron studies of C_2H, an important combustion intermediate, have not yet been made.

Publications of DOE sponsored research (1998-2000)

1. R. C. Shiell, M. Evans, S. Stimson, C.-W. Hsu, C. Y. Ng, and J. W. Hepburn, "A High Resolution Study of the Low Lying Correlation Satellites in Xenon", *Phys. Rev. Lett.* **80**, 472 (1998).
2. C.-H. Hsu, P. Heimann, M. Evans, S. Stimson, and C. Y. Ng, "High Resolution Photoelectron Spectroscopy Using Multibunch Synchrotron Radiation: Rotational-Resolved Photoelectron Bands of $O_2^+(b^4\Sigma_g^-, v^+)$", *Chem. Phys.*, (invited article), **231**, 121 (1998).
3. S. Stimson, Y.-J. Chen, M. Evans, C.-L. Liao, C. Y. Ng, C.-W. Hsu, and P. Heimann, "A High Resolution Pulsed Ionization Photoelectron Bands for $H_2^+(X^2\Sigma_g^+, v^+=0, 2, 9, \text{and } 11)$", *Chem. Phys. Lett.* **289**, 507 (1998).
4. S. Stimson, M. Evans, C. Y. Ng, C.-W. Hsu, P. Heimann, C. Destandau, G. Chambaud, and P. Rosmus, "High Resolution Pulsed Field Ionization Photoelectron Band for $OCS^+(X^2\Pi)$: An Experimental and Theoretical Study", *J. Chem. Phys.* **108**, 6205 (1998).
5. S.-W. Chiu, Y.-S. Cheung, N.-L. Ma, W.-K. Li, and C. Y. Ng, A G2 ab initio Study of $C_2H_5S^+$, I. Structures, Energetics, and Unimolecular Isomerizations of Non-Carbenoid Isomers", *J. Mol. Struct. (TheoChem.)*, **452**, 97 (1998).
6. C.-W. Hsu, M. Evan, S. Stimson, and C. Y. Ng, "Rotationally Resolved Photoelectron Spectroscopic Study of O_2: Identification of Vibrational Progression for the $O_2^+(2^2\Pi_u, ^2\Sigma_u^-)$ States", *J. Chem. Phys.* (communication), **108**, 4701 (1998).
7. Y. J. Chen, S. Stimson, P. T. Fenn, and C. Y. Ng, "A Study of the Dissociation of $CH_3CH_2SH^+$ by Collisional Activation: Evidence of Nonstatistical Behavior", J. Chem. Phys. **108**, 8020 (1998).

8. M. Evans, S. Stimson, C. Y. Ng, and C.-W. Hsu, "High Resolution Pulsed Field Ionization Photoelectron Study of O_2: Predissociation Lifetimes and High-n Rydberg Lifetimes Converging to $O_2^+(c^4\Sigma_u^-, v^+=0,1)$", *J. Chem. Phys.* **109**, 1285 (1998).
9. Y.-S. Cheung, J.-C. Huang, and C. Y. Ng, "Vacuum Ultraviolet Laser Pulsed Field Ionization Photoelectron Spectroscopy: Accurate Ionization Energies of CH_3SH and CH_3CH_2SH", *J. Chem. Phys.* **109**, 1781 (1998).
10. Y.-S. Cheung, C.-W. Hsu, and C. Y. Ng, "Non-resonant pulsed field ionization photoelectron study of CH_3CH_2S", (invited article) *J. Electron Spectroscopy & Related Phenomena* **97**, 115 (1998).
11. Y.-S. Cheung and C. Y. Ng, "Vacuum Ultraviolet Single-Photon and Ultraviolet Non-Resonant Two-Photon Pulsed Field Ionization Photoelectron Study of CH_3SCH_3", (invited article) *Int. J. Mass Spectrom Ion Proc.* **185/186/187**, 533 (1999).
12. M. Evans, S. Stimson, C. Y. Ng, and C.-W. Hsu, "Rotationally Resolved Photoelectron study of $O_2^+(B^2\Sigma_g^-, {}^2\Sigma_u^-; v^+=0\text{-}7)$ at 20.2-21.3 eV", *J. Chem. Phys.* **110**, 315 (1999).
13. S.-W. Chiu, Y.-S. Cheung, N. L. Ma, W.-K. Li, and C. Y. Ng, "A Gaussian-2 *ab initio* study of $[C_2H_5S]^+$ ions: II. Fragmentation pathways of $CH_3SCH_2^+$ and $CH_2CHSH_2^+$ revisited", *J. Mol. Struct. (TheoChem.)* **468**, 21 (1999).
14. R. C. Shiell, M. Evans, S. Stimson, C.-W. Hsu, C. Y. Ng, and J. W. Hepburn, "Characterization of Correlation Satellites Below 25 eV in Xeon Probed by Pulsed Field Ionization Photoelectron Spectroscopy", *Phys. Rev. A.***59**, 2903 (1999).
15. L.-S. Sheng, S.-Q. Yu, and C. Y. Ng, "Recent Advances in High Resolution Photoelectron Studies Using Synchrotron Radiation and Lasers", *Progress in Chemistry*, **11**, 153 (1999).
16. K.-C. Lau, W.-K. Li, C. Y. Ng, and S. W. Chiu, "A Gaussian-2 Study of Isomeric $C_2H_2N/C_2H_2N^+$", *J. Phys. Chem.* **103**, 3330 (1999).
17. G. K. Jarvis, Y. Song, and C. Y. Ng, "High resolution pulsed field ionization photoelectron spectroscopy using multi-bunch synchrotron radiation: time-of-flight selection scheme", *Rev. Sci. Instrum.***70**, 2615 (1999).
18. G. K. Jarvis, Y. Song, and C. Y. Ng, "Rotational-Resolved Pulsed Field Ionization Photoelectron Study of $NO^+(a^3\Sigma^+, v^+ = 0\text{-}16)$ in the energy range of 15.6-18.2 eV", *J. Chem. Phys.* **111**, 1937 (1999).
19. Y. Song, M. Evans, C. Y. Ng, C.-W. Hsu, and G. K. Jarvis, "Pulsed Field Ionization Photoelectron Spectroscopy: Rotationally Resolved Photoelectron Bands for $O_2^+(X^2\Pi_{3/2,1/2}, v^+=0\text{-}38)$, *J. Chem. Phys.* **111**, 1905 (1999).
20. G. K. Jarvis, M. Evans, C. Y. Ng, and K Mitsuke, "Rotational-Resolved Pulsed Field Ionization Photoelectron Study of $NO^+(X^1\Sigma^+, v^+ = 0\text{-}32)$ in the energy range of 9.24-16.80 eV", *J. Chem. Phys.***111**, 3058 (1999).
21. G. K. Jarvis, K.-M. Weitzel, M. Malow, T. Baer, Y. Song, and C. Y. Ng, "High Resolution Pulsed Field Ionization Photoelectron-Photoion Coincidence Spectroscopy Using Synchrotron Radiation", *Rev. Sci. Instrum.* **70**, 3892-3906 (1999).
22. D. Fedorov, M. Evans, Y. Song, M. Gordon, and C. Y. Ng, "An Experimental and Theoretical Study of the Spin-Orbit Interaction for $CO^+(A^2\Pi_{3/2,1/2}, v^+=0\text{-}41)$ and $O_2^+(X^2\Pi_{3/2,1/2g}, v^+=0\text{-}38)$", *J. Chem. Phys.* **111**, 6413-6421 (1999).
23. S.-W. Chiu, K.-C. Lau, W.-K. Li, N. L. Ma, Y.-S. Cheung, and C. Y. Ng, "A Gaussian-2 *ab initio* study of $[C_2H_5S]^+$ ions: III. H_2 and CH_4 Eliminations from $CH_3SCH_2^+$ and $CH_2CHSH_2^+$", *J. Mol. Struct. (TheoChem.)*, **490**, 109 (1999).
24. D. S. Peterka, M. Ahmed, C. Y. Ng, and A. G. Suits, "Dissociative Ionization by Ion Imaging with Undulator Synchrotron Radiation: Dissociation Dynamics of SF_6^+", *Chem. Phys. Lett.* **312**, 108 (1999).
25. S.-H. Chien, K.-C. Lau, W.-K. Li and C.Y. Ng, "Energetics and Structure of the Carbonyl Chloride Radical and Oxalyl Chloride", *J. Phys. Chem.* **103**, 7913-7922 (1999).

26. C. Y. Ng, "Advances in Photoionization and Photoelectron Studies Using Third Generation Synchrotron Radiation", Proceedings for the IV International Meeting in Dissociative Recombination", June 15-20, Stockholm, Sweden (World Scientific, Singapore, 1999).
27. K.-M. Weitzel, M. Malow, G. K. Jarvis, T. Baer, Y. Song, and C. Y. Ng, "High-Resolution Pulsed Field Ionization Photoelectron Photoion Coincidence Study of CH_4: Accurate 0 K Dissociation Threshold for CH_3^+ ", *J. Chem. Phys. (Communication)* **111**, 8267-8270 (1999).
28. M. Evans and C. Y. Ng, "Rotational-Resolved Pulsed Field Ionization Photoelectron Bands for $CO^+(X, v^+=0\text{-}42)$", *J. Chem. Phys.* **111**, 8879-8892 (1999).
29. G. K. Jarvis, Y. Song, C. Y. Ng, and E. R. Grant, "A Characterization of Vibrationally Excited NO_2^+ by High-Resolution Threshold Photoionization Spectroscopy", *J. Chem. Phys.* **111**, 9568-9573 (1999).
30. R. C. Shiell, M. Evans, C. Y. Ng, and J. W. Hepburn, "A High Resolution Study of the $D^2\Pi$ and $3^2\Sigma^+$ Satellite States of CO^+", *Chem. Phys. Lett.* **315**, 390-396 (1999).
31. G. K. Jarvis, K.-M. Weitzel, M. Malow, T. Baer, Y. Song, and C. Y. Ng, "High-Resolution Pulsed Field Ionization Photoelectron Photoion Coincidence Study of C_2H_2: Accurate 0 K Dissociation Threshold for C_2H^+", *Phys. Chem. Chem. Phys. (Communication),* **1**, 5259 (1999).
32. C. Y. Ng, "Advances in photoionization and photoelectron studies using third generation synchrotron radiation and UV/VUV lasers", in "Photoionization, and Photodetachment", edited by C. Y. Ng (World Scientific, Singapore, 2000), *Adv. Ser Phys. Chem.* **10A**, in press.
33. C. Y. Ng, editor, "Photoionization and Photodetachment I" (World Scientific, Singapore, 2000), *Adv. Ser Phys. Chem.*, Vol. **10A**, in press.
34. C. Y. Ng, editor "Photoionization and Photodetachment II" (World Scientific, Singapore, 2000), *Adv. Ser Phys. Chem.*, Vol. **10B**, in press.
35. Y. Song, M. Evans, C. Y. Ng, C.-W. Hsu, and G. K. Jarvis, "Rotational-Resolved Pulsed Field Ionization Photoelectron Study of $O_2^+(A^2\Pi_u, v^+=0\text{-}12)$ in the Energy Range of 17.0-18.2 eV, *J. Chem. Phys.* **112**, 1271-1278 (2000).
36. Y. Song, M. Evans, C. Y. Ng, C.-W. Hsu, and G. K. Jarvis, "Rotationally Resolved Pulsed Field Ionization Photoelectron Study of $O_2^+(a^4\Pi_u, v^+=0\text{-}18)$ in the Energy Range of 16.0-18.0 eV, *J. Chem. Phys.* **112**, 1306 (2000).
37. G. K. Jarvis, R. C. Shiell, J. Hepburn, Y. Song, and C. Y. Ng, "Pulsed Field Ionization-Photoion Spectroscopy Using two-bunch Synchrotron Radiation: Time-of-Flight Selection Scheme", *Rev. Sci. Instrum.* **71**, 1325 (2000).
38. T. Baer, Y. Song, C. Y. Ng, J. Liu, and W. Chen, "High-Resolution PFI-PEPICO Studies of Ionic Dissociation at the Advanced Light Source", *Faraday Discussion* **115**, Apr. 3-5, 2000, accepted.
39. A. Yencha, M. C. A. Lopes, G. C. King, M. Hochlaf, Y. Song, and C. Y. Ng, "Ion-Pair Formation Observed in a Pulsed-Field Ionization Photoelectron Spectroscopic Study of HF", *Faraday Discussion* **115**, Apr. 3-5, 2000, accepted.
40. C. Y. Ng, "Advances in Photoionization and Photoelectron Studies Using Third Generation Synchrotron Radiation", *J. Electron Spectroscopy & Related Phenomena*, accepted.
41. T. Baer, Y. Song, C. Y. Ng, W. Chen, and J. Liu, "The Heat of Formation of $C_3H_7^+$ and Proton Affinity of C_3H_6 Determined by Pulsed Field Ionization-Photoelectron Photoion Coincidence Spectroscopy", *J. Phys. Chem.*.
42. W.-K. Li, K.-C. Lau, C. Y. Ng, H. Baumgärtel, and K.-M. Weitzel, "Energetics and Structure of Cl_2O_n and $Cl_2O_n^+$, n=1, 4, 6 and 7", *J. Phys Chem*, accepted.
43. J. Lau, W. Chen, C.-W. Hsu, M. Hochlaf, M. Evans, S. Stimson, and C. Y. Ng, "High-Resolution Pulsed Field Ionization-Photoelectron Study of $CO_2^+(X^2\Pi_g)$ in the energy range of 13.6-14.7 eV", *J. Chem. Phys.*, revised.

KINETICS AND MECHANISMS OF COMBUSTION CHEMISTRY

David L. Osborn
Combustion Research Facility, Mail Stop 9055
Sandia National Laboratories
Livermore, CA 94551-0969
Telephone: (925) 294-4622
Email: dlosbor@sandia.gov

Program Scope

The goal of this program is to elucidate mechanisms of elementary combustion reactions through the use of absorption and emission-based spectroscopy. The technique of time-resolved Fourier transform spectroscopy (TR-FTS) is employed to probe multiple reactants and products with broad spectral coverage (> 1000 cm^{-1}) and a wide range of temporal resolution (ns – ms). In addition to the measurement of thermal rate coefficients as a function of temperature and pressure, the inherently multiplexed nature of TR-FTS makes is possible to simultaneously measure product branching ratios, internal energy distributions, energy transfer, and spectroscopy of radical intermediates. Together with total rate coefficients, this additional information provides further constraints upon and insights into the potential energy surfaces that control chemical reactivity.

For reactions producing vibrationally or electronically excited molecules, emission-based TR-FTS may be used to study the reaction rate, product state, and branching ratios. While several groups have made great progress in gas phase emission-based time-resolved Fourier transform spectroscopy,[1-6] there is very little work in absorption.[7] Absorption techniques are being pursued in this program because they are more general than emission methods, and are not complicated by fluorescence lifetime effects or predissociation. Another thrust of this program is toward kinetic measurements of larger molecules. The development of absorption-based TR-FTS in the mid-infrared "fingerprint" region will enable reactivity studies of larger hydrocarbons (C3 – C6) found in practical fuels. In addition, Fourier transform spectroscopy offers throughput and multiplex advantages over dispersive instruments when used in the infrared. Finally, the broad band spectral detection offered by FTS can allow the identification of unexpected product channels that might go unnoticed by narrow band detection techniques.

Recent Progress

During the last year we designed and constructed the new Kinetics and Mechanisms laboratory in Phase II of the Combustion Research Facility. The time-resolved Fourier transform spectrometer is now operational. As an initial experiment to troubleshoot the system we have focused on the electronic emission from NH_2 $\tilde{A}$ ($^2A_1$), a system that has been studied extensively by Leone and coworkers.[8] When photolyzed at 193 nm, NH_3 fragments to form H + NH_2 $\tilde{A}$ ($^2A_1$). Emission from the ($\tilde{A} \rightarrow \tilde{X}$) transition of NH_2 is measured in both the time and frequency domain simultaneously, as shown in Fig. 1. This preliminary experiment demonstrates the broad spectral coverage (7000 – 15000 cm^{-1}) and fast time resolution (25 ns) capabilities now available in this laboratory. In the step-scan method of TR-FTS used here, the only limitation to the

achievable time resolution is the bandwidth of the detector and sampling rate of the digitizer,[9] with laser-limited rise times of 3 ns observed in the present system.

There are few examples of gas-phase TR-FTS absorption measurements. Absorption-based flash-photolysis experiments generally require long pathlengths to obtain sufficient detection sensitivity. For kinetics measurements, the overlap between the photolysis region and the probed region must have a narrow temperature distribution. One method of achieving both criteria is the use of Herriott multipass laser resonators to confine the overlap region to the center of a reaction cell, where the temperature is well defined.[10] Because broadband radiation used in Fourier transform techniques cannot be described as a Gaussian beam, this light cannot be mode-matched to the Herriott resonator. Nevertheless, we have developed a reentrant beam design for the Herriott resonator that allows it to be used with broadband radiation. In the current version, a total pathlength of over 15 m is achieved, with a photolysis-probe overlap length of ≈ 5 m.

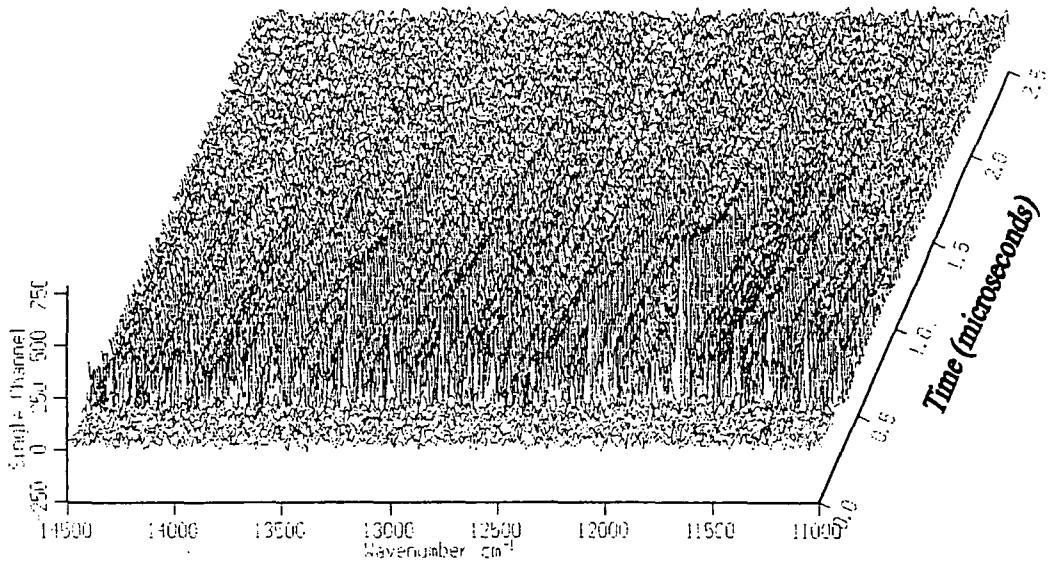

Figure 1. NH_2 emission $\tilde{A}\ (^2A_1) \rightarrow \tilde{X}\ (^2B_1)$.

Very recent emission experiments have focused on the Swan bands of C_2 ($d\ ^3\Pi_g \rightarrow a\ ^3\Pi_u$) produced by 266 nm photolysis of C_2H_2 at 1 – 25 torr. In the Advanced Imaging Laboratory at the Combustion Research Facility, planar laser induced fluorescence (PLIF) imaging of methane/air flames have suggested that laser-generated Swan band emission in these flames may offer a new detection method for C_2 hydrocarbon radicals.[11] The current TR-FTS investigation in the more controlled environment of a low-pressure cell, where the presence and concentration of various C_2 hydrocarbon intermediates can be systematically varied, will shed light on the details of this observation in the PLIF experiments.

Future Plans

The ketenyl radical (HCCO) is an important combustion intermediate, and its reaction with NO is critical in the chemistry of NO reburning. The reaction of ketenyl with NO has two major product channels:

$$\begin{aligned} HCCO + NO &\rightarrow HCNO + CO && (R1) \\ &\rightarrow HCN + CO_2. && (R2) \end{aligned}$$

To explain the removal of NO from reburning systems, modeling results from Miller *et al.*[12] conclude that (R2) is the dominant product channel. However, two experimental investigations of the product branching ratio at room temperature[13,14] find that (R1) is the dominant channel. The concurrent examination of rate constants and branching fractions by TR-FTS may shed further light on this reaction mechanism.

Another area of interest is the spectroscopy of the cyclopropyl radical (C_3H_5). Although it is the simplest cyclic hydrocarbon radical, little is know of its spectroscopy and reactivity. Its isomeric forms, the allyl and methylvinyl radicals, are better understood, and have differing reactivities. The C_3H_5 system is therefore a good candidate for the study of isomerization in combustion systems. However, spectroscopic characterization of cyclopropyl must first be obtained, and efforts are underway toward this goal.

Finally, high spectral brightness broadband sources for use in absorption-based studies are being explored in collaboration with research at Sandia National Laboratories in quasi phased-matched non-linear optical materials.

BES sponsored publications since 1998

David H. Mordaunt, David L. Osborn, and Daniel M. Neumark, "Nonstatistical unimolecular dissociation over a barrier," *J. Chem. Phys.* **108**, 2448 (1998).

References

[1] R. E. Murphy and H. Sakai, in *Proceedings of the Aspen International Conference on Fourier Transform Spectroscopy*, Aspen, p. 301 (1970).
[2] G. Hancock and D. E. Heard, *Adv. Photochem.* **18**, 1 (1993).
[3] T. R. Fletcher and S. R. Leone, *J. Chem. Phys.* **88**, 4720 (1988).
[4] G. V. Hartland, W. Xie, H. L. Dai, A. Simon, and M. J. Anderson, *Rev. Sci. Instrum.* **63**, 3261 (1992).
[5] P. W. Seakins, in *The Chemical Dynamics and Kinetics of Small Radicals*, ed. K. Liu and A. Wagner, Singapore, p. 250 (1995).
[6] G. E. Hall, J. T. Muckerman, J. M. Preses, R. E. Weston, and G. W. Flynn, *Chem. Phys. Lett.* **193**, 77 (1992).
[7] J. Eberhard, P. S. Yeh, and Y. P. Lee, *J. Chem. Phys.* **107**, 6499 (1997).
[8]a) R. A. Loomis, J. P. Reid, and S. R. Leone, *J. Chem. Phys.* **112**, 658 (2000). b) E. L. Woodbridge, M. N. R. Ashfold, and S. R. Leone, *J. Chem. Phys.* **94**, 4195 (1991).

[9] L. T. Letendre, H. L. Dai, I. A. McLaren, and T. J. Johnson, *Rev. Sci. Instrum.* **70**, 18 (1999).
[10] J. S. Pilgrim, R. T. Jennings, and C. A. Taatjes, "Temperature-controlled multiple-pass absorption cell for gas phase chemical kinetics studies," *Rev. Sci. Instrum.* **68**, 1875 (1997).
[11] J. Rehm and P. Paul, unpublished.
[12] J. A. Miller, J. L. Durant, and P. Glarborg, *Twenty-Seventh Symposium (International) on Combustion*, The Combustion Institute, Pittsburg, p. 235 (1998).
[13] U. Eickhoff and F. Temps, *Phys. Chem. Chem. Phys.* **1**, 243 (1999).
[14] K. T. Rim and J. F. Hershberger, *J. Phys. Chem. A* **104**, 293 (2000).

The Effect of Large Amplitude Motion on Spectroscopy and Energy Redistribution in Vibrationally Excited Methanol

David S. Perry, Principal Investigator
Department of Chemistry
University of Akron, Akron OH 44325-3601
DPerry@UAkron.edu

I. Introduction

Molecular vibrations play a fundamental role in chemical reactivity. Vibrationally excited products are produced by exothermic elementary reactions – sometimes preferentially. In a small molecule such as water, vibrations have been shown to cause a dramatic and mode-selective enhancement of subsequent bimolecular reactivity. In simple terms, a potentially reactive atom, whose bond is substantially extended in the course of a molecular vibration, is more easily picked off by an attacking reagent.

In larger molecules above a certain threshold energy, vibrational energy initially deposited in a particular mode will spontaneously and collisionlessly redistribute into other vibrational degrees of freedom and thereby frustrate the search for mode-selective chemistry. On the other hand, fast intramolecular vibrational redistribution (IVR) is the essential assumption in the RRKM theory of unimolecular reactions.

Previous research under this grant has pointed to two important conclusions:

First, large amplitude torsional motion has been identified with acceleration of IVR. Faster IVR has been found when the torsional barrier is low, when the torsional bond is adjacent to an excited vibration, and when internal rotation results in isomerization. This conclusion is also based on work of other groups. See particularly C. S. Parmenter and B. M. Stone, *J. Chem. Phys.* **84**, 4710-4711 (1986), and A. McIlroy and D. J. Nesbitt, *J. Chem. Phys.* **101**, 3421-3435 (1994).

Second, IVR in methanol is not a single process but occurs on multiple timescales following a particular vibrational excitation. The fastest timescales (< 1 ps) reflect the largest spectral splittings and correspond to energy transfer between modes involved in strong low-order resonances. Smaller splittings reflect slower (≈ 1 ps) energy transfer to additional modes. After 10 or so ps energy randomization is thought to occur by multiple indirect coupling pathways. In ethanol, we have indirect information about processes that occur on even longer timescales – such as the decay of molecular alignment, which continues well after the initially prepared vibration has decayed.

Methanol was selected as the model system for the present studies of IVR because it is one of the smallest molecules that incorporates large amplitude motion and has a sufficient number of vibrational modes to offer a diversity of resonances and coupling pathways. It is the objective of this project to use high resolution spectroscopy to explore and quantify vibrational couplings in methanol and thereby to obtain new qualitative insights into the nature of IVR. These studies go beyond the well-studied OH overtone manifold to explore new regions of phase space. The experiments involve sub-Doppler spectroscopy of the fundamental region and lowest overtones in Akron and IRLAPS spectra throughout the overtone region in collaboration with

Rizzo's group in Lausanne Switzerland. The work also includes the development of spectroscopic Hamiltonians and *ab initio* calculations.

II. Vibrational Couplings in the Methanol CH Stretch Manifold

In the fundamental region, our high resolution spectra have shown that the torsional tunneling splittings for the ν_2 and ν_9 vibrations are inverted relative to the ground state [1, 4]. Because this energy level structure was not consistent with existing Hamiltonians, we developed an internal coordinate Hamiltonian to explain the results. The model includes the tunneling of the OH group between the three equivalent potential minima and the three CH stretch vibrations. Since the CH bond *trans* to the OH is in a chemically distinct position from the other two CH bonds, it will have a different force constant. Therefore a vibrational excitation of the *trans* CH bond has to tunnel to the other CH bonds as the OH tunnels to the other equivalent potential minima. This effect, when included to lowest order in a properly symmetrized internal coordinate Hamiltonian, was able to account for the tunnelling behavior of all three CH stretches [4]. The coupling of the CH stretches with the torsion is strong enough to produce a spectral splitting of 42 cm^{-1}.

Based on Hougen's treatise on symmetry considerations is systems with 3-fold internal rotation (J. T. Hougen, *J. Mol. Spectrosc.* **181**, 287 (1997).) and on an analysis of our Hamiltonian, we proposed [4] that inverted torsional structure should be a general phenomenon applicable to other modes and other systems. That expectation is now supported by *ab initio* calculations (L.-H. Xu, submitted for publication) and confirmed by assignment of high resolution spectra of the ν_{11} methyl rock in methanol (R. M. Lees and L. H. Xu., submitted for publication).

Extensive single resonance IRLAPS jet spectra in the first overtone region have been obtained including the OH overtone $2\nu_1$ and the CH overtone stretch-bend polyad containing 39 individual bands. Also found with intensity comparable to the CH overtone polyad are the CH + OH combinations, $\nu_1+\nu_3$ and $\nu_1+(\nu_2/\nu_9)$, and the OH stretch-bend combination, $\nu_1+2\nu_6$. In addition, we have found and rotationally assigned two combination vibrations, $2\nu_1+\nu_{12}$, and $2\nu_1+2\nu_{12}$, that include torsional excitation.

Additional IRLAPS jet spectra have been obtained in the regions of 3 and 4 quanta of CH stretch. Although the number of bands in each polyad increases dramatically, the spectra appear simplified at the higher overtones. This simplification, which is consistent with the transition to local mode behavior and a partial detuning from the CH stretch-bend resonance, provides a key to the interpretation of the spectra.

David Rueda, a doctoral student at the EPFL in Lausanne, recently spent two months in Akron to begin the task building a Hamiltonian to model the CH overtone data. The internal coordinate model constructed, contains all of the CH stretch combinations and nearly isoenergetic combinations with HCH bends. The polyad quantum number is $v_{CH}=v_2+v_3+v_9+(v_4+v_5+v_{10})/2$. Initial results support a convergence toward local mode behavior by $v_{CH}=4$. While this kind of reduced-dimensional internal co-ordinate model has been used in the literature, fundamental limitations can be expected because the bending vibrations, ν_4 ν_5 and ν_{10}, are not well described as linear combinations of local HCH bends but contain also significant amounts of methyl rock, CO stretch, and COH bend. Therefore, this work will explore the limitations of reduced-dimensional internal coordinate Hamiltonians.

III. The Role of a Potentially Reactive Pathway

Consider two results from our recent publications on vibrational mode coupling in methanol:

1. The 50 cm^{-1} splitting observed in the $5\nu_1$ region of the OH stretch overtone manifold is assigned to an interaction between the OH and CH stretch vibrations [3]. Specifically, the coupling matrix element between the $5\nu_1$ and $4\nu_1+\nu_2$ bands is found to be 23.5 cm^{-1}. The assignment of this interaction is based on its tuning through the $4\nu_1$, $5\nu_1$, and $6\nu_1$ regions and was confirmed by isotopic studies. Note that the vibrational amplitude ν_2 CH stretch is predominantly on the CH bond *trans* to the OH bond and that interactions with the other two CH stretches, ν_3 and ν_9, are not observed in the spectra. An internal coordinate analysis (L Halonen, *J. Chem. Phys.* **106**, 7931 (1997).) also supports the assertion that the dominant interaction is between the OH bond and the *trans* CH bond.

2. Rotationally resolved and state-selected spectra in the OH stretch manifold show a monotonic decrease in the torsional tunneling splitting from 9.1 cm^{-1} in the ground state to 1.6 cm^{-1} in the $6\nu_1$ band [6]. This behavior indicates an increase in the torsional barrier height from 373 cm^{-1} in the vibrational ground state to more than 600 cm^{-1} when 6 quanta of the OH stretch are excited. We have now confirmed this trend with data on ^{13}C methanol including sub-Doppler slit jet spectra of the ν_1 fundamental and state-selected IRLAPS spectra in the overtone region. The variation of the torsional barrier with OH stretch excitation reflects a strong coupling between these degrees of freedom.

To shed light on these results, *ab initio* calculations on methanol were undertaken at a variety of levels. At the *MP2/6-311+G(2d,p)* level, a grid of points was calculated for different combinations of OH bond lengths and bond lengths of the *trans* CH. At each point, all of the other nuclear degrees of freedom were optimized to achieve a minimum energy geometry. In this way, the effect of changes in the OH and CH bond lengths, either separately or in combination, on the molecular geometry could be deduced.

The qualitative results are summarized as follows. When both the OH and *trans* CH bonds are substantially extended, the CO bond shortens and the geometry adjusts to reflect the potentially reactive pathway

$$CH_3OH \rightarrow CH_2O + 2H\,.$$

Because of the formation of a CO double bond in formaldehyde, the resulting energy is substantially less than would be predicted by independent OH and CH bond extensions. The *ab initio* calculations show that the effect of this potentially reactive pathway extends well down into the bound region and accounts for the OH – CH coupling observed in the experiments. In fact the effect of formaldehyde channel is felt even when only the OH bond is extended. At an OH extension corresponding to the energy of $6\nu_1$, the CO bond shortens slightly reflecting about a 1% double bond character. Because double bonds are torsionally rigid with barriers to internal rotation of 30,000 cm^{-1} or more (e.g., in ethylene), the addition of 1% double bond character is sufficient to almost double the barrier height.

Therefore, the existence of a potentially reactive pathway is able to explain two different kinds of vibrational mode coupling that, at first, appeared to be unrelated. The formaldehyde reaction channel is not a simple bond dissociation, but it involves the formation of a new chemical bond and it is the incipient bond formation that is responsible for the vibrational mode coupling.

IV. Plans for the Coming Year

The CH overtone manifold will provide the focus for the next year's work.

The first task is to understand the course structure in the various polyads. We will look for the v_{CH}=5 polyad to confirm the trend toward local behavior. Spectra of the isotopomer CH_3OD will be free of overlap of the $3\nu_1$ band with the v_{CH}=4 polyad. Spectra of isotopomers with a single methyl hydrogen, CHD_2OH and CHD_2OD, will be much simpler and provide an important check on the assignment and modeling of regular methanol spectra. The coarse structure of the overtone spectra provides information on the fastest IVR timescales (10 – 100 fs) and the strongest interactions including local-local coupling and stretch-bend coupling.

To understand the subsequent timescales including torsion-vibration coupling, rotationally resolved and assigned spectra are needed. Because double resonance IRLAPS spectra in the CH overtone manifold have not yet been possible, this is the task of high resolution spectroscopy. CW cavity ringdown spectroscopy will be developed based on an external cavity diode laser. Target vibrations include the CH – OH combination bands and bands in the v_{CH}=2 polyad to be selected based on the results of the modeling effort. The high resolution spectra provide additional information including the symmetry and torsional structure of each band that could be crucial in verifying a model.

V. Publications, 1997 - 99

[1] L.-H. Xu, X. Wang, T.J. Cronin, D.S. Perry, G.T. Fraser, and A.S. Pine, *Sub-Doppler infrared spectra and torsion-rotation energy levels of methanol in the CH stretch region, J. Mol. Spectrosc.*, **185**, 158-172 (1997).

[2] D.S. Perry, *Timescales and mechanisms of intramolecular energy redistribution*, in *Highly Excited Molecules: Relaxation, Reaction, and Structure*, Amy S. Mullin and George C. Schatz, eds. (ACS Publishing, Washington DC 1997) pp 70-80.

[3] O.V. Boyarkin, L. Lubich, R.D.F. Settle, D.S. Perry, and T.R. Rizzo, *Intramolecular energy transfer in highly vibrationally excited methanol. I. Ultrafast dynamics, J. Chem. Phys.*, **107**, 8409-8422 (1997).

[4] X. Wang and D. S. Perry, *An internal coordinate model of coupling between the torsion and C-H stretch vibrations in methanol, J. Chem. Phys.* **109**, 10795-10805 (1998).

[5] O.V. Boyarkin, T.R. Rizzo, and D.S. Perry, *Intramolecular energy transfer in highly vibrationally excited methanol. II. Multiple time scales for energy redistribution, J. Chem. Phys.*, **110**, 11359-11367 (1999).

[6] O.V. Boyarkin, T.R. Rizzo, and D.S. Perry, *Intramolecular energy transfer in highly vibrationally excited methanol. III. Rotational and torsional analysis, J. Chem. Phys.*, **110**, 11346-11358 (1999).

[7] T. J. Cronin, X. Wang, and D. S. Perry, *High resolution infrared spectra in the C-H region of CH_2F_2: The ν_6 and $2\nu_2$ bands, J. Mol. Spectrosc.*, **194**, 236-242 (1999).

Partially-Premixed Flames in Internal Combustion Engines

Professor Robert W. Pitz, Program Manager and Co-Principal Investigator
Department of Mechanical Engineering, Vanderbilt University, Nashville, TN 37235
robert.w.pitz@vanderbilt.edu
Dr. Michael C. Drake and Dr. Todd D. Fansler, Co-Principal Investigators
General Motors R & D Center, 30500 Mound Road, Warren, MI 48090-9055
michael_c._drake@gmr.com, tfansler@gmr.com
Professor Volker Sick, Co-Principal Investigator
Department of Mechanical Engineering and Applied Mechanics, University of Michigan
2023 W. E. Lay Automotive Laboratory, Ann Arbor, MI 48109-2121
vsick@umich.edu

Program scope

The purposes of this joint university-industry research program are: 1) to use advanced laser diagnostics and detailed chemistry models to understand partially-premixed flames in unique laboratory burners, 2) to use advanced laser diagnostics to observe and characterize partially-premixed combustion in optically-accessible direct injection gasoline engines, and 3) to more fully develop laser diagnostic techniques for temperature and flame front imaging in partially-premixed flames and IC engines. The work is being done primarily at Vanderbilt University, General Motors Research and Development Center, and the University of Michigan.

The goals of this research are 1) a better understanding of the effects of strain and curvature on partially-premixed flame structure, 2) better conceptual models of partially-premixed combustion in highly stratified direct injection engines for automotive applications, and 3) improved and more robust laser diagnostic methods for use in university and industrial environments.

Recent progress

At Vanderbilt University, premixed and partially-premixed laminar flames with curvature are being studied both experimentally and numerically, and at the University of Michigan, in-cylinder turbulent flames are being studied experimentally. The laminar flame work at Vanderbilt focuses on flames produced in a unique burner that provides a cylindrical flame whose flame stretch is constant everywhere on the flame surface. Similar burners have been used or modeled by others (Yamamato et al. 1994; Nishioka et al. 1991; Smooke and Giovangigli 1990; Kobayashi and Kitano 1989) but all of these experimental and numerical investigations were for premixed flames only, where only one reactant flow travels radially inward. The unique feature of the Vanderbilt cylindrical burner is that it has an inner nozzle, made of a porous sintered metal tube, through which a second reactant flow travels radially outward, as shown in Fig. 1a. This type of flowfield can be numerically modeled using a quasi-one-dimensional analysis, similar to that used for planar counterflow flames created in opposed jet flows, whose geometry is shown in Fig. 1b. With the Vanderbilt Cylindrical Burner, laminar flames can be created that are subject to both partial premixedness and flame curvature, both of which are important in stratified charge direct injection spark ignition (DISI) engines, where highly curved flames travel from burnable, near-stoichiometric regions into adjacent very-lean or very-rich regions (Haworth et al. 2000). The relatively high hydrocarbon emissions resulting from stratified charge operation need to be addressed before widespread use of these energy-saving engines occurs in North America.

Recent progress at Vanderbilt includes the construction and operation of the partially-premixed cylindrical burner. An end view (nearly along the cylindrical axis) is shown in Fig. 2, where a cylindrical methane-fueled pure diffusion flame is shown created by issuing methane (equivalence ratio, ϕ, of ∞) from the inner nozzle onto an inwardly traveling flow of pure air ($\phi = 0$). Figure 3 shows an end view exactly along the cylindrical axis, showing the circular nature of the flame. Figure 4 shows a view of the same flame, looking in the radial direction from an optical port that forms part of the outer nozzle. To-date, pure diffusion flames, partially-premixed, and premixed flames have been created in the burner.

However in all situations the radially-inward traveling flow has been air only with no partial premixing. Future efforts will include adding fuel to the outer flow to create a lean stoichiometry for the outer flow. This will allow a "triple flame" to be established, where lean reactants from the outer flow burn and then impinge upon the rich, burned reactants coming from the inner flow, producing a third flame (a diffusion flame) between the rich and lean premixed flames. This is a situation expected in stratified charge operation of the DISI engine. Flat, partially-premixed propane air flames are currently being investigated at Vanderbilt using a visible Raman system (Osborne et al. 2000) that provides major species and temperature information. These flat flames are produced in a conventional opposed jet burner (see Fig. 1b) and provide information to allow decoupling of the combined effects of strain rate and flame curvature in the cylindrical flames.

Vanderbilt researchers, collaborating with Dr. C. J. Sung at Case Western Reserve University, are in the process of modifying a formerly freeware version of the Oppdiff code (Kee et al. 1999) to allow it to model curved, partially-premixed laminar flames. The present status of these modifications allows modeling of premixed flames with the premixed reactants inwardly traveling from the outer nozzle. Others have modeled these types of premixed flames in the past, using their own in-house codes (Nishioka et al. 1991; Smooke and Giovangigli 1990). Figure 5 shows a comparison of numerical results using either the modified Oppdiff code or an in-house code used by Nishioka et al. (1991) to model a stoichiometric methane-air flame entering a cylindrical burner with a moderate velocity (200 cm/sec) at a burner radius of 8.5 mm. Both sets of numerical data are based on the same reaction mechanism (from Nishioka et al.) and predict the same radial location for the flame, thus giving confidence to the modifications made to-date on the Oppdiff program. Experimental flame structure data for cylindrical flames is almost nonexistant, except for thermocouple-measured flame temperatures obtained in stoichiometric propane-air flames (Kobayashi and Kitano 1989). These experimental data are reproduced in Fig. 6 and are compared to numerical predictions, again obtained using the modified Oppdiff code but now using a propane-air mechanism (Smooke and Giovangigli 1988). There is a substantial difference between numerically predicted and experimentally measured flame location for both boundary velocities, indicating further experimental work is needed to assess the performance of this and other propane-air reaction mechanisms, especially if used to model curved laminar flames.

At the University of Michigan, the following progress has occurred: Advances in the optical setup for in-cylinder fuel measurements have been made. A tunable excimer laser has been used to form a counter-propagating pair of light sheets that illuminate a cross section in a static gasoline direct injection engine model. This model was built using a pent-roof cylinder head, equipped with both a high-pressure fuel injector and windows for optical access. A single-cylinder engine with similar optical access is currently under construction. The counter-propagating beam arrangement helps to minimize laser beam attenuation effects on measured LIF and Mie scattering signals from fuel sprays.

The evolution of the fuel distribution in space and time is studied using the model engine with a combination of LIF and Mie scattering images, obtained simultaneously from a single laser pulse. A high throughput filter is used to separate Mie scattering signals from LIF that originates from 3-pentanone. The 3-pentanone molecule is used as a fluorescence tracer and is added in small quantities to the isooctane fuel. The combination of LIF and Mie images yields information about the Sauter-Mean diameter of the fuel droplets, and the change of this quantity in both time and space is addressed. As expected from a spray with an evaporative liquid, the mean droplet diameter decreases over time. Using the engine model, the setup has been shown to be robust and reliable and will be used in its current design for the actual engine experiments.

With a single pulse from the tunable excimer laser and one ICCD camera it is now possible to simultaneously obtain any of the following pairs of measurements: fuel and OH, fuel and NO, liquid and vaporized fuel (limited by dynamic range of ICCD cameras), or two different fuel components. For the simultaneous measurement of temperature and any of the named quantities, tests were performed to measure Rayleigh scattering images in the engine model. However, scattering from the cylindrical quartz liner produces a substantial background signal, in particular when using vertical light sheets and side-view detection. A somewhat better result is obtained when viewing through the piston window. At this

point it seems that a temperature measurement strategy, as shown by Einecke et al. (1998),which is based on two-line LIF of 3-pentanone, will be better suited for the measurements in the direct injection engine.

Future plans

At Vanderbilt the modified Oppdiff code will undergo its last modification: transformation of the inner boundary condition from an axis of symmetry at the radial origin into a prescribed set of velocity, temperature, and mole fraction values at a nonzero radial location. This will allow modeling of curved and partially-premixed flames. Experimentally, the cylindrical burner will be inserted into the visible Raman system at Vanderbilt, allowing nonintrusive temperature and mole fraction measurements to be obtained. Both propane and methane will be used as fuels, in order to determine the effects of Lewis number variation upon flame structure for curved, strained, partially-premixed flames.

At Michigan, a robust setup for the two-line temperature imaging will be realized and tested before setting it up at the engine. The excimer laser setup will be installed at the optical engine and measurements of flame front evolution will be performed. The same setup can be directly used for NO imaging by tuning the excimer laser to the appropriate wavelength and changing the ICCD camera filter.

References

Einecke, S., C. Schulz, V. Sick, R. Schiessl, A. Dreizler, and U. Maas, (1998), "Two-dimensional temperature measurements in the compression stroke of a SI engine using two-line tracer LIF," SAE Transactions, Vol. 107 Journal of Engines, Section 4, 1060-1068, and also SAE Technical Paper 982468, San Francisco

Kee, R. J., F. M. Rupley, J. A. Miller, M. E. Coltrin, J. F. Grcar, E. Meeks, H. K. Moffat, A. E. Lutz, G. Dixon-Lewis, M. D. Smooke, J. Warnatz, G. H. Evans, R. S. Larson, R. E . Mitchell, L. R. Petzold, W. C. Reynolds, M. Caracotsios, W. E. Stewart, and P Glarborg, (1999), "CHEMKIN Collection," Release 3.5, Reaction Design, Inc., San Diego, CA.

Kobayashi, H., and M. Kitano, (1989), "Extinction Characteristics of a Stretched Cylindrical Premixed Flame," *Combustion and Flame*, 76, pp. 285-295.

Haworth, D. C., R. J. Blint, B. Cuenot, and T. J. Poinsot, (2000), "Numerical Simulation of Turbulent Propane-Air Combustion with Nonhomogenous Reactants," *Combustion and Flame*, 121, pp. 395-417.

Nishioka, M., K. Inagaki, S. Ishizuka, and T. Takeno, (1991), "Effects of Pressure on Structure and Extinction of Tubular Flame," *Combustion and Flame*, 86, pp. 90-100.

Osborne, R. J., J. A. Wehrmeyer, and R. W. Pitz, (2000), "A Comparison of UV Raman and Visible Raman Techniques for Measuring Non-Sooting Partially Premixed Hydrocarbon Flames." AIAA Paper 2000-0776 presented at the 38th Aerospace Sciences Meeting, Reno, NV, Jan. 10-13.

Smooke, M. D., and V. Giovangigli, (1990), "Extinction of Tubular Premixed Laminar Flames with Complex Chemistry." in *Twenty-Third Symposium (International) on Combustion*, pp. 447-454, The Combustion Institute, Pittsburgh.

Yamamoto, K., S. Ishizuka, and T. Hirano, (1994), "Effects of Rotation on the Stability and Structure of Tubular Flame," in *Twenty-Fifth Symposium (International) on Combustion*, pp. 1399-1406, The Combustion Institute, Pittsburgh.

Publications acknowledging DOE support

Osborne, R. J., J. A. Wehrmeyer, and R. W. Pitz, (2000), "A Comparison of UV Raman and Visible Raman Techniques for Measuring Non-Sooting Partially Premixed Hydrocarbon Flames." AIAA Paper 2000-0776 presented at the 38th Aerospace Sciences Meeting, Reno, NV, Jan. 10-13.

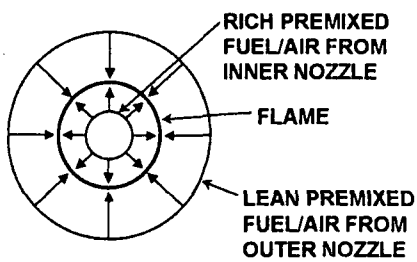

Fig. 1a. Cylindrical counterflow burner geometry.

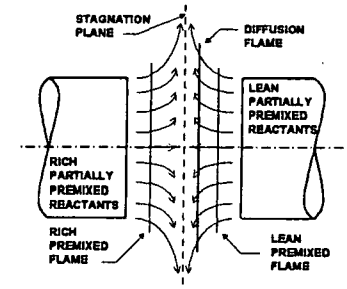

Fig. 1b. Opposed jet counterflow burner geometry.

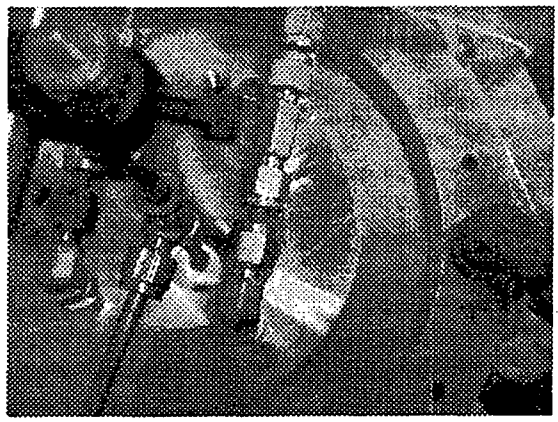

Fig. 2. End view of methane-air diffusion flame looking almost along cylindrical axis.

Fig. 3. End view of methane-air diffusion flame with co-flow tubing removed to show circular flame edge. Flame diameter ~1 cm.

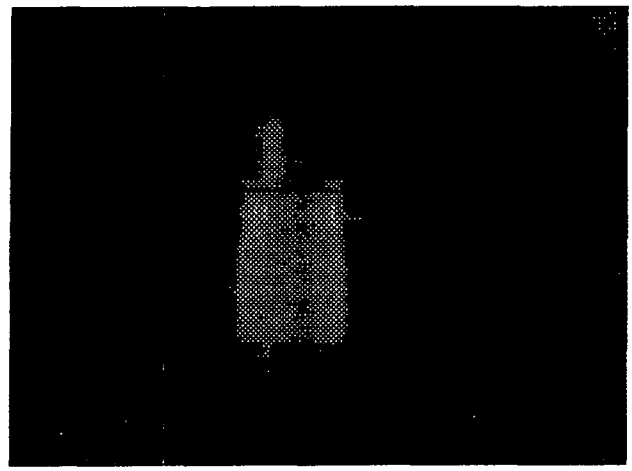

Fig. 4. View of cylindrical methane-air diffusion flame, looking radially inward through optical access port. Flames axial length ~ 2cm.

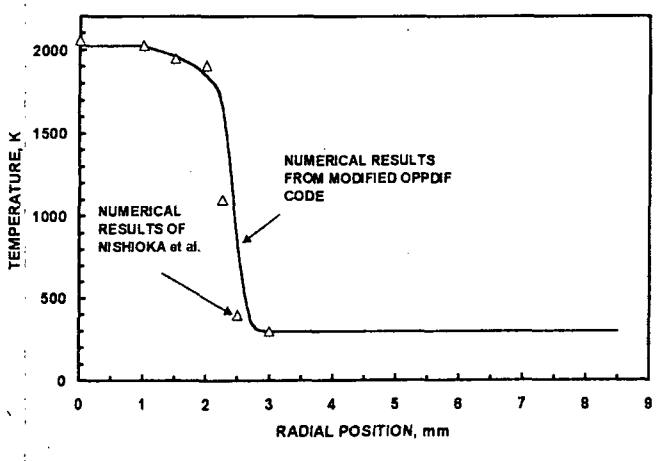

Fig. 5. Numerically predicted temperature profiles for stoichiometric, premixed methane-air flames in cylindrical burner with boundary velocity of 200 cm/sec at 8.5 cm radius.

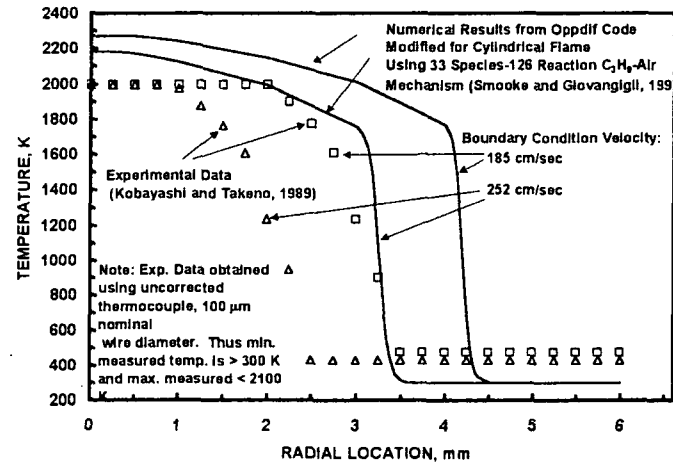

Fig. 6. Numerical and experimental temperature profiles for stoichiometric, premixed propane-air flames in cylindrical burner with 6 mm radius.

INVESTIGATION OF NON-PREMIXED TURBULENT COMBUSTION

Grant: DE-FG02-90ER14128

Principal Investigator: Stephen B. Pope
Sibley School of Mechanical & Aerospace Engineering
Cornell University
Ithaca, NY 14853
pope@mae.cornell.edu

Introduction

It is desirable to design combustion equipment to maximize the efficient utilization of the fuel, while minimizing the environmental impact of the combustion products. In most of the industries involved, turbulent combustion models are employed as a primary design tool. These are computer models that predict the combustion performance by solving a set of equations that model the fundamental physical and chemical processes involved. The aim of the current research is to apply the best available turbulent combustion models to turbulent flames for which there are reliable experimental data, in order to test (and if necessary improve) the submodels involved.

The turbulent combustion models considered are PDF methods, in which a modelled transport equation is solved for the joint probability density function of velocity, turbulence frequency, and the thermochemical composition of the fluid (species mass fractions and enthalpy). The modelled PDF equation is solved numerically using a particle/mesh method. Considerable effort has been devoted to improving the accuracy and efficiency of these methods.

Improved PDF Algorithms

The code PDF2DV is the basic computational tool that we have been using to perform PDF calculations over the past five years. It uses a particle/mesh method to solve the modelled transport equation for the joint PDF of velocity, turbulent frequency, and thermochemical composition. It does so for statistically two-dimensional (plane or axi-symmetric) recirculating flows—a class of flows that includes most of the relevant laboratory experiments.

While PDF2DV can be used to obtain accurate solutions to the modelled PDF transport equation, there are two motivations to develop alternative algorithms. The first is the fact that the bias in PDF2DV is unexpectedly large, and hence a large number of particles is required in order to make this numerical error acceptably small (Xu & Pope 1999). An alternative algorithm, with smaller bias, would achieve the same accuracy at lower computational cost. The second motivation is to develop a PDF algorithm that can be combined with existing finite-volume codes, to facilitate technology transfer and the incorporation of the PDF methodology within existing LES codes.

The alternative numerical approach that has been developed is a completely consistent hybrid algorithm (Muradoglu et al. 1999, Jenny et al. 1999a), consisting of a finite-volume (FV) code and particle code. The FV code solves the standard mean equations for the conservation of mass, momentum and energy, along with the mean equation of state. The particle method solves the modelled transport equation for the fluctuating velocity and thermochemical composition. In fact, two separate codes have been developed to implement this hybrid approach, with the coupling between the FV and particles codes being effected by different strategies.

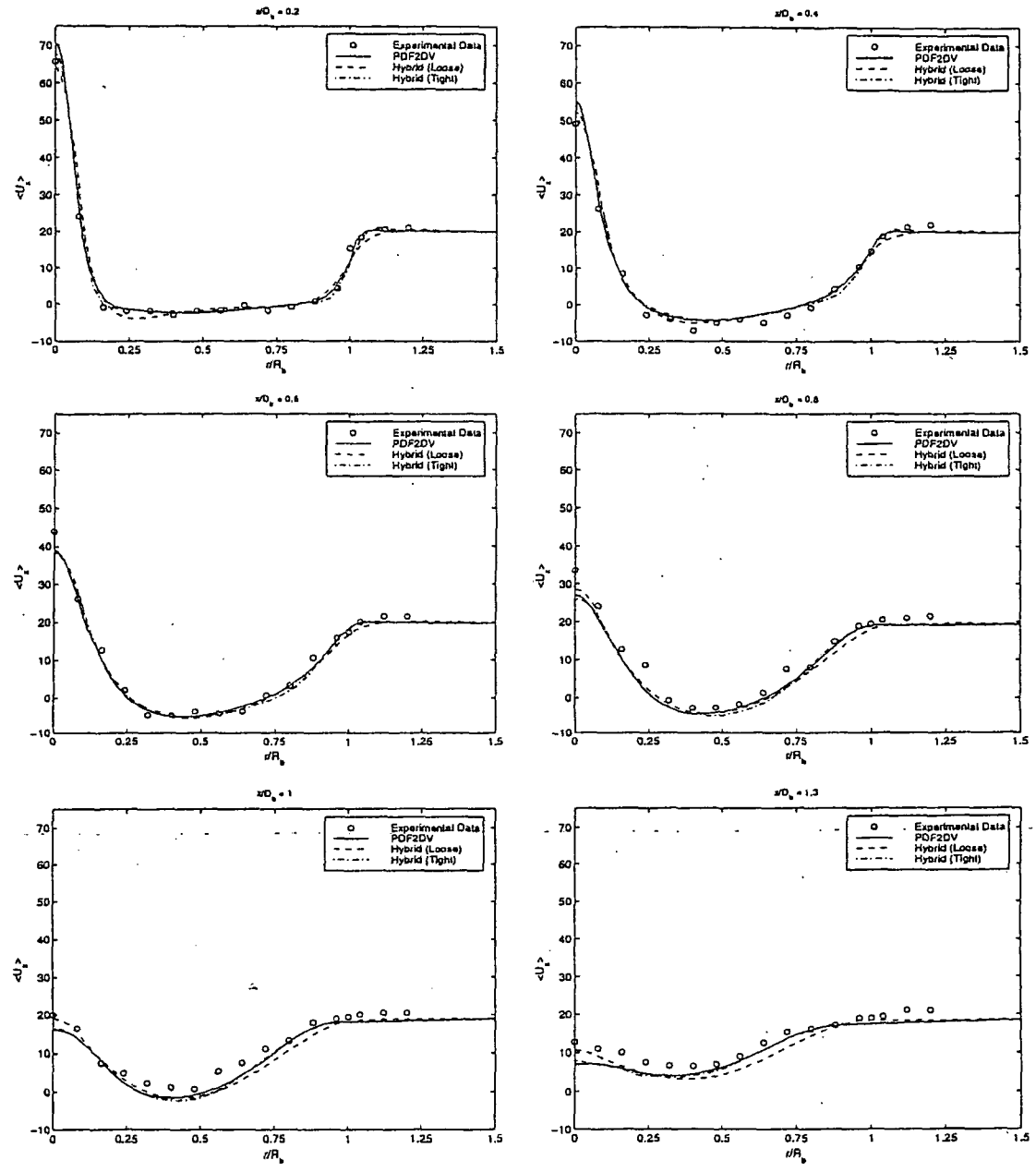

Figure 1: Radial profiles of mean axial velocity in a bluff body flow: symbols, experimental data of Dally et al. 1998; lines, PDF calculations using three different numerical methods.

In the paper Jenny et al. (1999b), these three methods are compared (i.e., PDF2DV and the two different hybrid methods). As an example, Fig. 1 shows the calculated mean velocity profiles in a bluff-body flow compared to experimental data (see Dally et al. 1998). As may be seen from the figure, there is excellent agreement between the three codes, and also with the experimental data.

Quantitative examination of the numerical errors reveals that indeed the bias in the hybrid methods is very small. As a consequence, the computational efficiency of the new methods is greater than that of PDF2DV by at least a factor of 40. That is, for the given accuracy requirement of 5% numerical errors in mean quantities, the new methods require less CPU time by at least a factor of 40. This greatly reduced computational requirement significantly increasing our ability to test different turbulent-combustion submodels.

PDF Calculations of Turbulent FLames

The objective of this part of the work is to apply the most advanced PDF methods to make detailed calculations of the non-premixed flames for which there are reliable experimental data. This is part of the international collaborative effort being led by R.S. Barlow of Sandia National Laboratories.

Using the base model, comprehensive calculations have been performed of the piloted jet flames measured by Barlow & Carter (1998). The calculations of Xu & Pope (2000) show quantitative agreement for the degree of local extinction as a function of axial distance and jet velocity. The calculations of Tang, Xu and Pope (2000) include NO_x and the effects of radiation.

Work on the bluff-body flames is in progress and will be reported at the next Turbulent Non-premixed Flame Workshop (Delft, July 2000).

Turbulent nonpremixed swirl-stabilized flames are common in practical combustors and form the next level of complexity after piloted and bluff-body stabilized flames. Modeling swirling flows remains a challenge especially when the swirl level is high enough to induce vortex breakdown and recirculation. In a collaboration with the University of Sydney, PDF calculations have been made of a new swirl burner (Masri et al. 2000). This burner is capable of stabilizing turbulent nonpremixed flames which have high swirl numbers and which may have a significant degree of turbulence-chemistry interactions. In the PDF calculations, a simple flamelet library is used to represent chemistry. These simple computations reproduce the correct flow structure and compare well with the measured velocity field.

Future Plans

Topics of current and future work are:

1/ to improve the accuracy and efficiency of the particle-mesh method used to solve the PDF equations

2/ for the piloted-jet and bluff-body flames, examine the accuracy of the calculations obtained using different submodels (e.g., the modified Curl mixing model instead of EMST; the LIPM model instead of SLM; and various reduced chemical mechanisms).

References

1. R.S. Barlow and J.M. Frank (1998) Twenty-seventh Symp. (Int'l) on Combust., p. 1087, Pittsburg, The Combustion Institute.

2. B.B. Dally, D.F. Flectcher and A.R. Masri (1998) "Flow and mixing fields of turbulent bluff body jets and flames." Combust. Theory Modelling. **2**, 193–219.

3. J. Xu and S.B. Pope (1999) "Assessment of numerical accuracy of PDF/Monte Carlo Methods for Turbulent Reactive Flows," Journal of Computational Physics, **152**, 192–230.

4. M. Muradoglu, P. Jenny, S.B. Pope and D.A. Caughey (1999). "A Consistent Hybrid Finite-Volume/Particle Method for the PDF Equations of Turbulent Reactive Flows," Journal of Computational Physics **154**, 342–371.

5. P. Jenny, S.B. Pope, M. Muradoglu and D.A. Caughey (1999) "A new hybrid algorithm to solve the fully joint PDF equation for turbulent reactive flows," J. Comp. Phys. (submitted).

6. P. Jenny, M. Muradoglu, K. Liu, S.B. Pope, D.A. Caughey (1999) "PDF simulations of a bluff-body stabilized flow", J. Comp. Phys. (submitted).

7. A.R. Masri, S.B. Pope and B.B. Dally (2000) "PDF computations of a strongly swirling nonpremixed flame stabilised on a new burner", Twenty-Eighth Symp. (Int'l) on Combust. (to be published).

8. Q. Tang, J. Xu and S.B. Pope (2000) "PDF calculations of local extinction and NO production in piloted-jet turbulent methane/air flames", Twenty-Eighth Symp. (Int'l) on Combust. (to be published).

9. J. Xu and S.B. Pope (1999) "Assessment of numerical accuracy of PDF/Monte Carlo Methods for Turbulent Reactive Flows," Journal of Computational Physics, **152**, 192–230.

10. J. Xu and S.B. Pope (2000) "PDF calculations of turbulent nonpremixed flames with local extinction," Combust. Flame (to be published).

Publications from DOE research, 1998–2000

1. M.R. Overholt and S.B. Pope (1998) " A deterministic forcing scheme for direct numerical simulations of turbulence," Computers & Fluids, **27**, 11–28.

2. M.R. Overholt and S.B. Pope (1999) "Direct Numerical Simulation of a Statistically Stationary Turbulent Reacting Flow," Combustion Theory and Modelling, **3**, 371–408.

3. M. Muradoglu, P. Jenny, S.B. Pope and D.A. Caughey (1999). "A Consistent Hybrid Finite-Volume/Particle Method for the PDF Equations of Turbulent Reactive Flows," Journal of Computational Physics **154**, 342–371.

4. P. Jenny, S.B. Pope, M. Muradoglu and D.A. Caughey (1999) "A new hybrid algorithm to solve the fully joint PDF equation for turbulent reactive flows," J. Comp. Phys. (submitted).

5. P. Jenny, M. Muradoglu, K. Liu, S.B. Pope, D.A. Caughey (1999) "PDF simulations of a bluff-body stabilized flow", J. Comp. Phys. (submitted).

6. A.R. Masri, S.B. Pope and B.B. Dally (2000) "PDF computations of a strongly swirling nonpremixed flame stabilised on a new burner", Twenty-Eighth Symp. (Int'l) on Combust. (to be published).

OPTICAL PROBES OF ATOMIC AND MOLECULAR DECAY PROCESSES

S.T. Pratt
Building 200, D-177
Argonne National Laboratory
9700 South Cass Avenue
Argonne, Illinois 60439

Telephone: (630) 252-4199
E-mail: stpratt@anl.gov

PROJECT SCOPE

The study of molecular photoionization and photodissociation dynamics provides insight into (1) the intramolecular mechanisms by which energy and angular momentum are exchanged and redistributed among the internal degrees of freedom of highly excited molecules and (2), more specifically, into the mechanisms that determine the decay pathways and product-state distributions for the excited molecules. This project is aimed at addressing how these mechanisms can give rise to mode-specific effects (that is, decay rates, products, or branching ratios) showing a significant dependence on the quantum numbers of the excited state. An important aspect of this project is that multiple detection techniques are used to provide a more complete characterization of the decay processes, including the determination of product ionic-state distributions, neutral-state distributions, and their relative yields. Excited-state absorption spectroscopy, which reflects the total excitation probability, is also used for comparison with measurements made by monitoring specific decay channels. The wide variety of complementary experimental techniques employed include single- and multiphoton excitation techniques, mass spectrometry, dispersive and threshold photoelectron spectroscopy, and laser-induced fluorescence.

RECENT PROGRESS

In the past year, the principal emphasis of our work was on understanding several different aspects of the mechanisms for vibrational autoionization in ammonia. Vibrational autoionization is a form of intramolecular vibrational-to-electronic energy transfer in which a quasibound resonance above the ionization threshold of a neutral molecule decays into the continuum by the conversion of vibrational energy of the molecular core into electronic (and, ultimately, translational) energy of the escaping electron. Among the questions we have addressed are: (1) for a given set of vibrational quantum numbers of the quasibound state, which vibrational levels of the ion are populated? (2) for autoionization involving an odd number of quanta in nontotally symmetric vibrations, how is the total symmetry of the isolated molecule preserved? and (3) when two or more vibrational modes are populated in the resonance, for which mode is vibrational autoionization most efficient? As discussed below, progress has been made toward answering all three questions. This work focuses on vibrational-to-electronic energy transfer and ionization dynamics. However, through the application of the concept of microscopic reversibility, it is hoped that the results will also provide information on processes involving intramolecular electronic-to-vibrational energy transfer such as internal conversion and intersystem crossing. In particular, this work may provide insight into promoting modes, i.e., vibrational modes that promote radiationless transitions, and into the involvement of rotational degrees of freedom in these intramolecular processes.

To address question (1), we have used photoelectron spectroscopy to study the vibrational branching ratios for autoionization of a wide variety of planar Rydberg states of ammonia converging to the NH_3^+ $\tilde{X}\,^2A_2''(0200)$ and (1300) ionization thresholds. These Rydberg states were populated by double-resonance excitation via the corresponding vibrational level of the $C'\,^1A_1$ state. (Here, ν_1 is the symmetric stretch and ν_2 is the umbrella vibration.) These states can autoionize by a variety of different changes in the vibrational quantum numbers, but in all cases $\Delta v = -1$ processes were found to dominate. Similar behavior has been observed in a number of other molecules and is consistent with the vibrational propensity rule that states that processes with the minimum allowed change in vibrational quantum numbers are fastest.

To address question (2), we have used very high resolution photoelectron spectroscopy to record rotationally resolved photoelectron spectra of autoionizing nd Rydberg states converging to the NH_3^+ $\tilde{X}\,^2A_2''(0200)$ threshold. These states preferentially autoionize by $\Delta v_2 = -1$ processes into the NH_3^+ $\tilde{X}\,^2A_2''(0100)$ continuum. Because the ν_2 vibration is nontotally symmetric in planar NH_3, this process results in a change in the vibrational symmetry of the system, which must be compensated by a change in either the electronic symmetry or the rotational symmetry. The selection rules for photoionization place severe restrictions on the rotational energy levels that can be populated in the $\tilde{X}\,^2A_2''(0100)$ state, and it turns out that each allowed level is correlated with either even or odd ℓ photoelectrons. Thus, by recording rotationally resolved photoelectron spectra, it is possible to determine whether the rotational or electronic degrees of freedom compensate for the change in vibrational symmetry. The results of these experiments indicate that while changes in the electronic symmetry occur more frequently, in some instances changes in the rotational symmetry are equally important. This result also provides insight into the mechanism of the autoionization process. In particular, the electronic symmetry changes are driven by the normal coordinate dependence of the odd multipole moments of the system, which will then mix states with even and odd values of ℓ. In contrast, the rotational symmetry changes are more closely related to Coriolis interactions. We are currently examining the data in more detail to try to predict which types of Rydberg series will display which types of behavior.

To address question (3), we have studied the vibrational branching ratios for autoionization of Rydberg series converging to the NH_3^+ $\tilde{X}\,^2A_2''(1300)$ threshold. These states are expected to decay most efficiently either by $\Delta v_1 = -1$ to the NH_3^+ $\tilde{X}\,^2A_2''(0300)$ state or by $\Delta v_2 = -1$ to the NH_3^+ $\tilde{X}\,^2A_2''(1200)$ state. Interesting, the photoelectron band corresponding to the $\Delta v_2 = -1$ process is approximately 30 times more intense than the band corresponding to the $\Delta v_1 = -1$ process, indicating that the former process is significantly faster than the latter. We are attempting to develop a qualitative model for this observation based on the character of the Rydberg orbitals how they change along the two normal coordinates.

In an attempt to study a more complex system with many different types of normal modes, we have performed analogous double-resonance photoelectron spectroscopy studies on aniline (essentially an ammonia molecule with one hydrogen replaced with a phenyl ring). Although rotational resolution was not possible, photoelectron spectroscopy was performed on a number of Rydberg states converging to ionic vibrational levels in which two or more vibrational modes were excited. The photoelectron spectra provided a direct measurement of the vibrational branching ratios, thus

indicating which modes were most efficient at inducing vibrational autoionization. The results of these studies are currently being analyzed.

FUTURE PLANS

Although we have made significant progress toward understanding vibrational autoionization in ammonia, a number of questions remain to be addressed. First, studies will be performed using other combination bands in the C' state to characterize the mode dependence of the autoionization process more fully. A particular effort will be made to study the other two vibrational modes of NH_3, which correspond to a degenerate asymmetric stretch and a degenerate asymmetric bend. The asymmetric stretch is particularly interesting as it appears to be the beginning of the path to dissociation. Second, studies will be performed using a different electronic intermediate levels in the two-step excitation process to allow the access of different autoionizing states. Such studies should provide insight into how the vibrational autoionization process depends on the electronic character of the resonance. In addition to our continued work on ammonia and aniline, we will also investigate the generality of those results by studying the photoionization dynamics of other small polyatomic molecules, including H_2O and CH_3.

In the coming year, studies will also be performed on processes such as predissociation that compete with autoionization. In particular, we will work to use fluorescence dip spectroscopy to record excited-state absorption spectra for the C' state of ammonia. Analogous studies may also be performed on aniline. When compared with the ionization spectrum, such absorption spectra can provide information on the relative amounts of dissociation and ionization. We are also developing an ion-imaging apparatus to obtain information on the dissociation dynamics directly, particularly with respect to the branching ratios between different neutral fragments.

DOE-SPONSORED PUBLICATIONS SINCE 10/1/97

1. S. T. Pratt
   Vibrational Autoionization And Predissociation In High Rydberg States Of Nitric Oxide
   J. Chem. Phys., **108**, 7131 (1998).

2. E. F. McCormack, F. DiTeodoro, J. M. Grochocinski, and S. T. Pratt
   Dynamics Of Rydberg States Of Nitric Oxide Probed By Two-Color Resonant Four-Wave Mixing Spectroscopy
   J. Chem. Phys., **109**, 63 (1998).

3. W. Yun, S. T. Pratt, R. M. Miller, Z. Cai, D. B. Hunter, A. G. Jarstfer, K. M. Kemner, B. Lai, H. R. Lee, D. G. Legnini, W. Rodrigues, and C. I. Smith
   X-Ray Imaging And Microspectroscopy Of Plants And Fungi
   J. Synchrotron Rad., **5**, 1390 (1998).

4. W. L. Glab, M. S. Child, and S. T. Pratt
   Rotationally Resolved Photoelectron Spectroscopy Of Autoionizing States Of Water
   J. Chem. Phys., **109**, 3062 (1998).

5. S. T. Pratt
   Competition Between Autoionization And Predissociation In Molecular Rydberg States
   in *Adv. Ser. in Phys. Chem., Vol. 10.: Photoionization and Photodetachment*, edited by C. Y. Ng (World Scientific, Singapore, 1998) p. XXX.

6. K. M. Kemner, W. Yun. Z. Cai, B. Lai, H.-R. Lee, D. G. Legnini, W. Rodrigues, J. Jastrow, R. M. Miller, S. T. Pratt, M. A. Schneegurt, C. F. Kulpa, Jr., and A. J. M. Smucker
Using X-Ray Microprobes For Environmental Research
43rd Optical Science, Engineering, and Instrumentation Conference Proceedings,
X-Ray Microfocusing: Applications and Techniques. SPIE, Vol. **3449**, 45 (1998).

7. K. M. Kemner, W. Yun. Z. Cai, B. Lai, H.-R. Lee, D. G. Legnini, W. Rodrigues, J. Jastrow, R. M. Miller, S. T. Pratt, and A. J. M. Smucker
Using Zone Plates for X-Ray Microimaging and Microspectroscopy in Environmental Science
J. Synchrotron Rad., **6**, 639 (1999).

8. C. A. Raptis and S. T. Pratt
Rotational Autoionization in Ammonia
Chem. Phys. Lett., **303**, 281 (1999).

9. J. A. Bacon and S. T. Pratt
Photoelectron Spectroscopy of Rydberg States of the Methyl Radical
Chem. Phys. Lett., **311**, 346 (1999).

10. C. A. Raptis, J. A. Bacon, and S. T. Pratt
Double-Resonance Spectroscopy of Autoionizing States of Ammonia
J. Chem. Phys., **112**, 2815 (2000).

11. J. A. Bacon, and S. T. Pratt
Photoelectron Spectroscopy of Autoionizing Rydberg States Ammonia
J. Chem. Phys. **112**, 4153 (2000).

GAS-PHASE MOLECULAR DYNAMICS: STUDIES OF THE CH_3 + O RADICAL-RADICAL REACTION

Jack M. Preses (preses@bnl.gov) and Christopher Fockenberg (fknberg@bnl.gov)
Chemistry Department, Brookhaven National Laboratory, Upton, NY 11973-5000

PROGRAM SCOPE

The goal of our program is the understanding of elementary chemical and physical processes important in the combustion of fossil fuels, including reactions and properties of short-lived chemical intermediates using laser-based techniques, mass-spectrometric methods, and theoretical studies. In reaction schemes describing combustion of fossil fuels, the majority of the reactions involved are radical-radical reactions, about which little is known. This particular part of our program is a collaborative endeavor bringing together the efforts and expertise of several principal investigators applying time-of-flight mass spectrometry (TOFMS) and infrared diode laser spectroscopy to determinations of the chemical kinetics and reaction yields for radical-radical reactions of importance to combustion.

TOFMS as a primary detection technique allows simultaneous detection of all constituents of a photoionized gas sample from a flow reactor. Using a cw VUV hollow cathode lamp in combination with a high-repetition-rate electronic gating and extraction mechanism, we are able to probe the concentration in the reactor every 50 μs. This enables us to collect time-resolved concentration profiles on multiple species simultaneously. Also, we are using infrared diode laser spectroscopy to complement the TOFMS studies where this technique provides complementary information either not accessible to mass spectrometric studies or where spectroscopic methods provide advantages in state specificity, signal to noise, or freedom from interferences.

RECENT PROGRESS

Last year we reported a TOFMS study of the reaction between CH_3 radicals and O atoms. To summarize briefly, there are several possible channels accessible to this reaction:

$$CH_3 + O(^3P) \rightarrow CH_2O + H \qquad \Delta H = -294.1 \text{ kJ/mol} \qquad (1a)$$
$$\rightarrow HCO + H_2 \qquad \Delta H = -354.2 \text{ kJ/mol} \qquad (1b)$$
$$\rightarrow CO + H + H_2 \qquad \Delta H = -228.7 \text{ kJ/mol} \qquad (1c)$$
$$\rightarrow CH + H_2O \qquad \Delta H = -43.9 \text{ kJ/mol} \qquad (1d)$$
$$\rightarrow OH + CH_2 \qquad \Delta H = +29.2 \text{ kJ/mol} \qquad (1e).$$

One quadrupole mass spectrometric study[1] reported that reaction (1a) was the only important channel between 294 and 900 K. Another FTIR-based investigation determined that the overall yield for CO from reactions (1) was 0.4 ± 0.2.[2] We decided to attempt resolving this discrepancy using our new TOFMS apparatus.[3] The result, at room temperature, was 0.17 ± 0.11, a value considerably different from the FTIR result, but which indicates that the CO-producing channel cannot be neglected. With mass spectrometry the error limits on this value cannot be reduced owing to unavoidable interferences at mass 28, the mass of CO. We therefore undertook a diode laser absorption experiment in an attempt to refine the determination of the CO channel.

A cw beam from a lead-salt 2077 cm^{-1} diode laser is counterpropagated through a 1.3 m-long Pyrex or quartz cell along with a beam from a 193-nm excimer laser. After unwanted modes are removed with a monochromator, the IR beam is focused onto an InSb detector. The diode laser is either locked to an absorption peak and time-resolved absorptions are recorded or the diode is swept across absorption lines and portions of absorption spectra are recorded.

The concept of the experiment is simple: generate methyl radicals and O atoms photolytically, let them react and, after completion, determine the concentration of CO generated by reactions using the intensity of the absorption of the diode laser by a single CO rovibrational transition. In practice there are a number of difficulties to be overcome. First, the best 193-nm photolytic source of CH_3 is acetone, CH_3COCH_3, which produces photolytic CO as well. (The source of O atoms is SO_2). Second, we want to avoid a determination of CO concentration that depends on absolute measurements. Third, the effects of secondary chemistry need to be minimized.

The first problem is overcome by using commercially available acetone labeled with ^{13}C only on the methyl groups as the source of CH_3. Photolysis of this compound yields ^{12}CO directly and ^{13}CO only as a product of reaction (1c). There are two spectral regions near 2073 and 2077 cm^{-1} where identifiable ^{12}CO and ^{13}CO rovibrational transitions are adjacent to one another and sufficiently close that both absorptions can be encompassed by current-sweeping the diode. Absolute measurements are avoided by recording two spectra: the first is a simultaneously acquired absorption spectrum of the ^{12}CO and ^{13}CO lines in a sample of known isotopic composition, either natural abundance or ^{13}C enriched. The second spectrum is that of the CO reaction product. Comparison of the intensities of the two spectra permits determination of the CO yield using only ratios of intensities. Third, modeling the reaction mechanism represented by reactions (1) and others demonstrates that we have chosen conditions where interferences from other radical-radical reactions that would produce ^{13}CO, such as $H^{13}CO + O \rightarrow OH + {}^{13}CO$ are negligible.

In the absence of processes that scramble ^{12}CO from labeled acetone photolysis and ^{13}CO from the reaction of $CH_3 + O$, the branching fraction, b for the production of CO from this reaction is given by

$$b = \frac{1}{2}\frac{[^{13}CO]}{[^{12}CO]}.$$

A plot of this quantity is shown in Fig. 1. Extrapolating to zero extent of reaction to remove minor effects of product buildup, the branching fraction is 0.18 ± 0.04 in excellent agreement with the TOFMS result.

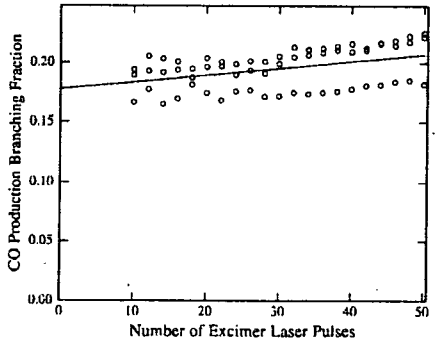

Figure 1: A plot of $[^{13}CO]/2[^{12}CO]$ vs. The number of excimer laser pulses on a mixture of 4 mT labeled acetone

TOFMS studies on this reaction have been extended to temperatures up to 925 K. Under these conditions, wall effects as well as secondary chemistry, in particular the reaction of formaldehyde with oxygen atoms leading to HCO radicals and subsequently CO, can no longer be ignored. Rinsing the flow reactor with a boric acid solution and heat treating it at 450° C alleviates the problem somewhat, but wall-loss rates, especially for O atoms, can range up to 150 s^{-1}. Although much slower than reaction (1), the CH_2O + O reaction has a profound effect on the maximum concentration of formaldehyde, lowering it up to 15 %. These effects have to be incorporated into the analysis with respect to the branching fraction of the reaction CH_3 + O. Preliminary results on the overall rate constant of reaction (1) show an increase from $k_1 = 1.4\times10^{-10}$ cm^3s^{-1} at (354±15) K to $k_1 = 2.2\times10^{-10}$ cm^3s^{-1} at (925±30) K (see Fig. 2). However, a general trend has to be confirmed at intermediate temperatures.

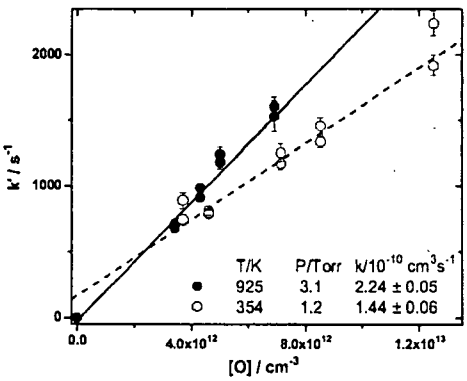

Figure 2: Rate coefficients obtained from methyl radical decay and formaldehyde increase. Ar-ionization (hν ≈ 11.6 eV)

FUTURE WORK

Studies of the temperature dependence of CH_3 + O using TOFMS and diode laser spectroscopy are continuing. Building on expertise in our group concerning CH_3 and C_2H_5 spectroscopy, we plan to undertake further diode laser studies of reactions of these radicals. Availability of diodes in the 3000 and 1440 cm^{-1} spectral regions opens new opportunities for us. Previous diode studies of CH_3 radicals had to be performed using deuterated compounds in the 2300 cm^{-1} region. Since relatively few deuterated compounds are available, our choice of molecules was severely limited. We will be able to use absorptions in the 3000 cm^{-1} C-H stretching region and the 1400-1500 cm^{-1} C-H bending region. Joint TOFMS and diode laser studies of CH_3 + O, C_2H_5 + O, and CH_3 + OH are planned. After completion of the investigation of the reaction involving methyl radicals, the TOFMS research will focus on reactions of propargyl radicals (C_3H_3). The self-reaction of these radicals is considered to be a candidate for the production of benzene, which subsequently leads to the formation of soot in combustion systems. Therefore, the chemistry of propargyl radicals might be key to understand soot production on a molecular basis.

ACKNOWLEDGMENT

This research was carried out at Brookhaven National Laboratory under Contract DE-AC02-98CH10886 with the U.S. Department of Energy and supported by its Division of Chemical Sciences, Office of Basic Energy Sciences.

REFERENCES

1. I.R. Slagle, D. Sarzyński, D. Gutman, *J. Phys. Chem.* **1987**, *91*, 4375.
2. P.W. Seakins, S.R. Leone, *J. Phys. Chem.* **1992**, *96*, 4478.
3. C. Fockenberg, G.E. Hall, J.M. Preses, T.J. Sears, J.T. Muckerman, *J. Phys. Chem. A* **1999**, *103*, 5722.

PUBLICATIONS SINCE 1998

C. Fockenberg, T.J. Sears, and B.-C Chang

Near-Infrared High Resolution Diode Laser Spectrum of the CH_2 $b\ ^1B_1 \leftarrow a\ ^1A_1$ Transition

J. Molec. Spectrosc. **187**, 119-125 (1998)

C. Fockenberg, H.J. Bernstein, G.E. Hall, J.T. Muckerman, J.M. Preses, T.J. Sears, and R.E. Weston Jr.

Repetitively Sampled Time-of-Flight Mass Spectrometry for Gas-Phase Kinetics Studies

Rev. Sci. Instrum. **70**, 3259-3264 (1999)

C. Fockenberg, G.E. Hall, J.M. Preses, T.J. Sears, and J.T. Muckerman

Kinetics and Product Study of the Reaction of CH3 Radicals with O(3P) Atoms using Time Resolved Time-of-Flight Spectrometry

J. Phys. Chem. A 103, 5722-5731 (1999)

R.A. Holroyd, and J.M. Preses

Radiation Chemical Effects of X-rays on Liquids. In Chemical Applications of Synchrotron Radiation

T. K. Sham, Ed., World Scientific Publishing (in press)

R.A. Holroyd, J.M. Preses, and T.K. Sham

Ion Yields for tetramethylgermane Exposed to X-Rays near the Ge K-Edge

J. Phys. Chem. A 104, 2859-2864 (2000).

J. M. Preses, C. Fockenberg and G.W. Flynn

A Measurement of the Yield of Carbon Monoxide from the Reaction of Methyl Radicals and Oxygen Atoms

J. Phys.Chem. A (submitted)

STUDIES IN CHEMICAL DYNAMICS

Herschel Rabitz (hrabitz@princeton.edu)
Tak-San Ho (taksan@chemvax.princeton.edu)

Department of Chemistry
Princeton University
Princeton, NJ 08544

Program Scope.

This program deals with fundamental issues in chemical dynamics pertinent to combustion processes in three principal areas: (A) construction of accurate, smooth and rapidly interpolated potential energy surfaces using reproducing kernel Hilbert space (RKHS) techniques, (B) development and application of efficient and robust time-dependent methods based on the quantum fluid dynamics (QFD) for numerical simulations of molecular dynamics, and (C) development of efficient means for globally mapping potential energy surfaces into dynamical observables.

Recent Progress.

Recently, we have successfully developed initial aspects of the RKHS method with applications to several PES's: (i) global surfaces for the $1A'$ and $2A''$ states of $O(^1D) + H_2$ and $N(^2D) + H_2$ have been constructed (in collaboration with Larry Harding and George Schatz). These surfaces were subjected to various quantum and quasi-classical trajectory reactive calculations, and the results compared favorably with recent experimental data; (ii) a global surface of the lowest quartet state of Na_3 has been constructed based on accurate CCSD(T) *ab initio* calculations (in collaboration with Giacinto Scoles and Kevin Lehmann). This surface has been used for large-scale bound-state calculations, and the results are in very good agreement with high quality vibronic spectra; (iii) global surfaces for $S+H_2$ and CH_3 are being constructed (in collaboration with Larry Harding). A user-friendly RKHS software package has been implemented to automatically construct smooth global PES's for triatomic reactive systems using high-level *ab initio* data. The package will be made available to the dynamics community.

In the past year, we have been developing efficient and accurate computational machineries for treating quantum dynamics phenomena based on the complementary techniques of quantum fluid dynamics (QFD) and RKHS. The QFD formulation is capable of significantly accelerating time integration, by taking advantage of the generally slowly varying density and phase variables in the QFD equations coupled with highly efficient fluid dynamics algorithms. A flux conserving transport code was very successful in preliminary studies of the dissociation

dynamics of NOCl and NO_2, as well as the dynamics of wave packets in up to four dimensions. Preliminary numerical implementation of the QFD equations has also been carried out within the Lagrangian moving grid approach, in conjunction with the RKHS interpolation procedure. Our results indicate that the combined RKHS-QFD method, for its low storage requirement and its uniform accuracy, presents a very significant improvement, especially in three and higher dimensional cases, over the existing ones, including the split-operator (SO) and Chebyschev expansion (CE) methods, in computational efficiency for time-dependent wave packet dynamics.

Finally, we have been studying a high-dimensional model representation (HDMR) of global mapping between a large class of polyatomic Hamiltonians and experimental data. Preliminary results show that a global HMDR map (table) can be efficiently and accurately computed for a large number of heteronuclear diatomic potentials and a variety of observables involved in collisional dynamics, including total cross sections, differential cross sections, and various transport cross sections.

Future Plans.

In the coming year, we plan to continue research in the general areas of developing the RKHS, QFD and HDMR methods, and their applications, along the following lines: (1) refining the RKHS method to allow for *ab initio* data points, including gradients and Hessians, distributed in arbitrarily shaped regions in accordance with the dynamics of a particular system; (2) developing flexible and portable RKHS software packages for PES's construction using high quality *ab initio* data for polyatomic reactive systems; (3) extending the RKHS method for the construction of multi-valued PES's by incorporating non-adiabatic couplings; (4) performing reactive dynamics through full development of the QFD-RKHS formulation; and (5) computing efficient and accurate HDMR maps for a large class of triatomic potential energy surfaces and various observables associated with both non-reactive and reactive dynamics.

Publications Resulting from DOE-Sponsored Research (1998 – Present).

1. Inversion of absorption spectral data for relaxation matrix determination II: Application to Q-branch line mixing in HCN, C_2H_2 and N_2O, R. Boyd, T.-S. Ho, and H. Rabitz, *J. Chem. Phys.*, **108**, 1780-1793 (1998).

2. Inversion of absorption spectral data for relaxation matrix determination I: Application to line-mixing in the 106 $\leftarrow$ 000 overtone transition of HCN, R. Boyd, T.-S. Ho, and H. Rabitz, *J. Chem. Phys.*, **108**, 392-401 (1998).

3. Variational reproducing kernel Hilbert space (RKHS) method for quantum mechanical bound-state problems, X.-G. Hu, T.-S. Ho, and H. Rabitz, *Chem. Phys. Lett.*, **288**, 719-726 (1998).

4. Identifying collective dynamical observables bearing on local features of potential surfaces, A.A. Lazarides, H. Rabitz, J. Chang, and N.J. Brown, *J. Chem. Phys.*, **109**, 2065-2070 (1998).

5. The collocation method based on a generalized inverse multiquadric basis for bound state problems, X.-G. Hu, T.-S. Ho, and H. Rabitz, *Computer Phys. Comm.*, **113**, 168-179 (1998).

6. Efficient input-output model representations, H. Rabitz, Ö.F. Alis, J. Shorter, and K. Shim, *Computer Phys. Comm.*, **117**, 11-20 (1999).

7. An Efficient Chemical Kinetics Solver Using High Dimensional Model Representation, J.A. Shorter, P.C. Ip, and H. Rabitz, *J. Phys. Chem. A*, **103**, 7192-7198 (1999).

8. Potential energy surface and quasiclassical trajectory studies of the $N(^2D) + H_2$ reaction, L.A. Pederson, G.C. Schatz, T.-S. Ho, T. Hollebeek, H. Rabitz, L.B. Harding, and G. Lendvay, *J. Chem. Phys.*, **110**, 9091-9100 (1999).

9. Quantum fluid dynamics in the Lagrangian representation and applications to photodissociation problems, F. Sales Mayor, A. Askar, and H. Rabitz, *J. Chem. Phys.*, **111**, 2423-2435 (1999).

10. Constructing Multi-Dimensional Molecular Potential Energy Surfaces from *Ab Initio* Data, T. Hollebeek, T.-S. Ho, and H. Rabitz, *Annu. Rev. Phys. Chem.*, **50**, 537-570 (1999).

11. Exploring the reaction dynamics of nitrogen atoms: A combined crossed beam and theoretical study of $N(^2D) + D_2 \rightarrow ND + D$, M. Alagia, N. Balucani, L. Cartechini, P. Casavecchia, G.G. Volpi, L.A. Pederson, G.C. Schatz, G. Lendvay, L.B. Harding, T. Hollebeek, T.-S. Ho, and H. Rabitz, *J. Chem. Phys.*, **110**, 8857-8860 (1999).

12. Solving the bound-state Schrödinger equation by reproducing kernel interpolation, X.-G. Hu, T.-S. Ho, and H. Rabitz, *Phys. Rev. E*, **61**, 2074-2085 (2000).

13. On the Importance of Exchange Effects on Three-Body Interactions: The Lowest Quartet State of Na_3, J. Higgins, T. Hollebeek, J. Reho, T.-S. Ho, K.K. Lehmann, H. Rabitz, G. Scoles, and M. Gutowski, *J. Chem. Phys.*, **112** 5751-5761 (2000).

14. Multivariate radial basis interpolation for solving quantum fluid dynamical equations, X.-G. Hu, T.-S. Ho, H. Rabitz, and A. Askar, *Computer and Mathematics with Application*, submitted.

15. Propagation of the Quantum Fluid Dynamical Equations, X.-G. Hu, T.-S. Ho, and H. Rabitz, *Phys. Rev. E*, in press.

16. Reproducing Kernel Technique for Extracting Accurate Potentials from Spectral Data: Potential Curves of the Two Lowest States $X^1\sum_9^+$ and $a^3\sum_u^+$ of the Sodium Dimer, T.-S. Ho, H. Rabitz, and G. Scoles, *J. Chem. Phys.*, in press.

Reactions of Atoms and Radicals in Pulsed Molecular Beams

Hanna Reisler
Department of Chemistry, University of Southern California
Los Angeles, CA 90089-0482
reisler@chem1.usc.edu

Program Scope

We study photoinitiated reactions of molecules and free radicals that involve competitive pathways and/or isomerization by exploiting multiple-resonance excitation schemes, state-selected product detection, and photofragment ion imaging for generation of correlated distributions.

Recent Progress:

The hydroxymethyl radical (CH_2OH) and its isomer, the methoxy radical (CH_3O) are important species in fuel combustion and in atmospheric and interstellar chemistry. CH_2OH, being much more reactive than CH_3O, is also of importance in polluted environments.[1] The isomerization $CH_2OH \leftrightarrow CH_3O$ is intriguing because the calculated barrier is comparable to the $H + CH_2O$ dissociation barrier.[2] However, despite considerable theoretical interest in this system, experimental studies of the uni- and bimolecular reactions of CH_2OH are sparse, due mainly to difficulties in preparing this reactive species.

Recently, we have succeeded in producing the radical in a molecular beam using the photoinitiated reaction $Cl + CH_3OH \rightarrow HCl + CH_2OH$. The reaction is carried out in a quartz tube extension to the pulsed valve under conditions that suppress the rapid consecutive reaction $Cl + CH_2OH \rightarrow CH_2O + HCl$.

Using this method for production of the radical and resonance enhanced multiphoton ionization (REMPI) for its detection, we obtained rotational envelopes of selected vibronic bands following excitation to the $3p$ Rydberg state, whose origin lies at ~ 243 nm.[1] Analysis of the rotational contours led to assignment of the $3p$ Rydberg state as $^2A''(3p_z)$. The 11 cm^{-1} homogeneous linewidth inferred from the spectral simulations implies that the upper state is predissociative, although no dissociation products have been observed.

We report here the first results identifying H(D) as a photodissociation product of $CH_2OH(D)$ following excitation in the origin band of the $^2A''(3p_z) \leftarrow {}^2A''(\pi^*)$ transition. Because of the large H background in our apparatus, the isotopomers CH_2OD and CD_2OH were used. The D photofragment was examined using the "core sampling" variant of time-of-flight (TOF) spectroscopy. Both the kinetic energy release and the effective recoil anisotropy parameter, β_{eff}, were determined.

The study of the photodissociation dynamics on the $^2A''(3p_z)$ surface is intriguing for several reasons. First, excitation accesses a vibronically resolved Rydberg state, and therefore Rydberg-valence interaction must influence the subsequent dynamics. Second, there is more than one pathway that can terminate in D photofragments. Third, the role of isomerization to the methoxy radical can be investigated by comparing the H and D signals obtained in the photolysis of CD_2OH and CH_2OD. We note that in the photodissociation of CH_3O from the first excited $^2A_1$ state, the $CH_2 + OH$ channel, which involves isomerization, has been

observed.[3] Fourth, there are additional distinct chemical channels that are energetically accessible from the $^2A''(3p_z)$ state, e.g. $CH_2 + OH$, $H_2 + HCO$ etc., but have not yet been observed. Last, the combination of a structured vibronic spectrum and multiple dissociation pathways opens the possibility of observing mode or bond specificity in the dissociation. Here we discuss in detail the D product obtained following excitation to the origin band.

Isotopomers of CH_2OH are detected with a combination of REMPI spectroscopy and TOF mass spectrometry, using the published assignments.[1] H(D) atoms are detected via 2-color (1+1) REMPI. The core sampling technique utilizes a spatial restriction in the ion detection in order to eliminate contributions from off-axis ions, thereby yielding the speed distribution of the recoiling fragments in a straightforward manner. This allows the measurement of differential cross-sections as a function of kinetic energy and the angular anistropy of the products.

Since other sources in the reactive mixture may give rise to D atom signal, it is imperative to establish a direct correspondence between the absorption features of CH_2OD and the observed D atom signal. For this reason, photofragment yield spectroscopy was carried out in selected regions of the absorption spectrum of CH_2OD. The top panel of Fig. 1 presents a (2+1) REMPI spectrum of jet-cooled CH_2OD radical, and the middle panel displays a (1+1) REMPI spectrum of the bands chosen for the photofragment yield study. The bottom panel shows the D-atom photofragment yield spectrum. The clear correspondence between the D and CH_2OD spectral features indicates that deuterium is a product of the dissociation of the excited hydroxymethyl radical. The co-fragment is most likely formaldehyde. In contrast, no H atom signal corresponding to the absorption features of CH_2OD was observed, and neither was a D atom signal from CD_2OH. We conclude therefore that it is the O–H(D) bond that preferentially breaks. Comparison of the D atom signals obtained from CD_2OH and CH_2OD indicates that the fraction of D atoms produced via the methoxy route is insignificant.

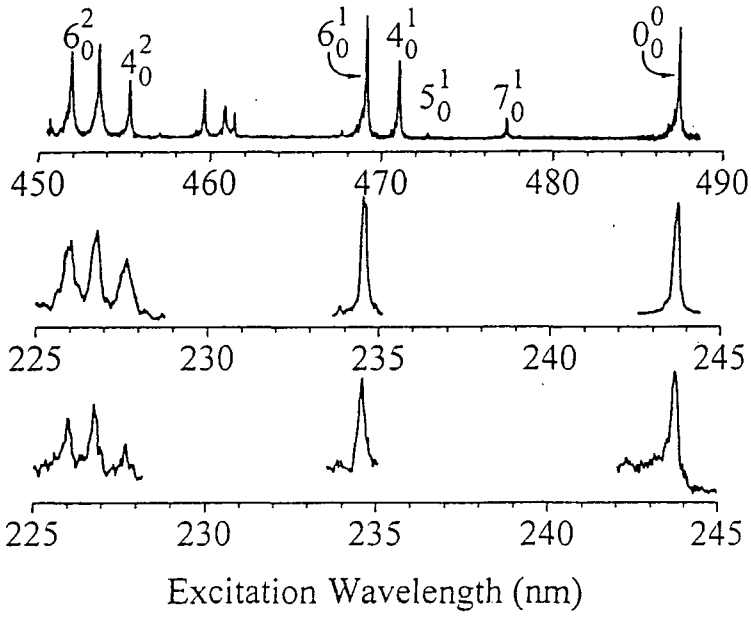

Fig. 1: REMPI and D-atom photofragment yield spectra of CH_2OD

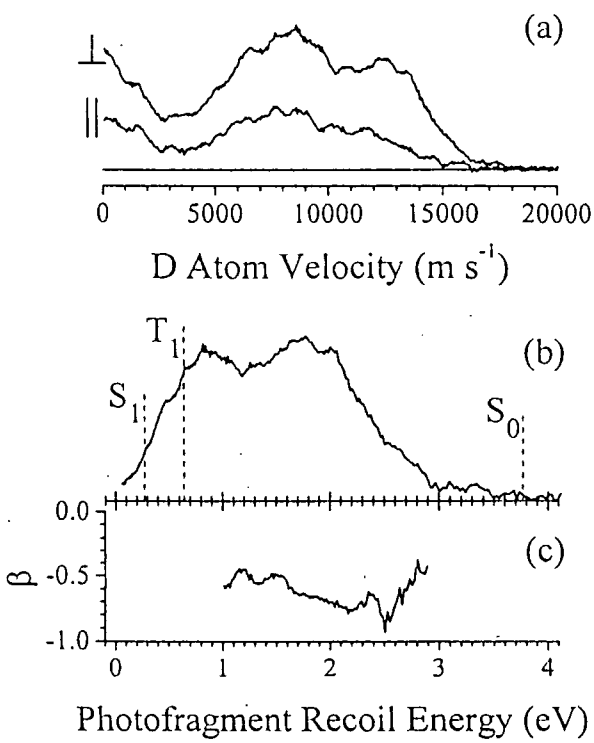

Fig. 2. D-atom velocity, recoil energy and anisotropy parameter for CH_2OD.

The velocity distribution of the D atom and the distribution of *total* translational energy of photofragments are shown in Fig. 2(a,b), which also indicates the kinetic energy limits associated with production of the formaldehyde co-fragment in the electronic states $S_0(^1A_1)$, $T_1(^3A_1)$, and $S_1(^1A_2)$. Clearly, the large fraction of D atoms with high kinetic energies identifies the ground-state of formaldehyde as the dominant co-fragment. The internal excitation of formaldehyde peaks at ~ 1–2 eV, exhibiting a broad, structureless distribution that decreases gradually beyond the maximum.

The angular distribution of the products was inferred from measurements carried out at parallel and perpendicular polarizations of the photolysis laser with respect to the TOF axis. The derived average anisotropy parameter (shown in Fig. 2(c)) is $\beta_{eff} = -0.6 \pm 0.3$. In CH_2OH, the C–O–H angles were computed *ab initio* to be 108.4 ° and 115.1°, for the ground and excited state, respectively,[1] while μ_e was found to be co-linear with the C–O bond. For axial recoil along the O–H (or O–D) bond, the expected anisotropy is –0.46 to –0.70, corresponding to the ground state and excited state geometries of CH_2OD (assuming that they do not change for the different isotopomers).

Excitation deposits 5.08 eV (40,950 cm^{-1}) in CH_2OD, making all the channels indicated in Fig. 2 energetically accessible. As shown above, the isomerization channel is not important. The large fraction of D fragments with high translational energies indicates that the channel terminating in ground-state formaldehyde must be a major pathway.

According to *ab initio* cacluations, three other Rydberg states lie below the $3p_z$ state ($3p_y$, $3p_x$ and $3s$).[4] All have planar geometries similar to that of ground state CH_2OH^+.[1] These states are located at energies lower than the $3p_z$ state by up to 1.2 eV. Because of the proximity of the $3p_z$ state to the other Rydberg states, Franck-Condon considerations would favor initial couplings to one or more of these states, leading to a sequential coupling mechanism finally terminating in a crossing to the ground state. No calculations including both valence and Rydberg states have yet been reported; thus, the issue of the specific nonadiabatic interactions leading to products remains open.

The short time scale for dissociation inferred in our studies is the clue to understanding the seemingly contradictory observations of a broad internal energy distribution in the formaldehyde product, which is nevertheless accompanied by no isotope scrambling in the products (no isomerization). The shape of the internal energy distribution is similar to what is expected from a statistical-like dissociation, in which case the energy would be fully

randomized in the activated complex. Since the excitation energy (5.1 eV) is much greater than the barrier to isomerization on the ground state (1.8 eV),[2] such a mechanism would imply a significant probability for isomerization during the dissociation. The absence of isomerization suggests that the high internal excitation of the formaldehyde fragment derives from dynamical biases in the exit channel for O–D(H) fission.

In summary, the work presented above demonstrates that the D + $CH_2O(S_0)$ channel is a major pathway in the dissociation of CH_2OD excited to the origin band of the $^2A''(3p_z)$ Rydberg state. Isomerization to the methoxy isomer is not an important pathway. The mechanism involves predissociation, and the dissociation lifetime is on the order of a picosecond. The final dissociation step possibly involves fast, direct cleavage of the O–D bond, and it is the exit-channel dynamics that gives rise to a formaldehyde product with a high degree of internal excitation. The direct sequence of nonradiative pathways is presently unknown.

Future Plans

The hydroxymethyl radical can exhibit rich photochemistry both on the ground and the excited potential energy surfaces. For example, additional product channels such as CH_2 + OH are likely to be important for some states, and isomerization may depend on the initial excitation as well. Work currently in progress in our laboratory examines the dependence of the D atom translational energy distributions on the $3p_z$ vibronic level. We also have preliminary results assigning the 3*s* Rydberg state. We also plan to commence experiments in which the OH or CH vibrations will be excited prior to electronic excitation.

1. Johnson, R. D.; Hudgens, J. W. *J. Phys. Chem.* **1996**, *100*, 19874, and references therein.
2. Adams, G. F.; Bartlett, R. J.; Purvis, G. D. *Chem. Phys. Lett.* **1982**, *87*, 311; Saebø, S.; Radom, L.; Schaefer, H. F. *J. Chem. Phys.* **1983**, *78*, 845.
3. Osborn, D. L.; Leahy, D. J.; Neumark, D. M. *J. Phys. Chem.* **1997**, *101*, 6583.
4. Rettrup, S.; Pagsberg, P.; Anastasi, C. *Chem. Phys.* **1988**, *122*, 45.

Publications in 1998-2000:

Endoergic reactions of hyperthermal C(^{3}P) with methane and acetylene, M.R. Scholefield, J.-H. Choi, S. Goyal, and H. Reisler, Chem. Phys. Lett. **288**, 487 (1998).

Symmetry and liftime of the hydroxymehtyl raidcal in the 3p Rydberg state, V. Aristov, D. Conroy and H. Reisler, Chem. Phys. Lett., **318**, 393 (2000).

HCO rovibrational distributions from the unimolecular decompositions of H_2CO at excess energies 1100-2655 cm^{-1}, L. Valachovic, M.J. Dulligan, M.F. Tuchler, Th. Droz-Georget, M. Zyrianov, A. Kolessov, H. Reisler and C. Wittig, J. Chem. Phys., **112**, 2752 (2000).

The electronic Origin and vibrational levels of the first excited singlet state of isocyanic Acid (HNCO), H. Laine Berghout, F. Fleming Crim, Mikhail Zyrianov and Hanna Reisler, J. Chem. Phys., in press.

Photoionization Studies of Transient and Metastable Species

Branko Ruscic
Chemistry Division, Argonne National Laboratory
9700 South Cass Avenue, Argonne, IL 60439-4831
ruscic@anl.gov

Program Scope

In most general terms, the fundamental goal of this program is to explore, understand, and utilize the basic processes of interaction of vacuum UV light with atoms and molecules. In more specific terms, the program uses photoionization mass spectrometry and other related methods to study transient and metastable species that are either intimately connected to energy-producing processes, such as combustion, or play prominent roles in the associated environmental issues. The ephemeral species of interest are produced *in situ* using various suitable techniques, such as sublimation, pyrolysis, microwave discharge, chemical abstraction reactions with H or F atoms, laser photodissociation, on-line synthesis, and others. The desired information is obtained by applying appropriate photoionization techniques, which use both conventional and coherent light sources in the vacuum UV region. The *spiritus movens* of our studies is the need to provide the chemical community with essential information on the species of interest to energy-related processes, such as accurate and reliable thermochemical, spectroscopic and structural data, and thus contribute to the global comprehension of the underlying chemical reactions. The scientific motivation is additionally fueled by the intent to extract, when possible, useful generalities such as bonding patterns within a class of related compounds, or unveil systematic behavior in the ubiquitous autoionization processes and other phenomena occurring during photoionization. In addition, results obtained in this program serve as testing ground for the state-of-the-art electronic structure calculations, and have historically generated a significant impetus for further theoretical developments. The experimental work of this program is coordinated with related experimental and theoretical efforts within the Chemical Dynamics Group to provide a broad perspective on this area of science.

Recent Progress

Photoionization Studies of HOCO Radical

The reaction OH + CO → H + CO_2 is the key oxidation pathway from CO to CO_2 during combustion. It is also responsible for vernal and aestival oxidative cleaning of the atmosphere and is implicated in tropospheric smog formation mechanisms by controlling the OH concentration and hence the rate of NO_x conversion. One of the salient features on the OH + CO potential energy surface is the existence of a stable HOCO well, directly responsible for the peculiar temperature and pressure dependence of the OH + CO rate constant. While the overall exothermicity of this reaction (24.476±0.072 kcal/mol at 0 K) is known quite accurately,[1,2] thermochemical information regarding HOCO (and hence the depth of the well) is meager. Neither the NBS Tables nor JANAF list HOCO, while the Russian compilation[2] essentially adopts the value $\Delta H°_{f0}$(HOCO) = -50±3 kcal/mol from the first edition of Benson's book, which was subsequently revised to –49±1 kcal/mol in the second edition.[3]

Roughly a decade ago,[4,5] we have attempted to shed some light on the enthalpy of formation of HOCO by using the positive ion cycle, which involves the ionization energy (EI) of HOCO and the enthalpy of formation of $HOCO^+$, or, equivalently, the proton affinity of CO_2. Our studies[4] have produced $\Delta H°_{f0}(HOCO^+)$ = 143.2±0.5 kcal/mol, corresponding to $PA_{298}(CO_2)$ = 129.2 ±0.5 kcal/mol, somewhat lower than the prevailing value at the time, but subsequently confirmed at least twice to within 0.1-0.2 kcal/mol and now listed as the preferred value in the NIST compilation of proton affinities.[6] The second quantity needed in the thermochemical cycle is the adiabatic ionization energy of HOCO. Here, our old upper limit[5] is the only measurement reported to date. HOCO has two stable conformers, *trans* and *cis* (higher in energy by ~0.1-0.2 eV). Upon ionization, the OCO angle becomes almost linear, and both CO

bonds shorten, causing dismal Franck-Condon factors and frustrating the experimental detection of the adiabatic ionization threshold. The lowest experimentally identifiable step, at 146.1±0.2 nm was the basis for our previous[5] upper limit of 8.486±0.012 eV. Taken at face value, it implies $\Delta H°_{f0}$(HOCO) > -52.5±0.6 kcal/mol, or a depth of the HOCO well (exclusive of barriers, but including ZPEs) of <10 kcal/mol relative to the H + CO_2 asymptote. The upper limit nature of this determination was reemphasized in the BEG review,[7] where HOCO was exemplified as a 'difficult case' and the true threshold was guesstimated to be perhaps lower by one quantum of the principal vibrational progression. In the meantime, direct experimental detection of a lower threshold continues to be quite difficult in practice (e. g., Washida's group[8] reported that they could not detect and monitor HOCO with a Xe resonance lamp, 8.44 eV, "consistent with the [measurement] by Ruscic et al.") Theory seems to provide only limited guidance on how much lower the true ionization energy might be. For example, a recent B3LYP/6-311++G(d,p) calculation reports 8.31 eV, slightly lower than (but very close to) our previous upper limit.[9] On the other hand, a presumably better CCSD(T)/6-311++G(3df,3pd) calculation[10] suggests a significantly lower value of 8.01 eV.

In view of the importance of this species, we have decided to carefully examine the ionization threshold region of this species again, hoping that by improving the experimental conditions we might be able to detect the presumed lower ionization energy. As before, HOCO was produced *in situ* by reacting F atoms with formic acid. Signal to noise was improved by adopting an extremely discriminatory approach while searching for the best experimental conditions. This resulted in a high rejection rate, requiring repeated attempts at careful cleaning, coating and curing of the surfaces of the radical source, combined with very patient adjustments of the conditions of the radical source. The final spectrum is a composite average of a dozen best runs, each providing only a handful of points collected at wavelengths corresponding to peaks in the H_2 discharge light source. The new spectrum clearly shows the previously detected step at 146.1 nm. However, at the improved experimental level of the present measurements, the data clearly show an additional, even weaker, step-like onset at 151.3±0.4 nm, corresponding to a new upper limit of EI(t-HOCO) ≤ 8.195 ± 0.022 eV. This translates into a lower limit to the enthalpy of formation, $\Delta H°_{f0}$(t-HOCO) ≥ -45.8±0.7 kcal/mol (≥ -46.5±0.7 kcal/mol at 298 K), implying that the t-HOCO well is not deeper than 3.5±0.7 kcal/mol relative to the H + CO_2 asymptote. The new spectrum corroborates our previous finding of a progression in the double C=O bond stretch of the ion of ~2300 cm^{-1}, suggests the presence of the single C-O bond stretch of ~1200-1300 cm^{-1}, and provides indirect evidence for the excitation of an even lower frequency, such as the OCO bend. The data also tentatively suggest an additional very weak onset at 8.06±0.03 eV. While the interpretation of the latter feature is still somewhat ambiguous, it most likely corresponds to ionization from the *cis* conformer, suggesting that its energy is ~3.1±0.7 kcal/mol higher than that of t-HOCO.

Methylene, Ketene, and Thermochemical Networks

The thermochemistry of methylene was further elucidated by carefully measuring the appearance onset of the CH_2^+ fragment from ketene. The underlying idea was to provide additional support for our recent study,[11] which reported the first direct determination of EI(CH_2) = 10.393±0.011 eV and , together with our $EA_0(CH_2^+/CH_3)$ = 15.120±0.006 eV, produced D_0(H-CH_2) = 109.0±0.3 kcal/mol and hence $\Delta H°_{f0}(CH_2, {}^3B_1)$ = 93.2±0.3 kcal/mol and $\Delta H°_{f0}(CH_2, {}^1A_2)$ = 102.2±0.3 kcal/mol. The CH_2^+/CH_2CO threshold was analyzed by an extension of our fitting approach, which had to accommodate the somewhat unusual vibrational autoionization structure (seldom present in fragment ion yields), and produced an appearance onset of 13.743±0.005 eV. Using the well-known dissociation energy of ketene,[12] this produces EI(CH_2) = 10.400±0.005 eV, fully corroborating our previous finding. The value can be further propagated through selected thermochemical cycles to yield D_0(H-CH_2) = 108.9±0.2 kcal/mol and $\Delta H°_{f0}(CH_2, {}^3B_1)$ = 93.1±0.2 kcal/mol.

However, rather than obtaining thermochemical values by sequential propagation through "best" measurements, a statistically much more significant set of thermochemical values can be obtained by

analyzing the relevant local thermochemical network. We have recently successfully used this approach[13] to establish accurate experimental thermochemistry of CF_3X, X=nil, H, Cl, Br, I, CF_3, CN. The present network involves CH_3, CH_3^+, CH_2, CH_2^+, and ketene, and includes 14 relevant experimental determinations. A complete statistical analysis of this overdetermined network provides over a dozen simultaneously adjusted thermochemical values, such as $\Delta H°_{f0}(CH_3)$ = 35.86 ±0.07 kcal/mol (35.05 ±0.07 kcal/mol at 298 K), $\Delta H°_{f0}(CH_2, {}^3B_1)$ = 93.18 ±0.20 kcal/mol (93.31 ± 0.20 kcal/mol at 298 K), $D_0(H_3C\text{-}H)$ = 103.42 ± 0.03 kcal/mol (104.99 ± 0.03 kcal/mol at 298 K), $D_0(H_2C\text{-}H)$ = 108.95 ± 0.20 kcal/mol (110.35 ± 0.20 kcal/mol at 298 K), etc. In addition, the network approach unambiguously demonstrates that the original NIST value for the enthalpy of formation of ketene[14] corresponds to the best available direct experimental determination, while the two newer values[15,16] are too low. The recommended enthalpy of formation of CH_2 implies that the reaction of singlet methylene with water is essentially thermoneutral (to within ±0.2 kcal/mol) at 0 K and 298 K, and slightly endothermic (0.5±0.2 kcal/mol) at 1000 K.

Development of radical sources at the Chemical Dynamics Beamline at ALS

We have recently embarked upon a program aiming to study free radicals and other transient species at the 9.0.2 Beamline at the ALS. Carrying out these experiments at the ALS has an obvious advantage, since the high brightness of the synchrotron can help alleviate some of the fundamental experimental challenges typically encountered in studies of ephemeral species. So far, we have installed a laser photoionization source both on Endstation 2 and 3. The source, which uses pulsed laser excitation but produces a quasi-continuous stream of radicals that are equilibrated at a known (selected) temperature, was constructed and initially tested at Argonne. After installation at the ALS, the performance of the source was probed and fine-tuned with respect to timing sequences by examining methyl radical and SO. The tests have indicated that the source works quite well and suggested that a sound general strategy would be to use Endstation 3 to generate overview spectra of radicals and Endstation 2 for high-resolution studies of selected spectral regions. Using this source we have now started to examine vinoxy, vinyl, and HOCO radicals, all of which have very unfavorable Franck-Condon factors for ionization. In parallel, we are continuing the implementation of a full complement of radical sources. These include a second laser photodissociation source that exploits the cooling capabilities of jet expansion, as well as a variation of our laboratory source that generates radicals either via chemical abstraction reactions using fluorine, chlorine and hydrogen atoms, or directly in the microwave discharge and has been proven in the past to be a clean and continuous source of a very large variety of radicals.

Future Plans

Future plans of this program pivot around the continued investigation of radicals and transient species that are intimately related to combustion processes, particularly those that potentially define the initial attack of O_2 on hydrocarbon moieties during combustion, as well as other ephemeral species that are implicated in subsequent atmospheric chemistry. These investigations will continue to be correlated with other ongoing activities in the Chemical Dynamics Group, and will be enhanced by complementing the research carried in our laboratory using classical and laser sources of radiation with measurements taking advantage of the Advanced Light Source at Lawrence Berkeley Laboratory. We also intend to further test and enhance our fitting method for accurate determination of fragment appearance potentials.

This work is supported by the U.S. Department of Energy, Office of Basic Energy Sciences, Division of Chemical Sciences, under Contract W-31-109-ENG-38

References

[1] J. D. Cox, D. D. Wagman, V. A. Medvedev, CODATA Key Values for Thermodynamics, Hemisphere, New York, 1989.
[2] L. V. Gurvich, I. V. Veyts, C. B. Alcock, Thermodynamic properties of Individual Substances, Hemisphere, New York 1989.

[3] S. W. Benson, Thermochemical Kinetics, Wiley, New York, 1968; 2nd ed., Wiley, New York, 1976.
[4] B. Ruscic, M. Schwarz, and J. Berkowitz, J. Chem. Phys. 91 (1989) 6772.
[5] B. Ruscic, M. Schwarz, and J. Berkowitz, J. Chem. Phys. 91 (1989) 6780.
[6] E. P. L. Hunter and S. G. Lias, J. Phys. Chem. Ref. Data 27 (1998) 413.
[7] J. Berkowitz, G. B. Ellison, and D. Gutman, J. Phys. Chem. 98 (1994) 2744.
[8] A. Miyoshi, H. Matsui, N. Washida, J. Chem. Phys. 100 (1994) 3532.
[9] C. A. Schalley, G. Homung, D. Schroder, and H. Schwartz, Int. J. Mass Spectrom. Ion Proceesses 172 (1998) 181.
[10] J. S. Francisco, J. Chem. Phys. 107 (1997) 9039.
[11] M. Litorja and B. Ruscic, J. Chem. Phys. 108 (1998) 6748.
[12] I. C. Chen, W. H. Green, Jr., and C. B. Moore, J. Chem. Phys. 89 (1988) 314.
[13] B. Ruscic, J. V. Michael, P. C. Redfern, L. A. Curtiss, and K. Raghavachari, J. Phys. Chem. A 102 (1998) 10889.
[14] R. L. Nuttall, A. H. Laufer, and M. V. Kilday, J. Chem. Thermodyn. 3 (1971) 167.
[15] V. M. Orlov, A. A. Krivoruchko, A. D. Misharev, and V. V. Takhistov, Bull. Acad. Sci. USSR Div. Chem. Sci. (1986) 2404.
[16] C. Aubry, J. L. Holmes, and J. K. Terlouw, J. Phys. Chem. A 101 (1997) 5958.

Publications Resulting from DOE Sponsored Research (1997-1999)

- On the Heats of Formation of Trifluoromethyl Radical, CF_3, and its Cation, CF_3^+
  R. L. Asher and B. Ruscic, J. Chem. Phys. **106**, 210-221 (1997)
- Absolute Photoionization Cross Sections
  J. Berkowitz, J. Phys. B: At. Mol. Opt. Phys. **30**, 583-592 (1997)
- Sum Rules and the Oscillator Strength Distribution in Helium
  J. Berkowitz, J. Phys. B: At. Mol. Opt. Phys. **30**, 881-892 (1997)
- A Photoionization Study of Trifluoromethanol, CF_3OH, Trifluoromethyl Hypofluorite, CF_3OF, and Trifluoromethyl Hypochlorite, CF_3OCl
  R. L. Asher, E. H, Appelman, J. L. Tilson, M. Litorja, J. Berkowitz, and B. Ruscic, J. Chem. Phys. **106**, 9111-9121 (1997)
- Evidence of Rotational Autoionization in the Threshold Region of the Photoionization Spectrum of CH_3
  M. Litorja and B. Ruscic, J. Chem. Phys. **107**, 9852-9856 (1997)
- Direct Observation of the Ionization Threshold of Triplet Methylene by Photoionization Mass Spectrometry
  M. Litorja and B. Ruscic, J. Chem. Phys. **108**, 6748-6755 (1998)
- A Photoionization Study of Hydroperoxyl Radical, HO_2, and Hydrogen Peroxide, H_2O_2
  M. Litorja and B. Ruscic, J. Electron Spectrosc. **97**, 131-146 (1998)
- Simultaneous Adjustment of Experimentally Based Enthalpies of Formation of CF_3X, X = nil, H, Cl, Br, I, CF_3, CN, and a Probe of G3 Theory
  B. Ruscic, J. V. Michael, P. C. Redfern, L. A. Curtiss, and K. Raghavachari, J. Phys. Chem. A **102**, 10889-10899 (1998)
- Sum Rules and the Photoabsorption Cross Section of C_{60}
  J. Berkowitz, J. Chem. Phys. **111**, 1446-1453 (1999)
- Ionization Energy of Methylene Revisited: Improved Values for the Enthalpy of Formation of CH_2 and the Bond Dissociation Energy of CH_3 via Simultaneous Solution of the Local Thermochemical Network
  B. Ruscic, M. Litorja, and R. L. Asher, J. Phys. Chem. A **103**, 8625-8633 (1999)
- Photoionization of HOCO Revisited: A New Upper Limit to the Adiabatic Ionization Energy and Lower Limit to the Enthalpy of Formation
  B. Ruscic and M. Litorja, Chem. Phys. Lett. (in press)

Research on Free Radical Reactions

Henry F. Schaefer III

Center for Computational Quantum Chemistry, University of Georgia

Athens, Georgia 30602-2525

email: hfsiii@arches.uga.edu

(706)542-2067

Our collaboration with the research group of Yuan Lee (Institute for Atomic and Molecular Science, Academia Sinica, Taiwan) is aimed at delineating and understanding the chemical reaction dynamics of free radical reactions by combining crossed beam experiments and quantum mechanical predictions. Such reactions are of fundamental importance for the formation of larger molecular species (for example polycyclic aromatic hydrocarbons, PAH's) both in terrestrial, e.g. combustion, and extraterrestrial environments. The collaboration has resulted in four publications to date.

The reaction of ground state ^3P_j carbon atoms with perdeuterobenzene (C_6D_6, $X\ ^1A_{1g}$) at extremely low collision energies results in the formation of the C_7D_5 radical, which could not be further characterized experimentally. However, our computational results combined with the experimental reaction energy strongly indicate that the species detected by mass spectroscopy is the didehydrocycloheptatrienyl radical **1**, which is formed in a slightly exothermic reaction. A detailed computational analysis indicates that **1** can be made from the reactants without barriers in the entrance and exit channels of the reaction, in agreement with experimental observations. The formation of other possible products could be ruled out because the overall energetics, or the energies and barriers of intermediates, or the barriers in the exit channels are not in agreement with experiment. The finding that ground state carbon atoms react with benzene without barriers is of fundamental importance for the chemistry of molecular clouds, and can also be envisioned as an alternative path towards PAH's in combustion flames.

Another hydrocarbon reaction studied in our interdisciplinary research environment was the reaction between phenyl radical (C_6H_5, $X\ ^2A_1$) and methylacetylene (CH_3CCH, $X\ ^1A_1$). At an average collision energy of 140 kJ mol^{-1} the formation of a phenylmethylacetylene (1-phenylpropyne) **2** was observed in an exothermic reaction. The reaction proceeds through a short lived C_9H_9 radical intermediate, but the observed reaction product **2** is thermodynamically not the most stable isomer, nor is it formed via the lowest barrier. Obviously, the lifetime of the highly rovibrationally excited intermediate, less than 0.1 ps, is too small to allow an energy randomization via internal vibrational relaxation. As the reaction involves a small barrier in the entrance channel, it might not be of importance in cold extraterrestrial environments, but it will likely be involved in the formation of PAH's.

Finally, we also studied the reaction of cyano radicals (CN; $X\ ^2\Sigma^+$) with benzene (C_6D_6, $X\ ^1A_{1g}$) and dimethylacetylene (2-butyne) (CH_3CCCH_3; $X\ ^1A_1'$). Again, the exchange of a hydrogen atom of the closed-shell molecule for the attacking radical is observed. The exothermic formation of cyanobenzene proceeds without a barrier in the entrance channel through a C_6H_6-CN radical. As the barrier in the exit channel is well below the energy of separated reactants, this reaction is also viable at extremely low temperatures. The formation of isocyanobenzene was not observed; indeed, our work indicates that this reaction is energetically much less favorable (by about 100 kJ mol^{-1}) with a high barrier (+ 30 kJ mol^{-1} with respect to separated reactants) in the exit channel. The product observed in the reaction between CN and 2-butyne is 2-cyano-2,3-butadiene, but according to our theoretical methods the CH_3 ejection (resulting in 1-cyanopropyne) should be thermodynamically and kinetically more favorable than H atom loss. The lifetime of the radical intermediate is sufficiently long to allow the energy averaging over vibrational modes, and Rice-Ramsperger-Kassel-Marcus (RRKM) calculations indeed indicate that the latter pathway is more

important. The failure to observe 1-cyanopropyne is due to unfavorable kinematics in the crossed beam experiment.

Research Supported by the U. S. Department of Energy 1998, 1999, 2000.

1. H. F. Bettinger, P. R. Schreiner, H. F. Schaefer, and P. R. Schleyer, "Rearrangements on the C_6H_6 Potential Energy Surface and the Topomerization of Benzene", *J. Amer. Chem. Soc.* **120**, 5741 (1998).
2. Y. Yamaguchi, S. S. Wesolowski, T. J. Van Huis, and H. F. Schaefer, "The Unimolecular Dissociation of H_2CO on the Lowest Triplet Potential Energy Surface", *J. Chem. Phys.* **108**, 5281 (1998).
3. E. F. Valeev and H. F. Schaefer, "The Protonated Water Dimer: Brueckner Methods Remove the Spurious C_1 Symmetry Minimum", *J. Chem. Phys.* **108**, 7197 (1998).
4. J. Gu, Y. Xie and H. F. Schaefer, "The Barrier Height for Decompostion of HN_2", *J. Chem. Phys.* **108**, 8029 (1998).
5. K. Fukuzawa, Y. Osamura, and H. F. Schaefer, "Are Neutral-Neutral Reactions Effective for the Carbon-Carbon Chain Growth of Cyanopolyynes and Polyactetylenes in Interstellar Space?" *Astrophysical Journal* **505**, 278 (1998).
6. Y. Yamaguchi, J. C. Rienstra-Kiracofe, J. C. Stephens, and H. F. Schaefer, "The Hydroxyethynyl Radical (CCOH): An Accessible Isomer of the Ketenyl Radical (HCCO)?" *Chem. Phys. Lett.* **291**, 509 (1998).
7. R. A. King, W. D. Allen, B. Ma, and H. F. Schaefer, "The Fragmentation Surface of Triplet Ketene", *Faraday Discussions of the Chemical Society,* **110**, 23 (1998).
8. H. F. Bettinger, P. R. Schleyer, and H. F. Schaefer, "Tetradehydrobenzenes: Singlet-Triplet Energy Separations and Vibrational Frequencies", *J. Amer. Chem. Soc.* **121**, 2829 (1999).
9. T. D. Crawford, J. F. Stanton, J. C. Saeh, and H. F. Schaefer, "Structure and Energetics of Isomers of the Interstellar Molecule C_5H", *J. Amer. Chem. Soc.* **121**, 1902 (1999).
10. J. C. Stephens, Y. Yamaguchi, and H. F. Schaefer, "The Adiabatic and Vertical Ionization Potentials of NH_2 to the Three Lowest-Lying States of NH_2^+", *Keiji Morokuma Issue, J. Molecular Structure (Theochem)* **461/462**, 41 (1999).
11. G. Tarczay, A. G. Csaszar, W. Klopper, V. Szalay, W. D. Allen, and H. F. Schaefer, "The Barrier to Linearity of Water", *J. Chem. Phys.* **110**, 11971 (1999).
12 M. Hofmann and H. F. Schaefer, "The $[C_6H_{10}]^{\cdot+}$ Hypersurface: The Parent Radical Cation Diels-Alder Reaction and Alternative Pathways", *J. Amer. Chem. Soc.* **121**, 6719 (1999).
13. N. Takagi, K. Fukuzawa, Y. Osamura, and H. F. Schaefer, "Ion-Molecule Reactions Producing HC_3NH^+ in Interstellar Space: Forbiddenness of the Reaction between Cyclic $C_3H_3^+$ and the N Atom", *Astrophys. J.* **525**, 791 (1999).
14. R. I. Kaiser, I. Hahndorf, L. C. L. Huang, Y. T. Lee, H. F. Bettinger, P. R. Schleyer, and H. F. Schaefer, "Crossed Beam Reaction of Atomic Carbon $C(^3P_j)$ with d_6-Benzene, C_6D_6 $(X\ ^1A_{1g})$: Observation of the Per-Deutero-1, 2-Didehydro-Cycloheptatrienyl Radical, $C_7D_5(X\ ^2B_2)$", *J. Chem. Phys.* **110**, 6091 (1999).
15. Y. Xie, H. F. Schaefer, X.-Y. Fu, and R.-Z. Liu, "The Infrared Spectrum of the NO Dimer Cation: Problems for Density Functional Theory and a Muddled Relationship to Experiment", *J. Chem. Phys.* **111**, 2532 (1999).
16. H. F. Bettinger, J. C. Rienstra-Kiracofe, B. C. Hoffman, H. F. Schaefer, J. E. Baldwin, and P. R. Schleyer, "Structural Isomerization of Cyclopropane: A New Mechanism Through 1-Propylidene", *J. Chem. Soc. Chem. Communications* 1515 (1999).
17. N. Balucani, O. Asvany, A. H. H. Chang, S. H. Lin, Y. T. Lee, R. I. Kaiser, H. F. Bettinger, P. R. Schleyer, and H. F. Schaefer, "Crossed Beam Reaction of Cyano Radicals with Hydrocarbon Molecules I: Dynamics of Cyanobenzene (C_6H_5CN; $X\ ^1A_1$) and Perdeutero Cyanobenzene (C_6D_5CN; $X\ ^1A_1$) Formation from Reaction of $CN(X\ ^2\Sigma^+)$ with Benzene, $C_6H_6(X\ ^1A_{1g})$ and d_6-Benzene, $C_6D_6(X\ ^1A_{1g})$", *J. Chem. Phys.* **111**, 7457 (1999).

18. N. Balucani, O. Asvany, A. H. H. Chang, S. H. Lin, Y. T. Lee, R. I. Kaiser, H. F. Bettinger, P. R. Schleyer, and H. F. Schaefer, "Crossed Beam Reaction of Cyano Radicals with Hydrocarbon Molecules II: Chemical Dynamics of 1,1-Cyanomethylallene ($CNCH_3CCCH_2$: $X\ ^1A'$) Formation from Reaction of $CN(X\ ^2\Sigma^+)$ with Dimethylacetylene, $CH_3CCCH_3(X\ ^1A_1')$", *J. Chem. Phys.* **111**, 7472 (1999).
19. M. Hofmann and H. F. Schaefer, "Pathways for the Reaction of the Butadiene Radical Cation $[C_4H_6]^{\bullet+}$ with Ethylene", *J. Phys. Chem.* A **103**, 8895 (1999).
20. N. A. Richardson, J. C. Rienstra-Kiracofe, and H. F. Schaefer, "Examining Trends in the Tetravalent Character of Group 14 Elements (C, Si, Ge, Sn, Pb) with Acids and Hydroperoxides", *J. Amer. Chem. Soc.* **121**, 10813 (1999).
21. J. C. Rienstra-Kiracofe, G. B. Ellison, B. C. Hoffman and H. F. Schaefer, "The Electron Affinities of C_3O and C_4O," *William A. Goddard Issue, J. Phys. Chem.* **A 104**, 2273 (2000).
22. R. A. King, W. D. Allen, and H. F. Schaefer II, "On Apparent Quantized Transition-State Thresholds in the Photofragmentation of Acetaldehyde", *J. Chem. Phys.*
23. R. I. Kaiser, O. Asvany, Y. T. Lee, H. F. Bettinger, P. R. Schleyer, and H. F. Schaefer, "Crossed Beam Reaction of Phenyl Radicals with Unsaturated Hydrocarbon Molecules. I. Chemical Dynamics of Phenylmethyacetylene ($C_6H_5CCCH_3$; $X\ ^1A'$) Formation from Reaction of C_6H_5 ($X\ ^2A_1$) with Methylacetylene, CH_3CCH (X^1A_1)", *J. Chem. Phys.* **112**, 4994 (2000).
24. S. T. Brown, Y. Yamaguchi, and H. F. Schaefer, "The $\tilde{X}\ ^3\Sigma^-$ and $\tilde{A}\ ^3\Pi$ Electronic States of Ketenylidene (CCO): Analysis of the Renner-Teller Effect in the Upper State", *Marilyn Jacox Issue, J. Phys. Chem.*
25. A. G. Csaszar, W. D. Allen, Y. Yamaguchi, and H. F. Schaefer, "*Ab Initio* Determination of Accurate Ground Electronic State Potential Energy Hypersurfaces for Small Molecules", in *Computational Molecular Spectroscopy*, Editors P. R. Bunker and P. Jensen (Wiley, New York, 2000).
26. T. D. Crawford, S. S. Wesolowski, E. F. Valeev, R. A. King, M. L. Leininger, and H. F. Schaefer, "The Past, Present, and Future of Quantum Chemistry", in *Science at the Turn of the Millennium*, editor E. Keinan.
27. I. S. Ignatyev, H. F. Schaefer, and P. R. Schleyer, "Triplet States of Carbenium and Silylium Cations", *Chem. Phys. Lett.*
28. M. Hofmann and H. F. Schaefer, "Structure and Reactivity of the Vinylcyclopropane Radical Cation", *J. Org. Chem.*
29. Y. Xie and H. F. Schaefer, "The Puzzling Infrared Spectra of the Nitric Oxide Dimer Radical Cation: A Systematic Application of Brueckner Methods", *Molecular Physics*
30. J. C. Rienstra-Kiracofe, W. D. Allen, and H. F. Schaefer, "The $C_2H_5+O_2$ Reaction Mechanism: High Level *Ab Initio* Characterizations", *Feature Article, J. Phys. Chem. A.*
31. S.-J. Kim and Henry F. Schaefer , Dimethyldioxirane, Carbonyl Oxide, and the Transition State Connecting Them: Electronic Structures, Relative Energies, and Vibrational Frequencies", *J. Phys. Chem.*
32. H. F. Bettinger, P. R. Schleyer, P. R. Schreiner, H. F. Schaefer, R. I. Kaiser, and Y. T. Lee, "The Reaction of Benzene with Ground State Carbon Atom, $C(^3P_j)$", *J. Chem. Phys.*

Theoretical Studies of Reaction Dynamics and Energy Transfer

George C. Schatz†
Theoretical Chemistry Group
Argonne National Laboratory
Argonne, Il 60439
(847)491-5657
schatz@chem.nwu.edu

† Mailing address: Department of Chemistry, Northwestern University, Evanston IL 60208-3113

This research program is concerned with using theoretical methods to study gas phase reactions important to combustion chemistry, with emphasis on the development of global potential energy surfaces and on high quality reaction dynamics calculations. Included in the reaction dynamics studies are quasiclassical and quantum scattering calculations of thermal rate constants, cross sections, angular distributions, internal state distributions and related information.

The primary focus of the present research program is on electronically nonadiabatic effects in chemical reactions. Three specific reactions being studied are: $O(^1D) + H_2$, $N(^2D) + H_2$ and $Cl(^2P) + HCl$. For all these reactions, accurate potential energy surfaces based on *ab initio* calculations have been determined and we are studying the dynamics using scattering theory methods and/or trajectory methods.

Our work on the reaction $O(^1D) + H_2 \rightarrow OH + H$ was described extensively in last year's report. We continue to study this reaction, as new experimental results have provided new clues concerning the role of nonadiabatic interactions in the reaction dynamics. In particular, we are currently studying the effect of rotational excitation on the reactive cross sections. In past work it has been assumed that rotation had no effect on the ground state (1A') potential surface, as this surface is weakly anisotropic and globally attractive. Reaction on the excited states (1A" and 2A') involves surmounting a collinear barrier, and in prior work we had suggested that this would suppress reactivity for low excitation, and enhance it for high excitation. Our recent studies have demonstrated that many of these earlier conclusions need to be revised. First of all, we find in both trajectory and quantum scattering calculations that rotational excitation suppresses reactivity on the ground state surface at low collision energies. Second, we find that the suppression in reactivity that we had previously found for the excited states is not observed for the most accurate states we now have available (due to Dobbyn and Knowles).

The reaction $N(^2D) + H_2$ is somewhat analogous to $O(^1D) + H_2$ but there are also important differences. This year we completed studies of the reaction dynamics on the two lowest potential energy surfaces, 1A" and 1A'. These are the only surfaces that are not repulsive, and the ground state, 1A", is the only one that correlates between the ground states of the reactants and products. The 1A' state correlates adiabatically to excited products, but can access ground state products very efficiently through its Renner-Teller coupling with the ground state. We have now completed detailed trajectory studies of the reaction dynamics on ground and excited states, and we find excellent agreement with recent molecular beam measurements due to Casavecchia, as well as very good agreement with a variety of laser chemistry and kinetics measurements.

Our work on $Cl(^2P)$ + HCl has also evolved considerably in the past year. Here we are interested in understanding the effect of spin-orbit interactions on reactivity. We have developed a quantum scattering code for doing these studies that incorporates spin-orbit coupling, electronic and nuclear Coriolis coupling, and electrostatic coupling accurately in the coupled channel expansion. In previous work we also developed a very high quality potential energy surface for describing the reaction dynamics. This year we completed a detailed dynamics study of reaction probabilities and resonances based on this surface. Using comparisons with experiment, we have determined that the reaction barrier is about 1 kcal/mol too high, and a new scaled surface has been determined that reproduces experimental rate data. Using this new surface, we have generated preliminary results that suggest that spin-orbit excited rate coefficients are larger than their ground state counterparts for this reaction. This result is in accord with recent molecular beam studies, and it suggests that the role of spin-orbit excitation on reaction kinetics, which has traditionally assumed that spin-orbit excitation does not actively contribute to motion needed in surmounting reaction barriers may need revision. Further work is underway.

This work was supported by the U. S. Department of Energy, Office of Basic Energy Sciences, Division of Chemical Sciences, under Contract No. W-31-109-ENG-38.

Publications (1998-present)

Quantum Scattering Studies of Spin-Orbit Effects in the $Cl(^2P)$ + HCl → ClH + $Cl(^2P)$ Reaction, G. C. Schatz, P. McCabe and J. N. L. Connor, Far. Disc. Chem. Soc., **110**, 139-157 (1998).

Coupled *ab initio* potential energy surfaces for the reaction $Cl(^2P)$ + HCl → ClH + $Cl(^2P)$ A. J. Dobbyn, J. N. L. Connor, N. A. Besley, P. J. Knowles and G. C. Schatz, Phys. Chem. Chem. Phys., **1**, 1141-1148, 1999.

Helicity decoupled quantum dynamics and capture model cross sections and rate constants for $O(^1D)+H_2 \rightarrow OH + H$, S. K. Gray, E. M. Goldfield, G. C. Schatz and G. G. Balint-Kurti, Phys. Chem. Chem. Phys., **1**, 957-966 (1999)

Potential energy surface and quasiclassical trajectory studies of the $N(^2D) + H_2$ Reaction, L. A. Pederson, G. C. Schatz, T-S Ho, T. Hollebeek, H. Rabitz, L. B. Harding and G. Lendvay, J. Chem. Phys., **110**, 9091-100 (1999).

A Combined Experimental and Theoretical Study of the Simplest Nitrogen Atom Reaction, M. Alagia, N. Balucani, L. Cartechini, P. Casavecchia, G.G. Volpi, L. A. Pederson, G.C. Schatz, G. Lendvay, L.B.Harding,T. Hollebeek, T. –S. Ho, H. Rabitz , J. Chem. Phys., 110, 8857-60 (1999).

Coupled *ab initio* potential energy surfaces for the reaction $Cl(^2P)$ + HCl → ClH + $Cl(^2P)$ A. J. Dobbyn, J. N. L. Connor, N. A. Besley, P. J. Knowles and G. C. Schatz, Phys. Chem. Chem. Phys., **1**, 957-966 (1999).

Helicity decoupled quantum dynamics and capture model cross sections and rate constants for $O(^1D)+H_2 \rightarrow OH + H$, S. K. Gray, E. M. Goldfield, G. C. Schatz and G. G. Balint-Kurti, Phys. Chem. Chem. Phys., **1**, 1141-1148 (1999).

Reaction of H with Highly Vibrationally Excited Water: Activated or Not?, G.C. Schatz, G. Wu, G. Lendvay, De-Cai Fang and L. B. Harding, Far. Disc. Chem. Soc., **113**, 151-66(1999).

Potential energy surface of the A state of NH_2, and the role of excited states in the $N(^2D) + H_2$ Reaction, L. A. Pederson, G. C. Schatz, T. Hollebeek, T. -S. Ho, H. Rabitz, and L. B. Harding, J. Phys. Chem., **112**, (2000), in press.

Quantum Wave Packet Study of Nonadiabatic Effects in $O(^1D) + H_2 \rightarrow OH + H$, S. K. Gray, C. Petrongolo, K. Drukker and G. C. Schatz, J. Phys. Chem. **103**, 9448-9459 (1999).

Quantum scattering on coupled ab initio potential energy surfaces for the $Cl(^2P) + HCl \rightarrow ClH + Cl(^2P)$ reaction, T. W. J. Whiteley, A. J. Dobbyn, J. N. L. Connor and G. C. Schatz, Chem. Phys. Phys. Chem., (2000) in press.

Theoretical Studies of Potential Energy Surfaces and Computational Methods

Ron Shepard
Chemistry Division
Argonne National Laboratory
Argonne, IL 60439
[email: shepard@tcg.anl.gov]

Program Scope: This project involves the development, implementation, and application of theoretical methods for the calculation and characterization of potential energy surfaces (PES) involving molecular species that occur in hydrocarbon combustion. These potential energy surfaces require an accurate and balanced treatment of reactants, intermediates, and products. This difficult challenge is met with general multiconfiguration self-consistent-field (MCSCF) and multireference single- and double-excitation configuration interaction (MRSDCI) methods. In contrast to the more common single-reference electronic structure methods, this approach is capable of describing accurately molecular systems that are highly distorted away from their equilibrium geometries, including reactant, fragment, and transition-state geometries, and of describing regions of the potential surface that are associated with electronic wave functions of widely varying nature. The MCSCF reference wave functions are designed to be sufficiently flexible to describe qualitatively the changes in the electronic structure over the broad range of molecular geometries of interest. The necessary mixing of ionic, covalent, and Rydberg contributions, along with the appropriate treatment of the different electron-spin components (e.g. closed shell, high-spin open-shell, low-spin open shell, radical, diradical, etc.) of the wave functions are treated correctly at this level. Further treatment of electron correlation effects is included using large scale multireference CI wave functions, particularly including the single and double excitations relative to the MCSCF reference space. This leads to the most flexible and accurate large-scale MRSDCI wave functions that have been used to date in global PES studies.

Electronic Structure Code Maintenance and Development: A major component of this project is the development and maintenance of the COLUMBUS Program System. The COLUMBUS Program System is maintained and developed collaboratively with several researchers including Isaiah Shavitt and Russell M. Pitzer (Ohio State University), and Hans Lischka (University of Vienna, Austria). During the past year, the COLUMBUS Program System of electronic structure codes has been maintained on the various machines used for production calculations by the Argonne Theoretical Chemistry Group, including the Sun workstations, the Cray C90 and J90 at NERSC, IBM RS6000 workstations, the parallel IBM SP QUAD machine at ANL, and the Theoretical Chemistry Group's IBM SP parallel supercomputer. In the next year, these codes will be ported also to the IBM SP at NERSC which is a distributed-memory parallel machine in which each node consists of two shared-memory CPUs. These computer codes are used in all of the production-level molecular applications by members and visitors of the Argonne Theoretical Chemistry Group.

In collaboration with Hans Lischka (University of Vienna, Austria) and Robert Harrison (Pacific Northwest National Laboratory), the parallel version of the CI diagonalization program CIUDG has been developed and ported to several large parallel machines. Using the TCGMSG library, this program also runs on networks of workstations, small-scale shared-memory parallel machines (e.g. Alliant and Cray), and small-scale distributed memory machines (e.g. Intel IPSC/i860). The latest version of this parallel code uses the Global Array library. The use of this library eliminates unnecessary synchronization steps from earlier versions of this code, and reduces the overall

communications requirements for larger numbers of nodes. Excellent scalability on as many as 320 nodes of the Intel Delta, 256 nodes of the IBM SP, and 512 nodes on the Cray T3D and T3E have been demonstrated. One benchmark calculation by Dachsel, et al [*J. Phys. Chem. A*, **103**, 152-155 (1999)] using this code employed a 1.3E9 CSF expansion of the wave function, the largest MRSDCI wave function ever reported. This is the first successful attempt to parallelize a production-level MRSDCI code, and this effort represents a major step forward toward using effectively the large-scale parallel supercomputers that are becoming available to scientists. Generalizations of the method are planned that will allow treatment of larger molecular systems. Future effort will be directed also to integrate the parallel version of the code with other parts of the COLUMBUS Program System to allow production-level PES calculations.

Initial applications of the MRSDCI analytic energy gradient code have begun and have included both ground and excited electronic states, and a variety of states including both closed- and open-shell systems and states of mixed valence and Rydberg character. Future developmental work of this code will include the addition of more orbital resolution options for additional flexibility in the wave function specification and the development of a parallel version to accompany the parallel MRSDCI code for large-scale wave functions. A study of geometry optimizations for several small molecules has been initiated with the current code. This allows direct comparisons with experimental results and with other electronic structure methods. These geometry comparisons demonstrate that even with modest MCSCF reference spaces, the MRSDCI geometries compare very well with the very best single-reference methods currently in use. This is encouraging because the flexible MRSDCI wave functions are expected to be comparably accurate over the entire PES, whereas it is known that the accuracy of single-reference methods is biased toward those regions of the PES that are dominated by the reference determinant (such as near equilibrium conformations). These initial comparisons are for ground-state singlet molecules, and future work will include similar comparisons for high-spin states, radicals, and excited electronic states.

The major computational step involved in MRSDCI analytic energy gradients after the energy calculation is the computation of the CI density matrices. This step typically requires about 10% of the effort of the energy calculation. Very large-scale wave functions can be optimized with the parallel MRSDCI code, reducing the (wall clock) time required for this step considerably. With this reduction in computation time for the energy and wave function optimization step, this leaves the CI density step as the most significant bottleneck in the time-to-solution for PES calculations and geometry optimizations. In the past year, a parallel version of the CI density code has been developed that is based on the same basic methodology that is used in the parallel CI code. This allows the density computation to again take 10% of the time of the energy computation for large-scale MRSDCI wave functions. The first applications have been initiated with this code–the geometry optimization of C_2H_4 with a flexible multireference wave function using three orbital basis sets. The smallest basis set (cc-pVDZ), results in 24M CSFs, the medium basis set (cc-pVTZ), results in 198M CSFs, and the largest basis (cc-pVQZ), results in 858M CSFs. These are the largest CI wave functions that have ever been used in an analytic energy gradient geometry optimization.

Public Distribution of the COLUMBUS Program System: The COLUMBUS Program System is available using the *anonymous ftp* facility of the internet. The codes and online documentation are now also available from the web address http://www.itc.univie.ac.at/~hans/Columbus/columbus.html. The latest code version, 5.5, was released in August, 1999. In addition to the source code, the complete online documentation, installation scripts, sample calculations, and numerous other utilities are included in the distribution. A partial implementation of an IEEE POSIX 1009.3 library has

been developed and is also available from the anonymous ftp server `ftp.tcg.anl.gov`. This library simplifies the porting effort required for the COLUMBUS codes, and also may be used independently for other Fortran programming applications.

Iterative Matrix Diagonalization: A new iterative subspace diagonalization method, called Subspace Projected Approximate Matrix (SPAM), has been developed. In a subspace method, a new trial vector is added to an existing vector subspace each iteration. The choice of expansion vectors determines the convergence rate. The traditional Davidson and Lanczos methods are examples of iterative subspace methods. In the SPAM approach, an approximate matrix is constructed each iteration using a projection operator approach, and the eigenvector of this approximate matrix is used to define the new expansion vector. The convergence rate is improved over the Davidson and Lanczos approaches by choosing an appropriate approximate matrix to define the expansion space. The efficiency of the procedure depends on the relative expense of forming approximate and exact matrix-vector products. In the past year this method has been extended in two different ways. First, it has been extended to simultaneous optimization of several roots. This is achieved by converging all of the roots at the approximate level before contracting and computing the exact matrix-vector products; this minimizes the overall effort required to optimize all of the desired eigenpairs. Second, the method has been extended to allow an arbitrary number of levels of matrix approximations. This results in a multiroot-multilevel SPAM algorithm that has a wide range of possible applications. In the next year, this matrix diagonalization method will be applied to ground and excited-state CI wave function optimization and to rational-function Direct-SCF optimization.

This work was supported by the U.S. Department of Energy, Office of Basic Energy Sciences, Division of Chemical Sciences, under Contract No. W-31-109-ENG-38.

Publications:

"Workshop Report on Large-Scale Matrix Diagonalization Methods in Chemistry Theory Institute", edited by C. H. Bischof, R. L. Shepard, and S. Huss-Lederman, ANL/MCS-TM-219 (1997). Also available online: `ftp://info.mcs.anl.gov/pub/tech_reports/reports/TM219.ps.Z`

"A Massively Parallel Multireference Configuration Interaction Program – The Parallel COLUMBUS Program", H. Dachsel, H. Lischka, R. Shepard, J. Nieplocha, and R. J. Harrison, *J. Computational Chem.* **18**, 430-448 (1997).

"A Systematic *Ab Initio* Investigation on the Open and Cyclic Structures of Ozone", T. Müller, S. S. Xantheas, H. Dachsel, R. J. Harrison, J. Nieplocha, R. Shepard, G. S. Kedziora, and H. Lischka, *Chem. Phys. Letters* **293**, 72-80 (1998).

"High-Performance Computational Chemistry: Hartree-Fock Electronic Structure Calculations on Massively Parallel Processors", J. L. Tilson, M. Minkoff, A. F. Wagner, R. Shepard, P. Sutton, R. J. Harrison, R. A. Kendall, A. T. Wong, *The Int. J. High Performance Computing Applications* **13**, 291-302 (1999).

"Ab Initio Determination of Americium Ionization Potentials", J. L. Tilson, R. Shepard, C. Naleway, A. F. Wagner, and W. C. Ermler, *J. Chem. Phys.* **112**, 2292-2300 (2000).

COMPUTATIONAL AND EXPERIMENTAL STUDY OF LAMINAR FLAMES

M. D. Smooke and M. B. Long
Department of Mechanical Engineering
Yale University
New Haven, CT 06520
mitchell.smooke@yale.edu

Program Scope

Our research has centered on an investigation of the effects of complex chemistry and detailed transport on the structure and extinction of hydrocarbon flames in coflowing axisymmetric configurations. We have pursued both computational and experimental aspects of the research in parallel. The computational work has focused on the application of accurate and efficient numerical methods for the solution of the boundary value problems describing the various reacting systems. Detailed experimental measurements were performed on axisymmetric coflow flames using two-dimensional imaging techniques. Spontaneous Raman scattering and laser-induced fluorescence were used to measure the temperature, major and minor species profiles.. Laser-induced incandescence has been used to measure soot volume fractions. Our goal has been to obtain a more fundamental understanding of the important fluid dynamic and chemical interactions in these flames so that this information can be used effectively in combustion modeling.

Recent Progress

The major portion of our work during the past year has focused on a combined computational and experimental study of time varying, axisymmetric, laminar, unconfined, methane-air diffusion flames and on a combined computational and experimental study of the formation of soot in axisymmetric, laminar, unconfined, ethylene-air diffusion flames. The time varying systems can enable the investigator to bridge the gap between laminar and fully turbulent systems. In addition, time varying flames offer a much wider range of interactions between chemistry and fluid dynamics than do steady-state configurations. The sooting flames can enable the investigator to understand the detailed inception, oxidation and surface growth processes by which soot is formed in hydrocarbon flames.

Time-Varying Flames

Atmospheric pressure, overventilated, axisymmetric, coflowing, nonpremixed laminar flames were generated with a burner in which the fuel flows from an uncooled 4.0 mm inner diameter vertical brass tube (wall thickness 0.038 mm) and the oxidizer flows from the annular region between this tube and a 50 mm diameter concentric tube. The oxidizer is air while the fuel is a mixture containing methane and nitrogen 65%/35% by volume, to eliminate soot. The burner includes a small loudspeaker in the plenum of the fuel jet, which allows a periodic perturbation to be imposed on the exit parabolic velocity profile. Perturbations of 30% and 50% of the average velocity have been investigated. Because the flame is slightly lifted, there is no appreciable heat loss to the burner.

Two-dimensional profiles of temperature, mixture fraction, and mole fractions of N_2, CO_2, CH_4, H_2, CO, and H_2O as well as CH* emission have been measured in the time-varying flame. We obtain CH* relative concentration from flame chemiluminescence, and species concentrations and temperature with vibrational Stokes-shifted Raman scattering and Rayleigh scattering using the second harmonic of a Nd:YAG laser. Each measurement is averaged over 1200 laser pulses, with separate data acquisitions for each orthogonal polarization of the scattered light. The signals are integrated over a spectral window large enough to account for spectral broadening due to temperature increases, but small enough

to minimize crosstalk with other species. Measurements are performed at heights above the burner ranging from 2.5 mm to 50 mm, in 0.5 mm increments. These line measurements are then tiled together to form images. Data are acquired for the steady state flame, and for five equally spaced phases of the forced flame over one forcing period.

As a relatively simple experiment, CH* in a flame can be measured from flame chemiluminescence (without a laser). Since CH* occurs in approximately the same location in a flame as CH, and since CH is a good flame front marker, we can easily determine the flame front. Images are obtained for the steady state flame, and for 10 equally spaced phases of the forced flame over one forcing period (five of these phases were identical to the phases for the species and temperature measurements.) Acquisitions are phase-locked and integrated over 200 intensifier gates. An Abel inversion converts the line of sight collection of CH* emission into an in-plane two-dimensional profile.

The modulated flame length increases in time, until the flame begins to pinch off downstream, forming two slightly attached high temperature regions. For the 50% modulation, the two regions break apart, leaving unattached high temperature zones. Eventually the downstream region moves farther downstream, and burns out. The pinch-off phenomenon is more drastic in the 50% modulation than the 30% modulation. For the 50% case, the flame has a larger curvature than for the 30% case. The flame width at the flame anchoring point varies significantly over time, with a larger fluctuation seen for the 50% case. The lift off height stays the same over time, comparable to the steady flame lift off height. There appears to be more soot production for the 50% than for the 30% modulation, and a large increase in soot as compared to the unforced flame. Further investigation into soot production of the forced flame is needed.

Soot Modeling

Soot kinetics are modeled as coalescing, solid carbon spheroids undergoing surface growth in the free molecule limit. The particle mass range of interest is divided into sections and an equation is written for each section including coalescence, surface growth, and oxidation. Sectional analysis makes it possible to obtain the particle size distribution without a-priori assumptions about the form of the distribution. For the smallest section, an inception source term is included. The transport conservation equation for each section includes thermophoresis, an effective bin diffusion rate, and source terms for gas-phase scrubbing. The gas and soot equations are additionally coupled through non-adiabatic radiative loss in the optically-thin approximation. The inception model employed here is based on an estimate of the formation rate of two- and three-ringed aromatic species (naphthalene and phenanthrene), and is a function of local acetylene, benzene, phenyl and molecular hydrogen concentrations. The contributions from the inception processes are incorporated in the first sectional bin, whose lower mass boundary is set equal to the mass of the smallest inception species. In the sectional representation, the sectional mass boundaries vary linearly on a logarithmic scale. The number of sections required for convergence must be examined for each problem and depends on the relative magnitudes of surface growth and inception. Oxidation of soot is by O_2 and OH. The surface growth rate is based upon that of Harris and Weiner [1] with an activation energy as suggested by Hura and Glassman [2].

Gas temperatures were measured with thermocouples and corrected for radiation heat transfer effects using standard techniques. A rapid insertion procedure was used to minimize errors due to soot deposition onto the thermocouple. In soot-free regions, the absolute uncertainty of these measurements is estimated to be ± 50 K and the relative uncertainty to be ± 10 K. Species concentrations were measured by extracting gas samples from the flames with a narrow-tipped quartz microprobe and analyzing these samples with on-line mass spectrometry. Acetylene and ethylene were quantified with an Extrel C50 variable-

ionization-energy electron-impact/quadrupole mass spectrometer, and C_3 to C_{12} hydrocarbons with a custom-built photoionization/time-of-flight mass spectrometer. Measurements were directly calibrated and have an absolute uncertainty of 30%. Profiles were generated by moving the burner with translation stages. The axial and radial coordinates, designated z and r, have a relative uncertainty of ± 0.2 mm and an absolute uncertainty of ± 0.5 mm.

Using planar laser imaging, we obtain two-dimensional fields of temperature, fuel concentration, and soot volume fraction in the C_2H_4/N_2 flame. The temperature field is determined using the two scalar approach of Stårner et al. [3] and included the measurement of Rayleigh scattering and the use of the computed fuel concentration. The soot volume fraction field is determined by laser-induced incandescence (LII). At sufficient laser intensities, the LII signal has been shown to be directly proportional to soot volume fraction. Probe measurements of the soot volume fraction are used for calibration.

The chemical kinetic mechanism for ethylene combustion has 52 species and 233 reactions. It was derived from GRIMech 1.2 [4], based upon comparisons to experimental data on ethylene from perfectly stirred and flow reactors and ignition delay data. It includes reactions describing the formation and oxidation of benzene, and related species. Fuel and nitrogen are introduced through the center tube (4mm id) utilizing a parabolic velocity profile and air through the outer coflow with a plug flow profile. Both velocity profiles were those employed in the experiments. Flames containing 40% (60%), 60% (40%) and 80% (20%) mole fractions of ethylene (nitrogen) with a bulk averaged velocity of 35 cm/sec were studied. The coflow air velocity was 35 cm/sec. Reactant temperatures were assumed to be 298 K. All radial velocities were assigned to zero at the flame base. Calculations were performed on an SGI Origin 2000 computer. The computations included 20 soot sections. Starting from a converged solution for an ethylene-air flame without the sectional equations, we typically obtained converged solutions for the complete gas-soot problem in several hours of computer time.

Variations in the base soot model surface growth, inception, and oxidation rates were carried out to gain understanding of the possible causes of the difference between the model and the experiments. These studies did not yield a clean explanation of the discrepancies. We conclude that the ability to make quantitative soot predictions remains limited by some fundamental uncertainties in the soot model (including the lack of aging and aggregate formation effects), by the ability of the chemical kinetic mechanism to predict accurately the concentrations of important species (benzene, propargyl, acetylene and diacetylene) and possibly by the lack of quantitative information concerning the production of translucent particles.

Future Plans

During the next year we hope to expand our research in two main areas. First, we will continue our study of sooting hydrocarbon flames with the goal of understanding the differences in soot distribution between the computational and experimental results. Second, we will continue our study of flickering diffusion flames with the goal of predicting acetylene and benzene concentrations as a function of time. We will then begin incorporating a detailed soot model into the gas phase system with the goal of predicting soot volume fractions as a function of time. Laser induced incandescence (LII) will be used to measure soot volume fractions.

References

1. Harris, S.J., and Weiner, A.M., *Combust. Sci. Tech.*, **31**, p. 155, (1983).

2. Hura, H.S. and Glassman, I., *Twenty-Second Symposium (International) on Combus-*

tion, The Combustion Institute, Pittsburgh, 1988, p. 371.

3. Stårner, S., Bilger, R. W., Dibble, R. W., Barlow, R. S., *Combust. Sci. Tech.*, **86**, p. 223, (1992).

4. Bowman, C.T., Hanson, R.K., Davidson, D.F., Gardiner, Jr., W.C. Lissianski, V., Smith, G.P., Golden, D.M., Frenklach, M., Wang, H., and Goldenberg, M., *GRI-Mech version 2.11*, http://www.gri.org (1995).

DOE Sponsored Publications 1998-2000

1. B. A. V. Bennett and M. D. Smooke, "Local Rectangular Refinement with Application to Fluid Flow Problems," **151**, *J. Comp. Phys.*, (1999).

2. B. A. V. Bennett and M. D. Smooke, "Local Rectangular Refinement with Application to Axisymmetric Laminar Flames," *Comb. Theory and Modelling*, **2**, (1998).

3. C. McEnally, A. Shaffer, M. B. Long, L. Pfefferle, M. D. Smooke, M. B. Colket and R. J. Hall, "Computational and Experimental Study of Soot Formation in a Coflow Laminar Ethylene Diffusion Flame, *27th Symposium (International) on Combustion*, (1998).

4. K. Walsh, M. A. Tanoff, M. B. Long and M. D. Smooke, *27th Symposium (International) on Combustion*, "Computational and Experimental Study of OH^* and CH^* Radicals in an Axisymmetric Laminar Diffusion Flame," (1998).

5. R. Mohammed, M. A. Tanoff, M. B. Long and M. D. Smooke, "Computational and Experimental Study of a Flickering Axisymmetric Laminar Diffusion Flame," *27th Symposium (International) on Combustion*, (1998).

6. B. A. V. Bennett and M. D. Smooke, "A Comparison of the Structures of Lean and Rich Axisymmetric Laminar Diffusion Flames: Application of Local Rectangular Refinement Solution-Adaptive Gridding," *Comb. Theory and Modelling*, **3**, (1999).

7. C. McEnally, L. Pfefferle, R. Mohammed, M. D. Smooke and M. B. Colket, "Mapping of Trace Hydrocarbon Concentrations in Two-Dimensional Flames Using Single-Photon Photoionization Mass Spectrometry, *Anal. Chem*, **71**, (1999).

8. J. Luque, J. B. Jeffries, G. P. Smith, D. R. Crosley, K. T. Walsh, M. B. Long, and M. D. Smooke, "CH(A-X) and OH(A-X) Optical Emisison in an Axisymmetric Laminar Diffusion Flame, to be published *Comb. and Flame*, (2000).

9. B. A. V. Bennett, C. McEnally, L. Pfefferle, and M. D. Smooke, "Computational and Experimental Study of Axisymmetric Coflow Partially Premixed Methane/Air Flames," to be published *Comb. and Flame*, (2000).

10. K.T. Walsh, J. Fielding, M.D. Smooke, and M.B. Long, "Experimental and Computational Study of Temperature, Species, and Soot in Buoyant and Nonbuoyant Coflow Laminar Diffusion Flames," to be published *28th Symposium (International) on Combustion*, 2000.

11. C.S. McEnally, L.D. Pfefferle, A.M. Schaffer, M.B. Long, R.K. Mohammed, M.D. Smooke, and M.B. Colket, "Characterization of a Coflowing Methane Air Nonpremixed Flame with Computer Modelling, Rayleigh-Raman Imaging, and On-Line Mass Spectrometry," to be published *28th Symposium (International) on Combustion*, 2000.

Universal/Imaging Studies of Chemical Reaction Dynamics

Arthur G. Suits
Chemical Sciences Division MS 6-2100
Ernest Orlando Lawrence Berkeley National Laboratory
Berkeley CA 94720
agsuits@lbl.gov

Program Scope

Our program seeks to study the global dynamics of systems of relevance to combustion and atmospheric chemistry, with emphasis on primary photodissociation events and the dynamics of bimolecular reactions under crossed-beam conditions. We exploit complementary techniques utilizing lasers and synchrotron radiation to perform state resolved and universal product detection. Tunable VUV undulator radiation on the Chemical Dynamics Beamline at the Advanced Light Source is used to ionize products formed in photodissociation and reactive scattering. This soft ionization technique provides *universal* and *selective* detection, allowing us to study molecules not accessible to laser-based probes. Furthermore, we use velocity map imaging in conjunction with tunable dye lasers to study the photodissociation dynamics of free radicals and molecules, perform photoelectron and photoionization spectroscopy of novel metastable species, and gather global snapshots of reactive scattering events. Future studies will take advantage of the new imaging endstation 3 on the Beamline and the associated high-throughput monochromator system to develop innovative new studies of the spectroscopy and dynamics of ions, radicals and clusters.

Recent Progress

Photodissociation of ethylene sulfide at 193nm

Photodissociation at 193nm of ethylene sulfide has been studied using photofragment translational spectroscopy with tunable VUV probe on the Chemical Dynamics Beamline to reveal new aspects of the photodissociation dynamics. The results suggest the presence of a channel giving $S(^3P)$ in conjunction with *triplet* ethylene C_2H_4 ($^3B_{1u}$) and allow for the first experimental measure of the energy of the latter species near its equilibrium geometry, in which the two methylene groups occupy perpendicular planes. In addition, a channel representing the production of H_2S with vinylidene also has been observed. The experimental results are supported by recent theoretical calculations. Details of the complex dissociation dynamics, involving multiple potential surfaces, have been inferred for all principal decay channels. In addition, strong alignment of the $S(^1D)$ atom is observed in state-resolved imaging experiments (see below) and the results aid in the interpretation of the PTS study.

Photodissociation of phenylacetylene at 193 nm

The gas phase ultraviolet (UV) photochemistry of phenylacetylene (PA) has been studied at 193nm using undulator radiation at the Chemical Dynamics Beamline . The primary dissociation pathway observed leads to the formation of acetylene + C_6H_4. Some of the latter molecules were found to undergo secondary decomposition to 1,3,5-hexatri-yne (triacetylene) + H_2, providing the first reported experimental value for the heat of formation of triacetylene.

193 nm photodissociation of thiophene using synchrotron radiation

Thiophene is an important sulfur-bearing aromatic in fossil fuel combustion. Using photofragment translational spectroscopy and undulator synchrotron radiation of the Chemical Dynamics Beamline, we have measured the time-of-flight spectroscopy and some photoionization efficiency spectra (PIE) of photofragments from photolysis of thiophene. Two radical channels and three closed shell channels were observed, in close analogy to the results reported earlier for furan. They are HCS + $HC{\equiv}C\text{-}CH_2$, HS + $H\text{-}C{\equiv}C\text{-}C{=}CH_2$ and C_4H_4 + S, C_3H_4 + CS, C_2H_2 + C_2H_2S respectively. Analysis suggests that all channels occur on ground state surface. The identity of the primary products are identified with photoionization efficiency curves which have been obtained for all products.

Reactive scattering studied by velocity map imaging

Ion imaging is a multiplexing method which provides simultaneous detection of all recoil velocities, both speed and angle, for the detected product, and deconvolution of the images does not require the simplifying assumption of uncoupled translational energy and angular distributions often employed in analyzing reactive scattering

experiments. Yet imaging has not fully lived up to its early promise for probing crossed-beam reaction dynamics, largely owing to the limited sensitivity of the two-photon probes generally employed. We have recently begun a series of investigations of crossed-beam reaction dynamics using velocity map imaging with a single photon ionization probe provided by an F_2 excimer laser at 157nm. This approach affords tremendous sensitivity, making detailed and systematic investigations of polyatomic reaction dynamics quite facile. Our initial studies have focused on the crossed beam reaction of ground state Cl ($^2P_{3/2}$) atoms with alcohols (CH_3OH, C_2H_5OH and 2-C_3H_7OH), with probe of the corresponding hydroxyalkyl radical. The double differential cross sections were obtained at collision energies of 8.7 kcal/mol for methanol, 6.0 and 9.7 kcal/mol for ethanol, and 11.9 kcal/mol for 2-propanol. In all cases, the scattering was predominantly in the backward-sideways direction suggesting direct rebound dynamics, with varying amounts of sideways-scattering. All of the translational energy distributions peaked at about 6 kcal/mol and on average 30-40% of the available energy was deposited into product translation for all the alcohols studied. These results are in contrast with previous H abstraction studies performed on Cl-hydrocarbon systems where some significant forward scattering was observed.

UV photodissociation of hydrocarbon radicals

Hydrogen emission is the principal decay mechanism of hydrocarbon radicals following UV photoexcitation, and the resulting energy release can provide a powerful probe of the energetics of the products and the dynamics of the event. We have recently begun a series of studies using velocity-map imaging of radical photodissociation. These investigations employ 2+1 REMPI probes of the H atom product, and dissociation the radical at the same UV wavelength. The radicals are generated via photolysis using 193nm light at the nozzle of a pulsed valve, with subsequent entrainment and cooling in the molecular beam. In the photodissociation of the vinyl radical (C_2H_3) at 243nm, we found evidence for formation of some cold vinylidene, with the bulk of the C_2H_2 product formed with more than 2 eV internal energy. In addition, a minor contribution was seen which is assigned to triplet acetylene. The inferred heat of formation of vinylidene is in agreement with literature values, and we also derived the first experimental excitation energy for this lowest triplet state of acetylene. We are in the course of extending these studies to the ethyl (C_2H_5), ethynyl (C_2H), and the propargyl (C_3H_3) radicals.

Orbital alignment in atomic photofragments

Photodissociation events, in general, give rise to photofragments whose angular momentum is polarized. If the *angular distribution* of this polarization can be measured, then the dissociation dynamics may be revealed *in the frame of the molecule*. Ion imaging represents a powerful means of probing this alignment angular distribution, as we have shown in a series of papers describing electronic angular momentum polarization in atomic photofragments. We demonstrated the first direct evidence of coherence in atomic orbital alignment following photodissociation in Cl_2, and have shown in NO_2 photodissociation that this coherence reveals that the electron cloud in the recoiling atom 'remembers' the plane of the molecule even in the asymptotic region, and this is likely to be a rather common feature of polyatomic photodissociation dynamics. We have extended these studies to investigations of the alignment and orientation of O(^{1}D) fragments formed in the photodissociation of N_2O at 193nm. Or most recent alignment study is for the S(^{1}D) product of ethylene sulfide photodissociation (see above). The results show three distinct maxima in the alignment as a function of recoil velocity, affording additional insight into the dissociation dynamics. We have also recently begun an investigation of the analogous dynamics leading to orbital orientation, and in ozone photodissociation at 266nm we have found that the principal means of producing oriented O(^{1}D) fragments is by photolysis using linearly polarized light, with the two different projections of the transition moment on the recoil axis giving rise to a torque on the electron cloud in the recoiling atom.

In addition to providing insight into important subtleties of the photodissociation event, orbital alignment can interfere with the spectroscopic determination of commonly sought photochemical quantities such as the angular and translational energy distributions. We have developed a general method of isolating these quantities free of interference from such alignment effects, and demonstrated one such approach in our study of N_2O photodissociation at 193nm.

Future plans

We will continue to expand on our studies of the photodissociation of hydrocarbon molecules and radicals, both in the laboratory and on the Beamline. We will extend our photodissociation studies of heterocyclic aromatics to

methylfuran and dimethylfuran, with an eye to understanding the detailed ground state dynamics in these systems and to developing radical sources for future crossed beam experiments. We will study the dissociation of a variety of alkyl and alkoxy halides, probing both the halogen atom and the radical to explore carefully the internal energy dependence of the VUV detection of the radical. Our studies on the unimolecular dissociation dynamics of large hydrocarbon radicals will be expanded, which will aid in the understanding of the role of polycyclic aromatic hydrocarbons (PAH) in combustion processes.

Complementary studies will be carried out in the laser laboratory. We will extend our photodissociation studies on hydrocarbon free radicals as described above, and demonstrate the general strategies for obtaining alignment-free anisotropy parameters in photodissociation experiments. Key questions in alcohol oxidation are the dynamics and relative branching between abstraction of α- and β- hydrogens. Unfortunately, the imaging experiments at 157nm are only sensitive to the former process because of the fixed 7.9 eV probe energy. Crossed-beam studies on Endstation 1 using the continuous pyrolytic Cl atom source can be used to probe the Cl reaction with ethanol and propanol. The tunable VUV, in conjunction with the energy dependence of the reaction dynamics, will allow discrimination among the different isomers of the hydroxyalkyl radical products, since the ionization energies differ significantly. The second, important issue concerns the relative reactivity and dynamics of spin-orbit excited Cl^*, since other studies have recently suggested distinct dynamics for this species. Complementary imaging studies using a photolytic Cl atom sources will be used to contrast the dynamics for ground state and spin-orbit excited Cl atoms. Finally, as we have seen, the sensitivity of imaging with a single-photon ionization probe is such that we expect to be able to record differential cross sections for $O(^3P)$ and OH reactions with alkanes as well.

DOE Sponsored Publications 1998-2000

D. A. Blank, N. Hemmi, A. G. Suits and Y. T. Lee, "A crossed molecular beam investigation of the reaction Cl + propane → HCl + C_3H_7 using VUV synchrotron radiation as a product probe," *Chem. Phys.* **231**, 261, (1998). LBNL-40947.

D. A. Blank, W. Sun, A. G. Suits, Y. T. Lee, S. W. North and G. E. Hall, "Primary and secondary processes in the 193nm photodissociation of vinyl chloride," *J. Chem. Phys.*, **108**, 5414, (1998). LBNL-41168.

D. A. Blank, A. G. Suits, Y. T. Lee, S. W. North and G. E. Hall, "Photodissociation of acrylonitrile at 193nm: a photofragment translational spectroscopy study using synchrotron radiation for product photoionization," *J. Chem. Phys.*, **108**, 5784, (1998). LBNL-40942.

W. M. Jackson, R. Price, J. Wrobel, D. Xu, M. Ahmed, D. Peterka, and A. G. Suits, "Velocity map imaging studies of the Lyman α photodissociation mechanism for H atom production from hydrocarbons," *J. Chem. Phys.*, **109**, 4703 (1998). LBNL-42029.

N. Hemmi and A. G. Suits, "The dynamics of hydrogen abstraction reactions: crossed-beam reaction Cl+*n*-C_5H_{12} → C_5H_{12}+HCl," *J. Chem Phys.*, **109**, 5338 (1998). LBNL-42023.

D. Stranges, M. Stemmler, X. Yang, J. D. Chesko, A. G. Suits, and Y. T. Lee, "UV Photodissociation dynamics of allyl radical by photofragment translational spectroscopy," *J. Chem. Phys.*, **109**, 5372 (1998). LBNL-41439R1.

A. S. Bracker, S. W. North, A. G. Suits, and Y. T. Lee, "The near ultraviolet dissociation dynamics of azomethane: correlated V-T energy disposal and product appearance times," *J. Chem Phys.*, **109** 7238 (1998). LBNL-42021.

M. Ahmed, D. S. Peterka, A. S. Bracker, O. S. Vasyutinskii, and A. G. Suits, "Coherence in polyatomic photodissociation: Aligned O (^3P) from photodissociation of NO_2 at 212.8 nm," *J. Chem. Phys.* **110**, 4115 (1999). LBNL-42489.

M. Ahmed, D, S. Peterka and A. G. Suits, "The photodissociation of vinyl radical at 243nm by velocity map imaging," *J. Chem. Phys.*, **110**, 4248 (1999). LBNL-42490.

W. Sun, J. Robinson, K. Yokoyama, A. G. Suits and D. M. Neumark, "Discrimination of product isomers in the photodissociation of propyne and allene at 193nm," *J. Chem. Phys.*, **110**, 4363 (1999). LBNL-42855.

M. Ahmed, D.S. Peterka, A.G. Suits "Crossed Beam Reaction of $O(^1D) + D_2 \rightarrow OD + D$ by Velocity Map Imaging," *Chem. Phys. Lett.*, **301**, 372 (1999). LBNL-42488.

D.S. Peterka, M. Ahmed, and A.G. Suits, "Unraveling the mysteries of metastable O_4," *J. Chem. Phys.*, **110**, 6095 (1999). LBNL-42662.

A.S. Bracker, E. Wouters, O. S. Vasyutinskii and A.G. Suits, "Imaging the alignment angular distribution: State symmetries, coherence, and nonadiabatic dynamics in photodissociation," *J. Chem. Phys.*, **110**, 6749 (1999). LBNL-42486.

O. Sorkhabi, F. Qi, A.H. Rizvi, and A.G. Suits, "UV photodissociation of furan probed by tunable synchrotron radiation," *J. Chem. Phys.*, **111**, 100 (1999) LBNL-42892.

M. Ahmed, E. R. Wouters, D. S. Peterka, O. S. Vasyutinskii and A. G. Suits, "Atomic orbital alignment and coherence in N_2O Photodissociation at 193.3 nm," *Faraday Discussion*, **113**, 425 (1999). LBNL-43097.

D. S. Peterka, M. Ahmed, C.-Y. Ng and A. G. Suits, "Dissociative photoionization dynamics of SF_6 by ion imaging with synchrotron undulator radiation," *Chem. Phys. Lett.*, **312**, 108 (1999). LBNL-43243.
D.S. Peterka, M. Ahmed, and A.G. Suits, "Erratum: Unraveling the mysteries of metastable O_4," *J. Chem. Phys.*, **111**, 5279 (1999).

F. Qi, O. Sorkhabi, A. H. Rizvi and A. G. Suits, "193nm Photodissociation of Thiophene Probed Using Synchrotron Radiation," *J. Phys. Chem. A*, **103**, 8351 (1999). LBNL-43495.

M. Ahmed, D. S. Peterka and A. G. Suits, "H abstraction dynamics by crossed beam velocity map imaging: $Cl+CH_3OH \rightarrow CH_2OH+HCl$," *Chem. Phys. Lett.*, **317**, 264 (2000). LBNL-44340.

M. Ahmed, D. S. Peterka and A. G. Suits, "Imaging H abstraction dynamics in crossed beams: Cl+ROH reactions," *Phys. Chem. Chem. Phys.*, **2**, 861 (2000). LBNL-44340.

M. Ahmed, D. S. Peterka and A. G. Suits, "Photodissociation of NO_2 near 225 nm by velocity map imaging," in **Advances in Atomic and Molecular Beam Research and Applications**, R. Campargue, ed., Springer-Verlag (in press). LBNL-42491.

W. S. McGivern, O. Sorkhabi, A. Rizvi, A. G. Suits and S. W. North, "Photofragment Translational Spectroscopy with State-Selective 'Universal Detection': the Ultraviolet Photodissociation of CS_2," *J. Chem. Phys.*, **112**, 5301 (2000). LBNL-44681.

A.G. Suits, "Photodissociation and Reaction Dynamics Studies Using Third-Generation Synchrotron Radiation." In **Chemical Applications of Synchrotron Radiation**, T.K. Sham, ed., (World Scientific, Singapore, 2000.) (In Press). LBNL-42663.

M. Ahmed, D. S. Peterka and A. G. Suits, "New directions in reaction dynamics using velocity map imaging," in **Imaging in Chemical Dynamics**, A. G. Suits and R. E. Continetti, eds., *ACS Symposium Series*, (American Chemical Society, Washington DC, in press).

E.R. Wouters, M. Ahmed, D.S. Peterka, A.S. Bracker, A.G. Suits and O.S. Vasyutinskii, "Imaging the Atomic Orientation and Alignment in Photodissociation," in **Imaging in Chemical Dynamics**, A. G. Suits and R. E. Continetti, eds., *ACS Symposium Series*, (American Chemical Society, Washington DC, in press).

A.G. Suits and R. E. Continetti, "Imaging in Chemical Dynamics: the State of the Art," in **Imaging in Chemical Dynamics**, A. G. Suits and R. E. Continetti, eds., *ACS Symposium Series*, (American Chemical Society, Washington DC, in press).

W.S. McGivern, O. Sorkhabi, A.G. Suits, A. Derecskei-Kovaks, and S.W. North, "Primary and Secondary Processes in the Photodissociation of $CHBr_3$," *J. Phys. Chem. A*, (in press).

Elementary Reaction Kinetics of Combustion Species

Craig A. Taatjes
Combustion Research Facility, Mail Stop 9055, Sandia National Laboratories, Livermore, CA 94551-0969
cataatj@ca.sandia.gov *www.ca.sandia.gov/LaserChemistry*

SCOPE OF THE PROGRAM

The scope of this program is to develop new laser-based methods for studying chemical kinetics and to apply these methods to the investigation of fundamental chemistry relevant to combustion science. The central goal is to perform accurate measurements over wide temperature ranges of the rates at which important free radicals react with stable molecules. In the past several years, the program has concentrated on the investigation of CH, C_2H, and Cl + stable molecule reactions, applying the extraordinarily precise techniques of laser photolysis/continuous-wave laser-induced fluorescence (LP/cwLIF) and laser photolysis/continuous-wave infrared long-path absorption (LP/cwIRLPA). The precision of these methods enables kinetic measurements to probe reaction mechanisms, utilizing thermal rate constant and product distribution measurements as indicators of detailed global reaction paths. Another aim has been the investigation and application of new detection methods for precise and accurate kinetics measurements. Absorption-based techniques are emphasized, since many radicals critical to combustion are not amenable to fluorescence detection. As an additional advantage, absorption-based techniques can be straightforwardly applied to determination of absolute concentrations in reacting systems.

RECENT PROGRESS

The efforts of the laboratory center on extending the capabilities of the laser-induced-fluorescence method to new reaction systems, on developing high-sensitivity absorption-based techniques for kinetics measurements, and on applying these techniques to investigate important combustion reactions. Recent work on the LP/cwLIF method has applied advances in resonant external-cavity doubling of cw lasers to extend the easily usable probe frequency range, for example to cw LIF detection of HCO in the $B \leftarrow X$ band. Absorption-based techniques for probing reactions, principally in the infrared, are extensively used. In the last year we have especially concentrated on the application of cw infrared frequency-modulation spectroscopy to measuring product formation in the reaction of alkyl radicals with O_2. In addition we have refined measurements of kinetic isotope effects in reactions of the CH radical and have begun applying long-path visible absorption to kinetics of the vinyl radical.

Product Formation in Alkyl + O_2 reactions

The LP/cwIRLPA method has now been applied to the reaction of several alkyl radicals with O_2. The alkyl + O_2 reactions are important in understanding autoignition. We have undertaken time-resolved measurements of HO_2 formation in the C_2H_5 + O_2 reaction using diode laser absorption in the overtone of the O-H stretch. Alkyl radicals are produced by the reaction of the corresponding alkane with Cl atoms from Cl_2

photolysis at 355 nm. The yield of HO_2 in the reaction is determined by comparison with HO_2 signals from the Cl + CH_3OH + O_2 system, which quantitatively converts Cl atoms to HO_2. In addition, possible formation of OH is simultaneously monitored by infrared absorption using an F-center laser co-propagating with the diode laser beam.

Ethyl + O_2 As reported previously, the prompt formation of HO_2 observed in our experiments at low temperatures becomes biexponential at approximately 600 K, implying redissociation of the ethylperoxy radical. The difference in time scales of the two HO_2 production mechanisms allows separation of "direct" HO_2 formation from HO_2 produced after thermal redissociation of an initial ethylperoxy adduct. We have completed investigations of the time constants and yields over the temperature range 298-700 K. The "slow" HO_2 production rate displays an effective activation energy of approximately 25 kcal mol^{-1}. The results can be successfully modeled using a parameterization based on the modified strong-collision treatment of Wagner, et al.. (J. Phys. Chem. **94**, 1853 (1990)).

Propyl + O_2 We have performed similar time-resolved measurements of HO_2 formation in the C_3H_7 + O_2 reaction. Propyl radicals are produced by the reaction of propane with Cl atoms from Cl_2 photolysis at 355 nm. Similar to the previous investigations of ethyl + O_2, formation of HO_2 from propyl + O_2 becomes biexponential above approximately 600 K, implying redissociation of the propylperoxy radical. The biexponential time behavior of the HO_2 production allows separation of "direct" HO_2 formation from HO_2 produced after thermal redissociation of a propylperoxy adduct. The direct HO_2 yields follow a smooth extrapolation from the lower temperature values, while the total yield, including the slower rise, show a rapid increase with temperature to reach 100% at 673 K. These results clearly indicate that the onset of increased metathesis yield arises from dissociation of the propylperoxy radical. We have investigated the formation of OH in the reaction of propyl radicals with O_2 using simultaneous time-resolved infrared probing of HO_2 and OH products from the reaction. Literature measurements suggest that *i*-propyl + O_2 yields 15% OH + propylene oxide at 750 K. We have found no evidence of OH production up to 700 K in our experiments, which generate approximately 1:1 *n*- and *i*- propyl radicals. We place an upper limit of < 3% for prompt formation of OH and a limit of ~ 10% on formation of OH from propylperoxy dissociation under these conditions.

Cyclopropyl + O_2 The formation of HO_2 in the alkyl + O_2 reactions occurs via a cyclic transition state. In order to investigate the effects of ring strain in the alkyl radical on this reaction, we have begun to study cycloalkyl radical reactions with O_2. Ring transition states occur in many critical combustion reactions and ring formation and ring opening help determine product branching fractions. The yield of OH and HO_2 in the *c*-C_3H_5 + O_2 reaction has been measured by simultaneous detection of HO_2 in the near IR and OH in its vibrational fundamental band. The cyclopropyl radical is a prototypical system because of the high degree of ring strain and its isomeric relationship to the allyl radical. Cyclopropyl is produced by the reaction of Cl atoms with cyclopropane Significant yields of OH and HO_2 from *c*-C_3H_5 + O_2 are detected even at room temperature, showing a markedly different behavior than the ethyl and propyl radical reactions. At temperatures above ~550 K the HO_2 yield once again increases dramatically. However, the nature of the increase in HO_2 yield in this case is somewhat uncertain. Since the barrier for ring-opening of cyclopropyl has been calculated at

between 20-30 kcal mol^{-1}, these results may have implications for the poorly understood isomerization to allyl. The temperature at which the rise in HO_2 yield occurs should be above the region of thermal stability of the cyclopropyl radical. However, measurements of the allyl (from Cl + propylene) + O_2 reaction have shown negligible HO_2 production under the conditions of our experiments.

OH-Initiated Oxidation of Unsaturated Hydrocarbons

The initiation of unsaturated hydrocarbon oxidation by OH radical addition contributes to aldehyde formation in pre-ignition chemistry, e.g., OH + $CH_3CH=CHCH_3$ $\rightarrow$ $CH_3CH\text{-}CH(OH)CH_3$ -(+O_2)$\rightarrow$ 2 CH_3CHO + OH. A similar reaction is thought to be responsible for the atmospheric oxidation of benzene, converting OH + benzene + O_2 to phenol + HO_2. We have undertaken an investigation of the OH-initiated oxidation of benzene in collaboration with Dr. Christa Fittschen (Univ. Lille). By simultaneous monitoring of OH disappearance and HO_2 formation we have directly observed HO_2 from the OH•benzene + O_2 reaction. Similar techniques will be applied to OH + alkene systems of relevance to combustion systems.

Kinetic Isotope Effects in CH Radical Reactions

Previous studies in our laboratory established the kinetic isotope effect for the reactions of CH radical with O_2, methane ethylene, and acetylene. The kinetic isotope effect for deuterium substitution on the hydrocarbon species is affected by the mechanism of the reaction. A negligible effect is observed for deuterium substitution of acetylene, whereas a large kinetic isotope effect is seen for deuterium substitution of methane. Using the commonly-implemented approximation of the center-of-mass separation as the reaction coordinate, variational transition state theory predicts only small isotope effects unless the conserved mode frequencies change. On the other hand, a variable reaction coordinate representation allows coupling of rotational motion to the reaction path and can produce isotope effects without changes in the conserved modes. We have been working with Stephen Klippenstein to interpret the experimental kinetic isotope effects using a variable reaction coordinate. A fixed reaction coordinate referenced to the radical orbital of the CH can reproduce the observed CH/CD kinetic isotope effect for a range of interaction potentials. This may provide a framework for mechanistic interpretation of kinetic isotope effects for similar reactions.

We have also reinvestigated the kinetic isotope effect in the CH + CO atom exchange reaction. As shown previously in our laboratory, the carbon atom exchange is facile and displays an inverse kinetic isotope effect. The rate coefficient for the exchange decreases slightly with temperature (at constant total pressure) over the range of 295-700 K, and the kinetic isotope effect disappears above 500 K. These results support the interpretation of the exchange as occurring from an excited HCCO adduct with a reaction coordinate for isomerization that involves only heavy atom motion.

Visible Absorption Probing of Vinyl Radical Kinetics

We have begun to apply our work on the spectroscopy of the vinyl radical to kinetic investigations. Vinyl radicals are important intermediates in hydrocarbon flames, contributing to carbon chain building and soot formation, but relatively little has been measured about their reactivity. Detection of the vinyl radical in LP/cwLPA apparatus

has been demonstrated using the $A \leftarrow X$ transition near 420 nm. Detectivities are sufficient to measure kinetics using vinyl radical concentrations of approximately 10^{12} cm^{-3}, which will enable this apparatus to measure vinyl radical reactions with rate coefficients above about 10^{-14} cm^3 $molecule^{-1}$ s^{-1}. Development of kinetics experiments using optical probing techniques will allow direct measurements of many important rate coefficients.

FUTURE DIRECTIONS

As part of the new Phase II laboratory the capability for investigating reactions at elevated pressure (10-20 atm) is being developed. There is a need to measure rate coefficients and especially branching ratios of key reactions at pressures approaching real combustion conditions. However, measurement of these quantities is extremely challenging, and few experimental values are available. Using optical techniques such as saturated LIF and direct absorption in combination with traditional chemical detection methods will allow branching fractions and reaction rate coefficients to be measured at elevated pressure. In addition, coupling between fundamental reaction kinetics and flame modeling will require that precise kinetics methods are applied to sub-mechanism validation on small controlled sets of elementary reactions. The long-term aim of the high-pressure kinetics effort is to establish a similar level of detail for the investigation of reactions at elevated pressure as is currently available in our lower pressure experiments. The efforts in simultaneous multiple optical probes for reaction kinetics will also be applied at high pressure in an effort to enable investigations of multiple step or competitive chemistry, e.g., pathways for the production of excited C_2 or the detailed chemistry following the R + O_2 reaction.

The use of multiple infrared probes has been applied in our measurements of product formation in several R + O_2 reactions, where simultaneous HO_2 and OH detection was used to determine an upper limit for OH formation. The characterization of R + O_2 reactions will continue. In the long term, detection of the purported hydroperoxy radical intermediate in the R + $O_2 \leftrightarrow RO_2 \leftrightarrow QOOH \rightarrow QO + OH$ mechanism may be possible in the infrared. Investigations of OH-initiated oxidation reactions, such as production of aldehydes from alkenes via OH-alkene adduct reactions with O_2, will also continue using this technique.

BES sponsored publications since 1998

John T. Farrell and Craig A. Taatjes, "Infrared Frequency-Modulation Probing of Cl + C_3H_4 (Allene, Propyne) Reactions: Kinetics of HCl Production from 292-850 K," *J. Phys. Chem. A*, 102, 4846 (1998).

Charles D. Pibel, Andrew McIlroy, Craig A. Taatjes, Sterling Alfred, Katina Patrick, and Joshua B. Halpern, "The Vinyl Radical ($\tilde{A}\ ^2A'' \leftarrow X\ ^2A'$) Spectrum between 530 and 415 nm Measured by Cavity Ring-down Spectroscopy," *J. Chem. Phys.* **110,** 1841-1843 (1999).

Craig A. Taatjes, "Infrared Frequency-modulation Measurements of Absolute Rate Coefficients for Cl + HD → HCl (DCl) + D (H) between 295 and 700 K," *Chem. Phys. Lett.* **306**, 33 (1999).

Craig A. Taatjes, Lene K. Christensen, Michael D. Hurley, and Timothy J. Wallington, "Absolute Rate Coefficients and Site-Specific Abstraction Rates for Reactions of Cl with CH_3CH_2OH, CH_3CD_2OH, and CD_3CH_2OH between 295 and 600 K," *J. Phys. Chem. A.*, **103**, 9805-9814 (1999).

Craig A. Taatjes, "Time-Resolved Infrared Absorption Measurements of Product Formation in Cl Atom Reactions with Alkenes and Alkynes," *Int. Rev. Phys. Chem.* **18**, 419-458 (1999).

A Scaling Theory for the Assignment of Spectra in the Irregular Region

Howard S. Taylor (taylor@chem4.usc.edu)

Department of Chemistry
University of Southern California
Los Angeles, CA 90089-0482

DOE Grant DE-FG03-94ER14458

Program Scope: The question posed in this program is "How do the atoms in molecules move when the molecule is in a high vibrational state." Put another way we wish to uncover, using spectral Hamiltonians derived from experiment, the internal molecular motions that when quantized yield the observed highly excited vibrational spectra. We have chosen two molecular systems to work on. The first is the highly excited bending spectra of acetylene in the 10,000 to 15,000 cm^{-1} region. The experimental part of this project was carried out by the Field group [1,2,3] using the dispersed fluorescence spectroscopic technique. The problem was that, even using both wave function inspection techniques (in various normal and local coordinate systems) and using wave packet propagation methods to study IVR, a complete insight valid for all eigenstates in this region could not be obtained. Last year we reported at this conference and published a paper [4] on how a combination of quantum and semiclassical techniques integrated into a classical nonlinear dynamic study of polyad 22 (the one just adjacent to the vinyladene barrier) could show how the complex spectra was really due to the intertwining of four regular simpler spectral sequences, each based on one of four types of internal molecular motion. Chaos played no role here; all could be explained without it. Two of the four types of motion were counter-rotor at the top of the polyad and local mode libration at the bottom of the polyad. In the center of the polyad two totally unexpected types of motion appeared. The first was a simultaneous, perpendicular to each other and the molecular bond, local mode hydrogenic motion which when viewed end on gave an appearance of a celtic cross. The second motion was a libration of one hydrogens (x direction) perpendicular to the bond (z direction) and a small amplitude elliptical rotation of the other hydrogen along the y axis, followed at fixed intervals by an axis switching motion that effectively interchanged periodically the x and y directions. Both this libration or the local mode libration could when highly excited, appear to be a "warming up exercise" for isomerization to vinyladene.

The second system we have chosen to work on was based on the spectral Hamiltonian, fitted by Quack's group [5,6], to the FTIR spectra of the chiral molecule bromochlorofluoromethane. In this work [5,6] wavepacket propagation was a key analytic tool as was a fitting potential surface to the data. A key and unexplained finding was that in some cases the packet propagated for picoseconds as if the Hamiltonian governing the dynamics was of C_s and not the chiral C_1 symmetry. Our purpose was to explain this observation based on our hope to assign detailed atomic motions to all highly excited states parameterized by the effective Hamiltonian. Here the hydrogen atom motion relative to the rest of the system was considered as Quack only excited the CH bond and the other modes had much lower frequencies allowing an adiabatic separation of the hydrogens' motion.

Recent Progress: For the methane based system, in polyad 5, the highest (11,000 cm^{-1} to 1400 cm^{-1}) for which the H_{eff} holds, four type of motion were observed to give sequences of levels. At the bottom and top of the polyad we see the effects of the soon to be born Fermi 2:1 stretch-bend resonance zones supporting levels showing the coupling of the lower and higher frequency bend

modes respectively to the CH stretch. These levels could be assigned with normal mode quantum numbers n_s, n_a, n_b representing the CH stretch, the bend of the hydrogen toward the fluorine and the bend of the hydrogen moving roughly in a semicircle going from Cl to Br and back. The motion here was regular and quantizable by EBK tori quantization. Other levels interspersed in the middle of the polyad were based on two other types of motions. One was a sequence of levels, which were deemed chaotic as the classical phase space analogue of wave functions of these states lay in classically chaotic regions of phase space. Second was a sequence of states with motion dominated by a Darling-Dennison bending exchange resonance, which when the two bending frequencies came into a match, yielded a most unexpected dynamics. This motion was the rotation of the hydrogen on the lip of a cone atop the "asymmetric pyramid" of the carbon-halogen system. As the hydrogen rotated the height of the cone on average oscillated with a frequency that was twice the rotation frequency. This rotation appeared in both clockwise and counter-clockwise senses, leading upon quantization to two states whose very weak mixing added and subtracted them into a' and a'', approximately energy degenerate (to five figures in cm^{-1}) eigenstates.

The wave functions of these levels when used to propagate packets, explained the observed non-chiral C_s type dynamics. Physically the rotation was so fast that it smeared over the hydrogen's view of the halogens. The dynamic situation is similar to particle motion at energies above barriers between asymmetric multiwell systems.

Roughly speaking the Hydrogen is rotating fast enough to reflect the double degeneracy of C_{3v} but not so fast as to be able to ignore the a' and a'' of the lower symmetry C_s arrangement. Dynamics is overriding the point group symmetry.

We have also completed an extended "bending spectra of acetylene "analyses for polyads 16 to 22. We have uncovered a deep correlation between the motions described above. Namely the motions can be based, for fixed polyad number and $l=0$ bending angular momentum, on a two mode picture. Each of the modes evolves differently from the bottom to the top of the polyad but merge at the bottom to local mode states and at the top to counter-rotor states. In the middle one mode shows the celtic cross motion and the other one the axis switching motion. Intermediate energy states have different numbers of quanta of excitation on each of these modes. The ones with zero quanta in one of modes were either perfect "crosses" or "switchers" and the ones with non zero excitations on both modes explain the states we previously deemed "distorted from the ideal motions" or which were deemed previously too complex to assign (about 10 out of 122 states in polyad 22). Hence every state could be assigned and associated with the motions of the evolving modes at its eigenenergy.

Future Plans: We hope to extend our work to the DCO spectra where some observed resonance states, which correspond to excitation in all modes, defy a simple motional explanation when wave function examination or packet propagation methods of analysis are used[7]. We will also treat CDBrClF[8]. The latter will be most challenging as Quack's fit to an H_{eff} indicates many resonances; now including resonances with the CF stretching motion. This extra dimension will force us to extend our methods of phase space analysis to cover such "larger" problems.

References

(1) Solina, S.A. B.; O' Brien, J.P.; Field, R.W.; Polik, W.D. J. Chem Phys. 1996, 100, 7797

(2) O; Brien, J.P.; Jacobson, M.P.; Sokol, J.J.; Coy, S.L.; Field, R.W. J. Chem Phys. 1998, 108, 7100

(3) Jacobson, M.P.Ph.D. thesis, Massachussets Institute of Technology, Cambridge, MA 1999

(4) M.P. Jacobson, C. Jung, H.S. Taylor and R.W. Field, J. Chem. Phys. 111, 600 (1998)

(5) A. Beil, D. Luckhaus and M. Quack, Ber. Bunsenges. Phys. Chem. 100, 1853 (1996)

(6) A. Beil, D. Luckhaus, M. Quack and J. Stohner, Ber. Bunsenges. Phys. Chem. 101, 311 (1997)

(7) F. Temps, private communication

(8) A. Beil, H. Hollenstein, O. Montc, M. Quack and J. Stohner, preprint.

Papers Published in 1998, 1999 & 2000

(1) All Adiabatic Bound States of NO2 (J=0), with R. Salzgeber, C. Schlier, and V. Mandelshtam, J. Chem. Phys., 109, 937-941 (1998).

(2) State by State Assignment of the Bending Spectrum of Acetylene at 15,000 cm^{-1}: A Case Study of Quantum-Classical Correspondence, with C. Jung, M. Jacobson & R. Field.

(3) All Non-Adiabatic (J=0) bound states of NO^2 with R. Salzgeber, C. Schlier, V. Mandelshtam, and H.S. Taylor, J. Chem. Phys., 110, 3756 (1999).

(4) Semi-Classical Quantization by Padé Approximant of Periodic Orbit Sums, with J. Main, P.A. Dando, D. Belkic, Europhys. Lett., 48 (3), 250-256 (1999).

(5) Decimated Signal Diagonalization for Obtaining the Complete Eigenspectra of Large Matrices, D. Belkic, P.A. Dando, H.S. Taylor, and J. Main, Chem. Phys. Lett., 315, 135-139 (1999)

VARIATIONAL TRANSITION STATE THEORY

Principal investigator, mailing address, and electronic mail

Donald G. Truhlar
Department of Chemistry, University of Minnesota, 207 Pleasant Street SE,
Minneapolis, Minnesota 55455
truhlar@umn.edu

Program scope

This project involves the development and application of variational transition state theory (VTST) and semiclassical transmission coefficients to gas-phase reactions. Our current work is focussed on developing and applying new methods for interfacing reaction-path dynamics calculations with electronic structure theory and new electronic structure methods that are especially well suited for applications in combustion kinetics. The work involves development of the theory, development of practical techniques for applying the theory to various classes of transition states, and applications to specific reactions, with special emphasis on combustion reactions and reactions that provide good test cases for methods needed to study combustion reactions. A theme that runs through our current work is the using of multiple levels of electronic structure for a given problem and their creative combination.

Recent progress

We have developed powerful new multi-coefficient correlation methods that allow accurate evaluation of bond energies and reaction energies at relatively low cost compared to previously available methods. We developed a multi-configuration version of molecular mechanics that allows a convenient interface of high-level ab initio calculations with molecular mechanics force fields. Recent applications of VTST include the reactions of H atoms with ethylene, diazene, and methanol, methyl cation transfer reactions, the reactions of O atoms with hydrogen chloride and methane, the reaction of Cl atoms with methane, and reactions of hydroxyl radicals with alkanes.

We have made our computer programs, POLYRATE, MORATE, GAUSSRATE, ABCRATE, and AMSOLRATE available to other workers in the field over the Internet. The URL for our software distribution site is http://comp.chem.umn.edu/Truhlar. We have filled the following license requests for these codes since 1998:

	Total	*academic*	*government*	*industry*
POLYRATE	193	161	17	15
MORATE	44	41	1	2
GAUSSRATE	90	75	9	6
ABCRATE	8	7	1	0
AMSOLRATE	12	12	0	0

Future plans

A critical issue to increase the applicability and reliability of variational transition state theory with semiclassical tunneling calculations for combustion reactions is further improvement of the interface with high-level electronic structure calculations. We will continue to develop the single-level and dual-level direct dynamics methods for carrying out rate calculations with implicit potential energy surfaces, and we will continue to

develop new multi-coefficient correlation methods for kinetcs.. We will soon report a new hybrid density functional method parameterized for kinetics. In addition to developing the methods, we are putting them into user-friendly packages that will allow more researchers to carry out calculations conveniently by the new methods.

VTST is being applied to selected reactions of three types: (i) important test cases for the new methods, (ii) reactions of fundamental importance for further development of dynamical theory, and (iii) important combustion reactions, for example, reactions of oxygen atoms and hydroxyl radicals and the reaction of hydrogen atoms with ethanol. We are also developing new methods for the calculation of substituent effects.

Publications, 1998-present

Journal articles

1. "Reaction-Path Dynamics in Redundant Internal Coordinates," Y.-Y. Chuang and D. G. Truhlar, Journal of Physical Chemistry A **102**, 242-247 (1998).
2. "ABCRATE: A Program for the Calculation of Atom-Diatom Reaction Rates," B. C. Garrett, G. C. Lynch, T. C. Allison, and D. G. Truhlar, Computer Physics Communications **109**, 47-54 (1998).
3. "Integrated Molecular Orbital Method with Harmonic Cap for Molecular Forces and its Application to Geometry Optimization and the Calculation of Vibrational Frequencies," J. C. Corchado and D. G. Truhlar, Journal of Physical Chemistry A **102**, 1895-1898 (1998).
4. "Interpolated Variational Transition State Theory by Mapping," J. C. Corchado, E. L. Coitiño, Y.-Y. Chuang, P. L. Fast, and D. G. Truhlar, Journal of Physical Chemistry A **102**, 2424-2438 (1998).
5. "Entropic Effects on the Dynamical Bottleneck Location and Tunneling Contributions for $C_2H_4 + H \rightarrow C_2H_5$. Variable Scaling of External Correlation Energy for Association Reactions," J. Villà, A. González-Lafont, J. M. Lluch, and D. G. Truhlar, Journal of the American Chemical Society **120**, 5559-5567 (1998).
6. "Variational Transition State Theory and Tunneling Calculations with Reorientation of the Generalized Transition States for Methyl Cation Transfer," A. González-Lafont, J. Villà, J. M. Lluch, J. Bertrán, R. Steckler, and D. G. Truhlar, Journal of Physical Chemistry A **102**, 3420-3428 (1998).
7. "Variational Transition State Theory Calculations of Thermal Rate Coefficients for the $O(^3P)$ + HCl Reaction," T. C. Allison, B. Ramachandran, J. Senekowitsch, D. G. Truhlar, and R. E. Wyatt, Journal of Molecular Structure Theochem **454**, 307-314 (1998).
8. "Dual-Level Direct Dynamics Calculations of Deuterium and Carbon-13 Kinetic Isotope Effects for the Reaction Cl + CH_4," by O. Roberto-Neto, E. L. Coitiño, and D. G. Truhlar, Journal of Physical Chemistry A **102**, 4568-4578 (1998).
9. "Dual-Level Direct Dynamics Calculations of the Reaction Rates for a Jahn-Teller Reaction: Hydrogen Abstraction from CH_4 or CD_4 by $O(^3P)$," by J. C. Corchado, J. Espinosa-Garcia, O. Roberto-Neto, Y.-Y. Chuang, and D. G. Truhlar, Journal of Physical Chemistry A **102**, 4899-4910 (1998).
10. "Variational Reaction Path Algorithm," P. L. Fast and D. G. Truhlar, Journal of Chemical Physics **109**, 3721-3729 (1998).
11. "The Calculation of Kinetic Isotope effects Based on a Single Reaction Path," P. L. Fast, J. C. Corchado, and D. G. Truhlar, Journal of Chemical Physics **109**, 6237-6245 (1998).

12. "Chemical Reaction Theory: Summarizing Remarks," D. G. Truhlar, Faraday Discussions Chemical Society **110**, 521-535 (1998).
13. "Explanation of Deuterium and Muonium Kinetic Isotope Effects for Hydrogen Atom Addition to an Olefin," J. Villà, J. C. Corchado, A. González-Lafont, J. M. Lluch, and Donald G. Truhlar, Journal of the American Chemical Society **120**, 12141-12142 (1998).
14. "A Mapped Interpolation Scheme for Single-Point Energy Corrections in Reaction Rate Calculations and a Critical Evaluation of Dual-Level Reaction-Path Dynamics Methods," Y.-Y. Chuang, J. C. Corchado, and D. G. Truhlar, J. Phys. Chem. A **103**, 1140-1149 (1999).
15. "Optimized Parameters for Scaling Correlation Energy," P. L. Fast, J. Corchado, M. L. Sanchez, and D. G. Truhlar, Journal of Physical Chemistry A **103**, 3139-3143 (1999).
16. "Simple Approximation of Core-Correlation Effects on Binding Energies," P. L. Fast and D. G. Truhlar, Journal of Physical Chemistry A **103**, 3802-3803 (1999).
17. "Multi-Coefficient Correlation Method for Quantum Chemistry," P. L. Fast, J. C. Corchado, M. L. Sánchez, and D. G. Truhlar, Journal of Physical Chemistry A **103**, 5129-5136 (1999); erratum: to be published.
18. "Multi-Coefficient Gaussian-3 Method for Calculating Potential Energy Surfaces," P. L. Fast, M. L. Sánchez, and D. G. Truhlar, Chemical Physics Letters **306**, 407-410 (1999).
19. "Variational Transition State Theory with Optimized Orientation of the Dividing Surface and Semiclassical Tunneling Calculations for Deuterium and Muonium Kinetic Isotope Effects in the Free Radical Association Reaction $H + C_2H_4 \rightarrow C_2H_5$," J. Villà, J. C. Corchado, A. González-Lafont, J. M. Lluch, and Donald G. Truhlar, Journal of Physical Chemistry A **103**, 5061-5074 (1999).
20. "Direct Dynamics for Free Radical Kinetics in Solution: Solvent Effect on the Rate Constant for the Reaction of Methanol with Atomic Hydrogen," Y.-Y. Chuang, M. L. Radhakrishnan, P. L. Fast, C. J. Cramer, and D. G. Truhlar, Journal of Physical Chemistry **103**, 4893-4909 (1999).
21. "Energetic and Structural Features of the $CH_4 + O(^3P) \rightarrow CH_3 + OH$ Abstraction reaction: Does Perturbation Theory from a Multiconfiguration Reference State (Finally) Provide a Balanced Treatment of Transition States?", O. Roberto-Neto, F. B. C. Machado, and D. G. Truhlar, Journal of Chemical Physics **111**, 10046-10052 (1999); erratum: to be published.
22. "Statistical Thermodynamics of Bond Torsion Modes," Y.-Y. Chuang and D. G. Truhlar, Journal of Chemical Physics **112**, 1221-1228 (2000).
23. "Multilevel Geometry Optimization," J. M. Rodgers, P. L. Fast, and D. G. Truhlar, Journal of Chemical Physics **112**, 3141-3147 (2000).
24. "Comment on Rate Constants for Reactions of Tritium Atoms with H_2, D_2, and HD," J. Srinivasan and D. G. Truhlar, Journal of Physical chemistry A, in press.
25. "How Should We Calculate Transition State Geometries for Radical Reactions? The Effect of Spin Contamination on the Prediction of Geometries for Open-Shell Saddle Points," Y.-Y. Chuang, E. L. Coitiño, and D. G. Truhlar, Journal of Physical Chemistry A **104**, 446-450 (2000).
26. "Improved Coefficients for the Scaling All Correlation and Multi-Coefficient Correlation Methods," C. M. Tratz, P. L. Fast, and D. G. Truhlar, PhysChemComm **2**, Article 14 (1999). (unpaginated, 10 pp.)

27. "Potential Energy Surface, Thermal and State-Selected Rate Constants, and Kinetic Isotope Effects for Cl + $CH_4 \rightarrow HCl + CH_3$" J. C. Corchado, D. G. Truhlar, and J. Espinosa-Garcia, Journal of Chemical Physics, in press.
28. "Multiconfiguration Molecular Mechanics Algorithm for Potential Energy Surfaces of Chemical Reactions" Y. Kim, J. C. Corchado, J. Villà, J. Xing, and D. G. Truhlar, Journal of Chemical Physics **112**, 2718-2735 (2000).
29. "Dynamics of the $Cl+H_2/D_2$ Reaction: A Comparison of Crossed Molecular Beam Experiments with Quasiclassical Trajectory and Quantum Mechanical Calculations," M. Alagia, N. Balucani, L. Cartechini, P. Casavecchia, G. G. Volpi, F. J. Aoiz, L. Bañares, T. C. Allison, S. L. Mielke, and D. G. Truhlar, Physical Chemistry Chemical Physics **2**, 599-612 (2000).

Long abstract

1. "Thermochemistry, Solvation, and Dynamics," D. G. Truhlar, Y.-Y. Chuang, E. L. Coitiño, J. C. Corchado, C. J. Cramer, D. Dolney, J. Espinosa-Garcia, P. L. Fast, G. D. Hawkins, Y. Kim, J. Li, B. Lynch, M. L. Radhakrishnan, O. Roberto-Neto, J. M. Rodgers, M. L. Sánchez, J. Villa, P. Winget, and T. Zhu, in *American Chemical Society Division of Fuel Chemistry Preprints of Symposia,* Vol. 44 (American Chemical Society, Washington, 1999), pp. 452-458.

Book chapters

1. "Transition State Theory," B. C. Garrett and D. G. Truhlar, in *Encyclopedia of Computational Chemistry*, edited by P. v. R. Schleyer, N. L. Allinger, T. Clark, J. Gasteiger, P. A. Kollman, and H. F. Schaefer III (John Wiley & Sons, Chichester, UK, 1998), Volume 5, pp. 3094-3104.
2. "Testing the Accuracy of Practical Semiclassical Methods: Variational Transition State Theory with Optimized Multidimensional Tunneling," T. C. Allison and D. G. Truhlar, in *Modern Methods for Multidimensional Dynamics Computations in Chemistry*, edited by D. L. Thompson (World Scientific, Singapore, 1998), pp. 618-712.
3. "Dual-Level Methods for Electronic Structure Calculations of Potential Energy Functions that Use Quantum Mechanics as the Lower Level," J. C. Corchado and D. G. Truhlar, in *Hybrid Quantum Mechanical and Molecular Mechanical Methods*, edited by J. Gao and M. A. Thompson, ACS Symposium Series volume 712, pp. 106-127.

Computer programs

"POLYRATE-version 8.0," Y.-Y. Chuang, J. C. Corchado, P. L. Fast, J. Villà, E. L. Coitiño, W.-P. Hu, Y.-P. Liu, G. C. Lynch, K. A. Nguyen, C. F. Jackels, M. Z. Gu, I. Rossi, S. Clayton, V. S. Melissas, R. Steckler, B. C. Garrett, A. D. Isaacson, and D. G. Truhlar, University of Minnesota, Minneapolis, August, 1998. Version 8.4.1, March 2000.

"MORATE-version 8.0/P8.0-M5.07," Y.-Y. Chuang, P. L. Fast, W.-P. Hu, G. C. Lynch, Y.-P. Liu, and D. G. Truhlar, August 1998. Version 8.4, December 1999.

"GAUSSRATE–version 8.0," J. C. Corchado, E. L. Coitiño, Y.-Y. Chuang, and Donald G. Truhlar, August 1998. Version 8.4, December 1999.

"AMSOLRATE-version 8.0," Yao-Yuan Chuang, Yi-Ping Liu, and Donald G. Truhlar, August 1998. Version 8.5, January 2000.

Chemical Kinetic Data Base for Combustion Modeling

Wing Tsang
National Institute of Standards and Technology
Gaithersburg, MD 20899
Wing.tsang@nist.gov

Program Scope or Definition

Computer simulation of combustion processes can be a very powerful tool for the design and optimization of the technology. It can expand the range of results from direct testing and frequently consider situations that are inaccessible to measurements. A key input to such efforts is a database of chemical kinetic information. The aim of this program is to provide such a database. The contents of the database are unimolecular (in the most general sense) and bimolecular rate constants. The determination of rate constants for the former is the most serious technical challenge in this effort. Although the broad principles have long been understood, quantitative treatment in terms of deriving rate constants have been generally based on single step thermal reactions and the assumption of a steady state distribution. These procedures are not readily extensible to the more general and realistic situation. These include multichannel processes (including reversible isomerizations) and when steady state distributions are no longer applicable. Chemical activation reactions are a special case of the former. Our work during the past year has been devoted to developing tools to handle these issues in a rigorous manner.

Recent Progress

A: Program for calculating rate constants for unimolecular reactions: At the onset of this work reliance was placed on the collection and evaluation of experimental data. However as we approached larger fuels and expanded the coverage to aromatic and soot formation chemistry it became clear that increasing emphasis must be placed on theory. This is due to the great increase in the number of reaction pathways and the importance of energy transfer effects under combustion temperatures. A principal thrust of the current year's activity has been the expansion and testing of a user friendly program designed to calculate rate constants for unimolecular reactions under all conditions.

Using the work of Knyazev[1,2] we have now incorporated into the program the capability for handling hindered rotors and making simple tunneling corrections. Thus the program can now generate its own JANAF type thermodynamic tables. It will produce rate constants for true bimolecular reactions on the basis of transition state theory. It is designed to take inputs from Gaussian calculations and directly calculate rate constants. Graphical comparisons with experiments can be made when it interfaced with the NIST Chemical Kinetics DataBase. The program can now produce all the chemical data needed for programs such as CHEMKIN.

A great deal of effort has been devoted to debugging the program. An unexpected problem was encountered for cases where reaction threshold is high or equivalently when E/RT is large. This is actually unimportant for most combustion applications since the temperature is high. However, there are much experimental results at or near room temperature and frequently they represent

the only available data. It is therefore important to be able to use this data as a basis for extrapolations. The source of this problem arises from the calculations being carried out to only 15 or 16 places. Errors arise when the differences between the quantities become of this magnitude. It is apparently endemic to many matrix techniques. For the present application this is the situation when steady state distributions will almost always be attained. Thus for thermal reactions we have implemented the Nesbitt procedure recommended by Gilbert and Smith[3]. For chemical activation processes it turns out that the "noise" which distorts the results occur in regions of the distribution function that does not contribute to the rate constants. Options have been added to the program to define ranges to be considered.

B: Chemically Activated Decomposition of 1,3 Butadiene: Many radicals are present in reactive organic systems. Their recombination leads to the formation of hot molecules that can then decompose. In the case of unsaturated radicals, the combination products can isomerize as well as decompose. This leads to an added degree of complication since the isomerized products unlike those from decomposition can recross the reaction barrier. In the following we report on work bearing on the chemically activated decomposition of 1,3 butadiene formed from vinyl radical combination. Aside from intrinsic interest in combustion applications, this represents an excellent opportunity to exercise our program.

There have been considerable experimental work on 1,3-butadiene decomposition [4-7]. This is a very complex process involving the possibility of 4 isomers as well as 5 decomposition processes. An energy level diagram can be found in Figure 1. An extra complication is the fact that the experimental studies were all carried out under conditions where energy transfer effects must be considered. We have analyzed the data on the basis of the solution of the time dependent master equation[8] and concluded that the data is only consistent with a main reaction (75-80%) involving the direct formation of ethylene and acetylene (or through a very short lifetime vinylidine). The important side reaction, in the 10-20% range, is. isomerization to form 1,2-butadiene and its subsequent decomposition to form propargyl and methyl. Details of the calculations have been given in last year's report. All measurements on vinyl combination have been at room temperature. Rate constants for combination are large[9] and except for the most recent studies[10], at the lowest pressure, 1 torr, butadiene was the main product. There may be some uncertainty on the nature of the butadiene isomers that are present.

The high pressure rate constants derived from the analysis of the thermal decomposition results can now be used to determine the branching ratios for chemically activated decompositions involving hot butadiene derived from vinyl combination using the same master equation approach. This is the first time such a complex system has been treated in this rigorous manner. The running times with a grid size of 100 cm^{-1} is of the order of several hours on a 450 mhz Pentium III PC. Since the run times scale as to the cube of the matrix size, it is not likely that we will be able to handle many more isomers with such high barriers. There are no limitations on the number of decomposition channels. As a practical matter, once the principal isomerization channels have been identified, the less important channels can be removed from the calculation. Results with a 400 cm^{-1} step size down can be found in Table 1. The direct formation of ethylene and acetylene (presumably from vinylidine) is the main channel. Stabilization is of importance at lower temperatures. The main radical producing process involves isomerization to

Figure 1. Energy level diagram involving butadiene decomposition and isomerization channels.

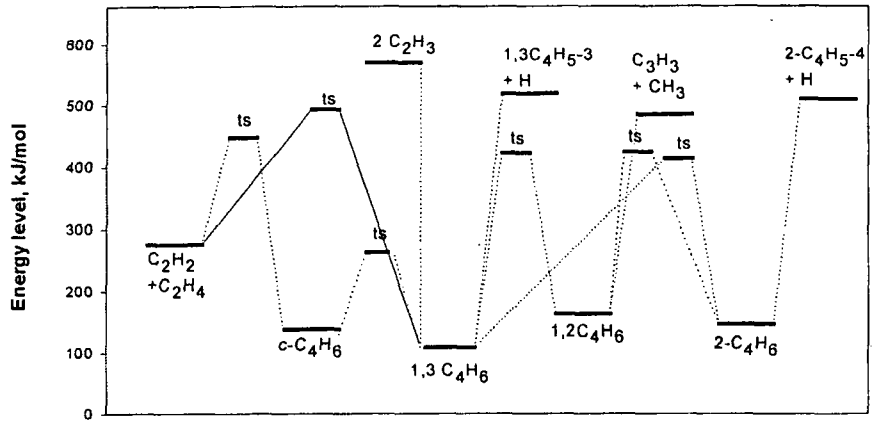

Table 1: *Branching ratios for the decomposition of chemically activated 1,3 butadiene formed from the combination of 2 vinyl radicals*

Activated molecule	Products	Branching Ratios					
		750 K		1000 K		1500 K	
		Bar		Bar		Bar	
		1	10	1	10	1	10
1,3-C_4H_6 From 2 C_2H_3	C_2H_2 + C_2H_4	.882	.499	.957	.82	.977	.976
	1,2-C_4H_6	.034	.022	.023	.022	.012	.013
	1,3-C_4H_5-2 +H	.0034	.002	.0043	.0037	.0045	.0044
	c- C_4H_6	.0028	.0015	.0023	.0019	.0014	.0014
	C_4H_6-2	.0093	.0096	.0041	.0077	.0020	.0019
	1,3-C_4H_6 (stab)	.068	.466	.0087	.14	0	0
	C_2H_3 + C_2H_3	.00016	.00012	.0007	.0006	.0031	.0031
1,2- C_4H_6 From 1,3-C_4H_6	2,3-C_4H_5-1 + H	.005	.0023	.01	.008	.024	.022
	C_3H_3 + CH_3	.792	.331	.944	.642	.976	.978
	1,2- C_4H_6 (stab)	.203	.667	.046	.35	0	0

to form 1,2 butadiene followed by decomposition to form propargyl and methyl. It is less important than in thermal decomposition. Note the complex pressure dependence. Extension of the analysis to room temperature and the lower pressures used experimentally leads to results that are consistent with the observation of Thorne et al.[9] on the absence of stabilization at 1 torr. Stabilization is only important at the upper end of the pressure range used by Fahr et al.[10]. It is suspected that it will be difficult to reconcile the two sets of experimental data.

Future Plans

We are beginning to distribute our program to interested users. Clearly there is a need for a tool of this type for the analysis of high temperature data. Hopefully this will assure some uniformity in data treatment. In our evaluative work, there is frequently insufficient information to properly assess published values. Our longer range plans is to use this program to build a data base of transition state structures and energetics so as to update the well known compilation of Benson and O'Neal[11]. Instead of just high pressure rate expressions, it will be possible to generate rate constants under any desired pressure or reaction environment. This is impossible to achieve with a printed format. In the shorter terms we will begin with the results derived from our work on building a database for ethanol combustion. It is expected that in the course of this work and with external investigators using the program it will be possible to continually upgrade the program through the removal of bugs and the addition of useful features.

References

1. Gilbert, R. and Smith, S. C., "Theory of Unimolecular and Radical Combination Reactions", Blackwell,London, 1990
2. Knyazev, V. D. and Slagle, I. R., J Phys. Chem.,100 16899, 1996
3. Knyazev, V. D., J. Phys. Chem.,A 102: 3916, 1998
4. Kiefer, J. H., Wei, H.C., Kern, R. D. and Wu, C. H., Int. J. Chem. Kin. 17, 225, 1985
5. Kiefer, J. H., Mitchell, K. I., and Wei, H.C., Int. J. Chem. Kin., 20, 787, 1988
6. Skinner, G., and Sokolski, E. M., Phys. Chem., 97, 1028, 1960
7. Hidaka, Y., Higashihara, T., Ninomiya, N., Masaoka, H., Nakamura, T. and Kawano, H., Int. J. Chem. Kin., 28, 137, 1996 .
8. Tsang, W. , Bedanov., V and Zachariah, M. R., Berichte der Busen-Gesellschaft fur Physikalische Chemie, 101, 491, 19978.
9. Thorne, R. P., Payne, W. A., Stief, L. J. and Tardy, D. C., J. Phys. Chem, 100, 13594, 1996
10.Fahr, A., Braun, W. and Laufer, A. H., J. Phys. Chem., 87, 1502, 1991
11. Benson, S. W. and O'Neal, H. E., "Unimolecular Reactions" NSRDS-24 US Government Printing Office, 1969

Publications of DOE sponsored research 1998 - 2000 .

1. Tsang W, Lifshitz A.,"Kinetic Stability of 1,1,1-trifluoroethane", Int. J. Chem. Kin.,30,621, 1998
2. Knyazev, V. D., Tsang, W., "Non-Harmonic Degrees of Freedom: Densities of States and Themodynamic Functions,", J. Phys. Chem., A102, 9167, 1998
3. Tsang, W., "Shock Tube Studies on the Stability of Polyatomic Moleculess and the Determination of Bond Energies" in "Energetics of Stable Molecules and Reactive Intermediates"(ed. Minas da Piedade, M. E.) Kluwer Academic Publisher, 1998, 323
4. Knyazev, V. D. and Tsang, W., "Incorporation of Non-Steady State Unimolecular and Chemically Activated Kinetics into Complex Kinetic Schemes. 1. Isothermal Kinetics at Constant Pressure", J. Phys. Chem., A103, 3944, 1999,
5. Tsang, W. and Lifshitz, A., "Single Pulse Shock Tube" in Part III "Chemical Reactions in Shock Waves, in Handbook of ShockWaves", Academic Press, New York, in press

SINGLE-COLLISION STUDIES OF ENERGY TRANSFER AND CHEMICAL REACTION

James J. Valentini
Department of Chemistry
Columbia University
New York, NY 10027
jjv1@chem.columbia.edu

PROGRAM SCOPE

This research program aims to understand fundamental chemical reaction dynamics of reactions that are actually important in combustion media, and those that are prototypes of such reactions. Study of reaction dynamics means asking many different questions. The one that we pose in our current work is how "many body" effects influence bimolecular reactions. By many-body effects we mean almost anything that results from having a reaction with a potential energy surface of more than three dimensions. These are polyatomic reactions, that is reactions in which one or both the reactants and one or both of the products are triatomic or larger molecules. Our current interest is in reactions for which the reactants offer multiple, identical reaction sites. Our aim is not to provide a complete description of any one molecular system, but rather to develop a general understanding of how the factors of energetics, kinematics, and reactant/product structure control the dynamics in a series of analogous systems.

Our experiments are measurements of quantum-state-resolved partial cross sections under single collision conditions. We use pulsed uv lasers to produce reactive radical species and thereby initiate chemical reactions. The reaction products are detected and characterized by resonant multi-photon ionization and time-of-flight mass spectroscopy.

RECENT PROGRESS

Our intent has been to expand our measurements to yield angle and speed resolved state-to-state cross sections. For that we built a crossed beam apparatus in which the reactant species were produced by photolysis in one molecular beam and the resultant beam of radicals intersected a second molecular beam. We were to use our spatially resolved POSTS (POsition Sensitive Translational Spectroscopy) method to determine the angle and speed distributions of products in individual quantum states. However, the molecular beam densities we were able to obtain were far below values calculated from hydrodynamic models of the free jet expansions from which the molecular beams were obtained. There are no reports from other labs of measurements of absolute molecular beam densities. However, our analysis of the experiments from other labs indicates that the densities are similar to ours. The lower than expected densities of reactants made the experiments we were attempting marginal at best. Repeated attempts and months of effort to make these experiments work were all unsuccessful. We have been redesigning the experimental

apparatus to make these experiments feasible even at the lower than expected molecular beam densities.

While these changes in apparatus are being incorporated by complete redesign of the apparatus, we have continued our study of the state-resolved dynamics of the H + RH → H_2 + R reactions, where RH is an alkane. We have measured partial cross sections for the straight-chain alkanes ethane, propane, pentane, and hexane, and have used partially deuterated hexane to distinguish primary from secondary abstraction. We have studied the abstraction reaction for the cyclic alkanes cyclopropane, cyclobutane, cyclopentane, and cyclohexane. For reference we have also recorded the product state distributions for the reaction H + HCl → H_2 + Cl. This reaction is the "reference" reaction for our alkane studies, since it is the atom + diatom analogue of the alkane reactions, having the same kinematics and energetics. We had previously measured the H + HCl reaction cross sections by CARS, but these do not have sufficient resolution to Doppler resolve the products. Doppler resolution is necessary to determine the translational energy for products in each quantum state.

Our results are: The products of the straight chain alkane reactions show less rotational energy for ground vibrational state products than for the products from the HCl reference reaction, but much more rotational energy for v'=1 products. There is a positive correlation of product rotational energy and product vibrational energy. For the cyclic alkanes there is at most a small positive correlation of rotational and vibrational energy release. This correlation shows up as much less rotational energy for v'=0 products and slightly more for the products in v'=1, relative to the H + HCl reference reaction. These results are summarized in Table 1.

	HCl	C_2H_6	C_3H_8	C_6H_{14}	C_5H_{10}	C_6H_{12}
E_{rot}/E_{avl}						
v'=0	0.20	0.12	0.13	0.13	0.08	0.11
v'=1	0.08	0.20	0.22	0.26	0.13	0.13
θ_r						
v'=0	3.7	7.6	7.2	7.0	12.7	8.4
v'=1	7.7	4.1	3.7	2.1	7.6	7.1

Table 1. Summary of energy disposal and rotational surprisal parameters for several H + RH → H_2 + R reactions and the analogous H + HCl reaction.

We believe that there are two effects operative here. First is an effect that we also see in the H + $CDCl_3$ reaction that removes the correlation of product rotational and vibrational excitation that is seen in all atom + diatom reactions, including H + HCl. We attribute this to having a radical product with low rotational constant. Rotational excitation of the radical product costs little energy even for states of high angular momentum. So, the rotations of the radical product serve as angular momentum "sinks" and effectively decouple the simultaneous constraints of conservation

of energy and angular momentum. It is the coupling of these constraints that results in the negative correlation of product rotational and vibrational energies.

The second effect is one that only the straight chain alkanes demonstrate, the positive correlation of product rotation and vibration. We believe that the availability of low frequency torsions and hindered rotations in the straight chain alkanes makes small impact parameter collisions more effective than large impact parameter collisions in producing rotational excitation. More specifically, the v'=1 products, are associated with small impact parameter collisions, which lead to more interaction of the H_2 product with the incipient radical product, giving rise to translation to rotation energy transfer in the exit channel. Since the translational energy of the products is high, even small transfer of energy can produce large increases in product rotational energy.

Our Doppler resolution of the products has proved inconclusive. We obtain Doppler line profiles that are not the shape we expect. They are Gaussian when we expect them to be predominantly flat-topped. The Doppler line profiles for all the H + RH reactions and for H + HCl, and H + HI as well, are all of this type. Though we cannot explain this, we believe that it is real and significant. That belief is based on the fact that we do get the expected lineshapes for H_2 from the H + H_2S reaction. A comparison of these Doppler-broadened lineshapes is shown in Fig. 1. The line profiles that we measure are those that have been observed by others for the H + HI reaction and H + H_2S reactions.

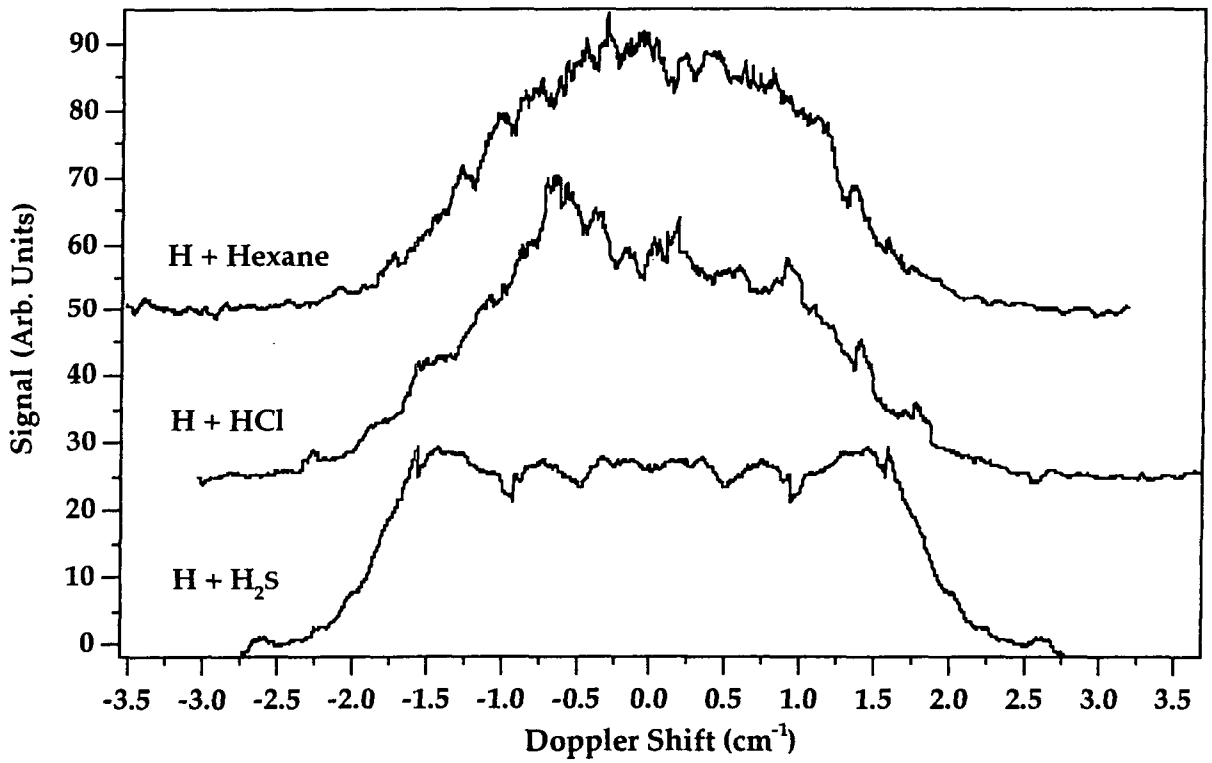

Figure 1. Doppler profiles in the REMPI spectra of the H_2 product of three H atom abstraction reactions.

FUTURE PLANS

In the next year our main plan is to get our redesigned crossed beam apparatus completed and to begin measurement of full state-resolved differential cross sections. In doing so we plan to take advantage of the special kinematics of these reactions, due to which the center-of-mass velocity vector and relative velocity vector are parallel and the center-of-mass velocity is much smaller than the relative velocity. We will get the speed and angular distributions from a measurement of the Doppler line profile for observation directly along the relative velocity vector.

Theoretical Studies of the Dynamics of Chemical Reactions

Albert F. Wagner

Gas Phase Chemical Dynamics Group
Chemistry Division
Argonne National Laboratory
Argonne, IL 60439
wagner@tcg.anl.gov

Program Scope

The goal of this program is to apply and extend dynamics and kinetics theories to elementary reactions of interest in combustion. Typically, the potential energy surfaces used in these applications are determined from ab initio electronic structure calculations, usually by other members of the group. Generally the calculated kinetics or dynamics is compared to experimental results, often generated by other members of the group.

Recent Progress

Studies of Initiation Reactions. We have completed experimental and theoretical work on two combustion initiation reactions:

$$H_2 + O_2 \rightarrow HO_2 + O$$
$$H_2CO + O_2 \rightarrow HO_2 + HCO.$$

The rates of both reactions were directly measured in a shock tube (see J. V. Michael). Potential energy surfaces of both reactions were examined (see L. B. Harding). The first reaction goes exclusively by abstraction as written. No four center transition state was discovered. For the second reaction, a bent transition state was found, giving rise to two nearly free rotors. Variational rate constant calculations were carried out on the computed surfaces adjusted for the correct endothermicity determined in part by photoionization thermodynamics studies carried out previously. Variational effects were found to be minor at the high temperatures of interest. For the first reaction, the theoretical rates compare well with the shock tube measurements and with reverse rate constant measurements carried out at room temperature, a span of tens of orders of magnitude in rate constant values when expressed in the forward direction. For the second reaction, the theoretical rates connect our high-temperature direct measurements with lower temperature indirect measurements by displaying substantial rate constant curvature due to the two free rotors. Treatment of either of these degrees of freedom harmonically degrades the agreement with experiment. For the second reaction, both DFT (B3LYP) and CCSD(T) methods were used to trace out the reaction path. Recently and independently, T. Truong (U. of Utah) have carried out similar calculations using a different DFT functional (BHLYP) with a different basis set to determine the reaction path. At the DFT level the transition state geometry, lower frequencies, and energetics are noticeably different for the two choices of functionals and are different from the CCSD optimized transition state. In collaboration with Truong the kinetic implications of these differences are being explored.

Anharmonic Effects in Recombination Reactions. In collaboration with Klippenstein and Dunbar (Case Western), Wardlaw (Queens University), Robertson (Leeds), and Diau (Caltech), we have released via web (http://chemistry.anl.gov/variflex) and anonymous ftp (ftp.tcg.anl.gov) the code VARIFLEX, a flexible transition state theory (FTST) code designed for direct and

complex-forming reactions with barrierless potentials. This code fully incorporates variable reaction coordinates (VRC) in which the definition of the reaction coordinate itself is optimized in the minimization of the rate constant. Advanced 1D Master Equation approaches as well as traditional harmonic-oscillator/rigid-rotor approaches combined with the RRKM approach for complex-forming reactions are included in VARIFLEX. The manual and example input and output display reactions where VRC is important (e.g., H+CCH and CF_xH_{3-x}+H) and where it is not (e.g., H_2+CH and CH_3+CH_3). This code is used in most of our kinetics calculations for barrierless reactions.

In recent VARIFLEX studies, we have examined the effect of ab initio versus simple semi-empirical potential energy surface models on the high-pressure limiting recombination kinetics of H + radical reactions including:

$$H+CCH \rightarrow HCCH \quad (1)$$

$$H+CF_{3-x}H_x \rightarrow CF_{3-x}H_{x+1} \quad (x=0,...,3) \quad (2)$$

$$H+NO_2 \rightarrow HNO_2 \text{ or } HONO \rightarrow HO+NO \quad (3)$$

The semi-empirical potential, which is an option in VARIFLEX, represents non-bonding interactions by pairwise additive potentials with well-known parameter tabulations for first row atoms and halogens (e.g., Mayo, et al., 1990) while bonding potentials can be input from either ab initio calculations or Morse oscillator (MO) parameters. The ab initio potential energy surfaces have all been generated by L. Harding in our group. In the above sequence of reactions, Rxn (1) has a single radical orbital pointing in one direction, Rxn (2) has a single radical orbital pointing front and back in two directions, and Rxn. (3) has in-plane radical orbitals on each atom in NO_2.

In all three reactions, use of the ab initio reaction path is necessary for reliable kinetics. While the ab initio reaction path can be represented by an MO, the beta parameter values can be very much different from those consistent with an MO fit to the experimental spectroscopy of the product bound molecules. In the case of Rxn. (2) the ab initio reaction path for both top and bottom attack of the splayed partially fluorinated methyl radical must be determined. Assuming the most attractive approach is sufficient will lead to factor of two errors in the kinetics for H+ CF_2H. For the first two reactions, the non-bonding interactions can be represented by semi-empirical models with only a modest effect on the kinetics. This despite the fact that prominent features in the ab initio surface (e.g., evidence of vinylidene in H+CCH) are entirely absent.

For Rxn. (3), the semi-empirical non-bonding potential works very poorly, producing too large a rate constant that rapidly falls with temperature. The ab initio rate constant is mildly increase with temperature. However, compared to published low temperature measurements on this reaction and unpublished high temperature measurements done by J. Michael in our group, the ab initio rate is about a factor of two too high, although with the correct temperature dependence. Only a limited region of the non-planar part of the potential energy surface has been sampled as yet by the ab initio calculations and further theoretical study of this reaction is in progress.

Potential Energy Surface Library: In collaboration with D. Truhlar (U. of Minnesota) and R. Duchovic (Purdue U. Indiana U. at Fort Wayne), we have constructed a potential energy surface subroutine library called POTLIB. Potential energy surfaces checked into the most developed part of this library obey an application interface protocol (AIP). As a consequence, any code that uses potential energy surfaces can check out any subroutine from the library and, via a single interface routine, compile, link, and execute with that subroutine. The library contains four example interface routines for POLYRATE (Truhlar et al.), VENUS (Hase et al.), VARIFLEX (Klippenstein et al.), and DYNASOLVE (Zhang et al.). This portion of the library currently contains about 100 members. A second portion of the library is archival in nature for surfaces

that work but do not yet conform to the AIP. The library is due to be officially released in the spring. We would be interested in any new potential energy subroutines and/or interface routines for this library.

Parallelization of Cumulative Reaction Probabilities. In collaboration with M. Minkoff (ANL Math. and Comp. Sci. Division), we are developing a parallelized code for the direct calculation of the cumulative reaction probability (CRP). Knowledge of the CRP allows a direct and trivial calculation of the exact rate constants (including quantum effects such as tunneling). In doing the parallelization, we are attempting to largely avoid custom coding but rely instead on generic subroutine libraries for common mathematical kernels, in this case the PETSc library (W. Gropp) developed at Argonne. Such libraries are portable and efficiently parallelized but their generic nature makes them unable to directly exploit the specifics of an application (e.g., the detailed structure of a matrix in doing matrix-vector multiplies). Use of such libraries reduces the human time in developing portable, parallel code but produces sub-optimal code because the specifics of the problem can not be fully exploited. Our effort is an attempt both to develop code to expand the number of degrees of freedom for which CRP calculations can be carried out and to assess the usefulness of generic subroutine libraries at this time. We have chosen a time-independent formulation of the CRP as initially developed by Miller et al. In this method, the CRP is a sum of eigenvalues of an operator containing two Green's functions. A DVR approach produces a representation of the operator that can have huge dimensions (10^5 or higher) but only a few eigenvalues are physically important. Consequently, the eigenvalue determination is done iteratively in a series of matrix-vector multiplies, each one of which requires the resolution of two Green's functions. Each resolution can be cast as an iterative solution to a linear equation. All of these operations are represented in the PETSc library. The sparse banded structure of the matrix used in the Green's function can be treated in PETSc but only at a sub-optimal level. We have applied our code to a model potential energy surface with an analytic CRP whose number of degrees of freedom can be varied from a triatomic to a tetra-atomic to a polyatomic reaction. Results on the T3E at NERSC as well as the Power Challenger at ANL show near ideal speed up over a range of ~100 processors for 5 degree of freedom problems or higher. For the 5 degree of freedom problem the T3E time-to-solution is on the order of a minute per eigenvalue per energy.

Future Plans

We plan to continue to study anharmonic effects in radical-radical reactions and in particular examine how of the relevant portion of the surface needs to be characterized by ab initio studies as opposed to simpler semi-empirical models. In this regard, see L. Harding for a variety of ab initio surfaces that could be targets for comparison to semi-empirical models. We also want to contrast trajectory and FTST-VRC calculations to understand more fully the implications of the VRC model.

We also intend to study specifically two reactions unmentioned above. The first is CH_3+O_2 where recent measurements by both J. Michael and J. Hessler in our group have determined rate constants into each of the two products, H_2CO+OH and CH_3O+O. There are a number of measurements available in the literature on this reaction and there is not experimental consensus on several aspects of the kinetics. We hope to carry out theoretical calculations on this reaction. Both the entrance and one of the exit channel is barrierless, making an FTST-VRC approach to the kinetics appropriate. The second reaction is OH+OH. Since our initial theoretical study on this reaction more than 10 years ago, recent experimental studies on isotope effects at low temperature (G. Poulet, CNRS, France) and rate constants at high temperature (see J. Hessler), motivate a more detailed study. Such a study could entail an application of the CRP code discussed above.

Finally, an emerging experimental program to study soot morphology (see J. Hessler) at the Advanced Photon Source at ANL has lead to an increase theoretical interest in soot chemistry. This interest could be expressed in reaction rate calculations of soot precursors under experimental study elsewhere (e.g., A. Fahr at NIST). It could also be expressed in simulations with coupled kinetics models (e.g., those of M. Frencklach, Berkeley) aimed directly at morphology.

Publications from DOE Sponsored Work from 1997-2000.

Flexible Transition State Theory for a Variable Reaction Coordinate: Derivation of Canonical and Microcanonical Forms
S. Robertson, D. M. Wardlaw, and A. F. Wagner, J. Chem. Phys. (in press)

Initiation in H2/O2: Rate Constants for H_2+O_2 -> $H+HO_2$ at High Temperature
J. V. Michael, J. W. Sutherland, L. B. Harding, and A. F. Wagner, 28th Symposium (International) on Combustion, (in press)

Variational Transition State Study of CN + H_2 -> HCN +H and Its Isotopic Variants
G. He, A. F. Wagner, and L. B. Harding, J. Chem. Phys. (in press).

High-Performance Computational Chemistry: Hartree-Fock Electronic Structure Calculations on Massively Parallel Processors
J. L. Tilson, M. Minkoff, A. F. Wagner, R. Shepard, P. Sutton, R. J. Harrison, R. A. Kendall, and A. T. Wong, Int. J. High Performance Computing Applications **13**, 291-302 (1999).

The Influence of Hindered Rotations on Recombination/Dissociation Kinetics
A. F. Wagner, L. B. Harding, D. M. Wardlaw, S. H. Robertson, Ber. Gunsenges. Phys. Chem. 101, 391-399 (1997).

A Quasiclassical Trajectory Study Of Product State Distributions From The CN + H_2 -> HCN + H Reaction
G. A. Bethardy, A. F. Wagner, G. C. Schatz and M. A. ter Horst, J. Chem. Phys.106, 6001, 1997.

Electronic Spectroscopy of Jet-Cooled Combustion Radicals

James C. Weisshaar
Department of Chemistry
University of Wisconsin-Madison
Madison, Wisconsin 53706-1396
email: weisshaar@chem.wisc.edu

Program Scope

The goal of our work has been to obtain and analyze new spectra of important combustion radicals cooled in supersonic expansions. An auxiliary fundamental goal is to measure and understand methyl rotor torsional potentials in the near vicinity of radical centers. Such torsional potentials strongly influence the density of rovibrational states that enters statistical calculations of unimolecular radical decay rates and product branching. Our techniques include laser induced fluorescence and dispersed fluorescence, as well as *ab initio* electronic structure calculations to assist in interpreting our results. Collaborations with Dr. Larry Harding (Argonne National Labs) and Dr. John Stanton (U. Texas) have been very fruitful when the need for state-of-the-art, multi-reference calculations arises.

Recent Progress

Vinoxy radicals are important primary products of the reactions of oxygen atoms with alkenes in combustion systems. We have obtained jet-cooled LIF spectra of two different methyl-substituted vinoxy radicals, 1-methylvinoxy and 2-methylvinoxy (unknown mixture of *cis-* and *trans-*). The spectrum of the $\tilde{B} \leftarrow \tilde{X}$ electronic transition 1-methylvinoxy radical has been assigned, including both hot and cold bands. The barrier to methyl internal rotation in both $\tilde{X}$ and $\tilde{B}$ states is determined by fitting pure torsional transitions to a one-dimensional hindered rotor model. The resulting threefold torsional barrier parameters are $V_3' = -740 \pm 30$ cm^{-1} for the $\tilde{B}$ state (minimum energy conformation having one methyl CH bond *cis* to the frame CO bond) and $V_3'' = +130 \pm 30$ cm^{-1} for the $\tilde{X}$ state (methyl CH bond *trans* to CO). The intensity pattern clearly indicates a change in the preferred methyl conformation upon excitation, while *ab initio* calculations provide the absolute conformations in each state.

A variety of *ab initio* methods including CASSCF, multi-reference CI, and coupled cluster techniques were applied to both the $\tilde{X}$ and $\tilde{B}$ states of 1-methylvinoxy. The multi-reference CI calculations were carried out by Dr. Larry Harding; the coupled-

cluster calculations were carried out by Dr. John Stanton. Only the largest coupled-cluster calculations yield a $\tilde{B}$-state barrier in good quantitative agreement with experiment.

In unsubstituted vinoxy, a $\tilde{B}$-state geometry adjusted earlier to fit experimental rotational constants due to T. Miller and co-workers (J. Chem. Phys. 81, 2339, 1984) is evidently in error.

Also recently assigned is the jet-cooled LIF spectrum of a mixture of *cis* and *trans*-2-methylvinoxy radicals. Both $\tilde{X}$ and $\tilde{B}$-state methyl torsional barriers were determined for the *cis* isomer as above by fitting hot and cold bands respectively to a one-dimensional hindered rotor model. For the *cis*-2-methylvinoxy radical, the experimental threefold torsional barriers are V_3'= -268 ± 30 cm^{-1} for the $\tilde{B}$ state (minimum energy conformation placing one methyl CH bond *cis* to the vicinal CC bond) and V_3''= +200 ± 30 cm^{-1} for the $\tilde{X}$ state (methyl CH bond *trans* to vicinal CC bond). As with 1-methylvinoxy, the intensity pattern of the torsional envelope clearly indicates a change in the methyl conformational minimum upon $\tilde{B} \leftarrow \tilde{X}$ excitation. For the *trans* isomer, only the $\tilde{B}$-state barrier to methyl internal rotation was determined (V_3'= +200 ± 30 cm^{-1}). The *trans*-2-methylvinoxy does not undergo a change in preferred methyl conformation, a methyl CH bond *cis* to the vicinal CC bond, upon $\tilde{B} \leftarrow \tilde{X}$ excitation.

The intensity patterns anomalous in the 2-methylvinoxy. Repetitions of the torsional structure analyzed at both the *cis* and *trans* origin should occur at roughly the same vibrational intervals that produce activity in the spectrum of plain vinoxy, but they do not. Instead, a few intense bands and many weak bands appear. We suspect that the well-known photochemical channel has distorted the LIF intensities; if so, the mode dependence of the photochemical yield is erratic.

Both CASSCF and MRCI *ab initio* methods have been applied to the 2-methylvinoxy species, the latter by Dr. Larry Harding. Coupled-cluster calculations are in progress. Thus far, agreement is again better for the ground state than for the $\tilde{B}$ state.

FUTURE PLANS

This concludes our efforts in the DOE combustion program. One additional publication describing the assignment of the 1-methylvinoxy spectrum (joint with Larry Harding and John Stanton) is now submitted to J. Phys. Chem. A. We anticipate one final manuscript regarding our assignment of the 2-methylvinoxy spectra and corroborating calculations with the same co-authors.

Publications Citing DOE Support, 1997-99.

1. R.A. Walker, E.C. Richard, K.-T. Lu, and J.C. Weisshaar, Effects of ionization on methyl internal rotation in substituted toluenes, chapter in *Advances in Gas Phase Ion Chemistry*, Vol. 3 (Eds. N.G. Adams and L.M. Babcock, JAI Press, Greenwich, Connecticut, 1998).
2. S. Williams, E. Zingher, and J.C. Weisshaar, $\tilde{B} \leftarrow \tilde{X}$ Vibronic Spectra and $\tilde{B}$-State Fluorescence Lifetimes of Methyl-Vinoxy Isomers, J. Phys. Chem. A **102**, 2297 (1998).
3. K.-T. Lu, E.C. Richard, R.A. Walker, and J.C. Weisshaar, Methyl internal rotation in substituted toluenes: effects of substituents, electronic excitation, and ionization, chapter in NATO Advanced Study Institute on *Fundamentals and Applications of Gas Phase Ion Chemistry*, Keith Jennings, ed. (1998).

Kinetic Modeling of Combustion Chemistry

Charles K. Westbrook and William J. Pitz
Lawrence Livermore National Laboratory
P. O. Box 808, Livermore, CA 94550

Program Goals

The goals of this program are to develop the techniques of developing detailed chemical kinetic reaction mechanisms for the combustion of hydrocarbon and related chemical species, and then to use those reaction mechanisms to study combustion in practical combustion systems. During the course of mechanism development, the value of many theoretical chemistry techniques are determined, and needs for further theoretical and experimental studies can be assessed. Finally, kinetic sensitivity analyses are used to determine what elementary reactions and reaction rates require further attention to improve modeling capabilities.

Background

Over the past 30 years, chemical kinetic modeling has developed into a very significant part of the overall field of combustion chemistry. The ability to interpret experimental data, the ability to predict the results of proposed experiments, and the possibility of using kinetic modeling to motivate further studies all contribute to the value of this technique. The building block of this discipline is the detailed chemical kinetic reaction mechanism, and LLNL has a long history in the study and development of these mechanisms. LLNL has focused in particular on models for larger hydrocarbon species, with more than 4 carbon atoms and extending to 8, 10 and as many as 16 carbon atoms. This is true in a field where most kinetic models treat only 2 or 3 carbon atoms. As a result, LLNL has been able to address a range of practical modeling problems that would be unaccessible if models for only 2 or 3 carbon atoms were available. Such applications include studies of engine knock, ignition in diesel engines, propagation of detonations in practical fuels, and incineration of many practical fuels.

In addition, the more general case of combustion of other chemicals related to hydrocarbons can be addressed. This includes halogenated hydrocarbons and hydrocarbons with organophosphate elements. The techniques required to develop models for hydrocarbons are then applied to other species, enabling modeling to study many new classes of problems.

Accomplishments

During the past two years, the LLNL program has emphasized several major features of combustion and related chemistry modeling. These are the production of soot precursors, combustion of smaller core hydrocarbon molecules, extension of modeling to ever-larger fuel species, development of

reaction mechanisms to new classes of fuels, and applications of modeling to important practical problems.

We have continued to advance the identification of reaction pathways that lead to production of small aromatic and polycyclic aromatic hydrocarbon species, those which eventually lead to soot production. This work has emphasized thermochemistry and electronic structure of hydrocarbon species. This work will lead to development of soot production models in practical engine simulations.

We have carried out studies of smaller species including dimethyl ether, dimethoxy methane, neopentane, and a variety of small oxygenated hydrocarbons, evaluating the role that oxygenation plays in reducing sooting in diesel engines. We have continued to refine and develop kinetic models for the larger hydrocarbon species that are characteristic of practical automotive and other fuels. A comprehensive reaction mechanism was published for the combustion of n-heptane, and an accompanying mechanism is being developed for the other primary reference fuel for spark ignition engines, iso-octane. We are also studying principles of reducing the size of reaction mechanisms for practical fuels to make their computational modeling much less computationally expensive.

Reaction mechanisms for new classes of fuels have been pursued, testing the capabilities of available theoretical tools. During the past year, we have focused on organophosphate species that are characteristic of chemical warfare nerve agents. We have developed reaction mechanisms for many real nerve agents and for their related surrogate species, in order to be able to guide development of such activities as destruction of nerve agent weapons using combustion technologies such as incineration and supercritical water oxidation.

We have continued to use kinetic models to examine practical combustion problems in spark-ignition and diesel engines. This work has had significant impacts on a variety of engine problems. In addition, we have studied an interesting new engine concept, that of homogeneous charge compression ignition (HCCI) combustion, which offers the possibility of very low NOx emissions but with the penalty of high unburned hydrocarbon species emissions.

Future Plans

We expect to continue to carry out detailed chemical kinetic model development and applications to new theoretical and applied problems. At the extremely low level of funding provided by BES/Chemical Sciences, we are supported primarily to participate in the program review and annual contractors conferences. This enables us to exchange information with other program participants and communicate our recommendations for further research, but it is much too low to have consistent impacts on overall program objectives.

email addresses
westbrook1@llnl.gov and pitz1@llnl.gov

Recent Publications

Marinov, N. M., Pitz, W. J., Westbrook, C. K., Castaldi, M. J., Senkan, S. M., and Melius, C. F. "Aromatic and Polycyclic Aromatic Hydrocarbon Formation in a Laminar Premixed n-Butane Flame," **Combustion and Flame** 114, 192-213 (1998).

Curran, H. J., Pitz, W. J., Marinov, N. M., Westbrook, C. K., Dagaut, P., Boettner, J.-C., and Cathonnet, M. "A Wide Range Modeling Study of Dimethyl Ether Oxidation," **International Journal of Chemical Kinetics** 30, 229-241 (1998).

Curran, H. J., Gaffuri, P., Pitz, W. J., and Westbrook, C. K. "A Comprehensive Modeling Study of n-Heptane Oxidation," **Combustion and Flame** 114, 149-177 (1998).

Marinov, N.M., Pitz, W.J., Westbrook, C.K., Lutz, A.E., Vincitore, A.M., and Senkan, S.M. "Chemical Kinetic Modeling of a Methane Opposed-Flow Diffusion Flame and Comparison to Experiments", **Twenty-Seventh Symposium (International) on Combustion**, pp. 605-613, The Combustion Institute, Pittsburgh, 1998.

Westbrook, C.K., Curran, H.J., Pitz, W.J., Griffiths, J.F., Mohamed, C., and Wo, S.K. "The Effects of Pressure, Temperature, and Concentration on the Reactivity of Alkanes: Experiments and Modeling in a Rapid Compression Machine", **Twenty-Seventh Symposium (International) on Combustion**, pp. 371-378, The Combustion Institute, Pittsburgh, 1998.

Curran, H.J., Pitz, W.J., Westbrook, C.K., Callahan, C.V., and Dryer, F.L., "Oxidation of Automotive Primary Reference Fuels at Elevated Pressures", **Twenty-Seventh Symposium (International) on Combustion**, pp. 379-387, The Combustion Institute, Pittsburgh, 1998.

Hori, M., Matsunaga, N., Marinov, N.M., Pitz, W.J., and Westbrook, C.K. "An Experimental and Kinetic Calculation of the Promotion Effect of Hydrocarbons on the NO-NO2 Conversion in a Flow Reactor", **Twenty-Seventh Symposium (International) on Combustion**, pp. 389-396, The Combustion Institute, Pittsburgh, 1998.

Marinov, N.M., Curran, H.J., Pitz, W.J., and Westbrook, C.K. "Chemical Kinetic Modeling of Hydrogen under Conditions Found in Internal Combustion Engines", **Energy and Fuels** 12, 78-82 (1998).

Flynn, P.F., Durrett, R.P., Hunter, G.L., zur Loye, A.O., Akinyemi, O.C., Dec, J.E., and Westbrook, C.K. "Diesel Combustion: An Integrated View Combining Laser Diagnostics, Chemical Kinetics, and Empirical Validation", Society of Automotive Engineers paper SAE-1999-01-0509 (1999).

Aceves, S.M., Smith, J.R., Westbrook, C.K., and Pitz, W.J. "Compression Ratio Effect on Methane HCCI Combustion", **J. Engineering for Gas Turbines and Power** 121, 569-574 (1999).

Wang, S., Miller, D. L., Cernansky, N. P., Curran, H. J., Pitz, W. J., and Westbrook, C. K., "A Flow Reactor Study of Neopentane Oxidation at 8 Atmospheres: Experiments and Modeling", **Combustion and Flame** 118, 415-430 (1999).

Montgomery, C. J., Cremer, M. A., Heap, M. P., Chen, J.-Y., Westbrook, C. K., and Maurice, L. Q., "Reduced Chemical Kinetic Mechanisms for Hydrocarbon Fuels", 35th AIAA/ASME/SAE/ASEE Joint Propulsion Conference, June 1999.

Aceves, S.M., Flowers, D.L., Westbrook, C.K., Smith, J.R., Pitz, W.J., Dibble, R., Christensen, M., and Johansson, B., "A Multi-Zone Model for Prediction of HCCI Combustions and Emissions", Society of Automotive Engineers publication SAE 2000-01-0327, February, 2000.

Curran, H. J., Fisher, E., Glaude, P.-A., Marinov, N. M., Pitz, W. J., Westbrook, C. K., Flynn, P. F., Durrett, R. P., zur Loye, A. O., and Akinyemi, O. C. "Detailed Chemical Kinetic Modeling of Diesel Combustion with Oxygenated Fuels", submitted for publication (2000).

Flynn, P. F., Hunter, G. L., Farrell, L. A., Durrett, R. P., Akinyemi, O. C., Westbrook, C. K., and Pitz, W. J. "The Inevitability of Engine-Out NOx Emissions from Spark-Ignition and Diesel Engines", submitted for publication (2000).

Ribaucour, M., Minetti, R., Sochet, L. R., Curran, H. J., Pitz, W. J., and Westbrook, C. K. "Ignition of Isomers of Pentane: An Experimental and Kinetic Modeling Study", submitted for publication (2000).

Fisher, E. M., Pitz, W. J., Curran, H. J., and Westbrook, C. K. "Detailed Chemical Kinetic Mechanisms for Combustion of Oxygenated Fuels", submitted for publication (2000).

Glaude, P.-A., Curran, H. J., Pitz, W. J., and Westbrook, C. K. "Kinetic Study of the Combustion of Organophosphorus Compounds", submitted for publication (2000).

Kaiser, E. W., Wallington, T. J., Hurley, M. D., Platz, J., Curran, H. J., Pitz, W. J., and Westbrook, C. K. "Experimental and Modeling Study of Premixed Atmospheric-Pressure Dimethyl Ether-Air Flames", submitted for publication (2000).

PROBING FLAME CHEMISTRY WITH MBMS, THEORY, AND MODELING

Phillip R. Westmoreland
Department of Chemical Engineering
University of Massachusetts Amherst
159 Goessmann Laboratory, P. O. Box 33110
Amherst, Massachusetts 01003-3110
Phone 413-545-1750
FAX 413-545-1647
westm@ecs.umass.edu
http://www.ecs.umass.edu/che/westmoreland.html

Program Scope

The program's objective is to establish kinetics of combustion and molecular-weight growth in hydrocarbon flames as part of an ongoing study of flame chemistry. Our approach combines molecular-beam mass spectrometry (MBMS) experiments on low-pressure flat flames; *ab initio* thermochemistry and transition-state structures; rate constants predicted by transition-state and collision-mediated reaction theories; and whole-flame modeling using mechanisms of elementary reactions. The MBMS technique is powerful because it can be used to measure a wide range of species quantitatively, including radicals, with high sensitivity and low probe perturbation. Ethene, propene, and allene-doped ethene flames are presently being studied.

Recent Progress

Summary. In the past year, we have:

- Begun upgrading our MBMS apparatus to obtain higher sensitivity and more species;
- Collected and added data sets to a Web site of flame-profile data;
- Begun developing a flame apparatus for photoionization MBMS at the LBL Synchrotron;
- Modeled MBMS data from the fuel-rich propadiene-ethene flame; and
- Begun developing new approaches for high-accuracy flat-flame modeling.

MBMS upgrade. Our MBMS apparatus is evolved from the first US flame MBMS apparatus, which was built and used for a classic set of experiments on chemical suppression of flames by Biordi, Lazzara, and Papp at the Bureau of Mines (Pittsburgh) in the early 1970's. Many of its components have been altered or replaced during the 14 years we have had it, but the Extranuclear Laboratories mass spectrometer and electronics have still been the originals.

A new Extrel quadrupole mass spectrometer will give higher mass resolution, higher signal sensitivity, negative- as well as positive-ion capability, and more stable operation. Electron-impact ionization will be used in the transverse-mounted MS with both analog and pulse-counting detection modes. Mass ranges will be 1-50 amu (ultra-high resolution for separation of oxygenates from hydrocarbons), 1-500, and 4-2000. The equipment has been delivered and is being installed. Testing should begin this summer.

Web repository of flame-profile data. A Web site, http://www.ecs.umass.edu/MBMS/, was created last year as a repository of flame-profile data, emphasizing the comprehensive sets available from MBMS experiments. Having these complete sets of data in digital form is important for testing models; however, most literature data have been reported in graphical form. Data from this research and from other studies are being collected and prepared in tabular, downloadable form for our use and for general use by the flame-modeling community. Initial sets have been focused on ethylene flames.

Proposed LBL photoionization MBMS. With Tom Baer, Terry Cool, and Andy McIlroy, we are developing a flame apparatus at the LBL Synchrotron that can be used for photoionization MBMS. Hot-wire electron-impact ionization is normally used in MBMS, operated just above the ionization potential to avoid fragmentation. The experimentally observed ionization potential is also valuable for identifying the species being ionized. This gives excellent results when a single isomer dominates or when two isomers have greatly different ionization potentials. However, signal does not appear abruptly at the ionization potential because the thermal electrons have a distribution of energies. With finely tuned photons from the Chemical Dynamics Beamline at the ALS, we should be able to discriminate many isomeric species by their photoionization thresholds.

Developing a new flame modeling method. We are developing a solution method for solving the nonadiabatic energy equation in a flat flame. This work is motivated by finding that the use of a temperature profile for modeling can account for failures by us and by others to successfully model our slightly lean ethene flame.[3] An accurate physical model of the flat flame will give new power to using flat-flame data for kinetics.

MBMS data from flat flames have proven to be useful for obtaining and testing flame kinetics for two main reasons. First, overall net reaction rates can be extracted for each species using experimental convection, diffusion, and flow-divergence terms in the steady-state mass-transport equations. Second, modeling the flame species has been possible and rather successful by using the mass-transport equations with experimentally based temperature profiles.

The conventional approach of using a measured temperature profile is imperfect, but it avoids important complications:

- Calculating radiative heat losses from the gas-phase flame;
- Accounting for uncertain heat loss to the burner, which has never been measured successfully;
- Difficulty in converging to a solution, which is hard even in an adiabatic flame because of Arrhenius and other nonlinear temperature dependences of the kinetics.

Temperature profiles are usually adapted and aligned using rules from earlier microprobe and optical measurements. The usual approach is to begin with an accurate optical or thermocouple measurement of an unperturbed flame. Conventionally, the profile is pinned to a measured surface temperature, measured temperatures are reduced by 100 K as correction for local cooling by the probe, and temperature profiles may be shifted axially because of enhanced convective heat transfer in a thermocouple's wake. Another approach is to measure temperatures just ahead of the probe tip, but the specific location to be used is uncertain. A coupled issue is shifting MBMS profiles 2 to 5 orifice diameters closer to the burner because the sample comes from in front of the probe tip rather than at the tip. By comparison, Vandooren, Van Tiggelen, and Peeters shift the temperature profile until the Lewis numbers throughout the flame are closest to unity. In most cases, these compromises have been quite acceptable.

To establish whether the ethene flame's inputted temperature profile could be at fault, we tested five variations, corresponding to different conventions. The unchanged experimental profile was used for one set of predictions. Alternatively, profiles were increased by 100 K, decreased by 100K, or shifted 0.5 mm away from the burner. A fifth profile was perturbed more strongly and arbitrarily: shifted 0.5 mm, decreased by 100 K, and given a less steep gradient near the burner. Only the fifth profile gave predictions of C_2H_4 that were very close to the data and an H-atom profile that matched the shape of the experimental profile well. Other major species were also much improved.

A reactive burner boundary condition was tested using a surface reaction H+H = H_2. However, even when the rate constant was increased to unit collision efficiency, the H profile only changed near the burner and not sufficiently.

Solving the full mass and energy equations with correct boundary conditions would not only be more intellectually satisfying, but it would avoid the danger of violating energy balances. That problem was observed even in the first study that modeled MBMS mole fraction profiles.[2] Predictions from a poorly performing mechanism gave low conversion, which could not have generated the amount of energy release needed to give flame temperatures. In hindsight, conversion occurred only because flame temperatures were imposed in the solution.

We are developing modifications to the Chemkin II version of the Sandia Premix code that will explicitly incorporate radiative losses and burner losses into the energy equation and boundary conditions. An empirical heat loss to the burner must be used for a given flame on a given burner. We and others have established that burner heat loss depends sensitively on the particular burner

---

[1] A. Bhargava and P. R. Westmoreland, *Combustion and Flame* **115**, 456-467 (1998).

[2] P.R. Westmoreland, J.B. Howard, and J.P. Longwell, *Twenty-First Symposium (International) on Combustion*, The Combustion Institute, Pittsburgh, PA, 773 (1986).

design. However, heat loss has not been measured successfully in previous studies. The problem is that if there is a detectable rise in burner cooling-water temperature, the burner surface temperature becomes too high. We are developing two approaches: (1) inference of the heat loss by applying the energy equation to the flame data and (2) extrapolating measurable heat losses to experimental cooling-water flowrates. Applying method 2 to the lean flame, we obtained 11.8±0.7 kW/m^2 with no definite trend up or down.

Propadiene-ethene flame modeling. We have modeled our recent allene-doped (0.50%), fuel-rich (ϕ=1.90) ethene flame and re-examined key reactions of C_3 hydrocarbons using the literature and theoretical kinetics. The corresponding ethene flame was fairly well modeled. Improved predictions due to new kinetics then add credence to the new reaction set.

Experimentally, mole fraction profiles were measured for 39 species (Table 1), and upper bounds were measured for two others. Because the flame was so similar to the earlier ethene flame,[1] data and predictions can be compared between the two. The main data differences were seen in C_3H_4 and in higher HCO and C_6H_6 profiles.

Table 1. Species measured in low-pressure flat flames of ethene/oxygen/50.0% argon and 0.50% propadiene/ethene/oxygen/49.7% argon at fuel-rich (ϕ=1.90) conditions.

Species	Ethene	Propadiene/ethene	Species	Ethene	Propadiene/ethene
H	Profile	Profile	CH_2CO	Profile*	Profile
H_2	Profile	Profile	CH_2CHO **	Profile	Profile
CH_2	Profile	Profile	CH_3CHO	Profile	Profile
CH_3	Profile	Profile	CO_2	Profile	Profile
CH_4	Profile	Profile	C_4H_2	Profile	Profile
OH	Profile	Profile	C_4H_3	-	Profile
H_2O	Profile	Profile	C_4H_4	Profile	Profile
C_2H_2	Profile	Profile	C_4H_5	-	Profile
C_2H_3	Profile	Profile	C_4H_6	-	Profile
C_2H_4	Profile	Profile	C_3H_3O/C_4H_7	-	Profile
CO	Profile	Profile	C_3H_4O/C_4H_8	Profile	Profile
HCO	Profile	Profile	C_3H_6O/C_4H_{10}	Profile	Profile
H_2CO	Profile	Profile	C_5H_4	Profile	Profile
O_2	Profile	Profile	C_5H_6	Profile	Upper bound
HO_2	-	Profile	C_4H_3O/C_5H_7	Profile	Upper bound
H_2O_2	-	Profile	C_4H_4O/C_5H_8	Profile	-
C_3H_2	Profile	Profile	C_4H_6O/C_5H_{10}	Profile	-
C_3H_3	Profile	Profile	C_4H_8O/C_5H_{12}	Profile	-
C_3H_4	Profile	Profile	C_6H_2	Profile	Profile
Ar	Profile	Profile	C_6H_4	Profile	Profile
HCCO	-	Postflame profile	C_6H_5	Profile	Profile
C_3H_5	Profile	Profile	C_6H_6	Profile	Profile

*Reported previously as C_3H_6.

**Possibly CH_2CHO^+ ionization fragment of CH_3CHO.

Principal changes in kinetics were H abstraction from the allene:

$CH_2=C=CH_2 + H \rightarrow C_3H_3 + H_2$, $k=3.7\cdot10^7T^{2.17}\exp(-13.4$ kcal/mol $/RT)$, ethene analog
$CH_2=C=CH_2 + OH \rightarrow C_3H_3 + H_2O$, $k=5.5\cdot10^5T^{2.31}\exp(-2.9$ kcal/mol $/RT)$, ethene analog
$CH_2=C=CH_2 + O \rightarrow C_3H_3 + H_2O$, $k=1.8\cdot10^{15}\exp(-10.4$ kcal/mol $/RT)$, BAC-MP4
$CH_2=C=CH_2 + HO_2 \rightarrow C_3H_3 + H_2O_2$, $k=2.0\cdot10^{14}\exp(-19.0$ kcal/mol $/RT)$, BAC-MP4
$CH_2=C=CH_2 + CH_3 \rightarrow C_3H_3 + CH_4$, $k=3.4\cdot10^{14}\exp(-14.3$ kcal/mol $/RT)$, BAC-MP4
$CH_2=C=CH_2 + CH_2\ (^3B_2) \rightarrow C_3H_3 + CH_3$, $k=7.9\cdot10^{14}\exp(-13.5$ kcal/mol $/RT)$, BAC-MP4

H transfer from HO_2 to allene and its reverse:

Allyl + O_2 <=> $CH_2=C=CH_2 + HO_2$, $k=5.8\cdot10^{14}\exp(-41.8$ kcal/mol $/RT)$, BAC-MP4

H addition to allene and its reverse:

$CH_2=C=CH_2$ + H <=> Allyl, $k_\infty=1.1\cdot10^{15}\exp(-7.8$ kcal/mol $/RT)$ plus falloff, BAC-MP4

formation of phenyl from propargyl:

$C_3H_3 + C_3H_3$ <=> Phenyl + H, $k_o=1.1\cdot10^{15}$ plus inverse falloff, BAC-MP4

and improved kinetics to form, destroy, and isomerize 1,3- and 1,2-butadiene. Predicted profiles were slightly nearer the burner, and the benzene magnitude was too low although the shape and position were much improved.

Future Plans

The ability to solve nonadiabatic energy balances will greatly enhance the value of flat-flame modeling to test and obtain kinetics. The next experiments will be on fuel-lean ethene flames doped with propadiene, allowing more direct study of C_3H_4 and C_3H_3 oxidation kinetics and exploiting the higher sensitivity of the new mass spectrometer. *Ab initio* calculations on the intermediates and whole-flame modeling will give improved oxidation kinetics.

Publications of DOE-sponsored Research, 1998-2000

1. A. Bhargava and P. R. Westmoreland, "Measured Flame Structure and Kinetics in a Fuel-Rich Ethylene Flame," *Combustion and Flame* **113**, 333-347 (1998).
2. A. Bhargava and P. R. Westmoreland, "MBMS Analysis of a Fuel-Lean Ethylene Flame," *Combustion and Flame* **115**, 456-467 (1998).
3. P.-A. Bui, D. G. Vlachos, and P. R. Westmoreland, "On the local stability of multiple solutions and oscillatory dynamics of spatially distributed flames," *Combustion and Flame* **117**, 307-322 (1999).

Investigations of the Reactions and Spectroscopy of Radical Species Relevant to Combustion Reactions and Diagnostics

David R. Yarkony, Department of Chemistry, Johns Hopkins University, Baltimore, MD 21218
e-mail:yarkony@jhuvms.hcf.jhu.edu

Our research employs computational techniques to study spin-nonconserving and spin-conserving electronically nonadiabatic processes involving radical species that are relevant to combustion reactions and combustion diagnostics. Photoexcitation is a key initial step in the detection of combustion intermediates. Thus the ultimate disposition of the excitation energy is an important question in combustion chemistry. A principal thrust of our current research is the nonadiabatic radiationless decay of this excitation, that is internal conversion, induced by conical intersections.

Electronic Structure Algorithms

The vicinity of a conical intersection can be described in terms of four characteristic parameters, which define the two dimensional branching space and the intersection adapted coordinates.[1] While the two dimensional branching space is uniquely defined locally, the intersection adapted coordinates are not. This is a consequence of the degeneracy at the conical intersection which leaves the two electronic wave functions arbitrary up to a one parameter rotation. We have shown this one parameter rotation can be used to guarantee the vectors defining the branching space:

$$2\mathbf{g}^{IJ} = \mathbf{c}^{I\dagger}(\tau_x)\left[\nabla_\tau \mathbf{H}(\tau)\right]c^{I}(\tau_x) - \mathbf{c}^{J\dagger}(\tau_x)\left[\nabla_\tau \mathbf{H}(\tau)\right]c^{J}(\tau_x) \quad \text{and}$$

$$\mathbf{h}^{IJ} = \mathbf{c}^{I\dagger}(\tau_x)\left[\nabla_\tau \mathbf{H}(\tau)\right]\mathbf{c}^{J}(\tau_x)$$

are orthogonal.[2] Here τ are the internal coordinates, τ_x and $(\mathbf{H}-\mathbf{I}E_I)\ \mathbf{c}^I=0$ is the electronic Schrödinger equation in the configuration state function basis. $\mathbf{g}^{IJ}$ and $\mathbf{h}^{IJ}$ chosen in this manner have several advantages over their 'nascent' counterparts in that they:(i) necessarily carry irreducible representations of the point group in question, (ii) reveal any local symmetry that may be responsible for the intersection in question and (iii) assure the continuity of the characteristic parameters along a seam of conical intersection. This later property has been used to advantage in the DoE funded work described below.

Conical Intersections and Molecular Dynamics

(a) $OH(A^2\Sigma^+)+ H_2$ (Ref[3])

The collisonal quenching of $OH(A^2\Sigma^+)$ is a question considerable importance in combustion diagnostics.[4] The electronic quenching of $OH(A^2\Sigma^+)$ by H_2 had previously been the object of a combined experimental/theoretical study[4] that demonstrated that conical intersections of the $1,2^2A'$ states, states correlating with $H_2 + OH(X^2\Pi)$ and $H_2 + OH(A^2\Sigma^+)$, play a role in the quenching process. However that study considered only the C_{2v} portion of the seam of conical intersection for which the states in question have different 1^2A_1, 1^2B_2 symmetry. We showed that C_{2v} and $C_{\infty v}$ seams of conical intersection exist in OH-H_2 and that they are connected by a C_s $1^2A' - 2^2A'$ conical intersection seam. This C_s seam was expected to play a key role in the quenching of $OH(A^2\Sigma^+)$ by H_2.[3]

In a work currently being prepared for submission this analysis has been extended considerably. The role of the C_{2v} ($1\ ^2B_2 - 1\ ^2A_1$), C_s ($1\ ^2A' - 2\ ^2A'$), and $C_{\infty v}$ ($1\ ^2\Pi - 1^2\Sigma^+$) seams of conical intersection in the dynamics of the captioned reaction was investigated in detail. The locus of the C_{2v},

$C_{\infty v}$ conical intersections and the C_s seam bridging them have been re-determined using a more flexible wavefunction and the accessibility of these seams was examined using linear interpolation pathways Transition state searches motivated by the energetics of these pathways indicate that a small barrier, ~ 1.26kcal/mol above the dissociation limit, due primarily to a required rotation of the OH molecule relative to H_2, exists between the Franck-Condon region and the seams. Finally, gradient descent paths from the conical intersections were determined to identify the possible products of the non-adiabatic quenching. For each symmetry distinct portion of the seam, pathways leading to both OH+ H_2 and H_2O + H were found.

(b) $S_1 \rightarrow S_0$ internal conversion in NHCO

The photodissociation of HNCO has the subject of many DoE supported experimental studies. The $S_1 \rightarrow S_0$ internal conversion is first radiatonless step in the reaction sequences

$$HNCO(S_0=X^1A')+h\nu \rightarrow HNCO(S_1={}^1A'') \rightarrow HNCO(S_0) \rightarrow H+NCO(X^2\Pi) \quad (2a)$$

$$HNCO(S_1={}^1A'') \rightarrow HNCO(S_0) \rightarrow HNCO(T_1={}^3A'') \rightarrow HN(X^3\Sigma^-)+CO(X^1\Sigma^+) \quad (2b)$$

This internal conversion is implicated in the production of H + NCO at energies below that of the NH + CO channel and the production of ^{3}NH is thought to occur through the sequence $S_1 \rightarrow S_0 \rightarrow T_1$. At photon energies above the S_1 threshold direct dissociation on S_1 competes with the reactions (2a), (2b). The competition between internal conversion and direct dissociation is an important issue. The outcome of this competition reflects the topography S_1 and the locus of the $S_1 - S_0$ seam of conical intersection at energies, above the S_1 threshold. Knowledge of the energetics and interstate couplings in the vicinity of the seam of conical intersection is essential for a reliable treatment of the nuclear dynamics leading to internal conversion. The characterization of the $S_1 - S_0$ seam of conical intersection, a rather challenging task,[5] is perhaps the only essential feature of these potential energy surfaces that has not been subject to careful theoretical scrutiny.

During the current performance period we determined a significant portion of the S_1 - S_0 seam of conical intersection using MCSCF/CI wavefunctions comprised of ~3.5 x 10^6 CSFs. The energetically relevant portions of the $S_1 - S_0$ seam of conical intersection have been determied as a function of R(N-H) and R(N-C) for both cis and trans configurations of the H and O with respect to the NC bond. The seam as function of R(C-N) and of R(N-H) for cis-HNCO is pictured on the following page.

(c) S_1 to S_0 internal conversion in ketene (Ref. [6])

The photodissociation of ketene

$$H_2CCO(S_0=X^1A_1) + h\nu \rightarrow H_2CCO(S_1={}^1A'') \rightarrow H_2CCO(S_0) \rightarrow$$
$$H_2CCO(T_1={}^3A'') \rightarrow {}^3CH_2 + CO(X^1\Sigma^+) \quad (1)$$

continues to be a problem of significant interest due to the lack of theoretical confirmation of the detailed steplike structure in the rate constant observed in the experiments.[7] This has motivated theoretical studies of the premises of analysis including the neglect of nonadiabatic processes that precede dissociation on T_1.

With this in mind we are currently extending our recent the electronic structure treatment of the internal conversion, $S_1 \rightarrow S_0$.[6] In that work the energy minimized portion of the $S_1(^1A'')$ - $S_0(^1A')$ seam of conical intersection near the minimum energy crossing point was studied as a function of R(CC) and $\angle$CCO and the accessiblity of the seam from the Franck-Condon region of the $S_0 \rightarrow S_1$ photoexcitation

was considered. Barrierless paths exist to $\mathbf{R}_{mex}$ the minimum energy point on the $S_1 - S_0$ seam of conical intersection and to $\mathbf{R}_e(A^1A')$, the equilibrium geometry of S_1 ketene. Following internal conversion onto S_0 near $\mathbf{R}_{mex}$ the gradient directed paths lead to $\mathbf{R}_e(\tilde{X}\ ^1A_1)$, the equilibrium geometry of ground state ketene.

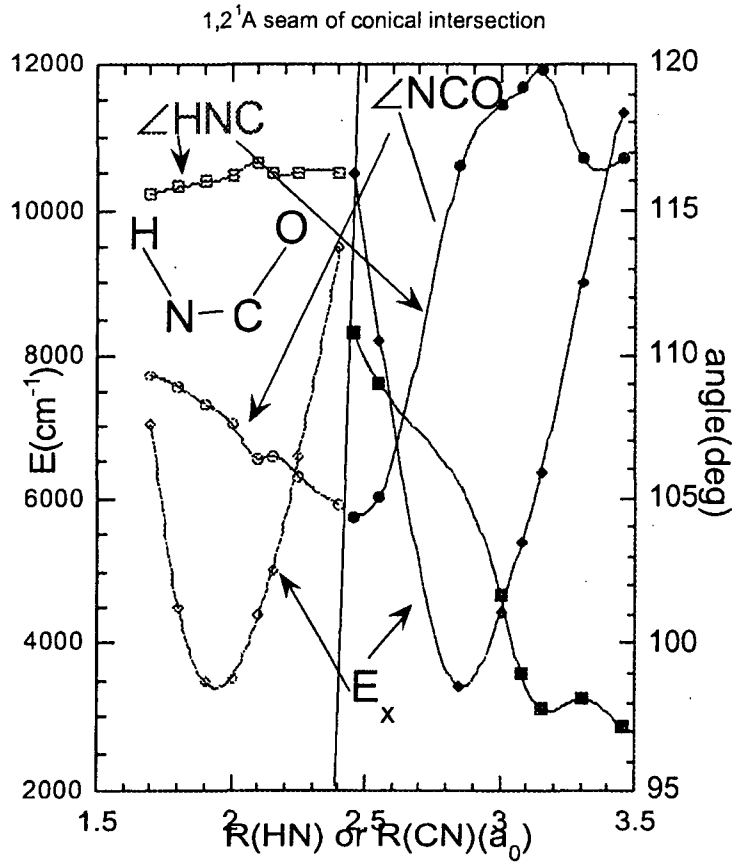

Figure 1: Seam of conical intersection in NHCO. Energies relative to S_1 equilibrium geometry.

Based on this analysis an initial reducecd dimensionality representation of the $1,2^1A$ potential energy surfaces appropriate is being determined based on *ab initio* MCSCF/CI calculations using R(CC) and $\angle CH_3$–C–O as parameters and the remaining internal coordinates chosen to minimize the energy of the 2^1A state.

Future Plans

Perhaps the most exciting aspect of our anticipated research during the coming year will be our effort to combine our expertise in the electronic structure aspects of conical intersections with time dependent dynamics techniques to better understand the way in which conical intersections funnel 'reactants' on the upper surface into the various product channels available on the lower surface. To this end, we have written a program to solve the time dependent Schrodinger equation in the vicinity of a

conical intersection in either the adiabatic or diabatic representations. During the coming year we intend to use this program to consider the product branching in OH+H_2 and HNCO. Subsequently using the insights gained from the wave packet analyses we will develop reduced dimensionality potential energy surfaces for the OH + H_2 and HNCO reactions described above. This work will benefit from that analogous treatment of ketene currently in progress. Dynamics on the reduced dimensionality potential energy surfaces for ketene will be performed in collaboration with H. Köeppel in Heidelberg, Germany

References

(1) G. J. Atchity, S. S. Xantheas, and K. Ruedenberg, *J. Chem. Phys.* **95,** 1862 (1991).
(2) D. R. Yarkony, *J. Chem. Phys.* **112,** 2111-2120 (2000).
(3) D. R. Yarkony, *J. Chem. Phys.* **111,** 6661-6664 (1999).
(4) M. I. Lester, R. A. Loomis, R. L. Schwartz, and S. P. Walch, *J. Phys. Chem. A* **101,** 9195-9206 (1997).
(5) A. L. Kaledin, Q. Cui, M. C. Heaven, and K. Morokuma, *J. Chem. Phys.* **111,** 5004-5016 (1999).
(6) D. R. Yarkony, *J. Phys. Chem. A* **103,** 6658-6668 (1999).
(7) S. K. Kim, E. R. Lovejoy, and C. B. Moore, *Science* **256,** 1541 (1992).

DEPARTMENT of ENERGY SPONSORED PUBLICATIONS 1998-2000

(1) *A compact representation of the energies and derivative couplings and locally diabatic bases for the HOH and OHH portions of the $1^1A'$ - $2^1A'$ seam of conical intersection in water,* David R. Yarkony, Molec. Phys.***93,*** 971-983 (1998)

(2) *Nonadiabatic Derivative Couplings*
D. R. Yarkony, in Encyclopedia of Computational Chemistry, editor-in-chief P. von Ragué Schleyer (John-Wiley, 1998).

(3) *Conical Intersections: Diabolical and Often Misunderstood*
David R. Yarkony, Accounts of Chemical Research, **31**, 511-518 (1998).

(4) *On the mechanism of the spin-nonconserving chemical reaction $O(^3P)$ + HCCH → $CH_2(\tilde{a}\ ^1A_1)$ + $CO(X^1\Sigma^+)$. I. Feasibility*
David R. Yarkony, J. Phys. Chem. A. **102**, 5305-5311(1998)

(5) *A theoretical analysis of the state-specific decomposition of $OH(A^2\Sigma^+, v', N', F1 / F2)$ levels, including the effects of spin-orbit and Coriolis interactions*
Gérard Parlant and David R. Yarkony, *J. Chem. Phys.* **110,** 363-376 (1999).

(6) *On the S_1 - S_0 Internal Conversion in Ketene:I.The Role of Conical Intersections*
David R. Yarkony, J. Phys. Chem. A. **103,** 6658-6668 (1999).

(7). *Diabatic potential curves and avoided crossings for diatomic molecules*
in Theoretical High Resolution Molecular Spectroscopy, editors Per Jensen and Phil Bunker, J. Wiley, 2000, to appear

(8). The geometric phase effect. Perspective on:*Some Recent Developments in the Theory of Molecular Energy Levels*: by H. C. Longuet-Higgins(Advances in Spectroscopy 2, 429-472 (1961)].
David R. Yarkony, Theoretical Chemistry Accounts, **103**, 242-246(2000)

(9) *Substituent effects and the noncrossing rule: The importance of reduced symmetry subspaces. I. The quenching of $OH(A^2\Sigma^+)$ by H_2*
David R. Yarkony , J. Chem. Phys. ***111,*** 6661-6664, (1999).

Laser Studies of the Chemistry and Spectroscopy Of Excited State Hydrocarbons

Timothy S. Zwier
Department of Chemistry
Purdue University
West Lafayette, IN 47907-1393
zwier@purdue.edu

Program Definition/Scope

The goal of this project is to identify and spectroscopically characterize the primary products of reactions of photo-activated molecules such as diacetylene and vinylacetylene with the hydrocarbons present in abundance in sooting flames. The lower energy of the triplet states of these longer-chain hydrocarbons and their comparative longevity toward quenching raises the possibility that they may be involved in the molecular chemistry important in moderate-temperature, sooting flames. The rich chemistry of the triplet states of these molecules also leads to products with unusual structures and unexplored spectroscopy, which we wish to pursue.

We continue to divide our efforts between developing the spectroscopic methods needed to achieve the long-term goals of the project and applying these methods to new reactions of metastable diacetylene (C_4H_2*) and vinylacetylene (C_4H_4*).

Recent Progress

Our studies of metastable diacetylene's chemistry utilize one tunable ultraviolet laser pulse to resonantly excite diacetylene to a singlet state from which intersystem crossing to the triplet manifold produces the metastable state responsible for the ultraviolet photochemistry. The high reactivity of C_4H_2 toward polymerization necessitates the use of a small reaction tube (1 cm long, 2 mm dia.) or constrained expansion in which reaction is initiated by the first UV laser pulse, but is quenched a few microseconds later as the gas mixture expands from the tube or channel into vacuum. VUV photoionization, resonant two-photon ionization/time-of-flight mass spectroscopy, and resonant ion-dip infrared spectroscopy (RIDIRS) have been used to detect, mass-analyze, and spectroscopically characterize the products of the reactions of C_4H_2* with the hydrocarbons of interest.

We have now completed our study of the reaction of metastable diacetylene with benzene and toluene which is complicated by the unusual reactivity of such mixtures. The two dominant primary products of the C_4H_2* reaction with benzene are phenylacetylene ($C_6H_5C_2H$) and phenyldiacetylene ($C_6H_5C_4H$):

$$C_4H_2^* + C_6H_6 \rightarrow C_6H_5C_2H\ (+ C_2H_2) \quad (1a)$$
$$\rightarrow C_6H_5C_4H\ (+ H_2, 2H). \quad (1b)$$

In collaboration with J. Buriak's group at Purdue, we have synthesized a sample of phenyldiacetylene, and recorded its room-temperature ultraviolet absorption spectrum for comparison with the R2PI spectrum of the $C_{10}H_6$ photochemical product. The comparison has enabled a positive identification of $C_{10}H_6$ as phenyldiacetylene.

In the reaction of $C_4H_2^*$ with toluene ($C_6H_5CH_3$), the dominant product channels are:

$$C_4H_2^* + C_6H_5CH_3 \rightarrow C_9H_8\ (+ C_2H_2) \quad (2a)$$
$$\rightarrow C_{11}H_8\ (+ H_2, 2H). \quad (2b)$$

Resonant two-photon ionization scans of the C_9H_8 product proves that a single ethynyltoluene isomer is formed exclusively; namely, the ortho isomer. This is a dramatic example of the highly-specific reaction routes taken by $C_4H_2^*$.

In collaboration with Prof. Lisa Pfefferle's group at Yale University, we have now completed a study of the effects of doping diacetylene and vinylacetylene at 1% concentration into non-premixed methane flames. In this study, the concentrations of species along the centerline of the flame were monitored by sampling the flame directly into the ion source region of a time-of-flight mass spectrometer using 118 nm VUV photoionization. Diacetylene and vinylacetylene produce larger increases in aromatic hydrocarbon concentrations and soot than did propadiene or acetylene. Furthermore, the phenylacetylene to benzene ratios were higher in the diacetylene-doped and vinylacetylene-doped flames than in the others. These observations and profiles of individual hydrocarbons indicate that two pathways in addition to propargyl self-reaction, n-C_4H_3 addition to acetylene and diacetylene, can be important sources of aromatics in flames.

Finally, we have undergone a major restructuring of our laboratory in anticipation of the acquisition of a seeded, Nd:YAG-pumped infrared parametric converter for generating high-power, pulsed tunable infrared for the DOE experiments. This system has recently been installed and initial characterization experiments carried out with it.

Future Plans

We will study the reactions of $C_4H_2^*$ with styrene and phenylacetylene to establish the potential for forming fused aromatic rings in metastable diacetylene's reactions. Anticipated products include aromatics with long side chains, multiple side chains, and possibly fused aromatic rings (naphthalene), like those shown on the next page. In many of these cases, several isomers

(ortho, meta, and para) are possible and will need to be explored. Spectroscopic characterization of these products will proceed first using resonant two-photon ionization to record ultraviolet spectra, and then resonant ion-dip infrared spectroscopy (RIDIRS) to record infrared spectra of the products in the CH stretch and C≡C stretch regions.

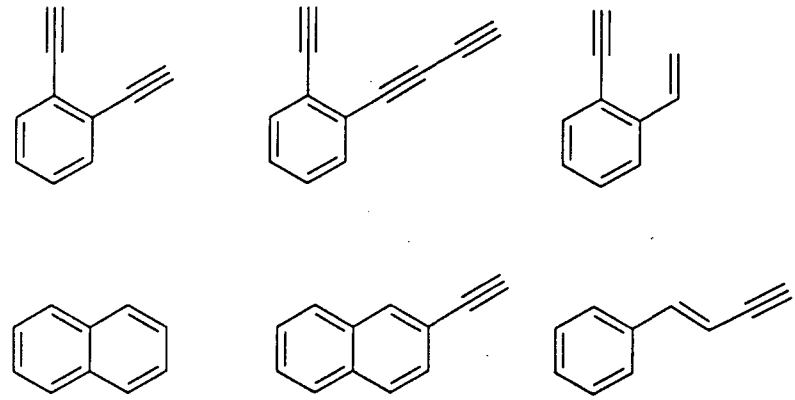

With the newly-installed infrared parametric converter, we hope to apply the method of RIDIRS to several molecular and free radical products. In addition, since so little is known about the triplet states of diacetylene whose chemistry we are studying, we have designed and built a flow cell which can be used for photoacoustic detection of the infrared spectrum of metastable diacetylene. CASPT2 calculations done in collaboration with K.D. Jordan predict that the CH stretch of C_4H_2* is shifted by about 100 cm^{-1} from the ground state frequency. The parametric converter has a resolution of about 0.15 cm^{-1}, which is sufficient to resolve rotational structure for C_4H_2, enabling structural characterization of the triplet state.

Publications acknowledging DOE support, 1998-present

- C.A. Arrington, C. Ramos, A.D. Robinson, and T.S. Zwier, "Aromatic Ring-Forming Reactions of Metastable Diacetylene with 1,3-butadiene", J. Phys. Chem. A **102**, 3315-3322 (1998).
- F.C. Hagemeister, C.A. Arrington, B.J. Giles, B. Quimpo, L. Zhang, and T.S. Zwier, "Cavity ringdown methods for studying intramolecular and intermolecular dynamics", chapter in "Cavity ring-down spectroscopy – An Ultratrace-Absorption Measurement Technique", ed. K.S. Busch and M.A. Busch, ACS Symposium Series 720, Chap. 14, pp. 210-232 (1999).
- C.A. Arrington, C. Ramos, A.D. Robinson, and T.S. Zwier, "The ultraviolet photochemistry of diacetylene with alkynes and alkenes: Spectroscopic characterization of the products", J. Phys. Chem. **103**, 1294-1299 (1999).

Electronic Structure, Molecular Bonding and Potential Energy Surfaces

Klaus Ruedenberg
Ames Laboratory USDOE, Iowa State University, Ames, Iowa, 50011
ruedenberg@iastate.edu

Scope

Potential energy surfaces provide the unifying conceptual basis as well as the essential quantitative constructs for understanding adiabatic as well as non-adiabatic physico-chemical processes. This group's work is focused on basic potential energy surface properties and their electronic origins, in particular for molecular systems involved in combustion reactions. Through quantum theoretical methods including electron correlations, electronic structures are determined for oxy- and hydroxy-compounds of carbon, nitrogen and sulfur and electronic structure changes are elucidated along reaction paths on potential energy surfaces. Ab-initio methods are developed for the analysis and interpretation of the attendant bonding pattern changes in terms of interactions between atoms in molecules.

Recent Results

The determination of energetic changes on reaction paths is an important quantum chemical goal. Along most such paths, molecular electronic wavefunctions undergo significant, often drastic changes in the mix of the *essential* configurations so that, in the transition-state regions, multi-configurational representations, describing non-dynamical correlations, are called for in zeroth-order. The optimal determination of such zeroth-order multi-configurational wavefunctions requires MCSCF calculations onto which higher-order dynamical corrections of various types can then be grafted. This approach is the only one to preserve the *variational* character of the quantitative results as far as possible beyond the SCF stage and it therefore deserves to be thoroughly pursued. Open questions have remained regarding the most appropriate *configuration* selection for the zeroth-order stage and the most appropriate *orbital* choice for the higher order stage, both with the objective of most effectively achieving size-consistent chemical accuracy. Progress on these problems is made by our current developments.

Various zeroth-order configuration spaces have been examined regarding their ability to accurately recover the binding energy. FORS 1 is the full configuration space generated by as many orbitals as there are formal atomic SCF valence orbitals. FORS 2 is the full configuration space generated by twice as many orbitals as there are valence electrons. FORS 3 is the full space generated by as many orbitals as there are in the first atomic correlation shells. In each case, the reduction of the configuration space size with respect to the degree of excitations as well as electron hopping needed is explored so that larger systems can be treated. Transformation of the zeroth-order configuration expansions to quasi-atomic configuration bases furthermore yields expressions in terms of MCSCF molecular orbitals that have quasiatomic character, including directed hybrid orbitals with localized bonding interactions. The most effective orbital choice outside the zeroth-order space has also being analyzed.

The capability of executing such investigations has been contingent on the formal development and computer implementation of new, fast and robust configuration interaction and multi-configuration-self-consistent-field methods and algorithms that can deal efficiently with large configuration spaces as well as arbitrary configuration selections. A new direct determinant-based CI method has been formulated and implemented for full as well as arbitrary configuration expansions. It has been coupled to a new orbital optimization procedure that is based on sequential Jacobi rotation optimizations rather than Newton- Raphson-type iterations.

The described method is currently applied to O, OH, H_2O, HNO. It is planned to complete and refine it and to consolidate it in a production code. It will be used for oxidation reactions of carbon and hydrogen compounds. A cooperative application to surface reactions relevant to catalysis is also underway.

Publications 1998, 1999, 2000

Robert S. Hansen, the Second Director of the Ames Laboratory USDOE
K. Ruedenberg,
Golden Alumni, Chemistry Department, Iowa State University, March 1999.

A Local Understanding of the Quantum Chemical Geometric Phase Theorem.
G. J. Atchity and K. Ruedenberg
J. Chem. Phys., **110**, 4208-4212 (1999)

Orbital Transformations and Configurational Transformations of Electronic Wave Functions
G. J. Atchity and Klaus Ruedenberg
H. J.Chem.Phys., **111**, 2910-2920 (1999)

Direct Recurrence Relations for the Rapid and Stable Determination of Rotation Matrices between Spherical Harmonics
Cheol Ho Choi, Joseph Ivanic, Mark S. Gordon, Klaus Ruedenberg
J. Chem. Phys., submitted

Oriented Atoms Least Squares. I. Equations and Methodology
L Miller, R. A. Jacobson, K. Ruedenberg, J. E. Niu, W. H. E. Schwarz
Acta Crystallogeaohica, submitted

Reactions of Small Molecular Systems

Curt Wittig
Department of Chemistry
University of Southern California
Los Angeles, CA 90089-0482
wittig@chem1.usc.edu

Program Scope

The focus of our program is reaction mechanisms of species that display phenomena which are relevant to combustion chemistry. We have examined numerous small polyatomics by using the high-n Rydberg time-of-flight (HRTOF) method to probe H atom products of elementary reactions. Recently we began employing double resonance in conjunction with HRTOF. We had carried out several studies using double resonance, so this method was not new to us. However, these earlier studies were concerned solely with the photodissociation of small molecules.

It has been a goal of ours to examine long-range interactions in chemical systems. This is a frontier area for theory and experiment. For radical-radical and radical-molecule systems, long-range interactions contain contributions from several PES's which become degenerate at large separation. The van der Waals well depths are comparable to spin-orbit energies (both of which are comparable to collision energies), and the role of anisotropy is subtle and hard to assess.

In principle, it is possible to probe long range interactions by using weakly bound precursors. We used this strategy previously, but the focus was on a unique form of hot hydrogen atom chemistry. Progress was limited by higher-than-binary clusters. Two years ago we extended the technique to the regime of chemical systems that are sensitive to the long range part of the potential. The idea was to probe the long-range region of Cl-HCl. There are three PES's due to the Cl spin-orbit levels in combination with the anistropic electrostatic interaction.

To implement double resonance (DR) a laser source was stabilized at the transitions of species that are present in low concentrations and are not chemically stable. This problem exists when carrying out DR studies of radicals, clusters, excited states, etc. In the present experiments overtones are probed in a molecular beam. Such experiments and their extensions may result in a new era of detailed studies. The work has been published, so only a brief overview is given here. Following this, our current studies with water are described.

The strategy is given in Fig. 1. HCl dimer is excited to first overtone ($2\nu_1$) levels of the free HCl. Subsequently, 193 nm radiation dissociates the tagged bond. Excited dimers also undergo vibrational predissociation, resulting in correlated product state distributions of the monomer pairs. This is expected to occur with low (acceptor) and high (donor) rotational excitation. The $2\nu_1$ predissociation lifetime is $\geq$ 3 ns, based on linewidth. Both tagged dimers and internally excited monomers produced via predissociation can be photolyzed. By varying the IR-UV delay, it is possible to separate these contributions. A cavity ringdown spectrometer was integrated into the setup to locate dimer transitions (Fig. 2). Jet-cooled dimers were generated in a pulsed expansion. Tunable IR radiation (20 mJ at 1.77 μm) was produced in an OPO capable of long-term locking to a single mode.

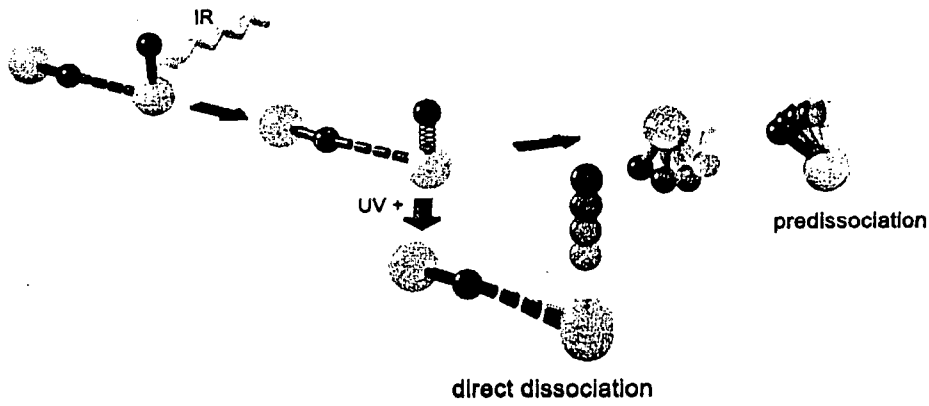

Figure 1. An IR photon excites the free HCl bond, thereby tagging the cluster. The upper pathway shows predissociation; the donor HCl is expected to acquire more angular momentum than the acceptor. The other pathway is UV photodissociation of the tagged dimer; the H atom leaves behind the Cl-HCl complex.

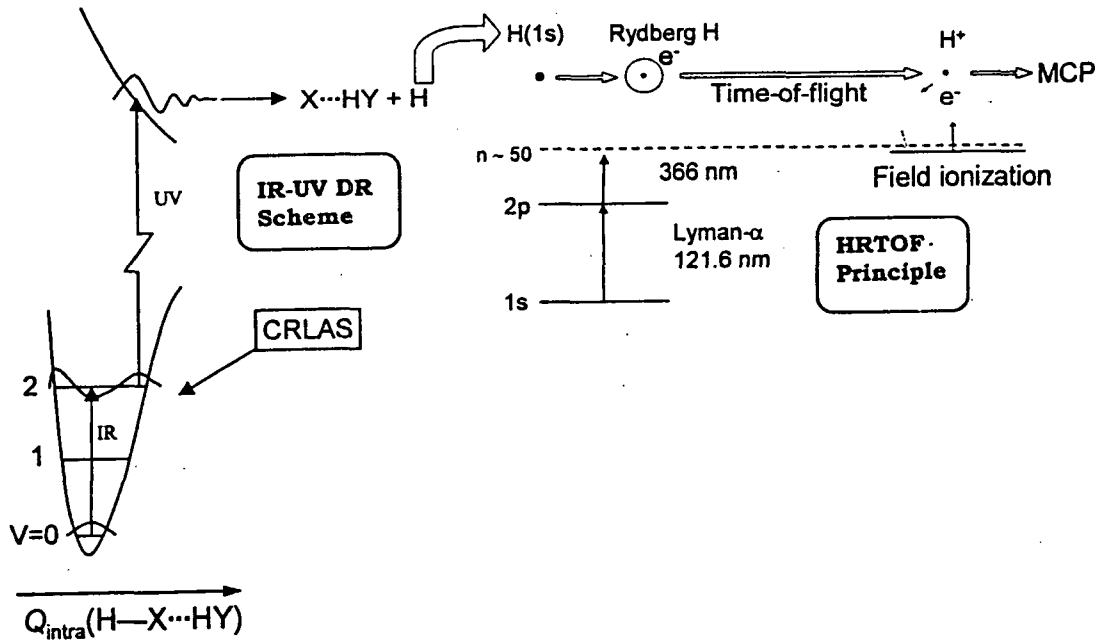

Figure 2. Cavity ringdown (left) and HRTOF (right) are combined.

Photodissociation was done with an ArF laser, and two other beams (121.6 and 366 nm) excited H atoms to high-n Rydberg states. For double resonance, data were collected with the IR alternately on and off. Figure 3 shows translational energy distributions; the upper traces show the UV pulse delayed 10 and 70 ns relative to the IR pulse.

The signal at 70 ns delay derives mainly from predissociated monomer pairs, while the short delay data contain contributions from both direct and predissociation channels. We do not know the predissociation lifetime (τ_{PD}) of the dimer at the first overtone of free HCl. However, on the basis of studies of the vibrational dependence of the predissociation lifetime in $(HF)_2$ and the predissociation of $(HCl)_2$ at the free fundamental ($\tau_{PD} \geq 100$ ns), we assume that the lifetime is < 100 ns. The peaks in the signal lie at energies which cor-

respond to highly excited HCl. For example, the two highest-energy peaks differ by the energy difference between J = 20 and 21 of HCl(v = 0). In the present case, two quanta in the free HCl are transferred to internal excitation of one of the recoiling monomers (presumably the donor) upon predissociation. We are currently attempting to explain this surprising observation.

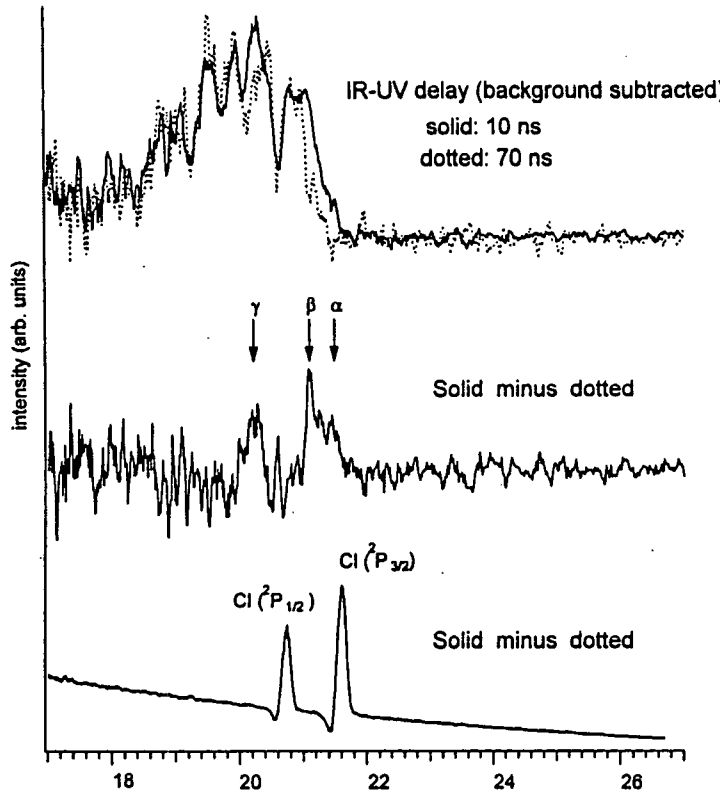

Figure 3 (left): CM translational energy distributions (10^3 cm^{-1}); UV is delayed relative to IR by 10 and 70 ns. Photodissociation of tagged dimers is identified by subtracting the 70 and 10 ns traces; The lower trace shows $Cl(^2P_{3/2})$ and $Cl(^2P_{1/2})$ deriving from photodissociation of overtone-excited HCl monomer.

Signals from $(HCl)_2^{\dagger} + h\nu_{UV} \rightarrow H + Cl\text{-}HCl$ can be obtained from differences between DR spectra taken at short and long delays. Such a contribution is identified in the difference spectrum. The lower entry displays the spectrum of $H^{35}Cl$ monomer tagged by the first overtone $R(0)$ transition.

The departing H atom carries information about Cl-HCl. This complex does not undergo significant decomposition on the rapid timescale characteristic of H-atom removal. At low resolution, one can expect to see the Cl-atom spin-orbit levels, whereas with better resolution, the PES's of the Cl-HCl system will be reflected. Note that rapid H-atom removal creates a coherent superposition of electronic and vibrational levels of the Cl-HCl complex. At even higher resolution, it may be possible to resolve vibrational structure and widths arising from Cl-HCl decomposition.

The trace shown in Fig. 3, despite low S/N, reflects the PES's of Cl-HCl. The main features are associated with the Cl spin-orbit levels; they are broader than those associated

with photodissociatiion of unclustered HCl. We believe this broadening is due to Cl-HCl vibrational and electronic excitations; it is present at all levels of signal averaging.

Resolution is limited by the excimer linewidth, as seen in the monomer widths. However, dimer features are broader. This is believed to reflect the fact that the free HCl bond dissociates with a range of recoil angles relative to the intermolecular axis with probabilities as per the squares of the acceptor bending wavefunction, producing Cl-HCl complexes with a range of internal excitations. With improved resolution and S/N, one might observe vibrational structure, providing a stringent test of the PES's.

Current Work

Following the above studies of the HCl dimer, we have initiated a long-term program focused on water — its intramolecular dynamics and unimolecular decomposition on the ground PES. The strategy is to use overtone-combination band excitation to promote the system to the region from just below to just above D_0. This system is amenable to a high level of theory and can serve as a benchmark against which calculations can be judged. As a warm-up experiment, the OPO system was tuned to the (011) ← (000) combination band and the excited molecules were photodissociated at 193 nm. The S/N was good, showing the distribution of OH rotational levels. Theory matches experiment very well (A. McCoy, unpublished). Next, we plan to use $4 \leftarrow 0$ or $5 \leftarrow 0$ local mode excitation and then move to higher energies by pumping $10 \leftarrow 4$, $11 \leftarrow 5$ and other high overtones (and combination bands). It is expected that the S/N will be good for $4 \leftarrow 0$ and $5 \leftarrow 0$, in fact better than the case of (011) ← (000). Major challenges will arise in trying to reach energies near D_0.

DOE Publications: 1997 – Present

1. HCO rotational excitation in the photoinitiated unimolecular decomposition of H_2CO, M.J. Dulligan, M.F. Tuchler, J. Zhang, A. Kolessov and C. Wittig, Chem. Phys. Lett. 276, 84 (1997).
2. Photodissociation of HCl at 193.3 nm: spin-orbit branching ratio,J. Zhang, M. Dulligan and C. Wittig, J. Chem. Phys. 107, 1403 (1997).
3. Quenching of interconversion tunneling: The free HCl stretch first overtone of $(HCl)_2$, K. Liu, M. Dulligan, I. Bezel, S. Kolessov, C. Wittig, J. Chem. Phys. 108, 9614 (1998).
4. Probing the Cl-HCl Complex via Bond-Specific Photodissociation of $(HCl)_2$, K. Liu, A. Kolessov, J.W. Partin, I. Bezel and C. Wittig, Chem. Phys. Lett. 299, 374 (1999).
5. Photoinitiated H_2CO unimolecular decomposition: accessing H + HCO products via S_0 and T_1 pathways, L.R. Valachovic, M.F. Tuchler, M. Dulligan, Th. Droz-Georget, M. Zyrianov, A. Kolessov, H. Reisler and C. Wittig, J. Chem. Phys. 112, 2752 (2000).
6. Highly Specific Rotational Excitations in the Vibrational Predissociation of HCl Dimer, A. Kolessov and C. Wittig, unpublished.

List of Conference Participants

Conference Participants

Dr. William T. Ashurst
Combustion Research Facility
MS9051
Sandia National Laboratories
Livermore, California 94551-0969
Phone: 925.294.2274
ashurs@ca.sandia.gov

Prof. Tomas Baer
Department of Chemistry
University of North Carolina
Chapel Hill, North Carolina 27599-3290
Phone: 919.962.1580
baer@unc.edu

Dr. Robert S. Barlow
Combustion Research Facility
MS9051
Sandia National Laboratories
Livermore, California 94551-0969
Phone: 925.294.2688
barlow@ca.sandia.gov

Prof. Richard Bersohn
Department of Chemistry
Columbia University
116th Street and Broadway
New York, New York 10027
Phone: (212)854-2192
rb18@columbia.edu

Prof. Joel M. Bowman
Department of Chemistry
Emory University
1515 Pierce Drive
Atlanta, Georgia 30322
Phone: (404)727-6590
bowman@euch3g.chem.emory.edu

Prof. C. Thomas Bowman
Department of Mechanical Engineering
Stanford University
Stanford, California 94305
Phone: 650.723.1745
bowman@navier.stanford.edu

Professor Kenneth Brezinsky
Chemical Engineering Dept.
810 S. Clinton
The University of Illinois at Chicago
Chicago, Illinois 60607-7022
Phone: (312)996-9430
kenbrez@uic.edu

Dr. Nancy Brown
Energy and Environment Division
Lawrence Berkeley Laboratory
One Cyclotron Road
Berkeley, California 94720
Phone: (510)486-4241
njbrown@lbl.gov

Prof. Laurie J. Butler
The James Franck Institute
The University of Chicago
5640 S. Ellis Avenue
Chicago, Illinois 60637
Phone: 773.702.7206
ljb4@midway.uchicago.edu

Prof. Barry K. Carpenter
Department of Chemistry
Cornell University
Ithaca, NY 14853-1301
Phone: (607)255-3826
bkc1@cornell.edu

Dr. David W. Chandler
Combustion Research Facility
MS 9055
Sandia National Laboratories
Livermore, California 94551-0969
Phone: 925.294.2091
chandler@ca.sandia.gov

Dr. Jacqueline H. Chen
Combustion Research Facility
MS9051
Sandia National Laboratories
Livermore, California 94551-0969
Phone: 925.294.2586
jhchen@sandia.gov

Dr. Robert K. Cheng
Energy and Environment Division
University of California
Lawrence Berkeley Laboratory
One Cyclotron Road
Berkeley, California 94720
Phone: 510.486.5438
rkcheng@lbl.gov

Dr. Andrew V.G. Chizmeshya
Center for Solid State Science
Arizona State University
Tempe, Arizona 85287-1704
chizmesh@asu.edu

Prof. Jerzy Cioslowski
Supercomputer Comp. Res. Inst.
406 Science Center Library
Florida State University
Tallahassee, Florida 32306-4052
Phone: (904)644-4885
jerzy@scri.fsu.edu

Prof. Philip Colella
Department of Mechanical Engineering
University of California, Berkeley
Berkeley, California 97420
Phone: (510)642-2652
pcolella@euler.me.berkeley.edu

Prof. Robert E. Continetti
Department of Chemistry, 0314
University of California, San Diego
9500 Gilman Drive
La Jolla, CA 92093-0314
Phone: (619)534-5559
rcontinetti@ucsd.edu

Prof. F. Fleming Crim
Department of Chemistry
University of Wisconsin
1101 University Avenue
Madison, Wisconsin 53706
Phone: (608)263-7364
fcrim@chem.wisc.edu

Prof. Robert F. Curl, Jr.
Department of Chemistry
Rice University
P.O. Box 1892
Houston, Texas 77251
Phone: (713)527-4816
rfcurl@rice.edu

Prof. Hai-Lung Dai
Department of Chemistry
University of Pennsylvania
Philadelphia, Pennsylvania 19104
Phone: 215.898.2033
dai@a.chem.upenn.edu

Dr. Michael Davis
Chemistry Division
Argonne National Laboratory
9700 South Cass Avenue
Argonne, Illinois 60439
Phone: 630.252.4802
davis@tcg.anl.gov

Dr. Anthony M. Dean
Exxon Research & Engineering Co.
Clinton Township, Route 22 East
Annandale, NJ 08801
Phone: 908.730.2727
amdean@erenj.com

Dr. Michael C. Drake
Physical Chemistry Department
General Motors R&D and Planning
Box 9055
Warren, Michigan 48090-9055
Phone: 810.986.1320
mdrake@gmr.com

Prof. Frederick L. Dryer
Department of Mechanical & Aerospace Engineering
Princeton University
Princeton, New Jersey 08544
Phone: (609)258-5206
fldryer@princeton.edu

Prof. G. Barney Ellison
Department of Chemistry
University of Colorado
Boulder, Colorado 80309
Phone: 303.492.8603
barney@jila.Colorado.EDU

Prof. Kent M. Ervin
Department of Chemistry/216
College of Arts and Sciences
University of Nevada, Reno
Reno, Nevada 89557-0020
Phone: 775.784.6676
ervin@chem.unr.edu

Prof. James M. Farrar
Department of Chemistry
University of Rochester
Rochester, New York 14627
Phone: 716.275.5834
farrar@chem.rochester.edu

Dr. Roger Farrow
Combustion Research Facility
MS 9055
Sandia National Laboratories
Livermore, California 94551-0969
Phone: 925.294.3259
farrow@sandia.gov

Prof. Robert W. Field
Department of Chemistry
Massachusetts Institute of Technology
18-390 Massachusetts Ave.
Cambridge, Massachusetts 02139
Phone: 617.253.1489
rwfield@mit.edu

Prof. George Flynn
Department of Chemistry
Mail Stop 3109
Columbia University
3000 Broadway
New York, New York 10027
Phone: (212)854-4162
flynn@chem.columbia.edu

Dr. Christopher Fockenberg
Chemistry Department
Brookhaven National Laboratory
Upton, NY 11973-5000
Phone: 631.344.4372
fknberg@bnl.gov

Dr. Jonathan H. Frank
Combustion Research Facility
MS 9051
Sandia National Laboratories
Livermore, California 94551
jhfrank@ca.sandia.gov

Prof. Michael Frenklach
Department of Mechanical Engineering
Lawrence Berkeley Laboratory
University of California at Berkeley
Berkeley, California 94720-1740
Phone: (510)643-1676
myf@me.berekley.edu

Prof. Graham P. Glass
Department of Chemistry
Rice University
P.O. Box 1892
Houston, Texas 77251
Phone: 713.737.5683
gglass@rice.edu

Dr. Philip M. Goldberg
National Energy Technology Laboratory
P.O. Box 10940
U.S. Department of Energy
626 Cochrans Mill Road
Pittsburgh, Pennsylvania 15236-0940
Phone: 412.386.5806
goldberg@netl.doe.gov

Prof. Edward R. Grant
Department of Chemistry
Purdue University
West Lafayette, Indiana 47907
Phone: (765)494-9006
egrant@chem.purdue.edu

Dr. Stephen K. Gray
Chemistry Division
Argonne National Laboratory
9700 South Cass Ave.
Argonne, Illinois 60439
Phone: 630.252.3594
gray@tcg.anl.gov

Prof. William H. Green, Jr.
Department of Chemical Engineering
66-448
Massachusetts Institute of Technology
77 Massachusetts Ave.
Cambridge, Massachusetts 02139
Phone: 617.253.4580
whgreen@mit.edu

Prof. Christopher M. Hadad
Department of Chemistry
Ohio State University
120 West 18th Avenue
Columbus, Ohio 43210
Phone: 614.688.3141
hadad.1@osu.edu

Dr. Gregory E. Hall
Chemistry Department
Brookhaven National Laboratory
Upton, New York 11973
Phone: 631.344.4376
g_hall@bnl.gov

Prof. Ronald K. Hanson
Department of Mechanical Engineering
Stanford University
Stanford, California 94305
Phone: 650.723.4023
hanson@cdr.stanford.edu

Dr. Lawrence Harding
Chemistry Division
Argonne National Laboratory
9700 South Cass Avenue
Argonne, Illinois 60439
Phone: (630)252-3591
harding@tcg.anl.gov

Dr. Carl C. Hayden
Combustion Research Facility
MS 9055
Sandia National Laboratories
Livermore, California 94551-0969
Phone: 925.294.2298
cchayde@sandia.gov

Prof. Martin Head-Gordon
Department of Chemistry
University of California at Berkeley
Berkeley, California 94720
Phone: 510.642.5957
mhg@bastille.cchem.berkeley.edu

Prof. John Hershberger
Department of Chemistry
North Dakota State University
Fargo, ND 58105-5516
Phone: (701)237-8225
hershber@prairie.nodak.edu

Dr. Jan P. Hessler
Chemistry Division
Argonne National Laboratory
9700 South Cass Avenue
Argonne, Illinois 60439
Phone: (630)252-3717
hessler@anl.gov

Prof. Paul L. Houston
Department of Chemistry
122 Baker Laboratory
Cornell University
Ithaca, New York 14853-1301
Phone: 607.255.4175
plh2@cornell.edu

Prof. Jack B. Howard
Department of Chemical Engineering
Massachusetts Institute of Technology
Cambridge, Massachusetts 02139
Phone: (617)253-4574
jbhoward@mit.edu

Prof. Robert Hurt
Division of Engineering, Box D
Brown University
182 Hope Street
Providence, RI 02912
Phone: (401)863-2685
robert_hurt@brown.edu

Dr. Karl Irikura
Physical and Chemical Properties Division
Natl. Inst. of Stds. and Tech. 8380
100 Bureau Drive
Gaithersburg, MD 20899-8380
Phone: 301.975.2510
karl.irikura@nist.gov

Prof. Philip M. Johnson
Department of Chemistry
State University of New York
at Stony Brook
Stony Brook, New York 11794
Phone: (631)632-7912
Philip.Johnson@sunysb.edu

Prof. Michael E. Kellman
Department of Chemistry
University of Oregon
Eugene, Oregon 97403
Phone: 541.346.4196
kellman@oregon.uoregon.edu

Prof. R. D. Kern, Jr.
Department of Chemistry
University of New Orleans
New Orleans, LA 70148
Phone: (504)280-6847
rdkern@uno.edu

Dr. Alan R. Kerstein
Combustion Research Facility
MS9051
Sandia National Laboratories
Livermore, California 94551-0969
Phone: 925.294.2390
arkerst@sandia.gov

Prof. John Kiefer
Department of Chemical Engineering
University of Illinois at Chicago
Chicago, Illinois 60607
Phone: (312) 996-571
john.h.kiefer@uic.edu

Dr. William H. Kirchhoff
Fundamental Interactions Branch, ER-141
Chemical Sciences Division
Office of Basic Energy Sciences
U.S. Department of Energy
19901 Germantown Road
Germantown MD 20874-1290
Phone: (301)903-5809
william.kirchhoff@oer.doe.gov

Dr. Dahv A. V. Kliner
Combustion Research Facility
MS 9051
Sandia National Laboratories
Livermore, California 94551-0969
Phone: 925.294.2821
dakline@sandia.gov

Prof. Stephen J. Klippenstein
Department of Chemistry
Case Western Reserve University
Cleveland, Ohio 44106-7078
Phone: (216)368-6916
sjk5@po.cwru.edu

Prof. Stephen R. Leone
Department of Chemistry
University of Colorado
Campus Box 215
Boulder, Colorado 80309
Phone: (303)492-5128
srl@jila.colorado.edu

Prof. Marsha I. Lester
Department of Chemistry
University of Pennsylvania
231 South 34th Street
Philadelphia, Pennsylvania 19104-6323
Phone: (215)898-4640
lester@a.chem.upenn.edu

Prof. William A. Lester, Jr.
Department of Chemistry
University of California at Berkeley
Berkeley, California 94720
Phone: 510.643.9590
walester@cchem.berkeley.edu

Prof. John C. Light
The James Franck Institute
The University of Chicago
5640 S. Ellis Avenue
Chicago, Illinois 60637
Phone: 773.702.7197
light@pclight.uchicago.edu

Prof. Ming-Chang Lin
Department of Chemistry
Emory University
1515 Pierce Drive
Atlanta, Georgia 30322
Phone: (404)727-2825
chemmcl@emory.edu

Prof. Marshall B. Long
Department of Mechanical Engineering
Yale University
P.O. Box 208284
New Haven, Connecticut 06520-8284
Phone: 203.432.4229
long-marshall@yale.edu

Prof. Robert P. Lucht
Department of Mechanical Engineering
315 Engineering/Physics Building
Texas A&M University
College Station, TX 77843-3123
Phone: 409.862.2623
rlucht@mengr.tamu.edu

Dr. R. Glen Macdonald
Chemistry Division
Argonne National Laboratory
9700 South Cass Avenue
Argonne, Illinois 60439
Phone: (630)252-7742
macdonald@anlchm.chm.anl.gov

Dr. Michael J. McKelvy
Center for Solid State Science
Arizona State University
Tempe, Arizona 85287-1704
mckelvy@asu.edu

Dr. Andrew Mcilroy
Combustion Research Facility
MS 9055
Sandia National Laboratories
Livermore, California 94551-0969
Phone: 925.294.3054
amcilr@sandia.gov

Dr. Joe V. Michael
Chemistry Division
Argonne National Laboratory
9700 South Cass Avenue
Argonne, Illinois 60439
Phone: (630)252-3171
michael@anlchm.chm.anl.gov

Prof. William H. Miller
Department of Chemistry
University of California at Berkeley
Berkeley, California 94720
Phone: (510)642-0653
miller@neon.cchem.berkeley.edu

Dr. James A. Miller
Combustion Research Facility
MS-9055
Sandia National Laboratories
Livermore, California 94551-0969
Phone: 925.294.2759
jamille@sandia.gov

Dr. David Moncrieff
Supercomputer Comp. Res. Inst.
496 Science Center Library
Florida State University
Tallahassee, Florida 32306-4130
Phone: 850.644.4885
moncrieff@csit.fsu.edu

Prof. C. Bradley Moore
Department of Chemistry
University of California at Berkeley
Berkeley, California 94720
Phone: 510.642.3453
cbmoore@socrates.berkeley.edu

Dr. James Muckerman
Chemistry Department
Brookhaven National Laboratory
Upton, NY 11973
Phone: 631.344.4368
muckerma@bnl.gov

Dr. Habib Najm
Combustion Research Facility
MS9051
Sandia National Laboratories
Livermore, California 94551-0969
Phone: 925.294.2054
hnnajm@ca.sandia.gov

Prof. Daniel M. Neumark
Department of Chemistry
University of California at Berkeley
Berkeley, California 94720
Phone: 510.642.3502
neumark@cchem.berkeley.edu

Prof. Cheuk-Yiu Ng
Department of Chemistry
Iowa State University
Ames, Iowa 50011
Phone: (515)294-4225
cyng@ameslab.gov

Dr. David L. Osborn
Combustion Research Facility
MS 9055
Sandia National Laboratories
Livermore, California 94551-0969
Phone: 925-294-4622
dlosbor@sandia.gov

Dr. Phillip H. Paul
Combustion Research Facility
MS-9051
Sandia National Laboratories
Livermore, California 94551-0609
Phone: 925.294.1465
phpaul@sandia.gov

Prof. David S. Perry
Department of Chemistry
University of Akron
Akron, Ohio 44325
Phone: 330.972.6825
dperry@uakron.edu

Prof. Robert W. Pitz
Department of Mechanical Engineering
Vanderbilt University
Box 1592, Station B
Nashville, Tennessee 37235
Phone: 615.322.2950
pitzrw@vuse.vanderbilt.edu

Dr. William J. Pitz
Lawrence Livermore National Laboratory
P. O. Box 808
Livermore, California 94550
Phone: 925.422.7730
pitz@llnl.gov

Prof. Stephen B. Pope
Department of Mechanical and Aerospace Engineering
Cornell University
106 Upson Hall
Ithaca, New York 14853
Phone: (607)255-4314
pope@mae.cornell.edu

Dr. Stephen Pratt
Chemistry Division
Argonne National Laboratory
9700 South Cass Avenue
Argonne, Illinois 60439
Phone: 630.252.4199
stpratt@anl.gov

Dr. Jack M. Preses
Chemistry Department
Brookhaven National Laboratory
Upton, New York 11973
Phone: 631.344.4371
preses@bnl.gov

Prof. Herschel A. Rabitz
Department of Chemistry
Princeton University
Princeton, New Jersey 08544
Phone: (609)258-3917
hrabitz@chemvax.princeton.edu

Dr. Larry A. Rahn
Combustion Research Facility
MS 9056
Sandia National Laboratories
Livermore, California 94551-0969
Phone: 925.294.2091
rahn@sandia.gov

Prof. Hanna Reisler
Department of Chemistry
University of Southern California
Los Angeles, California 90089-0482
Phone: (213)740-7071
reisler@chem1.usc.edu

Prof. Klaus Ruedenberg
Department of Chemistry
Iowa State University of Science and Technology
Ames, Iowa 50011
Phone: (515)294-5253
ruedenberg@iastate.edu

Dr. Branko Ruscic
Chemistry Division
Argonne National Laboratory
9700 South Cass Avenue
Argonne, Illinois 60439
Phone: 630.252.4079
ruscic@anl.gov

Prof. Henry Frederick Schaefer III
Department of Chemistry
University of Georgia
Athens, Georgia 30602
Phone: (706)542-2067
hfsiii@uga.cc.uga.edu

Prof. George Schatz
Department of Chemistry
Northwestern University
2145 Sheridan Road
Evanston, Illinois 60201
Phone: 847.491.5657
g-schatz@nwu.edu

Dr. Trevor Sears
Chemistry Department
Brookhaven National Laboratory
Upton, New York 11973
Phone: 631.344.4374
sears@bnl.gov

Dr. Ron Shepard
Chemistry Division
Argonne National Laboratory
9700 South Cass Avenue
Argonne, Illinois 60439
Phone: 708.252.3584
shepard@tcg.anl.gov

Prof. Volker Sick
2023 Automotive Laboratory
Department of Mechanical Engineering
and Applied Mechanics
University of Michigan
1231 Beall Avenue
Ann Arbor, Michigan 48109-2121
Phone: 734.647.9607
vsick@umich.edu

Prof. Robert Silbey
Department of Chemistry
Massachusetts Institute of Technology
Cambridge, Massachusetts 02139
Phone: 617.253.1470
silbey@mit.edu

Prof. Irene Slagle
Department of Chemistry
The Catholic University of America
Michigan Avenue at 7th Street, N.E.
Washington, D.C. 20064
Phone: (202)319-5384

Prof. Mitchell Smooke
Department of Mechanical Engineering
Yale University
P.O. Box 208284
New Haven, Connecticut 06520-8284
Phone: (203)432-4344
mitchell.smooke@yale.edu

Dr. Arthur G. Suits
Mailstop 6-2100
Chemical Sciences Division
Lawrence Berkeley Laboratory
University of California
Berkeley, California 94720
Phone: 510.486.4754
agsuits@lbl.gov

Dr. Craig Taatjes
Combustion Research Facility
MS 9055
Sandia National Laboratories
Livermore, California 94551-0969
Phone: 925.294.2764
cataatj@california.sandia.gov

Prof. Lawrence Talbot
Department of Mechanical Engineering
6173 Etcheverry Hall
University of California, Berkeley
Berkeley, California 94720-1740
Phone: 510.642.6780
talbot@me.berkeley.edu

Prof. Howard S. Taylor
Department of Chemistry
University of Southern California
Los Angeles, California
Phone: 213.932.1624
taylor@chem1.usc.edu

Prof. Donald G. Truhlar
Department of Chemistry
139 Smith Hall
University of Minnesota
207 Pleasant St. SE
Minneapolis, Minnesota 55455
Phone: (612)624-7555
truhlar@chem.umn.edu

Dr. Wing Tsang
Chemical Kinetics Division
Center for Chemical Technology
A147 Chemistry Building
Natl. Inst. of Standards and Technology
Gaithersburg, Maryland 20899
Phone: (301)975-2507
wtsang@enh.nist.gov

Dr. Frank P. Tully
Combustion Research Facility
Sandia National Laboratories
Livermore, California 94551-0969
Phone: 925.294.2316
tully@sandia.gov

Prof. James J. Valentini
Department of Chemistry
Columbia University
116th Street and Broadway
New York, New York 10027
Phone: (212)854-7590
jjv1@chem.columbia.edu

Dr. Albert F. Wagner
Chemistry Division
Argonne National Laboratory
9700 South Cass Avenue
Argonne, Illinois 60439
Phone: (630)252-3597
wagner@tcg.anl.gov

Prof. James C. Weisshaar
Department of Chemistry
University of Wisconsin
1101 University Avenue
Madison, Wisconsin 53706
Phone: 608.262.0266
weisshaar@chem.wisc.edu

Dr. Charles K. Westbrook
Division of Computational Physics
Lawrence Livermore National Laboratory
P. O. Box 808, L-014
Livermore, California 94551
Phone: 925.422.4108
westbrook1@llnl.gov

Prof. Phillip R. Westmoreland
Department of Chemical Engineering
University of Massachusetts
Amherst, Massachusetts 01003
Phone: (413)545-1750
westm@ecs.umass.edu

Dr. Michael G. White
Department of Chemistry
Brookhaven National Laboratory
Upton, New York 11973
Phone: 516.344.4301
mgwhite@bnl.gov

Prof. Curt Wittig
Department of Chemistry
University of Southern California
Los Angeles, California 90089-0484
Phone: (213)740-7368
wittig@chem1.usc.edu

Prof. David R. Yarkony
Department of Chemistry
Johns Hopkins University
Charles and 34th Streets
Baltimore, Maryland 21218
Phone: 410.516.4663
yarkony@jhuvms.hcf.jhu.edu

Prof. Timothy S. Zwier
Department of Chemistry
Purdue University
West Lafayette, Indiana 47907
Phone: (765)494-5278
zwier@chem.purdue.edu

Index

Author Index